BJR

THE BRITISH JOURNAL OF RADIOLOGY

Volume 62 Number 733 January 1989

CUK-H06096-16-P25849

16

X-ray Diagnosis • Ultrasound • Interventional Radiology
Radiotherapy • Oncology • Hyperthermia
Nuclear Medicine • Nuclear Magnetic Resonance
Radiation Physics • Radiobiology • Radiation Protection

BJR is published by The British Institute of Radiology BIR

You Can Depend On Our Diode Detectors For Patient Dose Verification During Treatment

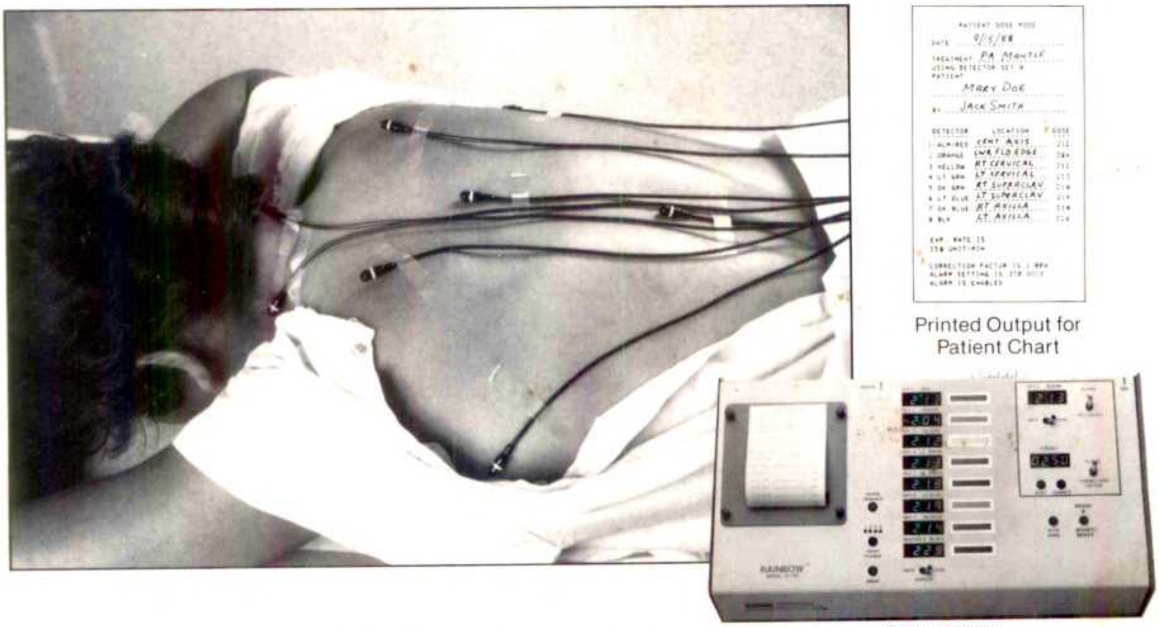

Printed Output for Patient Chart

RAINBOW™

Patient Dose Verification and QA Beam Analyzer with 8 Displays for 8 Detectors

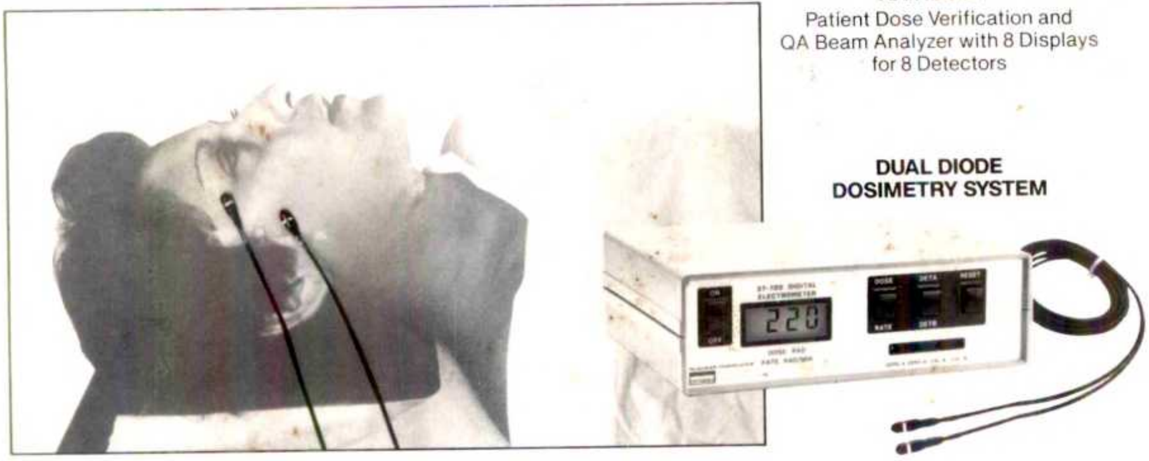

DUAL DIODE DOSIMETRY SYSTEM

- **Instant measurements will help prevent accidental overexposure to patients.**
- **Over 10 years of proven, reliable, dependable performance in the clinical environment.**
- **Detectors for photons and electrons.**
- **Unlimited versatility — use with your electrometer or ours.**

When coupled with a precision electrometer, our Diode Detectors offer the unique combination of high accuracy, ruggedness, small size, immediate readout, and simplicity of operation. The use of noble metal dopings, sophisticated mounting methods and special low noise cable have substantially reduced radiation induced damage, directional sensitivity and induced noise from cable movements, making these detectors perfect for the application of patient dose verification.

For complete details on our Diode Detectors and Diode Dosimetry Systems, request Bulletin 371-14

NUCLEAR ASSOCIATES

VICTOREEN

A Division of VICTOREEN, INC
100 VOICE ROAD
CARLE PLACE, NY 11514-1593 U.S.A.
(516) 741-6360
FAX (516) 741-5414

*Victoreen, Inc

P25849

BJR THE BRITISH JOURNAL OF RADIOLOGY

Established 1896

The Editorial Committee

Honorary Editors
J. T. Patton, FRCP, FRCR
N. J. McNally, BSc, MSc, PhD

Deputy Editors
D. G. Shaw, FRCP, FRCR
C. K. Bomford, BSc, MPhil, FInstP

Associate Editors
J. E. Adams, MB, BS, FRCP, FRCR
P. R. Blake, MB, BS, BSc, FRCR
J. A. Bullimore, MB, BS, MRCS, LRCP, DMRT, FRCR
R. G. Dale, MSc, PhD, CPhys, FInstP
P. Dawson, BSc, PhD, MB, BS, MRCP, MInstP, FRCR
S. Dische, MD, FRCR
F. A. Duck, PhD, MIEEE
A. H. Freeman, MB, BS, FRCR
R. M. Harrison, BSc, MSc, PhD, FInstP
J. W. Hopewell, BSc, PhD
W. D. Jeans, MB, BS, FRCR
D. M. King, MB, BS, FRCR, DMRD
H. W. C. Loose, DMRD, FRCR
D. W. Pilling, MB, ChB, DCH, DMRD, FRCR
M. J. Raphael, MA, MD, FRCP, FRCR, DMRD
J. R. K. Savage, DSc
R. A. Shields, PhD
D. M. Tait, MB, ChB, MRCP, FRCR
J. Tudor, MB, BS, FRCR
A. R. Valentine, MB, BS, MRCS, LRCP, FRCR, DMRD
G. H. Whitehouse, MB, BS, FRCP, FRCR, DMRD
A. G. Wilson, FRCP, FRCR
E. P. Wraight, MB, BChir, PhD, DMRT

Associate Editors Overseas
P. Armstrong, MB, BS, FRCR, DMRD (North America)
H. K. Baddeley, MB, BS, DMRD, FRCR, MRACR (Australasia)
S. G. A. Chenery, PhD, FCCPM (North America)
B. J. Cremin, MD, FRCR, FRACR (South Africa)
R. Fox, DPhil (Australia)
M. Takahashi, MD (Japan)
D. M. Taylor, DSc, CChem, FRSC (Continental Europe)

Managing Editor: Roderick Smith, BSc

The British Journal of Radiology is published monthly by the British Institute of Radiology, 36 Portland Place, London W1N 4AT. Telephone 01-580 4189 (editorial). Editorial communications should be addressed to the Honorary Editors in accordance with the Instructions to Authors published in the January issue each year, and copies of which may be obtained from the Managing Editor upon request.

Advertisements. Communications should be addressed to the Advertising Manager at the above address. Tel. 01-631 1168.

Subscriptions. The monthly fulfilment and distribution are carried out by Butterworth Scientific Ltd, PO Box 63, Westbury House, Bury Street, Guildford, Surrey GU2 5BH, UK. Telephone 0483 300966.

UK and Overseas subscription orders should be sent to: Westbury Subscription Services, PO Box 101, Sevenoaks, Kent TN15 8PL, UK. Telephone 0732 885833. Telex 95678. Facsimile 0732 884079. Cable Westbury, Sevenoaks, Kent. North American orders should be sent to: Journals Fulfilment Department, Butterworths, 80 Montvale Avenue, Stoneham, MA 02180, USA. Telex 880052. Telephone (617) 438 8464.

The annual subscription to *The British Journal of Radiology* (12 issues) for UK readers is £115.00. Overseas rates are £125.00. These prices include delivery by sea mail; airmail rates are available on request. Copies of this journal sent to subscribers in Bangladesh, Canada, India, Japan, Pakistan, Sri Lanka and USA are air-speeded for quicker delivery at no extra cost. Subscriptions are on a calendar year basis only.

All claims for unfulfilled subscriptions should be sent to Westbury Subscription Services at the above address.

Back issues prior to the current volume are available from Wm Dawson & Sons Ltd, Cannon House, Folkestone, Kent, England CT19 5EE. Telephone 0303 57421.

US mailing agents: Mercury Airfreight International Ltd Inc. Second class postage paid at Rahway, NJ, USA. Postmaster: send address corrections to The British Journal of Radiology, c/o Mercury Airfreight International Ltd Inc., 10B Englehard Avenue, Avenel, NJ 07001, USA.

THE BRITISH INSTITUTE OF RADIOLOGY

BIR

Founded 1897
Incorporated by Royal Charter
Patron: Her Majesty The Queen

The British Institute of Radiology is an association of persons interested in radiology and allied subjects. Meetings are held monthly from October until May. Particulars of membership and other information may be obtained on application to the General Secretary at the Institute, 36 Portland Place, London W1N 4AT.
Telephone: 01-580 4085 and 01-580 4189.
Cable Address: Britology, London W1.

President
B. S. Worthington, BSc, LIMA, MB, BS, LRCP, MRCS, DMRD, FRCR

Honorary Secretaries
M. Gowland, MB, ChB, FRCR, MRCP(Hon)
M. J. Harvey, TDCR, DMS

Honorary Treasurer
D. S. McIntosh, BSc, PhD, ARIC, MPS

General Secretary
Susan M. Johnstone, BA

The answer is 'YES'

Can APEX systems reconstruct SPECT slices in under 2½ seconds?

Does the rectangular field system have the largest commercially available detector head?

Is the APEX 409M the only mobile large-field camera system in the U.K.?

Does the range include a dedicated cardiac mobile Gamma Camera/ Computer?

Can I generate a gated heart report automatically before the patient leaves my department?

Will an APEX system let me perform bone densitometry scanning?

Can I produce hard copy of images on film and on paper?

Could Elscint install an APEX system in less than three days?

Can I depend on Elscint to provide me with fully comprehensive service contracts and operator training? Plus software support and assistance in developing programmes at no extra charge?

If I ask nicely, will Elscint provide me with more information about the APEX Series? And even arrange a visit to one of their working Local Area Networks in the U.K. so that I can see all the features and benefits of their APEX systems for myself?

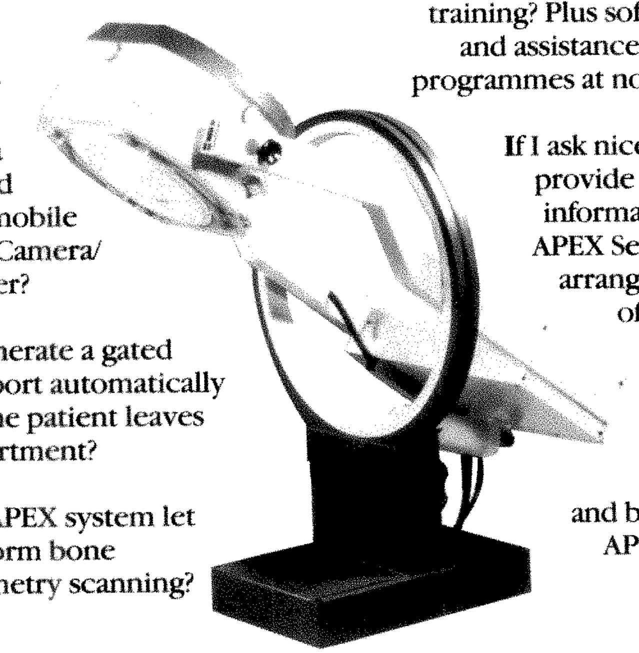

For further information or the chance to see for yourself, just call Mike Barker.

THE APEX DIGITAL NM SERIES

Elscint (G.B.) Ltd

Focused on the future.

Colonial Way, Watford, Herts WD2 4PT. Tel No: Watford (0923) 39511

VOL 62 NO 733 JANUARY 1989

The British Journal of Radiology

Contents

Papers

Page

High-resolution computed tomography in pulmonary cystic fibrosis 1
D. M. Hansell and B. Strickland

Hepatic venography in the surgical assessment of hepatic tumours 6
A. Odurny, M. J. McLoughlin, R. F. Colapinto and K. W. Sniderman

Clinically unsuspected complications of arterial surgery shown by post-operative digital subtraction angiography 13
C. Teeuwen, B. C. Eikelboom and J. W. Ludwig

Some indicative parameters on diagnostic radiology in Spain: first dose estimations 20
E. Vañó, L. González, A. Calzado, P. Morán and V. Delgado

Transient diverticula of the colon 27
J. Rawlinson and F. J. Brunton

Technetium-99m hydroxymethylene diphosphonate scanning of acute injuries to the lateral ligaments of the ankle 31
H. Maurice and I. Watt

Aortic tumours: report of a case and review of the literature 35
J. Schipper, J. A. van Oostayen, J. C. den Hollander and A. J. van Seyen

Cell kinetic changes in the follicular epithelium of pig skin after irradiation with single and fractionated doses of X rays 41
G. M. Morris and J. W. Hopewell

Precision of determining compliance with prescribed fields from conventional portal films 48
P. B. Dunscombe and K. Fox

Radiotherapy of epidermoid anal canal cancer 53
W. Dobrowsky

Discriminant analysis on the treatment results of interstitial radium tongue implants 59
M. Hoshina, H. Shibuya, J.-I. Horiuchi, S. Matsubara, S. Suzuki and M. Takeda

Results of treatment of carcinoma of the uterine cervix using the Newcastle afterloading technique 64
P. J. D. K. Dawes, E. M. Dean and G. D. Lambert

Technical notes

An indwelling intrauterine tube to facilitate intracavitary radiotherapy of carcinoma of the cervix 68
B. J. Smit, J. P. du Toit and W. A. Groenewald

A source localizing technique for the microSelectron-HDR afterloading system 69
C. H. Jones

Installation requirements for an argon laser angioplasty system 71
P. H. Smithson, W. D. Jeans and P. Murphy

Case reports

Van Buchem's disease with classical radiological features and appearances on cranial computed tomography 74
J. V. Cook, P. D. Phelps and J. Chandy

Anomalous superior vena cava causing non-visualization of the lungs in perfusion scintigraphy 78
A. Morgan and N. Evans

Ossified leiomyoma of the stomach: demonstration on computed tomography 79
R. M. Savit, M. M. Horrow and P. Agarwal

Primary extranodal lymphoma in muscle 81
J. Scally and A. Garrett

Polyorchidism diagnosed by ultrasound 82
P. Cadigan

Renal neoplasms in a family 83
V. M. Laurence and A. C. R. Robinson

Case of the month

A colonic double bubble 85
A. Harrison, L. Machin and A. Grundy

Short communication

Functional changes in the irradiated rat ureter: assessment by transit-time renography 87
J. F. Knowles and C. C. Nimmon

Correspondence

Late normal tissue reactions in patients with breast carcinoma 91
M. J. Tomlinson

Authors' reply 91
T. D. Bates and O. C. A. Scott

Diagnostic radiation, pregnancy and termination 92
J. G. B. Russell

Leakage from a caesium-137 needle 94
D. G. Clarkson

Costing imaging procedures 94
J. G. B. Russell

Author's reply 95
P. M. Bretland

Proceedings

Proceedings of The British Institute of Radiology
Too much radiation in radiodiagnosis? March 9, 1988 96

Instructions to authors 99

Book reviews

Magnetic resonance imaging of the central nervous system. *M. Brant-Zawadzki and D. Norman* (Eds) 101
Head and neck imaging. Handbooks of diagnostic imaging. *J. M. Unger* 101
Interpretation of the chest roentgenogram. *M. J. Landay* 101
Manual for the videofluorographic study of swallowing. *J. A. Logemann* 101
Transvaginal sonography. *I. E. Timor-Tritsch and S. Rottem* (Eds) 102
Percutaneous biopsy, aspiration and drainage. *J. G. Letourneau, M. K. Elyaderani and W. R. Castañeda-Zuñiga* 102
Safety and efficacy of radiopharmaceuticals 1987. *K. Kristensen and E. Norbygaard* (Eds) 102
Chernobyl: the real story. *R. F. Mould* 103
Ionizing radiation exposure of the population of the United States. *NCRP Report 93* 103
Lung cancer risk from indoor exposure to radon daughters. ICRP Publication 50. *H. Smith* (Ed.) 103
Data for use in protection against external radiation. ICRP Publication 51. *H. Smith* (Ed.) 104
Protection of the patient in nuclear medicine. ICRP Publication 52. *H. Smith* (Ed.) 104
The management of bladder cancer. *D. Raghavan* (Ed.) 105
Management of advanced cancer of prostate and bladder. *P. H. Smith and M. Pavone-Macaluso* (Eds) 105
Mesothelioma. Diagnosis and management. *C. F. Kittle* 106
International Agency for Research on Cancer. Biennial report 1986/87 106

BIR Bulletin and calendar events *facing page* 106

Featured in the next issue

Radiological evaluation of temporal bone disease: high-resolution computed tomography versus conventional X-ray diagnosis
P. Fritz, K. Rieden, T. Lenarz, J. Haels and K. zum Winkel

Films, screens and cassettes for mammography
J. Law and A. E. Kirkpatrick

© 1989 The British Institute of Radiology. This publication is copyright under the Berne Convention and the Universal Copyright Convention. All rights reserved, apart from any relaxations permitted under national copyright laws, no part of this publication may be reproduced, stored in a retrieval system or transmitted in any form or by any means without the prior permission of the copyright owners. Permission is not, however, required to copy abstracts of papers or of articles on condition that a full reference to the source is shown. Multiple copying of the contents of the publication without permission is always illegal.
Published by The British Institute of Radiology, 36 Portland Place, London W1N 4AT. Printed in Great Britain by The Whitefriars Press Ltd., Tonbridge. ISSN 0007 1285

VOL 62 NO 734 FEBRUARY 1989

The British Journal of Radiology

Contents

Papers

Page

Radiological evaluation of temporal bone disease: high-resolution computed tomography versus conventional X-ray diagnosis 107
P. Fritz, K. Rieden, T. Lenarz, J. Haels and K. zum Winkel

Basic concepts of femoral neck anteversion: comparison of two definitions 114
A. Høiseth, O. Reikerås and E. Fønstelien

Intravenous digital subtraction angiography in non-specific aorto-arteritis 117
S. Sharma, S. Aggarwal, K. K. Talwar and M. Rajani

Assessment of angioplasty balloon catheters: further studies 121
W. D. Jeans, J. H. L. Henson, T. M. A. Holloway, A. G. G. Forman and A. Blakeborough

Percutaneous drainage of subphrenic abscesses 127
D. van Gansbeke, C. Matos, M. Gelin, P. Müller, M. Zalcman, J. Devière and J. Struyven

Experiences at the new magnetic resonance imaging centre at Bristol 134
J. L. G. Thomson

Patient doses from computed tomography in Manitoba from 1977 to 1987 138
W. Huda, G. A. Sandison and T. Y. Lee

Radical radiotherapy for carcinoma of the vulva 145
N. J. Slevin and R. C. S. Pointon

Possibility of retrospective dosimetry for persons accidentally exposed to ionizing radiation using electron spin resonance of sugar and mother-of-pearl 148
T. Nakajima

Interstitial iridium-192 implantation for malignant brain tumours. Part I: Techniques of dosimetry planning 154
A. Wu, M. Chun, D. Kasdon, D. Heros, P. McKeough and H. Chang

Interstitial iridium-192 implantation for malignant brain tumours. Part II: Clinical experience 158
M. Chun, P. McKeough, A. Wu, D. Kasdon, D. Heros and H. Chang

Films, screens and cassettes for mammography 163
J. Law and A. E. Kirkpatrick

Case reports

Unusual long bone changes in thalassaemia: findings on plain radiography and computed tomography 168
T. Singcharoen

Sickle-shaped scapulae in a patient with the Pierre Robin syndrome 171
D. R. Bezirdjian and R. Szucs

Re-irradiation of astrocytoma of the brain 173
A. Y. Rostom and K. Sunderland

Autopsy assessment of the Gunther vena caval filter 174
M. Mahendran, D. J. Gwilt, O. P. Fitzgerald Finch and S. Jalloh

Demonstration on computed tomography of tracheomalacia in tracheobronchomegaly (Mounier-Kuhn syndrome) 176
A. J. Doyle

Lipoma arborescens of the knee 178
S. J. Armstrong and I. Watt

Cystic haemangioma of the spleen: findings on ultrasound and computed tomography 180
M. J. Duddy and C. J. Calder

Case of the month

The jockey with a mass in the thigh 183
A. M. Davies, N. Evans and R. J. Grimer

Short communications

Radiation dose to urological surgeons during X-ray fluoroscopy for percutaneous stone extraction 185
J. Law, J. A. Inglis and D. A. Tolley

Intraoperative radioactive localization of an osteoid osteoma: a useful variation in technique 187
B. D. Todd, L. W. Godfrey and R. N. Bodley

Alteration of cardiac myosin isozymes after whole-body irradiation 189
R. Z. Litten, T. L. Walden, G. T. Gainey and R. Nagai

Correspondence

Variation of image quality with X-ray tube potential in mammography 192
J. Law, K. Faulkner and S. Smith

Aid to localization for computed tomographic biopsy and aspiration procedures 193
M. J. Turner and P. Ball

Stress changes of the wrist in adolescent gymnasts 194
M. R. T. F. Read

The cost of imaging procedures 194
W. D. Jeans

Book reviews

Radiation dose to patients from radiopharmaceuticals: a report of a task group of Committee 2 of the ICRP. *ICRP Publication 53* 195
Non-ionising radiation: microwaves, ultraviolet and laser radiation. *H. Moseley* 195
Quality assurance and image artifacts in magnetic resonance imaging. *R. James, R. Knowles and J. A. Markisz* 196
Clinimetrics. *A. R. Feinstein* 196
Nuclear and atomic data for radiotherapy and related radiobiology. Proceedings of a meeting at Rijswijk, 16–20 September, 1985 196
Physical aspects of brachytherapy. *T. J. Godden* 197
Pediatric tumors of the genitourinary tract. *B. H. Broecker and F. A. Klein* (Eds) 197
Essentials of clinical MRI. *T. H. M. Falke* (Ed.) 197
MRI: a teaching file approach. *J. H. Bisese* 198
MRI of the brain, head, neck and spine. A teaching atlas of clinical applications. *J. Valk* 198
Magnetic resonance imaging of the brain, head and neck. A text atlas. *W. G. Bradley Jr, W. R. Adey and A. N. Hasso* 198
Cranial and spinal magnetic resonance imaging. An atlas and guide. *D. L. Daniels, V. M. Haughton and T. P. Naidich* 199
Atlas of axial, sagittal and coronal anatomy (with CT and MRI). *A. J. Christoforidis* (Ed.) 199
Magnetic resonance imaging of the knee. *J. H. Mink, M. A. Reicher and J. V. Crues III* 200
Clinical applications of Doppler ultrasound. *K. J. W. Taylor, P. N. Burns and P. N. T. Wells* (Eds) 200

BIR Bulletin and calendar events *facing page 200*

Featured in the next issue

Paediatric brachytherapy. Part I: The role of brachytherapy in the multidisciplinary therapy of localized cancers
P. N. Plowman, D. Doughty and A. N. Harnett

Paediatric brachytherapy. Part II: Brain implantation
E. S. Thomson, F. Afshar and P. N. Plowman

A new high-definition microfocal X-ray unit
J. C. Buckland-Wright

Clinical applications of high-definition microfocal radiography
J. C. Buckland-Wright and C. R. Bradshaw

© 1989 The British Institute of Radiology. This publication is copyright under the Berne Convention and the Universal Copyright Convention. All rights reserved, apart from any relaxations permitted under national copyright laws, no part of this publication may be reproduced, stored in a retrieval system or transmitted in any form or by any means without the prior permission of the copyright owners. Permission is not, however, required to copy abstracts of papers or of articles on condition that a full reference to the source is shown. Multiple copying of the contents of the publication without permission is always illegal.

Published by The British Institute of Radiology, 36 Portland Place, London W1N 4AT. Printed in Great Britain by The Whitefriars Press Ltd., Tonbridge.
ISSN 0007 1285

VOL 62 NO 735 MARCH 1989

The British Journal of Radiology

Contents

Papers

Page

A new high-definition microfocal X-ray unit 201
J. C. Buckland-Wright

Clinical applications of high-definition microfocal radiography 209
J. C. Buckland-Wright and C. R. Bradshaw

Paediatric brachytherapy. I. The role of brachytherapy in the multidisciplinary therapy of localized cancers 218
P. N. Plowman, D. Doughty and A. N. Harnett

Paediatric brachytherapy. II. Brain implantation 223
E. S. Thomson, F. Afshar and P. N. Plowman

Radiation dose to neonates on a Special Care Baby Unit 230
K. Faulkner, J. L. Barry and P. Smalley

Experimental intra-arterial administration of SR-2508 in the rabbit V2 carcinoma model 234
D. M. Coldwell, J. Huff, H. Marcellus and S. G. Coldwell

A comparison of two different T-grain films in rare-earth screens with a standard film–screen combination for intravenous pyelography and bone examinations 237
H. Logan, L. Daly and J. Masterson

Radiobiological assessment of permanent implants using tumour repopulation factors in the linear-quadratic model 241
R. G. Dale

Evaluation of response following irradiation of juvenile angiofibromas 245
A. C. R. Robinson, G. G. Khoury, D. V. Ash and B. D. Daly

Contribution of computed tomography in the aetiology and prognosis of cerebral palsy in children 248
E. Schouman-Claeys, A. Picard, G. Lalande, G. Kalifa, P. Lacert, E. Brentanos and G. Frija

Outpatient myelography: an acceptable and cost-effective technique 253
A. H. Choudhri, P. C. Rowlands, C. J. Barber, J. Johnson and J. M. Stevens

Radiological appearances of colonic ring staple anastomoses 256
B. D. Daly and B. M. Crowley

A large trial of intravenous Conray 325 and Niopam 300 to assess immediate and delayed reactions 260
M. McCullough, P. Davies and R. Richardson

Technical note

An iodine-125 applicator designed for irradiating blood vessels growing into the cornea of the eye 266
E. R. Hering, R. Sealy, J. B. Korrubel and J. Hill

Case reports

Value of bone scanning and computed tomography in fibrodysplasia ossificans progressiva 269
S. R. Carter, A. M. Davies, N. Evans and R. J. Grimer

Ultrasound diagnosis of gallbladder perforation in a case of xanthogranulomatous cholecystitis 273
J. P. Houston, M. A. Sampson and M. C. Collins

Giant central disc prolapse: a pitfall in computed tomographic diagnosis 274
G. Buirski

Submarine escape training, lung cysts and tension pneumothorax 276
W. R. Saywell

Case of the month

The misleading pre-operative chest radiograph 279
J. Ipinyomi and I. Watt

Short communications

Effects of inhibition of intercellular communication on repair of damage induced by ionizing radiation 281
J. Madhoo and G. Blekkenhorst

Precipitation of radiation injury in kidney epithelium reveals a low fractionation sensitivity ($\alpha/\beta = 12.5$ Gy) 283
C. Ewen and J. H. Hendry

Autoradiographic imaging of pion stopping distribution utilizing scanning laser stimulated luminescence 285
H. Shirato, C. C. Gaffney and G. B. Goodman

Primary orbital lymphoma: staging by computed tomographic scanning 287
P. Mills and C. A. Parsons

Demonstration of vertebral body end plate veins by magnetic resonance imaging 290
W. R. Saywell, H. V. Crock, J. P. S. England and R. E. Steiner

Correspondence

An analysis of referrals for primary diagnostic ultrasound to a general X-ray department 293
R. Fitzgerald, G. Mackie and R. Manns

Reply 293
K. C. Dewbury

Sarcoidosis mimicking metastatic testicular tumour 293
S. K. Morcos

New developments in the field of acute myocardial infarct imaging 294
D. Jain, A. Lahiri, J. C. Crawley and E. B. Raftery

Reply 294
D. Bell, A. M. Millar, R. Grayshan and A. L. Muir

The unseen radiation hazards of ultrasound 295
A. C. Havard

Incorporating the time factor into the linear-quadratic model 296
J. van de Geijn

Post-operative neutron irradiation 298
A. Courdi

Reply 298
J. Glaholm and C. Harmer

Book reviews

Doppler echocardiography. The quantitative approach, 2nd edn. *A. J. Labovitz and G. A. Williams* 300
Ultrasonography of the neck. *J.-N. Bruneton* 300
The use of transrectal ultrasound in the diagnosis and management of prostate cancer. *F. Lee and R. D. McLeary* (Eds) 300
Cerebral angio-CT. *K. Sadamoto and K. Fukui* 301
Normal anatomy for multiplanar imaging. I. The trunk and extremities. II. Head, neck and spine. *B. Raval, J. W. Yeakley and J. H. Harris Jr* 301
Computed tomography of the chest: a teaching file. *M. E. Gale and J. B. Karlinsky* 301
Renal and adrenal tumors: pathology, radiology, ultrasonography, magnetic resonance (MRI), therapy, immunology, 2nd edn. *E. Löhr and L.-D. Leder* (Eds) 301
Rational use of diagnostic imaging in paediatrics. Report of a WHO study group. *World Health Organization Technical Report Series 757* 302

BIR Bulletin *facing page* 302

Featured in the next issue

Acute rhabdomyolysis: evaluation with magnetic resonance imaging compared with computed tomography and ultrasound
A. E. Lamminen, P. E. Hekali, E. Tivla, I. Suramo and O. A. Korhola

The ICRU recommendations for reporting intracavitary therapy in gynaecology and the Manchester method of treating cancer of the cervix uteri
J. M. Wilkinson and T. P. Ramachandran

Treatment of persistent and recurrent nasopharyngeal carcinoma by brachytherapy
J. S. T. Sham, W. I. Wei, D. Choy, C. M. Ho, P. T. H. Tai and P. H. K. Choi

© 1989 The British Institute of Radiology. This publication is copyright under the Berne Convention and the Universal Copyright Convention. All rights reserved, apart from any relaxations permitted under national copyright laws, no part of this publication may be reproduced, stored in a retrieval system or transmitted in any form or by any means without the prior permission of the copyright owners. Permission is not, however, required to copy abstracts of papers or of articles on condition that a full reference to the source is shown. Multiple copying of the contents of the publication without permission is always illegal. Published by The British Institute of Radiology, 36 Portland Place, London W1N 4AT. Printed in Great Britain by The Whitefriars Press Ltd., Tonbridge.

ISSN 0007 1285

1989, *The British Journal of Radiology*, 62, 1–5

VOLUME 62 NUMBER 733 JANUARY 1989

The British Journal of Radiology

High-resolution computed tomography in pulmonary cystic fibrosis

By David M. Hansell, MRCP, FRCR and Basil Strickland, FRCP, FRCR

Department of Radiology, Brompton Hospital, London

(*Received March 1988 and in revised form June 1988*)

Abstract. Twenty-one patients with established cystic fibrosis were examined using high-resolution, narrow-section computed tomography. The bronchiectasis of cystic fibrosis is described and is shown to be characteristic in many respects. Computed tomography was found to be more accurate than standard radiography in locating the disease process and demonstrated pleural involvement which was not apparent on chest radiographs.

The typical radiological features of bronchiectasis are evident on the chest radiograph of virtually all patients with established cystic fibrosis. The thickened bronchial walls are manifest as either parallel lines when seen in profile or ring shadows when seen end-on. In addition to the radiographic signs of bronchiectasis, other features may be present on a chest radiograph: overinflated lungs, atelectasis, thin-walled cystic spaces, and hilar enlargement due to lymphadenopathy or pulmonary arterial hypertension (Friedman et al, 1981).

On a chest radiograph, the extent and pattern of bronchiectasis in cystic fibrosis is masked by the summation of shadows from bronchial wall thickening, mucus plugs and superadded parenchymal consolidation. Even in patients with little additional shadowing, the chest radiograph is not sufficiently sensitive to assess the full extent of bronchiectasis (Currie et al, 1987a). Bronchography is contraindicated in these patients and the only detailed studies of the bronchiectasis of cystic fibrosis have been of the appearances at post-mortem examination (Andersen, 1962). Using narrow-section computed tomography (CT) we have studied a number of patients with cystic fibrosis, most of whom were being assessed prior to heart–lung transplantation.

Methods

Twenty-one patients were studied and their ages ranged from 15 to 43 years (median 29 years). The age at diagnosis of cystic fibrosis varied from 2 months to 3 years. Computed tomography was performed on all patients and concurrent postero-anterior (PA) chest radiographs were assessed in 17 cases. Computed tomography was performed using an Elscint 2002 scanner with a scanning time of 5.5 s. A standard protocol (contiguous 10 mm slices) and a high-resolution protocol (interspaced 3 mm slices) were both used in the majority of cases (16 out of 21). In some cases the patients were scanned prone as well as supine to clarify subpleural opacification (Strickland et al, 1986). In one case, scans in full expiration were obtained to determine the degree of air-trapping. Intravenous contrast was not given so the contribution to hilar enlargement by pulmonary artery dilatation or lymph node enlargement could not be accurately assessed.

The chest radiographs and CT scans were assessed separately and in random order. The distribution of abnormalities was described in terms of lobes on CT scans and in zones on the available PA chest radiographs. On both CT scans and chest radiographs the following features were recorded: (i) the presence or absence of lung overinflation, (ii) bronchial dilatation —(a) proximal or distal, or (b) cylindrical, varicose or cystic, (iii) the presence or absence of volume loss (zone or lobe), (iv) pleural thickening, and (v) complications.

The division of bronchiectasis into cylindrical, varicose and cystic types follows the classification of Reid (1950). The distinction between proximal and distal bronchial involvement was taken arbitarily as a point midway radially from the hilum to the chest wall. The degree of dilatation of the bronchiectatic airways on CT was graded as mild, moderate or severe. Pleural thickening was described as limited (*i.e.* pleural tags) or extensive and the site recorded.

Results

Bronchiectasis was present in 84 out of 102 zones in 16 out of 17 cases on plain chest radiography compared with 124 out of 126 lobes in all patients (21) who had CT scans.

Chest radiography consistently underdiagnosed the

Address correspondence to: Dr D. M. Hansell, Department of Radiology, Westminster Hospital, Dean Ryle Street, London SW1P 2AP.

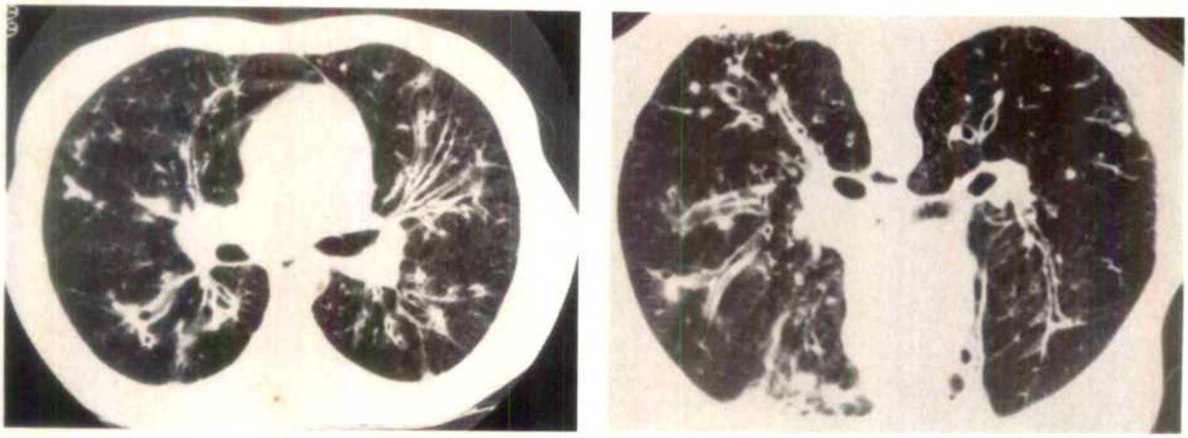
(a) (b)

Figure 1. Two examples (a) supine and (b) prone of the cylindrical type of bronchiectasis seen in cystic fibrosis. Note the areas of pleural thickening posteriorly.

extent of bronchiectasis: 58 (69%) of the 84 zones affected were reported as showing only proximal involvement, the remainder showing both proximal and distal bronchiectasis (26 out of 84, 31%). However, CT demonstrated bronchiectasis extending distally in 73 out of the 124 affected lobes (59%). No case showed distal bronchiectasis without proximal involvement.

All three patterns of bronchiectasis were seen on CT and these sometimes coexisted in the same lobe. The predominant type was cylindrical (Fig. 1) (116 out of 124) with cystic (42 out of 124) and varicose (13 out of 124) bronchiectasis seen much less frequently. In individual patients the type of bronchiectasis was remarkably constant at all sites involved, as was the degree of bronchial dilatation. The features of bronchiectasis in cystic fibrosis demonstrated on CT are summarized in Table I.

Cases which showed large, cystic, thin-walled air spaces were analysed to determine whether there were any features which discriminated between dilated bronchi and air cysts. Twelve cases had cystic spaces and seven of these were identified as dilated bronchi either because of their continuity with bronchi or because of the presence of the signet-ring sign (Fig. 2) of the accompanying pulmonary artery (Naidich et al, 1984). In two cases the cystic spaces were peripheral and discontinuous with the bronchiectatic airways. In three cases the distinction between air spaces having the appearances of bullae and grossly dilated bronchi could not be made (Fig. 3).

Volume loss as a result of either atelectasis or fibrosis was identified on CT in 21 out of 126 lobes in 10 patients and this occurred most frequently in the upper lobes (upper, 12; middle, 5; lower, 4). Evidence on CT of pleural thickening was found in 15 of the 21 patients studied (compared with eight cases on plain radiography). The extent of pleural disease in each case is summarized in Table II. Pleural thickening was demonstrated most often in the upper zones and was almost

Table I. Features of bronchiectasis in cystic fibrosis in computed tomography

Features	Lobes (total = 126)	%
Bronchiectasis present	124	98
Distribution of bronchiectasis		
Proximal only	51	41
Proximal and distal	73	59
Distal only	0	0
Pattern of bronchiectasis		
Cylindrical	116	94
Varicose	13	11
Cystic	42	34

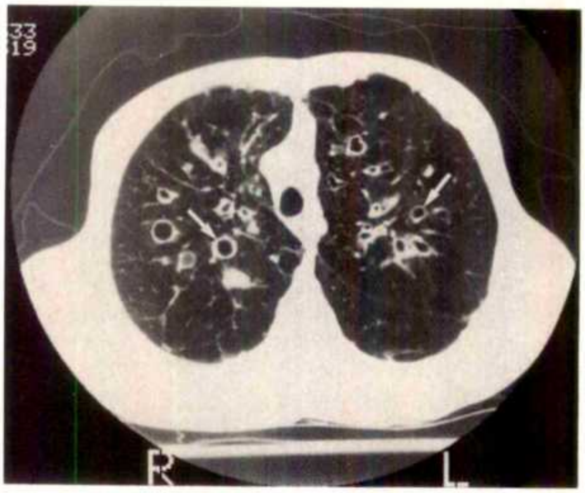

Figure 2. The "signet-ring" sign of pulmonary arteries accompanying dilated bronchi (arrows) running vertically in the upper lobes.

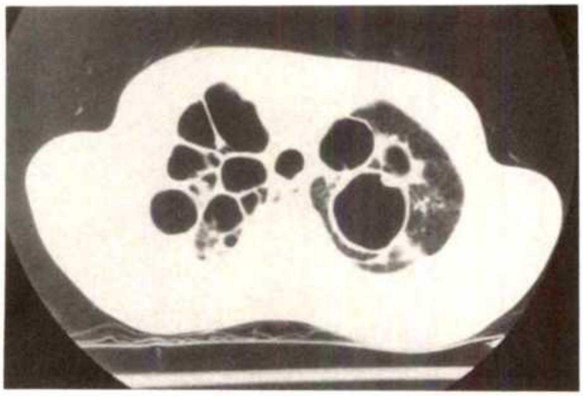

Figure 3. Large cystic spaces in the upper lobes. The distinction between severe cystic bronchiectasis and bullae cannot be made.

invariably posterior (14 out of the 15 cases showed a predominantly posterior distribution) (Fig. 4).

Overinflation of the lungs, as judged subjectively on CT, was present in 19 of the 21 patients. The single case in which scans were taken in full expiration showed virtually no change in cross-sectional diameter of the chest at the extremes of respiration, indicating severe air-trapping. Focal lobar consolidation was seen in six cases but there was no specific lobar predilection. Two patients were thought to have pneumothoraces on plain chest radiographs; one was confirmed by CT, the other was shown to be a bulla at the left apex. In one patient an air–fluid level was demonstrated in an empyema on CT; the chest radiograph showed the same air–fluid level in the left upper zone and this was interpreted as a lung abscess.

Table II. Extent of pleural thickening on computed tomography

	Limited (12 patients)		Extensive (3 patients)	
	R	L	R	L
Upper zone	8	5	3	2
Mid zone	5	2	1	0
Lower zone	1	0	1	0

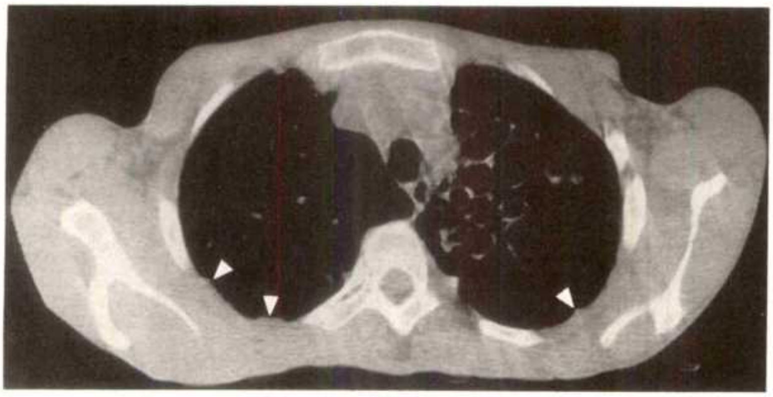

(a)

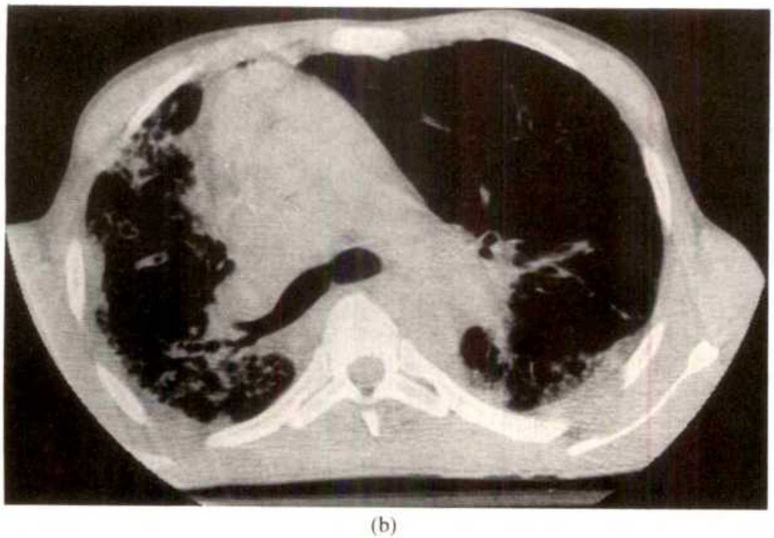

(b)

Figure 4. (a) Limited pleural tags posteriorly in the upper chest (arrowheads) which were confirmed macroscopically and on histology following removal of the recipient lungs. (b) Extensive pleural thickening bilaterally. There is marked contraction of the right lung because of fibrosis.

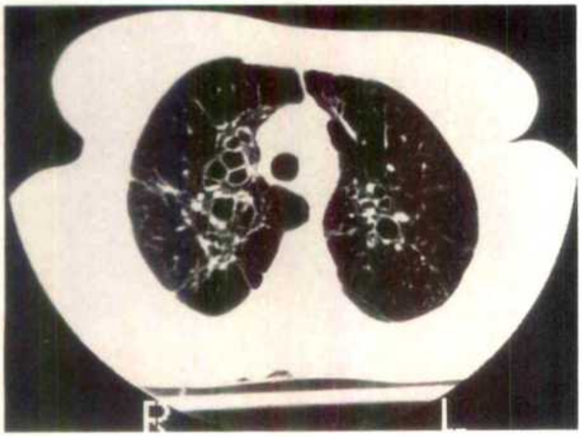

Figure 5. The proximal varicose and cystic bronchiectasis of allergic broncho-pulmonary aspergillosis.

Discussion

Widespread bronchiectasis is a cardinal feature of cystic fibrosis (Friedman, 1987). To date, studies of the type and distribution of bronchiectasis have relied on post-mortem specimens and inferences drawn from chest radiographs (Hodson & France, 1962; Friedman et al, 1981). Our study of patients with cystic fibrosis, using narrow-section CT, shows that cylindrical bronchiectasis is the commonest pattern and that bronchial involvement extending to the periphery of the lung is seen in most cases (Fig. 1). This pattern was seen in at least two lobes in 17 out of the 21 patients studied. The division of bronchiectasis into cylindrical, varicose and cystic types by Reid (1950) supposedly gives an indication of the degree of bronchial wall damage with end-stage bronchiectasis being characterized by a cystic pattern. The predominance of cylindrical bronchiectasis in our series is at variance with the only other published study which has employed CT in the assessment of pulmonary cystic fibrosis (Jacobsen et al, 1986). In that study, only four out of the 12 patients showed a cylindrical pattern, the remainder were reported as showing a varicose or saccular pattern. The apparent difference in the frequency of the types of bronchiectasis in cystic fibrosis in the latter study may relate to differences of interpretation or the use of wider CT sections.

The CT features of the bronchiectatic airways in cystic fibrosis are in marked contrast to those seen in allergic broncho-pulmonary aspergillosis. In the latter, the bronchiectasis is proximal and varicose or cystic (Fig. 5) (McCarthy et al, 1970; Currie et al, 1987b). The clinical, biochemical and immunological differences between cystic fibrosis and allergic broncho-pulmonary aspergillosis almost invariably allows the correct diagnosis to be made. However, the plain radiographic appearances of relatively mild cystic fibrosis and severe allergic broncho-pulmonary aspergillosis may be deceptively similar. Whilst the bronchial wall thickening seen in these two conditions may be apparent on plain radiographs, the characteristic pattern and extent of the bronchiectasis is readily delineated by CT.

The exact nature of the large cystic spaces in the lungs shown on CT in half the cases studied was difficult to assess. Grossly dilated airways are indistinguishable from bullae unless the cystic spaces can be seen to be in continuity with bronchi on adjacent sections (Friedman, 1987). These air-containing cysts were confined to the upper lobes and most were peripheral, a distribution confirmed in a pathological study which also found that the largest cysts were bronchiectatic in origin (Tomashefski et al, 1985). Most of the cysts (classified as bronchiectasis cysts, emphysematous bullae or interstitial air cysts) in this latter study were found in a subpleural distribution, perhaps accounting for the high incidence of pneumothorax in patients with cystic fibrosis. In our study the frequency of the finding of contracted upper lobes containing large cysts was striking and, in the past, the plain chest radiograph appearances of the upper lobes in longstanding cystic fibrosis were sometimes erroneously attributed to pulmonary tuberculosis (Wood et al, 1976).

The reason for submitting these patients to CT prior to heart–lung transplantation was to assess the amount of pleural thickening present. The separation of pleural adhesions during surgery may be a cause of severe haemorrhage. In this series, three patients were found to have extensive pleural thickening which was thought likely to cause significant difficulty at surgery; in one case, the pleural fibrosis was due to previous pleurodesis. The frequency of pleural thickening demonstrated on CT (15 out of 21) was surprising and this high incidence has not been previously reported. Metaplastic changes in the visceral pleura in cystic fibrosis have been described in a single case report (Dunnill, 1959) in which there was considerable thickening of the fibrous part of the mesothelium and evidence of intracellular vacuolation. Dunnill ascribed these changes to the rupture of small bronchiectatic abscesses into the pleural cavity.

The extent of pleural thickening may have a critical bearing on a patient's suitability for heart–lung transplant. Plain chest radiography is inadequate for assessing accurately the presence and extent of pleural thickening especially given its typical distribution posteriorly in the upper part of the chest.

Acknowledgments

We would like to thank all the clinicians at the Brompton Hospital, particularly Dr M. Hodson, who referred their patients for CT scanning.

References

ANDERSEN, D. H., 1962. Pathology of cystic fibrosis. *Annals of the New York Academy of Science*, *93*, 500–517.

CURRIE, D. C., COOKE, J. C., MORGAN, A. D., KERR, I. H., DELANY, D., STRICKLAND, B. & COLE, P. J., 1987a. Interpretation of bronchograms and chest radiographs in patients with chronic sputum production. *Thorax*, *42*, 278–284.

CURRIE, D. C., GOLDMAN, J. M., COLE, P. J. & STRICKLAND, B., 1987b. Comparison of narrow section computed tomography and plain chest radiography in chronic allergic bronchopulmonary aspergillosis. *Clinical Radiology*, *38*, 593–596.

DUNNILL, M. S., 1959. Metaplastic changes in the visceral pleura in a case of fibrocystic disease of the pancreas. *Journal of Pathology and Bacteriology*, *77*, 299–302.

FRIEDMAN, P. J., 1987. Chest radiographic findings in the adult with cystic fibrosis. *Seminars in Roentgenology*, *22*, 114–124.

FRIEDMAN, P. J., HARWOOD, I. R. & ELLENBOGEN, P. H., 1981. Pulmonary cystic fibrosis in the adult: early and late radiologic findings with pathologic correlation. *American Journal of Roentgenology*, *136*, 1131–1144.

HODSON, C. J. & FRANCE, N. E., 1962. Pulmonary changes in cystic fibrosis of the pancreas. A radio-pathological study. *Clinical Radiology*, *13*, 54–61.

JACOBSEN, L. E., STUART HOUSTON, C., HABBICK, B. F., GENEREUX, G. P. & HOWIE, J. L., 1986. Cystic fibrosis: a comparison of computed tomography and plain chest radiographs. *Journal of the Canadian Association of Radiologists*, *37*, 17–21.

MCCARTHY, D. S., SIMON, G. & HARGREAVE, F. E., 1970. The radiological appearances in allergic broncho-pulmonary aspergillosis. *Clinical Radiology*, *21*, 366–375.

NAIDICH, D. P., ZERHOUNI, E. A. & SIEGELMAN, S. S., 1984. Airways. In *Computed Tomography of the Thorax* (Raven Press, New York), pp. 104–105.

REID, L. M., 1950. Reduction in bronchial subdivision in bronchiectasis. *Thorax*, *5*, 233–247.

STRICKLAND, B., BRENNAN, J. & DENISON, D. M., 1986. Computed tomography in diffuse lung disease: improving the image. *Clinical Radiology*, *37*, 335–338.

TOMASHEFSKI, J. F., BRUCE, M., STERN, R. C., DEARBORN, D. G. & DAHMS, B., 1985. Pulmonary air cysts in cystic fibrosis: relation of pathologic features to radiologic findings and history of pneumothorax. *Human Pathology*, *16*, 253–261.

WOOD, R. E., BOAT, T. F. & DOERSHUK, C. F., 1976. Cystic fibrosis (state of the art). *American Review of Respiratory Diseases*, *113*, 833–878.

1989, *The British Journal of Radiology*, 62, 6–12

Hepatic venography in the surgical assessment of hepatic tumours

By Allan Odurny, MB, FRCS, FRCR, Michael J. McLoughlin, MB, FRCR, FRCP(C), Ronald F. Colapinto, MD, FRCP(C) and Kenneth W. Sniderman, MD, FRCP(C)

Department of Radiological Sciences, Toronto General Hospital, 200 Elizabeth Street, Toronto, Ontario M5G 2C4, Canada

(*Received April 1988 and in revised form July 1988*)

Abstract. Hepatic venography was performed on 80 patients with hepatic tumours for the pre-operative assessment of resectability. Sixty-six patients subsequently underwent laparotomy, 27 undergoing hepatic resection. Forty-two patients had metastases from colo-rectal primaries, 19 hepatocellular carcinoma and 19 a variety of other tumours. The type and frequency of the abnormalities shown on venography were noted for each tumour category and for their hepatic segmental distribution. The results of venography were compared with those of arteriography, computed tomography and ultrasound and with the findings at laparotomy. Displacement was the commonest abnormality seen while encasement or obstruction occurred less frequently and tumour invasion was rare. The sensitivity of venography in correctly identifying the segmental distribution of tumour deposits was 41%. Sensitivity was poorest with tumours in the left lobe (31%) and bilobar tumours (0%). Venography was most sensitive in detecting tumour involvement of the major segmental hepatic veins and inferior vena cava (100%). Peripheral colo-rectal metastases frequently produced no venographic abnormality. Hepatic venography provides no additional information to arteriography, computed tomography or ultrasound in patients with peripheral or bilobar tumour deposits. Some additional information may be obtained with central tumours and venography is the most accurate means of detecting tumour involvement of the major segmental hepatic veins.

The prognosis for primary hepatocellular carcinoma (HCC) is poor, with a 5-year survival of 4–8% (Marks et al, 1979b). Metastatic deposits in the liver from colo-rectal tumours are present in 15–25% of patients at diagnosis. A further 5–7% will develop metachronous deposits (Bengmark & Hafstrom, 1969; Foster & Berman, 1977; Bengtsson et al, 1981; Taylor et al, 1983). For both primary and secondary hepatic tumours, resection is now an accepted form of treatment, with 5-year survival rates of 25% being reported, compared with 0–3% at 5 years for unresected deposits (Taylor et al, 1983; Adson et al, 1984; Wagner et al, 1984; Taylor, 1985).

Since the technique of hepatic resection is determined by the segmental distribution of the hepatic vascular supply, demonstration of both arterial and venous anatomy is essential. In order to demonstrate venous anatomy, we have performed hepatic venography on all patients being considered for hepatic resection. To assess the value of venography in predicting resectability and to assess the comparative diagnostic accuracy of venography, arteriography, ultrasound and computed tomography (CT) in determining the segmental distribution of tumour deposits, we reviewed the medical records of all patients with hepatic tumours undergoing hepatic venography over a 5-year period.

Materials and methods

The medical records of 80 consecutive patients with hepatic tumours who underwent hepatic venography between November 1981 and October 1986 were reviewed. The spectrum of venographic abnormalities demonstrated and the relationship of such abnormalities to the type and position of tumour deposits were noted. The results of arteriography, ultrasound and CT were also reviewed in those patients in whom these investigations had been performed. Hepatic resection or laparotomy was performed in 66 patients. The extent and distribution of tumour deposits as predicted by arteriography, venography, CT and ultrasound were compared with the findings at surgery.

Particular attention was given to the accuracy of venography in determining tumour proximity to the major hepatic veins and inferior vena cava (IVC) and to the sensitivity of hepatic venography in predicting spread of tumour across hepatic segmental boundaries. Tumour distribution was defined as: (a) peripheral; lying peripherally in the right or left lobes, (b) central; in close relationship to the middle hepatic vein whether in the right or left lobe, (c) major hepatic veins/IVC; involving posteriorly the hepatic IVC or origins of the major hepatic veins and (d) bilobar; deposits in the periphery of both lobes.

Hepatic venography was usually performed via a cut-down onto a vein in the antecubital fossa using a 7 F Cournand catheter. Occasionally, if the arm veins were unsuitable, an internal jugular vein approach was used. Alternatively, a femoral vein puncture was performed, using either a pre-shaped 6.5 F Kifa or 5.5 F Simmons-type catheter. The hepatic veins are located just below the junction of the IVC and right atrium, the veins normally arising antero-laterally. The middle and left hepatic veins usually have a common trunk. The orifices

---

Address reprint requests to: Dr A. Odurny, Department of Radiology, Southampton General Hospital, Tremona Road, Southampton, Hants SO9 4XY.

Table I. Abnormalities detected on hepatic venography

	Number of venograms	Number abnormal	Abnormalities			
			Displacement	Encasement	Obstruction	Invasion
Colorectal carcinoma	42	19 (45%)	16	5	3	—
Hepatocellular carcinoma	19	14 (74%)	10	12	7	2
Others	19	13 (68%)	7	5	6	—

of the veins were located by searching with the catheter tip, then selectively cannulated. Correct positioning of the catheter was confirmed with a test injection of contrast medium. The procedure was generally easier from the cubital fossa or jugular approach because of the angle of origin of the hepatic veins. Biplanar views of right, middle and left hepatic veins were obtained following injection of 15–20 ml of contrast medium into each vein. Major accessory veins were also catheterized; minor accessory veins and veins supplying the caudate lobe were not injected.

Computed tomography was performed on EMI 5005 or 7070 scanners. Scans were performed with a 1 cm slice at 1–1.5 cm intervals, usually both before and after an intravenous bolus of 100 ml of contrast medium. Ultrasound examinations were performed on a variety of real-time scanners using 3.5 and 5.0 MHz transducers. Because of the retrospective nature of the study, neither CT nor ultrasound scans were performed specifically to visualize hepatic veins and not all examinations delineated these structures completely.

Results

Hepatic venography was performed in 80 patients, 52 male and 28 female, with ages ranging from 22 to 74 years (mean 53 years). Metastatic deposits from colonic or rectal carcinoma were present in 42 patients. Nineteen patients had hepatocellular carcinoma (HCC). Ten patients had metastases from other sources: two breast carcinomas, two ovarian carcinomas, two carcinoid tumours and one each of pancreatic gastrinoma, adrenal, renal and gastric carcinoma. Hepatic sarcoma was pre-

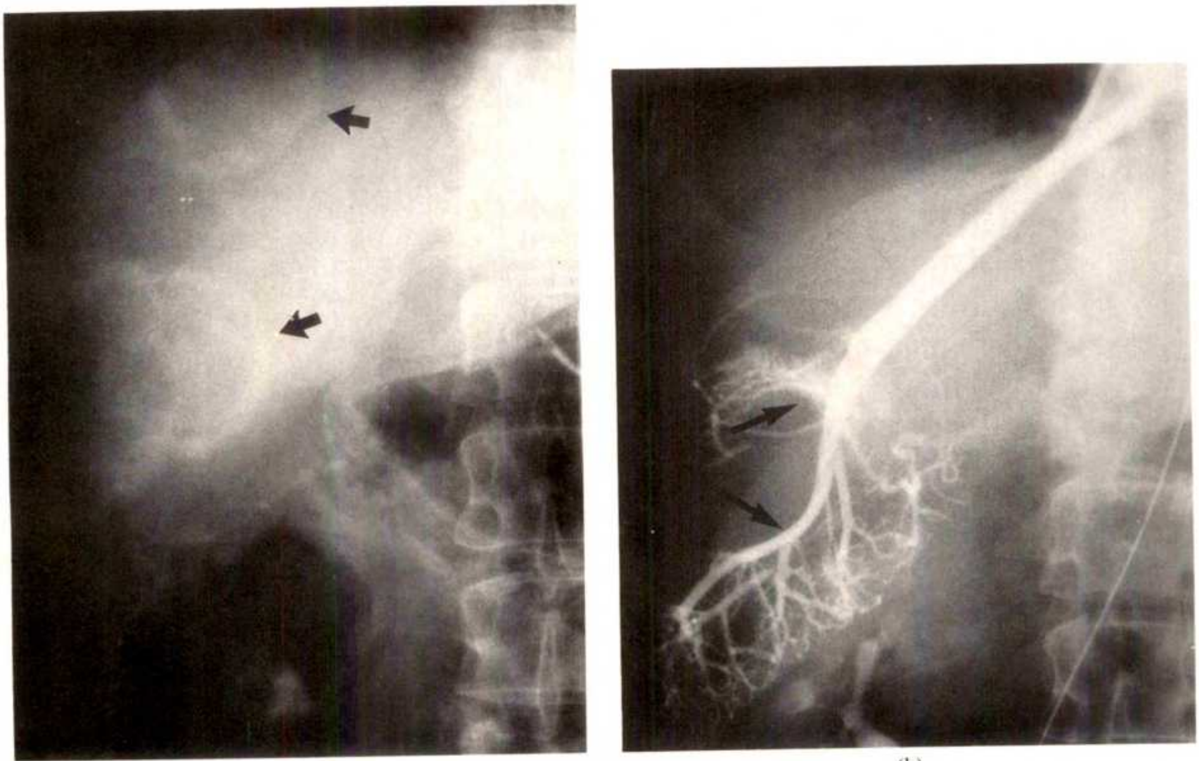

(a) (b)

Figure 1. (a) Late radiograph from a selective hepatic arteriogram showing several large hypovascular metastatic deposits from a colonic carcinoma in the right lobe of the liver (arrows). (b) Selective right hepatic venogram showing displacement of the peripheral branches of the posterior segmental veins by the metastatic deposits (long arrows).

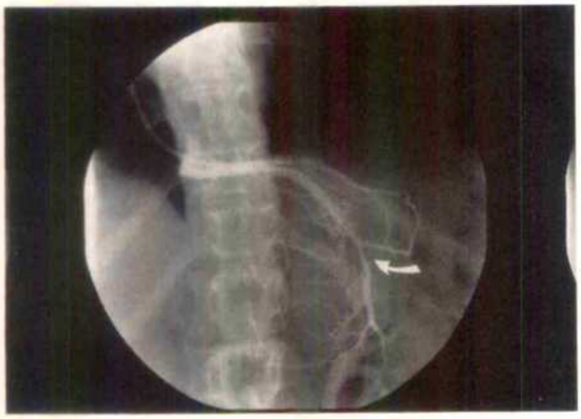

Figure 2. Selective left hepatic venogram in a patient with hepatocellular carcinoma showing marked irregularity of both medial and lateral segmental branches because of tumour encasement (arrow).

sent in three patients, three had cholangiocarcinoma, two lymphoma and one a benign hepatic adenoma.

The results of venography are shown in Table I. Hepatic venography was abnormal in 46 (58%) of the patients, 19 (45%) of those who colonic metastases and 14 (74%) with hepatocellular carcinoma. Venous displacement was the commonest venous abnormality seen, occurring in 16 (84%) with colonic metastases and 10 (71%) with HCC (Fig. 1). Venous encasement was present in five patients with colonic metastases and 12 patients with HCC (Fig. 2). Venous obstruction was seen in three patients with colonic metastases and seven patients with HCC (Fig. 3).

Tumour invasion of the hepatic veins was rare, occurring in only two patients, both with HCC (Fig. 4). Laparotomy was performed in 66 patients (83%), hepatic resection being performed in 27 (41%) of these.

Venography correctly predicted the distribution of tumour in 27 patients (41%). In the remainder, further tumour deposits or spread of tumour across segmental boundaries were found which had not been predicted by venography. When tumour was situated peripherally in either the right or left hepatic lobe, only 22 (58%) of the examinations were abnormal (Table II). When tumour was situated centrally, hepatic venography was abnormal in 11 patients (73%); however, the lobar distribution of tumour was correctly predicted by venography in only six (40%) of central tumours. Venography correctly predicted involvement of the proximal portions of the major hepatic veins and inferior vena cava in all four patients in whom this was detected at laparotomy. Of the nine patients with bilobar metastases, venography failed to detect abnormalities in the left lobe in all nine. No complications related to hepatic venography were experienced.

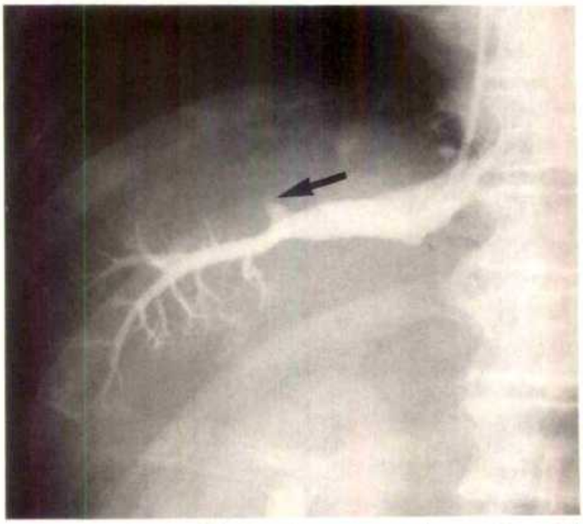

Figure 3. Selective right hepatic venogram in a patient with metastatic colonic carcinoma showing obstruction of a posterior superior segmental branch by a metastatic deposit (arrow).

The results of venography were compared with those of arteriography, CT and ultrasound (Table III) to assess the comparative sensitivity of each technique.

Venography and arteriography

Arteriography was performed in 76 (95%) patients who underwent venography. Only one patient with abnormal venography had normal arteriography, but venography was normal in 20 (26%) patients with abnormal arteriograms. The predicted segmental distribution of tumour deposits was the same with both arteriography and venography in 22 (33%) patients. Venography supplied additional information not provided by arteriography in five (8%) patients. In four, encasement at the origins of major hepatic veins was seen. One patient with normal arteriography had encasement of veins in the periphery of the right hepatic lobe.

Table II. Results of venography related to site of tumour deposits

	Peripheral		Central	Major veins and IVC	Bilobar
	Right lobe	Left lobe			
Number abnormal	15/25	7/13	11/15	4/4	7/9
% Abnormal	60	54	73	100	78

Results refer to 66 patients undergoing laparotomy.

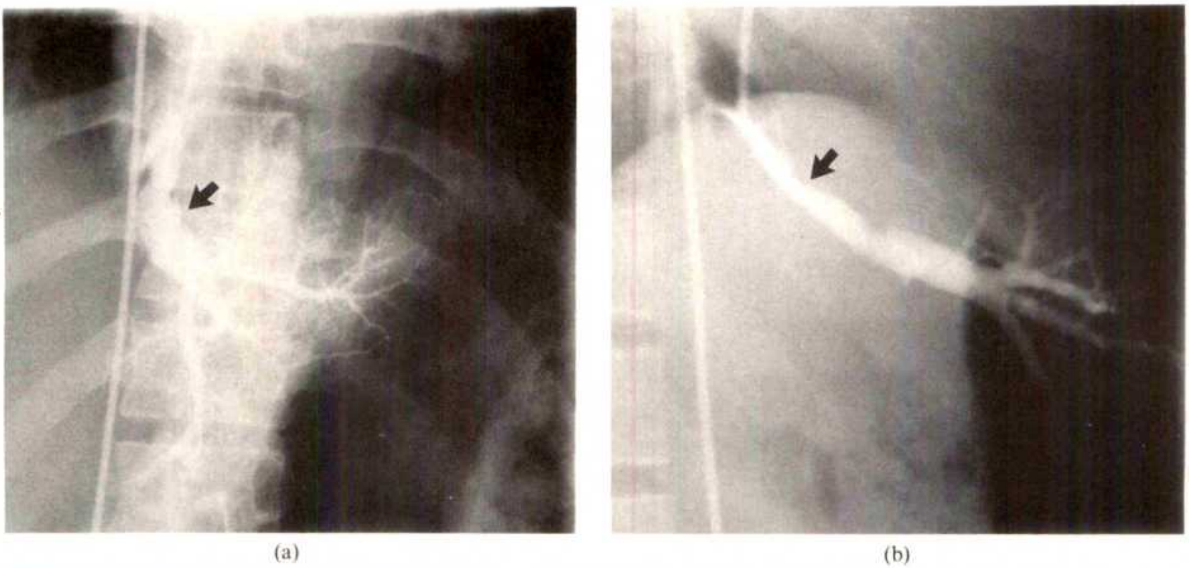
(a) (b)

Figure 4. (a) Antero-posterior and (b) lateral views from a selective left hepatic venogram in a patient with a large central hepatoma showing encasement of the origin of the left hepatic vein indicating invasion (arrows).

Venography and computed tomography

Computed tomography was performed in 53 (66%) patients, laparotomy being performed in 43. There was agreement between CT and venographic prediction of tumour distribution in 12 (28%) patients. In a further 12 patients CT correctly predicted segmental distribution of tumour. In five patients, venography provided information not given by CT. Encasement of major hepatic veins was seen in four patients and displacement of veins in the left hepatic lobe was seen in one patient. In two of these patients, both with hepatoma, small hepatic venous emboli were detected. Major hepatic veins were reliably visible in only nine (17%) of the CT scans; CT failed to detect invasion of these veins in the four patients in whom this was detected at laparotomy. Computed tomography failed to predict the extent of tumour distribution in 19 (36%) patients including all seven with bilobar metastases who underwent CT.

Venography and ultrasound

Ultrasound was performed in 44 (55%) patients of whom 30 underwent laparotomy. There was agreement between sonographic and venographic prediction of tumour distribution in 13 (43%). Ultrasound correctly predicted the distribution of tumour in 20 (67%) patients. Venography provided further information not provided by ultrasound in only one patient, encasement of a left hepatic vein being demonstrated.

The ultrasound examinations were not specifically performed to visualize hepatic veins. However, tumour involvement of major veins was demonstrated in one of the two cases in which ultrasound was performed.

The overall accuracy of arteriography, CT and ultrasound combined in predicting the segmental distribution of tumour was 73%. With the addition of venography the accuracy rose to 74%, there being only one case in which venography provided additional information, encasement of the origin of a middle hepatic vein being demonstrated (Fig. 5).

Discussion

Despite the controversy that exists over various forms of treatment for patients with hepatic tumours it is generally accepted that hepatic resection is beneficial for

Table III. Sensitivity (%) of hepatic imaging studies related to site of tumour at laparotomy

	% Sensitivity			
	Venography	Arteriography	CT	Ultrasound
Right lobe ($n = 25$)	54	79	75	100
Left lobe ($n = 13$)	31	60	64	71
Central ($n = 15$)	40	60	40	50
Major veins or IVC ($n = 4$)	100	50	50	50
Bilobar ($n = 9$)	0	22	0	66
Overall sensitivity ($n = 66$)	41	61	53	69

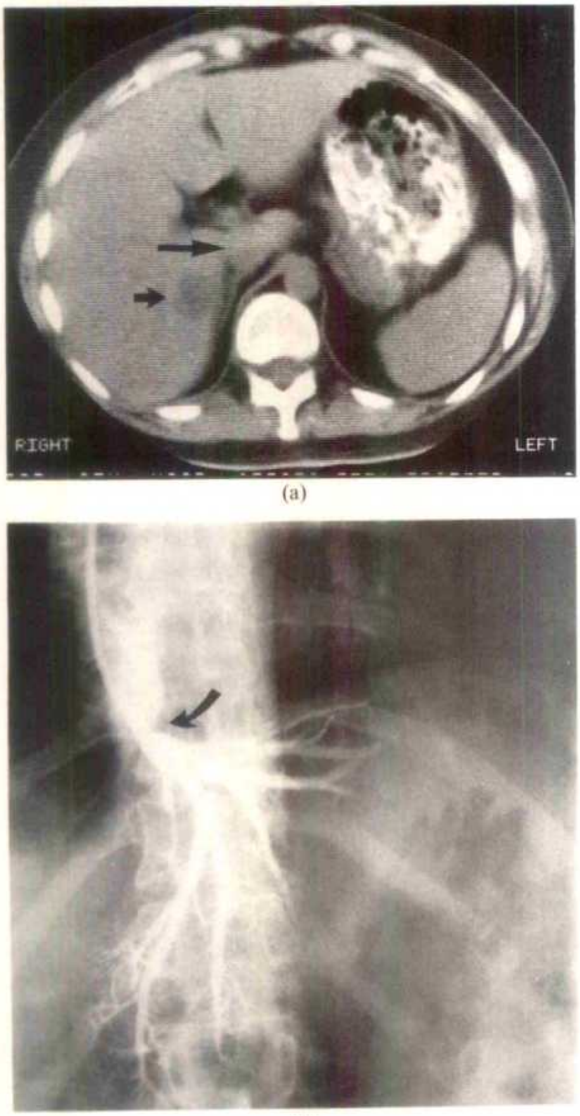

(a)

(b)

Figure 5. (a) Enhanced CT scan at the level of the porta hepatis in a patient with metastatic rectal carcinoma showing an apparently solitary deposit in the posterior segment of the right lobe (short arrow) lying some distance from the IVC (long arrow). (b) Selective injection of a combined middle and left hepatic venous trunk in the same patient showing encasement of the trunk proximally by an unsuspected metastatic deposit (curved arrow).

patients with unilobar primary or secondary hepatic tumours (Okuda, 1980; Adson et al, 1984; Langer, 1985; Taylor, 1985). The benefit of resection for more extensive lesions is less clear, tumour involving the portal vein or inferior vena cava being a contraindication to surgery (Foster & Berman, 1977; La Berge et al, 1984; Taylor, 1985). Collective mortality rates of 5% result from hepatic resection, much of this arising from intraoperative difficulties producing haemorrhage (Foster & Berman, 1977; Taylor, 1985; Olak et al, 1986).

It is therefore essential to obtain as much information as possible about the extent of tumour involvement and its relationship to hepatic vasculature prior to laparotomy. Computed tomography and ultrasound are efficient screening procedures for selecting those patients who may benefit from surgery (Snow et al, 1979; La Berge et al, 1984; Schreve et al, 1984). Arteriography provides further information regarding tumour extent and the relationship of tumour deposits to portal veins (Marks et al, 1979b; Reuter et al, 1986; Takayasu et al, 1986). Hepatic veins are not visualized at arteriography and lie in different anatomical planes from hepatic arteries and portal veins. Hepatic veins lie intersegmentally and are thus important in classical segmental resections both in terms of reducing operative haemorrhage and in maintaining venous drainage of residual liver tissue (Nakamura & Tsuzuki, 1981).

Involvement of hepatic veins by tumour may preclude resection in some instances or alter the planned extent of resection in others. Hepatic veins and segmental architecture can be visualized with both CT and ultrasound (Marks et al, 1979a; Pagani, 1983; Subramanyam et al, 1984; Cosgrove et al, 1987; Mukai et al, 1987). Technical improvements in ultrasound transducers and the introduction of duplex scanning and colour Doppler imaging now permit excellent visualization of hepatic vascular structures (Becker & Cooperberg, 1988). Despite these improvements, technical difficulties related to intestinal gas may result in inaccurate examinations with ultrasound. Moreover, extensive tumour deposits may produce only subtle changes and some areas of the liver are difficult to scan or visualize with both CT and ultrasound (Snow et al, 1979; Sexton & Zeman, 1983). Recent reports of the use of magnetic resonance imaging suggest that this technique may offer a reliable, non-invasive means of visualizing venous anatomy (Fisher et al, 1985; Mukai et al, 1987). However, the technique is limited in its availability and controversy still exists over the most appropriate pulse sequences for visualizing hepatic metastases (Glazer, 1988). Theoretically, hepatic venography should provide more accurate information regarding the relationship of tumour to hepatic veins.

Williams and Peterson (1976) were among the first to describe the use of selective hepatic venography in the pre-operative assessment of a patient with metastatic HCC. In their case, a venography previously thought to be unresectable was resected after hepatic venography had shown normal venous drainage of a hepatic segment.

Our results show that metastatic colonic tumours in the periphery of the right and left lobes frequently produce no venographic abnormality. Colonic metastases primarily displace veins with encasement and invasion being rare. The degree of displacement may be small and as hepatic venous anatomy is variable, subtle changes may be missed (Nakamura & Tsuzuki, 1981). Peripheral HCC produced venographic abnormalities more frequently, although negative examinations were not uncommon.

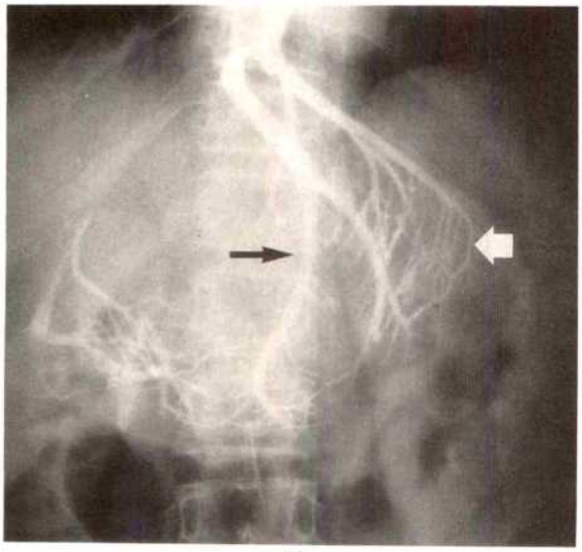

(a)

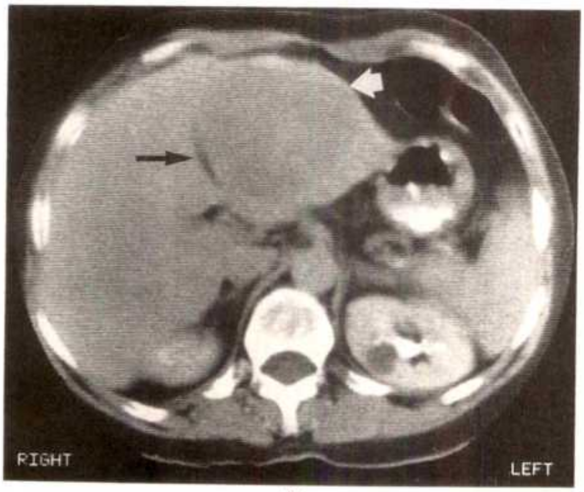

(b)

Figure 6. (a) Selective injection of combined middle and left hepatic venous trunk showing displacement of branches of the left hepatic vein around a left-lobe colonic metastasis (white arrow). Displacement of the middle hepatic vein to the left suggests involvement of the anterior segment of the right lobe (black arrow). (b) Enhanced CT scan in the same patient at the level of the coeliac axis showing a large metastatic deposit in the lateral segment of the left lobe (white arrow). The tumour abuts the left medial segment but does not involve it (black arrow).

There was no particular venous abnormality that could reliably differentiate between HCC and colonic metastases. Although encasement was more common with HCC this also occurred with metastases. The thread and streaks appearance of venous invasion described by Okuda et al (1975) was seen in the portal vein in three out of 19 (16%) HCC cases but neither of the two cases of HCC invasion of hepatic veins showed this sign. A higher incidence of positive examinations was present with tumours situated centrally in the liver. Tumour involvement of the middle hepatic vein is an especially important feature to recognize as this vessel separates right from left lobes. Tumour involvement of this vessel precludes either a simple right or left lobectomy.

In the absence of venous invasion or encasement, it was difficult to predict extension of tumour across intersegmental boundaries even when displacement of veins was marked; in several instances, apparent involvement of the left lobe as predicted by venography was not confirmed at laparotomy (Fig. 6). Venography was particularly inaccurate in detecting abnormalities in the left lobe in the presence of bilobar peripheral deposits. Of the four imaging modalities, hepatic venography demonstrated tumour involvement of the proximal major hepatic veins most reliably. In all four cases undergoing laparotomy this was predicted by venography and in four cases of advanced HCC which did not undergo laparotomy, two showed venous invasion at venography. Moreover, hepatic venography demonstrated venous anatomy more accurately than CT or ultrasound.

The place of hepatic venography in the pre-operative investigation of hepatic tumours is debatable. Although there are few complications attributable to the procedure, it is frequently time consuming, as all the major hepatic veins need to be catheterized, resulting in a high percentage of negative examinations. This may in part be related to technique. Satisfactory visualization of both main hepatic, segmental and subsegmental veins down to 4th and 5th order branches is difficult. Frequently, either underfilling or a wedged venogram results. Use of a balloon occlusion technique would prevent visualization of the main segmental veins. This problem can be overcome by using two injections of contrast medium with the balloon inflated and deflated, but this doubles the contrast dose (Novak et al, 1977). A double balloon technique as described by Rappaport et al (1966) or digital subtraction angiography (Yamauchi et al, 1987) are further alternatives.

For metastatic colonic tumours in the periphery of the right or left lobes, no further information regarding tumour extent was provided by venography than was already available from arteriography, CT and ultrasound. Because of the tendency for HCC to encase and invade veins, venography was more effective in defining the segmental distribution of tumour than either CT or ultrasound. For tumours situated centrally, venography gives more information than either arteriography, CT or ultrasound, especially regarding involvement of the middle hepatic vein.

The ultrasound scans in our series were not specifically performed to visualize hepatic veins. Whilst several studies have shown that these veins can be readily seen on ultrasound, many of these studies relate to scans performed on normal livers (Cosgrove et al, 1987; Mukai et al, 1987). The venous anatomy in livers involved with tumour may be considerably distorted. In both ultrasound and CT, only intravascular filling defects can be considered a specific sign of venous invasion (La Berge et al, 1984). Hepatic venous thrombi are uncommon, occurring in only two of our cases. Although serpiginous encasement, pathognomonic of tumour invasion in arteries does not occur in veins, we feel that the venographic demonstration of irregularity and obstruction of major hepatic veins is a reliable indicator of invasion. Venography, CT and ultrasound are all accurate in demonstrating the presence of tumour in the region of the main segmental veins, but only venography reliably demonstrated venous invasion.

We therefore believe that hepatic venography is of value in those patients in whom CT and/or ultrasound have shown tumour to be situated centrally or at the junction of hepatic veins and IVC. Of the current imaging modalities, hepatic venography provides the best anatomical demonstration of the junction of hepatic veins and IVC.

References

Adson, M. A., van Heerden, J. A., Adson, M. H., Wagner, J. S. & Ilstrup, D. M., 1984. Resection of hepatic metastases from colorectal cancer. *Archives of Surgery, 119,* 647–651.

Becker, C. D. & Cooperberg, P. L., 1988. Sonography of the hepatic vascular system. *American Journal of Roentgenology, 150,* 999–1005.

Bengmark, S. & Hafstrom, L., 1969. The natural history of primary and secondary malignant tumours of the liver. The prognosis for patients with hepatic metastases from colonic and rectal carcinoma at laparotomy. *Cancer, 23,* 198–202.

Bengtsson, G., Carlsson, G., Hafstrom, L. & Jonsson, P. E., 1981. Natural history of patients with untreated liver metastases from colorectal cancer. *American Journal of Surgery, 141,* 586–589.

Cosgrove, D. O., Arger, P. H. & Colman, B. G., 1987. Ultrasonic anatomy of hepatic veins. *Journal of Clinical Ultrasound, 15,* 231–235.

Fisher, M. R., Wall, S. D., Hricak, H., McCarthy, S. & Kerlan, R. K., 1985. Hepatic vascular anatomy on magnetic resonance imaging. *American Journal of Roentgenology, 144,* 739–746.

Foster, J. H. & Berman, M. M., 1977. Solid liver tumours. *Major Problems in Clinical Surgery, 22,* 209–303.

Glazer, G. M., 1988. MR imaging of the liver, kidneys and adrenal glands. *Radiology, 166,* 303–312.

La Berge, J. M., Laing, F. C., Federle, M. P., Jeffrey, R. B. & Lim, R. C., 1984. Hepatocellular carcinoma. Assessment of resectability by computed tomography and ultrasound. *Radiology, 152,* 485–490.

Langer, B., 1985. Colorectal cancer: managing distant metastases. *Canadian Journal of Surgery, 28,* 419–421.

Marks, W. M., Filly, R. A. & Callen, P. W., 1979a. Ultrasonic anatomy of the liver: a review with new applications. *Journal of Clinical Ultrasound, 7,* 137–146.

Marks, W. M., Jacobs, R. P., Goodman, P. C. & Lim, R. C., 1979b. Hepatocellular carcinoma: clinical and angiographic findings and predictability for surgical resection. *American Journal of Roentgenology, 132,* 7–11.

Mukai, J. K., Stack, G. M., Turner, D. A., Gould, R. J., Petasnick, J. P., Matalon, T. A. S., Doolas, A. M. & Murakami, M., 1987. Imaging of surgically relevant hepatic vascular and segmental anatomy. Part I. Normal anatomy. *American Journal of Roentgenology, 149,* 287–292.

Nakamura, S. & Tsuzuki, T., 1981. Surgical anatomy of the hepatic veins and inferior vena cava. *Surgery, Gynecology and Obstetrics, 152,* 43–50.

Novak, D., Butzow, G. H. & Becker, K., 1977. Hepatic occlusion venography with a balloon catheter in portal hypertension. *Radiology, 122,* 623–628.

Okuda, K., 1980. The liver cancer study group of Japan. Primary liver cancers in Japan. *Cancer, 45,* 2663–2669.

Okuda, K., Musha, H., Yoshida, T., Kanda, Y., Yamakazi, T., Jinnouchi, S., Moriyami, M., Kawaguchi, S., Kubo, Y., Shimokawa, Y., Kojiro, M., Kuratomi, S., Sakamoto, K. & Nakashima, T., 1975. Demonstration of growing casts of hepatocellular carcinoma in the portal vein in celiac angiography: the thread and streaks sign. *Radiology, 117,* 303–309.

Olak, J., Wexler, M. J., Rodriguez, J. & McLean, A. P., 1986. Hepatic resection for metastatic disease. *Canadian Journal of Surgery, 29,* 435–439.

Pagani, J. J., 1983. Intrahepatic vascular territories shown by computed tomography (CT). *Radiology, 147,* 173–178.

Rappaport, M., Holmes, R. B., Stolberg, H. O., McIntyre, J. L. & Baird, R. J., 1966. Cinévéinographie hépatique et rénale. *Revue Internationale d'Hépatologie, 16,* 1045–1062.

Reuter, S. R., Redman, H. C. & Cho, K. J., 1986. Tumors: hepatic neoplasms. In *Gastrointestinal Angiography,* 3rd edn, ed. by D. Manke (W. B. Saunders, Philadelphia), pp. 156–192.

Schreve, R. H., Terpstra, O. T., Ausema, L., Lameris, J. S., van Siejen, A. J. & Jeekel, J., 1984. Detection of liver metastases. A prospective study comparing liver enzymes, scintigraphy, ultrasonography and computed tomography. *British Journal of Surgery, 71,* 947–949.

Sexton, C. C. & Zeman, R. K., 1983. Correlation of computed tomography, sonography and gross anatomy of the liver. *American Journal of Roentgenology, 141,* 711–718.

Snow, J. H., Goldstein, H. M. & Wallace, S., 1979. Comparison of scintigraphy, sonography and computed tomography in the evaluation of hepatic neoplasms. *American Journal of Roentgenology, 132,* 915–918.

Subramanyam, B. R., Balthazar, E. J., Halton, S., Lefleur, R. S., Horii, S. C. & Raghavendra, B. N., 1984. Hepatocellular carcinoma with venous invasion. Sonographic–angiographic correlation. *Radiology, 150,* 793–796.

Takayasu, K., Shima, Y., Muramatsu, Y., Goto, H., Moriyama, N., Yamada, T., Makuuchi, M., Yamasaki, S., Hasegawa, H., Okazaki, N., Hirohasi, S. & Kishi, K., 1986. Angiography of small hepatocellular carcinomas. Analysis of 105 resected tumours. *American Journal of Roentgenology, 147,* 525–529.

Taylor, B., Langer, B., Falk, R. E. & Ambus, U., 1983. Role of resection in the management of metastases to the liver. *Canadian Journal of Surgery, 26,* 215–217.

Taylor, I., 1985. Colorectal liver metastases—to treat or not to treat. *British Journal of Surgery, 72,* 511–516.

Wagner, J. S., Adson, M. A., van Heerden, J. A., Adson, M. H. & Ilstrup, D. M., 1984. The natural history of hepatic metastases from colorectal cancer. *Annals of Surgery, 199,* 502–508.

Williams, R. D. & Peterson, C., 1976. Selective hepatic venography in primary liver cell carcinoma. *American Journal of Surgery, 131,* 350–351.

Yamauchi, T., Furui, S., Ohtomo, K. & Hai, Y., 1987. Stereoscopic digital subtraction angiography of hepatic artery and vein. *American Journal of Roentgenology, 148,* 825–826.

1989, *The British Journal of Radiology*, *62*, 13–19

Clinically unsuspected complications of arterial surgery shown by post-operative digital substraction angiography

By C. Teeuwen, *B. C. Eikelboom and J. W. Ludwig

Departments of Radiology and *Surgery, St Antonius Hospital, Koekoekslaan 1, 3435 CM Nieuwegein/Utrecht, The Netherlands

(*Received April 1988 and in revised form August 1988*)

Abstract. Intravenous digital subtraction angiography was performed within 20 days of 678 vascular reconstructions as a routine post-operative evaluation. After 339 carotid endarterectomies, 34 patients showed a stenosis of >30% and six occlusions were seen. In 157 patients after aortic aneurysm repair, we found five anastomotic aneurysms and seven stenoses of >30%. After aortic bypass surgery, 77 patients were evaluated and nine stenoses were found; no anastomotic aneurysms were seen. In 105 patients with femoro-distal bypass procedures, occlusion was reported in 11 cases and stenosis in 13 cases. One patient had two anastomotic aneurysms. To summarize, major abnormalities were present in 81 cases (12.7%) and consisted of 59 stenoses of >30%, 17 occlusions and six patients with anastomotic aneurysms. Most of these were unexpected and were reason for more critical follow-up or re-operation.

Because of its invasive nature, conventional angiography is used with reluctance for early post-operative evaluation of vascular reconstruction. Direct ultrasound studies such as duplex scanning are not always feasible in this period. Intravenous digital subtraction angiography (DSA) has made it easier to obtain post-operative angiographic information and, in our hospital, is now used routinely after almost all arterial reconstructions before discharge of the patient.

This report gives the findings after carotid endarterectomy, abdominal aortic grafting procedures and peripheral bypass procedures in order to determine whether late sequelae may be caused by silent abnormalities already present in the early post-operative period.

Routine post-operative conventional angiography before discharge of the patient is rarely reported in the literature (Szilagyi et al, 1975). This is understandable on clinical grounds because one does not expect to find sufficient abnormalities to justify such an invasive and expensive procedure. The long-term results of the above-mentioned vascular procedures are good, but if complications occur, they are usually such that re-operation is necessary. This is the case for late occlusions as well as false or anastomotic aneurysm formation. Rupture of an anastomotic aneurysm or the formation of an aorto-enteric fistula, in particular, represent life-threatening complications.

These considerations, together with our favourable experiences with the DSA technique since 1980, with low risk and good patient acceptance (de Vries, 1986), has led to its routine use in the early post-operative period after almost all our vascular reconstructions.

Materials and methods

The DSA studies were performed with a Philips DVI-IV with a 512 × 512 image matrix and a depth of 10 bits. We use an XTV-VI TV chain with a 14 in image intensifier, changeable to 10 and 6 in for fine detail information.

A routine investigation consisted of from one to a maximum of five injections of 40 ml contrast medium followed by 15 ml glucose through a short intravenous cannula in the elevated right arm. The glucose solution is given to wash the contrast medium into the superior caval vein. All patients were investigated within the first 20 days after the operation, while still in hospital. It was not possible to investigate all patients because of contra-indications, such as renal insufficiency, cardiac failure, a poor post-operative general condition or patient refusal.

In practice, 70–90% of the patients were actually investigated (Table I). We have listed only those patients who were operated on for the first time. Re-operations were not included in the series.

Results

Of 436 patients examined, 339 carotid arteries were operated upon with the following results.

Forty-three stenoses of <30% and 11 stenoses of >30% were found proximal (caudal) to the carotid bifurcation. Thirty-two stenoses of <30% and 23 stenoses of >30% were found distal (cranial) to the carotid bifurcation. Six carotid arteries were found to be occluded.

In conclusion, we found significant stenosis in 34 cases and six occlusions. None of the patients showed

Table I. Numbers of post-operative intravenous DSA studies in operated patients

	Operated	DSA	%
Abdominal procedure	327	234	71.5
Peripheral procedure	129	105	81.4
Carotid procedure	436	339	77.7

Table II. Results of early post-operative intravenous DSA after carotid endarterectomy

	Proximal to the bifurcation	Distal to the bifurcation	Total
Normal	—	—	224 (66%
Stenosis < 30%	43	32	75 (22%)
Stenosis > 30%	11	23	34 (10%)
Occlusion	3	3	6 (2%)
Total	57	58	339 (100%)

Table IV. Results of early post-operative intravenous DSA after femoro-popliteal and femoro-crural bypass procedures

	Femoro-popliteal bypass	Femoro-crural bypass	Total
Normal	59	18	77 (74%)
Stenosis > 30%	11	5	16 (15%)
Occlusion	4	7	11 (10%)
Slow flow		1	1 (1%)
Total	74	31	105 (100%)

any neurological abnormality which could be related to the lesions discovered. The results are listed in Table II.

After abdominal procedures the following abnormalities were found.

(1) *Elective aneurysm repair (106 patients).* Minor abnormalities were present in 13 patients and consisted of a stenosis <30% or a slight bulging of an anastomosis. Major abnormalities were found in another nine patients. There were six stenoses >30% and three anastomotic aneurysms.

(2) *Ruptured aneurysm repair (51 patients).* This group consisted of 43 patients with normal appearances on DSA and five with minor stenoses. One patient had an 80% stenosis at the proximal anastomosis. Two patients had a total of three anastomotic aneurysms, all at the distal end of the graft. After implantation of an aortic tube graft we found remaining aneurysms in the iliac arteries in seven patients. A disturbed renal perfusion or renal artery stenosis was present in five patients.

(3) *Aortic bifurcation bypass operations (77 patients).* Minor stenoses were found in three cases and stenoses of >30% in nine patients. There were no anastomotic aneurysms in this group.

A summary of these findings is given in Table III. Major abnormalities were present in 33 patients or 14% of all operations and consisted of 16 stenoses (7%), five anastomotic aneurysms (2%), seven remaining aneurysms (3%) and five patients with abnormalities in renal perfusion (2%).

After peripheral bypass procedures the following pathology was reported.

(1) *Femoro-popliteal bypass procedures (74 patients).* In 74 patients examined, we found four occlusions and 11 stenoses of >30%.

(2) *Femoro-crural bypass procedures (31 patients).* In 31 patients examined, we found seven occlusions, five stenoses of >30% and one bypass with a very slow flow.

Major abnormalities were reported in 28 patients. The results are listed in Table IV.

Discussion

The carotid arteries are very well suited to intravenous DSA evaluation (de Vries, 1986). They are relatively wide, have a good flow, are situated in an area of equal tissue densities and no local application in the area of the wound has to be made (Fig. 1). The clinical impact of a residual stenosis is still under discussion (Szilagyi et al, 1975; Thompson & Talkington, 1976; Callow, 1980). From our own experience we know that some of these stenoses smooth out during the first year after operation, whereas others show progression towards haemodynamically significant lesions (Sanders et al, 1987).

Patients with a residual stenosis are followed with duplex scanning to determine whether the stenosis becomes smoother than immediately after the operation. The duplex investigation is done 3 months post-operatively, when the wound is completely healed.

Table III. Results of early post-operative intravenous DSA after elective aneurysm repair, ruptured aneurysm repair and aortic bypass surgery

	Elective aneurysm repair	Ruptured aneurysm repair	Aortic bypass surgery	Total
Normal	84	31	65	180 (77%)
Stenosis < 30%	13	5	3	21 (9%)
Stenosis > 30%	6	1	9	16 (7%)
Anastomotic aneurysms	3	2	0	5 (5%)
Remaining aneurysms	0	7	0	7 (3%)
Renal complications		5		5 (2%)
Total	106	51	77	234 (100%)

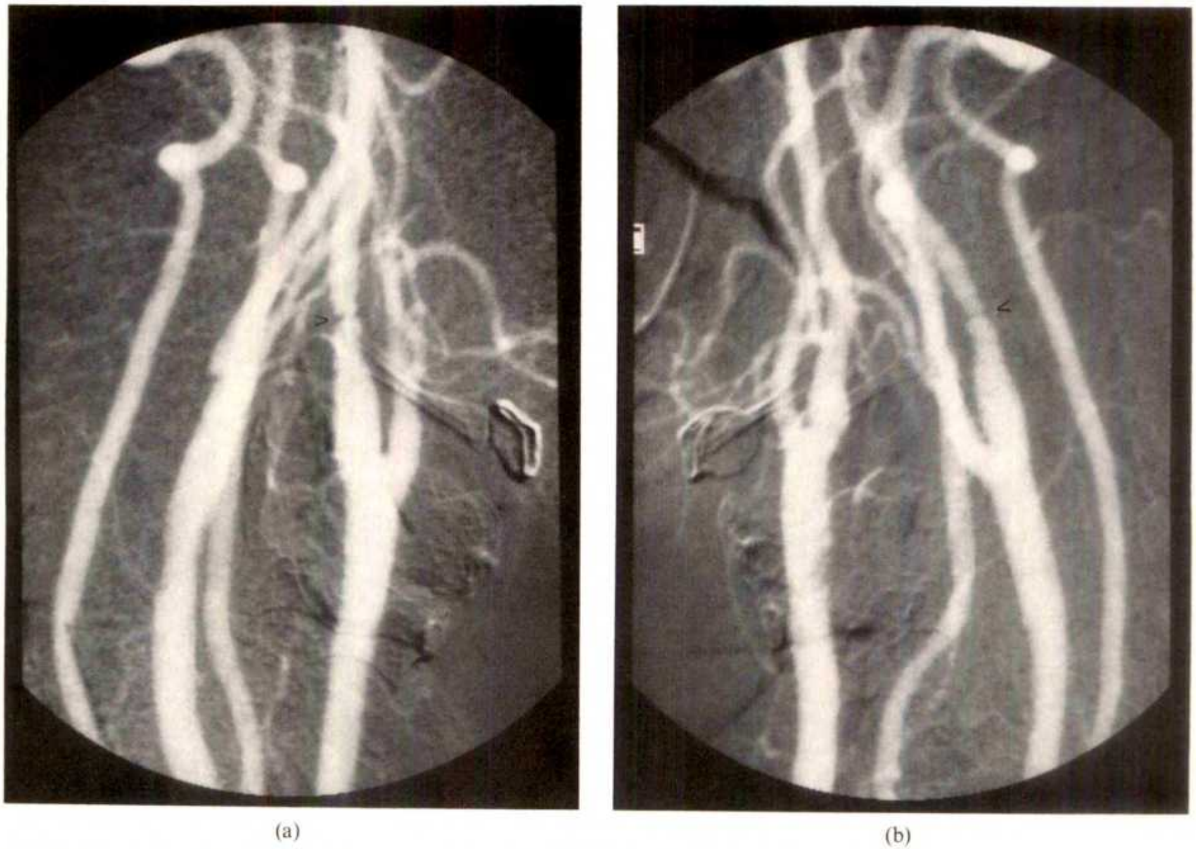
(a) (b)

Figure 1. Short stenosis in the internal carotid artery after endarterectomy. (a) Left and (b) right oblique projection.

We know already from our series that intravenous DSA and duplex scanning give similar results in 80% of cases, and in the remaining 20%, duplex indicates more severe stenosis in 15% and less severe stenosis in 5%, compared with DSA. Several factors can explain these findings.

First, when there is significant stenosis in the contralateral carotid artery, a compensatory high flow can be found in the operated artery. We also found that in women, especially those operated upon without venous patch, duplex scanning demonstrates more severe stenosis than intravenous DSA. This might be caused by the thinner arteries found in women or difficulties encountered with duplex scanning, because of turbulent flow in an artery after endarterectomy and with a venous patch (small and large calibre vessel interchanging). In addition, intravenous DSA does not always demonstrate well short septum-like lesions found after endarterectomy. Both investigations have their advantages and disadvantages. Intravenous DSA can be used shortly after operation and gives anatomical information whilst duplex scanning gives a good indication of the flow in a stenotic area. In most cases we use both investigations.

Patients are not re-operated upon for correction of a residual stenosis immediately after endarterectomy. Initially, the residual stenosis is followed to see if it is diminishing. If it gets worse in the following month to years, re-operation is considered if a residual stenosis is severe (>70%) and causing clinical symptoms. We found four patients with a stenosis of 60% or more; two with a stenosis of 60% showed improvement on intravenous DSA after 1 year, one with a stenosis of 70% showed a better patency on duplex scanning 3 months later, and one with a 95% stenosis occluded shortly after operation. Only this last patient might have been a candidate for re-operation.

The finding of an asymptomatic occlusion is not surprising. All our patients were operated upon because of haemodynamic lesions of >70%. Many of these patients had a stenosis of 95–99%. Pre-operatively, these vessels are not contributing significantly to the cerebral perfusion and in these patients there must already be a good collateral perfusion. If these vessels occlude shortly after operation, the cerebral perfusion is not significantly changed from the pre-operative situation. Because of the possibility of silent occlusions, re-operation is not considered.

Reconstruction of the abdominal aorta for aneurysmal dilatation or occlusive disease is a common

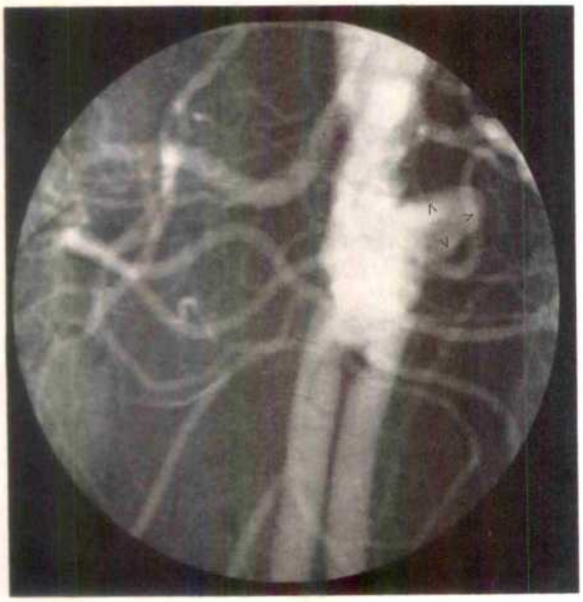

Figure 2. Anastomotic aneurysm of the proximal end-to-end anastomosis of a bifurcation inlay prosthesis.

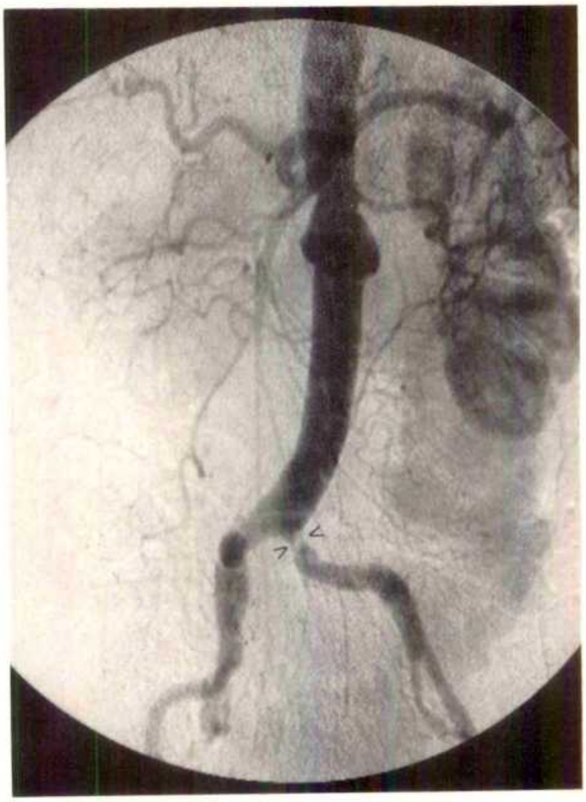

Figure 3. Bulging of the aorta cranial to the proximal end-to-end anastomosis and a stenosis of the left common iliac artery after emergency aneurysm repair with a tube prosthesis.

procedure that has been shown to be durable. Major late complications include anastomotic aneurysm formation and graft occlusion (Fig. 2). Although these conditions are relatively rare, they present such a significant morbidity and mortality rate that attempts to obtain early diagnosis are warranted. The true incidence of anastomotic aneurysms is hard to determine (Horsch et al, 1979; Bosman, 1983). Although an aneurysm in the groin may be felt as an enlarging pulsating mass, the first signs of an intra-abdominal anastomotic aneurysm are often those of rupture or bleeding into the bowel, both of which may lead to sudden death. For this reason, the incidence of anastomotic aneurysms may be higher than is reported in the literature (Szilagyi et al, 1975). Even less is known about the time interval between operation and anastomotic aneurysm formation as few prospective serial angiographic or ultrasound studies exist. In retrospect, most authors mention a period of 5 years, but there have been reports on "early" diagnosis after 3 months (Thompson et al, 1977; Greenhalgh, 1979; Millili et al, 1980).

The finding of an anastomotic aneurysm in five patients was surprising. One patient even showed two false aneurysms at both distal anastomoses. It is of particular interest that all these false aneurysms were found after aneurysm repair and not after bypass grafting, which suggests that the quality of the vessel wall may be an important aetiological factor. To our knowledge there are very few reports in the literature on these very early anastomotic aneurysms and it has yet to be determined what the natural course of these lesions will be.

As yet, we have no firm criteria for re-intervention. We found five patients with an anastomotic aneurysm, two of whom were candidates for re-operation because of the size of the aneurysm, but had a bad cardiac prognosis and died of cardiac failure in the first year after operation. One patient with a smaller aneurysm was followed for 3 years and in this case the aneurysm did not grow. The remaining two patients were not followed in our hospital.

Although this study shows that anastomotic aneurysms are more frequent than expected, the true number may be even higher. We examined one patient with normal appearances on DSA. However, B-mode imaging was used to investigate abdominal pain and showed an anastomotic aneurysm, which was confirmed by computed tomography. This finding can be explained by the smooth lining of the aneurysmalic vessel or anastomosis by a thrombotic mass (Hilton et al, 1982; Mark et al, 1982).

The implantation of tube grafts for ruptured aortic aneurysms is gaining more widespread acceptance and has the advantage of limiting the surgical procedure, thereby reducing the time of operation (Fig. 3). However, one has to be cautious not to overlook iliac aneurysms (Fig. 4). It is not always easy to judge whether or not these arteries are normal if a large

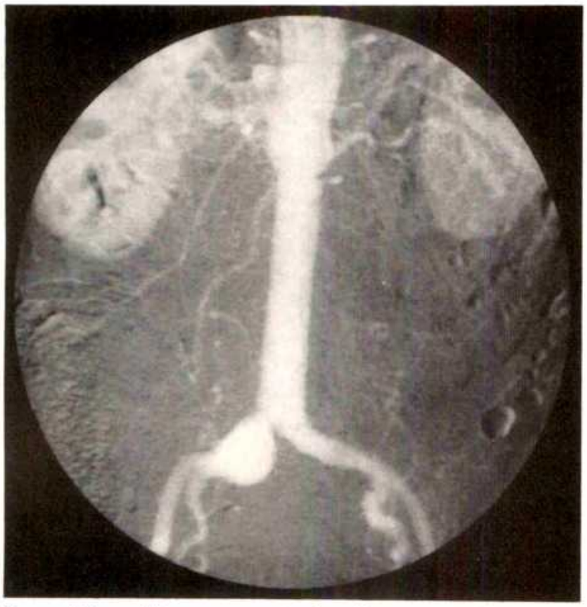

Figure 4. Remaining aneurysm in the right common iliac artery after emergency aneurysm repair with a tube prosthesis.

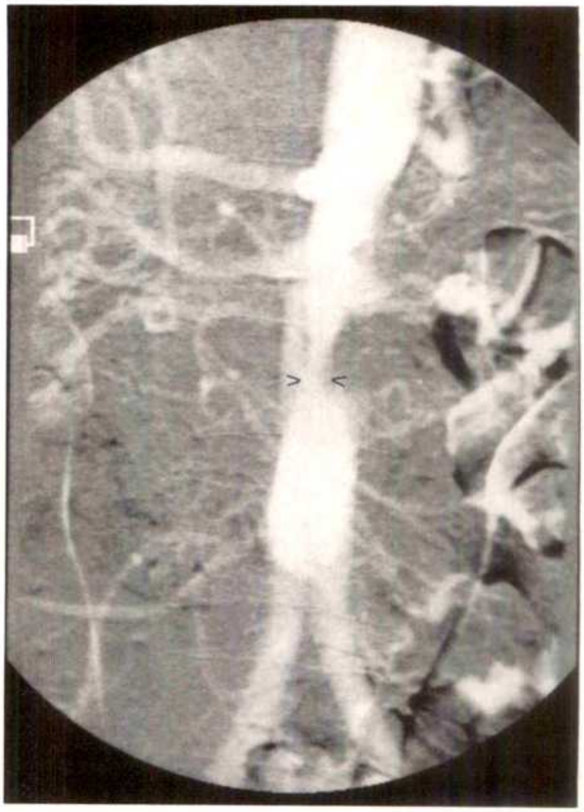

Figure 5. Stenosis cranial to the proximal end-to-end anastomosis of a bifurcation bypass prosthesis.

haematoma is present. After operation, patients with a remaining iliac aneurysm are usually checked with ultrasound or intravenous DSA. Of seven patients, one patient was corrected 1 year later, one ruptured while still in hospital, four patients showed an unchanged situation with a small aneurysm not gaining calibre, and one patient was not checked in our hospital. A number of unexpected renal abnormalities were also encountered after emergency aneurysm repair, including renal artery stenosis and abnormal kidney perfusion.

The reasons for graft occlusion may include the presence of residual lesions left behind or new stenotic lesions formed at the time of operation. Data on these technical problems are scarce. In our series there were far more abnormalities than expected. After elective aneurysm repair, we found six patients with stenoses left after operation. Two patients had a stenosis of 40% and 70%, respectively, at the proximal anastomosis, which were found without difficulty during check-up. One patient with a 70% stenosis was not checked in our hospital and three patients showed stenoses at the distal anastomosis of 40%, 40% and 50%. All did well during follow-up. After ruptured aneurysm repair one patient had a severe 80% stenosis at the proximal anastomosis. This patient also did well, but had a loud bruit in both groins. After aortic bypass surgery, five patients showed a 40% or 50% stenosis at the proximal anastomosis, two of which also had a 40% stenosis in one distal anastomosis. These patients did well during follow-up. One patient had a proximal stenosis of 50% revised later because of progression. One patient with a 70% stenosis in the right distal anastomosis also progressed well with no complaints being recorded. One patient was found to have an occluded right limb of his bifurcation prosthesis. Thrombectomy was performed, followed by a femoro-politeal bypass to improve the flow in the limb, after which the patient recovered without problems. Major stenoses, as high as 80%, may be present with good femoral pulses and almost no complaints from the patient (Fig. 5). These lesions might very well lead to graft occlusion. It has yet to be determined what the natural history of minor lesions in this area will be.

Evaluating peripheral bypass surgery to the popliteal artery or the lower leg is not as helpful as in the abdomen. The quality of intravenous DSA images may be poor because of poor perfusion in thin vessels (Fig. 6). Most surgeons will be satisfied with good peripheral pulsations, a normally coloured foot and a normal ankle pressure measurement. In some clinics it is routine to evaluate the graft with pre-operative angiography. Although the quality of post-operative intravenous DSA is not as good, we nevertheless found a large number of complications (van de Pavoordt et al, 1983). That unsuspected occlusions are present is not surprising, because this type of surgery is performed frequently for limb salvage on very thin vessels and the perfusion of the leg is only slightly improved because of poor run-off. Even the judging of stenosis might be

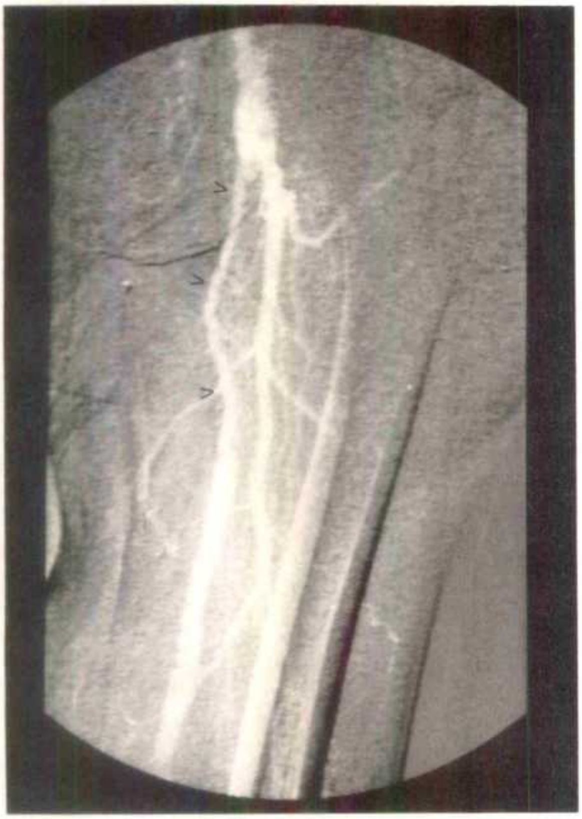

Figure 6. Diminished calibre of the first part of femoro-popliteal bypass prosthesis.

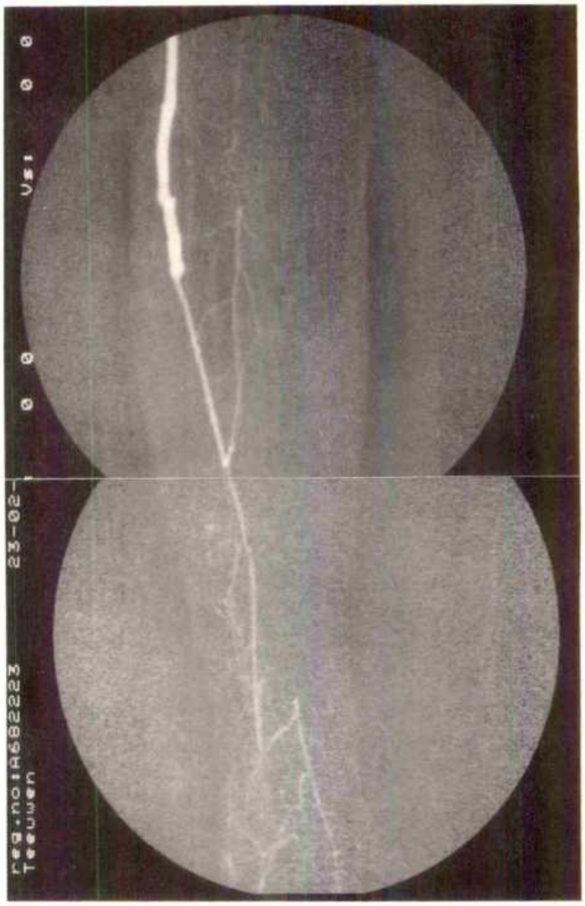

Figure 7. Distal anastomosis of a femoro-crural bypass prosthesis composed of several sections of venous material.

rather difficult, and all stenoses counted were at least 30% because the resolution of the intravenous DSA does not allow judging of stenoses <30%. Nevertheless, most of these investigations gave a good demonstration of the bypass and of its effectiveness. In these circumstances, good visibility means enough contrast medium in the graft and a good flow (Fig. 7).

Femoral-popliteal bypass surgery reviewed later showed that in 11 patients with a stenosis of >30%, seven bypasses remained patent and four occluded in the first year after operation. Most grafts with a 40% or 50% stenosis remained open. Occlusion was found in two patients with a 50% stenosis, one with a 70% proximal stenosis and one patient with a bad proximal part of the graft. Of the group with a patent graft and a stenosis, one patient had to be operated upon after 1 year because of an increasing stenosis.

After femoro-crural bypass surgery, three grafts with reported stenoses remained open and three grafts were occluded after 1 year. Occlusion was found in a patient with a 40% stenosis in the distal anastomosis, a patient with a slow blood flow through the graft and a patient with narrowing of the proximal part of the graft. In several investigations we were able to demonstrate stenotic residual lesions which required careful follow-up and re-operation. Residual arterio-venous fistulae after *in situ* bypass grafts can be visualized, as well as remaining valves.

In our opinion, even in this group of post-operative patients, intravenous DSA has given useful information about anatomical configuration and function of the graft. We do not recommend intra-arterial DSA for post-operative follow-up of peripheral reconstructions. Only in patients where there is malfunction of the graft or severe stenosis found after intravenous DSA should intra-arterial DSA be performed, usually in combination with dilatation of the stenosis. At present we are evaluating duplex investigation of the lower limbs, which might be a more promising method of investigation.

Conclusions

Routine post-operative conventional angiography before discharge of the patient is rarely reported in the literature. This is understandable because on clinical grounds one does not expect to find sufficient abnormalities to justify an invasive and expensive procedure. The long-term results of the abovementioned procedures are good, but if complications occur, they are usually such that re-operation is necessary. This consideration, together with our favourable impression of the intravenous DSA technique since 1980, showing low risk and good patient acceptance, has led us to its routine use in the early post-operative period after almost all vascular reconstructions. In principle, the only patients excluded are those with renal insufficiency, poor cardiac output or those who refuse the investigation. The performance of intravenous DSA after operation is not stressful for the patient and did not prolong the time in hospital. The benefits of this policy have been such that we continue to use it. There were far more abnormalities discovered than expected. Early post-operative application of intravenous DSA has provided important clinical information leading to changes in surgical technique, improvement in operative results and better patient care.

References

Bosman, C. H. R., 1983. *AAAA Report on 20 Years of Experience with Athersclerotic Aneurysms of the Abdominal Aorta*, Thesis, University of Leiden (A. Jongbloed & Son, The Hague).

Callow, A. D., 1980. An overview of stroke problem in the carotid territory. *American Journal of Surgery*, *140*, 181–191.

Greenhalgh, R. M., 1979. Dilatation and stretching of knitted Dacron grafts associated with failure. In *Surgery of the Aorta and its Body Branches*, ed. by J. J. Bergan & J. S. T. Yao (Grune & Stratton, London), pp. 621–626.

Hilton, S., Megibow, A. J., Naidich, D. P. & Bosniak, M. A., 1982. Computed tomography of the postoperative aorta. *Radiology*, *145*, 403–407.

Horsch, S., Imig, H., Zehle, A. & Ichlmaier, H., 1979. Spätergebnisse nach Resection infrarenaler Bauchaortenaneurysmen. *Langenbecks Archiv für Chirurgie*, *349*, 546.

Mark, A., Moss, A. A., Lusby, R. & Kaiser, J. A., 1982. CT evaluation of complications of abdominal aortic surgery. *Radiology*, *145*, 409–414.

Millili, J. J., Lanes, J. S. & Nemir, P., 1980. A study of anastomotic aneurysms following aortofemoral prosthetic bypass. *Annals of Surgery*, *192*, 69–73.

Pavoordt, H. D. W. M. van de, Bast, T. J., Eikelboom, B. C., Engels, P. H. C., De Geest, R., Taks, A. C. J. M. & Vermeulen, F. E. E., 1983. A comparison of conventional and digital intravenous arteriography in the follow-up of femoro-crural bypass operations. *Journal of Cardiovascular Surgery*, *24*, 641–645.

Sanders, E. A. C., Hoeneveld, H., Eikelboom, B. C., Ludwig, J. W., Vermeulen, F. E. E. & Ackerstaff, R. G. A., 1987. Residual lesions and early recurrent stenosis after internal carotid endarterectomy. *Journal of Vascular Surgery*, *5*, 731–737.

Szilagyi, D. E., Smith, R. F., Elliot, J. P., Hageman, J. H. & Dall'Olmo, C. A., 1975. Anastomotic aneurysms after vascular reconstruction: problems of incidence, etiology, and treatment. *Surgery*, *78*, 800–816.

Thompson, J. E. & Talkington, C. M., 1976. Carotid endarterectomy. *Annals of Surgery*, *184*, 1–15.

Thompson, W. M., Johnsrude, I. S., Jackson, D. C., Older, R. A. & Wechsler, A. S., 1977. Late complications of abdominal aortic reconstructive surgery. *Annals of Surgery*, *185*, 326–334.

Vries, A. R. de, 1986. Digital substraction angiography and catheter angiography in examinations of the carotid artery. In *Digital Substraction Angiography in Clinical Practice* (Philips Medical Systems, Best, The Netherlands), pp. 59–67.

1989, *The British Journal of Radiology*, 62, 20–26

Some indicative parameters on diagnostic radiology in Spain: first dose estimations

By E. Vañó, PhD, L. González, PhD, A. Calzado, PhD, P. Morán, PhD and V. Delgado, PhD

Medical Physics Group, Medical School, Complutense University of Madrid, 28040 Madrid, Spain

(*Received February 1988*)

Abstract. The Medical Physics Group at the Complutense University of Madrid has been co-ordinating, for approximately 1 year, a project on optimization of radiation protection in diagnostic radiology, in co-operation with the other states of the European Community. Exhaustive data on the subject, which offer accurate results on patient dosimetry for the different types of examination, are the final aim of the project. So far, it has been possible to analyse in detail the data from the National Institute of Health (NIH), which manages the care of about 96% of the Spanish population, plus the findings from several hospitals, outpatient centres and private clinics of the community of Madrid, which allowed us to perform the first dose estimations and to extrapolate them to the rest of Spain. The following estimations are presented: annual frequency of different examinations, their variation from 1985 to 1986, number of diagnostic rooms used for a given minimum of annual examinations, organ doses for different examinations, effective dose-equivalent, genetically significant dose for some examinations, as well as the collective dose.

The Medical Physics Group at the School of Medicine of the Complutense University of Madrid initiated a study of radiation doses in relation to diagnostic radiology in the area of Madrid in 1986, in co-operation with the Department of Health and Consumer Affairs and several Madrid hospitals (San Carlos University Hospital, Primero de Octubre and La Princesa Hospitals, and Gomez Ulla Military Central Hospital), as well as some outpatient centres. Although many of the results and conclusions obtained may be extrapolated to the rest of Spain, a second phase of the study is currently under design in co-operation with the Department of Health, which will involve sampling throughout Spain.

The project has the technical and economic support of the European Economic Community (EEC), the Advisory Committee on Scientific and Technical Research (CAICYT), the Department of Health and Consumer Affairs and the Nuclear Safety Council (NSC), during this first stage.

Although it is still too early to obtain sufficiently reliable data for the different types of examination, we feel it is important to report a first assessment, inevitably using preliminary figures and a few indirect estimations. We hope this may facilitate comparisons between diagnostic radiology in Spain and in the other EEC countries and the rest of the world, even at this level of approximation. It is hoped that accuracy will improve during the project (which is expected to last 3 years in its initial stage), leading to a higher degree of awareness on the part of those providing the information, who are relatively distant from our base. Data on the population numbers cared for at the different centres, number and distribution of X-ray examinations in private medicine, etc., were provided and proved to be useful in the completion of this work.

In Spain, the National Health Service (NHS), through the National Institute of Health (NIH), cares potentially for the health of approximately 96% of the population (NIS, 1986a; NIH, 1987a, g). This responsibility is being transferred from the NIH to the regional institutions (this has already occurred in Cataluña and Andalucia Autonomous Communities). Each person affiliated to the NHS has a card which entitles his/her family to receive health care in the NHS network. Radiological examinations are performed mainly in hospitals and outpatient centres, the latter being the first link in the patient's radiological diagnosis. Private diagnostic radiology is used by the remaining population (not counting the population served by military hospitals), and by patients who, in spite of having access to NHS diagnostic radiology services, prefer to choose the private sector for different reasons.

During this first year of study, data have also been furnished by national, regional and local health institutions including the NSC. The Deputy Directorate of Food, Health and Consumer Protection also contributed valuable advice and help throughout the data-collection process.

Hospitals involved in the project comprise between 700 and 1500 beds and serve 36% of the population of the Autonomous Community of Madrid (ACM). The data available from outpatient centres refer to 31% of the ACM population and those from the private sector were obtained from 16 centres, according to the documentation presented at the NSC by these centres, for licensing of their corresponding installation (NSC, 1987, personal communication; Vañó & Alvarez, 1987, unpublished) with comprehensive data from one centre (Morillo, 1987).

Data were available from all the Autonomous Communities through the Directorate General of the NIH, except for Andalucia and Cataluña, and amounted to 67% of the Spanish population. Any possible variation presented by these two Communities will not be significant, since as a whole their

Table I. Growth in the number of physicians in Spain

	1981	1982	1983	1984	1985
Population (millions)	37.62	37.96	38.17	38.39	38.60
Licensed physicians	96 569	104 759	115 251	121 362	127 195
Dentists	4032	4065	4458	4682	5137
No. of inhabitants per physician	391	362	331	316	303
No. of inhabitants per physician (without dentists)	408	378	345	329	316

The Official Bulletin of the General Council of Physicians, (GCP, 1987) note that the current number of unemployed phsicians is 27 000 and that this figure will reach 51 000 by 1992.

The possibility of double licensing (motivated by the need to meet this requirement in order to have access to jobs in different counties and the fact that the number of members of Physician Colleges may be out date could affect the accuracy of the data.

Sources: NIS (1986b), DHCA, (1984) and GCP (1987).

characteristics must be close to the nation's average, although they may show individual difrerences. We therefore assumed that the results obtained for that 67% of population could be extended to the whole of Spain.

The report from the National Institute of Statistics (NIS, 1986a, b), enabled us to analyse the population of the different Autonomous Communities. From their age distribution and number of offspring, it was possible to derive the child expectancy as a function of age (Taylor, 1980), which was assumed to be identical for the whole of the Spanish territory in the absence of better sources of data (Delgado et al, 1987), and to calculate the genetically significant dose. In some cases, it has been possible to obtain detailed information on the characteristics of the population cared for (NIH, 1986b, 1987c; ACM, 1987).

Some parameters relating to diagnostic radiology in Spain

One of the fundamental parameters in assessing the health care level of different countries, which is directly related to the number of radiological examinations performed, is the number of inhabitants per physician. Table I shows the evolution of this figure throughout the past few years. At present, Spain has about 300 inhabitants/physician.

Table II presents some significant data on Spain's public health care, obtained from official reports (NIH, 1986a; NIH, 1987a). Among the most significant would be the ratio of 22 316 inhabitants per NIH radiologist and 82.3 public hospital beds per hospital radiologist.

A detailed survey of diagnostic X-ray equipment is still not available. The NSC performed a survey in 1983 (NSC, 1987, personal communication) with this objective, but the level and detail of the answers has not

Table II. Population covered by the National Institute of Health

Autonomous community	Beds in service	Diagnostic radiology specialists		Population NIH card[a]	Population census
		Hospital	Outpatient		
Aragón	3285	33	33	1165 701	1184 295
Asturias	2382	34	16	1061 248	1112 186
Baleares	1138	7	16	671 332	680 933
Canarias	1846	22	22	1401 184	1449 758
Cantabria	1173	31	8	482 942	522 664
C. La Mancha	2959	23	33	1598 967	1675 715
Castilla León	5729	58	52	2472 319	2582 327
C. Valenciana	6527	67	81	3617 712	3732 679
Extremadura	1942	12	16	1050 025	1086 420
Galicia	3847	31	46	2673 741	2843 498
La Rioja	513	5	5	257 341	260 024
Madrid	9554	181	119	4494 557	4780 572
Murcia	1430	28	14	964 503	1006 788
Navarra	638	6	11	509 697	523 787
País Vasco	3406	26	50	2038 267	2136 100
Melilla	151	0	1	35 605	52 388
Ceuta	—	0	2	47 893	65 151
Sub-total	46 414	564	538	24 543 034	25 695 285
Andalucia[b]				6670 257	6789 772
Cataluña[b]				5760 462	6073 258
Estimated total	69 275	842	803	36 973 753	38 558 315

[a] Total number of inhabitants included on NHS cards. [b] The Andalusian and Catalan Communities are no longer included in NIH reports since responsibility in health care matters has been transferred from the central Government. Sources: NIH (1987a,f), NIS (1986a).

P25849

Table III. Estimate of the amount of diagnostic radiology equipment performing over 1000 examinations per year[a]

	Mean number of rooms or equipment assumed
328 Outpatient centres (49 in Cataluña and 26 in Madrid)	× 4 rooms
124 Residences	× 9 rooms
44 Hospital centres	× 15 rooms
6 Special centres	× 20 rooms
17 General residences	× 15 rooms
27 Other	× 2 rooms
Total Department of Health and Autonomous Communities	3517 rooms
Department of Defence 36 centres × 10 rooms	360 rooms
Local administration and other 297 centres × 3 rooms	891 rooms
Private clinics 438 centres × 3 rooms	1314 rooms
Private offices and other	2718 rooms
Total	8800 rooms

[a] Excluding dental X-ray units.

(The number of centres was taken from the Annual Statistical Report of 1986 (NIS, 1986b) and refers to 1983).

yet made it possible to establish the correct figures. In Cataluña, a study during 1986 revealed a total of 5626 such installations (NSC, 1987, personal communication), including public and private hospitals, occupational medical services, dental equipment, private clinics and offices, primary care centres, etc.

A preliminary analysis of the results of this study carried out jointly by us and technicians from the NSC (Vañó & Alvarez, 1987, unpublished) allowed to us to estimate the number of machines performing over 1000 examinations per year, from an estimation of the number of machines attributed to each centre (Table III) and the number of examinations per machine (Table IV). From these estimations, a figure of 0.23 machine per 1000 inhabitants was derived or, alternatively, 4400 inhabitants per machine.

To estimate the annual number of radiological examinations, partial analyses of different diagnostic radiology sectors have been made. As indicated earlier, there are three well differentiated types of diagnostic radiology practice in Spain: one, performed in hospitals belonging to the Department of Health network (or to the Department of Health of the Autonomous Communities, as in the case of Andalucia and Cataluña), a second performed in outpatient centres (also depending on the corresponding Department), and a third performed in the private sector (private hospitals, clinics and offices).

Table IV. Estimate of the number of annual examinations per X-ray machine

Health care unit	Range
Hospital centre	4000–8000
Outpatient centre	5000–9000[a]
Private office	2500–11 500[b]

[a] Mean value of eight outpatient centres in Madrid: 8115.

[b] The figure of 11 500 is reliable for a general radiology private office working mornings and afternoons.

A sampling of 16 private centres (NSC, 1987, personal communication; Vañó & Alvarez, 1987, unpublished) shows an average value of 2240 examinations per machine.

The diagnostic radiology performed in any of the 36 centres of the Department of Defence (NIS, 1986a) or in local administration centres is not included. However, since one of the participating hospitals in this project is the Gomez Ulla Central Military Hospital, it will in future be possible to obtain some parameters in relation to diagnostic radiology at this type of centre.

The most difficult information to collect is that from the private sector. Except on very rare occasions, it is not possible to obtain precise information in this area. The most important private health care groups were consulted but a response was received from only one of them (SANITAS, 1987, personal communication). On the other hand, data presented to the NSC for licensing such installations are scarce and of questionable reliability, especially in relation to the number of examinations undertaken each year.

Information concerning the amount of X-ray film purchased in Spain each year has not been available from the different manufacturers and suppliers. One agreed fact, which has even been reflected in the Department of Health and Consumer Affairs internal reports (DDHET, 1987), is that about 20% of the total radiographic film sold annually in Spain is used in private radiology. We have assessed the average number of films/examination (excluding mammography and CT scans, where special types of films are used), as well as the average film area. The latter ranges from $0.100\,m^2$ in private radiology to $0.118\,m^2$ in hospitals and outpatient centres (Table V), which enabled us to establish that 26% of examinations were performed in the private sector.

With this figure added to the detailed information obtained from hospitals participating in the project, and

Table V. Use of films in the Autonomous Community of Madrid

	No. of films per examination	Mean area per film[a] (m^2)	Percentage of examinations	Percentage of area
Hospital centres	2.7	0.118	34	43
Outpatient centres	2.0	0.118	40	37
Private radiology	2.0	0.100	26	20
Mean weighted value		2.24 films per examination		

[a] Excluding mammography and CT.

the data from outpatient centres obtained by different sources (Ramírez, 1986, personal communication; Ruiz, 1987, personal communication), it was possible to estimate the number of annual examinations per 1000 inhabitants in the ACM. To extrapolate this figure to the remainder of Spain, NIH official data (NIH, 1986b), along with the assumption of an equal private sector contribution (26%) in all the country, have been considered. The latter has been deduced from requests for the licensing of facilities, which are centralized by the NSC for all the Spanish territory (Vañó & Alvarez, 1987, unpublished). The amount of private practice can be explained in terms of compensation for the less varied public health available in medium and small cities.

One of the most critical aspects of these estimates refers to the population which may potentially be served by the different centres (when an attempt is made at distributing the number of examinations performed in a hospital or outpatient centre by a given number of inhabitants). Wide discrepancies may be found, due partially to the lack of reliable figures on the mean number of people included on an NHS card, as well as the care rendered to patients not assigned to a given centre, by virtue of the freedom of choice of physicians. Values ranging from 2.1 to 3.0 persons per card are found. The most current official data supplied by the NIH, ranging from 2.2 to 2.4 (Lamata, 1986; NIH, 1987e), were used in our case.

Hospitals in large cities also serve a small percentage of patients from other counties. In the Autonomous Community of Madrid in 1986, this amounted to 7.14% of the total number of admissions and 0.9% of the hospital visits (NIH, 1987e).

Another factor to consider, and which should also make some adjustments to the final results, refers to the number of centres contracted by the NIH to serve NIH patients. Although this number has progressively decreased, 1.93% of the total visits in the Community of Madrid and 26.3% of the hospital admissions were in 1986 to contracted hospitals (comprising 40% in non-NIH public hospitals and 60% in private hospitals). Nevertheless, part of the effect this may have on the number of annual examinations per 1000 inhabitants is offset by the percentage attributed to private radiology.

The following figures can be established from the above information.

In the ACM (population 4.8 million, 12% of the whole of Spain), the annual number of X-ray examinations per 1000 inhabitants is distributed by sectors in the following way: 200 in hospitals, 230 in outpatient centres and 150 in the private sector, giving a total of 580 examinations per year and per 1000 inhabitants.

For the whole nation, and according to official data for 1986 (NIH, 1986a), a total of 20 888 000 radiographs were obtained (44% in hospitals and 56% in outpatient centres), for a total of 24 592 723 potential users (the whole of Spain except the Autonomous Communities of Andalucia and Cataluña, which amount to 33% of the total Spanish population).

It could be inferred from the average number of radiographs per examination deduced by us in Madrid (2.7 in hospitals and 2.0 in outpatient centres), that about 9 501 000 X-ray examinations were performed in NIH centres in 1986 (39% in hospitals and 61% in outpatient centres). The hospital ratio was fixed at 2.5 for the whole of the nation, according to the partial analysis based on data from regional and local reports (Lamata, 1986; NIH, 1987c; NIH, 1987d).

If these results are extrapolated to the nation as a whole, and assuming (as has already been mentioned) that private radiology accounts for 26% of the examinations, as in the case of the Community of Madrid, we would have, for a population of 38.8 million, a total annual number of examinations per 1000 inhabitants of 490, shared by hospitals (140), outpatient centres (223) and private practice (127). In both cases (ACM and Spain) estimates were made without considering labour and military mass screening or dental examinations.

Table VI. Increase in the number of radiological examinations

	Year		Increase (%)
	1985	1986	
Hospital centre (31 machines)	133 409	141 578	6.1
Outpatient centre (6 machines)	46 103	47 393	2.8
Private office (2 machines)	23 076	22 656	−1.8

Variation of annual frequency of examinations

A detailed analysis was performed on the variation of the annual frequency of examinations in some centres in Madrid between 1985 and 1986. The centres chosen did not show any substantial changes with regard to equipment, personnel or population attended. The results of this analysis are shown in Table VI.

The average increase in the number of examinations for the area of Madrid would be 2.7%, while the average for the whole of Spain, if we were to apply the same percentages, would be 2.5%. The difference is due to the different incidence of the various types of radiology attributed to the Community of Madrid (34% hospital, 40% outpatient and 26% private) and to the nation as a whole (28% hospital, 46% outpatient and 26% private).

Frequency of some examinations per 1000 inhabitants

In order to perform an analysis of the frequency of hospital radiological examinations (Tables VII and VIII), data obtained from the San Carlos University Hospital (HUSC) were used, as this centre does not present distortions with regard to its functioning and the patient population served during the year of the analysis (1986). Also, this hospital has a very good data-processing centre which enabled some of the data obtained to be compared using different methods of analysis.

The San Carlos University Hospital has 1406

Table VII. Estimate of the frequency of radiological examinations by sectors in the Autonomous Community of Madrid

	No. of examinations (per 1000 inhabitants per year)		
	Hospitals (%)	Outpatient centres (%)	Private centres (%)
Total	200	230	150
Extremities	30 (15)	30 (13)	30 (20)
Skull	6 (3)	7 (3)	5 (3)
Simple abdomen	16 (8)	23 (10)	14 (9)
Spine	14 (7)	58 (25)	38 (25)
Hip and pelvis	6 (3)	7 (3)	5 (3)
Chest	62 (31)	62 (27)	30 (20)
GI tract	5 (2.5)	23 (10)	17 (11)
Urology	3 (1.5)	7 (3)	5 (3)
CT scan	6 3.2)	—	4 (2)
Other	52 (25.8)	14 (6)	6 (4)
Mammography	(1.2)		
Vascular	(2.0)		
HSG	(0.2)		
Myelography	(0.2)		

Table VIII. Estimate of the frequency of radiological examinations in the Autonomous Community of Madrid and the whole of Spain

	No. of examinations (per 1000 inhabitants per year)		
	Autonomous Community of Madrid	Whole of Spain[a]	%
Skull	18	15	3.1
Spine	110	97	19.8
Chest	154	128	26.0
Mammography	17	14	2.9
Abdomen	53	45	9.2
GI tract	45	40	8.2
Urography	15	13	2.6
Hip and pelvis	18	15	3.1
Extremities	90	75	15.3
CT	10	7	1.4
Other	50	41	8.4
Total	580	490	100

[a] Values for Spain as a whole were extrapolated assuming the same frequency distribution of examinations as in the Autonomous Community of Madrid.

The table does not include mass labour and military screening or dental examinations.

operative beds, 18 radiodiagnostic rooms and 13 portable X-ray machines (not including the catheterization room or dental equipment). The hospital serves 690 000 potential users (14.2% of the ACM population) and performed 141 578 radiological examinations during 1986 (ultrasound examinations, which amounted to 19 291, or 12% of the total number of examinations performed in the Diagnostic Radiology Services, are not included). In 1986, 414 265 radiographs were taken.

Of the total number of radiological examinations, 137 197 were conventional examinations (excluding CT scans), involving 391 865 films, which amounts to an average of 2.86 films per examination in this centre.

In 1986, the HUSC had 26 348 patient admissions, 191 355 outpatient visits and 72 898 emergency admissions, making a total of 265 990 (HUSC, 1987), with an index of 0.53 radiological examinations per attended patient. Similar values have been obtained in other centres (NIH, 1987b, d; Nuñez, 1987, personal communication), albeit in some instances (NIH, 1987c), as for the La Fe Hospital of Valencia, with 1992 beds and a value of 0.42 examinations per attended patient. However, this figure excluded maternity hospital care (204 552 examinations and 489 094 patients served), as in this hospital the care burden is higher than the rest, since the centre holds 30% of the hospital beds in the Community of Valencia.

The analysis of examination frequency in outpatient centres (Ramirez, 1986, personal communication; Ruiz, 1987, personal communication) has supplied a total number of 302 893 examinations per year referred to nine outpatient centres in Madrid.

For the private sector, data from a national insurance company (SANITAS, 1987, personal communication) along with those for one private centre of Madrid (Morillo, 1987) have been analysed. In addition, the results from 16 private centres, comprising 43 rooms and 96 320 annual examinations, were used (NSC, 1987, personal communication; Vañó & Alvarez, 1987, unpublished).

Patient dose estimation

As noted previously, we have not yet carried out all the necessary measurements and evaluations in order to obtain accurate dose values for all types of examination. Nevertheless it was possible, during the first year of the project, to obtain information on over 60 000 hospital examinations with details of the technical parameters employed, operator and equipment involved, place where performed, patient sex and age, as well as a smaller number of examinations performed in outpatient centres (Ramirez, 1986, personal communication; Ruiz, 1987, personal communication) and private offices (NSC, 1987, personal communication; Vañó & Alvarez, 1987, unpublished).

Using mean and range values of those parameters (kVp, mAs, screening time, etc.) exposure measurements were made at skin level (without backscattering), in several rooms of the different centres and for a large number of examination modes (Vañó et al, 1987a), with properly calibrated Victoreen Radcheck ion chambers. Measurements of the exposure times per area for some complex examinations (digestive tract, intravenous urography, etc) were also made by using a Diamentor (PTW Freiburg) transmission ionization chamber.

Similarly, in urography, measurements have been

Table IX. Estimate of organ doses in computed tomography

Organ	Dose (μGy)
Ovary	730
Testes	82
Bone marrow	3 400
Thyroid	310
Breast	1 600[a]
Pancreas	7 600
Liver	20 700
Kidney	22 600
Intestine	7 000
Stomach	20 000
Spleen	22 000
Muscle entrance	26 800
Lung	1 200
Effective dose equivalent for liver CT	6.3 mSv
Estimated effective dose equivalent (Drexler et al, 1984)	
Head	2.8 mSv
Chest	4.4 mSv
Liver	6.1 mSv

[a] Male phantom, measured at the surface

Measurements were performed on a Remab phantom from Alderson, with TLD, for a 14 contiguous slices liver scan with a CT General Electric CT/T scanner.

Table XI. Estimate of dose in gonads for some types of examination

Type of examination	Female (mSv)	Male (mSv)
Intravenous urography	5.3	3.1
GI tract	1.1	0.13
Chest	0.025	0.005
Liver CT	0.73	0.082

Sources (Calzado et al (1987), Delgado et al (1987), Morán et al (1987), Vañó et al (1987a)).

made of the absorbed dose (in muscle) at point of entry, directly on patients, using TLD-100 dosemeters from Harshaw (Morán et al, 1987). This type of measurement is currently being co-ordinated among some EEC states.

Organ dose measurements have been initiated on a Remab phantom from Alderson, specially designed for diagnostic radiology, using between 40 and 50 TLD-100 chips for dose estimations in each radiological examination (Calzado et al, 1987). We have results from digestive tract examinations (following introduction of the corresponding contrast medium into the stomach), chest, conventional chest tomography, computed tomography and urology. A Rando phantom has also been used, following a similar procedure, to perform several measurements in chest (González et al, 1987b) and skull examinations.

With all this information, and bearing in mind the variations recorded within the same centre and between the different centres participating within the project, we have made an estimation (Vañó et al, 1987b) of the organ doses, using both the phantom measurements and the values derived from data from Jones and Wall (1985) and Drexler et al (1984).

In the case of chest and urographic examinations, it has already been possible to perform a more detailed analysis (Delgado et al, 1987; González et al, 1987a; Moran et al, 1987), which enabled us to derive the genetically significant dose in these cases.

Table X. Estimate of effective dose equivalent for different medical diagnostic X-ray examinations in the Autonomous Community of Madrid

Type of examination	Estimated effective dose equivalent[a] (mSv)	Mean effective dose equivalent weighted by frequency				
		Hospital (mSv)	Outpatient (mSv)	Private (mSv)	Total (mSv)	Total (%)
Skull	0.2	0.006	0.006	0.006	0.006	0.3
Spine	1.0	0.070	0.250	0.250	0.189	10.4
Chest	0.16	0.050	0.043	0.032	0.043	2.4
Abdomen	1.5	0.120	0.150	0.135	0.136	7.5
GI tract	10.2	0.255	1.020	1.122	0.781	43.1
Urology	7.0	0.105	0.210	0.210	0.174	9.6
Hip and pelvis	2.8	0.084	0.084	0.084	0.084	4.6
Extremities	0.1	0.015	0.014	0.020	0.016	0.9
CT	5.0	0.160	—	0.100	0.080	4.4
Others	3.0	0.774				
	0.5		0.030	0.025	0.282	15.6
Subtotal (mSv)		1.640	1.810	1.980	1.810	
Examination percentages		34%	40%	26%		
Effective dose equivalent per inhabitant 1.04 mSv						

[a] These values are to be more precisely evaluated.

The table does not include mass labour and military radiological controls and dental radiology.

With regard to computed tomography, the results presented correspond to the experimental results measured in the phantom already described for a liver CT scan, with 14 contiguous slices and using a General Electric CT/T (MSI) machine. The doses for head and chest CT scans have been derived from the data of Drexler et al (1984), using reference values from this equipment. The different results obtained are indicated in Tables IX–XI. A first estimation of the mean effective dose equivalent per radiological examination in the Madrid area gave a value of 1.81mSv, leading to 1.04 mSv per inhabitant per year.

If we assume that the 1.81 mSv value can be extrapolated, once properly corrected with the percentages of hospital, outpatient and private radiology, to the national whole (1.71 mSv), the 490 examinations per 1000 inhabitants per year would imply 0.84 mSv per inhabitant per year in Spain. The collective dose equivalent which would be attributed to diagnostic radiology would then be 32 510 man-Sv.

The genetically significant dose for chest and urinary tract examinations (without taking into account the incidence in the paediatric population), turned out to be 0.1 and 17 μGy, respectively (Delgado et al, 1987; González et al, 1987a; Morán et al, 1987).

Acknowledgments

This study was partially supported by the CEC (contract B16-214-EA), the CAICYT, the Department of Health and Consumer Affairs, and by the Nuclear Safety Council.

References

ACM, 1987. *Health and Social Services Picture. II. Demography and Social Structure Profile of Areas, Districts and Basic Zones* (Autonomous Community of Madrid, Health and Social Welfare Council, Madrid) (in Spanish).

Calzado, A., Vañó, E., Moran, P., Castellote, C., Marco, M., Delgado, V. & Gonzalez, L., 1987. Preliminary organ dose estimations for radiological procedures on a REMAB phantom. In *Proceedings of the Second National Congress on Radiation Protection*. Toledo, November 1987 (in Spanish).

DDHET, 1987. *Criteria for evaluation of medical X-ray films* (I) (Deputy Directorate of Health Evaluation and Technology, Department of Health and Consumer Affairs, Madrid) (in Spanish).

Delgado, V., Moran, P., Vañó E., Gonzalez, L. & Calzado, A., 1987. Hospital X-ray chest examinations contribution to GSD in the region of Madrid. In *Proceedings of the Second National Congress on Radiation Protection*, Toledo, November 1987 (in Spanish).

DHCA, 1984. *Physicians Supply and Demand in Spain* (Department of Health and Consumers Affairs, Madrid) (in Spanish).

Drexler, G., Panzer, W., Widenman, L., Williams, G. & Zankl, M., 1984. *The Calculation of Dose from External Photon Exposures using Reference Human Phantoms and Monte Carlo Methods. Part III: Organ Doses in X-ray Diagnosis*. GSF-Bericht S-1026.

GCP, 1987. *Information Bulletin of the General Council of Physicians*, no. 107 (in Spanish).

Gonzalez, L., Vañó, E., Calzado, A., Delgado, V., Moran, P., Lopez, P. & Bezares, M., 1987a. Dosimetric evaluation in diagnostic radiology installations in Spain. In *Proceedings of the Sixth European Congress of Radiology, Excerpta Medica International Congress Series*, No. 749 (Elsevier Science Publishers, Amsterdam), pp. 497–500.

Gonzalez, L., Vañó, E., Fernandez, P. & Manzanas, M. J., 1987b. Biological tissue equivalent phantom dosimetry for X-ray chest examinations. In *Proceedings of the Sixth National Congress of Medical Physics*, Badajoz, September 1987 (in Spanish).

HUSC, 1987. *Annual Report 1986*. (Department of Health and Consumer Affairs, San Carlos University Hospital, Madrid) (in Spanish).

Jones, D. G. & Wall, B. F. 1985. *Organ Doses from Medical X-ray Examinations Calculated using Monte Carlo Techniques*. NRPB Report NRPB-R186 (HMSO, London).

Lamata, F., 1986. Private communication.

Moran, P., Vañó, E., Morillo, A., Calzado, A., Gonzalez, L., Castellote, C., Delgado, V. & Marco, M., 1987. A first estimation of dose to adult patients for X-ray urinary tract examinations. In *Proceedings of the Second National Congress on Radiation Protection* Toledo, November 1987 (in Spanish).

Morillo A., 1987. Private communication.

NIH, 1986a. *Annual Report* (Department of Health and Consumers Affairs, National Institute of Health, Madrid) (in Spanish).

NIH, 1986b. *Health Diagnosis, Outpatient Centres, 10th Sector* (Department of Health and Consumer Affairs, National Institute of Health, Madrid) (in Spanish).

NIH, 1987a. *Report on Functional Economy of Health Institutions 1985*, Volume II (Department of Health and Consumer Affairs, National Institute of Health, Madrid) (in Spanish).

NIH, 1987b. *Management Reports* (Department of Health and Consumer Affairs, National Institute of Health, Provincial Directorate, Madrid), (in Spanish).

NIH, 1987c. *Annual Report 1986. Affairs* (National Institute of Health, Provincial Directorate, Avila), (in Spanish).

NIH, 1987d. *Annual Report 1986. La Fe Hospital* (Department of Health and Consumers Affairs, National Institute of Health, Valencia), (in Spanish).

NIH, 1987e. *Management Report 1982–1986* (Department of Health and Consumer Affairs, National Institute of Health, Provincial Directorate, Leon), (in Spanish).

NIH, 1987f. *Annual Report 1986* (Department of Health and Consumer Affairs, National Institute of Health, Provincial Directorate, Madrid), (in Spanish).

NIH, 1987g. *Budget for the Coming Year (draft document)*, Volume I. *Economical Area* (Department of Health and Consumer Affairs, National Institute of Health, Madrid, (in Spanish).

NIS, 1986a. *1985 Fecundity Inquiry (preliminary results)* (National Institute of Statistics, Madrid), (in Spanish).

NIS, 1986b. *Annual Statistical Report of Spain* (National Institute of Statistics, Madrid (in Spanish).

Taylor, F. E., 1980. *Estimation of Child Expectancy for the Population of the United Kingdom in 1974 to be used in the Calculation of Genetically Significant Dose*, NRPB Report NRPB-M49 (HMSO, London).

Vañó, E. et al., 1987a *Optimization of Protection in Medical Diagnostic Radiology Project. First Stage (April 1986–February 1987), Preliminary Report*, (in Spanish).

Vañó, E., Moran, P., Calzado, A., Gonzalez, L. & Delgado, V., 1987b. A first estimation of doses associated with diagnostic radiology in the region of Madrid. In *Proceedings of the Second National Congress on Radiation Protection*, Toledo, November 1987 (in Spanish).

1989, *The British Journal of Radiology*, *62*, 27–30

Transient diverticula of the colon

By J. Rawlinson, MA, FRCS and F. J. Brunton, FRCP, FRCR

Department of Radiodiagnosis, Southampton General Hospital, Southampton

(*Received May 1988*)

Abstract. Transient diverticula are radiological phenomena that can be observed in a minority of patients undergoing barium enema. Radiographs before and after smooth muscle relaxation are required. Diverticula seen on the early radiographs may, in some patients, disappear following the intravenous administration of 20 mg hyoscine-N-butylbromide (Buscopan). Using this technique in 441 examinations, transient diverticula have been observed in 18 patients (4.1%). They exhibit many features of established diverticula which suggests that they represent an incipient stage of the disease.

The observation that diverticula may be affected by the pharmacological action of drugs on colonic muscle was first made by Arfwidsson (1964). Following injection of the potent, smooth muscle stimulant prostigmine into a patient undergoing barium enema, questionable diverticula in the sigmoid colon became more apparent. More recently, in the Wessex region, transient diverticula have been observed by the action of muscle relaxants rather than stimulants. They were initially a chance finding in two patients (Fig. 1). Because of the barium enema technique now routinely practised, transient diverticula have been observed more frequently (Figs 2,3). These radiological phenomena confirm the important role of colonic muscle in the pathogenesis of diverticula and we suggest that they represent an early stage of diverticular disease.

Patients and methods

A standard technique was used in 441 consecutive barium enemas performed by the authors over the period 1985–86. Following barium infusion and air insufflation, an erect radiograph was taken to include the splenic flexure. Returning the patient to the supine position, 20 mg of Buscopan was administered intravenously. In those suffering from ischaemic heart disease, the dose was reduced to 10 mg and a few patients had Glucagon (1 mg). After further air insufflation decubitus, Hampton and lateral rectal views together with appropriate spot radiographs were taken to ensure that the whole colon and abnormalities therein were adequately visualized in double contrast. Post-evacuation radiographs were taken if indicated.

Examinations which had shown diverticula on the

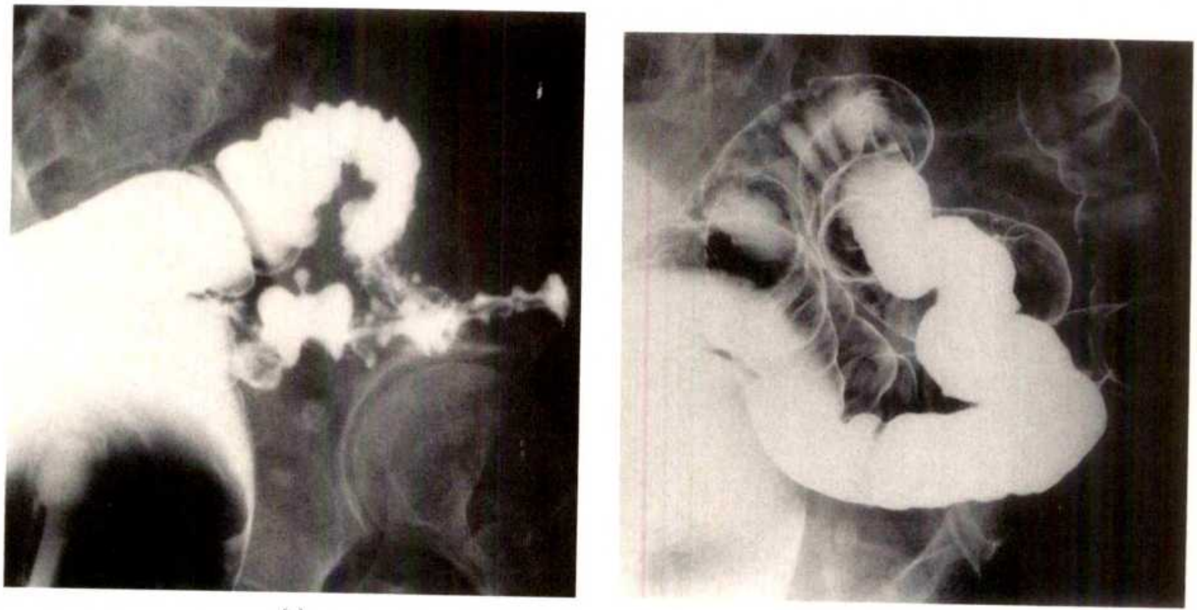
(a) (b)

Figure 1. (a) Sigmoid spasm obstructed the flow of barium in this 60-year-old man, who presented with change of bowel habit. Note also the sigmoid diverticula. (b) Following 20 mg intravenous Buscopan, both the spasm and the diverticula have disappeared. Similar findings were also noted in a 76-year-old woman.

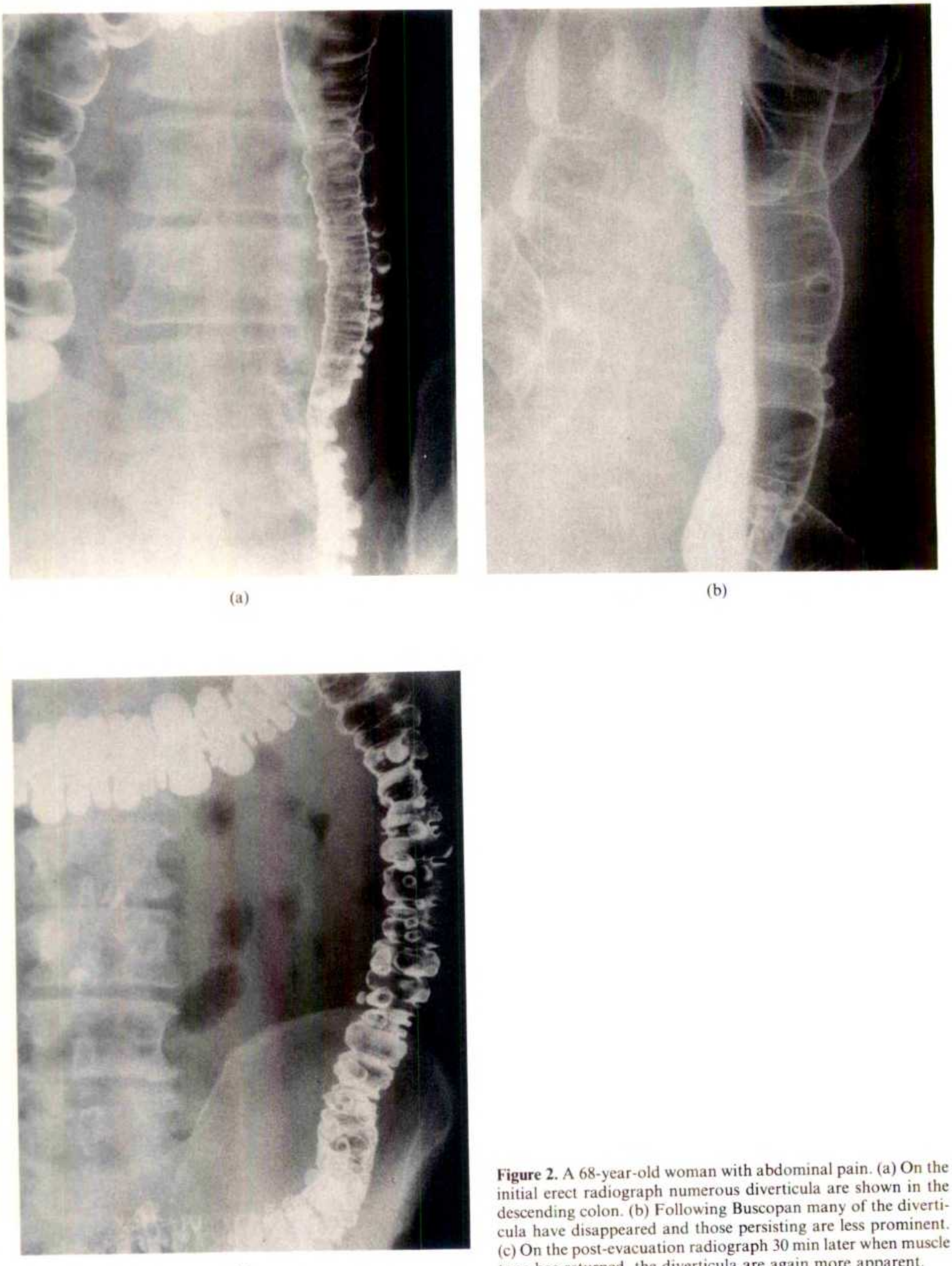

(a)

(b)

(c)

Figure 2. A 68-year-old woman with abdominal pain. (a) On the initial erect radiograph numerous diverticula are shown in the descending colon. (b) Following Buscopan many of the diverticula have disappeared and those persisting are less prominent. (c) On the post-evacuation radiograph 30 min later when muscle tone has returned, the diverticula are again more apparent.

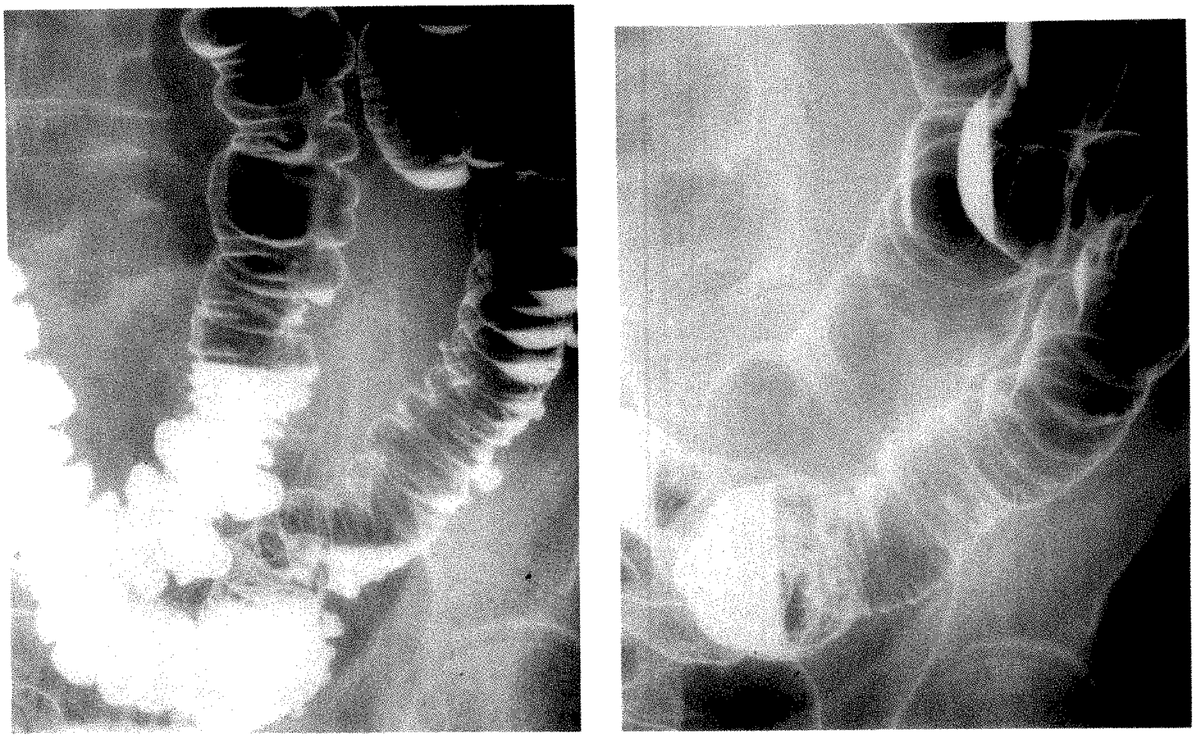

(a) (b)

Figure 3. (a) Diverticula are seen in the sigmoid and distal descending colon of this 56-year-old man. (b) After smooth muscle relaxation, those diverticula in the descending colon have disappeared.

initial erect radiograph but not on subsequent views were reviewed and the clinical details and radiological features recorded.

Results

Transient diverticula were observed in 18 examinations, an incidence of 4.1%. They were twice as common in women as in men and occurred in patients ranging in age from 47 to 88 years (mean 64.5 years). Eight patients presented with abdominal pain, six with change in bowel habit, two with anaemia and two had rectal bleeding. The 14 patients with pain and changed bowel habit were thought clinically to have irritable colon or diverticular disease. In the anaemic patients, the causes were unrelated to the gastrointestinal tract. One patient with bleeding had haemorrhoids but in the other no cause was found.

Transient diverticula were most commonly observed in the left hemicolon and evenly distributed throughout this region. In four patients they occurred in the proximal colon. They were associated with prediverticular spasm in four patients and with sigmoid diverticular disease in six.

Discussion

These radiological phenomena give a useful insight into the natural history of diverticula. In their predilection for the left hemicolon, the older age group and the female sex, transient diverticula exhibit many features of the established condition (Goligher, 1984). Their association with recognized manifestations of diverticular disease in 10 patients (56%) and the presentation of the majority with abdominal pain or change in bowel habit suggests that they do in fact represent an early stage of the disease. We might therefore expect them to occur at an earlier age, but no significant difference in the mean ages of those with transient as compared with established diverticula could be demonstrated. However, the difference in numbers between the groups is large (18 versus 179) and six patients had both forms of diverticula, so statistically the comparison is unsatisfactory.

The use of muscle relaxants during barium enema has been advocated by several workers on the basis that it improves distension and facilitates the identification of small mucosal abnormalities (Young, 1964; Welin, 1967; Ferrucci & Benedict, 1971; Lee, 1982). For these reasons muscle relaxants are nearly always used in this department. If given routinely before the start of the examination, in a minority of patients diverticula will disappear and the diagnosis of early disease will be missed. A normal report in such a patient with pain or change in bowel habit may lead to further investigation to account for the symptoms. A radiograph before the injection of Buscopan overcomes this problem while the advantages afforded by muscle relaxation are preserved for the remainder of the examination. This technique may confer some immediate benefit to the patient as well as allowing the visualization of transient diverticula. When the injection is administered the patient is supine and thereafter only turned into prone and decubitus positions. Given that the erect posture facilitates filling of the caecal pole (Dreyfuss & Janower, 1980), we prefer to achieve this position before the injection and so minimize drug-induced side-effects.

This response of diverticula to muscular relaxation clarifies some points about their pathogenesis. The muscle abnormality in diverticular disease was recognized towards the end of the 19th century (Lane, 1885) but its importance has only recently been emphasized (Morson, 1963). It was postulated by Painter et al (1965) that the thickened muscle, by segmental contractions, increased the intraluminal pressure sufficiently to cause mucosal herniation at points of weakness in the colonic wall. The demonstration of raised pressures in diseased colons (Arfwidsson & Kock, 1964; Painter & Truelove, 1964; Parks & Connell, 1969), the pathological finding of herniated mucosa alongside perforating vessels between the taenia coli (Slack, 1962), the beneficial effects of sigmoid myotomy (Attisha & Smith, 1969) and our own findings, would support this hypothesis. Such a view is challenged by the normal pressures found in many asymptomatic patients with the disease (Weinreich & Anderson, 1976; Eastwood et al, 1978). This apparent discrepancy may be explained by regarding the condition as a disease spectrum (Almy & Howell, 1980). At one extreme are patients with high intracolonic pressures, few diverticula and severe pain and at the other are those with normal pressures, multiple defects in the colonic wall with numerous diverticula and no symptoms. Whatever the significance of these interacting factors, the constancy of the muscular thickening in affected individuals and the response of some diverticula to a smooth muscle relaxant confirm that the uncomplicated disease is primarily a disorder of colonic muscle.

Acknowledgments

We would like to thank the radiographic and nursing staff for their help during the examinations. We are grateful to Dr P. Guyer for contributing the case illustrated in Fig. 1. We also thank the Department of Medical Illustration for preparing the photographs from the original radiographs.

References

ALMY, T. P. & HOWELL, D. A., 1980. Diverticular disease of the colon. *New England Journal of Medicine*, *302*, 324–331.

ARFWIDSSON, S., 1964. General aspects on the pathogenesis of multiple diverticula in the sigmoid colon and on diverticular disease. *Acta Chirurgica Scandinavia* (Suppl.), *342*, 56–62.

ARFWIDSSON, S. & KOCK, N. G., 1964. Intraluminal pressure in the sigmoid colon of normal subjects and of patients with diverticular disease. *Acta Chirurgica Scandinavia* (Suppl.), *342*, 11–26.

ATTISHA, R. P. & SMITH, A. N., 1969. Pressure activity of the colon and rectum in diverticular disease before and after sigmoid myotomy. *British Journal of Surgery*, *56*, 891–894.

DREYFUSS, J. R. & JANOWER, M. L., 1980. Techniques of colon examination. In *Radiology of the Colon*, ed. by J. R. Dreyfuss & M. L. Janower (Williams & Wilkins, Baltimore, USA), p. 73.

EASTWOOD, M. A., SMITH, A. N., BRYDON, W. G. & PRITCHARD, J., 1978. Colonic function in patients with diverticular disease. *Lancet*, *i*, 1181–1182.

FERRUCI, J. T. & BENEDICT, K. T., 1971. Anticholinergic-aided study of the gastro-intestinal tract. *Radiologic Clinics of North America*, *9*, 23–39.

GOLIGHER, J. C., 1984. Diverticulosis and diverticulitis of the colon. In *Surgery of the Anus, Rectum and Colon*, ed. by J. C. Goligher (Balliere Tindall, London), p. 1084.

LANE, W. A., 1885. The pathology of extravasation of urine and of sacculation of the urethra and bladder. *Guy's Hospital Report*, *43*, 29–52.

LEE, J. R., 1982. Routine use of hyoscine-N-butylbromide (Buscopan) in double-contrast barium enema examinations. *Clinical Radiology*, *33*, 273–276.

MORSON, B. C., 1963. The muscle abnormality in diverticular disease of the sigmoid colon. *British Journal of Radiology*, *36*, 385–392.

PAINTER, N. S., TRUELOVE, S. C., GORDON, M., ARDRAN, G. M. & TUCKEY, M., 1965. Segmentation and the localization of intraluminal pressures in the human colon, with special reference to the pathogenesis of colonic diverticula. *Gastroenterology*, *49*, 169–177.

PAINTER, N. S. & TRUELOVE, S. C., 1964. The intraluminal pressure pattern in diverticulosis of the colon. *Gut*, *5*, 201–213.

PARKS, T. G. & CONNELL, A. M., 1969. Motility studies in diverticular disease of the colon. *Gut*, *10*, 534–542.

SLACK, W. W., 1962. The anatomy, pathology and some clinical features of diverticulitis of the colon. *British Journal of Surgery*, *50*, 185–190.

WEINREICH, J. & ANDERSON, D., 1976. Intraluminal pressure in the sigmoid colon. II. Patients with sigmoid diverticula and related conditions. *Scandinavian Journal of Gastroenterology*, *11*, 581–586.

WELIN, S., 1967. Results of the Malmo technique of colon examination. *Journal of the American Medical Association*, *199*, 369–371.

YOUNG, A. C., 1964. The Malmo enema at St. Mark's Hospital: a preliminary report. *Proceedings of the Royal Society of Medicine*, *57*, 275–278.

1989, *The British Journal of Radiology*, *62*, 31–34

Technetium-99m hydroxymethylene diphosphonate scanning of acute injuries to the lateral ligaments of the ankle

By *Hugh Maurice, FRCS and Iain Watt, MRCP, FRCR

Departments of Orthopaedic Surgery and Radiodiagnosis, Bristol Royal Infirmary, Bristol BS2 8HW

(*Received April 1988 and in revised form August 1988*)

Abstract. Technetium-99m hydroxymethylene diphosphonate scans were performed on 29 consecutive patients with acute ankle ligament injuries. Scanning reliably differentiated a severe from a minor injury. Severe injuries gave a diffuse uptake on the scan and the minor injuries a more localized increase in uptake.

Many publications (Hughes, 1980; Galasko & Weber, 1984) have commented on the use of technetium-99m labelled bone scans in the diagnosis of osseous trauma. A previous study of technetium-99m hydroxymethylene diphosphonate (^{99}Tc^{m}-HDP) scanning in patients with foot pain following trauma revealed a number of patients with increased activity but no bony injury. The activity was thought to be due to uptake in injured capsule and ligaments (Maurice et al, 1987). The clinical significance of this finding has not been assessed previously. This paper reports the results of a prospective study of ^{99}Tc^{m}-HDP scanning in a consecutive series of acute ankle ligament injuries of varying severity.

Funder et al (1982) showed that swelling of 4 cm or more over the lateral malleolus correlated well with a significant ankle injury, 70% having a positive ankle arthrogram indicating torn ligaments and capsule. Staples (1975) and Fordyce and Horn (1972) advocate ankle arthrography to diagnose significant ligamentous tears, whereas Blanchard et al (1986) advocate peroneal tenography. Both of these procedures are locally invasive.

If a non-invasive technique, such as ^{99}Tc^{m}-HDP scanning, were to differentiate reliably a severe injury from a minor injury, it would be useful in clinical management.

The aim of this study was to demonstrate whether or not a ^{99}Tc^{m}-HDP scan can differentiate a severe ankle injury from a minor one.

Materials and methods

Twenty-nine consecutive patients with acute injuries to the lateral ligament complex of the ankle, presenting to the Accident and Emergency Department of the Bristol Royal Infirmary between March and May 1986, were included in this study.

There were 22 men and seven women, average age 31 years (range 16–78 years) and 18 (62%) sustained their injury playing sport.

All patients were assessed within 3 days of injury by one surgeon (H.D.M.), the diagnosis confirmed and given a clinical grading—minor, intermediate or severe—the grading depending on the size of swelling, site of tenderness and the patient's ability to bear weight (Table I). Soft-tissue swelling was assessed on the plain radiograph and quantified by a soft-tissue index (STI) (Fig. 1) (Blanchard et al, 1986). A ^{99}Tc^{m}-HDP scan of the ankles was then performed within 2 weeks of injury. The early and delayed scans were obtained by a standard method (Maurice et al, 1987).

Treatment for all cases unable to bear weight was 2 weeks in a plaster cast followed by active mobilization with an elasticated support, whereas those able to weight bear were given an elasticated support at once.

The patients were followed-up to full recovery, which was defined as a return to pre-injury functional level and no complaints with the injured ankle.

Inversion and antero-posterior shift stress radiographs were taken following recovery, to demonstrate any residual instability.

Statistical significance was assessed using Student's *t*-test.

Results

Those patients clinically graded as severe had more soft-tissue swelling on plain radiographs and took longer to recover than those in the minor group (Table II); both differences are highly significant ($p < 0.01$).

In nine of the 11 patients classified as severe (Fig. 2), the ^{99}Tc^{m}-HDP scan showed a diffuse increase in uptake in the whole of the lateral ligament complex, extending variably across the whole ankle capsule, and present in

Table I. Clinical grading of acute ankle injuries

Severe	Marked swelling >4 cm Unable to bear weight Tenderness throughout ligament complex
Minor	Minimal swelling <4 cm Able to bear weight Tenderness localized to one ligament only *i.e.* anterior talofibular
Intermediate	Any combination of minor or major features

---

*Current address and address for reprints: 59 Beaulieu Avenue, Sydenham, London SE26.

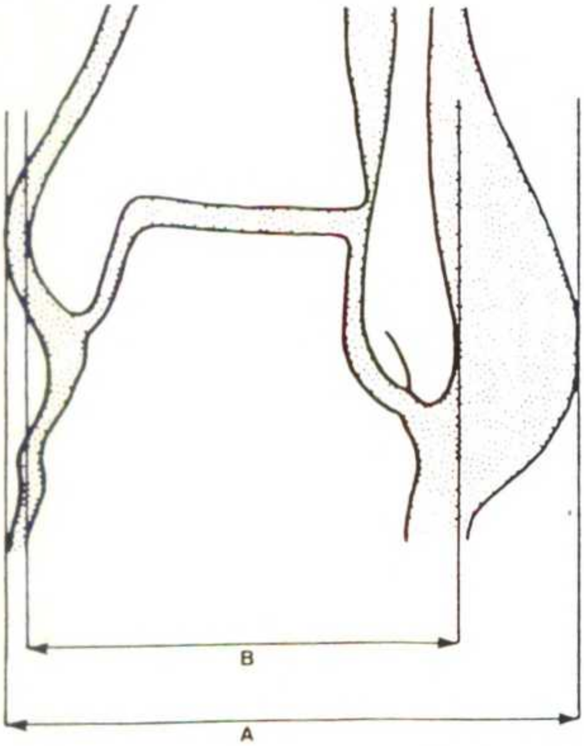

Figure 1. Calculation of the soft-tissue index. $\mathrm{STI} = \frac{\mathrm{A} - \mathrm{B}}{\mathrm{B}} \times 100$

both the perfusion and delayed images (Table III). One patient in the severe group had activity localized to the tibiofibular syndesmosis and another had a normal scan—both of these had little soft-tissue swelling on their radiographs (STI 17.1 and 16.9, respectively).

Those classified as minor (Table III) had either a normal scan or activity well localized to the injured ligament (Fig. 3). One patient in this group had a more diffuse uptake but had a low STI and behaved as a minor sprain in that full recovery was in 5 weeks.

Those patients with a diffuse scan made a full recovery in a mean of 7.5 weeks, whereas those with a localized or normal scan took a mean of 5.5 weeks to recover. This difference is significant ($p < 0.05$). The mean STI was also significantly greater for those with a diffuse scan (mean STI of 25.6) than the localized or normal scans (mean

Table II. Patients clinical grading following ankle ligament injury

Clinical grading	n	Mean STI	Mean recovery time (in weeks)
Severe	11	23.5	8
Intermediate	7	22.4	6
Minor	11	14.5	5

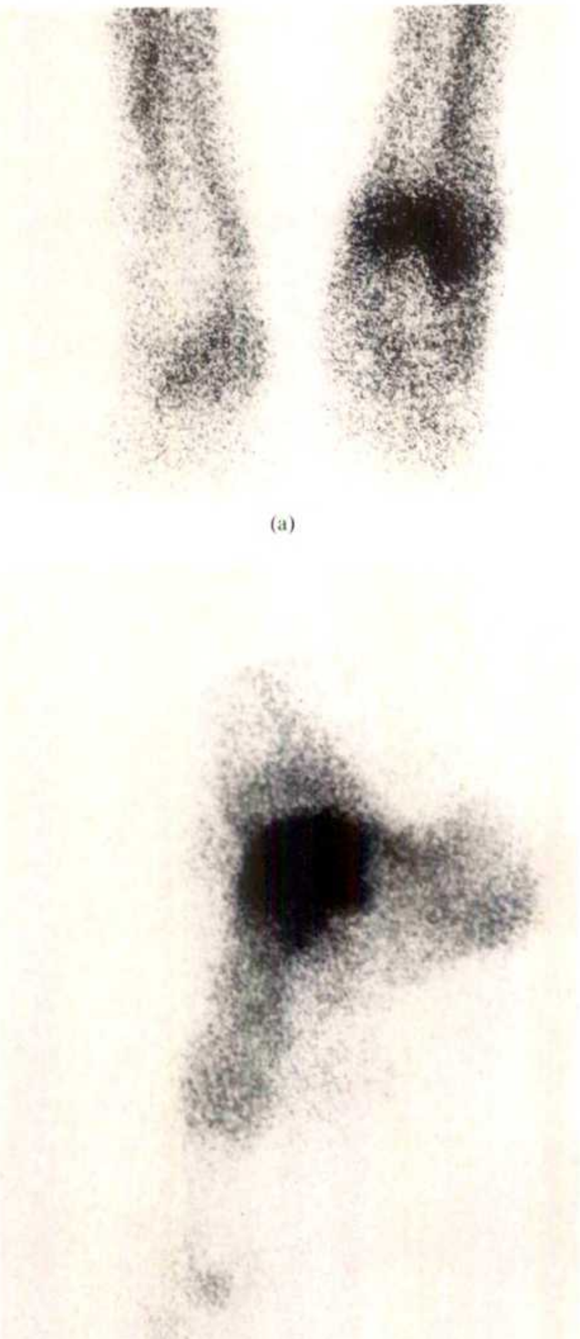
(a)

(b)

Figure 2. *Case 1.* A 19-year-old footballer with a severe lateral ligament injury of the left ankle. Plain radiographs showed no bony injury. (a) Anterior $^{99}\mathrm{Tc}^{\mathrm{m}}$-HDP scan of both ankles showing marked increased activity of the region of the left ankle. (b) Lateral $^{99}\mathrm{Tc}^{\mathrm{m}}$-HDP scan of the left ankle showing marked activity over the capsule of the left ankle.

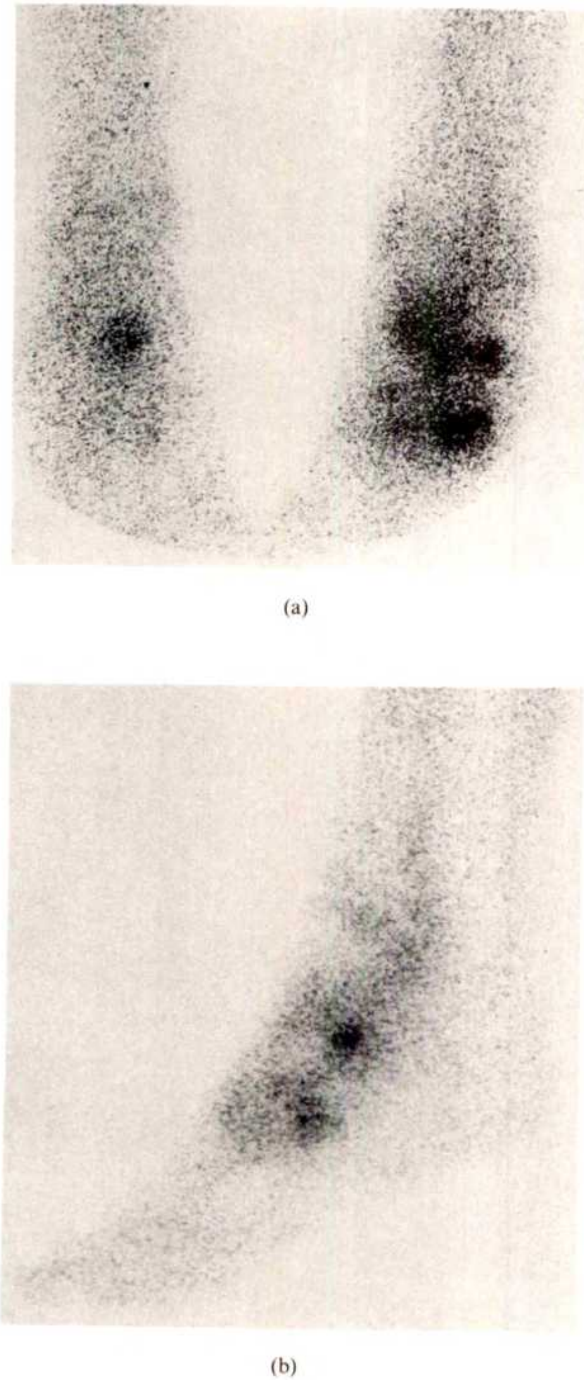

Figure 3. *Case 2.* A 35-year-old woman with a minor sprain of the left ankle and tenderness over the distal attachments of the talofibular ligament. No bony injury was seen on plain radiographs. (a) Anterior ^{99}Tc^{m}-HDP scan of both ankles showing increased activity in the left ankle region and maximal activity localized laterally along the talofibular ligament. (b) Lateral ^{99}Tc^{m}-HDP scan of the left ankle showing activity mainly over the distal insertion of the talofibular ligament.

Table III. ^{99}Tc^{m}-HDP scan features following ankle ligament injury

Clinical grading	Diffuse activity	Localized	Normal	Total number of patients
Severe	9	1	1	11
Intermediate	3	4	—	7
Minor	1	6	4	11

STI of 15.2), $p<0.02$ (Table IV). This indicates that a diffuse scan represents a more severe injury than those injuries giving a localized or normal scan.

All patients except two made a full recovery. These two had returned to their pre-injury functional level but complained of minor pain which did not require treatment.

Twenty of the patients had stress radiographs taken following recovery. None showed significant instability, and the other nine were clinically stable.

Discussion

These results confirm the earlier observation that soft-tissue injury alone may cause increased ^{99}Tc^{m}-HDP activity. Iimori et al (1975) noted that soft-tissue damage alone may cause abnormalities on a bone scan but did not comment on the significance or value of this. Rosenthall et al (1976) called this activity spurious and suggested that it should not mislead management. We recommend that when observing increased activity on a bone scan following trauma, where plain radiographs have shown no fracture, the possibility of soft-tissue injury should be borne in mind. The current report indicates how this activity may be of use in clinical management.

A radionuclide scan will differentiate a severe from a minor ankle ligament injury, the severe injuries giving a diffuse uptake on the scan and the minor injuries a more localized increase in uptake. Scan findings correlated well with a careful clinical assessment, a slower recovery time being seen in those with a clinically severe injury and a diffuse scan. Those patients with equivocal clinical features, classified as intermediate, could be separated into severe or minor on the basis of their scan findings.

In this study a number of the scans were not performed until the 2nd week following injury; however, there was no correlation between scan findings and time following ankle sprain. It is important to stress that the radionuclide scan should be performed as soon as

Table IV. Recovery time and ^{99}Tc^{m}-HDP scan features

Scan features	n	STI (mean)	Recovery time (in weeks)
Diffuse	13	25.6	7.5
Localized/normal	16	15.2	5.5

possible following injury, because excessive delay may invalidate its use.

The management of severe ankle ligament injuries is controversial. Funder et al (1982), Fordyce and Horn (1972) and Staples (1975) advocate an aggressive approach with surgical repair of proven ruptured ligaments, but Freeman (1965) advocates mobilization alone. All the patients in this series made a good recovery with a mobilization regime, which concurs with Freeman's findings. If a conservative regime is being adhered to then there is no place for investigating these patients by radionuclide scanning or locally invasive techniques. However, if an aggressive surgical policy is used then a radionuclide scan is an excellent method of assessment. Only those with a diffuse scan need be subjected to arthrography or tenography to confirm rupture of the ligament complex.

Scanning is also useful in patients with persistent ankle pain following a sprain (Maurice et al, 1987). Activity will be present until healing is complete. The scan will indicate and localize the lesion, allowing appropriate treatment to be started.

Conclusions

A technetium-99m radionuclide scan will differentiate a severe ankle ligament injury from a minor one. The severe injury gives a diffuse increase in uptake throughout the lateral ligament complex extending variably throughout the capsule of the ankle, whereas a minor injury gives increased activity accurately localized to the injured ligament. A scan will classify ligament injuries with equivocal physical signs and localize abnormality in those complaining of persistent pain.

References

Blanchard, K. S., Finlay, D. B. L., Scott, D. J. A., Ley, C. C., Siggins, D. & Allen, M. J., 1986. A radiological analysis of lateral ligament injuries of the ankle. *Clinical Radiology, 37*, 247–251.

Fordyce, A. J. W. & Horn, C. V., 1972. Arthrography in recent injuries of the ligaments of the ankle. *Journal of Bone and Joint Surgery, 54B*, 116–121.

Freeman, M. A. R., 1965. Treatment of ruptures of the lateral ligament of the ankle. *Journal of Bone and Joint Surgery, 47B*, 661–668.

Funder, V., Jorgensen, J. P., Anderson, A., Bryde Andersen, S., Lindholmer, E. & Niederman, B., 1982. Ruptures of the lateral ligaments of the ankle. *Acta Orthopaedica Scandinavica, 53*, 997–1000.

Galasko, C. S. B. & Weber, D. A., 1984. *Radionuclide Scintigraphy in Orthopaedics* (Churchill Livingstone, Edinburgh).

Hughes, S., 1980. Radionuclides in orthopaedic surgery. *Journal of Bone and Joint Surgery, 62B*, 141–150.

Iimori, M., Hisada, K. & Suzuki, Y., 1975. Technetium 99^m pyrophosphate bone scanning in evaluation of trauma. *Journal of Nuclear Medicine, 16*, 538.

Maurice, H. D., Newman, J. H. & Watt, I., 1987. Bone scanning of the foot for unexplained pain. *Journal of Bone and Joint Surgery, 69B*, 448–452.

Rosenthall, L., Hill, R. & Chunang, S., 1976. Observations on the use of 99^m Tc pyrophosphate imaging in peripheral bone trauma. *Radiology, 119*, 637–641.

Staples, O. S., 1975. Ruptures of the fibular collateral ligaments of the ankle. *Journal of Bone and Joint Surgery, 57A*, 101–107.

1989, *The British Journal of Radiology*, 62, 35–40

Aortic tumours: report of a case and review of the literature

By Jaap Schipper, MD, *Jacques A. van Oostayen, MD, †Jan C. den Hollander, MD and *Andries J. van Seyen, MD

Department of Radiology, University Hospital Leiden, and Departments of *Radiology and †Pathology, University Hospital Rotterdam "Dijkzigt"

(*Received June 1987 and in revised form December 1987*)

Abstract. We present a case of a leiomyosarcoma originating in the wall of the descending aorta and give a review of 27 previously reported cases of aortic neoplasms. An extraluminal aortic leiomyosarcoma has not been reported before in the literature.

Primary tumours of the aortic wall are extremely rare and, because of this and the fact that these tumours can mimic various other clinical conditions, they are seldom diagnosed pre-operatively or at ante-mortem examination. We present a case of a leiomyosarcoma originating in the wall of the descending aorta and give a review of 27 previously reported cases of aortic neoplasms.

Case report

A 74-year-old White woman presented with a 2-month history of back pain and a short period of severe, acute back and chest pain. On examination she appeared in good general condition and routine laboratory findings were normal.

A chest radiograph showed a large, left-sided, retrocardiac and para-aortic mass which could not be distinguished from the aortic contour (Fig. 1). Previous medical history included a cholecystectomy, a bilateral lumbar sympathectomy and a deep venous thrombosis of the lower legs many years before. An electrocardiogram (ECG), bronchoscopy, endoscopy of the oesophagus and barium swallow showed no abnormalities. Transfemoral arterial digital subtraction angiography (DSA) was performed and showed only moderate dilatation of the descending aorta at the level of the tumour. The aortic contour was smooth and there were no signs of a dissecting aneurysm (Fig. 2).

A subsequent examination of the chest by computed tomography (CT) revealed more of the nature of the abnormal mass seen on the chest radiograph. An inhomogeneous, lobulated mass in close contact with the descending aorta was visualized and punctate calcifications were visible in the periphery of the mass, which was seen to be separate from the oesophagus.

Except for slight discontinuity in the posterior margin, the lumen of the aorta was uninvolved (Fig. 3). Hounsfield Unit (HU) measurements on the pre-contrast scans varied from 80–120 HU. There was no significant enhancement of the mass itself on post-contrast images.

Although the radiological findings were indecisive, clinical signs and symptoms favoured the pre-operative diagnosis *viz.* partly thrombosed or ruptured aneurysm of the descending aorta. At operation, a firm mass was palpated originating from the distal part of the thoracic descending aorta which had no relation to the adjacent oesophagus or heart.

The mass was interpreted macroscopically as an old, organized haematoma. The aortic lumen was opened but no site of perforation could be identified, ruling out the possibility of a dissecting aneurysm. A vascular prosthesis was placed and the aortic wall was closed over the prosthesis. Parts of the mass were resected for pathological examination.

Microscopically, the tumour consisted of broad bundles of pleomorphic, elongated cells with oval,

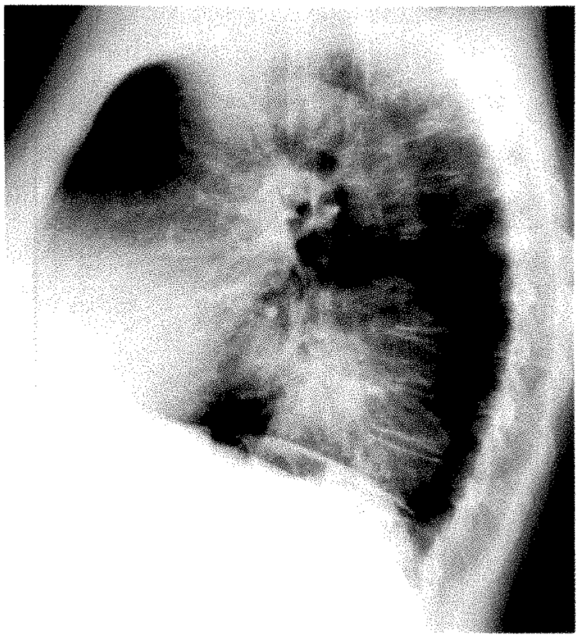

Figure 1. Lateral chest radiograph showing a large retrocardiac mass with loss of the aortic contour.

Address correspondence and reprint requests to: J. Schipper, Department of Radiology, University Hospital Leiden, Postbox 9600, 2300 RC Leiden, Netherlands.

Table I. Clinical, pathological and radiological features of primary aortic tumours

Reference	Sex/age (years)	Symptons and signs	Radiological findings	Site	Size (cm)	Type	Histology
Browdowski 1873	M/52	Weight loss, abdominal pain, paraesthesiae of hands and feet	—	Thoracic	11 × 8	I	Medullary sarcoma
Miura, 1891	M/38	Pathological fracture of right femur, thoracic and sacral pain	—	Thoracic, 7 cm below left subclavian artery to 6 cm above coeliac axis	9	I	Spindle and giant cell sarcoma
Aufferman, 1912	M/38	Abdominal pain, weight loss	—	Abdominal, 1.5 cm above coeliac axis to iliac arteries	4.5	M	Spindle and giant cell sarcoma
Nencki, 1946	M/46	Abdominal pain suggesting appendicitis or cholecystitis	—	Abdominal	3.5 × 3.5 × 2	M	Fibrosarcoma
Karhoff, 1952	M/55	Headache, abdominal pain, hypertension	—	Thoracic and abdominal, 4 cm below isthmus to below renal arteries	3.5 × 2.5	I	Primitive mesenchymal cell tumour
Kovaleva & Press, 1959	M/65	Abdominal pain radiating into right leg, hypertension, osseous metastases	—	Abdominal, level of renal arteries to 2 cm above bifurcation	?	I	Fibrosarcoma
Dètrie, 1960; Kattus et al, 1960	F/22	Hypertension, diminished femoral pulses	Angiography: occlusion of left renal artery	Thoracic and abdominal, cast-like tumour	30	I	Fibromyxoma
Zeitlhofer et al, 1963	M/3 months	Dyspnoea, tachycardia	—	Thoracic and abdominal, extension into coeliac artery	6.5 × 2 × 0.5	I	Fibromyxo-sarcoma
Kaigorodova & Berezovskaya, 1963	F/62	Headache, weight loss, fever, absent pulses in right arm	—	Thoracic, extension into right subclavian artery	13	I	Fibrosarcoma
Sladden, 1964	M/64	Lumbago and sciatica, swelling of right leg	Angiography: filling defect in lower aorta	Abdominal, 3–5 cm above bifurcation	2.5 × 2.5 × 0.5	I	Intimal sarcoma
Sladden, 1964	M/59	Bilateral leg pain, absent pulses in right leg	—	Abdominal at bifurcation, extension into both iliac arteries	?	I	Intimal sarcoma
Smeloff et al, 1965	F/65	Hypertension, dizziness, upper body oedema	Angiography: blockage of arch at left subclavian artery	Thoracic and abdominal, extension into left subclavian and left renal artery	20 × 1	I	Fibromyxo-sarcoma
Stevenson et al, 1971	M/60	Low back pain, abdominal pain, hypertension	—	Abdominal, level of renal arteries	4 × 2	I	Fibromyxo-sarcoma
Winkelmann et al, 1971	M/65	Pain in both legs, cutaneous metastases	Angiography: filling defect with aorta–iliac obstruction	Abdominal, level of bifurcation	?	I	Angiosarcoma

Table I—*continued*

Reference	Sex/age (years)	Symptons and signs	Radiological findings	Site	Size (cm)	Type	Histology
Silverman & Wexler, 1972	F/62	Headache, dizzy spells, hypertension	Angiography: filling defect	Thoracic, arch extension in right subclavian and left carotid artery	?	I	Myxoma
Salm, 1972	F/60	Backache, pathological fracture of right hip	—	Thoracic	3.5 × 2 × 2	M	Fibrosarcoma
Kimbrell & Kaasa, 1973	F/58	Headache, chest pain, hypertension	—	Abdominal and thoracic, arch to renal arteries	18 × 2	I	Myxoma
Stefelaar et al, 1975	M/70	Claudication, diminished pulses in both legs	Angiography: filling defect, obstruction above bifurcation	Abdominal, level of bifurcation	4	I	Undifferentiated malignant tumour
Crum et al, 1978	F/58	Pleuritic pain	—	Thoracic, distal to left subclavian artery	6 × 4 × 4	M	Fibroxanthosarcoma
Hernandez et al, 1979	M/42	Back pain, testicular pain, pulsatile abdominal mass	Angiography: aneurysm	Abdominal	12 × 7.5 × 5	M	Leiomyosarcoma
Weinberg & Maini, 1980	M/48	Hypertension, abdominal aneurysm	Angiography: extensive atherosclerosis, aneurysm, occlusion of several arteries	Thoracic	7.5 × 1.5 × 2	M	Malignant fibrous hystiocytoma
Milili et al, 1981	M/64	Severe pain in lower extremities, diminished pulses in both legs	Angiography: complete occlusion 3 cm distal to renal arteries	Abdominal	4 × 5 × 3	M	Leiomyosarcoma
Fehrenbacher et al, 1981	M/67	Pain and absent distal pulses in right leg	Angiography: filling defect, stenosis of right superficial femoral artery	Abdominal	6 × 2	I	Angiosarcoma
Mason et al, 1982	M/70	Abdominal pain, anorexia, weight loss	Angiography: filling defect. CT: intraluminal tumour	Abdominal, coeliac axis to below renal arteries	5 × 4	I	Angiosarcoma
Schmid et al, 1984	M/75	Symptoms of bilateral femoral arterial occlusion	Angiography: filling defect, descending aorta femoral arterial occlusion	Thoracic	8 × 4.5	I	Endothelioma
Hermanek et al, 1985	F/47	Back pain, abdominal pain	Angiography: aneurysm, pathologic vessels. CT: aneurysm, liver metastases. Ultrasound: same	Abdominal	?	I	Histiocytoma
Wright et al, 1985	F/46	Symptoms of bowel infarction	—	Abdominal	5 × 4	I	Intimal sarcoma

I = intimal; M = mural.

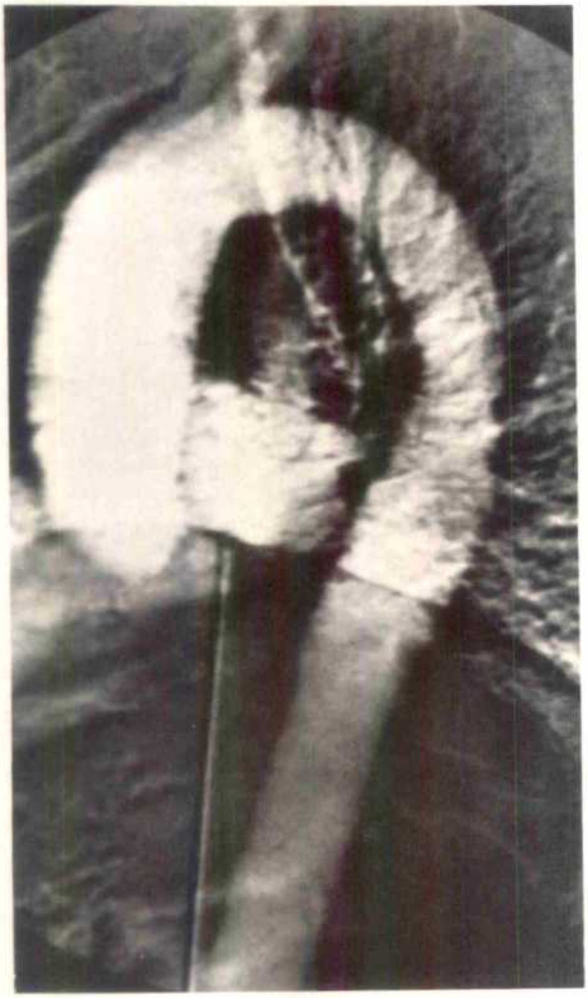

Figure 2. Intra-arterial digital subtraction arteriogram showing mild fusiform dilatation of the distal part of the thoracic aorta.

sometimes blunt, nuclei and a moderate amount of eosinophilic cytoplasm. The cells were enmeshed in a delicate framework of reticulin fibres with frequent mitotic figures (Fig. 4). Parts of the tumour were necrotic. Immunoperoxidase staining with anti-desmine was positive in the cytoplasm of many cells. On electron microscopy, small bundles of myofilaments were seen regularly within the tumour cells and many tumour cells also showed intracytoplasmic glycogen. The pathological diagnosis was leiomyosarcoma of the aortic wall.

Post-operatively, there were no complications; the patient was discharged in good condition and will receive palliative radiotherapy.

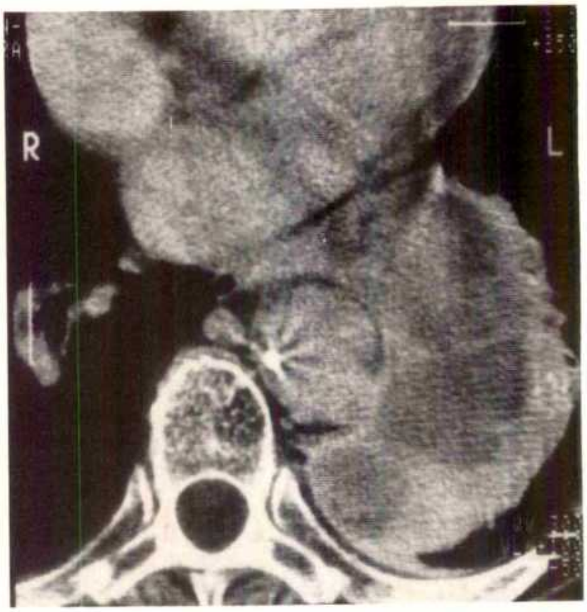

Figure 3. A CT scan of a large, left-sided para-aortic mass. Note punctate calcifications in the periphery of the tumour and minimal pleural effusion on the left side. The angiography catheter is visible within the aortic lumen.

Discussion

A primary tumour of the aortic wall is a very rare lesion, the first case of an aortic tumour being described by Browdowski in 1873. A review of the world literature disclosed 27 previously reported cases of primary aortic tumour (Table I). One report describes two cases (Salm, 1972) and one case is described in two different reports (Détrie, 1960; Kattus et al, 1960). Clinical, pathological and radiological features of these 27 cases are listed in Table I. The sites of origin of the tumours are distributed over the various aortic segments in the following way. Seven arose from the thoracic aorta, 12 from the abdominal aorta and the remaining eight involved both the thoracic and abdominal aorta. There were 18 male and nine female patients. The mean age of these patients was 54 years.

Although several authors (Kevorkian & Cento, 1973;

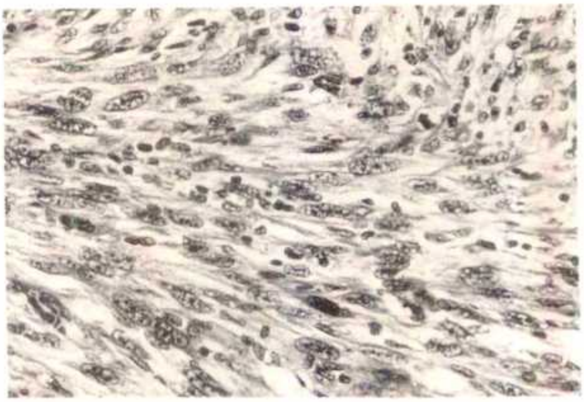

Figure 4. Microscopic section of leiomyosarcoma of the aortic wall. Haematoxylin azophloxin staining (× 236).

Mason et al, 1982) have pointed out that the histopathological classification is handicapped by the varied interpretation, there is a predominance of fibrosarcomatous tumours (Table I). There are two reports of a malignant aortic tumour associated with vascular graft material (Weinberg & Maini, 1980; Fehrenbacher et al, 1981). Vascular leiomyosarcoma (apart from the aorta, as presented in this case) mostly occur in the inferior vena cava or other large veins. These locations are about five times more frequent than in arteries in which the pulmonary artery is affected twice as often as systemic arteries (Kevorkian & Cento, 1973). Wright et al (1985) suggest a classification of aortic tumours into two categories based on their site of origin within the aortic wall.

(1) Tumours primarily involving the intima. These tend to grow in the direction of the aortic lumen forming polypoid masses or extend along the intima. Clinical signs and symptoms are referrable to luminal obstruction: diminished pulses distal to the tumour or severe hypertension when the renal arteries are involved. These tumours frequently give rise to thrombo-embolic metastases and because they can resemble atherosclerosis they may sometimes be overlooked at operation.

(2) Tumours arising in the media or adventitia. These form aggressive mass lesions with an intramural or extraluminal extension. They are less common (eight out of 27 cases) and seldom give rise to metastases, probably because the intima is usually not involved. Clinical signs and symptoms are non-specific: back-pain, fever or symptoms of dissecting aneurysm. The tumour presented here fits into this category. An origin in the wall of the vasa vasorum cannot be excluded but seems unlikely. The episode of sudden chest pain may be explained by intratumoral bleeding.

Because these diverse clinical manifestations mostly preclude an adequate pre-operative diagnosis, aortic tumours are almost always identified during operation or at autopsy. Information of radiological findings in aortic tumours is scarce. Thirteen reports give information of angiographic findings; all but three refer to intima-based lesions. In their book on aortic diseases, Crawford and Crawford (1984) reported three additional cases of aortic tumour, two with information of angiographic findings. The characteristic angiographic appearance is a polypoid intraluminal filling defect reflecting the morphology of the tumour while the remaining aorta is smooth and of normal calibre.

There are only two previously published CT scans of aortic tumours (Mason et al, 1982; Hermanek et al, 1985). Computed tomography cannot differentiate intraluminal tumour from a thromboid mass but can exclude extra-aortic disease. The inability of angiography to detect the tumour in the current case lay in the fact that this tumour originated in the media with the intima unaffected. It is not clear whether the slight aortic dilatation at the level of the tumour in this case is coincidental or represents weakening of the wall. Computed tomography revealed the relationship of the lesion with the aorta and the degree of extra-aortic extension. The HU measurement was probably due to intralesional haemorrhage as was suggested clinically.

The therapeutic management of aortic tumours is unclear. Surgical methods (primary resection with reconstruction) and non-surgical methods (radiotherapy, chemotherapy) have poor results: the average survival of patients with vascular sarcomas is 1.5 years (Kevorkian & Cento, 1973). Although these tumours are very rare, they should be added to the differential diagnosis in cases of an intraluminal filling defect on aortography and in an otherwise unexplained para-aortic mass.

Acknowledgment

We thank Mrs A. W. Laken for her help in preparing the manuscript.

References

Aufferman, H., 1912. Primäre Aortengeschwulst mit eigentümlichen Riesenzellen. *Zeitschrift für Krebsforschung, 11*, 294–301.

Browdowski, W., 1873. Primäres Sarkom der Aorta thoracica mit Verbreitung des Neugebildes in der unteren Körperhälfte. *Jahresbuch Leistungen Gesellschaft Medizin, 8*, 243–246.

Crawford, F. & Crawford, J. L., 1984. *Diseases of the Aorta* (Williams & Wilkins, Baltimore, USA), pp. 387–393.

Crum, C. P., Feldman, P. S. & Nolan, S. P. 1978. Primary fibroxanthosarcoma of the thoracic aorta. *Virchows Archiv A: Pathological Anatomy and Histopathology, 379*, 351–358.

Détrie, P., 1960. Tumeur primitive intravasculaire de l'aorte. *Journal de Chirurgie, 80*, 666–668.

Fehrenbacher, J. W., Bowers, W., Strate, R. & Pittman, J., 1981. Angiosarcoma of the aorta associated with a Dacron Graft. *Annals of Thoracic Surgery, 32*, 297–301.

Hermanek Jr, P., Gentsch, H. H. & Scheele, J., 1985. Maligne Tumoren der grössen Gefässe. Zwei Fall Berichte. *Chirurg, 56*, 120–122.

Hernandez, F. J., Stanley, T. M., Ranganath, K. A., Rubinstein, A. I., 1979. Primary leiomyosarcoma of the aorta. *American Journal of Surgical Pathology, 3*, 251–256.

Kaigorodova, P. E. & Berezovskaya, E. K., 1963. Endothelioma of the thoracic aorta. *Grudnaya Khirurgiya, 4*, 88–90 (in Russian).

Karhoff, B., 1952. Primärtumor der Aorta. *Zentralblatt für Allgemeine Pathologie und Pathologische Anatomie 89*, 46.

Kattus, A. A., Longmire, W. P., Cannon, J. A., Webb, R., Johnston, C., 1960. Primary intraluminal tumor of the aorta producing malignant hypertension. Successful surgical removal. *New England Journal of Medicine 262*, 694–700.

Kevorkian, J. & Cento, D. P., 1973. Leiomyosarcoma of large arteries and veins. *Surgery, 73*, 390–400.

Kimbrell, O. C. & Kaasa, L. J., 1973. Primary intraluminal aortic myxoma with involvement of several vertebrae. *Journal of the American Medical Association, 226*, 459–460.

Kovaleva, A. N. & Press, B. O., 1959. A case of primary sarcoma of the intima of the aorta. *Arkhiv Patologii, 21*, 62–65, (in Russian).

Mason, M. S., Wheeler, J. R. & Gregory, R. T., 1982. Primary tumours of the aorta: report of a case and review of the literature. *Oncology, 39*, 167–172.

Milili, J. J., La Flare, A. G. & Nemir, P., 1981. Leiomyosarcoma of the abdominal aorta: a case report. *Surgery, 89*, 631–634.

Miura, M., 1891. Das primäre Riesenzellensarcom der Aorta thoracica. *Internationale Beiträge Wissenschaftliche Medizinische Fortschritte Rudolf Virchow 2*, 249–255.

Nencki, L., 1946. Zur Kenntnis der primärtumoren der grossen Gefässstämme. Ueber einen fall von primären Sarcom der Aorta abdominalis. *Cardiologia (Basel)*, *10*, 1–24.

Salm, R., 1972. Primary fibrosarcoma of aorta. *Cancer*, *29*, 73–83.

Schmid, E., Port, S. J., Carroll, R. M. & Friedman, N. B., 1984. Primary metastasizing aortic endothelioma. *Cancer*, *54*, 1407–1411.

Silverman, J. F. & Wexler, L., 1972. Primary intraluminal tumor of the aorta. Case report with pre-operative angiographic diagnosis. *Radiology*, *102*, 581–582.

Sladden, R. A., 1964. Neoplasia of aortic intima. *Journal of Clinical Pathology*, *17*, 602–607.

Smeloff, E. A., Reece, J. M. & Masters, J. H., 1965. Primary intraluminal malignant tumor of the aorta. *American Journal of Cardiology*, *15*, 107–110.

Steffelaar, J. W., vd Heul R. O., Blackstone, E., Vos, A., 1975. Primary sarcoma of the aorta. *Archives of Pathology and Laboratory Medicine*, *99*, 139–142.

Stevenson, J. E., Burkhead, H., Trueheart, R. E., McLaren, J., 1971. Primary malignant tumor of the aorta. *American Journal of Medicine*, *51*, 553–559.

Weinberg, D. S. & Maini, B. S., 1980. Primary sarcoma of the aorta associated with a vascular prosthesis: a case report. *Cancer*, *46*, 398–402.

Winkelmann, R. K., van Heerden, J. A. & Bernatz, P. E., 1971. Malignant vascular endothelial tumor with distal embolization. *American Journal of Medicine*, *51*, 692–694.

Wright, E. P., Glick, A. D., Virmani, R, & Page, D. L., 1985. Aortic intimal sarcoma with embolic metastases. *American Journal of Surgical Pathology*, *9*, 890–897.

Zeitlhofer, J., Holzner, J. H. & Krepler, P., 1963. Primäres Fibromyxosarkom der Aorta. *Krebsarzt*, *18*, 259–269.

1989, *The British Journal of Radiology*, *62*, 41–47

Cell kinetic changes in the follicular epithelium of pig skin after irradiation with single and fractionated doses of X rays

By G. M. Morris and J. W. Hopewell

CRC Normal Tissue Radiobiology Research Group, Research Institute (University of Oxford), Churchill Hospital, Oxford

(*Received January 1988 and in revised form July 1988*)

Abstract. Changes in the cell kinetics of the follicular epithelium of the pig have been studied after irradiation with single and fractionated doses (30 fractions/39 days) of X rays and the results compared with previously published data for the epidermis. In the follicular epithelium there was an initial degenerative phase, during which the rate of cell depletion was independent of the radiation dose and the mode of administration. Evidence for repopulation was seen between the 14th and 18th days after single doses (15 or 20 Gy) and by the 28th day after the start of irradiation with fractionated doses (52.3–80.0 Gy). However, the degree of cell depletion and the subsequent rate of repopulation were independent of dose. The regenerative phase was characterized by an increased cell proliferation as indicated by an elevation of the labelling index. Islands of cells (colonies), with an appearance similar to cells in the normal follicular epithelium, were seen 18 days after a single dose of 20 Gy and 42 days after the start of fractionated irradiation. When compared with the epidermis, the follicular epithelium exhibited considerably less evidence of damage after both single and fractionated doses of X rays. There was a lower incidence of degenerate cells and reduced levels of cell depletion in the follicular epithelium, suggesting that cells from this region play an important role in the repopulation of the epidermis after high-dose irradiation.

In recent years the pig has been used with increasing frequency in biomedical research. Particular attention has been given to studies involving the skin because of its morphological and histological similarity to human skin (Winter, 1972; Donovan, 1975). There have been many reports on the effects of radiation on mammalian skin. However, the majority of such reports have dealt with the gross visual changes in the appearance of the skin after irradiation. Many of the more recent experimental investigations, involving the study of gross skin reactions, have been carried out on rodents and have compared the effects of single and fractionated doses of radiation (Field et al, 1975; Douglas & Fowler, 1976; van Rongen & Kal, 1984). Similar studies have also been undertaken on pig skin (Hopewell et al, 1978; van den Aardweg et al, 1988) and on human skin (Dutreix et al, 1973; Turesson & Notter, 1984).

Direct observations of radiation-induced changes in the epidermis have been less extensively studied and there have been comparatively few cell kinetic investigations. Again most of this work has been undertaken on rodent skin (Hegazy & Fowler, 1973; Denekamp et al, 1976; Etoh et al, 1977; Hansen et al, 1984) with only three detailed reports on pig skin (Archambeau et al, 1979; Morris & Hopewell, 1986, 1988).

The follicular epithelium constitutes a significant proportion of the total epithelial area of the skin in many mammalian species. For pig skin, Osanov et al (1976) calculated that more than half of the skin's epithelial basal cells were situated in hair follicles. Follicular epithelium has been demonstrated to play an important role in the regeneration of the epidermis after the mechanical wounding of pig skin (Winter, 1972) and after high doses of X rays in the mouse (Al-Barwari & Potten, 1976).

To our knowledge, the present report is the first to document the effects of single and fractionated doses of X rays on the cell proliferation kinetics of the follicular epithelium of the pig. Fractionated irradiation was given in the form of a conventional radiotherapy schedule (30 fractions in 39 days).

Materials and methods

Twenty female Large White pigs, 3–4 months of age (25 kg), were used in this study. All procedures were carried out with the animals under anaesthesia using a mixture of nitrous oxide, halothane and oxygen (Berry et al, 1974).

Three to four days prior to irradiation, eight 4 cm × 4 cm fields, spaced 4 cm apart, were tattooed with India ink on the left flank of each animal. In a group of 12 pigs the fields were irradiated with single doses of 15 or 20 Gy of 250 kV X rays (HVL 1.4 mm Cu; FSD 50 cm) at a dose rate of 0.69 Gy/min. Small crescent shaped skin biopsies (1–1.5 cm long, up to 0.5 cm wide) were taken at intervals of 1, 4, 7, 11, 14, 18, 22, 25, 35, 42, 49 and 56 days after irradiation. In a further group of eight pigs, skin fields were irradiated daily, five times per week, over a 6-week period (*i.e.* 30 fractions/39 days). Total doses of 52.3, 61.5, 70.7 and 80.0 Gy were used. Skin biopsies were taken at 14, 28 and 42 days after the start of irradiation (*i.e.* after 10, 20 or 30 fractions) and at 14 days after the final fraction.

The labelling of cells synthesizing DNA was carried out prior to biopsy using procedures described in detail previously (Morris & Hopewell, 1985). Briefly, local *in vivo* labelling was achieved by the intradermal injection of 0.1 ml of tritium (^{3}H) labelled thymidine (TdR). The radiolabel was diluted in normal saline containing disulphine blue (0.1 ml per 5 ml saline) to mark the position of each injection site. Flash labelling was with a single injection of 10μCi of ^{3}H-TdR (specific activity 45 Ci/mmol); biopsies were taken 60 min after injection.

Biopsies were fixed in Bouin's fluid, dehydrated through graded alcohols, cleared and embedded in paraplast. Histological sections, 5 μm thick, were cut perpendicular to the skin surface such that the hair follicles were viewed in transverse section. Observations on the follicular epithelium were restricted to the external root sheath. The hair matrix and surrounding epithelium were not examined.

Autoradiographs were prepared using standard techniques (Morris & Hopewell, 1985), after which they were examined to determine the labelling index (LI) in the basal layer (L_1) and first suprabasal layer (L_2) of the follicular epithelium. A minimum of 100 labelled cells were scored in cell layer L_1 and 50 cells in cell layer L_2, per biopsy. The cell density in these two cell layers was determined by counting cells along a minimum of 5 mm of basement membrane. Results were expressed as the count per millimetre length of basement membrane. The degenerate cells, *i.e.* those cells exhibiting pycnosis and shrinkage necrosis, were excluded from these calculations. The results obtained for the follicular epithelium were compared with those for the epidermis, published previously (Morris & Hopewell, 1986, 1988).

Results

Single dose studies

Cell density. There was a progressive decline in the cell density (CD) in the basal layer (L_1) and first suprabasal layer (L_2) of the follicular epithelium in the first 14 days after irradiation. Thereafter values remained constant until Day 25 (Fig. 1). The rate of cell loss from both cell layers appeared to be linearly related to the time after irradiation (Fig. 2). The maximum reduction in cell number was not related to the dose, being similar in both dose groups from 14 to 25 days after irradiation (Fig. 1). The presence of colonies of cells coincided with the period of maximal cell depletion (Fig. 1). Cells in the colonies had an appearance similar to those in

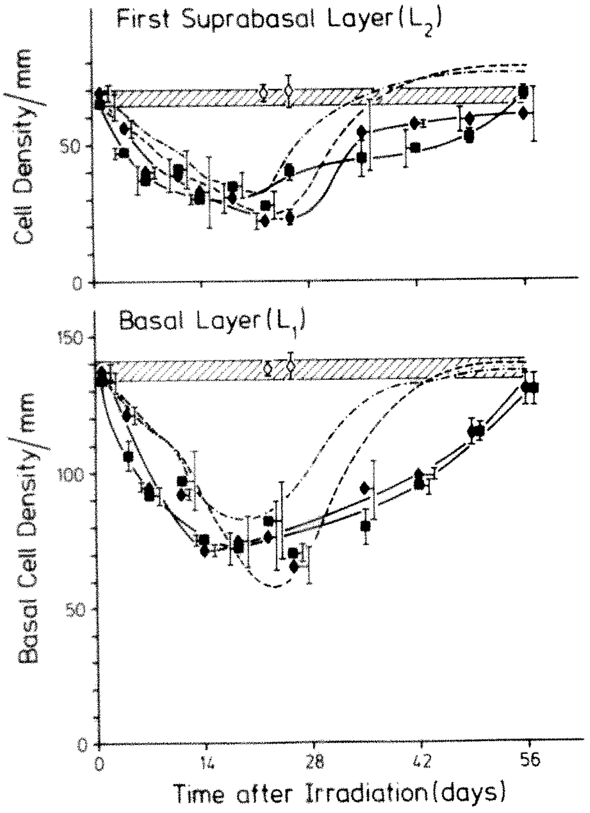

Figure 1. Time-related changes in the cell density in the basal cell layer (L_1) and first suprabasal cell layer (L_2) of the follicular epithelium of pigs after single doses of X rays. ■, 15 Gy; ◆, 20 Gy; ◇, 20 Gy (cell colonies). Shaded area indicates unirradiated control values ±SE. Error bars indicate ±SE. Changes in the epidermis after single doses of 15 Gy (–·–·–) and 20 Gy (– – –) are given for comparison (from Morris & Hopewell, 1988).

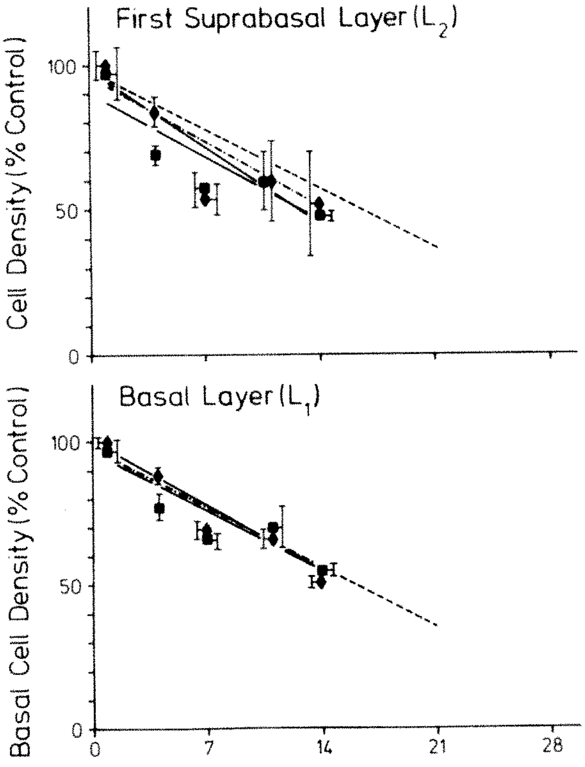

Figure 2. Time-related changes in the relative cell density over the period of cell loss (degenerative phase) in cell layers L_1 and L_2 of the follicular epithelium of pigs after single doses of X rays. (For key to symbols see Fig. 1.)

unirradiated follicular epithelium. Colonies were only seen after the higher of the two single doses (20 Gy) and the CD in the colonies was similar to that in unirradiated skin. The follicular epithelium had apparently recovered by 56 days after irradiation.

Degenerate cells. Degenerate cells, *i.e.* those cells exhibiting pycnosis or necrosis, were present in the follicular epithelium both before and after irradiation. Although mean values for the percentage of degenerate cells were highest over the period of maximum epithelial damage, the variability was great and as a consequence these values were not significantly different ($p > 0.05$) from those in the unirradiated follicular epithelium.

Number of viable cell layers. The number of cell layers in the viable follicular epithelium, excluding the stratum corneum, was 6.0 ± 0.5 in unirradiated skin. After 15 Gy, the mean counts of the number of cell layers were not statistically different ($p > 0.05$) from those in the unirradiated follicular epithelium until 25 days after irradiation (Fig. 3). After 20 Gy there was a clearly defined decline in the number of cell layers from 14 days after irradiation with a nadir at 22 days. At 35 days after irradiation slight hyperplasia of the follicular epithelium was seen. In the cell colonies, seen after a dose of 20 Gy, there were usually only 1 or 2 cell layers present at 22 days. However, by Day 25 the number of cell layers in the colonies had increased to 3.6 ± 0.5.

Labelling index. There was an initial reduction in the LI after irradiation. The reduction was maximal between 4 and 7 days after irradiation when very few, if any, cells were labelled (Fig. 4). There was a sharp increase in the LI in the basal layer (L_1) after 11 days in the 20 Gy dose group. A peak value was reached at 14 days, whereafter values fell, approaching values in unirradiated controls, by 35 days (Fig. 4). In the 15 Gy dose group, the increase in the LI in L_1 was less dramatic by 14 days after irradiation and a peak LI value (13.2 ± 0.3%) was not reached until Day 22. This was considerably lower than the peak in the LI (20.0 ± 0.6%) in the higher dose group. Thereafter LI values declined progressively, reaching values similar to those of unirradiated controls at 42–49 days after irradiation (Fig. 4). In the first suprabasal cell layer (L_2) the initial depression in the LI was followed by recovery to values similar to unirradiated follicular epithelium by 14 days. There was no significant overshoot in the LI after this time (Fig. 4). The LI values in the cell colonies were very high with up to 36% of basal cells labelled (Fig. 4).

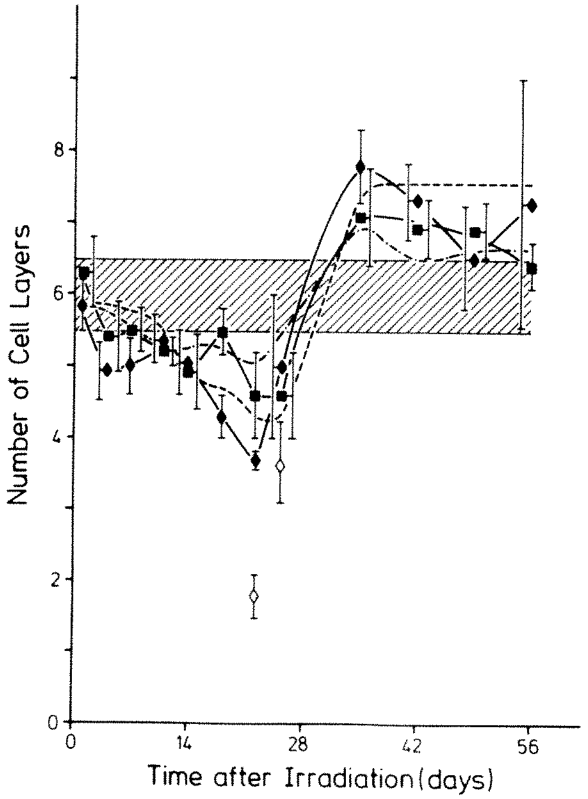

Figure 3. Time-related changes in the number of cell layers in the follicular epithelium of pigs after single doses of X rays. (For key to symbols see Fig. 1.)

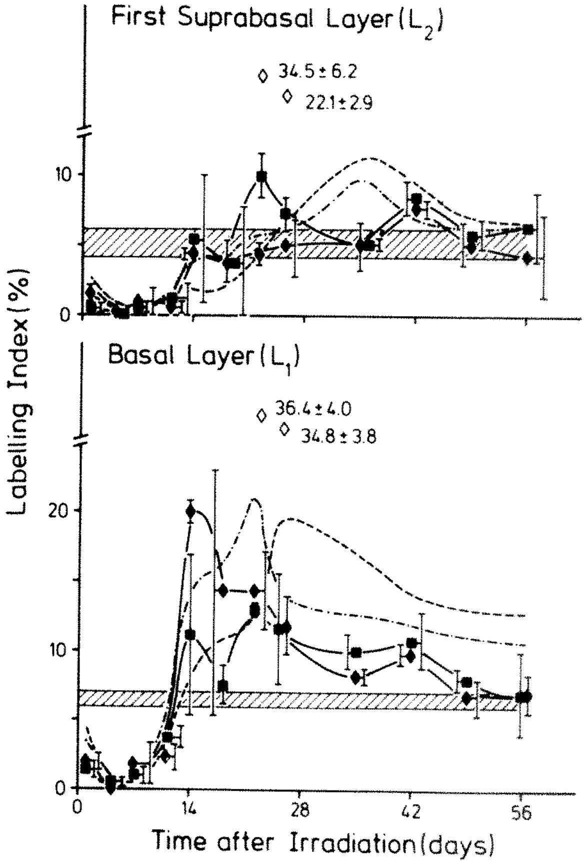

Figure 4. Time-related changes in the labelling index in cell layers L_1 and L_2 of the follicular epithelium of pigs after single doses of X rays. (For key to symbols see Fig. 1.)

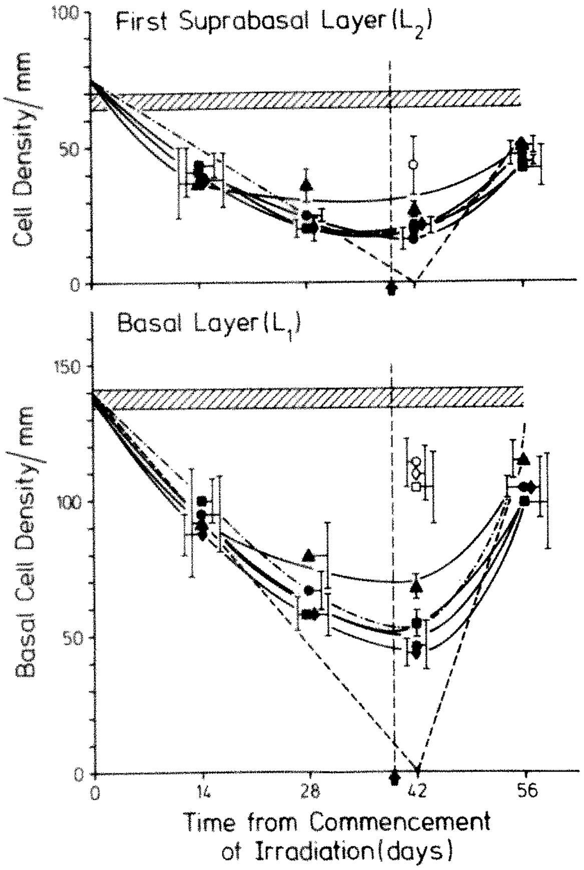

Figure 5. Changes in the cell density in cell layers L_1 and L_2 of the follicular epithelium of pigs with time from the start of fractionated irradiation. ▲, 52.3 Gy; ●, 61.5 Gy; ■, 70.7 Gy; ◆, 80.0 Gy; open symbols indicate corresponding values for cell colonies. Shaded areas indicate unirradiated control values. Error bars indicate ±SE. Changes in the epidermis after 52.3 and 61.5 Gy (-·-·-) and 70.7 and 80.0 Gy (- - -) are given for comparison (from Morris & Hopewell, 1986). ↑ indicates end of irradiation.

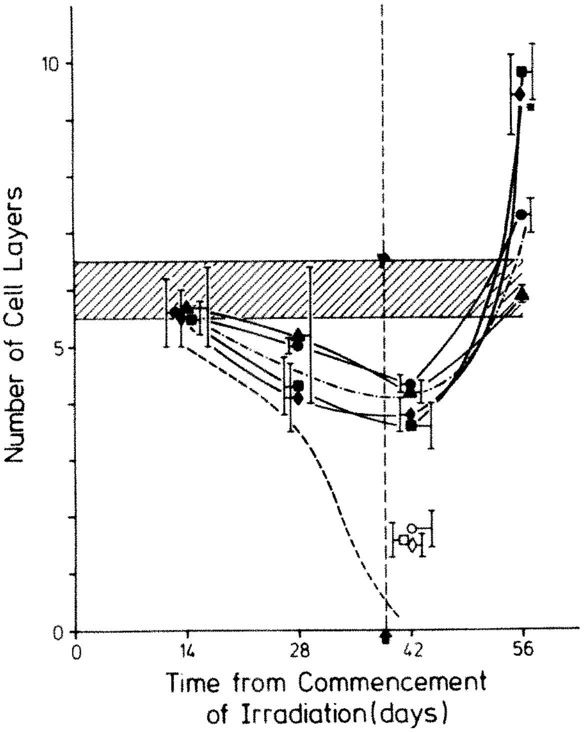

Figure 6. Variation in the number of viable cell layers in the follicular epithelium of pigs with time from the start of fractionated irradiation. (For key to symbols see Fig. 5.)

Fractionated dose studies

Cell density. The CD of the follicular epithelium declined over the course of the fractionated irradiation schedule (Fig. 5). After 28 days (20 fractions) there was a 50% reduction in cellularity. However, between 28 and 42 days (30 fractions) there was no further appreciable cell loss, even after the highest of the fractionated doses (80.0 Gy). Almost complete recovery of the follicular epithelium had occurred by 14 days after the final fraction, when values for the CD approached those of the unirradiated follicular epithelium (Fig. 5). Cell colonies were seen by the end of irradiation in all but the lowest dose group (52.3 Gy). The basal cell density in the colonies was not significantly different from that in the unirradiated follicular epithelium ($p > 0.05$).

Degenerate cells. Degenerate cells were present in the follicular epithelium before, during and after fractionated irradiation. The incidence of degenerate cells was very low and at no time exceeded 1.4%.

Number of viable cell layers. After 10 fractions the number of cell layers in the follicular epithelium was similar to that in unirradiated follicular epithelium. However, after 20 fractions (28 days) the number of cell layers had decreased in all but the lowest dose group (Fig. 6), and at the end of irradiation the number of cell layers was reduced further to approximately 4.2 layers in the two lowest dose groups and to approximately 3.7 layers in the highest two dose groups. The follicular epithelium had fully recovered by 14 days after the final fraction in the 52.3 Gy dose group, with evidence for hyperplasia after higher doses (Fig. 6). With the exception of the 52.3 Gy group, cell colonies were observed in all other dose groups. The number of cell layers in these colonies was similar at each dose level (1.5–1.8).

Labelling index. With the exception of the 52.3 Gy dose group, LI values in the basal cell layer (L_1) were approximately half those in the unirradiated follicular epithelium after 10 fractions (14 days). After 28 days (20 fractions) the mean values for the LI in the lowest dose group were still similar to those of the unirradiated follicular epithelium, although after higher doses the mean LI values had increased above those of the unirradiated follicular epithelium. However, due to the large associated errors the differences were not

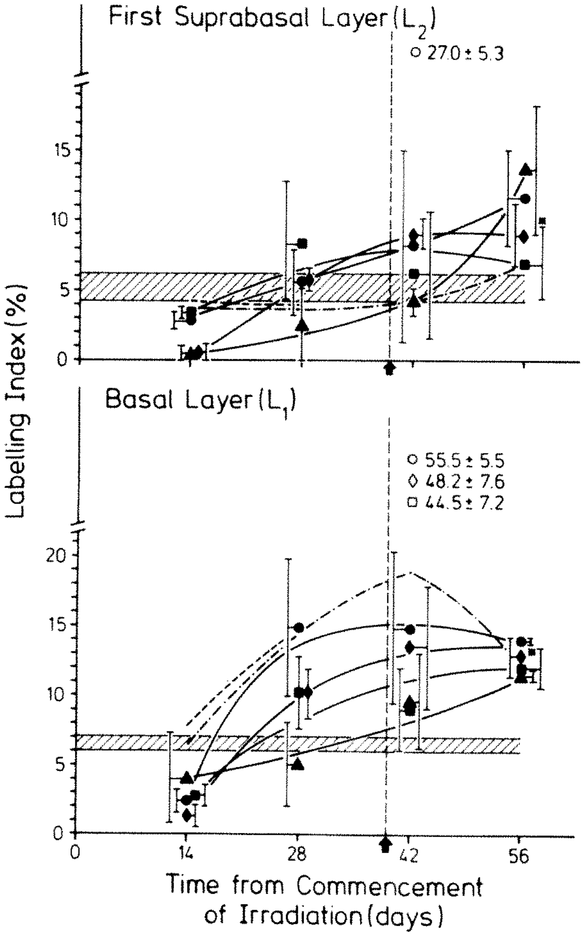

Figure 7. Changes in the labelling index (%) in cell layers L_1 and L_2 of the follicular epithelium of pigs with time from the start of fractionated irradiation. (For key to symbols see Fig. 5.)

statistically significant ($p > 0.1$). There was no further change in the LI by the end of irradiation (Fig. 7). At 14 days after the final fraction the mean LI values were similar to those found immediately after 30 fractions; however, there was considerably less variability and these values were significantly higher ($p < 0.02$) than those in the unirradiation follicular epithelium (Fig. 7). The trend in the changes in the LI values in cell layer L_2 was similar to that in layer L_1. However, at 14 days after the end of irradiation, although mean values were higher than in the unirradiated epithelium, they were not significantly different ($p > 0.1$). The LI values in the cell colonies were very high, with up to 50% of cells labelled in cell layer L_1.

Discussion

The histological sections of pig skin used in the present investigation have previously been used to assess the effects of single and fractionated doses of X rays on the epidermis (Morris & Hopewell, 1986, 1988). An indication of the general trend of these results has been included in the figures to enable a direct comparison to be made of the cell kinetic responses of the follicular epithelium and the epidermis to X rays.

In the initial degenerative phase after irradiation with single doses, or during irradiation with fractionated doses, the rate of cell loss from the follicular epithelium was independent of the X-ray dose. The rate of cell loss was similar after both single and fractionated doses, *i.e.* approximately 3% per day. A similar value was obtained for the epidermis (Morris, 1987). Assuming a turnover time for the whole epidermis (including the stratum corneum) of 30 days in the pig (Weinstein, 1965), the normal rate of cell loss in the absence of cell division would be approximately 3.3% per day. This is close to the value calculated after irradiation. A slightly higher estimate of 4% per day was obtained for the epidermis of the Yorkshire pig after single doses of X rays (Archambeau et al, 1979). In the epidermis of rodents, the rate of cell loss after irradiation was also found to be similar to that for the normal rate of cell migration/desquamation. For example, the rate of cell loss from the basal layer of guinea pig flank skin was 5.6% per day (Etoh et al, 1977) and in mouse dorsal skin it was 8.3% per day (Potten et al, 1983). Both sets of calculations were made after single doses of radiation.

Despite the similarity in the rates of cell loss from the follicular epithelium and epidermis of the pig there was a distinct difference both in the severity of the radiation damage and the rate at which recovery occurred. In marked contrast to the epidermis the follicular epithelium showed no clear dependence on dose in the degree of cell depletion after either single or fractionated doses of X rays. The follicular epithelium remained intact after fractionated doses of 70.7 and 80.0 Gy whereas the epidermis was completely denuded after these doses. This suggests that the follicular epithelium is more radioresistant than the epidermis. A similar conclusion was reached by Hendry et al (1980). They reported a D_0 value of 6.0 Gy for hair follicles in the dorsal skin of mice, compared with a value of 1.3 Gy for the epidermis of the dorsum for the same species (Emery et al, 1970). Hypoxia was suggested as being a factor contributing to the greater radioresistance of the hair follicles (Hendry et al, 1980). The presence of a number of species of anaerobic micro-organisms at the base of the hair follicle of the pig also points to the occurrence of hypoxia in this region (Sieber & Wells, 1986).

The initial stages of recovery of the follicular epithelium were marked by the continued proliferation of cells, many of which exhibited varying degrees of radiation damage. However, cells showing pycnosis and shrinkage necrosis did not appear to undergo mitosis and were termed degenerate cells. Although the number of degenerate cells did increase with time after single doses of X rays and over the course of fractionated irradiation, in pig epidermis no clear dependence on dose was seen. In the follicular epithelium this trend was not observed and the proportion of degenerate cells remained very low, both after single and during fractionated doses of X rays. This provides further evidence in support of the view that the follicular epithelium is more radioresistant than the epidermis. There have been few studies on the incidence of degenerate cells after irradiation and these have been confined to murine epidermis (Hegazy & Fowler, 1973; Al-Barwari as quoted by Potten et al, 1983; Morris & Hopewell, 1986, 1988). The results of these studies indicated that the incidence of degenerate cells was not dependent on dose, for doses in the range 5–35 Gy. As in the present study, the number of degenerate cells in irradiated murine epidermis never exceeded 10%.

Although the mitotic index was not assessed in the present or in previous studies on pig epidermis (Morris & Hopewell, 1986, 1988), an absence of labelled cells for the first 4 to 7 days after single doses of radiation suggests a period of mitotic delay of at least 3 days. A likely consequence of this is that a proportion of the initial increase in the LI in the pig follicular epithelium and in the epidermis was due to cell synchrony induced by this mitotic block. The difference in the timing of the peaks in the LI after single doses of 15 and 20 Gy was probably due, in part, to a longer mitotic delay after the higher of the two doses. It has been demonstrated that the duratioin of mitotic delay is proportional to the radiation dose and the cell cycle time (Denekamp, 1982). After fractionated doses it was not possible to establish with the same degree of clarity whether there was a pronounced mitotic delay at the start of the irradiations since the first samples were not taken until Day 14 (10 fractions). However, LI values for the irradiated follicular epithelium were below those of unirradiated skin at this time, suggesting that there was indeed an initial period of mitotic delay.

Evidence for the initiation of repopulation in the follicular epithelium, as indicated by an elevated labelling index and the appearance of cell colonies, was found at 14–18 days after single doses of X rays. An identical timing for the onset of repopulation was also found in the epidermis (Morris & Hopewell, 1988). Using split-dose experiments in the same strain of pig, van den Aardweg et al (1988) reported a similar time for the onset of repopulation, while in the Yorkshire pig epidermal repopulation started between 14 and 17 days after comparable single doses of X rays (Archambeau et al, 1979).

Repopulation is initiated at an earlier time after single doses of radiation in the mouse epidermis. This was estimated to be about 7 days in unplucked skin and after 2 days in plucked skin (Emery et al, 1970; Fowler & Denekamp, 1976).

Repopulation of the pig follicular epithelium was delayed until 28 days during fractionated irradiation. This is a timing identical to that reported for pig epidermis (Morris & Hopewell, 1986) and for human epidermis (Turesson & Notter, 1984) during an identical dose fractionation schedule.

Evidence for cell colony formation was seen at 14 days after single doses and at 28 days after the start of fractionated irradiation, when small clusters of 2–10 normal-looking cells were observed in the basal layer. By 25 days after single doses of radiation and after the last dose in the fractionated irradiation scheme the colonies were well developed. Colonies were seen less frequently in the follicular epithelium than in the epidermis (Morris & Hopewell, 1986, 1988). They were also detected after a lower dose in the epidermis, again suggesting a greater radiosensitivity for this region.

In areas of the epidermis of pigs that had degenerated by the end of the course of fractionated irradiation, there was evidence for the migration of viable cells from follicular colonies onto the basement membrane of the epidermis (Morris, 1987). A number of cell kinetic studies have been carried out on regenerative cell colonies in mouse skin (Potten & Al-Barwari, 1985). It was concluded from these studies that there was a steady flow of cells from the deeper regions of the follicular epithelium into the epidermis; from as early as the 3rd day after 12 Gy approximately half of the cell colonies surrounded or were immediately adjacent to the necks of hair follicles. These observations clearly implicated the follicular epithelium as a major source of cells in the repopulation of the epidermis after irradiation (Al-Barwari & Potten, 1976).

In the pig, regeneration of the follicular epithelium occurred after the maximum level of cell depletion had been reached at 14–25 days after single doses. Although cell colonies with very high labelling indices were obvious "foci of regeneration", many radiation-damaged cells also continued to proliferate. This was suggested by the fact that many of these cells were labelled and also by the presence of multinucleate cells and of bizarre mitotic figures. Other workers have made similar observations (Potten, 1978; Archambeau et al, 1979). It remains uncertain what proportion of these proliferating, radiation-damaged cells retain long-term viability. If it is assumed that the hierarchical concept of cell proliferative organization applies to stratified epithelia (Michalowski, 1981) then the majority of these damaged proliferative cells would be transit cells, destined to be removed from the follicular epithelium by the processes of cell differentiation and desquamation

In conclusion, the major difference between the response of the follicular epithelium to single and fractionated doses of radiation was the timing of repopulation. This occurred earlier after single doses.

The rates at which cells were lost from the follicular epithelium and the epidermis were similar. In both cases the cell loss rate was not influenced by the dose or mode of irradiation. This finding is inconsistent with the occurrence of a homogeneous proliferative compartment containing cells of similar radiosensitivity, in either of these two regions of the skin.

There was considerably less evidence of radiation damage to the follicular epithelium than to the epidermis. In contrast to the epidermis there was no clear dose dependence in the degree of cell depletion of the follicular epithelium after single doses or during fractionated irradiation. The number of degenerate cells was low and the follicular epithelium remained intact even after high fractionated doses. These findings, when taken together with the observed migration of follicular cell colonies onto the denuded epidermal/dermal interface (Al-Barwari & Potten, 1976; Morris, 1987), indicate that the follicular epithelium plays an important role in the repopulation of the epidermis after high doses of radiation.

Acknowledgments

The authors would like to thank Miss S. Messenger, Mr F. Dickinson and Mr N. Hubbard for excellent technical assistance and for the day-to-day care of the animals. The Research Group at the Churchill Hospital is supported by the Cancer Research Campaign. This study was in part supported by grants from the Commission of the European Communities (EURATOM) and the Central Electricity Generating Board (CEGB).

References

VAN DEN AARDWEG, G. J. M. J., HOPEWELL, J. W. & SIMMONDS, R. H., 1988. Repair and recovery in the epithelial and vascular connective tissues of pig skin after irradiation. *Radiotherapy and Oncology, 11*, 73–82.

AL-BARWARI, S. E. & POTTEN, C. S., 1976. Regeneration and dose-response characteristics of irradiated mouse dorsal epidermal cells. *International Journal of Radiation Biology, 30*, 201–216.

ARCHAMBEAU, J. O., BENNETT, G. W., ABATA, J. J. & BRENNEIS, H. J., 1979. Response of swine skin to acute single exposure of X-rays: quantification of the epidermal cell changes. *Radiation Research, 79*, 298–337.

BERRY, R. J., WIERNIK, G. W. & PATTERSON, J. J. S., 1974. Skin tolerance to fractionated X-irradiation in the pig—how good a predicter is the NSD-formula? *British Journal of Radiology, 47*, 185–190.

DENEKAMP, J., 1982. *Cell Kinetics and Cancer Therapy* (Charles C. Thomas, Illinois).

DENEKAMP, J., STEWART, F. A. & DOUGLAS, B. G., 1976. Changes in the proliferation rate of mouse epidermis after irradiation: continuous labelling studies. *Cell and Tissue Kinetics, 9*, 19–29.

DONOVAN, W. E., 1975. Experimental models in skin flap research. In *Skin Flaps*, ed. by W. C. Grabb & M. B. Myers (Little, Brown and Co., Boston), pp. 11–20.

DOUGLAS, B. G. & FOWLER, J. F., 1976. The effect of multiple small doses of X rays on skin reactions in the mouse and a basic interpretation. *Radiation Research, 66*, 401–426.

DUTREIX, J. WAMBERSIE, A. & BOUNIK, C., 1973. Cellular recovery in human skin reactions: application to dose fraction number, overall time relationship in radiotherapy. *European Journal of Cancer, 9*, 159–167.

EMERY, E. W., DENEKAMP, J. & BALL, M. M., 1970. Survival of mouse skin epithelial cells following single and double doses of X rays. *Radiation Research, 41*, 450–466.

ETOH, H., TAGUCHI, Y. H. & TABACHNICK, J., 1977. Cytokinetics of regeneration in β-irradiated guinea pig epidermis. *Radiation Research, 71*, 109–118.

FIELD, S. B., MORRIS, C. & DENEKAMP, J., 1975. The response of mouse skin to fractionated X rays. *European Journal of Cancer, 11*, 291–299.

FOWLER, J. F. & DENEKAMP, J., 1976. Regulation of epidermal stem cells. In *Stem Cells of Renewing Cell Populations*, ed. by A. B. Cairnie, P. K. Lala & D. G. Osmond (Academic Press, New York), pp. 111–134.

HANSEN, L. S., COGGLE, J. E., WELLS, J. & CHARLES, M. W., 1984. Changes in the DNA labelling index after β-irradiation of mouse epidermis. *Cell and Tissue Kinetics, 17*, 475–481.

HEGAZY, M. A. & FOWLER, J. F., 1973. Cell population kinetics and desquamation skin reactions in plucked and unplucked mouse skin. II, Irradiated skin. *Cell and Tissue Kinetics, 6*, 587–602.

HENDRY, J. H., EDMUNDSON, J. M. & POTTEN, C. S., 1980. The radiosensitivity of hair follicles in the mouse dorsum and tail. *Radiation Research, 84*, 87–96.

HOPEWELL, J. W., FOSTER, J. L., GUNN, Y., MOUSTAFA, J. F., PATTERSON, T. J. S., WIERNIK, G. & YOUNG, C. M. A., 1978. Role of vascular damage in the development of late radiation effects in the skin. In *Late Biological Effects of Ionizing Radiation* (International Atomic Energy Agency, Vienna), Vol. 1, pp. 483–492.

MORRIS, G. M., 1987. *Epidermal Cell Kinetics in Normal and X-irradiated Pig Epidermis*. PhD Thesis (University of London).

MORRIS, G. M. & HOPEWELL, J. W., 1985. Pig epidermis: A cell kinetic study. *Cell and Tissue Kinetics, 18*, 407–415.

MORRIS, G. M. & HOPEWELL, J. W., 1986. Changes in the cell kinetics of pig epidermis after repeated daily doses of X rays. In *Radiation Damage to Skin, British Journal of Radiology*, Suppl. 19, (BIR, London), pp. 34–38.

MORRIS, G. M. & HOPEWELL, J. W., 1988. Changes in the cell kinetics of pig epidermis after single doses of X rays. *British Journal of Radiology, 61*, 205–211.

MICHALOWSKI, A., 1981. Effects of radiation on normal tissues: Hypothetical mechanisms and limitations of *in situ* assays of clonogenicity. *Radiation and Environmental Biophysics, 19*, 157–172.

OSANOV, D. P., RAKOVA, V. A., KLYKOV, O. V. & FILATOV, V. V., 1976. Effect of depth distribution of basal cells on their survival after irradiation of skin with beta particles of different doses (various energies). *Radiobiologica, 16*, 59–63.

POTTEN, C. S., 1978. The cellular and tissue response of skin to single doses of ionising radiation. In *Current Topics in Radiation Research*, ed. by M. Ebert & A. Howard (North Holland, Amsterdam), pp. 153–185.

POTTEN, C. S. & AL-BARWARI, S. E., 1985. Micro-colonies in mouse epidermis. In *Cell Clones: Manual of Mammalian Cell Techniques*, ed. by C. S. Potten & J. H. Hendry (Churchill Livingstone, Edinburgh), pp. 81–86.

POTTEN, C. S., HENDRY, J. & AL-BARWARI, S. E., 1983. A cellular analysis of radiation injury in epidermis. In *Cytotoxic Insult to Tissues*, ed. by C. S. Potten & J. H. Hendry (Churchill Livingstone, London), pp. 153–185.

VAN RONGEN, E. & KAL, H. B., 1984. Acute reactions in rat feet exposed to multiple fractions of X-rays per day. *Radiotherapy and Oncology, 2*, 141–150.

SIEBER, V. K. & WELLS, J., 1986. The use of plucked hairs as a biological dosimeter. In *Radiation Damage to Skin, British Journal of Radiology*, Suppl. 19 (BIR, London), pp. 92–95.

TURESSON, I. & NOTTER, G., 1984. The influence of the overall treatment time in radiotherapy on the acute reaction: comparison of the effects of daily and twice-a-week fractionation on human skin. *International Journal of Radiation Oncology, Biology, Physics, 10*, 607–618.

WEINSTEIN, G. D., 1965. Autoradiographic studies or turnover time and protein synthesis in pig epidermis. *Journal of Investigative Dermatology, 44*, 413–419.

WINTER, G. D., 1972. Epidermal regeneration studied in the domestic pig. In *Epidermal Wound Healing*, ed. by H. Maibach & D. Rove, (Year Book Medical Publishers, Chicago), pp. 71–112.

1989, *The British Journal of Radiology*, 62, 48–52

Precision of determining compliance with prescribed fields from conventional portal films

By P. B. Dunscombe, PhD, FCCPM and *K. Fox, RT(T)

Departments of Medical Physics and *Radiotherapy Technology, Manitoba Cancer Treatment and Research Foundation, Winnipeg, Manitoba, Canada R3E 0V9

(*Received March 1988 and in revised form June 1988*)

Abstract. Three hundred and seventy measurements of field placement errors (FPEs) have been made by a total of 16 observers on 20 prescription-treatment film pairs taken during routine radiotherapy for cancer of the prostate. Analysis of the distributions of the measured FPEs has yielded the precision of the measurement under a variety of conditions. We report here the influence on the precision of determining FPEs of the following factors: the clinical duties of the observers, the quality of the treatment film, the relative magnification of prescription and treatment films, and whether double-exposure techniques were employed.

It is one of the tenets of radiotherapy that accurate field placement is essential if maximum tumour response is to be achieved with minimum morbidity. In one of the earliest studies of field placement errors (FPE), Marks et al (1974) reported an error rate of 36% in extended mantle fields. They were unable to demonstrate a convincing relationship between FPE and local recurrence, although this was later confirmed during a Patterns of Care Study (Kinzie et al, 1983). The data produced in this latter survey showed an increase in infield or marginal recurrence from 7% for adequate portals to 33% for portals judged to be inadequate. Both of these studies employed a subjective clinical assessment of portal adequacy. Quantitative comparison with the prescribed fields, which could themselves have been inadequate, was not performed.

Byhardt et al (1978) reported a comprehensive and quantitative comparison between the prescribed field as indicated on a simulator film and treatment field deduced from the portal films taken during either the whole or the initial portion of a treatment. Field placement errors in excess of 5 mm occurred at a rate of 15% overall, with a maximum rate of 27% observed in the pelvic region.

More recently, Rabinowitz et al (1985) have studied both the accuracy with which the prescribed field can be reproduced on the treatment machine and the day-to-day variation in portal position with respect to patient anatomy. Day-to-day reproducibility was surprisingly good with a measured standard deviation of 3 mm.

Whilst data on the accuracy of current clinical practice are being amassed, the consequences of FPEs as a function of the magnitude of the error remain unclear. An interesting theoretical analysis has been offered by Goitein and Busse (1975) for two representative sites. These authors have calculated the changes in tumour control probabilities consequent upon field malposition and demonstrated dependence particularly on the slope of the dose–response curves. Clinical confirmation of such predictions is, of course, some way off.

The literature cited above reflects the sporadic interest shown in field placement until fairly recently. However, the last few years have seen both an increased awareness of the significance of accurate field placement and, particularly with the widespread availability of digital techniques in the clinic, a more strenuous effort to develop and implement portal verification programmes on a routine basis.

The overall objective of a portal verification programme may be summarized by the question "Is the treated portal identical to the prescribed portal?" If the answer when a portal film is taken is "yes", the procedure will be repeated after some predetermined interval without changes in machine or patient set-up. A negative answer at any time during a course of treatment will provoke set-up changes and further confirmation will be sought that the agreement between prescribed and treated fields is acceptable. It is implicit in the question posed that some level of acceptability has been established for the treatment under consideration, and further that this level of acceptability, expressed in terms of the magnitude of the allowable FPE, exceeds the error in its determination.

Whether therapy field placement is to be assessed by conventional film techniques or by the newer real-time approaches (Lam et al, 1987), it is pertinent to investigate the precision with which FPEs can be quantified and the factors influencing this precision. With such information it is possible both to optimize the procedures in a portal verification programme and to establish the upper limit of precision that is clinically achievable.

In this paper we describe a study of the precision with which treatment (portal) and prescription (simulation) films may be quantitatively compared under conditions obtaining in a busy clinic. The site chosen for the study was the pelvis, which has been shown to have a high frequency of FPEs (Byhardt et al, 1978). In addition, such treatments form a large proportion of our clinical load and there is a high degree of uniformity in treatment technique. Both of these factors simplified the logistics of this study. We have been particularly interested in the influence on the precision of determining FPEs of the following factors: the clinical duties of the observers, the quality of the treatment film, the relative magnification of prescription and treatment films, and whether double-exposure techniques were employed.

Materials and methods

The images used in this study were obtained as part of the routine treatment of 20 males receiving radiotherapy for cancer of the prostate. These patients ranged in anterior–posterior (A–P) separation from 17 to 25 cm and each was treated with four square fields of side 12 cm (box technique). Although the clinical success of such a treatment clearly depends on the accurate positioning of all four fields, the purposes of this study were adequately served by including only the A–P fields. Simulation of the patient was performed on an AECL Therasim 750 simulator, with subsequent isocentric treatment on a CGR Sagittaire 25 MV linear accelerator. Both machines are subject to regular quality assurance according to commonly accepted procedures (American Association of Physicists in Medicine (AAPM), 1983).

The film used on the simulator and therapy machine was Kodak T-mat G. For the simulator, the film was exposed within a Kodak X-omatic cassette with lanex regular screens. On the treatment machine, a Dupont Cronex Radiation Therapy cassette with lead screens was employed. This latter film–screen combination resulted in an optical density of ~1 following the delivery of 5 cGy to the patient and hence the film would be known variously as a beam film (Byhardt et al, 1978) or a localization film. Prescription films were taken within a few days before the start of treatment. Treatment films were taken at some arbitary time during the first 2 weeks of treatment.

As the primary objective of this study was to establish, under routine clinical conditions, the precision with which prescription and treatment films can be compared, it was necessary to repeat measurements many times on one pair of films. Marking directly on the films was therefore not allowed, and instead the following procedure was adopted. A transparent plastic sheet was taped to the treatment film. With the aid of a standard light box, and in the absence of special viewing conditions, observers were asked to indicate, using fine-tipped markers, identifiable anatomical landmarks, together with the centre and four field edges, on the plastic sheet. For comparison with a prescription film of similar magnification, the observer then superimposed both the plastic sheet and the treatment film information over the prescription film and aligned the selected anatomical landmarks. The locations of the centres of the simulator delineator wires were traced on the plastic sheet to indicate the positions of the prescribed field edges.

In those studies in which the magnifications of the films being compared were different, both prescription and treatment film data were transferred to the plastic sheets, but in these cases superimposition was not possible. The greater element of subjectivity could be expected to be reflected in an inferior precision for this part of the study.

Each comparison yielded a plastic sheet with selected anatomical landmarks together with prescribed and treated field boundaries as identified by each observer. A total of 185 such comparisons was accumulated during this study.

No limit was imposed on the time allowed for each comparison. However, as time of observation has been shown to be an important factor in the interpretation of low-contrast portal films (Reinstein et al, 1987), this was recorded.

In the first part of the study the precision with which different groups, intimately connected with clinical radiotherapy, could compare prescribed and treated fields was investigated. A series of five simulator–portal film pairs was compared by a group of four radiotherapists, a group of five treatment planning and simulator technologists and a group of seven treatment unit technologists. Following this initial study, and for reasons of organizational simplicity, observers for the remaining investigations comprised the seven treatment unit technologists only.

In the studies involving the influence of film quality, a diagnostic quality "treatment" film was produced on the simulator. In this centre, patients receiving radiotherapy for cancer of the prostate routinely return to the simulator about half-way through their treatment course to have their marks checked. For the nine patients who provided diagnostic quality treatment films for this study the usual simulator procedure was preceded by an A–P exposure taken with the field borders defined by the X-ray collimators as opposed to the delineator wires. This high-quality film could then be compared with the original simulator or prescription film.

Studies of the influence of magnification were performed by selecting the position of the treatment film cassette to yield magnifications of about 1.43 or 1.25. Prescription films were always obtained with a magnification of 1.46 ± 0.03.

Double-exposure techniques involved opening the collimators of the treatment machine or simulator to a field size of 15 cm × 18 cm (width) for approximately 60% of the exposure, which had been found subjectively to yield the best image. (With this field size the femoral heads were visible and provided additional anatomical information.) The collimators were then closed down to the prescribed treatment field for the remaining 40% of the exposure.

Three independent steps can be identified in the measurement of an FPE from the film pairs collected. Step 1 is the delineation, on the pairs of images, of the prescribed and treated field boundaries; Step 2 is the comparison, by superimposition or otherwise, of the two images resulting in the identification of the relative positions of these boundaries; and Step 3 is the measurement of the difference in location of the boundaries, *i.e.* the quantification of the FPE, at pre-selected points on the field periphery. Owing to the independence of these processes, the errors associated with each can be added quadratically to yield the total precision of the measurement.

Steps 1 and 2 were carried out by the observers participating in the study as described earlier. The overall procedure was simplified, without loss of useful information, by having one individual (K.F.) perform all the measurements of Step 3. Thus the plastic sheets, with anatomical landmarks traced from treatment films together with both prescribed and treated field boundaries, were assembled and FPEs were measured in the middle of each of the four sides.

Step 1, as performed by each observer, consisted of independent pairs of assessments of the locations of the four field boundaries. The error components injected into the measurements of FPEs at different locations in the field from this procedure are expected to be uncorrelated. In contrast, errors associated with Step 2, which requires the comparison of the prescribed and treated fields, result in correlations between FPEs determined at opposite sides of the field. For example, a greater than average FPE on the superior border of a field will be accompanied by a greater than average FPE on the inferior border. It was important to avoid distortion of the statistical comparison of the results obtained under different conditions because of this effect. In the data reduction which follows, only the FPEs on the left lateral and inferior borders have been combined for analysis as these measurements are independent.

All the measurements of FPE made on the left lateral and inferior borders of each film pair were tabulated and the deviation of each measurement from the mean for that film pair was calculated. Between four and seven measurements were available to estimate the mean FPE at any location. Estimates of the precision of determining the FPE under a given set of conditions are based on observations on at least three film pairs. In general, each border on each film pair displayed a different FPE. It was assumed that the magnitude of the FPE did not influence the precision with which it could be measured and hence a standard deviation could be computed from the n deviations measured under a given set of conditions. Finally, the measured FPEs and associated precisions were demagnified to yield values in millimetres at the position of field definition, the isocentre.

Results

Table I summarizes the results of 370 measurements on 20 film pairs (Groups 1, 2 and 3 used the same five film pairs). The number of measurements per group is the product of 2 (for the two borders assessed), the number of observers and the number of film pairs per group. The observer group is indicated by T for treatment unit technologists, P for treatment planning and simulator technologists and R for radiotherapists. Two qualities of treatment film were assessed as described in the previous section: "T" indicates that the film was obtained at 25 MV and "D" indicates that an image obtained at diagnostic energies was compared with the prescription film. The magnification of the simulator film on which the treatment prescription was drawn was maintained at 1.46 ± 0.03, whilst the portal film was obtained with a magnification of either about 1.43 or about 1.25, as indicated in Table I. The column headed "Exposure" differentiates between single- and double-exposed treatment films.

The main results of the study are tabulated in the eighth column of Table I in which are shown the standard deviations of the FPEs as measured under the different sets of conditions employed during the study. Standard deviations are reported in mm at the location of field size definition. The final column shows the average time required to complete Steps 1 and 2 in the comparison of prescribed and treated fields, and to produce the plastic sheet with anatomical and boundary information indicated.

Before proceeding to a discussion of the results, it is noted that the average FPE measured during this study (summing measurements of the moduli of the FPEs at all four field borders for the 20 film pairs) was 2.1 mm and hence considerably smaller than that reported by Rabinowitz et al (1985). There is no obvious reason for this difference, although it may in part be a consequence of different clinical practice at the two centres. A further contributing factor may be the manner in which the two studies were conducted. The present study was limited to square fields which can be expected to be easier to set up precisely than the blocked and irregular fields which were

Table. I The precision with which the relative positions of prescribed and treated field boundaries can be quantified. See text for explanation of symbols.

Group	No. of film pairs	No. of measurements (n)	Observers	Treatment film quality	Average treatment film magnification	Exposure	σ_{n-1} (mm)	Observation time (min)
1	5	70	T	T	1.43	1	0.9	6.3
2	5	50	P	T	1.43	1	0.5	—
3	5	40	R	T	1.43	1	0.8	—
4	3	42	T	D	1.47	1	0.7	5.0
5	3	42	T	T	1.27	1	2.2	10.0
6	3	42	T	D	1.25	1	1.5	7.6
7	3	42	T	T	1.25	2	1.5	7.0
8	3	42	T	D	1.3	2	1.4	5.9

included by Rabinowitz et al (1985). In addition, and possibly of greater significance, is the fact that the locations of measurements in this study were pre-determined and identical for all film pairs whereas in the study by Rabinowitz et al the observer selected the points at which the measurements were made. Any bias towards those regions where FPEs were largest would tend to exaggerate the magnitude of the average FPEs recorded.

Discussion

On the assumption that the measured FPEs are normally distributed, the *F* test of significance may be applied to the variances of the different groups in Table I. In comparison with Group 1, all Groups except 3 and 4 represented different populations with a probability exceeding 0.95. Group 4 differed at the 0.9 level.

A comparison of Groups 1, 2 and 3 in Table I leads to the conclusion that experience in interpreting such films results in a more precise estimate of FPEs. The treatment planning and simulation technologists in this institution are responsible for assessing therapy field placement, in the first instance, and it is therefore not surprising that they display a higher degree of consistency than the other two groups. Groups 1 and 3 were different from Group 2 at the $p > 0.95$ level, but not from each other.

The influence of film quality on the precision of determining FPEs can be assessed by comparing Groups 4 and 1. In both these groups the magnifications of the prescription and treatment films were similar. With unlimited viewing time, only a marginal improvement in precision was observed over that obtainable with the poorer-quality 25 MV portal films. This result is consistent with the study by Reinstein et al (1987), who found that the advantage of superior film quality in identifying low-contrast features of a phantom decreased with increased observation time. It should also be noted from Table I that improved image quality, Group 4, leads to a reduction in the time required for a quantitative assessment of FPE, although this reduction is modest.

A comparison of Groups 5 and 1 illustrates the importance of the relative magnification of the films being compared. The inability to overlay the two images not only results in a deterioration of the precision of quantifying the FPE of more than a factor of two but also results in a lengthier procedure than when equal magnification is employed.

If, under these conditions of different magnification, image quality is improved as in Group 6, a significant reduction in both the standard deviation and the observation time associated with the measurement of FPE ensues. However, these quantities are still much larger than those observed with a therapy quality image when compared with a prescription film of the same magnification (Group 1).

Groups 7 and 8 summarize an investigation of the commonly employed double-exposure technique for the assessment of field placement. Our results indicate that under these conditions portal image quality does not greatly influence the precision of FPE measurement, although a better quality image may be assessed more rapidly. Double exposure does not appear to offer any advantage over high-quality single-exposure portal films, Group 6. However, the technique does lead to higher precision than the use of single-exposure therapy-quality film, Group 5.

In order to generate statistically significant results, data from only one site in the pelvis have been used. In general it can be expected that the precision of FPE measurement will depend upon the size and location of the treatment field and these are likely to influence particularly the comparison of double- and single-exposure techniques. However, although the standard deviations presented in Table I are almost certainly site dependent, the conclusions drawn above are expected to remain qualitatively valid for other treatment sites.

In addition to the specific comparisons already described, several general observations may be made. The highest level of precision found in this study is certainly adequate for the quantification of clinically encountered FPEs and, given the margin allowed around known tumour under most conditions, is adequate for almost all clinical purposes. The Group 4 data were obtained under close to optimum conditions, and hence a standard deviation of 0.7 mm is expected to be close to the limit of precision in the measurement of FPEs.

Routine analysis of portal films allows the continuous assessment of systematic errors under the full range of treatment conditions. For practical reasons a quality assurance programme cannot be expected to be as comprehensive and hence could be augmented and possibly, to some extent, replaced by a portal verification programme. With the advent of independently controllable field delineator wires and the availability of comprehensive quantitative FPE data, the interesting possibility develops of simulating not only the ideal treatment machine parameters but also the systematic mechanical errors present for any type of patient set-up. Systematic contributions to FPEs could be significantly reduced by the implementation of such an approach.

Whilst this study has shown that the manual quantitative comparison of prescribed and treated fields may be made with high precision, it has also demonstrated the impracticality of this approach in the busy clinical environment. The observation times recorded and tabulated in Table I would result in too great a demand on scarce resources were a comprehensive quantitative portal verification programme, based on the manual comparison of films, to be introduced. A possible solution to this difficulty, which is under active investigation in many centres, is the implementation of computer-based techniques (Lam et al, 1987). The results presented here may assist in identifying the salient features of software developed for the quantitative assessment and analysis of field placement errors.

Conclusions

With prescription and therapy-quality treatment films of the same magnification, the precision of quantifying field placement errors lies between 0·5 and 0·9 mm. The use of treatment films of diagnostic quality results in a significant improvement in precision only if the films being compared are of different magnification. Comparison of prescription and treatment films of different magnification requires a longer observation time and is less precise than when films of the same magnification are used.

Double-exposure techniques enhance the precision of quantitatively evaluating therapy-quality films of magnification different from the prescription film. Such an improvement is not observed when comparing double- and single-exposure techniques with diagnostic-quality treatment films.

Acknowledgments

The authors are grateful to the physicians and technologists who gave their time to generate the data analysed in this study.

References

AAPM, 1983. *Proceedings of a Symposium on Quality Assurance of Radiotherapy Equipment* (American Institute of Physics, New York).

Byhardt, R. W., Cox, J. D., Hornburg, A. & Liermann, G., 1978. Weekly localization films and detection of field placement errors. *International Journal of Radiation Oncology, Biology, Physics, 4,* 881–887.

Goitein, M. & Busse, J., 1975. Immobilization error: some theoretical considerations. *Radiology, 117,* 407–412.

Kinzie, J. J., Hanks, G. E., MacLean, C. J. & Kramer, S., 1983. Patterns of Care Study: Hodgkin's disease relapse rates and adequacy of portals. *Cancer, 52,* 2223–2226.

Lam, W. C., Partowmah, M., Lee, D. J., Wharam, M. D. & Lam, K. S., 1987. On-line measurement of field placement errors in external beam radiotherapy. *British Journal of Radiology, 60,* 361–367.

Marks, J. E., Haus, A. G., Sutton, H. G. & Griem, M. L., 1974. Localization error in the radiotherapy of Hodgkin's disease and malignant lymphoma with extended mantle fields. *Cancer, 34,* 83–90.

Rabinowitz, A., Broomberg, J., Goitein, M., McCarthy, K. & Leong, J., 1985. Accuracy of radiation field alignment in clinical practice. *International Journal of Radiation Oncology, Biology, Physics, 11,* 1857–1867.

Reinstein, L. E., Alquist, L., Amols, H. I. & Lagneux, B., 1987. Quantitative evaluation of a portal film contrast enhancement technique. *Medical Physics, 14,* 309–313.

1989, *The British Journal of Radiology*, 62, 53–58

Radiotherapy of epidermoid anal canal cancer

By *W. Dobrowsky, MD

Department of Radiotherapy and Radiobiology, University of Vienna, A–1090 Vienna, Alserstrasse 4, Austria

(*Received April 1988 and in revised form July 1988*)

Abstract. Forty-eight patients with anal canal cancers were treated with surgery and irradiation or irradiation alone during the period 1970–1982. All cases were treated by external megavoltage equipment. The overall 5-year survival was 50%, and the local recurrence rate 33%. According to the therapy, four major groups were analysed: radical surgery followed by post-operative irradiation (5-year survival 43%, local recurrence rate 38%), incomplete major surgery and post-operative irradiation with very inferior prognosis (none of the patients surviving beyond 52 months). Two groups of patients had sphincter-saving procedures: local surgery followed by irradiation (5-year survival 78%, local recurrence rate 22%) and primary irradiation (5-year survival 57%, local recurrence rate 14%). Lymph node positive patients showed a median survival of 24.5 months against 52 months in N0 cases (5-year survival 21% against 50%). Side-effects of radiotherapy were transient and mild, and no late severe sequelae were seen. The data indicate that post-operative external radiotherapy seems insufficient and unable to decrease the local recurrence rate, especially when surgery is incomplete. Both spincter-saving surgery and radiotherapy, as well as primary irradiation, are effective treatment modalities. These data are analysed and future aspects considering combined radiochemotherapy are discussed.

Epidermoid cancer of the anus is a rare disease comprising 1–4% of malignant colo-rectal cancer, though 30% of all ano-rectal malignancies are anal cancers. About 75% of anal cancers are anal canal cancers and are more common in women than in men (ratio 3 : 2–5 : 1) (Kuehn et al, 1968; Quan, 1978; Beahrs, 1979; Eschwege et al, 1985). Histologically most cancers are of the squamous cell type of different keratinization. The lymphatic spread is mainly in three directions. The anal margin drains in the inguinal superficial region, anal canal tumours primarily in lymph nodes along the great vessels (A. mesenterica inferior, A. iliaca) and perirectal/anal lymph nodes.

Treatment of anal canal cancer is mainly a loco-regional problem, distant metastases being uncommon. The age of patients has a wide range from 25 to 80 years with a median age of about 60 years. About 75% of patients have uncharacteristic symptoms with haemorrhoids, fistulas, pruritus or leucoplakia which may delay the correct diagnosis.

In Europe, irradiation always has played a more important role in the therapy of these tumours, compared with North America where surgery is often preferred as the initial therapy. Radiotherapy was abandoned in some centres during the early decades of this century because of severe side-effects. With the introduction of combined modality treatment, the use of concomitant radiochemotherapy has again changed the treatment policy towards a conservative radiotherapeutic approach to these cancers.

The present study analyses the patients referred to the Department of Radiotherapy and Radiobiology, University of Vienna from 1970 to 1982 (assessment October 1987).

Materials and methods

During a 12-year period from 1970 to 1982, 48 patients with anal canal cancer were treated at the Department of Radiotherapy and Radiobiology, University of Vienna, and followed up for at least 5 years. The patients were divided into four main groups depending on their disease status and therapy.

Radical surgery and post-operative irradiation

Abdomino-perineal resection was performed in 21 patients who were subsequently irradiated. The median age of these patients was 68 years (range 47–76 years). Four men and 17 women, all presenting with squamous cell cancer, were irradiated 4 to 6 weeks following operation. Table I shows the stage distribution according to the TNM system of 1982 (UICC, 1982).

All patients were treated with megavoltage equipment, the tumour region being given 45–67 Gy in 5–7 weeks. In two cases Bleomycin ± 5-fluorouracil was applied concomitantly with irradiation.

Incomplete abdomino-perineal resection and post-operative irradiation

Four patients were referred for radiotherapy after incomplete abdomino-perineal resection of their anal canal cancer. Three women and one man, aged 61–72 years (mean age 65 years), presenting with squamous cell cancers were treated post-operatively with 40–60 Gy (mean dose 56 Gy) in 4–6 weeks. The stage of disease in these patients was T3N0, T4N0, T3N1 and T4N1.

Tumour excision and post-operative irradiation

Nine patients were treated initially by a conservative surgical procedure. Local excision was performed in eight women and one man, aged 45–79 years (median 67 years); two patients also underwent groin dissection and removal of metastatic lymph nodes. In eight cases the operative specimen showed a squamous cell cancer and in one patient a basaloid cancer was found.

---

*Address for correspondence: Department of Radiation Oncology, Princess Margaret Hospital, Toronto M4X 1K9, Canada.

Table I. Abdomino-perineal resection and postoperative irradiation ($n = 21$). Stage distribution according to the TNM-classification(UICC, 1982)

	N0	N1
T1	2	—
T2	5	4
T3	4	3
T4	2	1

Seven patients were treated post-operatively, and two patients were treated for a local recurrence 12 and 16 months post-operatively. Table II shows the initial tumour stage in these patients. They were treated with 45–70 Gy in 4–7 weeks (mean dose 60 Gy).

Primary irradiation of anal canal cancer

Fourteen patients with a histologically confirmed anal canal cancer had radiation as the primary treatment; 13 patients had squamous cell cancer and one had basaloid cancer. Eight women and six men aged 47–86 years (median 72 years) were irradiated with doses of 45–70 Gy in 4–7 weeks (median 60 Gy). The stage distribution is shown in Table III.

Technique of irradiation

All patients were treated with external-beam irradiation, using megavolt equipment, either ^{60}Co, 6 MeV or 42 MeV photons or high-energy electron beams.

The target volume comprised the pelvic region, with the cranial border at L5/S1, the lateral margin being 1 cm lateral of the osseous small pelvis. The distal margin of the field encompassed the perineal skin. Two types of field arrangement mainly were applied. Usually anterior–posterior fields were used, but in some patients this technique was used with an additional perineal field. Primary irradiation of anal canal cancer was performed by a direct perineal field in some cases. This group of patients had no elective irradiation of the inguinal region unless involved.

In patients who underwent operation prior to irradiation, the medial inguinal lymph node region was generally included in the treatment field; in node positive patients the total extent of the inguinal region was enclosed in the irradiated field.

Table II. Local tumour excision and postoperative irradiation. Stage distribution according to the TNM-classification (UICC, 1982)

	N0	N1
T1	2	2
T2	4[a]	—
T3	1[a]	—
T4	—	—

[a] In each of these stages one patient with local recurrence was treated.

Table III. Primary radiotherapy of anal canal cancer. Stage distribution according to the TNM-classification (UICC, 1982)

	N0	N1
T1	—	1
T2	10	—
T3	1	—
T4	1	1

Results

Survival and local recurrence

Radical surgery and post-operative irradiation. The crude 5-year survival in this group of 21 patients was 9/21 (43%). The median survival was 48 months (range 10–68 months). Analysing the survival according to the lymph nodal status, the following was found. Patients with lymph node metastases had a mean survival of 35 months (range 10–62 months) and a 5-year survival of 2/8 (25%) against 54 months (range 20–86 months) and a 5-year survival of 7/13 (53%) in node negative patients. Thirteen of 21 treated patients did not survive 5 years. Eight of these patients recurred loco-regionally and two patients had distant metastases (lung, liver), one also presenting with a pelvic failure. The cause of death in the other four patients is unknown. Both patients receiving chemotherapy had an inferior prognosis because of the advanced stage of disease (survival 14 and 20 months).

Incomplete abdomino-perineal resection and post-operative irradiation. These patients, initially presenting with large tumours, all died with tumour progression. Death occurred at 17, 23, 39 and 52 months, survival being shorter in node positive patients.

Tumour excision and post-operative irradiation. These patients, presenting with less extensive tumours than the previous groups, showed a 5-year survival of 7/9 (78%), with a range of 24–118 months (mean survival of 60 months). The two patients with a local recurrence after sphincter-saving surgery survived 24 and 60+ months after irradiation. The patient surviving 24 months died with tumour progression and inguinal lymph node metastases. Another patient died with a local recurrent tumour at 25 months. All other patients are alive and without evidence of tumour.

Primary irradiation of anal canal cancer. The 5-year survival in this group was 8/14 (57%) and the mean survival was 60 months (range 25–125 months). Two patients died without evidence of tumour at 67 and 75 months post-treatment, one patient (T4N1) died at 25 months with tumour progression (persistent tumour and distant metastases). One patient (T2N0) showed a local recurrence after 24 months and was treated by abdomino-perineal resection. He was well for 2 years longer, then presented with a new local recurrence which could not be treated curatively. This patient died 53 months after initial irradiation. Another two patients died with tumour-unrelated disease. Metachronous lymph node metastases in the inguinal region were not

Table IV. Treatment of anal canal cancer according to the mode of therapy.

Therapy	No. of patients	Crude 5-year survival (%)	Local recurrence rate (%)
Radical surgery + irradiation	21	43	38
Incomplete major surgery + irradiation	4	0	100[a]
Sphincter-saving surgery + irradiation	9	78	22
Primary radiotherapy of primary tumour	14	57	14[a]
All	48	50	33

[a] Persistence of tumour included.

Table V. Survival and local recurrence of anal canal carcinoma according to modality of treatment

Treatment	No. of patients	5-year survival (%)	Local recurrence (%)
Major surgery			
Klotz et al (1967)	194	50	26
Greenall et al (1984)	103	55	27
Hardcastle & Bussey (1968)	92	48	27
Boman et al (1984)	114	71	40
Local excision			
Kuehn et al (1968)	26	75.2	8
Stearns & Quan (1970)	30	66	63
Klotz et al (1967)	33	61	33
Radiotherapy (external)			
Eschwege et al (1985)	64	46	19
Green et al (1980)	16	81	25
Cummings et al (1982)	51	71	27
Present series	14	57	14
Radiotherapy (external + interstitial)			
Papillon & Montbarbon (1987)	222	66	21
Delouche et al (1973)	22	45	25

seen in any of the patients in this group. The results of treatment according to the mode of therapy are shown in Table IV.

Survival according to lymphonodal status. In this series there were 34 patients without lymph node secondaries and 14 with lymph node metastases. The survival in patients without lymph node metastases is 29–118+ months (median survival 52 months) with 17 patients surviving 5 years or more. In patients with positive lymph nodes, the median survival was 24.5 months (range 10–60+ months) with only three of 14 (21%) surviving at least 5 years.

Distant metastases. Only three of the 48 patients have shown distant metastases (liver or lung). The true number of patients with distant metastases is probably greater, because not all patients had an autopsy or radiologically diagnosed secondaries.

Side-effects. Generally treatment was well tolerated and only a few patients presented increased skin reactions. Transient moist desquamation occurred in some patients, and healed without sequelae in all patients. Gastrointestinal disturbances (diarrhoea or proctitis) were present in one-third of patients at the end of therapy. While diarrhoea persisted for only few weeks after therapy, the proctitis lasted longer and in five patients with normal anal function a mild rectal stenosis was present. None of the patients have shown a severe stenosis, fibrosis or fistula requiring surgical intervention and none have shown small bowel obstructions.

Discussion

Anal canal cancers are rare and large series are seldom reported. The therapeutic approach has changed markedly during the last decades, and while surgery has been the choice of therapy in most North-American series, traditionally in Europe radiotherapy has played a more important role.

Table V shows the survival of patients treated for anal canal cancer according to different therapy modalities (Klotz et al, 1967; Hardcastle & Bussey, 1968; Kuehn et al, 1968; Stearns & Quan, 1970; Delouche et al, 1973; Green et al, 1980; Cummings et al, 1982; Boman et al, 1984; Eschwege et al, 1985; Greenall et al, 1985; Papillon & Montbarbon, 1987). Analysing the survival in the present study, there does not seem to be a major benefit of post-operative irradiation following radical surgery. The survival of 43% in the present series is quite comparable to the survival rates found after radical surgery without post-operative irradiation (see Table V).

Hohm and Jackman (1964) found a survival rate of 50% in patients irradiated after radical surgery compared with 65% in patients treated by radical surgery only. Schulz et al (1982) found a recurrence-free survival in 6/14 patients following post-operative irradiation. The follow-up in their series was 14–60 months. Frost et al (1984) also did not find any survival benefit in patients receiving post-operative irradiation after major surgery, although the local recurrence rate decreased (17% against 25%).

Post-operative irradiation after incomplete major surgery apparently does not result in an increased survival. However, one must bear in mind that few patients have been treated in this category. The reason for its ineffectiveness is the advanced nature of these large unresectable lesions and biological behaviour of persisting tumour following surgery, with a high proportion of anoxic, less radiosensitive tumour cells.

Anal canal cancer should be treated in the light of two major problems. First, the tumour must be controlled, which is possible either by surgery or radiotherapy, and secondly one should choose the most conservative treatment modality, sparing the patient a permanent colostomy. Sphincter-saving surgery is only feasible in a few selected, small cancers, accounting for about 25% of all anal canal cancers (Eby & Sullivan, 1969). Radiotherapy as a non-invasive, curative treatment modality can be applied to about 80% of patients (Papillon & Montbarbon, 1987).

The crude 5-year survival in patients treated conservatively by local excision and irradiation (nine patients) or irradiation alone (14 patients) was 15/23 (65%), which can be compared with other conservative therapies showing similar survival rates (Klotz et al, 1967; Kuehn et al, 1968; Stearns & Quan, 1970).

Comparing the results of local excision and local excision followed by post-operative irradiation, it seems that post-operative irradiation could decrease the local recurrence rate. Greenall et al (1985) found only 10% of all cases of anal canal cancer suitable for local excision; of these patients 65% experienced a recurrent tumour. In the series presented here, the local recurrence rate after local excision and post-operative irradiation was quite low. When the two patients treated with recurrent tumour after local excision are excluded, the local recurrence rate in these patients is 1/7 (14%) and the 5-year survival rate of 6/7 (86%) is quite comparable to the data of Hohm and Jackman (1964), who found a survival rate of 81% (13/16) in their patients treated by local excision and subsequent irradiation.

The results obtained for the 14 patients treated by primary irradiation show that radiotherapy is as effective as limited surgery (local excision). Obviously the number of patients treated is small and the tumour stage distribution shows that mainly earlier stages were treated. The corrected survival rate of 83% (10/12) shows the irradiation of these tumours is an adequate therapy. The local recurrence rate of 14% is also less than expected after local excision only. The reason for the low loco-regional recurrence rate may be that not only the tumour region is treated but also pelvic lymph node regions are included in the treatment volume.

According to the literature, the frequency of pelvic nodal disease varies from 10 to 45% (Grinell, 1954; Dargent, 1958; Dillard et al, 1963; Klotz et al, 1967; Hardcastle & Bussey, 1968; Kuehn et al, 1968; Stearns & Quan, 1970) and depends on histology, tumour stage and localization. Basaloid carcinoma metastasizes earlier than squamous cell cancers. Boman (1984) found lymph node metastases in 35% of patients with basaloid cancers against 6% in patients with squamous cell cancers (tumour smaller than 2 cm). This difference is also present in 2–3 cm tumours (50% against 29% lymph node metastases). In more extensive tumours there is no significant difference (50% against 46%).

Since a local excision of a small anal canal cancer does not include any therapy of pelvic lymph nodes, this may be a reason for the high incidence of recurrence following limited surgery (Klotz et al, 1967; Beahrs, 1979; Stearns & Quan, 1970; Frost et al, 1984; Greenall et al, 1985).

The frequency of inguinal node secondaries does not differ from the incidence of pelvic node metastases (Kuehn et al, 1968; MacConell, 1970; Stearns & Quan, 1970; Beahrs & Wilson, 1976; Loygue et al, 1981; Cummings et al, 1982; Glimelius et al, 1987). The inguinal region was not electively irradiated in the patients referred to in the present report. Only patients with inguinal lymph node metastases were irradiated to the groins after lymphadenectomy. So far no metachronous lymph node metastases have occurred in node-negative patients. This would justify a watch policy, especially since the inguinal region is easily examined and metachronous lymph node secondaries have a better prognosis than synchronous metastases (Golden & Horsley, 1976; Papillon, 1982). In the literature different statements can be found. Rousseau et al (1973) and Delouche et al (1973) recommended elective irradiation, whereas Cummings et al (1982) found no difference in inguinal failure rates in patients treated with elective inguinal irradiation. Generally the trend shows that elective irradiation is not of much benefit. Another reason for not performing an elective irradiation to the groins is potential radiation-induced morbidity with possible lymphoedema and gastrointestinal reactions.

There is no doubt that the lymph nodal status is an important prognostic factor. The survival in patients treated in this series was 21% when lymph nodes were involved against 50% in N0 patients. These data can be compared with others showing 5-year survival from 0 to 40% (Dillard et al, 1963; Hightower & Judd, 1967; Kuehn et al, 1968; Brennan & Stewart, 1972; Beahrs & Wilson, 1976; Corman & Haggit, 1977; Pyper & Parks, 1985) in patients with lymph node secondaries. Using radiotherapy, possible micrometastases in lymph nodes can be sterilized by a dose of 50 Gy in 5 weeks. This dose can safely be applied without major complications and should be the dose delivered to subclinical disease. A dose lower than 50 Gy is ineffective and cannot be recommended in curative treatment. The primary tumour or enlarged metastatic lymph nodes require an increased radiation dose.

Tumour control clearly depends on the tumour volume and the dose of irradiation. Eschwege et al (1985) found a local recurrence rate of 9% in T1–T2 tumours when irradiation was performed with 60–65 Gy, while in T3 tumours the rate was 24% and in T4 tumours 33%. Thus, 65 Gy seems to be a sufficient dose to eradicate small tumours (T1–T2). The dose in larger tumours should be increased, thus achieving a higher local control. This is possibly difficult when using external beams alone. Papillon (1982) therefore advocates the use of additional curietherapy to increase the tumour dose, without extensive irradiation of normal pelvic tissue and he has reported a 66% 5-year survival rate.

In the present study the dose was 40–75 Gy. The dose of 40 Gy was delivered palliatively to one patient with large residual tumour after abdomino-perineal resection. In most cases the dose was adopted according to the tumour situation, *e.g.* post-operative dose ("low risk") 45–50 Gy. In patients with larger initial tumours the post-operative dose was 55–70 Gy. A similar policy was used in the treatment of primary tumours. One patient with a large (T3) cancer interrupted treatment (at 45 Gy), but all others were treated as initially planned (55–70 Gy).

The number of patients treated and the various doses used in the present study do not enable any conclusions to be made about the comparison of dose and control. Both irradiation techniques used gave a similar effect, except for a slight increase of perineal skin reaction when a perineal field was added to the opposed fields.

Since Nigro et al (1974) first reported on radiochemotherapy with mitomycin C (MMC) and 5-fluorouracil (5-FU) the therapy of choice has changed markedly to more conservative sphincter-saving procedures, abandoning the Miles operation, sparing most patients a permanent colostomy. The combination of radiation and MMC and 5-FU has resulted in a clear therapeutic benefit. Papillon and Montbarbon (1987) found a significant decrease of local recurrence when MMC and 5-FU were added to irradiation during the first 5 days of radiotherapy (recurrence rate 19% against 34%, $p = 0.02$). A similar treatment regime has been used at the Department of Radiotherapy and Radiobiology, University of Vienna since 1985 (Dobrowsky, 1988). Since 1985, nine patients have been treated with radiochemotherapy using 15 mg MMC/m^2 on Day 1 and 750 mg 5-FU/m^2 per day for Days 1–5. Irradiation was given to 50 Gy in 4 weeks, starting on Day 1. Six weeks following irradiation an implant with iridium 192 was performed (15–20 Gy in target volume). So far none of the patients has experienced a recurrence and all patients are alive and well.

In conclusion, external radiotherapy seems to be able to eradicate smaller tumours. For therapy of larger cancers brachytherapy or chemotherapy should also be given to increase the local therapy. Post-operative irradiation (following abdomino-perineal resection) does not seem to be of great benefit either for survival or recurrence. Post-operative irradiation following local surgery decreases the rate of local recurrence. Initial results from irradiation and concomitant chemotherapy (MMC and 5-FU) are encouraging, showing high tumour clearance, low local recurrence and a normal sphincter function in a great majority of cases. Future studies will show if the combined modality treatment will replace surgery and be accepted as the treatment of choice for all stages of anal cancer.

References

BEAHRS, O. H., 1979. Management of cancer of the anus. *American Journal of Roentgenology, 133,* 791–795.

BEAHRS, O. H. & WILSON, S. M., 1976. Carcinoma of the anus. *American Surgeon, 184,* 422–428.

BOMAN, B. M., MOERTEL, C. G., O'CONNELL, M. J., SCOTT, M., WEILAND, L. H., BEART, R. W., GUNDERSON, L. L. & SPENCER, R. J., 1984. Carcinoma of the anal canal—a clinical and pathologic study of 188 cases. *Cancer, 54,* 114–125.

BRENNAN, J. T. & STEWART, C. F., 1972. Epidermoid carcinoma of the anus. *Annals of Surgery, 176,* 787–790.

CORMAN, M. L. & HAGGITT, R. C., 1977. Carcinoma of the anal canal. *Surgery, Gynecology and Obstetrics, 145,* 674–676.

CUMMINGS, B. J., THOMAS, G. M., KEANE, T. J., HARWOOD, A. R. & RIDER, W. D., 1982. Primary radiation therapy in the treatment of anal canal carcinoma. *Diseases of the Colon and Rectum, 25,* 778–782.

DARGENT, M., 1958. Le cancer de l'anus. *Revue de Praticien, 8,* 731–741.

DELOUCHE, G., BACHELOT, F., COHEN, M. & GEST, J., 1973. La radiothérapie des cancers malpighiens de l'anus. *Journal de Radiologie d' Electrologie et de Médecine Nucléaire, 54,* 642–646.

DILLARD, B. M., SPRATT, J. S., ACKERMANN, L. V. & BUTCHER, H. R., 1963. Epidermoid carcinoma of the anal margin and canal. *Archives of Surgery, 86,* 772–777.

DOBROWSKY, W., 1988. *Radio-Onkologie beim Rektum-und Analkarzinom.* (Springer Verlag, Vienna.)

EBY, L. S. & SULLIVAN, E. S., 1969. Current concepts of local excision of epidermoid cancer of the anus. *Diseases of the Colon and Rectum, 12,* 332–337.

ESCHWEGE, F., LASSER, A., CHARY, P., WIBAULT, KAC, J., ROUGIER, P. & BOGNEL, C., 1985. Squamous cell carcinoma of the anal canal: treatment by external beam irradiation. *Radiotherapy and Oncology, 3,* 145–150.

FROST, D. B., RICHARDS, P. C., MONTAGUE, E. D., GIACCO, G. G. & MARTIN, R. G., 1984. Epidermoid cancer of the anorectum. *Cancer, 53,* 1285–1293.

GLIMELIUS, B. & PÅHLMAN, L., 1987. Radiation therapy of anal epidermoid carcinoma. *International Journal of Radiation Oncology, Biology, Physics, 13,* 305–312.

GOLDEN, G. T. & HORSLEY, J. S., 1976. Surgical management of epidermoid carcinoma of the anus. *American Journal of Surgery, 131,* 275–280.

GREEN, J. P., SCHAUPP, W. G., CANTRIL, S. T. & SCHALL, G., 1980. Anal carcinoma: current therapeutic concepts. *American Journal of Surgery, 140,* 151–155.

GREENALL, M. J., QUAN, S. H. Q., URMACHER, C. & DE COSSE J. J., 1985. Treatment of epidermoid cancer of the anal canal. *Surgery, Gynecology and Obstetrics, 161,* 509–517.

GRINELL, R. S., 1954. An analysis of forty-nine cases of squamous cell carcinoma of the anus. *Surgery, Gynecology and Obstetrics, 98,* 29–39.

HARDCASTLE, J. D. & BUSSEY, H. J. R., 1968. Results of surgical treatment of squamous cell carcinoma of the anal canal and the anal margin. *Proceedings of the Royal Society of Medicine, 61,* 629–630.

HIGHTOWER, B. M. & JUDD, E. S., 1967. Carcinoma of anal canal and anus therapy. *Mayo Clinic Proceedings, 42,* 271–275.

HOHM, W. H. & JACKMAN, R. J., 1964. Anorectal squamous-cell carcinoma: conservative or radical treatment? *Journal of the American Medical Association, 188,* 241–244.

KLOTZ, R. G., PAMUKOGLU, T. & SOUILLARD, D. H., 1967. Transitional cloacogenic carcinoma of the anal canal. Clinicopathological study of 373 cases. *Cancer, 20,* 1727–1745.

KUEHN, P. G., EISENBERG, H. & REED, J. F., 1968. Epidermoid carcinoma of the perianal skin and anal canal. *Cancer, 22,* 932–938.

LOYGUE, J., LAUGIER, A., PARC, R. & WEISGERBER, G., 1981. Carcinoma épidermoide de l'anus, à propos de 149 observations. *Chirurgie, 109,* 710–716.

MACCONNELL, E. M., 1970. Squamous carcinoma of the anus: a review of 96 cases. *British Journal of Surgery, 57,* 89–92.

NIGRO, N. D., VAITKOVICIUS, V. K. & CONSIDINE, B., 1974. Combined therapy for cancer of the anal canal: a preliminary report. *Diseases of the Colon and Rectum, 17,* 354–356.

PAPILLON, J., 1982. *Rectal and Anal Cancers. Conservative Treatment by Irradiation: An Alternative to Radical Surgery.* (Springer Verlag, Berlin.)

PAPILLON, J. & MONTBARBON, J. F., 1987. Epidermoid carcinoma of the anal canal. *Diseases of the Colon and Rectum*, *30*, 324–333.

PYPER, P. C. & PARKS, T. G., 1985. The results of surgery for epidermoid carcinoma of the anus. *British Journal of Surgery*, *72*, 712–714.

QUAN, S. H. Q., 1978. Anal and para-anal tumours. *Surgical Clinics of North America*, *58*, 591–603.

ROUSSEAU, J., MATHIEU, G., FENTON, J. & CUZIN, J., 1973. Radiothérapie des cancers malpighiens de l'anus. *Journal de Radiologie d' Electrologie et de Médecine Nucléaire*, *54*, 622–626.

SCHULZ, U., BAMBERG, M., GROSS, E. & NIEBEL, 1982. Die kombinierte chirurgisch-radiologische Therapie der Plattenepithelkarzinome des Analkanals und der perianalen Haut. *Strahlentherapie*, *158*, 327–335.

STEARNS, M. W. & QUAN, S. H. Q., 1970. Epidermoid carcinoma of the ano-rectum. *Surgery, Gynecology and Obstetrics*, *131*, 953–957.

UICC, TNM-ATLAS, 1982. *Illustrated Guide to the Classification of Malignant Tumours*, ed. by B. Spiessl, O. Scheibe & G. Wagner (Springer Verlag, Berlin).

1989, *The British Journal of Radiology*, *62*, 59–63

Discriminant analysis on the treatment results of interstitial radium tongue implants

By *Masao Hoshina, BMSc, Hitoshi Shibuya, MD, Jun-Ichi Horiuchi, MD, Sho Matsubara, MD, Soji Suzuki, MD and †Masamune Takeda, DDS

Departments of Radiology and †Dental Radiology, Tokyo Medical and Dental University, 5–45 Yushima 1-chome, Bunkyo-ku, Tokyo 113, Japan

(*Received June 1988 and in revised form July 1988*)

Abstract. Discriminant analysis was carried out for 48 tongue cancer patients who were treated with radium single-plane implantation. The 48 patients were grouped into 32 successfully cured without complications, five successfully cured with complications, six successfully cured but requiring additional boost therapy and five with local recurrence. To evaluate the relation between the dose distribution and the local treatment results, the analysis was based on a volume–dose relationship. The functions introduced by this discriminant analysis were linear, and the parameters used were modal dose, average dose and shape factors of histograms. Each group of treatment results had a correction rate of >80%, except for the successfully cured group with ulcers. The discriminant functions were useful as an index to obtain a final clinical treatment result at the early time of implantation, and these functions could be used as a criterion for the optimal treatment of tongue carcinoma. We were also able to recognize the limitation of the actual arrangement of sources in the single-plane implant.

Several brachytherapy systems have been described using interstitial implants (Laughlin et al, 1963; Meredith, 1967; Goodwin et al, 1970; Pierquin et al, 1978), and the dosimetry of ideal arrangements of the sources has been reported (Gillin et al, 1984; Marinello et al, 1985; Muller-Runkel & Vijayakumar, 1987).

In practice, the dose distributions can be obtained with the aid of a computer and then a particular isodose can be selected from a series of isodose curves. However, even if we confirm the distribution inside a particular isodose curve selected for dose prescription, the results obtained can be conflicting. This is because the dose distribution in a target volume is decided from only the isodose curve, which is only one index. Therefore, an isodose curve needs to be selected on the basis of the integrated index which has a direct relation with the local treatment results.

Quantitative analyses of dose distributions have been attempted using the volume–dose relation (Awwad et al, 1974; Tokita et al, 1980; Burgers et al, 1985; Anderson, 1986; McCrae et al, 1987). Although this relationship cannot present information about positions for individual doses, it seems able to compress the whole dose distribution in a target volume into basic statistics (average dose, modal dose, etc.). If the interstitial treatment results can be estimated by the statistics obtained from the volume–dose histogram, predictive mathematical models will be obtained. They can function as criteria for quality control in brachytherapy or for the selection of a proper isodose for dose prescription.

Although iridium sources are now used for brachytherapy, we have performed the first examination of the predictive models using cases treated with radium needles (Horiuchi et al, 1982, 1986). The technique we use is discriminant analysis, employing a method of multivariate analysis of the results obtained by local treatment of carcinoma of the tongue.

Materials and methods

Forty-eight patients with carcinoma of the tongue were treated with single-plane radium implants between 1971 and 1986 (Horiuchi et al, 1982, 1986). They were divided into five groups according to their clinical outcome after treatment: 32 locally-cured cases with no complications, two locally-cured cases with ulcers, three locally-cured cases with necrosis, six locally-cured cases requiring additional boost therapy by electron beams, and five cases with local recurrences. The minimum follow-up period was 1 year. All patients had had no previous treatment such as surgery, external irradiation or chemotherapy. According to the UICC TNM classification, there were 10 patients with T1 and 38 patients with T2 tumours. The planned doses ranged from 60 to 70 Gy in 114 to 194 h.

Thirty-eight of the 48 patients were taken as initial samples in order to compute the discriminant functions, and the other 10 locally-cured cases were utilized as "external" samples to verify whether the functions acquired from the initial samples were valid. Pretreatment calculation of needle selection and treatment time was done according to the Paterson–Parker rules.

Clinically, not all needles can be inserted exactly as planned. Therefore, the plane of the sources in single-plane implantation was approximately determined so as to cross the geometrical centre of an actual source arrangement. The area of this plane was equal to that of the treatment plan. The calculated region was established as a box 10 mm wide centred on the plane of sources and the width between calculation points was

---

*Author for correspondence.

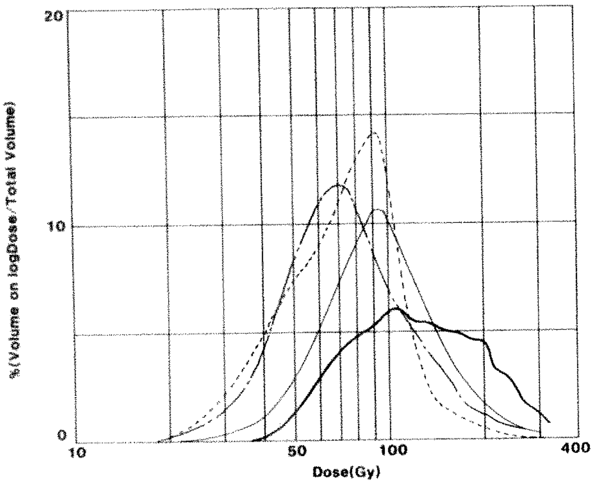

Figure 1. Volume–dose histogram normalized by total volume for single-plane radium implants of four groups as (———) locally cured case without complications, (**———**) locally cured case with necrosis, (– – –) locally cured case requiring boost therapy and (– · –) uncontrolled case.

1 mm. The distribution of volume per dose was established for the region within this box. The frequency of volume was obtained in each dose interval for the dose range from 10 to 320 Gy, divided into 31 intervals. To demonstrate effectively the differences in volume per dose among cases, logarithmic dose transformation was necessary.

The *k*th moments were used as general variables to determine the shape of the histogram. Four parameters (an average dose, a modal dose, skewness and kurtosis) were used in the discriminant analysis (Lachenbruch, 1975). Skewness and kurtosis, calculated from the second to fourth moments around the average, were used as the shape factors of the histogram (Fisher, 1950).

The analysis was restricted only to the assessment of dose distribution, and clinical parameters were not taken as variables for discriminant functions. As the material was limited to single-plane implants, the differences in the clinical parameters were assumed to be relatively small.

The initial 38 patients were divided into three object groups according to the treatment results:

(I) CR group: locally-cured group, 22 patients.

(II) B&R group: locally-cured group requiring additional boost therapy and local recurrence group, 11 patients.

(III) COMP group: locally-cured group with ulcer and necrosis, five patients.

Cases with different final outcomes were included in the B&R group. These cases were not treated successfully with brachytherapy.

Results

Figure 1 shows the typical volume–dose relationship for the four groups in the calculated region. The difference between the histograms for the CR cases and the COMP cases is evident (Fig. 1). The shape of the volume–dose histogram for the CR cases was similar to that of a lognormal distribution. By contrast, the shape of the histogram for the COMP cases reveals a plateau and was shifted to higher doses. The peak of the histogram for the recurrent cases was lower than that for the CR cases. In cases requiring boost therapy, the volume showed a steep fall-off in the high-dose region.

As the number of cases in each group was limited, the distribution of each variable (modal dose, average dose, skewness, kurtosis) was expected to be lognormal when plotted as a probability scale. The discriminant analysis was then done after the logarithmic transformations such that each variable had a normal distribution. As the skewness and kurtosis each had a negative value (β), the transformations were done by log $(1+\beta)$.

Figure 2 shows the correlations between each pair of the four parameters in the analysis. As shown in Fig. 1, a histogram for an appropriate implant concentrates on a given dose and is symmetrically distributed. Then skewness and kurtosis have values close to zero and the histogram has a distribution similar to that of the lognormal distribution. The cases which met the above condition, are found close to the origin of Fig. 2a, and if the average dose is sufficient, these cases are in the CR group. Because sources are distributed in the calculated region, the histogram usually has a long tail extending to the higher dose level, *i.e.* the histogram is skewed to the right. Therefore, in addition to the vicinity of the origin on Fig. 2a, the first quadrant of Fig. 2a also becomes a

Table I. Comparison between dose, shape factors and local results

	CR (n = 22)	B&R (n = 11)	COMP (n = 5)
Modal dose (cGy)	8439 ± 117	9234 ± 123	6602 ± 184
Average dose (cGy)	10226 ± 109	9829 ± 113	10970 ± 122
Skewness	0.016 ± 0.108	−0.068 ± 0.144	−0.121 ± 0.146
Kurtosis	−0.019 ± 0.149	−0.088 ± 0.187	−0.289 ± 0.212

CR, locally-cured group without complications; B&R, locally-cured group requiring boost therapy and uncontrolled group; COMP, locally-cured group with complications (ulcers and necrosis). Each variable was processed by logarithmic transformation for the discriminant analysis, but dose values in this table are returned to the original form. Results given as mean ± SD.

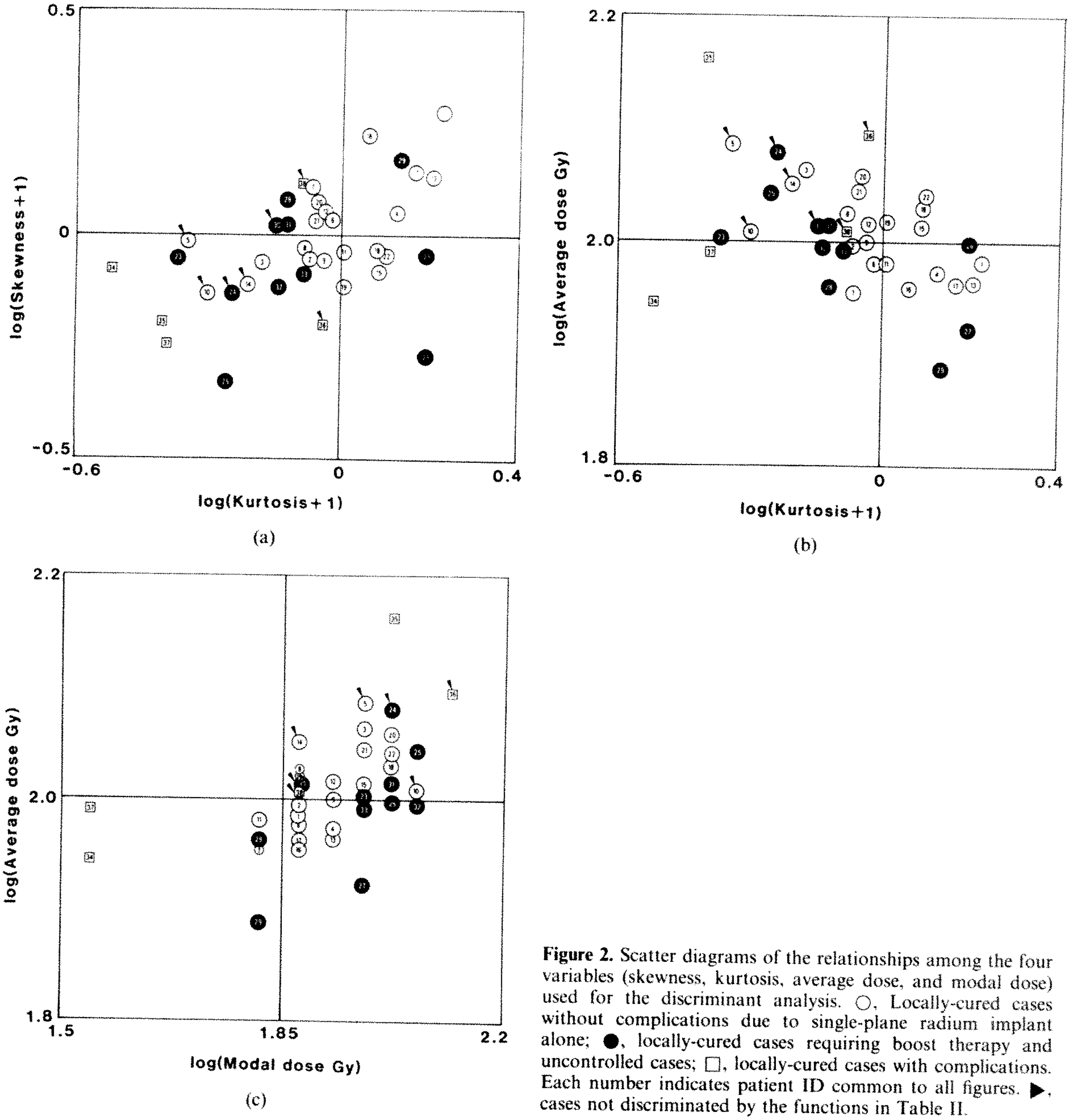

(a)

(b)

(c)

Figure 2. Scatter diagrams of the relationships among the four variables (skewness, kurtosis, average dose, and modal dose) used for the discriminant analysis. ○, Locally-cured cases without complications due to single-plane radium implant alone; ●, locally-cured cases requiring boost therapy and uncontrolled cases; □, locally-cured cases with complications. Each number indicates patient ID common to all figures. ▶, cases not discriminated by the functions in Table II.

successful region under the condition that the average dose is sufficient. Kurtosis denotes the degree to which the volume is concentrated about an average dose; it has a negative correlation to average dose in Fig. 2b. Clearly the average dose for a given kurtosis in the B&R group is lower than that in the CR group. Average and modal dose are the same in a normal distribution and in a general volume–dose histogram the difference between them will be expected to be small. Figure 2c shows a positive correlation between them both, but the cases (34–37) in the COMP group had values separated from the CR and B&R groups.

Table I shows the parameters for the three groups of patients, subject to the above transformation. The linear discriminant functions for each pair of groups, acquired by using four parameters, and the apparent prediction rates (the number of cases discriminated correctly divided by the total number) are shown in Table II. As there were some correlations between parameters, the validity of them was examined by the *F* test using Mahalanobis' generalized distance. The results of the test are shown at the bottom of Table II. In the case of the relationship between the CR and B&R groups, the parameters average dose and kurtosis were demon-

Table II. Linear discriminant functions between pairs of groups

Coefficient	CR—B&R	CR—COMP	B&R—COMP
a	−88.5298	47.3442	89.2215
b	−15.6659	18.1024	29.2206
c	59.8172	−39.7956	−72.4029
d	8.0715	3.3385	−0.9490
e	8.8535	3.1938	−7.2835
$Z>0$	CR	CR	B&R
$Z<0$	B&R	COMP	COMP
Apparent correct rate	CR: 95.5% B&R: 81.8%	CR: 90.9% COMP: 60.0%	B&R: 81.8% COMP: 100%

$Z = a+bx_1+cx_2+dx_3+ex_4$.
$x_1 = \log_{10}$ (modal dose [Gy]), $x_2 = \log_{10}$ (average dose [Gy]), $x_3 = \log_{10}$ (skewness + 1), $x_4 = \log_{10}$ (kurtosis + 1).
The group corresponding to a given case is determined by a positive or negative sign of the linear discriminant function values ($Z>0$ or <0 in table). CR, locally-cured group without complications; B&R, locally-cured group requiring boost therapy and uncontrolled group; COMP; locally-cured group with complications (ulcers and necrosis). The apparent correct rate is the number of cases discriminated correctly divided by the total number × 100. Average dose ($p<0.01$) and kurtosis ($p<0.05$) between CR and B&R. Modal dose ($p<0.01$) and average dose ($p<0.05$) between B&R and COMP. None of the variables are significant between CR and COMP ($p<0.09$).

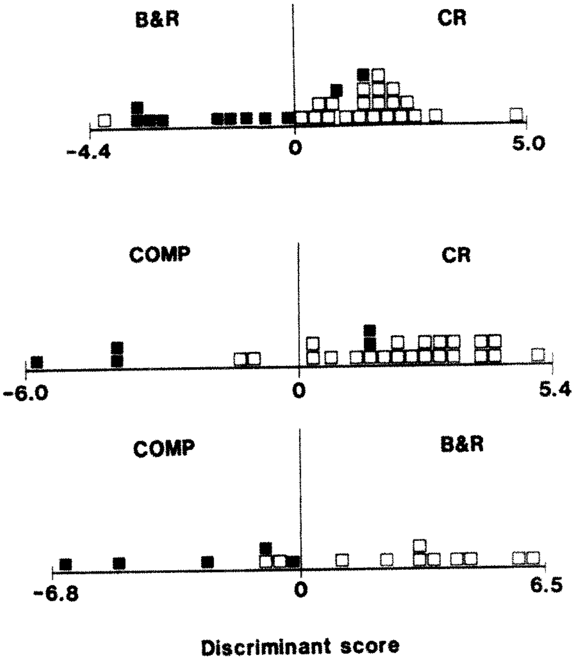

Figure 3. Discriminant scores of the three groups according to the functions in Table II. CR, locally-cured cases without complications; COMP, locally-cured cases with complications; and B&R, locally-cured cases requiring boost therapy and uncontrolled cases.

strated to be statistically significant, $p<0.01$ and $p<0.05$, respectively. The other parameters, modal dose and skewness, gave rise to no significance, $p<0.06$ and $p<0.13$, respectively.

The apparent prediction rate for each group was more than 80% except for the cases which discriminated between the CR and COMP groups (Table II). The arrowheads in Fig. 2 denote the cases that could not be discriminated and Fig. 3 shows the distributions of discriminant scores. The prediction rates for CR and B&R were high (96% and 82%). The controlled cases with ulcers (Cases 36 and 38) in the COMP group could not be discriminated from the CR group; the cases with necrosis in the COMP group were discriminated correctly. Cases 24 and 30 in the B&R group, given additional boost therapy, could not be discriminated from the other two groups. The recurrent Case 29 in the first quadrant of Fig. 2a was a man treated in a short overall time owing to the worsening of his general condition. He had a low average dose without any change in the shape of the volume–dose histogram. As there were no new cases in the COMP and B&R groups as "external" samples, it was not possible to test the functions on new cases, except for the CR group. In the new CR cases, the apparent prediction rate was 80% using the functions given in Table II.

Some cases in the B&R group (Cases 23–25, 27, 30, 32) had been subjected to additional external irradiation for an induration indicating remaining tumour soon after the interstitial implantation. Uncontrolled cases (Cases 26, 28, 31, 33) had no such induration immediately following the implantation. These cases were distributed at the periphery to the successful region in Fig. 2a, b. The low kurtosis and/or low average dose were suspected to have caused the failure of treatment.

Most of the cases with complications (Cases 34–37) were distributed in the third quadrant of Fig. 2a. Cases 34, 35 and 37 had a low kurtosis value and the histograms extend widely from a lower to a higher dose, *i.e.* a large deviation of dose. Two cases with ulcers (Cases 36, 38) had CR values of skewness and kurtosis; one (Case 36) had a higher average dose (125 Gy) and the other (Case 38) had an average dose (100 Gy), the same as that for the CR group (Fig. 2b). The ulcer in Case 38 was assumed to be caused by inappropriate local care after implantation.

Discussion

There have been several studies concerning the factors and dose specifications of importance for treatment results of brachytherapy (Awwad et al, 1974; Burgers et al, 1985). These approaches have tried to obtain a common basis for discussing data obtained from different institutions and thus to obtain common criteria for the application of brachytherapy.

In the present analysis, discriminant functions for the local treatment results were obtained by using volume–dose histograms. Statistically-defined dose and shape factors derived from the histograms were used for discrimination. No consistent trend was found as to how these factors contribute to discriminate the treatment results. In the case of the clinically most important discrimination, between the CR and B&R groups, the dose and shape were found to be the most valid factors. In particular, a statistical significance was found relating average dose and kurtosis. It may be that the function relating these groups classifies a case by measuring the degree of volume concentration around a specific dose.

The B&R and COMP groups had opposite relationships between kurtosis and skewness, and their volume distributions deviated from normal distributions (Fig. 2a). For these groups the dose factors were more important than the factors concerning shape. Comparing the CR and COMP groups no one parameter was found to be dominant and the prediction indicated the lowest value in the COMP group. Therefore, further investigation will be required for other complication-inducing factors.

It is sometimes necessary to modify the initial treatment plan. The functions presented here are useful for optimization in such a case. There will be two methods of modification: one is to alter the treatment time and the other is to change the positions of the needles. The shape of the volume–dose histogram, *i.e.* skewness and kurtosis, depends mainly on the arrangement of sources, and its position on the abscissa of the histogram (average dose) depends mainly on the overall time of implantation. Therefore, knowing the relationship between these parameters it is possible to predict the result of an implant and to describe the method of modification. For instance, the uncontrolled cases (Cases 28, 29 and 33), with the same skewness and kurtosis as the controlled cases (Fig. 2a), would be expected to improve with a change in the time factor, whereas in the cases with complications (Cases 35 and 37) it would be necessary for some of the needles to be repositioned.

The cases in this analysis were treated with radium, but the results should provide a basis for application to other sources, *e.g.* iridium.

Acknowledgment

The authors thank Dr T. Okuyama, Dr Y. Mochizuki, Prof. K. Noda, Mr Y. Kyuma, and Miss M. Ishii for the assistance in the preparation of the manuscript. This study was supported in part by a Grant-in-Aid for Scientific Research No. 62570469 from the Ministry of Education, Japan.

References

ANDERSON, L. L., 1986. A "natural" volume–dose histogram for brachytherapy. *Medical Physics*, *13*, 898–903.

AWWAD, H. K., BURGERS, J. M. V. & MARCUSE, H. R., 1974. The influence of tumor dose specification on the early clinical results of interstitial radium tongue implants. *Radiology*, *110*, 177–182.

BURGERS, J. M. V., AWWAD, H. K. & LOARSE, R. V. D., 1985. Relation between local cure and dose–time–volume factors in interstitial implants. *International Journal of Radiation Oncology, Biology, Physics*, *11*, 715–723.

FISHER, R. A., 1950. *Statistical Methods for Research Workers* (Oliver and Boyd, London).

GILLIN, M. T., KLINE, R. W., WILSON, J. F. & COX, J. D., 1984. Single and double implants: a comparison of the Manchester system with the Paris system. *International Journal of Radiation Oncology, Biology, Physics*, *10*, 921–925.

GOODWIN, P. N., QUIMBY, E. H. & MORGAN, R. H., 1970. In *Physical Foundation of Radiology*. 4th edn (Harper and Row, New York).

HORIUCHI, J., OKUYAMA, T., SHIBUYA, H. & TAKEDA, M., 1982. Results of brachytherapy for cancer of the tongue with special emphasis on local prognosis. *International Journal of Radiation Oncology, Biology, Physics*, *8*, 829–835.

HORIUCHI, J., SHIBUYA, H. & TAKEDA, M., 1986. Role of radiation therapy in the multimodal treatment of head and neck cancer. *Japanese Journal of Cancer Chemotherapy*, *13*, II, 1717–1724.

LACHENBRUCH, P. A., 1975. *Discriminant Analysis* (Hafner Press, New York).

LAUGHLIN, J. S., SILVER, W. M., HOLODNY, E. I. & RITTER, F. W., 1963. A dose description system for interstitial radiation therapy. Seed implant. *American Journal of Roentgenology*, *89*, 470–490.

MARINELLO, G., VALERO, H., LEUNG, S. & PIERQUIN, B., 1985. Comparative dosimetry between iridium wires and seed ribbons. *International Journal of Radiation Oncology, Biology, Physics*, *11*, 1733–1739.

MCCRAE, D., RODGERS, J. & DRITSCHILO, A., 1987. Dose–volume and complication in interstitial implants for breast carcinoma. *International Journal of Radiation Oncology, Biology, Physics*, *13*, 525–529.

MEREDITH, W. J., 1967. *Radium Dosage—The Manchester System*. (Livingstone, London).

MULLER-RUNKEL, R. & VIJAYAKUMAR, S., 1987. Brachytherapy implants with differently spaced Ir-192 seeds: a dosimetric study. *Radiology*, *165*, 271–274.

PIERQUIN, B., DUTRIX, A., PAINE, C. H., CHASSAGNE, D., MARINELLO, G. & ASH, D., 1978. The Paris system in interstitial radiation therapy. *Acta Radiologica Oncology*, *17*, 33–48.

TOKITA, N., KIM, J. H. & HILARIS, B. S., 1980. Time–dose–volume considerations in iodine-125 interstitial brachytherapy. *International Journal of Radiation Oncology, Biology, Physics*, *6*, 1745–1749.

1989, *The British Journal of Radiology*, 62, 64–67

Results of treatment of carcinoma of the uterine cervix using the Newcastle afterloading technique

By P. J. D. K. Dawes, MB, BS, FRCR, *E. M. Dean, BSc, MSc and *G. D. Lambert, BSc, MSc

Regional Radiotherapy Department and *Regional Medical Physics Department, Newcastle General Hospital, Newcastle upon Tyne

(*Received March 1988 and in revised form May 1988*)

Abstract. Eighty-seven patients with carcinoma of the uterine cervix were seen between 1 August 1977 and 31 December 1985. Seventy-one patients were treated radically. A combination of intracavitary radiotherapy, using the Newcastle manual afterloading technique, and external-beam radiotherapy was used. The actuarial 4-year survival for all Stage 1 cervical carcinomas was 84.9%. For Stage 2 cancers the actuarial local control rate was 71.1% and the survival 49.2%, and for Stage 3 cancers the 4-year actuarial local control rate was 24.3% and the survival 14.8%. Complications of treatment were confined to the bowel and bladder and occurred in 11.5% of cases. The results of treatment of Stage 1 cancer suggest that the intracavitary technique gives a satisfactory distribution of radiation. The results of treatment of more advanced cases are disappointing and suggest that improvements are possible for some patients (*i.e.* wedge malalignment patients). There is sufficient flexibility in the technique for it to be applied satisfactorily for most anatomical situations.

In 1972 a manual afterloading system for gynaecological intracavitary radiotherapy was commissioned in Newcastle upon Tyne (Clayton & Ross, 1975). This paper describes the results of treatment of a series of 87 cases of carcinoma of the cervix referred from 1 August 1977 to 31 December 1985. In January 1986 a remote afterloading version of the system was introduced (Dean et al, 1988).

Patients and methods

Patients were staged prospectively using the FIGO system. The division of cases by stage and treatment intent is shown in Table I. The eight cases who had had either a simple abdominal or vaginal (one case) hysterectomy as the initial procedure were treated at the time of referral to the radiotherapy department. In one of these cases referral was delayed for some months. The histological grade of the squamous cell carcinomas was given in 59 cases but the numbers are too small to correlate histological grade to outcome. Seven adenocarcinomas of the cervix were seen. The relationship between age at presentation and stage is shown in Table II. The distribution of Stage 1 cases with age is not significantly different ($\chi^2 = 2.206$) although the trend is for younger patients to have Stage 1 disease.

Table I. Stage of disease and treatment

Stage	Previous non-radical surgery	Radical radiotherapy	Palliative radiotherapy	Total
Stage 1	8	22	—	30
Stage 2	—	21	3	24
Stage 3	—	24	1	25
Stage 4	—	4	4	8
Total	8	71	8	87

The intention was to treat all patients by a combination of external-beam and intracavitary radiotherapy. For Stages 1b and 2 the treatment was initially by two intracavitary insertions 1 week apart, with 35 Gy being given to Point A on each occasion. This was delivered over an average of 45 h at the beginning of the study period but by 1983 the time had risen typically on average to 52 h. Therefore, at that time it was decided to use three intracavitary insertions giving 24 Gy to Point A. The insertions were made at weekly intervals. This total dose of 72 Gy to Point A in three insertions over 17 days was considered biologically equivalent to 70 Gy to Point A in two insertions over 9 days.

The external-beam radiotherapy given to Stage 1b and 2 patients was aimed to treat the parametria. The central 6 cm of the field (at 10 cm depth) was shielded by a shaped lead block (gynae wedge). The parametria received 36 Gy in 15 daily fractions to the mid-plane and the portion of the pelvis shielded by the gynae wedge received 6 Gy (16.7% of the mid-plane dose) from scattered radiation when 4 or 8 MV X rays were used (the gynae wedges were designed for each machine).

Table II. Stage of the disease and age

Age (years)	Stage 1	2	3	4	?	Total
20–35	4	—	1	1	—	6
36–50	7	4	3	1	1	16
51–65	13	11	14	2	—	40
66+	5	7	7	4	—	23
?	1	2	—	—	—	3
Total	30	24	25	8	1	88

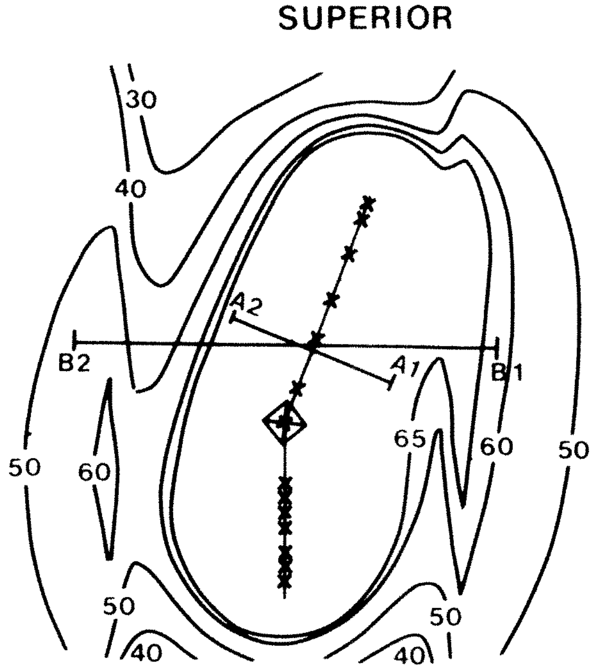

Figure 1. Arithmetical addition of three ^{137}Cs insertions and parametrial irradiation using 8 MV X rays. A total of 72 Gy was given to Point A in three insertions from the ^{137}Cs at weekly intervals. The parametria received 36 Gy in 15 daily fractions. The plane of calculation is coronal and there is no anteversion of the intrauterine source but it is tilted 10° to the left. X, ^{137}Cs sources; ⊠ origin, lowest uterine source.

For Stages 2b and 3 patients, if the above treatment regime could not be used, then 44 Gy modal dose was given in 20 daily fractions over 4 weeks to the true pelvis excluding the posterior two-thirds of the rectum. If possible an intracavitary treatment of 30 Gy to Point A was used at the end of treatment. Early in the series higher doses were given to the whole pelvis.

The treatment volume for the external-beam radiotherapy covered the following limits.

(1) The upper border of the volume was at the L5–S1 junction.
(2) The lower border of the volume was just below the obturator foramen (unless vaginal involvement by tumour suggested a lower level was appropriate).
(3) The lateral borders were each 1.0 cm clear of the bony pelvic side walls.

Patients were followed up at 3-monthly intervals for 3 years and then 6 monthly from then to 5 years. After 5 years follow-up was arranged close to the anniversary of treatment.

While Point A and B doses do not vary greatly with the lateral tilt of the uterine tube, major variations in dose occur in the tissues between Points A and B depending on the lateral tilt of the uterine tube (Fig. 1). It is not possible to apply these distributions retrospectively to the patients studied. However, the principle of high and low doses being due to lateral tilt of the uterine tube correlates with the result of treatment.

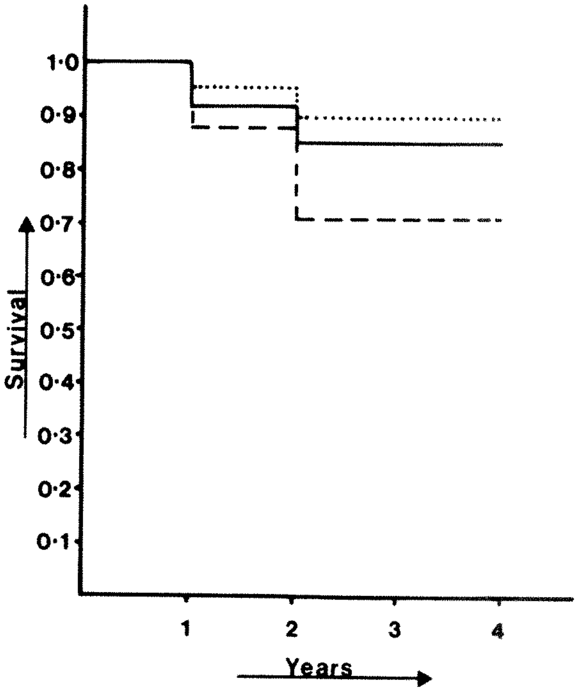

Figure 2. Actuarial survival for Stage 1 cervical cancers. (——) all cases, (– – –) simple hysterectomy cases and (. . .) radical radiotherapy cases.

Results

The actuarial 4-year survival for all Stage 1 cervical cancers was 84.9% (Fig. 2). For 22 Stage 1 cancers treated by radical radiotherapy alone the actuarial 4-year survival was 89.9% and for those Stage 1 cancers (eight) treated initially by a non-radical hysterectomy and radical radiotherapy the 4-year actuarial survival rate was 70·9%. This difference was not significant using statistical tests (χ^2).

For 21 Stage 2 cases treated radically the actuarial 4-year survival was 29.2% and the 4-year actuarial local control rate was 71.1% (Fig. 3). For Stage 3 cancers, the 4-year actuarial survival was 14.8%, for 24 cases treated radically and the 4-year actuarial local control rate was 24.3% (Fig. 3). Of nine Stage 4 cases, five were treated with radical intent and one of these has died. Of the 21 Stage 2 cases, only seven were Stage 2a and four of these seven survived. In one case the recurrence was associated with a low-dose region and in another widespread dissemination occurred despite local control. Of the 24 Stage 3 cancers, only four were Stage 3a and two of these four survived.

There is no evidence from this series that younger patients (<35 years) do worse in terms of either local control or survival when compared to older patients.

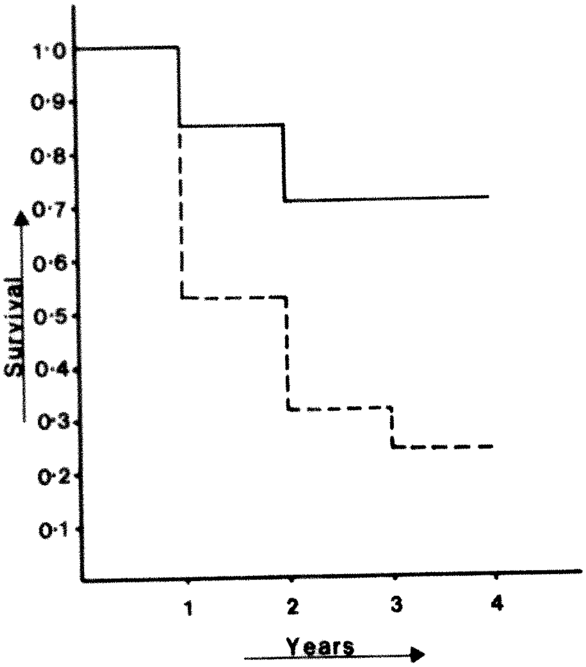

Figure 3. Actuarial local control for Stage 2 (——) and 3 (– – –) cervical cancers.

Examination of the combined external and intracavitary dose distributions in Stage 2 and 3 cases suggests that in two Stage 2 and two Stage 3 patients a fixed central position for the gynae wedge contributed to a failure due to low dosage of tumour bearing tissues secondary to a lateral tilt of the intrauterine tube.

Complications of treatment were confined to bowel and bladder. The details are shown in Table III. Total morbidity was 10/87 (11.5%). Nine of 10 cases suffering morbidity had serious morbidity and one of 10 died from complications. Four cases of bowel damage can be correlated with the position of the gynae wedge in relation to the intracavitary sources or in one case failure to achieve a satisfactory ^{137}Cs insertion for anatomical reasons. No cases of failure or morbidity can be attributed to the use of flexible uterine tubes to carry flexible uterine source trains.

Table III. Complications of radiotherapy

Stage	Complication	"Total" dose to Point B (Gy)
1B	Mild rectal	64.6
1B	Bladder (treated by partial cystectomy)	55.6
1B	Rectum (Colostomy)	54.9
2A	Rectum	53.2
2B	Fatal bowel	56.2
2B	Mild bowel	48.0
2B	Rectum	57.5
2B	Sigmoid (resection of affected area)	54.5
3B	Bowel	56.2
3B	Rectal	59.5

Discussion

A comparison of the results of treatment from a number of centres (Mould & Staffurth, 1979) showed a wide range of figures. The figures reported here are comparable but the results of treatment for Stage 2 and 3 cancers fall at the lower end of the ranges. Comparison with more recent reports leads to the same conclusions (Wiernik, 1986; Yeoh & Spittle, 1986; Meanwell et al, 1988.)

The physical features of the Newcastle system have been discussed in detail elsewhere (Dean et al, 1988). The dose around the cervix is high and comparable to that achieved by the Manchester system. The results of treatment for Stage 1 disease clinically confirm that this distribution is satisfactory and that an adequate radiation dose is used.

An examination of reported distributions suggests that serious morbidity is unusual below a combined intracavitary and external-beam radiation dose of 54.5 Gy at Point B. There are limitations when combining the dose contributions from low- and high-dose-rate regimes but the authors feel that some attempt is better than none. In this series seven of 10 cases suffering morbidity received a combined dose greater than 54.5 Gy to Point B. The intracavitary contribution was given at standard (57–83 cGy h^{-1} at Point A) dose rates. In six of the 10 cases with serious morbidity the greater contribution to this dose at Point B was from four-field external-beam therapy and in the other four cases the gynae wedge position cannot be regarded as satisfactory because the dose between Points A and B rose steeply (Fig. 1). Recent work has suggested that a redesigned gynae wedge (Dean et al, 1988) can obviate this type of problem.

Sutton (1986) has warned against rigid geometry in the design of intracavitary applicators because there is poor conformation of the radiation sources to the local anatomy if there is distortion caused by the presence of tumour. In the design of the Newcastle applicator a flexible uterine tube was considered essential to avoid splinting of the uterus. None of the morbidity in this series can be attributed to the uterine tube. The Newcastle applicators are made in four sizes both with and without rectal shields and an appropriate applicator to fit the anatomy can normally be found without difficulty.

In conclusion, the results of treatment of Stage 1 cancers of the cervix suggest that the intracavitary system employed in this series gives satisfactory dose distributions. The level of bowel and bladder complications at doses to Point B of less than 54.5 Gy (combined external and intracavitary doses) is acceptable. If an external-beam treatment to the parametria is used the shielding of the central volume must be carefully planned.

Acknowledgments

We would like to thank our colleagues Mr C. B. Clayton of the Regional Medical Physics Department and Dr R. G. B. Evans and Mr W. M. Ross of the Regional Radiotherapy Centre for their stimulation and interest, Mr R. Gillon and Mr D. Jewers of the Regional Medical Physics Department for practical technical advice, Mr K. Lambert of the Regional Medical Physics Department for drawing the figures and Mrs J. Deans for typing the manuscript. ICI Ltd kindly supplied the methyl methacrylate monomer used in the manufacture of the applicators without charge.

References

CLAYTON, C. B. & ROSS, W. M., 1975. Simple afterloading techniques. 2. The Newcastle technique. *British Journal of Radiology, 48*, 947.

DEAN, E. M., LAMBERT, G. D. & DAWES, P. J. D. K., 1988. Gynaecological treatments using the Selectron remote afterloading system. *British Journal of Radiology, 61*, 1053–1057.

MEANWELL, C. A., KELLY, K. A., WILSON, S., ROGIUSK, C., WOODMAN, C., GRIFFITHS, R. & BLACKLEDGE, G., 1988. Young age as a prognostic factor in cervical cancer: Analysis of population bases data from 10002 cases. *British Medical Journal, 296*, 386–391.

MOULD, R. F. & STAFFURTH, J. F. 1979. Carcinoma of the cervix at the Royal Marsden Hospital, London 1962–70. Survival and results. *British Journal of Radiology, 52*, 157–158.

SUTTON, M. L., 1986. Gynaecological radiotherapy. In *Radiotherapy in Clinical Practice*, ed. by H. F. Hope-Stone (Butterworth, Guildford) pp. 203–237.

WIERNIK, G., 1986. The combination of radiotherapy and surgery in the treatment of carcinoma of the uterine cervix. *British Journal of Radiology, 59*, 97–105.

YEOH, E. & SPITTLE, M. F., 1986. The treatment of carcinoma of the cervix and poor-risk endometrial carcinoma using the cathetron at the Middlesex Hospital: Experience since 1979. *Clinical Radiology, 37*, 165–168.

1989, *The British Journal of Radiology*, 62, 68–69

Technical notes

An indwelling intrauterine tube to facilitate intracavitary radiotherapy of carcinoma of the cervix

By B. J. Smit, MMedRadT(UCT), *J. P. du Toit, MMed(O&G), MD(Stell) and
†W. A. Groenewald, PhD(Stell)

Departments of Radiotherapy, *Gynaecological Oncology and †Medical Physics, University of Stellenbosch Medical School and Tygerberg Hospital, PO Box 63, Tygerberg 7505, Republic of South Africa

(*Received July 1988*)

This paper aims to show that the indwelling intrauterine tube (IIUT) is safe and can abolish repeated anaesthetics and large doses per fraction (Joslin et al, 1972) typical of high-dose-rate afterloading intracavitary treatment of carcinoma of the cervix. High-dose-rate schedules for Stage IB disease require as many as 12 (Liversage, 1969) to 17 (Dale, 1985) fractions for radiobiological equivalence with low-dose-rate schedules.

The purpose of the IIUT is to act as a semi-permanent channel for the applicator tube of the afterloading unit. We use the Gammamed II with a single high-activity ^{192}Ir source (Busch et al, 1977), but the IIUT could probably be adapted for use with any brachytherapy machine or even manual afterloading systems.

The tube (Fig. 1) is turned from nylon with a maximum outside diameter of 8 mm measured across the retaining ridges. Three holes of 2 mm diameter are drilled through the 15 mm diameter flange. A stainless steel marker is press-fitted into the middle hole and the other two holes are for suturing the tube to the cervix when necessary. A central canal of suitable diameter is drilled to within 2 mm of the tip and two lateral holes are drilled near the tip into this central canal, providing effective drainage, which is useful to avoid delay in cases of pyometra. The closed end of the tube prevents accidental perforation of the uterus by the applicator tube. Standard tubes are 50 mm in length, but shorter or longer tubes are useful on occasion.

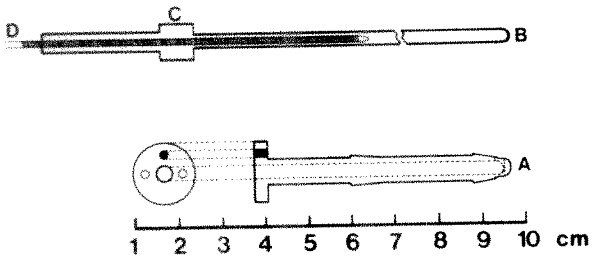

Figure 1. The indwelling intrauterine tube (A) with applicator tube (B); C is a coupling and D the drive cable with the 1 mm × 1 mm ^{192}Ir source welded to the tip.

The tube is inserted in theatre under sterile conditions (general or local anaesthesia). The cervix is dilated to 8 mm and the tube inserted till the flange is seated firmly against the cervix. If the cervical "grip" is good, no stitches are needed. The tube is left *in utero* for 4–25 days, depending on the number of fractions to be delivered.

Treatment is an outpatient procedure, because the IIUT eliminates the need to re-dilate the cervix. The specific technique is a matter of preference, but we used the technique of Kumar to displace the bladder and the rectum (Fig. 2) (Kumar et al, 1977). The reference

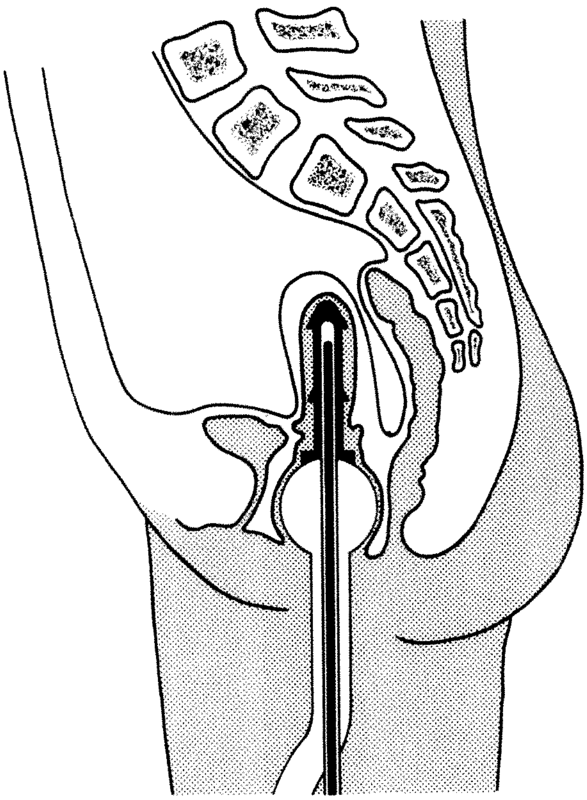

Figure 2. The indwelling intrauterine tube in position.

1989, *The British Journal of Radiology*, 62, 69–71

Table I. Fractionation schedules employed for ^{192}Ir and for ^{226}Ra

Nuclide	Patient no.	Fraction no.	Dose per fraction (cGy)	Total time (days)	Total dose (cGy)	TDF at Point A[a]
^{192}Ir	27	8	500	11	4000	105
	20	11	400	17	4400	105
	2	12	410	18	4920	116
	3	16	360	25	5760	116
^{226}Ra	34	3	2340	16	7020	125

[a] TDF values were calculated using the formulae of Orton and Ellis (1973) and Goitein (1976).

isodose surface is a cylindroid 40 mm × 40 mm × 90 mm; rectal and bladder dose on average were < 50% of the dose at Point A (International Commission on Radiological Units and Measurements (ICRU), 1985).

A subgroup of 86 patients with Stage IB disease was treated with a combination of pre-operative intracavitary radiotherapy followed by a Wertheim–Meigs radical hysterectomy 6 weeks later. In all these patients the effects of intracavitary radiation could be studied without the confusing effects of teletherapy. Of these, 51 were treated with the Gammamed II, and 34 with radium. The dose per fraction and total doses used were as shown in Table I.

The cervix was microscopically clear of tumour in 44/51 or 86.2% (^{192}Ir) and 32/34 or 94.1% (^{226}Ra). The 4-year actuarial survival rates (Kaplan & Meier, 1958) were 90.4% (^{192}Ir) and 94.1% (^{226}Ra). Minor acute reactions were seen in 3/51 (5.9%) and 2/34 (5.8%), respectively. No serious infections or late complications were seen.

In conclusion, the indwelling intrauterine tube caused no serious infection, eliminated multiple anaesthetics and made fractionated high-dose-rate remotely controlled intracavitary therapy a cost-effective, safe and easily tolerated outpatient procedure, with results similar to those of a comparable radium technique. The tube may also prove useful for low-dose-rate and manual afterloading techniques.

References

Busch, M., Makoski, B., Schulz, U. & Sauerwein, K., 1977. Das Essener Nachlade Verfahren. *Strahlentherapie*, *153*, 581–588.

Dale, R. G., 1985. The application of the linear-quadratic dose-effect equation to fractionated and protracted radiotherapy. *British Journal of Radiology*, *58*, 515–528.

Goitein, M., 1976. Review of parameters characterising response of normal connective tissue to radiation. *Clinical Radiology*, *27*, 389–404.

ICRU, 1985. *Dose and Volume Specification for Reporting Intracavitary Therapy in Gynaecology*, ICRU Report no. 38 (ICRU Publications, Bethesda).

Joslin, C. A. F., Smith, C. W. & Mallik, A., 1972. The treatment of cervix cancer using high activity ^{60}Co sources. *British Journal of Radiology*, *45*, 257–270.

Kaplan, E. L. & Meier, P., 1958. Non parametric estimation from incomplete investigations. *Journal of the American Statistics Association*, *53*, 475–481.

Kumar, P. P., Henschke, U., Ulrich, K. & Mahan, D. G., 1977. *Journal of the National Medical Association*, *69*, 27–28.

Liversage, W. E., 1969. A general formula for equating protracted and acute regimes of radiation. *British Journal of Radiology*, *42*, 432–440.

Orton, C. G. & Ellis, F., 1973. A simplification in the use of the NSD concept in practical radiotherapy. *British Journal of Radiology*, *46*, 529–537.

A source localizing technique for the microSelectron-HDR afterloading system

By Colin H. Jones, PhD, CPhys, FInstP

The Joint Department of Physics, Institute of Cancer Research and Royal Marsden Hospital, Fulham Road, London, SW3 6JJ

(*Received July 1988*)

The microSelectron-HDR is a high-dose-rate remote afterloading system which uses a single miniature 370 GBq (10 Ci) ^{192}Ir source. The source can be remotely afterloaded into a 1.9 mm diameter catheter for treatment of bronchial and oesophageal carcinoma or into an 18-channel indexing system for high-dose rate interstitial implants. It can also be used with applicators designed to treat gynaecological disease. The machine has a control unit which can be programmed to position the source for a specified period of time within each applicator. The source is cable driven and its position can be varied in steps of 2.5 mm. The relative position of a source configuration can also be altered in 1 mm intervals. This flexibility provides considerable clinical advantage over systems which rely on fixed source configurations. However, the very large number of source positions that are obtainable highlights the importance of carrying out source localization checks.

Programmed source positions within an applicator or catheter should be checked regularly to confirm that machine function is within acceptable limits. At the

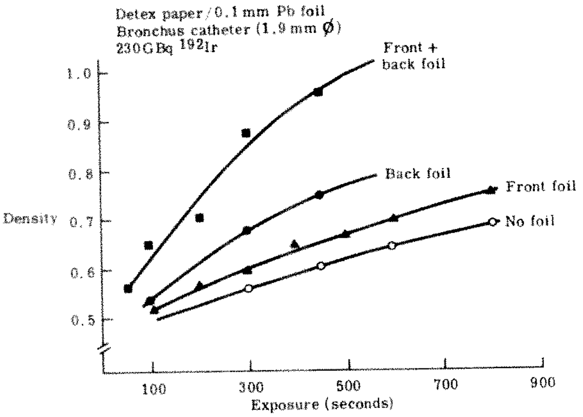

Figure 1. Density variation against exposure.

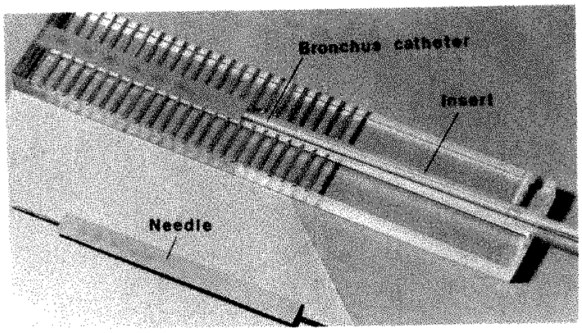

Figure 2. Perspex test jig for checking source positions in catheters and needles.

very least this will be necessary after every iridium source replacement, which takes place every 3 months or so.

In the case of low-dose-rate afterloading systems, quality assurance checks on source positioning are usually made with film. Kodak X Omat V film is useful for this purpose. It has a sensitivity which allows convenient exposure times of a few minutes and with the aid of lead foil markers it is possible to identify precisely where sources are located inside catheters or applicators (Jones, 1988). By contrast, the surface dose-rate of the microSelectron-HDR source is too high for optimal film exposure. For example, the dose-rate on the surface of a bronchus catheter will be about 30 kGy h^{-1} and consequently film exposure times become similar to the transit time of the iridium source.

We have found self-adhesive Detex radiation-sensitive paper to be a very useful alternative to film for recording radioactive source positions. Detex paper is designed to change colour when a specified dose of radiation is approached. Detex labels, for example, are used to indicate whether a product has received a sterilizing dose of radiation. Before exposure the paper is yellow in colour; under irradiation by γ rays or high-energy electrons, hydrochloric acid is released from the ink and the yellow azo dye turns red. The manufacturers emphasize that the shade of red does not indicate the amount of irradiation and that Detex paper is not a dosemeter in that specific levels of radiation are not indicated. However, the paper can be used in situations where the total radiation dose falls between 1 and 100 kGy. The colour change is less pronounced below 1 kGy and above 100 kGy the colour change may be lost altogether.

For a 370 GBq iridium source, the dose-rate on the surface of a microSelectron-HDR bronchoscope catheter is such that a 10 kGy exposure would be about 1000 s. Exposures of this magnitude are inconvenient, especially when multiple source positions have to be checked. This difficulty has been overcome with the aid of lead foil screens. Electron emission from the foil increases the local dose to the Detex paper analogous to the way in which film screens reduce exposure dose requirements in radiography. Detex paper is sandwiched between two thin lead foils and placed in contact with or wrapped around the catheter or applicator being investigated.

Table I shows that the back scatter is not dependent critically on the lead thickness. In contrast, forward scatter is increased by thin foil but for thicknesses > 0.1 mm radiation absorption in the lead and the inverse-square-law effect result in dose-rate reductions. Figure 1 shows the exposure against density curves for a 230 GBq ^{192}Ir source and illustrates the relative effects of front and back lead foils. Detex paper changes from yellow to red during exposure. The density measurements shown were made with a Macbeth reflection densitometer. A density increase of 0.3 measured with a magenta filter is readily detectable visually. There are obvious advantages in using foil that is malleable and easily cut, and with a front and back foil of 0.1 mm lead, a sixfold increase in sensitivity can be achieved.

Although Detex is unsuitable for dosimetry, it does provide a convenient and precise method of recording source location. We have found it to be particularly useful for machine commissioning measurements and for checking the microSelectron-HDR machine after source changes. It has been used for recording source positions in gynaecological applicators, implant needles and bronchus catheters. Optimal exposures are typically 200–600 s according to the source activity and the diameter of the applicator.

Table I. Variation of density with backscatter foil thickness for a constant exposure

Foil thickness (mm)	Density
0	0.56
0.1	0.73
0.2	0.73
0.3	0.70
0.4	0.72
40.0	0.71

The Perspex applicator jig shown in Fig. 2 has been designed to improve the precision of the source localization technique. The centre section of the device is removable and allows various Perspex inserts to be used for carrying needles, catheters or applicator tubes. Lead foil and strips of Detex paper (about 10 mm wide and as long as the active length of the configured source) are placed over the source carrier and an appropriate radiation exposure is made.

Detex is only slightly light sensitive and although it should not be exposed to bright light for long periods it can be used unwrapped. It is produced in sheet form by William Sessions Ltd of York, under licence by the United Kingdom Atomic Energy Authority (UKAEA).

Acknowledgment

The author gratefully acknowledges the advice of Mr B. Whittaker, UKAEA, Harwell.

Reference

JONES, C. H., 1988. Quality assurance in gynaecological brachytherapy. In *Dosimetry in Radiotherapy* (International Atomic Energy Agency, Vienna), IAEA-SM-298/58, Vol. 1, pp. 275–290.

Installation requirements for an argon laser angioplasty system

By P. H. Smithson, BEng, CEng, MIEE, *W. D. Jeans, FRCR and *P. Murphy, FRCR

Medical Equipment Management Organization and *Department of Radiology, Bristol & Weston Health Authority, Bristol

(Received December 1987 and in revised form July 1988)

The installation and running of an argon laser for angioplasty is described, together with the costs and safety aspects.

We have acquired a unit for the purpose of producing a passage through occluded arteries, and report here the pre-installation work required, the safety requirements and initial measurements on an argon laser (Optilase 900 supplied by Nycomed (UK) Ltd).

Installation

Argon lasers are similar to X-ray tubes in that they generate large amounts of heat for relatively small output powers (Carruth & McKenzie, 1986). Argon lasers have been used in laser-assisted angioplasty because they are stable and the blue/green frequency is absorbed well by blood.

A good water supply and drainage system is necessary to cool the laser. Interlocks are provided that will turn off the laser if the water pressure falls, so the water supply should preferably not have many other users as this will cause pressure fluctuations.

Most normal hospital water supplies would not be suitable without some modification. We have installed a high-pressure supply, normally taken to laboratories, but have still experienced changes in pressure, and a water pump may be necessary to ensure a good head of water. A simple pump could be used to maintain a flow of 18 litres/min at 50 lb/in^2. A flow-rate gauge or a pressure meter is also useful to check the flow. If the water has a high calcium or aluminium level, then softened water must be used. There are no water temperature limitations (Trimedyne, 1987).

On the electrical side, the power supply necessary is similar to that used on a modern X-ray generator. The three-phase supply must be clean—not connected to other generators—and capable of giving 23 kVA. An isolation step-down transformer is required to reduce the three-phase 415 V to 208 V. Its size is 0.65 m long by 0.31 m wide by 0.61 m high.

Figure 1 shows a typical gas laser. The laser mirror system is easily disturbed when the equipment is moved and it is preferable to use it in one room only. This also avoids the problem of providing multiple water supplies, drainage systems and transformers. The working system and power supply must be positioned in the X-ray room and space is also needed to one side for storage of the laser and its connections when not in use.

The argon laser is 2.29 m long by 0.56 m wide and 1.09 m high, and if it is not to be left permanently connected to water/electrical supplies, plugs and sockets for connection are needed. A maximum of 2–3 m of cabling is recommended to avoid staff tripping over cables during use. Figure 2 shows the laser in position in

Table I. Installation costs of the argon laser

	£
Water: pipes, connectors, meters and labour	200
Electrical supply: step-down transformer	1200
installation and connectors	1600
Safety goggles (two pairs for visitors)	360
Safety signs on two doors	35
Other warning signs (water pressure, shutter in/out, etc.)	45
Total	3440

These costs are for in-house (Works Department) labour. If outside contractors are used, the costs may be higher.

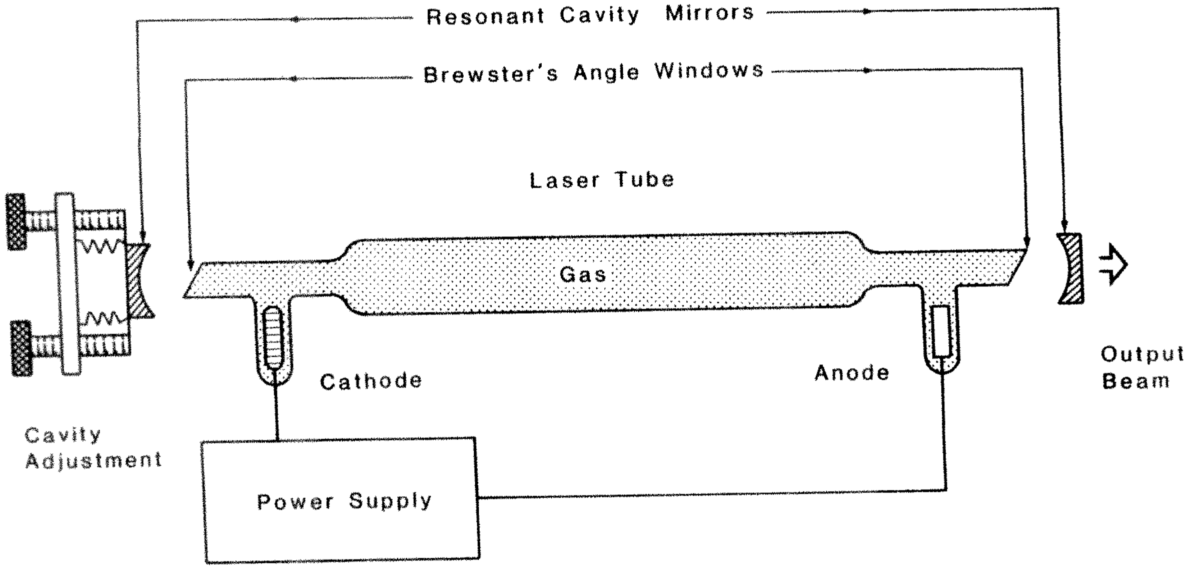

Figure 1. Diagram of a gas laser.

the angiography room. The costs of installation are shown in Table I.

Setting up

Gases

Nitrogen gas is used to keep the optical system dust-free. A small cylinder of oxygen-free nitrogen, using a flow rate of 0.1 litre/min, lasts about 50 h. Argon gas is used very slowly. A reservoir cylinder is plumbed permanently into the laser and a small amount of gas is taken from this every 3–6 months.

Frequency of checking/calibration

The laser needs to be run up weekly to keep the output to its normal level and to check the output power. The time needed for this is 1 h in total. The laser system is cleaned and calibrated fortnightly and a manufacturer's service representative carries out a full calibration and safety check every 3 months.

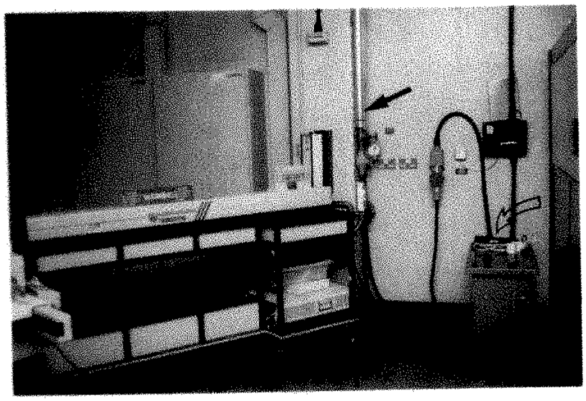

Figure 2. Argon laser system in position in the angiography room. Water supply with cables leading to the laser (→) and step-down transformer leading to the laser power supply (⇒).

Probes

The 2 mm Laserprobe (Trimedyne Inc.) is suitable for single use only, since coagulation occurs on the tip during use. It consists of a metal probe tip with a metal wire attached to this to enable the tip to be removed if it becomes detached. There is also a catheter "torque" wire and 4 m of Teflon-coated glass optical fibre. At the end of the fibre is a screw connector (Fig. 3).

Probes are supplied unsterilized coiled inside a plastic tube inside a sealed bag. Before use, the probe is sterilized by placing it inside the plastic tube container in a tray of sterilizing solution such as Cidex for 24 h. The probe remains in the tray until required for angioplasty. At that time, it is uncoiled from its tubing and cleansed of the sterilizing solution with saline. The proximal end is coupled to the laser and the distal end (metal tip) passed into the artery via an 8 F introducer.

Table II. Running costs of the argon laser (cost per case)

	£
Oxygen-free nitrogen gas (£8 per 50 h) (includes monthly cylinder rental charge)	0.32
Metal-tipped fibre-optic probes	300.00
Water costs at 2.6 m^3/case (costs are 25p/m^3 for water and 37p/m^3 for sewerage)	1.67
Electricity costs: 23 kVA, time 2 h (4.5p/unit)	2.07
Maintenance contract (£6400 per annum with an average of 50 patients/year)	128.00
Total cost per case	432.06

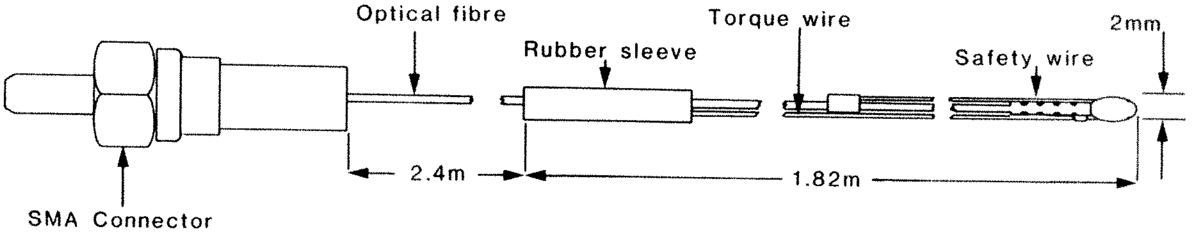

Figure 3. Diagram of the probe.

Maintenance

The potential purchaser should consider who will maintain the laser. The laser uses high voltages and high levels of ultraviolet radiation and experienced staff are needed, with both electrical and laser knowledge (Institute of Physical Sciences in Medicine (IPSM), 1987). Training can be provided by the manufacturer for local maintenance engineers. Most laser manufacturers will give first-line training to hospital staff to avoid service engineers having to attend to minor problems.

Safety aspects

The laser has an output of 12 W which makes it a Class IV laser and, therefore, it can only be used in a laser controlled area (BSI, 1983; DHSS, 1985).

A local Laser Protection Advisor should give advice in the same way as the Radiation Protection Advisor and local rules must be established. These rules must indicate the following.

(1) The boundaries of the controlled area.
(2) Control of access to the area.
(3) Who are the authorized users and maintenance staff.
(4) Who is the laser protection supervisor.
(5) Safety precautions to be employed.

In addition, doors must have warning notices and access must be restricted during use. Personnel closer than 2 m to the fibre or open laser should wear laser safety goggles, two pairs being provided with the equipment. The final aspect of safety is operator training. There is obviously a requirement for all users to be familiar with the laser operating procedures. In addition, however, the users should be taught about hazard control, use of personal protection equipment and accident reporting procedures.

Measurements

Beam divergence

As part of the initial acceptance tests, the physics staff measured the angle of divergence of the laser beam. This gives an indication of the spread of the beam as it leaves the open fibre. In normal practice the laser beam is totally contained in the fibre-optic to the patient.

Nevertheless, the chance of a broken fibre was considered as a remote possibility. Using the test fibre, the beam measured 50 mm in diameter at a distance of 300 mm from the end of the fibre. The resulting beam divergence of 9.5° has been used to calculate safe distances from a broken fibre (McKenzie, 1985). There is a considerable risk of damage to the eye at 15 cm from a break and a slight risk at 1.5 m.

Output power/heating effect

The argon laser described here is capable of giving 17 W output power. In contrast, the fibre-optic and metal probe have a design limit of 12 W. The output power has been measured before entering the fibre-optic and also at the end of a test fibre and it was found that there may be up to 2 W of loss in the coupling to the fibre and in the fibre itself. Areas of high loss show up as bright/hot spots on the fibre, and the coupling to the laser is a weak point at which breakage occurs.

It is necessary to check that adequate tip heating is present before inserting the probe into the patient. The probe tip is put into sterile water and, once activated, the laser should be able to boil the water around the tip within 30 s. Failure to do so indicates a faulty probe or coupling. The probe must only be energized when in contact with water or tissue to prevent damage.

Acknowledgments

We are grateful to Mr John Peters, Superintendent Radiographer, for his co-operation and Mr D. F. Follett, Laser Protection Advisor, for his technical help.

References

BSI, 1983. *Radiation Safety of Laser Products and Systems*, BS 4803 (British Standards Institution, Milton Keynes).
Carruth, J. A. S. & McKenzie, A. L., 1986. *Medical Lasers Science & Clinical Practice* (Adam Hilger, Bristol).
DHSS, 1985. *Guidance on the Safe Use of Lasers in Medical Practice* (Her Majesty's Stationery Office, London).
IPSM, 1987. *Medical Laser Safety*. Report No. 48 (Institute of Physical Sciences in Medicine, York).
McKenzie, A. L., 1985. Safety with surgical lasers. *Journal of Medical Engineering and Technology*, *8*, 207–214.
Trimedyne, 1987. *Optilase 900 Contact Laser System Service Manual* (Nycomed (UK) Ltd, Birmingham).

1989, *The British Journal of Radiology*, 62, 74–77

Case reports

Van Buchem's disease with classical radiological features and appearances on cranial computed tomography

By *J. V. Cook, MRCP, FRCR, P. D. Phelps, MD, FRCS, FRCR and J. Chandy, FRCR

Department of Radiology, Walsgrave Hospital, Coventry

(Received May 1988 and in revised form June 1988)

Van Buchem's disease is a rare hereditary sclerosing dysplasia of bone which was first described by van Buchem, Hadders and Ubbens in the Netherlands in 1955. Their original description was of an autosomal recessive disease which particularly affects the skull, mandible and long bones, the characteristic feature of the latter being the endosteal deposition of bone, particularly in the diaphyses.

We present a patient who has the classical recessive form of the disease and has developed auditory and visual symptoms due to encroachment on cranial foramina by hyperostotic bone. The appearances on computed tomography (CT) are described.

Case report

This patient had an unusual appearance at birth. Her birth weight was below the 10th centile for her gestational age and she was noted to have a prominent forehead, a long anteverted upper lip and coarse wrinkling of the skin. She was born of unrelated parents after a full-term, normal delivery and pregnancy and there was no family history of any congenital diseases.

Growth and development progressed normally but a year later she developed a mild chest infection during which she had a chest radiograph which showed sclerosis of the clavicles, ribs and spines of the scapulae. A diagnosis of a sclerosing bone dysplasia was made and a later skeletal survey showed classical features of van Buchem's disease (Figs 1, 2, 3). Allied investigations were normal apart from a raised alkaline phosphatase of 820 i.u./l. She had a normal female karyotype.

At the age of 11 years, although there was minimal clinical auditory impairment, it was considered prudent to radiograph her petrous bones to assess any narrowing of the auditory canals with a view to instituting some preventive measures.

Coronal and lateral tomograms of the internal auditory meati accompanied by axial CT scans were performed (Fig. 4). All the bones of the base of the skull were found to be sclerotic with dense bone from the petrous pyramids causing severe encroachment upon the internal auditory meati (maximum diameter 1 mm) and narrowing of the foramina ovale. Surprisingly her hearing has remained within normal limits despite the severity of the radiological findings.

Recently the patient has reported some visual disturbances but no definite field defect. Plain radiographs again demonstrated some narrowing of the optic foramina (Fig. 5) but in view of her minimal symptoms, any surgical measures have as yet been considered inappropriate.

Discussion

Van Buchem and his colleagues first described this condition as "hyperostosio corticalis generalisata familiaris" in 1955, following the discovery of a peculiar sclerosing disease of the skeleton in a pair of twins, which did not fit into any particular category of the known bone dysplasias. Fosmoe gave the eponym of van Buchem's disease in his case report in 1968 and under-

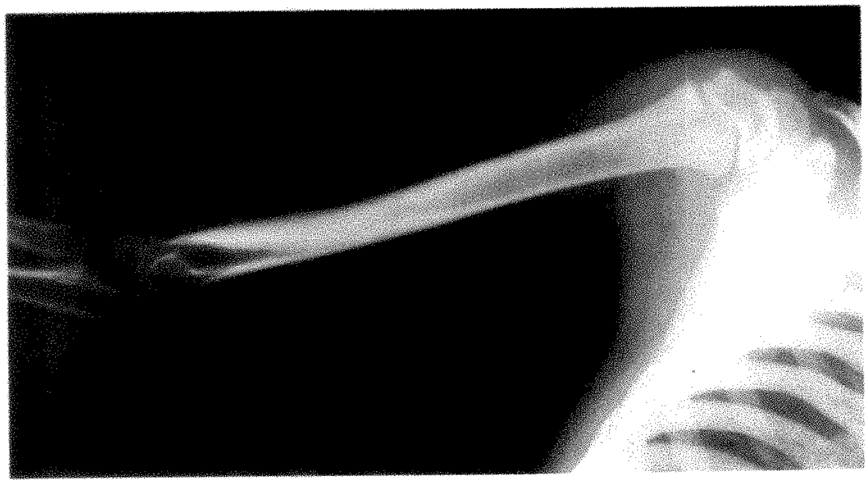

Figure 1. Antero-posterior view of the humerus showing classical endosteal deposition of bone in the diaphysis.

---

*Present address and address for correspondence: Department of Radiology, St George's Hospital, Tooting, London SW17.

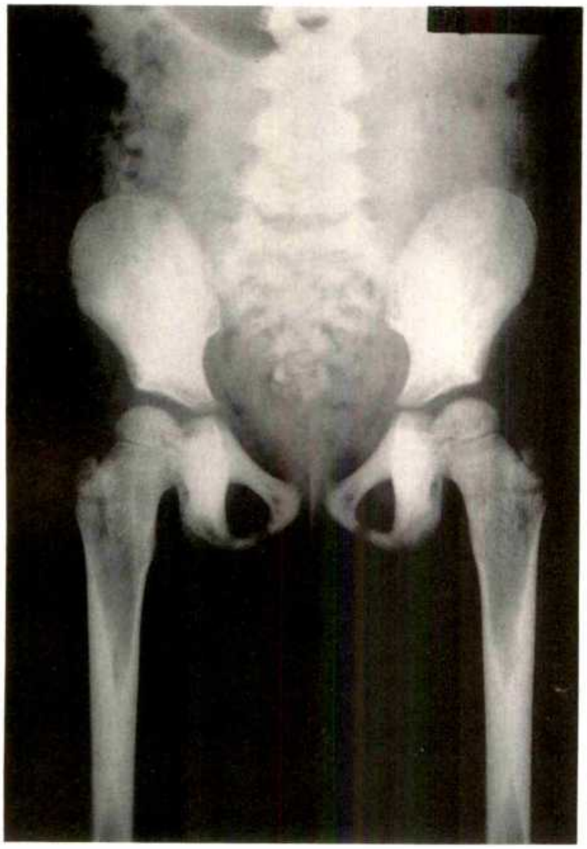

Figure 2. Antero-posterior view of the pelvis and upper femora demonstrating the dense endosteal sclerosis in the diaphyses of the femora, ischia, pubic arches and in the iliac bones adjacent to the acetabula.

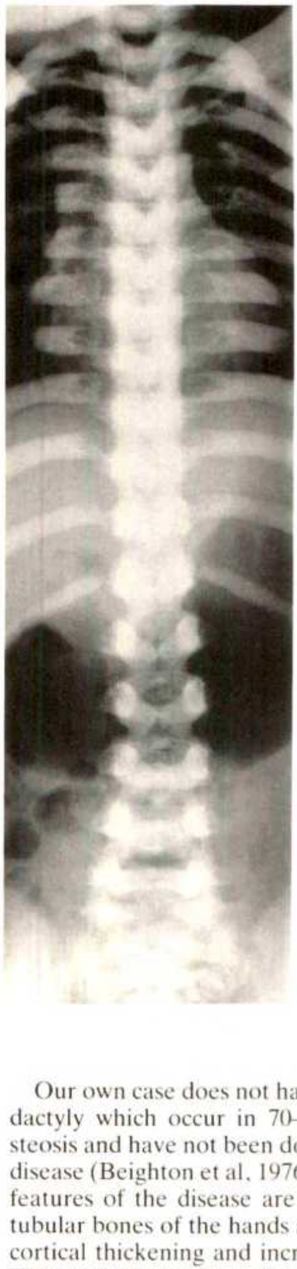

Figure 3. Antero-posterior view of the spine showing sclerosis particularly affecting the pedicles and posterior elements. The endosteal deposition of bone is also noted in the ribs and clavicles.

standably this is often used. Van Buchem added five further cases to the literature in 1962 and eight patients from the same family were described by him in 1971.

Additional cases have been described in the literature in various parts of the world and an increased incidence of rare bone dysplasias in the Afrikaner population of South Africa has been noted. The preponderance of the condition in people of Dutch origin is postulated to be the result of a plague in the Urk area of the Netherlands in 1637 where only 15% of the population survived and endogamous marriages were subsequently common (Jacobs, 1977). Our patient is not known to have any Dutch relations.

Van Buchem's original cases had an autosomal recessive inheritance, but autosomal dominant forms with endosteal hyperostosis have been reported. (Worth & Wollin, 1966; Owen, 1976; Gelman, 1977). The 1977 version of the Paris nomenclature on bone dysplasias described van Buchem's disease and sclerosteosis as separate entities but recent reports suggest that they may be phenotypic variants of the same condition (Beighton et al, 1984).

Our own case does not have the nail dysplasia or syndactyly which occur in 70–80% of cases with sclerosteosis and have not been documented in van Buchem's disease (Beighton et al, 1976). The classical radiological features of the disease are in the long bones and the tubular bones of the hands and feet where symmetrical cortical thickening and increased bone density occurs. This particularly affects the diaphyseal endosteum causing encroachment on the medullary canal. Our patient demonstrates these features particularly well (Figs 1, 2).

The posterior elements of the spine are more frequently involved than the vertebral bodies themselves. When the latter are affected, the density usually affects the central third of the vertebral body rather than the endplates (Fig. 3), in contrast to osteopetrosis. Distinguishing features from osteopetrosis include a raised alkaline phosphatase and absence of bone fragility.

The condition may be first detected in childhood, the typical features being ocular hypertelorism, mid-facial hypoplasia and prognathism. The latter usually becomes

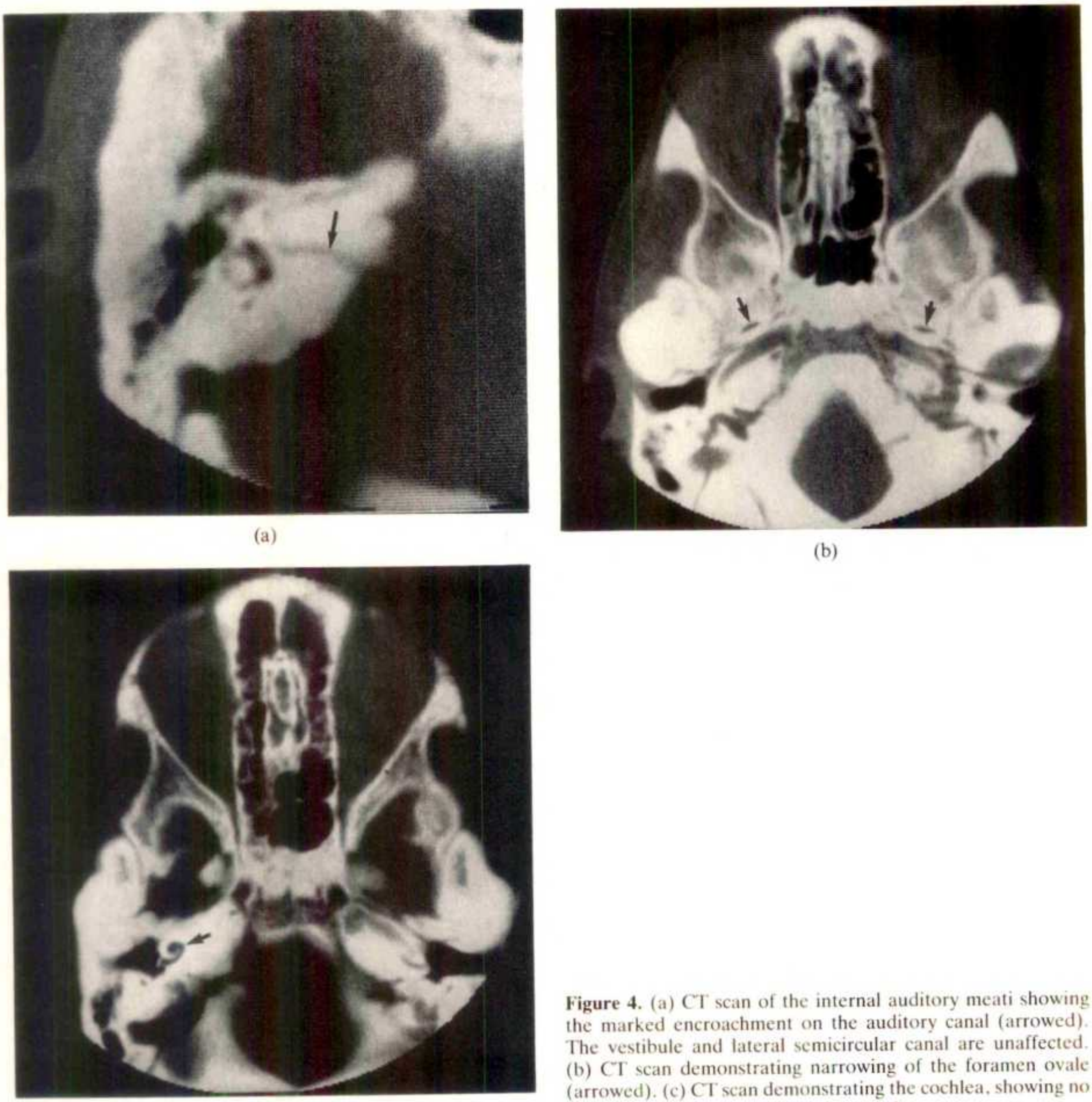

Figure 4. (a) CT scan of the internal auditory meati showing the marked encroachment on the auditory canal (arrowed). The vestibule and lateral semicircular canal are unaffected. (b) CT scan demonstrating narrowing of the foramen ovale (arrowed). (c) CT scan demonstrating the cochlea, showing no visible encroachment of bone (arrowed).

noticeable at puberty and all features progress with age. Some patients present later with facial nerve palsies, hearing loss or headaches due to raised intracranial pressure. The hearing loss is usually mixed conductive and sensorineural which commences about puberty.

Plain radiographs may be sufficient to show the degree of foraminal encroachment but CT is useful in providing a more complete demonstration of the anatomy. The appearances on CT include bony sclerosis of the petrous apices with loss of pneumatization of the mastoids and marked narrowing of the internal auditory meati involving the medial aspect first. The cochlear nerve and vessels are constricted in the narrowed internal auditory meatus and this is probably the cause of the sensorineural deafness. The conductive deafness is due to thickening and fusion of the ossicles, whose movement is also restricted by new bone formation in the surrounding epitympanic space.

The cranial foramina of the base of the skull are narrowed and although the actual measurements have a wide normal variation, the surrounding sclerosis is easily demonstrated and correlates with the clinical impairment. The foramen ovale is first affected. As in this case, radiology rarely shows changes in the cochlea, vestibule

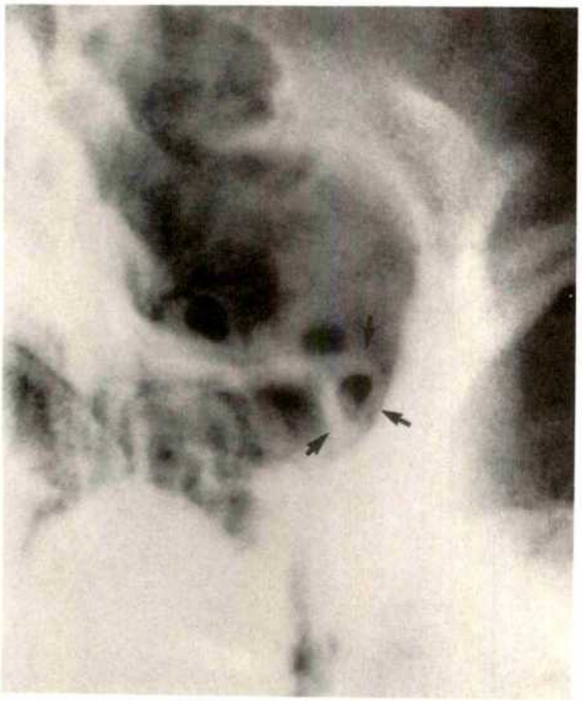

Figure 5. Optic foramen view showing the sclerosis around this foramen (arrowed).

or semicircular canals although the aqueducts may be narrowed. This was also noted in three cases of sclerosteosis reported by Hill et al (1986).

Exophthalmos is not unusual and may be associated with encroachment on the optic foramina causing early papilloedema followed by optic atrophy and visual field defects.

Cranial surgery may be debilitating and surgery on the ear can have high morbidity. Surgery is therefore usually reserved, as in craniectomy, for raised intracranial pressure or decompression of the optic canals when vision is threatened.

Because of its classical radiological features, the radiologist is often the first to make the diagnosis of van Buchem's disease. It is a chronic and incurable condition which may have considerable morbidity from cranial nerve encroachment and raised intracranial pressure.

Plain radiographs may show the degree of foraminal encroachment sufficiently but CT also plays a useful role in providing a more complete demonstration of the anatomy. However, investigation of these patients should be limited to those in which neurosurgical intervention is contemplated. The radiological features often appear far more severe than the clinical situation would suggest, and a careful clinical follow up is mandatory.

Acknowledgments

We would like to thank Mrs Pat Vecchi for her help with the preparation of the manuscript.

References

Beighton, P., Barnard, A., Hamersma, M. & Van Der Wouden, A., 1984. The syndromic status of sclereostosis and van Buchem's disease. *Clinical Genetics*, *25*, 175–181.

Beighton, P., Cremin, B. J. & Hamersma, H., 1976. The radiology of sclereostosis. *British Jounal of Radiology*, *49*, 934–940.

Fosmoe, R. J., Holm, R. S. & Roscoe, C. M., 1968. Van Buchem's disease (hyperostosis corticalis generalisata familiaris). A case report. *Radiology*, *90*, 771–774.

Gelman, M. I., 1977. Autosomal dominant osteosclerosis. *Radiology*, *125*, 289–296.

Hill, S. C., Stein, S. A., Dwyer, A., Altman, J., Dorwart, R. & Doppman, J., 1986. Cranial CT findings in sclerosteosis. *American Journal of Neuroradiology*, *7*, 505–511.

Jacobs, P., 1977. Van Buchem's disease. *Postgraduate Medical Journal*, *53*, 497–505.

Owen, R. H., 1976. Van Buchem's disease (hyperostosis corticalis generalisata). *British Journal of Radiology*, *49*, 126–132.

Van Buchem, F. S. P., 1971. Hyperostosis corticalis generalisata. Eight new cases. *Acta Medica Scandinavica*, *189*, 257–267.

Van Buchem, F. S. P., Hadders, H. N., Handsen, J. F. & Woldring, M. G., 1962. Hyperostosis corticalis generalisata. *American Journal of Medicine*, *33*, 387–397.

Van Buchem, F. S. P., Hadders, H. N. & Ubbens, R., 1955. An uncommon familial systemic disease of the skeleton. *Acta Radiologica*, *44*, 109–119.

Worth, H. M. & Wollin, D. G., 1966. Hyperostosis corticalis generalisata. *Journal of the Canadian Association of Radiologists*, *17*, 67.

1989, *The British Journal of Radiology*, 62, 78–79

Anomalous superior vena cava causing non-visualization of the lungs in perfusion scintigraphy

By A. Morgan, BSc and *N. Evans, MB, BCh

Department of Medical Physics and Bio-engineering, University Hospital of Wales, Heath Park, Cardiff, CF4 4XW and *Department of Radiology, Royal Gwent Hospital, Newport, Gwent

(*Received March 1988 and in revised form May 1988*)

^{99}Tc^{m}-labelled macro-aggregated albumin (MAA) is the most commonly used agent for lung perfusion imaging. In normal circumstances following intravenous injection, almost all of the MAA, after passage through the right heart, is trapped in the pulmonary capillaries. We present a case in which the lungs were not visualized following left antecubital vein injection of ^{99}Tc^{m}-MAA because of anomalous venous drainage from this side into the left atrium via a persistent left superior vena cava (SVC).

Case report

A 44-year-old, previously fit man presented with a 3-day history of right-sided, pleuritic type chest pain and dyspnoea. Physical examination revealed no evidence of finger clubbing or cyanosis but there were signs which suggested the presence of a right-sided pleural effusion. A blood count showed a normal haemoglobin level but a raised white cell count with neutrophilia. Chest radiography confirmed the presence of a right-sided, pleural effusion but, even in retrospect, was otherwise unremarkable. Pulmonary embolism was suspected and intravenous heparin therapy was commenced and a perfusion lung scan requested.

Following our standard technique, a left antecubital vein was selected and, using a butterfly needle and normal saline, 70 MBq of ^{99}Tc^{m}-MAA was administered. When imaging was commenced shortly afterwards the lungs were not visualized although activity was seen to be present in the kidneys. The immediate reaction was that a radiopharmaceutical other than that intended (*e.g.* ^{99}Tc^{m}-DTPA or some other renal agent) had been administered, despite the fact that the dispensing and checking procedures in the radiopharmacy based in the Medical Physics Department in Cardiff indicated that this was unlikely. During a repeat perfusion study performed 3 days later the gamma camera was placed in an anterior position over the patient's chest and data were acquired at a rate of 1 frame/s for the first 60 s following injection. This study showed that the whole injection passed directly into the left side of the heart and immediately into the aorta (Fig. 1).

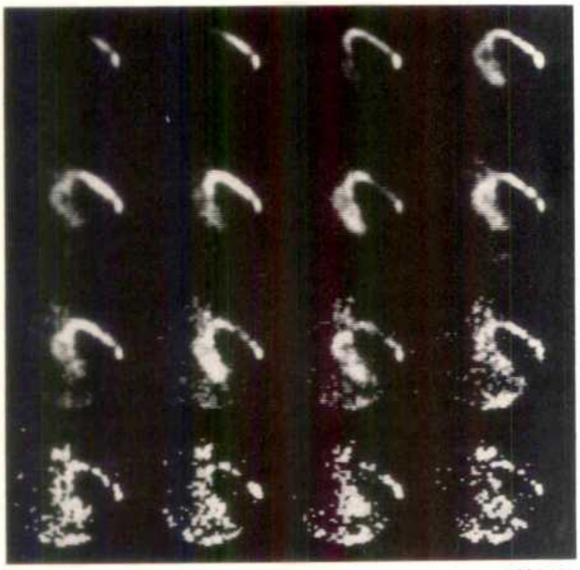

Figure 1. First-pass study following left arm injection of ^{99}Tc^{m}-MAA (anterior projection).

Nothing in the patient's history suggested any vascular abnormality but it was suspected that the findings were the result of anomalous drainage of a persistent left SVC into the left atrium. Subsequently, a perfusion lung scan was performed successfully following a right antecubital vein injection. Data were acquired dynamically for the first minute following injection and on this occasion showed normal passage of tracer into the right heart followed by a normal lung perfusion phase. The static images obtained indicated a low probability of pulmonary embolism and the final diagnosis was of post-pneumonic empyema.

It was felt that, under the circumstances, further investigations were not warranted and the patient was discharged from hospital.

Discussion

Persistent left SVC is a fairly frequent anomaly. Its incidence in the normal population has been estimated at 0.5% (Steinberg et al, 1953). In patients with congenital heart disease, the incidence is much higher and some authors suggest that it may be of the order of 10% (Sipila et al, 1955; Buirski et al, 1986). Various different classifications of SVC anomalies have been proposed, based on embryological, anatomical, physiological or angiographic features (Winter, 1954; Gensini et al, 1959; Fraser et al, 1961; Buirski et al, 1986).

The persistent left SVC usually drains via the coronary sinus into the right atrium. In such circumstances, echocardiography will clearly demonstrate enlargement of the coronary sinus in the parasternal, long axis plane (Huhta et al, 1982). A left SVC is usually of low radiographic density and is often not demonstrated on a conventional frontal chest radiograph.

In a recent large series of patients with congenital heart disease (Buirski et al, 1986), persistent left SVC was especially frequent in association with atrioventricular septal defects, double outlet right ventricle

1989, *The British Journal of Radiology*, *62*, 79–80

and situs abnormalities, but was rarely found in association with transposition of the great arteries. In the same series, 7% of left SVC drained into the left atrium. This compared with a previously reported incidence of 4% (Winter, 1954). Under these circumstances there will be systemic arterial desaturation to some degree. It is especially important to recognize the presence of SVC anomalies in patients with congenital heart disease (De Leval et al, 1975).

The case which we have presented is particularly interesting as the patient had been quite well until shortly before admission and there was nothing in his history to suggest any venous or cardiac anomaly. Although uncommon, drainage of a persistent left SVC into the left atrium should be considered when the lungs are not visualized following intravenous injection of $^{99}Tc^{m}$-MAA.

References

BUIRSKI, G., JORDAN, S. C., JOFFE, H. S. & WILDE, P., 1986. Superior vena cava abnormalities: their occurrence rate, associated cardiac abnormalities and angiographic classification in a paediatric population with congenital heart disease. *Clinical Radiology*, *37*, 131–138.

DE LEVAL, M. R., RITTER, D. G., MCGOON, D. C. & DANIELSON, G. K., 1975. Anomalous systemic venous connection. Surgical considerations. *Mayo Clinic Proceedings*, *50*, 599–610.

FRASER, R. S., DVORKIN, J., ROSSAC, R. E. & EIDEM, R., 1961. Left superior vena cava: a review of associated congenital heart lesions. Catheterization data and roentgenologic findings. *American Journal of Medicine*, *31*, 711–716.

GENSINI, G. G., CALBINI, P., CASACCIO, F. & BLOUNT, S. G., 1959. Persistent left superior vena cava. *American Journal of Cardiology*, *4*, 677–685.

HUHTA, J. C., SMALLHORN, J. F., MACARTNEY, F. J., ANDERSON, R. H. & DE LEVAL, M., 1982. Cross-sectional echocardiographic diagnosis of systemic venous return. *British Heart Journal*, *48*, 388–403.

SIPILA, W., HAKKILA, J., HEIKEL, P. E. & KYLLONEN, K. E. J., 1955. Persistent left superior vena cava. *Annales Medicinae Internae Fenniae*, *44*, 251–261.

STEINBERG, L., DUBILIER, W. & LUKAS, D., 1953. Persistence of left superior vena cava. *Disease of the Chest*, *24*, 479–488.

WINTER, F. S., 1954. Persistent left superior vena cava: survey of world literature and report of thirty additional cases. *Angiology*, *5*, 90–132.

Ossified leiomyoma of the stomach: demonstration on computed tomography

By Russ M. Savit, MD, Mindy M. Horrow, MD and *Pasha Agarwal, MD

Departments of Radiologic Sciences and *Pathology, The Medical College of Pennsylvania and Hospital, 3300 Henry Avenue, Philadelphia, Pennsylvania 19129, USA

(*Received July 1987 and in final form June 1988*)

Leiomyomas of the stomach with detectable calcification on plain radiographs are very uncommon, with only a few cases reported in the world literature (Garbarini & Price, 1950; Kolosky et al, 1950; Leigh, 1950; Steen & Newell, 1953; Crummy & Juhl, 1962; Graham et al, 1972; Kojima et al, 1981). We report a case of ossified leiomyoma of the stomach seen on computed tomography (CT) as well as plain radiography.

Case report

A 62-year-old white woman with a history of basal cell carcinoma of the face and melanoma of the right arm underwent a routine follow-up CT scan of the abdomen as an outpatient. The CT scan showed a 2.5 cm, densely calcified lesion near the splenic hilum (Fig. 1) and the possibility of a calcified splenic artery aneurysm was raised. An angiogram showed no aneurysmal filling but the scout radiograph for the angiogram showed an ossified lesion in the left upper quadrant, corresponding to the lesion seen on CT (Fig. 2). Laparotomy revealed a normal spleen and normal splenic vasculature. There was a calcified mass on the highest aspect of the greater curvature of the stomach, thought to be restricted to the subserosal area and the lesion was resected. The pathological diagnosis was ossified leiomyoma (Fig. 3) and the post-operative course was unremarkable.

Discussion

Gastric leiomyoma is the most common extramucosal tumour of the stomach. It is histologically identical to the more common uterine leiomyoma, consisting of collagenous stroma, hyaline changes and calcification. Gross calcification is often seen on plain radiographs of uterine leiomyoma but rarely in gastric leiomyoma. Calcification is probably dystrophic in nature owing to

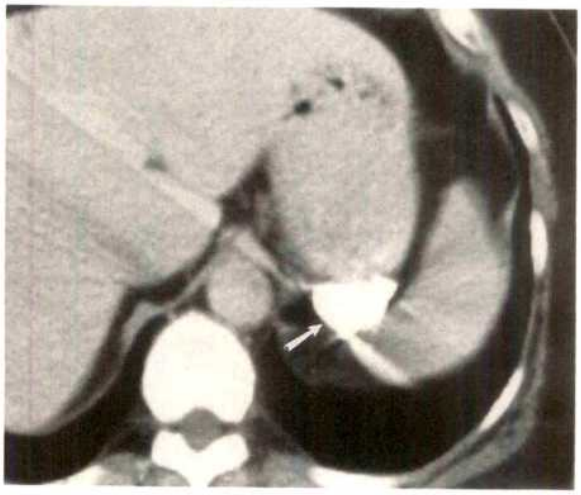

Figure 1. A CT scan of the upper abdomen showing a densely calcified lesion between the stomach and spleen (arrow).

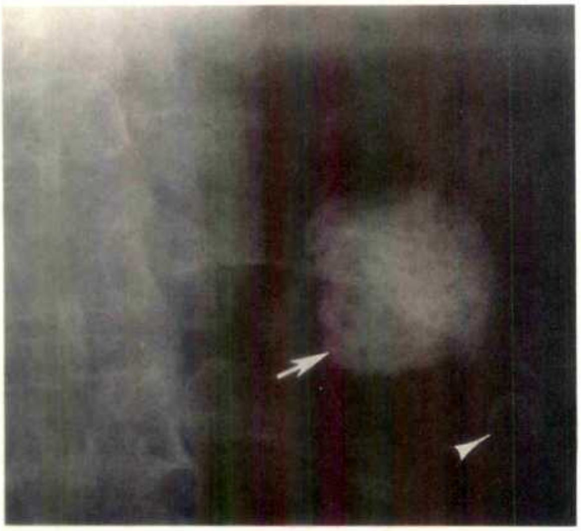

Figure 2. Scout radiograph for the angiogram showing an ossified lesion in the left upper quadrant (arrow) and splenic artery calcification (arrowhead).

cytoplasmic degeneration, liquefaction or haemorrhage.

An important entity to be distinguished from a calcified leiomyoma is a mucinous adenocarcinoma of the stomach. Rotondo et al (1986) discussed the differentiation of these lesions by virtue of their pattern of calcification. Mucinous adenocarcinomas have a fine, punctate or miliary pattern of calcification, whereas that in leiomyomas is usually more dense and patchy. In our case it was particularly dense, probably because the lesion actually contained ossification. Distinction between these lesions can also be made on barium examination, carcinoma being mucosal in location, leiomyoma being extramucosal.

Our case is unusual in that the leiomyoma contained not merely calcification, but frank ossification throughout. In addition, all previous case reports of calcified leiomyomata were in patients having only plain radiography, whereas this lesion was seen initially on CT. With the current widespread use of CT, it seems likely that we will encounter more leiomyomas of the stomach in which there are only small amounts of calcification. Densely calcified or ossified lesions seen on plain radiographs will presumably remain a rare occurrence. Recognition of this lesion on plain radiography or CT is important, however, because the radiologist can suggest gastric leiomyoma as the most likely diagnosis.

Acknowledgment

We would like to thank Joan Colombaro for the preparation of the manuscript.

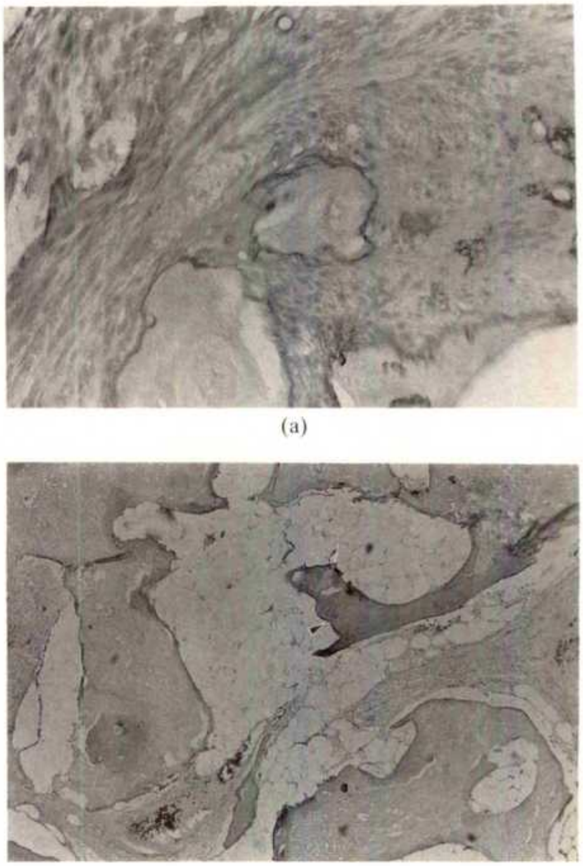

(a)

(b)

Figure 3. (a) Pathological specimen (low power, × 18). Leiomyoma of the stomach reveals the classic pattern of interlacing bundles and fascicles of well differentiated smooth muscle cells. (b) This illustrates frank ossification in the central part of the leiomyoma. Bone spicule (arrowhead).

References

CRUMMY, A. B. Jr & JUHL, J. H., 1962. Calcified gastric leiomyoma. *American Journal of Roentgenology*, *87*, 727–728.

GARBARINI, J. & PRICE, H. P., 1950. Calcified leiomyoma of the stomach. *New England Journal of Medicine*, *243*, 406–407.

GRAHAM, J. C. Jr, BLANCHARD, I. T. & SCATLIFF, J. H., 1972. Calcified gastric leiomyoma presenting as a mediastinal mass. *American Journal of Roentgenology*, *114*, 529–531.

KOJIMA, Y., FUJII, H., ASANO, E., JAKADA, M., NAKAGAWARA, G. & MIYAZKI, I., 1981. Calcified gastric leiomyoma—a case report. *Japanese Journal of Surgery*, *11*, 464–466.

KOLOSKY, E. L., SHALLENBERGER, P. L. & HAWK, G. W., 1950. Large partially calcified gastric leiomyoma. *American Journal of Surgery*, *80*, 245–248.

LEIGH, T. F., 1950. Calcified gastric leiomyoma—report of a case. *Radiology*, *55*, 419–422.

ROTONDO, A., GRASSI, R., SMALTINO, F., GRECO, A., LEUNG, A. W. L. & ALLISON, D. J., 1986. Calcified gastric cancer: report of a case and review of literature. *British Journal of Radiology*, *59*, 405–407.

STEEN, L. H. & NEWELL, W. G., 1953. Calcified gastric leiomyoma: case report. *Gastroenterology*, *24*, 124–129.

1989, *The British Journal of Radiology*, *62*, 81

Case reports

Primary extranodal lymphoma in muscle

By John Scally, FRCR and Anne Garrett, FRCR

Department of Radiodiagnosis, Countess of Chester Hospital, Liverpool Road, Chester

(*Received April 1988 and in revised form June 1988*)

Lymphomas can develop in any location where there is lymphomatous tissue, but extranodal presentation in the lower limb is unusual; involvement of skeletal muscle is also considered to be rare. Rosenberg et al (1961) reviewed 1269 cases of "lymphosarcoma" and none with muscle involvement was described. Significant involvement of skeletal muscle was noted in only 1.4% of 2147 cases of lymphoma reviewed in the *Annual of Pathologic Autopsy Cases* in Japan from 1976 to 1978 (Komatsuda et al, 1981). In a series of 97 patients who underwent computed tomography (CT) for lymphoma staging, in only five cases was significant muscle involvement noted (Pilepich & Carter, 1980). However, with improved imaging techniques, muscle involvement is beginning to be recognized, especially in the patient with established lymphoma. The site of muscular involvement in these rare cases is usually the thigh, although infiltration of the pectoral muscles has been reported in a case of diffuse disease (Komatsuda et al, 1981). Muscle involvement as the presenting feature of lymphoma is extremely rare.

Case report

A 51-year-old woman was referred to the orthopaedic clinic with a 3-week history of low back pain and left-sided sciatica. A disc prolapse was the initial clinical diagnosis but a lumbar radiculogram was normal. While in hospital, the patient experienced increasing pain and further examination revealed swelling of the left buttock and thigh. Ultrasound confirmed the presence of a buttock mass of mixed echogenicity and angiography revealed stretched and distorted gluteal and circumflex arteries but no pathological circulation. Computed tomography defined a large, slightly enhancing mass in the buttock and thigh (Fig. 1). Biopsy and histological examination revealed a B-cell non-Hodgkin's lymphoma. Cytotoxic chemotherapy rapidly reduced the tumour bulk and the patient was discharged home, pain free.

Discussion

The patient described presented with a diffuse mass in the buttock and thigh due to lymphomatous involvement of skeletal muscle. The symptoms initially suggested a root lesion secondary to a lumbar disc prolapse but clearly the pain was likely to have originated from direct pressure on or invasion of the sciatic nerve.

Presentation by lymphoma as a muscle mass has been reported in two cases by Kandel et al (1984), in a further two cases by Spector and Zimbler (1986) and in one of the three cases of muscle involvement described by Grem et al (1985). In all of the above, the thigh was the primary site of involvement.

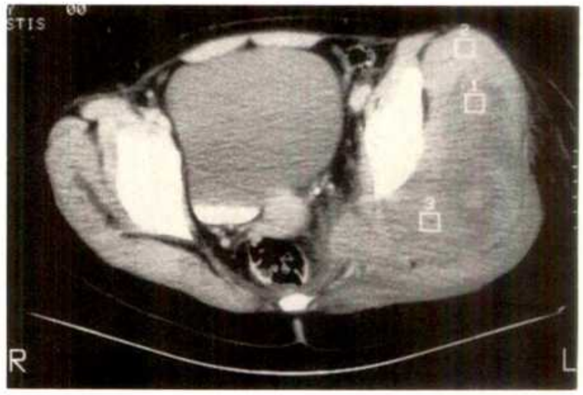

Figure 1. Enhanced CT scan showing the gluteal mass adjacent to the iliac blade with invasion through the sciatic notch into the pelvis. The tumour extends to the level of the distal femur.

In cases of localized swelling of the lower limb in which causes of generalized limb swelling have been excluded, CT is useful in defining the extent of the lesion and in determining the presence or otherwise of bone destruction and marrow involvement. Computed tomography may also be used in biopsy procedures, although in our case ultrasound guidance proved satisfactory. The presentation of lymphoma as muscle infiltration was accompanied by abnormalities on CT of the adjacent long bone in two out of the four cases reported in the literature (Grem et al, 1985; Kandel et al, 1985; Spector & Zimbler, 1986). In the case reported here, no such involvement was noted.

This report further supports the view stated by Spector and Zimbler (1986) that lymphoma should be included in the differential diagnosis of diffuse skeletal muscle enlargement in the lower limb.

References

Grem, J. L., Neville, A. J., Smith, S. C., Gould, H. R., Love, R. R. & Trump, D. L., 1985. Massive skeletal muscle invasion by lymphoma. *Archives of Internal Medicine*, *145*, 1818–1820.

Kandel, R. A., Bedard, Y. C. & Pritzker, K. P. H., 1984. Lymphoma presenting as an intramuscular small cell malignant tumour. *Cancer*, *53*, 1586–1589.

Komatsuda, M., Nagao, T. & Arimori, S., 1981. An autopsy case of malignant lymphoma associated with remarkable infiltration in skeletal muscle. *Rinsho Ketsueki*, *22*, 891–895.

Pilepich, M. V. & Carter, B. L., 1980. Muscle enlargement in lymphoma patients. *Radiology*, *134*, 521–523.

Rosenberg, S. A., Diamond, H. D., Jarlowitx, B. & Craver, L. F., 1961. Lymphosarcoma: a review of 1269 cases. *Medicine*, *40*, 31–84.

Spector, J. I. & Zimbler, H., 1986. Skeletal muscle involvement by lymphoma. *Archives of Internal Medicine*, *146*, 1232.

1989, *The British Journal of Radiology*, 62, 82–83

Polyorchidism diagnosed by ultrasound

By *P. Cadigan, FRCR

Department of Diagnostic Radiology, York District Hospital, Wigginton Road, York YO3 7HE

(*Received March 1988*)

Polyorchidism is a rare condition of uncertain embryological origin. It is most often diagnosed as an incidental finding in young males undergoing repair of an inguinal hernia (Sujka et al, 1987).

We report a case presenting as an intermittently painful scrotal swelling which was diagnosed pre-operatively by ultrasound. Although the ultrasound findings in polyorchidism have been described pre-operatively twice before (Rifkin et al, 1983; Goldberg et al, 1987), to our knowledge this is the first such report from Britain.

Case report

A 21-year-old man presented with a history of intermittent pain in the left testicle for 1 year. Examination revealed what was thought to be a swelling below the left testis and the patient was referred for ultrasound examination.

At ultrasound, two discrete structures of normal testicular echogenicity were identified in the left hemiscrotum. The upper was the larger of the two, although both appeared smaller than the single right testicle. There appeared to be an epididymis in relation to both structures which were diagnosed as testes.

Surgical exploration showed that the two left testicles were contained within a single tunica, sharing a common, elongated epididymis and a single vas deferens. It was felt that the upper testis was readily capable of undergoing torsion because of its narrow mesorchium and all three testicles were fixed. Biopsies of both the testicles on the left showed normal spermatogenesis.

Discussion

Less than 60 cases of polyorchidism have been described in the world literature (Nacey & Urquhart Hay, 1987). The anomaly is thought to result from either duplication or abnormal division of the genital ridge and usually results in two testes sharing a common epididymis and vas deferens. Complete duplication including epididymes and vasa occurs in less than 10% of cases (Al Hibbal & Izzidien, 1984). To our knowledge, there have been no reports of more than one supernumerary testicle and the majority occur on the left.

A previous report (Goldberg et al, 1987) suggests that when the ultrasound diagnosis is not in doubt, exploration of the scrotum need not be undertaken. This course of inaction must be considered against the background of the known associations of polyorchidism including torsion, hydrocele, varicocele, malignancy and epididymitis, together with the markedly increased incidence of incomplete descent and inguinal hernia (Nacey & Urquhart Hay, 1987). In this case the presence of pain, probably resulting from subacute torsion of the upper testicle, made exploration mandatory.

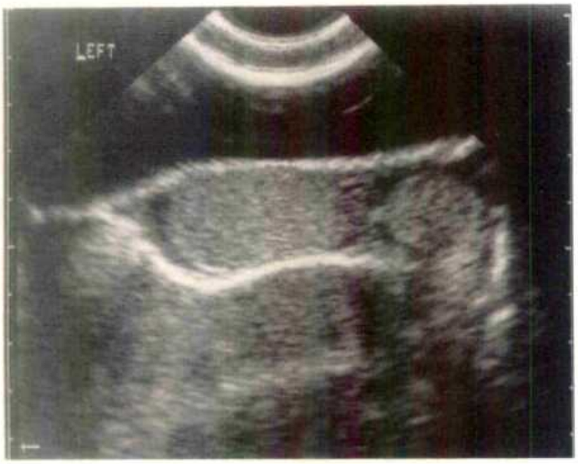

Figure 1. Longitudinal scan through the left hemiscrotum demonstrating the two left testicles. A trace of peritesticular fluid is present.

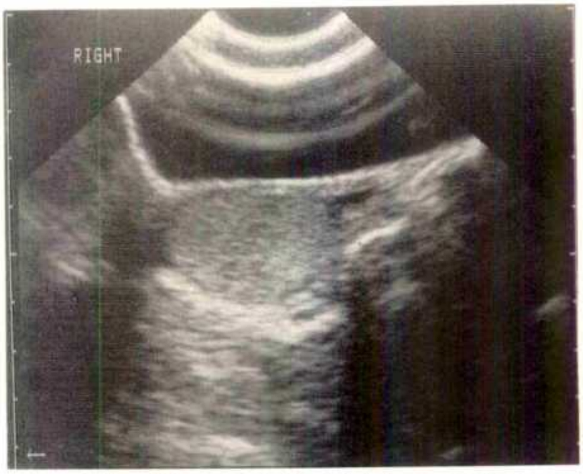

Figure 2. The right testicle is illustrated for comparison.

---

*Present address: Department of Radiology, Texas Tech University School of Medicine, 4800 Alberta Avenue, El Paso, Texas 79905, USA.

1989, *The British Journal of Radiology*, *62*, 83–84

References

Al Hibbal, Z. & Izzidien, A. Y., 1984. Polyorchidism: case report and review of the literature. *Journal of Paediatric Surgery*, *19*, 212.

Goldberg, R. M., Chilcote, W., Kay, R. & Bodie, B. H., 1987. Sonographic findings in polyorchidism. *Journal of Clinical Ultrasound*, *15*, 412–415.

Nacey, J. N. & Urquhart Hay, D., 1987. Polyorchidism. *British Journal of Urology*, *59*, 280–286.

Rifkin, M. D., Kurtz, A. B., Pasto, M. E. & Goldberg, B. B., 1983. Polyorchidism diagnosed pre-operatively by ultrasonography. *Journal of Ultrasound in Medicine*, *2*, 93–94.

Sujka, S. K., Ralabate, J. A. & Smith, R. A., 1987. Polyorchidism. *Urology*, *29*, 307–309.

Renal neoplasms in a family

By *V. M. Laurence, MRCP and †‡A. C. R. Robinson, MRCPI, FFR

Cookridge Hospital, Leeds and †University of Leeds, Department of Radiotherapy, Cookridge Hospital, Leeds

(*Received June 1988*)

Malignant tumours of the kidney are uncommon, renal cell carcinoma, the adult variety, accounting for 2% of all adult malignancies, whilst nephroblastoma, an enbryonic tumour of childhood, affects one per 200 000 children per year under the age of 15 years and constitutes 7% of childhood neoplasms (Bullimore & Mott, 1982). Both of these tumours occur in sporadic and hereditary forms. We report a family in which the mother had renal cell carcinoma and her son nephroblastoma. This has only been reported once before (Campbell et al, 1987).

Case reports

Case 1

In January 1975, a previously healthy 4-year-old boy presented with right-sided abdominal swelling. He had one healthy brother aged 9 months. Family history was otherwise unremarkable. Physical examination revealed a large abdominal mass. No other abnormalities were detected. In particular, there was no aniridia, hemi-hypertrophy or mental retardation. An intravenous urogram showed a horseshoe kidney with a mass occupying the right portion. A chest radiograph demonstrated metastatic nodules within the left lung which were confirmed by tomography. Haematological tests were normal, as was urine analysis.

At laparotomy, a massive tumour involving the right element of the horseshoe kidney was found. There was nodal spread which was compressing the inferior vena cava. The tumour and involved nodes, the whole of the right kidney and the bridge of the horseshoe were removed. Histology of the tumour was nephroblastoma. The patient was entered into the Medical Research Council (MRC) trial for nephroblastoma and received peri- and post-operative chemotherapy using actinomycin D, adriamycin and vincristine, as well as abdominal and pulmonary irradiation. A complete remission was achieved at the end of treatment. The patient remains disease-free 11 years later, but his weight and height are on the 10th percentile, having been on the 90th percentile at diagnosis. Chromosomal analysis was not carried out on the tumour specimen, nor were constitutional chromosomes evaluated.

Case 2

In April 1986, the mother of Case 1 presented with malaise and weight loss. She had a past history of Hashimoto's thyroiditis. Physical examination was unremarkable. In particular, the patient had no evidence of Von Hippel-Lindau syndrome and no accessory nipples. Her chest radiograph, haematological tests and urine analysis were all normal. Abdominal ultrasound and computed tomography (CT) of the abdomen showed a solid mass in the right kidney. At laparotomy a 5 cm tumour occupying the upper pole of the right kidney was found. A nephrectomy was performed. The tumour was a renal cell carcinoma of adeno-papillary structure. There was no evidence of capsular penetration and no invasion of the right renal vein or adjacent lymph nodes. Three months following surgery, the patient developed bony and cranial metastases which were treated by palliative radiotherapy. She eventually died from her disease 15 months after diagnosis. Chromosome analysis was not carried out.

Discussion

The malignant transformation of previously normal cells is thought to occur by a combination of genetic susceptibility and environmental exposure. Knudson has claimed that predisposition to almost every form of human cancer exists in both heritable and non-heritable forms (Knudson et al, 1973). Genetic predisposition is highest in retinoblastoma in which 40% of cases are inherited as an autosomal dominant trait. However, no clear familial pattern has emerged for most common solid tumours. Genetic factors have been implicated in the aetiology of both renal cell carcinoma and nephroblastoma. Urogenital neoplasms attributed to primary genetic factors occur more frequently in people with congenital genito-urinary anomalies, suggesting a link between teratogenesis and carcinogenesis. They tend to have an earlier age of onset, to be more frequently bilateral and more frequently multifocal than the same histological type of tumour of sporadic form.

---

*Author for correspondence.

‡Present address: Christie Hospital & Holt Radium Institute, Wilmslow Road, Withington, Manchester M20 9BX.

They have a higher incidence in families who have multiple primary cancers at varying anatomical sites (Lynch & Walzat, 1980).

The aetiology of renal cell carcinoma is still essentially unknown. Its incidence varies worldwide, being highest in Denmark where it affects 7 per 100 000/year of the population van der Werf-Messing & Schroeder, 1982). It is usually of the non-hereditary variety and occurs more commonly in men. Coke-oven workers and machinists have a higher than average incidence and other noted associations include tobacco smoking, coffee and a high consumption of animal protein.

The much rarer forms of hereditary renal cell carcinoma may result from several genetic mechanisms. Von Hippel-Lindau syndrome, an autosomal dominant disorder, may give rise to a multiplicity of neoplastic and cystic lesions at varying sites. There is a 10–25% incidence of renal cell carcinoma in this disorder which is commonly bilateral and multifocal and may occur in the walls of renal cysts (Lee et al, 1977).

Less common than this single gene trait is the association of renal cell carcinoma with a specific constitutional, balanced translocation between chromosomes 3 and 8. Cohen described a three-generation Italian American family in whom 10 members developed the tumour (Cohen et al, 1979; Campbell et al, 1987). The chromosomal defect was present in all five living members of the family with the tumour and at least three of the five deceased members. No other hereditary or environmental factor was identified. No family member with a normal karyotype developed the tumour. The inheritance was thought to be autosomal dominant and the estimated probability of developing this form of cancer in this family was 0.87 with a greater than 50% chance of it being bilateral. In comparison, the incidence of non-inherited renal cell carcinoma in the USA is 1 per 1000 and only 1–2% are bilateral. Of interest, by screening, three asymptomatic family members were found to have the tumour. Other families with a high incidence of the tumour have been reported (Lynch & Walzat, 1980). Finally, an association between renal cell carcinoma and accessory nipples has been described which is thought to be of multifactorial origin (Goedert et al, 1981).

Unlike renal cell carcinoma, nephroblastoma has a constant incidence worldwide and an equal sex incidence. It occurs in sporadic forms 50 times more commonly than the familial variety (Lynch & Walzat, 1980). No specific environmental factors have been implicated but associated phenotypic features include hemi-hypertrophy, hamartomas, pigmented naevi, renal anomalies and skeletal malformations.

Familial nephroblastoma is associated with a specific gene deletion at the IIp13 locus (Anderson et al, 1978). The tumour occurs in children who have sporadic aniridia in association with mental retardation. All of these children carry the gene deletion and one in three will subsequently develop the tumour. The mode of inheritance is thought to be autosomal dominant with a gene penetrance rate of 63%. Other chromosomal anomalies found in association with nephroblastoma include trisomy 8 and 18 and XX/XY mosaicism (Souhami & Tobias, 1986).

Kidney tumours arise in both adults and children by a combination of environmental and genetic mechanisms. Those tumours which are inherited are rarer and usually found in association with specific syndromes or genetic abnormalities. In the family described, it is likely that both tumours were sporadic and occurred in the same family by chance. However, it may be that chromosomal analysis would have shown an abnormality in the mother and child and that a mixture of environmental and hereditary factors contributed to the development of their tumours.

Acknowledgments

We wish to thank Dr S. C. Cartwright for allowing us to publish details of this case.

References

Anderson, S. R., Geertinger, P., Larsen, H. W., Mikkelsen, M., Parving, A., Vestermark, S. & Warburg, M., 1978. Aniridia, cataract and gonadoblastoma in a mentally retarded girl with deletion of chromosome 11. *Ophthalmologica, 176*, 171–177.

Bullimore, J. A. & Mott, M. G., 1982. Paediatric cancer. In *Treatment of Cancer*, ed. by K. E. Halnan (Chapman and Hall, London), pp. 755–756.

Campbell, A. N., Chan, H. S. L., O'Brien, A., Smith, C. R. & Becker, L. E., 1987. Malignant tumours in the neonate. *Archives of Disease in Childhood, 62*, 19–23.

Cohen, A. J., Li, F. P., Berg, S., Marchetto, D. J., Shien Tsai, S. M., Jacobs, S. C. & Brown, R. S., 1979. Hereditary renal cell carcinoma associated with a chromosomal translocation. *New England Journal of Medicine, 301*, 592–595.

Goedert, J. J., McKeen, E. A. & Fraumeni, J. F., 1981. Polymastia and renal adenocarcinoma. *Annals of Internal Medicine, 95*, 182–184.

Knudson, A. G., Strong, L. C. & Anderson, D. E., 1973. Heredity and cancer in man. *Progress in Medical Genetics, 9*, 113–158.

Lee, K. R., Wulfsberg, E. & Kepes, J. J., 1977. Some important aspects of the kidney in Hippel-Lindau syndrome: the value of prospective study in an affected family. *Radiology, 122*, 649–653.

Lynch, H. T. & Walzak, M. P., 1980. Genetics in urogenital cancer. *Urological Clinics of North America, 7*, 815–827.

Souhami, R. L. & Tobias, J. S., 1986. *Cancer and its Management* (Blackwell Scientific, Oxford), p. 414.

Werf-Messing, B. van der & Schroeder, F. H., 1982. Kidney. In *Treatment of Cancer*, ed. by K. E. Halnan (Chapman and Hall, London), p. 443.

1989, *The British Journal of Radiology*, 62, 85–86

Case of the month

A colonic double bubble

By Antony Harrison, BSc, MB, BS, *Louise Machin, MB, ChB and †Alan Grundy, MB, ChB, FRCR

Departments of Surgery, *Pathology and †Radiology, St George's Hospital, London SW17 0QT

(*Received January 1988 and in revised form April 1988*)

A 62-year-old woman presented with a 3-month history of two large abdominal swellings. There were no associated gastrointestinal or urinary symptoms and no history of previous abdominal surgery. On clinical examination, two 10 cm diameter, firm, mobile and non-tender masses were present in the left side of the abdomen. They were thought clinically to be arising within the abdominal wall. Clinical examination was otherwise unremarkable.

A supine abdominal radiograph (Fig. 1) was taken. Subsequently, a double-contrast brarium enema was performed (Fig. 2). What is the most likely diagnosis?

---

† Author for correspondence.

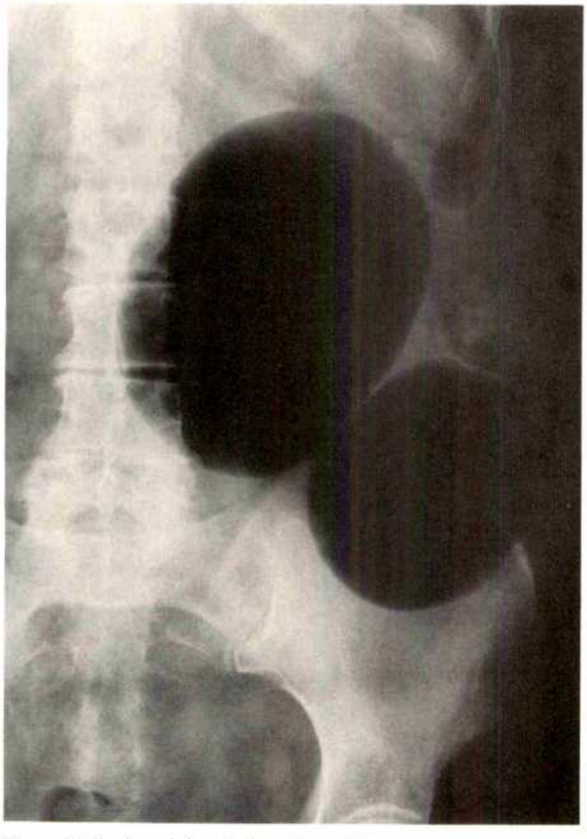

Figure 1. Supine abdominal radiograph.

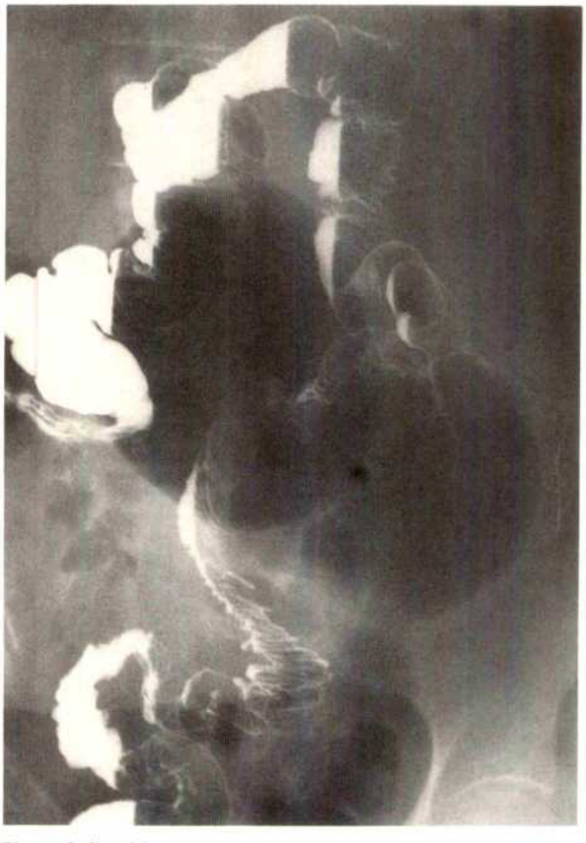

Figure 2. Double-contrast barium enema.

The plain abdominal radiograph shows two well circumscribed, oval, air-containing collections in the left side of the abdomen. The bowel gas pattern is otherwise unremarkable. The barium enema shows the sigmoid colon stretched around the two air-filled structures which do not fill with barium. There is evidence of diverticular disease in the adjacent sigmoid colon.

The patient underwent laparotomy at which two air-filled structures were identified attached to the sigmoid colon and communicating with each other. A segment of small bowel was adherent to the colon at this site. The involved segment of sigmoid colon was resected along with the segment of the adjacent small bowel (Fig. 3). The patient made an uneventful post-operative recovery.

Histological examination of the resected specimen showed two communicating fibrous-walled cysts within the serosa of the sigmoid colon. There was faecal debris in their walls which had elicited both acute and chronic granulomatous inflammation and a foreign-body giant cell reaction. Neither an epithelial lining, barium contents nor communication with the bowel lumen were demonstrated, although the presence of faecal debris within the cysts implied some previous communication.

Discussion

Giant colonic diverticula or giant air-cysts of the colon may present as an unusual gas collection arising from the large bowel and in the majority of cases they arise from the sigmoid colon (Kricun et al, 1980). They are usually solitary, multiplicity having been described in only a small number of cases (Gallagher & Welch, 1979). There is almost always evidence of diverticular disease elsewhere in the colon.

Giant colonic diverticula may be asymptomatic or may present with pain, vomiting, abdominal distension, malaena or more acute symptoms of diverticulitis (Kricun et al, 1980), including perforation, or rarely, as a palpable abdominal mass.

Giant colonic diverticula can be detected on plain radiographs as rounded or elliptical, well circumscribed air collections, usually in the left side of the abdomen (Rosenberg & Naidich, 1981). Such collections may exceed 20 cm in diameter. Differential diagnosis includes other causes of large air collections such as abscesses, which are usually less well circumscribed, or diverticula arising from other parts of the gastrointestinal tract, such as giant duodenal diverticula or a dilated air-containing Meckel's diverticulum.

On barium enema, these diverticula do not always fill with barium and a communication with the colonic lumen may be found in only 60% of cases (Kricun et al, 1980). They are invariably in close proximity to the sigmoid colon and the colon is often impressed by, or stretched around, the diverticula.

On histological examination the wall of a giant colonic diverticulum is often composed of acute and chronically inflamed tissue. Mucosal and muscular remnants may not be found. It is unusual not to find a communication with the colon (Muhletaler et al, 1981). In this case a communication was not visible on pathological examination although the presence of faecal debris within the lumen of the diverticula implies that a communication had existed.

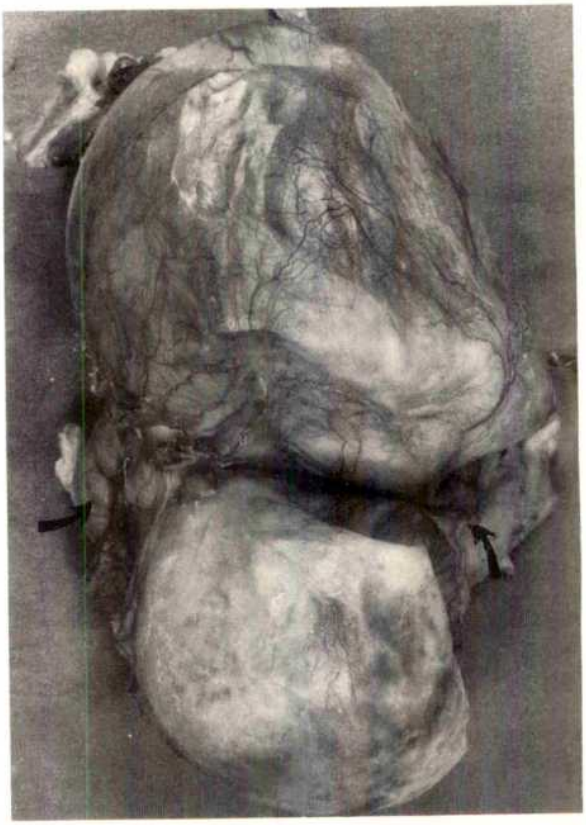

Figure 3. Resected specimen. Two giant sigmoid diverticula measuring 15 cm × 11 cm and 10 cm × 8 cm arising from and lying either side of the sigmoid colon (arrows).

Three mechanisms for the development of giant sigmoid diverticula have been proposed. Inflammation at the neck of a pre-existing diverticulum may lead to a ball-valve mechanism resulting in a massively enlarged pseudodiverticulum of mucosa and submucosa protruding through the wall of the colon. Alternatively, perforation of a diverticulum may have occurred leading to a progressively enlarging pseudocyst, secondary to a ball-valve mechanism. The other suggested mechanism is that the neck of a diverticulum is occluded and the diverticulum becomes distended by gas-forming organisms.

References

Gallagher, J. J. & Welch, J. P., 1979. Giant diverticula of the sigmoid colon: a review of differential diagnosis and operative treatment. *Archives of Surgery, 114*, 1079–1083.

Kricun, R., Stasik, J. J., Reither, R. D. & Dex, W. J., 1980. Giant colonic diverticulum. *American Journal of Roentgenology, 135*, 507–512.

Muhletaler, C. A., Berger, J. L. & Robinette, C. L., 1981. Pathogenesis of giant colonic diverticula. *Gastrointestinal Radiology, 6*, 217–222.

Rosenberg, R. F. & Naidich, J. B., 1981. Plain film recognition of giant colonic diverticula. *American Journal of Gastroenterology, 76*, 59–69.

1989, *The British Journal of Radiology*, 62, 87–90

Short communication

Functional changes in the irradiated rat ureter: assessment by transit-time renography

*J. F. Knowles, PhD and C. C. Nimmon, BSc

Department of Radiation Biology, Medical College of St Bartholomew's Hospital, London EC1M 6BQ and Department of Nuclear Medicine, St Bartholomew's Hospital, London EC1A 7BE

(*Received February 1988 and in final form August 1988*)

A primary requirement in the investigation of experimentally induced urinary tract obstruction is that there must be a reliable method of assessing the functional changes induced. In previous studies of the effects of X radiation on the rat urinary tract, assessment has used the relatively gross end-point of hydronephrosis development, as detected by regular renal palpation followed up by intravenous urography (Knowles, 1985; Knowles & Trott, 1987).

In order to detect early, subclinical changes and to obtain quantitative measures of radiation effects, more sensitive techniques are required. One such method which has proven successful in investigating human urinary tract obstruction is gamma camera renography. Deconvolution of the gamma camera renogram enables the estimation of radionuclide transit times through the kidney. Drawing of separate regions of interest round the pelvi-calyceal region allows separate whole kidney and parenchymal transit times to be calculated (Whitfield et al, 1978; Britton et al, 1979). Using these it is possible to obtain a measure of delay due to the obstruction and to determine whether or not nephron function is reduced.

We have been assessing the use of these techniques to examine changes occurring in the rat subsequent to localized irradiation of a length of ureter. This paper presents transit time results for the unobstructed urinary tract together with a description of the changes so far observed in radiation-induced obstructing uropathy.

Materials and methods

Animals

Male rats of the Wistar and F344 strains were used. They were supplied at ~8–10 weeks of age by the Imperial Cancer Research Fund, Clare Hall Laboratory and subsequently maintained in the animal house at St Bartholomew's Medical College. The rats were about 16 weeks old at irradiation for which they were anaesthetized with 100 mg/kg ketamine intraperitoneally (Ketalar). For renography, renal palpation and urography they were anaesthetized with 2–3% halothane in a 1 : 1, oxygen to nitrous oxide gas mixture which was supplied by a small face mask.

Irradiation

Full details of the X-irradiation procedure have been given previously (Knowles, 1985; Knowles & Trott, 1987). A 1 cm × 1.5 cm field was positioned over the left ureter and single doses of 20–30 Gy were given to a 1.5 cm length at 1.8 Gy/min using 320 kV, 10 mA, a focus–skin distance (FSD) of 37 cm and 0.5 mm Cu/0.9 mm Al added filtration.

Renal palpation and urography

Palpation of the kidneys was carried out at intervals of 2–3 weeks post-irradiation using the methods previously described (Knowles, 1985). Intravenous urography was carried out on all rats with prolonged transit time indices and all those where palpation indicated the possibility of renal enlargement, as well as occasional tests on apparently normal animals. Urographs were taken about 10 min after intravenous injection of contrast medium (Omnipaque 350, Schering) using a Phillips Metalix 300 LS machine at 52 kV with an FSD of 60 cm and 50 mAs exposure.

Gamma camera renography

The methods were essentially those previously described for humans (Whitfield et al, 1978; Britton et al, 1979). Anaesthetized rats were placed in a supine position on the medium-sensitivity/high-resolution collimator of a gamma camera (GE 400 AT, Ohio Nuclear), then 0.1–0.2 ml of a solution containing 10–20 MBq of $^{99}Tc^{m}$-labelled DTPA were injected into a tail vein and the gamma camera data recorded in 5 s frames over the following 15 min using an on-line computer (Varian 76). Data were recorded in frames of 64 × 64 pixels, each frame corresponding to a quarter of the field of view of the gamma camera. Regions of interest (ROI) were drawn round each kidney, each renal pelvis, the heart and a background area near each kidney. For each kidney the renal transit times were measured using a deconvolution technique based on a matrix algorithm method (Nimmon et al, 1981). Using background-subtracted activity–time curves from the carefully drawn ROI, mean transit times corresponding to both the whole kidney and parenchymal regions (*i.e.* excluding the renal pelvis) were obtained. These were corrected to give transit-time indices by subtracting the shortest transit time. This was done in order to reduce the effects of differences in urine flow rate between rats (Britton et al, 1979, 1987). In this way transit-time indices were obtained for the whole kidney (WTTI) and for the parenchymal region (PTTI). In addition, the relative uptake of the left kidney was calculated as described by Britton et al (1979). The total background-subtracted activity counted over the left kidney during the period 1.5–2.5 min after radionuclide injection was expressed as a percentage of the summer background-subtracted activities counted in right and left kidney ROI during this time.

Results

Control rats

Unirradiated rats of the Wistar strain only were investigated. Gamma camera renography was carried out on 14 occasions at irregular intervals during the period when they were 116–301 days old (irradiated rats were exposed at around 110 days of age). There was no significant difference between

---

*Present address: Ministry of Agriculture, Fisheries and Food, Directorate of Fisheries Research, Fisheries Laboratory, Lowestoft, Suffolk NR33 0HT.

Table I. A summary of increases in renal transit time indices and other changes following localized irradition of the rat ureter

Rat number	Rat strain	Dose (Gy)	Time of occurrence (days post-irradiation)				
			Onset of WTTI increase[a]	Recovery of normal WTTI[b]	Onset of PTTI increase[c]	Palpable change	Urographic change
2C	F344	30	35	77	None	None	None
1A	Wistar	20	98	None	98	None	98
13A	Wistar	25	108	None	None	None	None
13B	Wistar	25	195	–[d]	None	None	None
15A	F344	30	184	–[d]	184	None	None
17A	Wistar	30	35	None	35	109	109

[a]First occurrence of WTTI > 130 s; [b]Return to WTTI < 130 s; [c]First occurrence of PTTI > 120; [d]No test subsequent to onset.

right and left kidney for WTTI or PTTI ($p>0.6$ for both, Student's t-test). Regression analysis of the pooled results from both kidneys revealed no evidence of any age-related changes (correlation coefficients of -0.024 and 0.036 for WTTI and PTTI, respectively, $p > 0.1$ for both). The mean WTTI (± standard error) was 69.9 ± 4.4 s and the mean PTTI was 60 ± 3.7 s with upper limits of 130 and 120 s, respectively. The contribution of the left kidney to total uptake was always within the range 43–58%.

In a small proportion of the tests carried out on these control rats and on irradiated rats, very long TTI were obtained. As these abnormally prolonged transit times occurred both in unirradiated and irradiated animals and they were always found in both kidneys and never in one alone, this effect was obviously not radiation-induced. It was in fact observed to be due to the induction of too deep an anaesthesia and, with experience, was minimized by keeping the rats on the lowest effective concentration of halothane (2%). A very similar effect was observed for mini-pigs (S. Boddy, personal communication). We have excluded artefactually prolonged TTI from all the results and only rats with right kidney WTTI of less than 150 s are included (in irradiated rats, left kidney WTTI may exceed 150 s because of radiation-induced changes). This is justified by the fact that such TTI were so greatly prolonged as to be qualitatively different from the others; for example, amongst all Wistar rats (irradiated and unirradiated) right kidney WTTI had values less than 140 s on 33 occasions (less than 100 s on 27 occasions) and greater than 185 s on nine occasions (greater than 215 s on seven occasions) with no WTTI of between 140 and 185 s.

Irradiated rats

Gamma camera renography was carried out at least once on 18 irradiated rats (10 Wistar, eight F344) and 12 of these were tested on two or more occasions.

(i) *Rats showing no radiation-induced changes*. Seven of the irradiated Wistar rats had TTI in the normal range in all tests. These rats were called "irradiated Wistar controls". The mean WTTI and PTTI were 81.3 ± 4.9 and 71.1 ± 4.8 s, respectively. These values were not significantly different from those for unirradiated Wistars (WTTI $F = 3.0$, $p > 0.05$; PTTI $F = 3.5$, $p > 0.05$). Although no unirradiated F344 rats were tested, five of the eight irradiated animals showed no radiation effects and had TTI lower than the upper limits for control Wistars in all tests. These were called "irradiated F344 controls" and they had a mean WTTI of 91.0 ± 4.8 s and PTTI of 75.7 ± 4.4 s.

For various reasons, most notably computer failure, fewer successful tests than intended were carried out on unirradiated rats. In view of the lack of any difference between unirradiated Wistars and irradiated Wistar controls it was thought the larger sample size obtained by pooling results from these groups would give the best estimate of normal values for WTTI and PTTI (values for each individual group are, however, given above). When this pooling was carried out, mean WTTI of 75.4 ± 3.2 s and PTTI of 65.3 ± 3.0 s were obtained. Comparison of these indices with those of the irradiated control F344 rats showed that the WTTI of F344 rats was significantly longer ($F = 6.7$, $0.025 > p > 0.01$) but there was no difference for PTTI ($F = 3.5$, $p > 0.05$).

(ii) *Rats showing radiation-induced changes*. Results for the six rats which developed abnormally long WTTI are summarized in Table I. They include Wistar and F344 rats and at least one from each of the three dose groups. The time of onset of changes varied from 35 to 195 days and was not dose dependent. Only one rat showed a recovery, after an initial, relatively early change. Abnormal PTTI occurred at the same time as WTTI changes in three animals. In only one rat (17A) was the increase in WTTI associated with any palpable change in the left kidney and even here the change was not detected until much later on. This kidney also showed clear radiographic evidence of enlargement of the renal pelvis and proximal ureter and a definite reduction in uptake function (32%). Again, these changes only occurred long after the initial increase in WTTI. One other rat (1A) showed a very mild localized widening of the proximal left ureter at about the time of onset of WTTI increase.

Discussion

Control animals

The present study has shown that in spite of the relatively small size of the rat kidney it is possible to carry out gamma camera renography and obtain both whole kidney and parenchymal transit times. Animal studies of this type have previously only been carried out on dogs (Price et al, 1978) and mini-pigs (Boddy et al, 1988). Gamma camera studies on rats, however, have been carried out to evaluate changes in effective renal plasma flow after kidney irradiation (Chauser et al, 1976). These workers used a pinhole collimator but in initial trials comparing this with a medium-sensitivity/high-resolution collimator we obtained more satisfactory results using the latter.

Not surprisingly, there was no difference between left and right kidneys for either rat strain. However, the prolonged WTTI but not PTTI in irradiated control F344 compared with Wistar rats suggests that the renal pelvis in the F344 is larger or more distensible. A WTTI of 90 s is typical for humans and values of less than 170 s are regarded as normal (Nimmon et al, unpublished). Thus they are rather longer than for

Wistars (mean 75 s) but similar to F344 (mean 91 s). The mean PTTI for both strains (75 and 65 s, respectively) are a little shorter than for humans where they are typically 80 s and values less than 150–156 s are regarded as normal (Neal et al, 1985; Britton et al, 1987). The mean WTTI for mini-pigs was 129 s and the mean PTTI 70 s, with upper limits the same as humans at 170 and 156 s respectively (Boddy et al, 1988). However, the mean whole kidney transit time (*i.e.* uncorrected by subtraction of minimum transit time) for Large White pigs obtained using external probe renography was 412 s (Robbins et al, 1984) and a similar value can be deduced from the graphs for pigs shown by Wilkinson et al (1978). This is considerably longer than the equivalent values for rat, human or mini-pig. Two explanations for this are suggested: one is that the nephrons in the pigs were relatively longer and more time is required to pass through them; the other is that the pigs became deeply anaesthetized. The former suggestion is supported by the finding that the mean proximal tubule length in pigs is 30 mm compared with 16 mm for humans and 12 mm for rats (Mudge, 1982). The latter suggestion is prompted by the fact that in the present experiment, abnormally long transit time indices were found in both kidneys in a minority of rats and this was related to the rats becoming too deeply anaesthetized. The indices from these animals were thus artefactual and have not been presented. Similar prolonged transit times as a result of deep anaesthesia were obtained for mini-pigs (S. Boddy, personal communication). Wilkinson et al (1978) noted changes in Hippuran transit times in the pig and rabbit which were dependent on the anaesthetic being used.

Radiation-induced effects

Two strains of rat (Wistar and F344) rather than one were used in the present experiment because of the possibility of strain differences in radiation response. There is no evidence for such a difference. However, only a few rats from both strains developed radiation-induced changes and thus they both differ from the W/Nhg strain used in earlier experiments in Germany, which had a relatively radiosensitive ureter (Knowles, 1985; Knowles & Trott, 1986, 1987). The W/Nhg strain has also been shown to be relatively radiosensitive (compared with F344 rats) for heart (Lauk, 1986) and large bowel (Sassy & Breiter, 1986) damage.

Because of the small number of affected animals it has not been possible to establish dose–effect relationships or make generalizations. Nevertheless, the results suggest that gamma camera renography is a more sensitive test of rat urinary tract function than previously used methods. This is illustrated by the fact that among the six rats showing radiation-induced changes only one showed any urographic change by the time of onset of increased WTTI, and this was not a hydronephrosis but a very mild hydroureter. One other rat developed hydronephrosis but this was only detectable by palpation and renography more than 70 days after the WTTI increase. Thus among these rats radiation effects on the urinary tract were detected much earlier by gamma camera renography than by palpation or urography.

Previous studies, in which radiographically detectable hydronephrosis was an end-point, showed no recovery subsequent to onset (Knowles & Trott, 1986). One of the present rats did show recovery to a normal WTTI but it was notable that this was after an increase at an early post-radiation time which had occurred in the absence of any simultaneous increase in PTTI. Three rats showed an increase in PTTI, which is evidence of nephron damage (Britton et al, 1979), and in all three this was not preceded by an increase in WTTI but was observed at the same time.

It has recently been shown in mini-pigs that relatively mild distensions of the ureters causes a marked and rapid increase in transit time indices (Boddy et al, 1988) and in humans changes in ureters are well established as a sensitive measure of urinary obstruction (Whitfield et al, 1977; Buck et al, 1980; Piepsz et al, 1982; Neal et al, 1985; Britton et al, 1987). The present results suggest that ureters are equally sensitive in rats and that after ureteral irradiation at least, early changes in transit time indices may precede and predict later chronic hydronephrosis.

Acknowledgments

Dr Knowles is the holder of a research fellowship financed by the Imperial Cancer Research Fund. Some financial support was also received from the Deutsche Forschungsgemeinschaft. We wish to thank Professors H. N. Whitfield and K. E. Britton for use of the gamma camera facility and Professor K.-R. Trott for his helpful discussion and encouragement.

References

Boddy, S. M., Nimmon, C. C., Jones, S., Ramsay, J. W. A., Britton, K. E., Levison, D. A. & Whitfield, H. N., 1988. Acute ureteric dilatation for ureteroscopy. *British Journal of Urology, 61,* 27–31.

Britton, K. E., Nawaz, M. K., Whitfield, H. N., Nimmon, C. C., Carroll, M. J., Granowska, M. & Mlodowska, E., 1987. Obstructive nephropathy: comparison between parenchymal transit time index and frusemide diuresis. *British Journal of Urology, 59,* 127–132.

Britton, K. E., Whitfield, H. N., Hendry, W. F. & Wickham, J. E. A., 1979. Obstructive nephropathy: successful evaluation with radionuclides. *Lancet, i,* 905–907.

Buck, A. C., Macleod, M. A. & Blacklock, N. J., 1980. The advantages of 99m-Tc DTPA(Sn) in dynamic renal scintigraphy and measurement of renal function. *British Journal of Urology, 52,* 174–186.

Chauser, B. M., Hudson, F. R. & Law, M. P., 1976. Renal function in the rat following irradiation. *Radiation Research, 67,* 86–97.

Knowles, J. F., 1985. Radiation-induced hydronephrosis in the rat; a new experimental model. *International Journal of Radiation Biology, 48,* 737–744.

Knowles, J. F. & Trott, K.-R., 1986. Radiation damage to the rat ureter. *British Journal of Cancer, 53,* suppl. VII, 277–279.

——1987. Experimental irradiation of the rat ureter: the effects of field size and the presence of contrast medium on incidence and latency of hydronephrosis. *Radiotherapy and Oncology, 10,* 59–66.

Lauk, S., 1986. Strain differences in the radiation response of the rat heart. *Radiotherapy and Oncology, 5,* 333–335.

Mudge, G. H., 1982. Comparative pharmacology of the kidney: implications for drug-induced renal failure. *Monographs in Applied Toxicology, 1,* 504–518.

Neal, D. E., Simpson, W., Bartholomew, P. & Keavey, P. M., 1985. Comparison of dynamic computed tomography, diuresis renography and DTPA parenchymal transit time in the assessment of dilatation of the upper urinary tract. *British Journal of Urology, 57,* 515–519.

Nimmon, C. C., Lee, T. Y., Britton, K. E., Granowska, M. & Gruenwald, S., 1981. Practical application of deconvolution techniques to dynamic studies. In *Medical Radionuclide Imaging 1980.* (Internanational Atomic Energy Agency, Vienna), Vol. 1, pp. 367–388.

Piepsz, A., Ham, H. R., Erbsmann, F., Hall, M., Diffey, B. L., Goggin, M. J., Hall, F. M., Miller, J. A., LUMBROSO, J., DI PAOLA, R., BAZIN, J. P., DI PAOLA, M. & FRIES, D., 1982. A co-operative study on the clinical value of dynamic renal scanning with deconvolution analysis. *British Journal of Radiology, 55*, 419–433.

PRICE, R. R., TOUYA, J. J., BRANCH, R., GODDARD, J. & BRILL, A. B., 1978. Validation of renal transit time calculations using compartmental models and direct measurements. In *Information Processing in Medical Imaging*, ed. by A. B. Brill, R. R. Price, W. J. McClain & M. W. Landay (Oak Ridge National Laboratory Press, Tennessee), pp. 536–544.

ROBBINS, M. E. C., SOPER, M. & GUNN, Y., 1984. Techniques for the quantitative measurement of individual kidney function in the pig. *International Journal of Applied Radiation and Isotopes, 35*, 853–858.

SASSY, T. & BREITER, N., 1986. Differences in large bowel radiation damage between two rat strains. In *Experimental Tumour Therapy*, Annual Report of the Institut für Strahlenbiologie, Gesellschaft für Strahlen- und Umweltforschung, Munchen, pp. 81–83.

WHITFIELD, H. N., BRITTON, K. E., HENDRY, W. F., NIMMON, C. C. & WICKHAM, J. E. A., 1978. The distinction between obstructive uropathy and nephropathy by radioisotope transit times. *British Journal of Urology, 50*, 433–436.

WILKINSON, S. P., BERNARDI, M., PEARCE, P. C., BRITTON, K. E., BROWN, N. J. G., POSTON, L., CLARKE, M., JENNER, R. & WILLIAMS, R., 1978. Validation of 'transit renography' for the determination of the intrarenal distribution of plasma flow: comparison with the microsphere method in the anaesthetised rabbit and pig. *Clinical Science and Molecular Medicine, 55*, 277–283.

1989, *The British Journal of Radiology*, *62*, 91–92

Correspondence

(The Editors do not hold themselves responsible for opinions expressed by correspondents)

Late normal tissue reactions in patients with breast carcinoma

THE EDITOR—SIR,

I was interested to read the paper by Bates (1988) dealing with the late normal tissue reactions experienced by patients with breast carcinoma treated by mastectomy and post-operative radiotherapy given in either two or three fractions per week (a comparison of six fractions in 18 days with 12 fractions in 28 days). I would, however, suggest that the negative α/β ratio obtained indicates that the treatment of 51 Gy in 12 fractions is not equivalent to that of 35 Gy in six fractions.

Using the linear-quadratic model:

$$\text{Effect per fraction} = \alpha d + \beta d^2$$

where d is dose per fraction (Fowler, 1983).

For n fractions:

$$\begin{aligned}\text{Effect of total dose} &= n(\alpha d + \beta d^2)\\ &= nd(\alpha + \beta d)\end{aligned}$$

Dividing through by α:

$$\frac{\text{Effect}}{\alpha} = nd\left(1 + \frac{\beta d}{\alpha}\right) = nd\left(1 + \frac{d}{\alpha/\beta}\right) \text{ (Fowler, 1988).}$$

This can be used to compare the effects expected in the different fractionation schedules. Using the α/β ratio of 3 Gy for late-reacting tissues and assuming negligible proliferation, for the 12-fraction cervicoaxillary node schedule:

$$\begin{aligned}\frac{\text{Effect}}{\alpha} &= 51\left(1 + \frac{4.25}{3}\right)\\ &= 123 \text{ ``}\alpha 3\text{ damage units''}\end{aligned}$$

(Fowler, personal communication).

Similarly for the six-fraction schedule:

$$\begin{aligned}\frac{\text{Effect}}{\alpha} &= 35\left(1 + \frac{5.83}{3}\right)\\ &= 103 \text{ ``}\alpha 3\text{ damage units''.}\end{aligned}$$

Thus the 12-fraction schedule is 19.4% "hotter" than the six-fraction schedule, and one is therefore not surprised to learn that a higher percentage of late subcutaneous fibrosis, limitation of shoulder movement and lymphoedema of the arm occurred following the 12-fraction regime.

Considering the chest wall schedules, for 12 fractions:

$$\begin{aligned}\frac{\text{Effect}}{\alpha} &= 37\left(1 + \frac{3.08}{3}\right)\\ &= 75 \text{ ``}\alpha 3\text{ damage units''.}\end{aligned}$$

For six fractions:

$$\begin{aligned}\frac{\text{Effect}}{\alpha} &= 31.5\left(1 + \frac{5.25}{3}\right)\\ &= 87 \text{ ``}\alpha 3\text{ damage units''.}\end{aligned}$$

In this case one would expect more damage from the six-fraction schedule and that proved to be the case.

One can repeat the exercise using an α/β ratio of 10 Gy considered to be representative of acute-reacting tissues and tumours (Fowler, 1983). The values relating to the chest wall fractionation schedules are similar. However, with regard to the cervicoaxillary node schedules, the E/α is 31.2% greater for the 12-fraction schedule than the six-fraction schedule and therefore the regimes were not strictly biologically equivalent. This may be reflected by the greater metastatic and death rates in the six-fraction group, although this was not statistically significant.

Yours, etc.,
M. J. TOMLINSON

Bristol Radiotherapy and
Oncology Centre,
Horfield Road,
Bristol BS2 8ED
(*Received August 1988*)

(*Authors' reply*)

THE EDITOR—SIR,

We agree with Dr Tomlinson's algebra, but we question her conclusion. She points out that an assumed α/β ratio of 3 would correctly predict the direction of the difference in observed normal tissue response for γ rays and X rays. However, any value of α/β greater than -0.7865 and less than 9.35 would lead to the same predictions.

Dr Tomlinson's suggested value of $\alpha/\beta = 3$ would imply a total dose of nearly 39 Gy, using six fractions, *i.e.* 11% higher than the dose used in this trial. We believe that this would be a serious overdose. There is a very narrow margin of safety using six fractions. For instance, Dische et al (1981) found a sharp cut-off at 33.5 Gy, above which spinal cord damage was seen. In practice, we believe that it would be better in the future to reduce the γ-ray dosage with 12 fractions, rather than increase the six-fraction dose.

The late skin reactions on the chest wall are better matched than the axillary effects, being equal at 5 years. Equality would imply the relatively high α/β ratio of 9.35. Bates and Peters (1975) pointed out that the effect of changing fractionation is quite different, using γ rays or soft X rays. We therefore reject Dr Tomlinson's implied conclusion that a single value of α/β, *i.e.* 3, would fit the X-ray and γ-ray data.

As regards the tumour response, we question whether linear-quadratic (LQ) theory can be applied to a tumour, when the overall times of two regimes differ (see correspondence in *BJR*, *61*, 700–707, 1988). In general, we agree with the comment of R. T. Yaes "Nobody is suggesting that the LQ model, or indeed any model, should be a substitute for clinical trials or clinical experience".

Yours, etc.,
THELMA D. BATES
*O. C. A. SCOTT

South East London Radiotherapy Centre and
*Richard Dimbleby Department of Cancer Research,
United Medical and Dental Schools,
St Thomas' Hospital,
London SE1 7EH
(*Received August 1988*)

1989, *The British Journal of Radiology*, 62, 92–94

References

BATES, T. D., 1988. The 10-year results of a prospective trial of post-operative radiotherapy delivered in 3 fractions per week versus 2 fractions per week in breast carcinoma. *British Journal of Radiology, 61*, 625–630.

BATES, T. D. & PETERS, L. J., 1975. Dangers of the clinical use of the NSD formula for small fraction numbers. *British Journal of Radiology, 49*, 773.

DISCHE, S., MARTIN, W. M. C. & ANDERSON, P., 1981. Radiation myelopathy in patients treated for carcinoma of the bronchus using a six fraction regime of radiotherapy. *British Journal of Radiology, 54*, 29–35.

FOWLER, J. F., 1983. The second Klaas Breur Memorial Lecture—La Ronde. Radiation sciences and medical radiology. *Radiotherapy and Oncology, 1*, 1–22.

——1988. Intervals between multiple fractions per day. Differences between early and late radiation reactions. *Acta Oncologica, 27*, 181–183.

Diagnostic radiation, pregnancy and termination

THE EDITOR—SIR,

If a pregnant woman is exposed to diagnostic ionizing radiation, the possible sequelae may give cause for concern to the parents and to the medical advisors. If the exposure occurs in the first half of the pregnancy the question may arise as to whether the pregnancy should be terminated. To help allay these worries the Radiation Protection Committee of the British Institute of Radiology (BIR) issued a statement in 1973 expressing the consensus of national and international experts. This indicated that exposures of 100 mGy or less to the uterus did not justify abortion on radiological grounds.

Recently, new effects of radiation on human cerebral development have been identified (Otake & Schull, 1984) and this aspect has been reviewed and amplified by the International Commission on Radiological Protection (ICRP, 1986) and the Nuclear Energy Agency (NEA, 1988). The problem of the magnitude of carcinogenesis injury has also been the subject of further studies, although the size of this hazard is still debatable. Do these new data alter significantly our perception of the magnitude of the possible radiogenic injury to the fetus?

Cerebral injury

In the developing human fetus the formation of forebrain neurones by mitosis is almost entirely restricted to the period of 8–15 weeks after conception, *i.e.* a menstrual age of 10–17 weeks. This period is also associated with active migration of the primitive neurones to the cerebral cortical zones according to precise sequences in time of programmed spatial arrangements (ICRP, 1986). During a further stage of development, from the 16th to the 28th week, the primitive neurones develop further, forming axons and dendrites. Further brain growth lasting in particular up to the age of 2 years is associated mainly with the formation of functional connections between the neurones and with glial cell formation.

Dobbing and Sands (1973) initially pointed out that the time of increased sensitivity of the brain to radiation corresponded to the period of DNA synthesis in the forebrain. Studies on the Japanese atom bomb survivors (Otake & Schull 1984; Otake et al, 1987) show small doses of radiation, as low as 10–90 mGy, are associated with an increased incidence of mental retardation for exposure given to pregnancies from 8–15 weeks after conception, but the number of mentally retarded cases (two) who received this small dose is too small to be statistically significant. If one or two children were wrongly classified then risk estimates at low dose would be substantially changed (ICRP, 1986). The data are compatible with a linear relationship between dose and response and cannot exclude a threshold between zero and 100 mGy (ICRP, 1986). Further analysis shows, even when the mentally deficient had been excluded, that there is lowering of the IQ score of those exposed (ICRP, 1986). It is difficult to believe that a very small dose of radiation could stocastically damage the previously normal brain so as to cause mental deficiency, but this last observation might help to explain the findings.

If ionizing radiation causes a shift of the IQ distribution, lowering the mean, then more cases in the mentally deficient group will occur. Note the importance of the timing of the radiation exposure. No risk is seen resulting from small or moderate levels of radiation (*i.e.* less than 0.5 Gy) unless it is given during the post-conception age from 8 to 15 weeks. With exposures over 1 Gy—much greater than the doses used in diagnosis—brain damage is also seen in those exposed at post-conceptional ages of 16–25 weeks. Exposure at other gestational ages, even at very large exposures, did not affect brain growth or intelligence.

The ICRP (1986) assessed the risk of radiogenic mental deficiency at 0.4 Gy^{-1} during the gestational age of 8–15 weeks. A proportionality coefficient of 7–13 IQ points decrease Gy^{-1} was calculated for those in the 8–15 week gestational age period (NEA, 1988).

Other injuries to organogenesis

From the end of the 2nd week after conception, when organogenesis begins, to the 8th week of development, more than 90% of the 4500 identified structures seen in the adult are already formed (O'Rahilly, 1979). Radiation injuries to the formation of some of these structures have been described, although no injury at diagnostic doses in the human has been identified. Mole (1987) offers cogent argument to indicate that a threshold will usually be expected.

It is prudent, however, to bear in mind the possibility of injury; for example, an exposure in the period of 2–4 weeks after conception could lead to a spina bifida, and a careful ultrasound review of the fetus should be undertaken later with such an injury in mind. There is no human evidence to suggest that exposures in the first 2 weeks after conception, *i.e.* within the menstrual cycle, are dangerous to organogenesis.

Genetic risk

The latest United Nations Scientific Committee on the Effects of Atomic Radiation (UNSCEAR, 1986) assessment for the induction of mutations leading to abnormal children in the next generation lies in the range 0–20 per million live births per 0.01 Gy, or 0–0.20% Gy^{-1}.

Cancer risk

Reviews of the magnitude of the fatal cancer risk after fetal irradiation are available (UNSCEAR, 1982, 1986; Mole, 1987).

Estimates of magnitude of the risk of lethal cancer after irradiation *in utero* vary widely. The Japanese atom bomb survivors, on whom we rely so much for our adult radiation hazard assessment, showed no increase in childhood lethal cancer in those irradiated *in utero* (Jablon & Kato, 1970) but there is an increased cancer rate during adult life of those exposed *in utero* (Yoshimoto et al, 1988). The concensus figures of excess cancer deaths in the UNSCEAR report (UNSCEAR, 1986) is 2–2.5% Gy^{-1}.

Table I. Mean adult ovarian dose per examination

	mGy
Lumbar spine	6
Upper femur, hip	1
Pelvis	2
Abdomen	0.8
Barium enema	16
Barium meal	3.6
Intravenous urography	3.6
Cystography	14.2

Taken from Wall et al (1980).

In the latest report of the Oxford Survey of Childhood Cancers (Knox et al, 1987) this figure is 20% Gy^{-1} and higher in early pregnancy (Gilman et al, 1988). If these estimates are true it means that over half the childhood cancer deaths arise from the natural radiation exposure *in utero*, and we should see high rates of childhood cancer in areas of high natural radiation. This has been looked for and not found (Hanson & Komarov, 1983).

Full analysis of the new data from the Japanese bomb survivors (Preston & Pierce, 1987) is awaited but it seems likely that after irradiation of children a figure of fatal cancer induction of about 6% Gy^{-1} will be assessed. It seems unwise to assume a lower figure than this for the embryo or fetus.

Assessment of radiation dose

If there is a diagnostic exposure of a pregnancy an assessment of the radiation dose should be made. A medical physicist should be involved in the assessment; variations larger than a hundredfold may be found in different hospitals and individuals for a given examination (Shrimpton et al, 1986).

In nuclear medicine the radiation dose to the uterine contents is unlikely to be larger than the maternal tissue dose, with the exception of iodides, when the fetal dose may be assumed to be fivefold larger than the maternal dose (NEA, 1988).

Table I gives the mean ovarian dose for several examinations (Wall et al, 1980). As noted these can vary widely. In early pregnancy the ovarian dose and uterine dose are similar, but in later pregnancy assessment is more complex.

The average occupational exposure to radiographers was found to be 0.37 mGy^{-1} year and to radiologists 0.51 mGy year^{-1} (Hughes et al, 1983). These are film badge measurements and the uterus dose will be substantially less. If we assume the fetal brain exposure is half the film badge dose, then in the 8-week period of fetal brain growth sensitivity, the occupational radiation dose to the fetal brain will average only 0.06 mGy for radiographers and 0.08 mGy for radiologists.

Total risk

Taking a pessimistic view of the risk factors indicated above, the hazard of a fetal 1 mGy exposure will be as follows.

(1) Brain injury at a rate of 13 IQ points decrease Gy^{-1}, only during 8–15 weeks gestational age (corresponding to 10–17 weeks menstrual age): an IQ decrease of 0.013 of a point.

(2) Genetic risk to the next generation, at a rate of 0.20% Gy^{-1}, one abnormal child in half a million exposures.

(3) Childhood fatal cancer risk at a rate of 6% Gy^{-1}: one case in 16 000 such exposures. The natural incidence of fatal cancer in the United Kingdom is 1 in 1800 so this represents an increase of 11% in the natural incidence.

It can be seen that the cancer risk will be the most worrying of the hazards to the majority of people.

At this radiation dose to the fetus, it seems unlikely that fear of an injury from diagnostic radiation should ever be, *per se*, an indication for terminating a pregnancy. The final decision to ask for a termination rests with the mother, but the advice she gets from her attendants can be reassuring. At larger doses the matter should be discussed on the basis of a full understanding of the hazards.

Wherever possible, diagnostic radiation to a pregnancy should be avoided (National Radiation Protection Board (NRPB), 1985). Careful radiographic technique should always keep the dose as low as possible, especially for the gonads, whether a pregnancy is present or not. Radiation is unwelcome, but we do not live in a perfect world. Nora et al (1967) found women were exposed to an average 3.7 potentially teratogenic agents in the first 3 months of pregnancy.

Yours, etc.,
J. G. B. Russell

Department of Radiology,
Saint Mary's Hospital,
Whitworth Park,
Manchester M13 0JH

(Received July 1988)

References

BIR, 1973. *Diagnostic Radiology in Early Pregnancy and Grounds for Recommending Abortion.* Statement of Radiation Protection Committee (BIR, London).

Dobbing, J. & Sands, J., 1973. Quantitative growth and development of human brain. *Archives of Disease in Childhood, 48*, 757–767.

Gilman, E. A., Kneale, G. W., Knox, E. G. & Stewart, A., 1988. Pregnancy X-rays and childhood cancers: effects of exposure age and radiation dose. *Journal of the Society for Radiological Protection, 8*, 3–8.

Hanson, G. P. & Komarov, E., 1983. Health effects in residents of high background radiation regions. In *Biological Effects of Low Level Radiation* (International Atomic Energy Agency, Vienna).

Hughes, J. S., Roberts, G. C. & Stephenson, S. K., 1983. Occupational exposure in medicine—a review of radiation doses to hospital staff in North West England. *British Journal of Radiology, 56*, 729–735.

ICRP, 1986. *Developmental Effects of Irradiation on the Brain of the Embryo and Fetus* (Pergamon Press, Oxford).

Jablon, S. & Kato, H., 1970. Childhood cancer in relation to prenatal exposure to atomic bomb radiation. *Lancet ii*, 1000–1003.

Knox, E. G., Stewart, A. M., Kneale, G. W. & Gilman, E. A., 1987. Prenatal irradiation and childhood cancer. *Journal of the Society for Radiological Protection, 7*, 3–15.

Mole, R. H., 1987. Irradiation of the embryo and fetus. *British Journal of Radiology, 60*, 17–31.

NRPB, 1985. *Exposure to Ionising Radiation of Pregnant Women: Advice on the Diagnostic Exposure of those who are, or may be Pregnant* (Her Majesty's Stationery Office, London).

NEA, 1988. *The Biological Basis for the Control of Prenatal Irradiation* (Organization for Economic Co-operation and Development, Paris).

Nora, J. J., Nara, A. H., Sommerville, R. J. Hill, R. M. & McNamara, D. G., 1967. Maternal exposure to potential teratogens. *Journal of the American Medical Association, 202*, 1065–1069.

1989, *The British Journal of Radiology*, 62, 94–95

O'Rahilly, R., 1979. Early human development and the chief sources of information as staged human embryos. *European Journal of Obstetrics and Gynaecological Reproduction Biology*, 9, 273–280.

Otake, M. & Schull, W. J., 1984. *In utero* exposure to A-bomb radiation and mental retardation: a reassessment. *British Journal of Radiology*, 57, 409–414.

Otake, M., Yoshimaru, H. & Schull, W. J., 1987. *Severe Mental Retardation among the Prenatally Exposed Survivors of the Atomic Bombing of Hiroshima and Nagasaki: a Comparison of the T65D and the DS86 Dosimetry Systems*, RERF TR 16–87 (Radiation Effects Research Foundation, Hiroshima).

Preston, D. C. & Pierce, E. A., 1987. *The Effects of Changes in Dosimetry on Cancer Mortality Risk Estimates in the Atomic Bomb Survivors*, RERF 9–87 (Radiation Effects Research Foundation, Hiroshima).

Shrimpton, P. C., Wall, B. F., Jones, D. G., Fisher, E. S., Hillier, M. C., Kendall, F. M. & Harrison, R. M., 1986. Doses to patients from routine diagnostic X-ray examinations in England. *British Journal of Radiology*, 59, 749–758.

UNSCEAR, 1982. *Ionizing Radiation: Sources and Biological Effects* (United Nations, New York).

—— 1986. *Genetic and Somatic Effects of Ionizing Radiation* (United Nations, New York).

Wall, B. F., Fisher, E. S., Shrimpton, P. C. & Rae, S., 1980. *Current Levels of Gonadal Irradiation from a Selection of Routine Diagnostic X-ray Examinations in Great Britain* (NRPB, Harwell).

Yoshimoto, Y., Kato, H. & Schull, W. J., 1988. Risk of cancer among children exposed *in utero* to A-bomb radiations, 1950–84. *Lancet*, *ii*, 665–669.

Leakage from a caesium-137 needle

The Editor—Sir,

During routine leakage checks on our stock of iridio-platinum encased caesium-137 needles and tubes, an unacceptable level of activity was detected from a number of needles. On further testing it was found that 18 gave positive indication of free activity. It was known from our records that seven of these had never been used clinically since purchase from Amersham International in 1981. The suspect sources were returned to Amersham, at their request, for inspection.

They confirmed that one source consistently gave samples containing several hundred counts per minute when immersed in boiling water to remove surface contamination. The BS 5288 Appendix D limit is 200 Bq but Amersham use a pass limit of 18 Bq (0.5 nCi). The source was identified as a type CDC D2, one of the group which had never been used clinically. The other 17 needles passed the 4-h immersion test (British Standards Institution (BSI), 1988).

The test report from Amersham states "Visual examination at × 10 magnification found no damage, holes, blemishes or marks. Extra attention was paid to the resistance weld zones at the eylet and trocar ends but again no marks were visible. Careful wipe tests were made in these two areas. The eyelet end gave a 3.5 nCi result and the trocar end a 22.9 nCi result. Further close inspection of the trocar weld area again found no visible defects". The report concluded "There is a defective weld at the trocar end although there is no exterior visual evidence. The source passed its leak test at manufacture. One can only speculate that contamination between the inner shell and sheath has migrated over a period of time into an area of the weld that is faulty and contains a microscopic pathway for the Caesium 137".

The recently published *Guidance Notes for the Protection of Persons against Ionising Radiations arising from Medical and Dental Use* (National Radiation Protection Board (NRPB), 1988) states in Paragraph 9.23 that "sources should be re-tested at least once a year and whenever damage is suspected. This is necessary because brachytherapy sources are subject to wear through frequent use and sterilization". If the leak in our needle was the result of its use, namely three or four leak tests in 7 years, one might be tempted to forego such tests for sources which have never been used clinically, only performing a leak test when a request for the source arises. If, on the other hand, the leakage of active material is simply a migration during long-term storage, then it would be unwise to leave the source unchecked as contamination of nearby sources could become a serious problem. Paragraph 9.23 of the Guidance Notes can be interpreted in such a way that a source need not be tested until *after* its first use if a leakage test certificate has been issued by the manufacturer. This would be a dangerous interpretation in view of our experience, even allowing for the rarity of the occurrence.

Yours, etc.,

D. G. Clarkson

West of Scotland Health Boards,
Department of Clinical Physics and Bio-Engineering,
11 West Graham Street,
Glasgow G4 9LF

(*Received July 1988*)

Acknowledgment

Permission to reproduce parts of the report by the Technical Service Department of Amersham International is gratefully acknowledged.

References

BSI, 1988. *BS 5288. Sealed Radioactive Sources* (BSI, London).

NRPB, 1988. *Guidance Notes for the Protection of Persons against Ionising Radiations arising from Medical and Dental Use* (NRPB, Chilton Didcot).

Costing imaging procedures

The Editor—Sir,

Dr Bretland (1988b) has omitted an important factor from his calculations of the cost of oral cholecystography—that of the harm done by ionizing radiation. This has been calculated at £5–10 000 man-Sv $^{-1}$ (Russell & Webb, 1987). Since this estimate was made, our perception of fatal cancer induction has at least doubled (International Commission on Radiological Protection (ICRP), 1987) so it is reasonable to take £10 000 as the value of avoiding a man-Sv.

Shrimpton et al (1986) estimated the mean dose from oral cholecystography at 0.95 mSv (range 0.13 to 5.01 mSv) giving a value of the harm caused by radiation of £9.5/examination.

This increases the cost of an oral cholecystogram using Dr Bretland's figure to £39, which can be compared with his figure for a biliary ultrasound examination of £22.

The error of omission of a factor for the harm caused by ionization radiation flaws Bretland's earlier study (1988a).

Yours, etc.,

J. G. B. Russell

Department of Radiology,
Saint Mary's Hospital,
Whitworth Park,
Manchester M13 0JH

(*Received July 1988*)

(*Author's reply*)

THE EDITOR—SIR,
Dr Russell is quite right to suggest that an element representing in financial terms the harm done by ionizing radiation should be added to the costs of imaging procedures, but it is a different kind of cost, calculated in a different way.

The work on which my three articles (Bretland 1988a,b,c) were based was done in 1985 and was devoted to classifying and defining the elements to be included in the costing. It distinguished money actually spent within the District to cover variable, semi-variable and fixed costs in the financial year 1984/85 (the short-term costs) on the one hand, from the hypothetical capital costs of major equipment and existing buildings and the maintenance of those capital assets, (the medium-term costs) on the other, in accordance with standard commercial cost-accounting practice. It was concerned with ensuring that proper calculations could be made of the costs of maintaining an imaging service in the foreseeable future and that costing figures from different institutions could be properly compared because they had included similar cost elements in similar ways.

This work did not include estimates of "downstream" costs, *i.e.* the consequential, hypothetical, predicted costs entailed by undertaking or omitting a diagnostic procedure. There is an argument that any procedure which makes an earlier diagnosis reduces the costs and contributes to the success of future treatment and management of the patient, as well as improving the quality of life. Against this must be set not only the intrinsic cost of the diagnostic procedure but also the cost of its hazards and complications. Any sensible system of cost–benefit analysis will have to take these elements into consideration. There is remarkably little published work on this subject and much to be done in the future.

I suggest, therefore, that, however valid the concept of a cost element for the harm done by ionizing radiation, it is a probability-derived figure based on statistical evidence. Its place in the cost–benefit analysis is thus not with the basic intrinsic short- and medium-term local costs of maintaining the imaging service. Its place is with the hypothetical calculated "downstream" costs in the long-term cost–benefit analysis (preferably on a national basis) so that it can be set against the ultimate benefit of the procedure. Only then can its true relevance be properly assessed.

Yours, etc.,
P. M. BRETLAND

The Whittington Hospital,
St Mary's Wing,
Highgate Hill,
London N19 5NF

(*Received August 1988*)

References

BRETLAND, P. M., 1988a. Costing imaging procedures. *British Journal of Radiology, 61*, 54–61.

—— 1988b. The cost of imaging procedures. *British Journal of Radiology, 61*, 652–653.

—— 1988c. Costs of nuclear medicine. *Nuclear Medicine Communications, 9*, 25–35.

ICRP, 1987. *Como Statement* (Pergamon Press, Oxford).

RUSSELL, J. G. B. & WEBB, G. A. M, 1987. Valuing the man-Sievert in X-ray diagnosis. *British Journal of Radiology, 60*, 681–684.

SHRIMPTON, P.C., WALL, B. F., JONES, D. G., FISHER, E. S., HILLER, M. C., KENDAL, G. M. & HARRISON, R. M., 1986. *A National Survery of Doses to Patients undergoing a Selection of Routine X-ray Examination in English Hospitals, NRPB R200* (Her Majesty's Stationery Office, London).

1989, *The British Journal of Radiology*, 62, 96–98

Proceedings of The British Institute of Radiology

Too much radiation in radiodiagnosis?

Abstracts of papers presented at a meeting of the BIR, held at the University College and Middlesex School of Medicine, Windeyer Building, Cleveland Street, London W1 on Wednesday, March 9, 1988

Session 1

Chairman: Dr J. G. B. Russell

Theoretical overview of dose reductions, by C. Lawinski (abstract not received)
The potential and need for dose reductions in radiodiagnosis, by B. F. Wall
Optimization, by J. R. Croft
A clinical assessment of the image quality of radiographs obtained using dose reduction filters, by H. B. Meire and H. Jadva
Who makes the recommendations concerning radiation protection? by J. G. B. Russell, and A. P. Hufton
Legislation to limit radiation dose to patients, by B. E. Godfrey

Session 2

Chairman: Mr G. Mountford

Have intensifying screens changed to effect less radiation? by D. G. Rothery
Effects of films and screens on radiation dose reduction, by L. Astle (abstract not received)
Grids: changes in manufacture and design to effect lower dose, by P. de Hanika (abstract not received)
Processors, by A. N. Cropper
Dose reduction potential of carbon fibre table tops in diagnostic radiology, by L. G. Bevan
Cassettes: changes in design for more efficiency, by D. P. Roberts
Electronic imaging, by M. Moore (abstract not received)

The potential and need for dose reductions in radiodiagnosis

B. F. Wall
National Radiological Protection Board, Chilton, Didcot, Oxon

The potential for reducing the radiation exposure of the community is nowhere higher than in the field of radiodiagnosis, which accounts for nearly 90% of the dose to the population from all uses of ionizing radiation. Results of national surveys are presented which demonstrate wide variations in doses to patients from the same type of X-ray examination. Many of the higher doses could be dramatically reduced with no loss of diagnostic information and at little, if any, financial cost. A reduction of less than 1% in the population exposure from diagnostic radiology would balance the entire contribution from the UK nuclear power programme. Despite this potential, and unlike the case of nuclear power, there is little pressure from the public or the media to reduce doses from diagnostic X rays. This ambivalent attitude towards radiation no doubt stems from general appreciation of the direct and personal benefit of most health care activities, radiodiagnosis included, and a less than universal acceptance of the benefits of nuclear power. Patients will accept risks from medical procedures that promise relief from pain or disability, that they would not normally accept from other sources. The risks of radiation-induced health effects occurring in a patient after exposure to routine types of X-ray examination are shown to vary between about one in a million for a chest X ray to about 1 in 10 000 for an intravenous urogram or a barium enema. Considered individually, these risks are low, especially when compared with the risks of some surgical procedures, and can usually be justified in terms of the overriding medical benefit of the examination. However, with 35 million X-ray examinations taking place annually in Britain it is the collective radiation detriment that is the problem. If this detriment is expressed in terms of the number of years of life lost from the radiation delivered in a typical X-ray room, then the effectiveness of applying low-dose technology in the room in terms of the cost per year of life saved can be calculated. This is shown to compare favourably with other established medical procedures that extend or enhance life and already consume considerable health service resources.

Optimization

J. R. Croft
National Radiological Protection Board, Northern Centre, Cookridge, Leeds

The basic International Commission on Radiological Protection (ICRP) principle of optimization is applicable to radiodiagnosis and undoubtedly there exists a significant potential for dose reductions in this sphere. A variety of options to achieve this is available. The question is which of these should be considered reasonably practicable and implemented and can they be ranked in order of priority? To aid the judgments inherent in optimization, or as it is more commonly referred to, ALARA/ALARP, the Commission recommends the use of cost–benefit analysis. The current advice from the National Radiological Protection Board (NRPB) on the use of cost–benefit analysis and valuing the man-Sv is presented. Patient exposure is a special case as, unlike most other irradiations, the exposed person derives a personal benefit. This and other relevant factors have been considered by Russell and Webb and their proposals are discussed. The role of cost–benefit analysis in decision-making is discussed with reference to the level of decision and the use of structured approaches such as the ALARA Procedure and ALARA Audits. Brief examples of possible uses are presented and further studies are advocated. It is recognized that radiation protection in the medical field is competing for scarce resources and to demonstrate its cost effectiveness relative to medical procedures, other economic techniques such as cost–utility analysis are being explored. A common problem in the field of optimization, irrespective of whether quantitative decision aiding techniques are used, is the availability of appropriate databases. This problem is addressed and encouragement is given to the inclusion in quality assurance programmes of routine monitoring of doses to patients.

A clinical assessment of the image quality of radiographs obtained using dose reduction filters

Hylton B. Meire and Hansa Jadva
Department of Radiology, King's College Hospital, London SE5 9RS

Radiographs were taken over a 4-month period using three different filter materials: 3 mm aluminium (Al), 3 mm Al + 0.1 mm erbium and 3 mm Al + 0.1 mm ytrium. Examinations were confined to 11 main regions including chest, abdomen, pelvis, spine and limbs. Each patient was examined with only one filter material and all examinations were performed on a single basic radiographic unit. Nearly 1800 examinations were included in the study. Anatomical phantoms were used to establish the mAs factors necessary to achieve comparable clinical results with the different filter materials. The dose reductions obtained with the filters were measured and are reported separately. They were of the order of 30 to 70% of the dose with the 3 mm Al filter. During the study period 104 patients were examined with the erbium filter and 185 with the ytrium. At the conclusion of the study H.J. chose one example each of the 11 types of examination for each filter material on patients matched as closely as possible for size. The resulting radiographs were colour-coded for filter material, and other factors, using a complex code not known to the radiologists. The radiographs were then analysed separately by each of four radiologists and scored for image quality on a scale of 1 to 5. Image quality took into account overall image contrast with special reference to the diagnostic adequacy of the information in the lighter and darker areas of each radiograph.

The codes were then broken and totalled for each different filter material. The mean scores were: aluminium alone 3.45, aluminium + erbium 3.55, and aluminium + ytrium 2.82. The differences between these means are statistically significant. The high score for erbium is notable. This may be related to the unusual spectral distribution of the erbium-filtered radiation which tends more towards monochromatic with the peak value increased but the mean decreased. The mean values for the transmitted radiation for the three filters with a kVp of 80 were: Al 44.2 Kv, Er 43.2 Kv, and Yt 48.8 Kv. It seems possible that the radiologists subjective assessments had detected these differing values. The study suggests that the use of dose-reduction filters does not degrade image quality and that erbium may produce a small subjective improvement. The small but significant dose reductions obtained with these filters should be seen in the context of the huge range of different exposures for any given examination attributable to varying technique in different hospitals.

Who makes the recommendations concerning radiation protection?

J. G. B. Russell and *A. P. Hufton
*St Mary's Hospital, Manchester and *Regional Department of Medical Physics, Christie Hospital, Manchester*

The International Commission on Radiological Protection (ICRP) is the primary international body making recommendations on standards and practices in radiological protection. There are, however, many other international organizations having important roles in the field of radiation protection. A number of these are organized under the aegis of the United Nations. For example, the United Nations Scientific Committee on the Effects of Atomic Radiation (UNSCEAR) publishes an extensive review of the subject every 4 years, and both the World Health Organization and the International Atomic Energy Agency publish useful reports on specific radiation protection topics. The American Committee on the Biological Effects of Ionizing Radiation, (BEIR) and the National Council on Radiation Protection and Measurements, (NCRP) also produce reports in a similar way to UNSCEAR and ICRP, and these too have considerable influence in the international scene. In the United Kingdom the most important body dealing with radiation protection is the National Radiological Protection Board (NRPB). As well as being required to advise the Government on radiation protection matters, it publishes advice and reports on important topics. There are of course many other UK bodies, like the British Institute of Radiology, representing specific groups with interest in particular areas of radiation protection, and who, by various means, influence the advice which the Government receives through the DHSS and Health and Safety Commission. Ultimately, some of this advice may be incorporated into legal requirements for radiation protection. Examples of this, arising out of the 1974 Health and Safety at Work Act, and Directives from the Council of the European Communities, are the *Ionising Radiations Regulations 1985* and forthcoming Regulations concerning the protection of the patient.

Legislation to limit radiation dose to patients

B. E. Godfrey
Department of Health and Social Security, Elephant & Castle, London SE1 6BY

Specific requirements of the Medicines (Administration of Radioactive Substances) Regulations 1978, The Ionising Radiations Regulations 1985, and The Ionising Radiations (Protection of Persons undergoing Medical Examination or Treatment) Regulations (in draft), as they relate to the limitation of radiation dose to patients, are discussed. Current legislation is seen to be directed towards the achievement of dose limitation through regulation of the design, construction, installation and maintenance of equipment; the training of those who effect medical exposures; and procedures for medical exposures.

Have intensifying screens changed to effect less radiation?

D. G. Rothery
3M UK PLC, Bracknell, Berks RG12 1JU

It was, in fact, a phosphor coating that assisted Roentgen to discover X radiation; the phosphor, barium platino cyanide, was quickly changed at the turn of the century by Eddison who developed the phosphor calcium tungstate which formed the basis of medical intensifying screens up until the early 1970s. The only way to reduce radiation using $CaWO_4$ screens was to increase the size of the grains used in the phosphor coating. This led to a reduction in image quality. In 1972 Dr R. A. Buchanan was working on the absorption of radiation in space for the Lockheed Company. He proposed two new materials that would have a useful existence in medical applications. These two phosphors were rare-earth materials from the lanthanide series of elements, namely lanthanum oxysulphide and gadolinium oxysulphide. Light conversion from absorbed X-ray energy was four to six times better than calcium tungstate and gadolinium had a 50% better X-ray photon absorption than lanthanium above 50 kVp. However, both these two phosphors emitted a high intensity of green light when irradiated, which led to the development of oxybromide compounds to follow the direction of calcium tungstate. Today, phosphors are used in intensifying screens having ultraviolet, blue and green light emissions. Screen speeds now range as high as 1260 (relative speed) using rare-earth phosphors and high-speed film—this can offer exposure reductions of up to 90% compared with calcium tungstate (200 speed) systems. Furthermore, image quality is improved because of the small uniform grains and high packing densities achievable using rare-earth phosphor materials.

Reference

Buchanan, R. A., Finkelstein, S. & Wickersheim, K. A., 1972. Exposure reduction using rare earth oxysulphide screens. *Radiology, 105*, 185–190.

Processors

A. N. Cropper
Kodak Ltd, Hemel Hempstead, Herts HP1 1JU

Patient dosage and automatic processors may be approached from two directions. First, potential reduction of dose can be achieved by the use of the correct processing temperature as recommended by the manufacturer. The manufacturer will recommend the temperature that achieves the best possible result from their film and chemical products. Running a processor below this temperature results in an increase in exposure to achieve the necessary densities for diagnosis. With modern films, increases in temperature normally only result in increased fog and contrast, with higher visualization of mottle and a possibility of grain clumping. Informal surveys by this Company have demonstrated that well over 50% of processors are running at 2°C (or more) below recommended temperatures. This can result in an apparent speed loss in excess of 20%. Secondly, excess exposure can be prevented by reducing repeat examinations required by non-diagnostic radiographs. After installation, the correct operating temperatures and replenishment rates should be ensured throughout all the processors in each hospital, so that each processor is matched for speed and contrast monitoring of the sensitometric performance. Freshly exposed film, of the type used by the department should be used and the results plotted on a trend chart which will give advance warning of drifts away from the ideal. Corrective action may be taken before these changes become apparent on radiographs. Soon to be available will be a computer-based "Process Control Manager" comprising an "intelligent" densitometer interfacing with a computer and a software package that plots, diagnoses and recommends any corrective action(s) necessary. This will remove the tedium associated with the routine, daily plotting. Finally, the first person to touch an X-ray film is the person who opens the box. Film is manufactured in a totally automated process and is at its most sensitive in the post-exposure state prior to processing. Relatively few darkroom technicians receive any formal training, a deficiency generally attributed to lack of funds and/or time. Darkroom technicians who are also responsible for routine day-to-day processor monitoring and maintenance may contribute greatly to reduced film rejects and hence to dose reduction.

Dose reduction potential of carbon fibre table tops in diagnostic radiology

L. G. Bevan
Fothergill Composite and Polymer Technologies Ltd, Bridgwater, Somerset TA6 4TP

A significant portion of the dose received by a patient during a radiographic examination is a result of absorbtion in the various patient support structures through which the primary beam must pass. A significant reduction in dose to both patient and, equally importantly, the staff can be achieved by the use of carbon fibre materials. This has been confirmed by independent researchers. The use of carbon fibre in the construction of patient support structures was established in the 1970s. A major problem for CT scanner designers at that time was to design a patient support couch that would meet machine requirements of stiffness and strength yet have low attenuation. The problem with conventional materials was that they could satisfy one criterion but only at the expense of the other. Fothergill Technologies solved the problem by designing a carbon fibre skinned/foamed-filled couch that met the demanding requirements. Unless ill treated, the couches are hard wearing and can stand up to the rigours of a busy department. Well over 2000 installations worldwide have been made over the last decade and there has never, to our knowledge, been a service difficulty associated with the performance of the carbon couch. Carbon fibre materials are more costly than components made from conventional materials but the dose reduction made possible by carbon fibre components can be justified in cost–benefit terms. On average, a reduction of 10% in patient dose will save £5400 per room per year (Mufton et al, 1987). This means that the cost of a carbon fibre table can be recovered within a matter of months.

Reference

Mufton, A. P., Crosthwaite, C. M., Davies, J. M. & Robinson, L. A., 1987. Low attenuation materials for table tops, cassettes and grids: a review. *Radiography, 53*, 17–18.

Cassettes: changes in design for more efficiency

D. P. Roberts
Diagnostic Imaging Systems Division, Agfa-Gevaert Ltd, Brentford, Middlesex TW8 9AX

Like most sciences, radiography owes much of its modern developments to history. The cassette is no exception to this. Since the discovery of X rays there have been continuous attempts to improve the efficiency of examination of patients, particularly in attempts at dose reduction. For many years, the cassette was simply a box-like structure containing a pair of screens on each side of a film. The need for intimate contact between film and screens led to the relatively simple mechanical device of a curved, usually metal, cover exerting pressure on the film and screens. If film/screen contact could be maintained by sandwiching the screens between a thin metal foil and a sheet of magnetic rubber, a much lighter cassette could be constructed, since reliance need no longer be placed on the curved metal cover. Such a system was designed by Agfa-Gevaert using Novodur, an ABS plastic developed by Bayer. The resulting cassette is about 25% lighter than an equivalent metal cassette with significantly less absorption. The reduction in absorption can be as great as 40%. There are major advantages in such a construction, mainly due to the accuracy of modern moulding techniques. This accuracy is of great benefit in cassette transport and film-handling systems.

1989, *The British Journal of Radiology*, 62, 99–100

Instructions to authors

Please keep manuscripts brief and include only those illustrations essential to an understanding of the text. Much time and correspondence will be saved if authors pay careful attention to these detailed instructions especially as regards references.

Material published in *The British Journal of Radiology* includes full papers, case reports, the Case of the Month, technical and instrumental notes, short communications, letters to the editor and invited articles. Communications should ordinarily be addressed to the Honorary Editors, The British Journal of Radiology, 36 Portland Place, London W1N 4AT.

Communications from North America, Continental Europe, Australasia or South Africa should preferably be submitted to the most appropriate of the following Associate Editors:

Dr P. Armstrong, MB, BS, FRCR, DMRD, Department of Radiology, School of Medicine, University of Virginia, Charlottesville, Virginia 22901, USA (for diagnostic papers).

Professor H. K. Baddeley, MB, BS, DMRD, FRCR, MRACR, University of Queensland, Department of Radiology, Mater Misericordiae Hospitals, South Brisbane, Queensland 4101, Australia (for diagnostic papers).

Dr S. G. A. Chenery, PhD, Director, Physics Section, Radiation Oncology Center, 5271 F Street, Sacramento, CA 95819, USA (for non-diagnostic papers).

Professor B. J. Cremin, FRACR, FRCR, Department of Radiology, Red Cross Children's Hospital, Rondebosch, Cape Town 7700, South Africa.

Dr R. Fox, DPhil, Department of Medical Physics, Royal Perth Hospital, Perth, Western Australia (for non-diagnostic papers).

Professor M. Takahashi, Department of Radiology, Kumamoto University School of Medicine, 1-Chome, Honjo, Kumamoto, Japan 860.

Professor D. M. Taylor, Institute for Genetics and for Toxicology of Fissile Materials, Kernforschungszentrum, Postfach 3640, D-7500, Karlsruhe 1, Federal Republic of Germany.

The acceptance of a paper for publication in *The British Journal of Radiology* is at the discretion of the Editors and is subject to the understanding that the material contained in the paper has not already been published and is not intended for publication elsewhere.

If a paper has more than one author, the negotiating author is expected to bear responsibility for obtaining the agreement of all the other authors. **All** authors must sign the covering letter submitted with the manuscript.

The copyright of all publications resides with The British Institute of Radiology.

The Editors take no responsibility for the return of manuscripts, prints, etc., submitted for publication.

RESEARCH. Where relevant, authors will be required to sign a statement that permission for clinical trials has been obtained from the appropriate Ethical Committee. In animal experimentation, authors will be asked to provide a statement that this has been carried out in accordance with the Biological Council *Guidelines on the Use of Living Animals in Scientific Investigations*, 2nd edn.

MANUSCRIPT. The manuscript, *including* references, figure legends and tables, should be typewritten in English on one side of the paper only with **double spacing** and margins of at least 25 mm on both sides and at the top. Pages should be numbered. **Three** clear copies must be submitted. The address given in the title should be that of the department(s) or hospital(s) at which the work was carried out. If any author has subsequently moved to a new address, this should be given as a footnote. Degrees and diplomas of authors should be given but not more than three for each author. Tables (numbered I, II, etc.) should be given on separate sheets, and each should have a short descriptive title. Legends for illustrations, including diagrams and graphs, should be set out on a separate sheet, and denoted Figure 1, 2, etc. The initial letter of trade or proprietary names should be a capital. Mathematical expressions should be set out clearly. Up to three levels of headings may be used and paragraphs should be indented.

UNITS, SYMBOLS AND ABBREVIATIONS. Authors should use the International System of Units (SI) (NPL, 1982). Units of radiation should be given in SI with the old units in brackets if necessary; thus 1 Sv (100 rem), 1 Gy (100 rad), 1 MBq (27 μCi). *The British Journal of Radiology*, May 1981, contained two useful articles on this subject, by the BIR Working Party on SI units and by W. A. Jennings. On the question of quantities and units for radiation dosimetry, three recommendations from the British Committee on Radiation Units and Measurements (BCRU, 1980, 1982a, b) are worth consulting. The publication *Units, Symbols and Abbreviations: a Guide for Biological and Medical Editors and Authors* (Royal Society of Medicine, 1977) will also be found helpful.

DIAGRAMS AND GRAPHS. Three sets of artwork should be supplied. Diagrams and graphs, including numerals and lettering, should be clearly drawn in black ink for photographic reproduction to a width of 76 mm (exceptionally 156 mm). Good quality photographic prints or the original artwork should be supplied. Care should be taken that details such as numbering and experimental points remain legible after photographic reduction. Computer print-outs are seldom satisfactory. The figure number, author's name and title of article should be on the back of each illustration, pencilled lightly or on a sticky label. Authors of physics papers will find advice on drawing diagrams, particularly electrical circuits, in *Notes for Authors* issued by the Institute of Physics and the Physical Society in 1976 (revised 1983).

RADIOGRAPHS. Three sets of unmounted prints not larger than whole plate, 216 mm × 152 mm, and not smaller than half plate should be supplied with manuscripts; any extraneous areas which could be cropped off to highlight the area of interest should be indicated on a tracing-paper overlay. If the prints are not of sufficiently high standard for reproduction purposes the author will be required to submit the original radiographs and to defray the cost of making prints. Tracings of sections of prints are acceptable when necessary for additional clarification. Hospital illustrators and photographers are usually familiar with the style of drawing or print which will give the best reproduction.

COLOUR. Illustrations in colour are very expensive to print and are acceptable only if the author is prepared to pay the additional cost (likely to be at least £500).

All illustrations must have the top clearly marked.

REFERENCES. The Harvard system is used. In the text the names of authors and the year of publication should be given. When there are more than two authors only the first followed by et al should be used. In the bibliography references should be given *in full* and include the title of the paper, names of all authors and the full name of the journal or other publication in which the article cited appeared. Both first and last page numbers are required. The references must be arranged in alphabetical order, in the following form:

Examples

COHEN, M. D., SMITH, J. A. & GREENMAN, G. G., 1983. Ultrasound diagnosis of liquid-filled lesions in children. *British Journal of Radiology*, *56*, 527–530.

MICHAEL, B. D. & HARROP, H. A., 1980. Time scale and mechanism of radiosensitization and radioprotection at the cellular level. In *Radiation Sensitizers*, ed. by L. W. Brady (Masson, New York), pp. 164–170.

All references must appear both in the text and in the bibliography.

The accuracy of references is the responsibility of the author: references must be checked carefully at source before submitting the paper, otherwise publication may be delayed.

ABSTRACTS. Papers (other than case reports and technical notes) should be accompanied by an abstract. This abstract is not part of the paper, but is intended to convey the content of the paper and to draw attention to all new information and the main conclusions. It should be intelligible in itself without reference to the paper. An abstract should not normally exceed 200 words and should *not* contain references.

CORRESPONDENCE. Letters for publication in the correspondence section of the journal may be accepted on any matters of interest to readers of the journal.

SHORT COMMUNICATIONS. These are reports of initial studies in new areas, and comments which are too speculative or provocative for a normal paper. They should be kept as short as possible and must on no account exceed two pages of the journal. No abstract is required. They will be published with the minimum delay.

CASE OF THE MONTH. These are short papers reporting a recognised but rare abnormality, or are teaching cases with points of general interest that might be seen at an examination. They will occupy no more than two pages and should, therefore, be no more than 1700 words long, less approx. 200 words for each illustration included. The relevant history and initial radiographs will appear on a right-hand page, presenting a specific problem to the reader. Overleaf will appear comments, with the results of further investigations and a conclusion, followed by a brief and up-to-date review of the subject with a maximum of five references. The names of no more than three authors will be printed. Radiotherapy and oncology, as well as diagnostic, papers will be welcomed for this feature.

OFFPRINTS AND REPRINTS. Twenty-five free "as printed" offprints of each paper will be supplied. A form for ordering additional offprints, bound offprints etc. will be sent to the authors with proofs for correction. This form should be returned, giving the address for offprints, even when additional offprints are *not* required.

SUPPLEMENTS. Special monographs and reports of Working parties which are too long for publication within the journal may be considered for publication as a Supplement.

References

BCRU, 1980. Quantities for reporting the calibration of therapy-level dosemeters in photon beams. *British Journal of Radiology*, *53*, 917–918.

——1982a. Use of air kerma for photon dosimetry in air. *British Journal of Radiology*, *55*, 375–376.

——1982b. SI units for radiation protection—an interim measure. *British Journal of Radiology*, *55*, 376–377.

BIOLOGICAL COUNCIL, 1987. *Guidelines on the Use of Living Animals in Scientific Investigations*, 2nd edn. Obtainable from Mrs. B. Cavilla, c/o Institute of Biology, 20 Queensberry Place, London SW7 2DX.

BIR WORKING PARTY ON SI UNITS, 1981. Conversion to SI units in radiology. *British Journal of Radiology*, *54*, 377–380.

INSTITUTE OF PHYSICS, 1983. *Notes for Authors*. Obtainable from Institute of Physics Publications Dept., Techno House, Redcliffe Way, Bristol BS1 6NX.

JENNINGS, W. A., 1981. How much do you know about quantities and units? *British Journal of Radiology*, *54*, 381–383.

NATIONAL PHYSICAL LABORATORY, 1982. *The International System of Units, (SI)*. Ed. by D. T. Goldman and R. J. Bell. Her Majesty's Stationery Office, London (£3.95).

THE ROYAL SOCIETY OF MEDICINE, 1 Wimpole Street, London W1M 8AE, 1977. *Units, Symbols and Abbreviations: a Guide for Biological and Medical Editors and Authors* (£2).

1989, *The British Journal of Radiology*, 62, 101–106

Book reviews

Magnetic Resonance Imaging of the Central Nervous System. Ed. by M. Brant-Zawadzki and D. Norman, pp. xii + 404, 1987 (Raven Press, New York), $103.
ISBN 0-88167-240-8

This book has been written by a well proven team of North American teachers, all of whom have been fortunate enough to have acquired an extensive knowledge of magnetic resonance imaging (MRI), many being pioneers in the field, and all are actively involved in the continuing clinical applications of the technique.

Without presuming any prior knowledge of the subject or introducing any complex physics or mathematics, the contributors provide working concepts, which give sufficient insight to allow logical application of MRI to clinical problems. At the same time, all the important facts of the subject are covered and the book is extensively referenced, well indexed and illustrated with excellent magnetic resonance images and many diagrams.

It is divided into four sections covering (1) basic principles of MRI, (2) clinical aspects of brain imaging, (3) clinical aspects of spine imaging, and (4) imaging of the head and neck.

It is perhaps unfortunate that the orbit is not included. Many of the chapters are written as independent units embracing a particular subject, which inevitably results in a moderate amount of overlap with other chapters. Such repetition could have been edited out by using cross-referencing, but it does have the advantage of making easier reading.

The book serves as a textbook both for the needs of radiologists and clinicians commencing to use MRI and for more advanced students and as a reference book for practising neuroscientists.

It well deserves a place in all medical libraries in neuroscience departments and in centres performing neuroimaging, and for those considering it for personal acquisition it is good value for money.

BRIAN KENDALL

Head and Neck Imaging. Handbooks of Diagnostic Imaging. By June M. Unger, pp. ix + 232, 1987 (Churchill Livingstone, Edinburgh), £45.00.
ISBN 0-443-08471-8

This book is the second in a series of Handbooks of Diagnostic Imaging produced by the American division of Churchill Livingstone. If this handsome volume is anything to go by the rest of the series will be worth waiting for. The layout is pleasing and the contents are logically divided into eight chapters. Each chapter begins with a brief consideration of normal anatomy followed by subsections relating to specific diseases rather than to methods of imaging. This results in all the relevant techniques (from xeroradiography of the soft tissues through to magnetic resonance imaging) being brought to bear on each disease process described. The illustrations are meticulously selected with no redundancy and their reproduction is excellent. The suggestions on which imaging techniques to use to answer a clinical problem are particularly discriminating; for example there is a swift dismissal of the vogue for combined CT-sialography now that high-resolution CT machines are available.

The detail of this book allows it neatly to fill the gap between the necessarily cursory coverage of the head and neck given in the standard textbooks of radiology and the more specialized books such as *Computed Tomography and Magnetic Resonance Imaging of the Head and Neck* by Mancuso and Hanafee (2nd edn). The latter is something of a gold standard and remains the most detailed correlation of CT anatomy and pathology. The chapters relating to the head and neck in the first volume of *A Textbook of Radiological Diagnosis*, although good in parts, are remarkably uneven and there is no unified coverage of the head and neck. Coverage of this complex subject in Grainger and Allison's *Diagnostic Radiology* is far better and the illustrations used are of the highest quality. Overall, June Unger's book is the most comprehensive although it does not quite achieve the detail of Mancuso and Hanafee.

Although there should be no argument about which structures comprise the head and neck, the inconsistency with which the parathyroids and thyroid gland appear in the texts mentioned above is surprising; they are not included in this book, which is a pity. My only reservation is the rather sparse references (not surprisingly almost all American) given in the list of suggested further reading at the end of each chapter: only six are cited at the end of the beautifully illustrated chapter on facial trauma. Nonetheless, this is a superb effort which is well worth its price of £45.00.

DAVID HANSELL

Interpretation of the Chest Roentgenogram. By M. J. Landay, pp. x + 189, 1987 (Little, Brown and Co., Boston), £16.75.
ISBN 0-316-51352-0

The title of this little soft-backed book betrays its North American origins to any British reader. It is a delightful, profusely illustrated synthesis, full of concentrated wisdom.

Dr Landay has aimed his text at physicians, medical students and other health professionals. To any radiologist who is regularly involved in a similar spectrum of teaching it will be clear that the book is not totally suited to all its intended recipients. Physicians, surgeons and trainee radiologists — yes, but for undergraduate medical students — no. It relies on a certain level of knowledge and experience that these students do not possess.

The author, who may have provided excellent radiographs, has been let down by indifferent reproduction of the images. In some cases, it is not possible to see the object of interest despite lavish use of arrows and similar optical aids. In future editions the publishers might also consider placing text on left-hand pages and relevant images on right-hand pages so that readers do not constantly have to keep turning over pages to find the picture referred to in the narrative.

Dr Landay might consider advancing Chapter 16, on general guidance to observers of chest radiographs, to say Chapter 3 position, omitting the case reports, which add nothing to the important points he makes.

All in all a useful addition to radiological teaching which can be recommended to candidates for the United Kingdom Radiological Fellowship and the hordes of amateur radiologists who inhabit the wards of every hospital.

J. P. OWEN

Manual for the Videofluorographic Study of Swallowing. By Jeri A. Logemann, pp. ix + 71, 1986 (Taylor & Francis Ltd, London), £16.00.
ISBN 0-85066-635-X

If, like me, you are not really "au fait" with disorders of deglutition, then in this manual your prayers are answered. Jeri Logemann leads you, step by step, through 63 pages in which everything is explained so clearly and simply that frankly it's beyond embarrassment. The author explains the rationale and procedure for the use of the conventional and the modified barium swallows, indicating the anatomy and physiology of the oral cavity and pharynx during deglutition. A useful "worksheet" at the back of the book is included, and this acts as a check list to ensure that each facet of the examination is observed and hence assessed.

It is a pity that an index is not included so that one can refer to a particular aspect quickly, and also that there are no details of management or therapy for the various swallowing disorders, but this latter criticism is no doubt due to a previous publication on the subject by this author. Having said that, I think this book should be read by radiologists, radiographers and associated hospital staff concerned with swallowing and speech disorders.

T. Virjee

Transvaginal Sonography. Ed. by Ilan E. Timor-Tritsch and Shraga Rottem, pp. xviii + 165, 1988 (Heinemann Medical Books, London), £29.95.
ISBN 0–433–00038–4

This multi-author text has been produced following the introduction of one particular manufacturer's transvaginal ultrasound machine into their department and as such is very much a review of the capabilities of this particular machine. There is a short chapter on the physics of ultrasound with consideration of the particular features of the vaginal probe. There is a very good chapter dealing with the examination itself in considerable detail and giving helpful practical hints. The remaining chapters deal separately with each of the organs in the pelvis followed by the assessment of early pregnancy both normal and abnormal and finally chapters on ectopic pregnancy and a short chapter on the use of transvaginal sonography in infertility.

The quality of the illustrations is extremely good and the text is a good introduction to the possible uses of transvaginal sonography. There is some emphasis on the advantages of transvaginal sonography over transabdominal ultrasound but with the exception of the section on the uses in infertility, the authors do not attempt to give a judgement on how this affects clinical management in practice. The difficult problem of the adnexal mass is approached from the specific appearances of each pathological entity which means that from the practical point of view, it does not help in differentiating one condition from another when faced with a mixed-echo mass.

Overall the book gives a good introduction to the technique but a more critical appraisal of the place of transvaginal ultrasound in clinical practice and more emphasis on the commoner uses of the technique would have made an even more valuable text. I am sure this book will be of great interest to those considering taking up this technique.

D. W. Pilling

Percutaneous Biopsy, Aspiration and Drainage. By J. G. Letourneau, M. K. Elyaderani and W. R. Castañeda-Zuñiga, pp. x + 168, 1987 (Year Book Medical Publishers, Chicago), £38.50.

Unfortunately, I cannot enthuse about this book edited by three North American radiologists. Its stated main goal is to provide a concise practical guide to biopsy, aspiration and drainage for the practising radiologist. In effect, the advice is often *too* concise and insufficient emphasis is placed on possible severe complications of procedures.

The first and longest chapter is the best, covering general considerations of percutaneous biopsy and drainage. Many of the biopsy instruments and drainage sets used in the UK are included. Although the 14 F Trucut needle is included, there is no mention of newer automatic biopsy systems using a smaller gauge Trucut, nor any suggestion of a cytologist or cytotechnician being present at the time of aspiration biopsy using a fine-gauge needle.

Succeeding chapters cover biopsy in specific body regions and are well illustrated. It seems curious to have devoted 25 pages to percutaneous biopsy of kidneys and adrenals and drainage of perinephric collections and only five pages to percutaneous biopsy and drainage of pelvic masses. I was amazed that haematuria was not listed as a complication of renal biopsy and that the occasional necessity for embolization following liver or renal biopsy was not mentioned in text or index.

Virtually all of the references are pre-1985, and are non-European. It is surprising that there are none at all from the two main British journals of radiology, where there have certainly been key articles in areas such as biopsy of chest masses. Excluding references, there are 138 pages of text, which makes the publication expensive.

Robert Dick

Safety and Efficacy of Radiopharmaceuticals 1987. Ed. by K. Kristensen and E. Norbygaard, pp. xiv + 371, 1987 (Martinus Nijhoff, Dordrecht), Dfl 210.00, $100.00, £64.00.
ISBN 0–89838–986–0

This book contains the full text of review papers given at the 3rd European Symposium on Radiopharmacy and Radiopharmaceuticals, organized by the Danish Society of Clinical Physiology and Nuclear Medicine under the auspices of the European Joint Committee on Radiopharmaceuticals of the European Nuclear Medicine Societies, held in Elsinore, Denmark, in May 1987.

The book contains 27 chapters addressing issues such as the design and development of radiopharmaceuticals based on monoclonal antibodies, the new ^{99}Tc^{m}-labelled radiopharmaceuticals such as the brain, cardiac and renal agents, a review of labelling methods with radioactive iodine and radioactive indium 111, a perspective on animal models used for the evaluation of radiopharmaceuticals, discussion on the specifications and quality control methods for labelling cells and proteins, a discussion on the legal aspects of the introduction of new radiopharmaceuticals, the interaction between industry, hospital and government authorities, the design of hospital radiopharmacies, and a discussion on current trends in the training and education of pharmacists in radiopharmacies.

In contrast to so many other congress proceedings books, which are often put together in a hurry and contain very little useful information, this book is extremely well presented, has been published very rapidly after the conference, and contains a wealth of useful data. It is highly relevant in the fields of radiopharmacy and radiochemistry, but it also addresses issues which are of direct interest to the practising nuclear medicine physician or radiologist, with an interest in radioactive tracer work.

The practice of nuclear medicine is changing in that far more complex radiopharmaceuticals are being utilized in man today. The pace of development is rapid with new technetium-labelled tracers appearing in the fields of brain, heart and kidney work, protein (antibody) and cell labelling in particular. We feel this book is an essential addition to the library of nuclear medicine departments, and we would without hesitation recommend this book to libraries.

P. J. Ell

Chernobyl: The Real Story. By Richard F. Mould, pp. xiv + 256, 1988 (Pergamon, Oxford), £25.00.
ISBN 0–08–035718–0

This book is well titled, as Richard Mould is, among scientists, an outstanding story teller. He has used his personal links within the Soviet Union to assemble what must be the definitive collection of photographic records of the response to the Chernobyl nuclear accident. In his preface he states that his objective was to produce an historical account of what happened before, during and after the accident, rather than embroiling himself in the political issues of the implications of the Chernobyl accident for future exploitation of nuclear power. The Dickensian quotation "Now, what I want is facts" with which he begins is singularly apposite. The plant itself is described, as is the city and environment of Kiev. The accident itself is discussed chronologically, using as its source the extensive documentation provided by the Soviet Delegation at the Post-Accident Chernobyl Review Meeting, 25–29 August 1986, held at the IAEA in Vienna. In addition, he carried out hours of tape-recorded interviews and this material is efficiently included.

The chapter on the victims is spine-chilling, but factual. Further chapters cover the evacuation of the surrounding area, the decontamination of the environment, the influence of radioactive material released in the Chernobyl accident on the food chain, and finally the entombment of the damaged reactor. Basically, this is a source book; in many ways it is a reporter's notebook annotated with an amazing range of photographs—some more relevant than others but all full of interest. It can be read at many levels, from that of a fascinating (if perhaps morbidly so) traveller's tale, to that of a serious attempt at an annotated bibliography for the benefit of future historians of the nuclear age. It reflects perfectly the enthusiastic and irrepressible nature of its writer.

R. J. BERRY

Ionizing Radiation Exposure of the Population of the United States. NCRP Report 93, pp. viii + 87, 1987 (National Council for Radiation Protection, Bethesda, MD), $15.00.
ISBN 0–913392–91–X

This report aims to provide a comprehensive data base and dose assessment for exposure to radiation of the population of the USA. Every possible significant source has been considered and evaluated in making estimates and drawing up tables. These sources have been included within one of six categories which form the major sections of the report. Sandwiched between an Introduction and a Summary and Conclusions, the sections are as follows:

"Public Radiation Exposure from Natural Background"; dealing with naturally occurring radionuclides in the environment, external cosmic radiations and natural isotopes in the body.

"Occupational Exposure"; from radioactivity used in a medical, scientific or industrial context.

"Public Radiation Exposure from Nuclear Power Generation"; covering the whole fuel cycle from mining, enrichment, fabrication, utilization, storage to transportation and reprocessing.

"Public Radiation Exposure from Consumer Products"; deals with devices which use or produce low-level radiation in their operation, for example radioluminescence, smoke detectors, and tobacco products.

"Public Radiation Exposure from Miscellaneous Environmental Sources"; specialized sources not covered in previous sections, and including certain factories, chemical and smelting operations and some military and scientific research facilities. Also included here is a sub-section on fall-out from nuclear testing.

"Public Radiation Exposure from Medical Diagnosis and Therapy": hospital and dentistry sources.

Most of these sections either have been, or will be, the basis for more detailed individual reports.

To generalize for "the public" (the US population in 1980 was 2.3×10^8) in the face of enormous individual exposure variations in a meaningful way is a formidable task. The various committees responsible for compiling the sections have made a valiant and thorough assessment on the basis of data currently available, at the same time recognizing and admitting the uncertainties and limitations which inevitably exist in such an exercise. They have also made recommendations for improvements both to provide better source material and, where possible, to indicate situations where exposure reductions might be made.

Bearing in mind the uncertainties, the summary tables indicate that when all sources are considered, 82% of the average effective dose-equivalent for the American person comes from natural sources (55% from radon). Of the 18% man-made sources, 11% is from medical X rays and a further 4% from nuclear medicine. Radiation from all other sources constitutes the remaining 4% (nicely illustrated by a pie-chart, Fig. 8.1).

The Introduction (supported by a glossary) includes a section defining the various units used in the text, and their application. It is essential to grasp these before setting out to read the rest of the document or to attempt to interpret the tables. The reference list is also helpful to the English reader as an aid to interpreting the "initialese" which clearly plagues American governmental processes as it does British ones!

This is a reference work; not a text-book or for the general reader. Obviously it is of limited application in a non-American context, but will doubtless be a valuable compendium to those involved in environmental protection.

JOHN R. K. SAVAGE

Lung Cancer Risk from Indoor Exposures to Radon Daughters (Annals of the ICRP, Publication 50). Ed. by H. Smith, pp. vii + 60 (Pergamon Press, Oxford), £15.50, $25.00.
ISBN 0–08–035579–X
ISSN 0146–6453

This report of a Task Group of the International Commission on Radiological Protection is specifically concerned with *indoor* exposure to inhaled radon and radon daughter nuclides, and therefore with exposure of members of the public. It follows on from a previous report by the same Task Group, ICRP Publication 32 (1981), which dealt, however, with limits to inhalation exposure of radon for workers such as uranium miners and similarly exposed groups. For these workers, in the past, exposure was high enough to produce a significant excess incidence of lung cancer.

The topic of this report has been the subject of much debate and indeed public concern. It is therefore to be welcomed that the ICRP has produced a very detailed and thorough analysis of the potential risk faced by the public, a risk that may well be on the increase simply because of improvement in the quality of housing in some countries. In a sense it will be for the reader to judge the weight that should be placed on the risk from indoor radon levels: the dosimetric considerations presented in the report, coupled to risk coefficients for lung cancer that are derived *inter alia* from the uranium miners, lead via the ICRP system for risk evaluation to the conclusion that a significant fraction of observed lung cancer frequency may be attributed to this cause. At the same time, the admittedly limited epidemiological information now available does not yet firmly establish radon as a significant factor in variations in regional lung cancer incidence. As more such studies are reported, the subject will no doubt receive fresh attention.

The report reviews the environmental sources and levels of radon inside buildings. All the complicating factors in assessing the radon risk are fully discussed, including smoking as the dominant cause of lung cancer generally, and the differences governing exposure indoors as compared with in uranium mines. There is also an extensive treatment of the relative vs. absolute risk projection models, as applied to this problem.

By its thoroughness, this report is directed at an audience well versed in both the dosimetric analysis and the epidemiology of radiation risks. Nevertheless the arguments are clear and there is a useful appendix covering the necessary expressions and units used, as well as an excellent bibliography. There are very few typographical errors and the report is a valuable addition by which the Annals of the ICRP has reached its half-century.

G. Patrick

Data for Use in Protection Against External Radiation (Annals of the ICRP, Publication 51). Ed. by H. Smith, pp. xii + 132, 1987 (Pergamon Press, Oxford), £31.00, $50.00.
ISBN 0-08-035587-0
ISSN 0146-6453

This 131-page ICRP Publication 51 is very useful for a rather specialized readership, but will not be required routinely by all medical physicists. However if for no other reason than it is an ICRP Report, it ought to be purchased for the libraries of all medical physics departments.

Chapter 2, "Recommendations for the Limitation of External Radiation", extends over only three pages and is mainly extracts from earlier ICRP reports such as ICRP 26 (1977) and its later modification. Chapter 3 is entitled "Determination of Dose Distribution in The Human Body" and includes a section on phantoms of the human body which has a table recommending phantoms for measuring and calculating dose distributions, and sections on transport calculations and irradiation geometries. Chapter 4, "Conversion Coefficients for Idealized Circumstances", is the longest, and includes data for photons, muons, pions, neutrons, protons and for electrons. The section on photons (4.3), which is, I suspect, that relevant to most *BJR* readers, has sub-sections: anthropomorphic phantom, ICRU sphere, skin and eyes, and high energies. The section on neutrons (4.6) also gives ICRU sphere and anthropomorphic phantom. Electrons are dealt with on only one and a half pages and four paragraphs. Chapter 5, is "Application of the Conversion Coefficients".

The objective of ICRP 51 is "to provide information and advice on the relationships between radiometric, dosimetric and radiation protection quantities for external radiation and on their practical utilisation". However the cautionary note is sounded, in that "because of the large amount of data available for some types of radiation and the high rate at which they are being generated, change and refinement are inevitable, and responsible authorities should not hesitate to use more appropriate data as they become available". ICRP 51 also states (paragraph 2), that the main reason is "to adapt the data and the underlying approach to ICRP 26 (1977) and later relevant modifications" when considering ICRP 21 (1973), which contained data for protection against ionizing radiation from external sources, on the relationships between various radiation quantities and on shielding properties of various materials; ICRP 33 (1982) also contains some shielding data.

ICRP 51 also contains five appendices on Quantities and units, Transport calculations, Organ dose-equivalent data, Application of dose-equivalent quantities, and, reproduced directly from ICRP 21, Quality factors of charged particles. There are many tables and illustrations and in particular there is a lengthy Table extending over 12 pages for "Organ dose equivalent per unit fluence for photons incident in various geometries on a male anthropomorphic phantom" (part of the table for a male phantom and part for a female phantom), and a Table for neutrons, rather than for photons. In summary, therefore, if you already have ICRP 21 and 33 on your bookshelves, and have actually have used them, then it will be worthwhile spending £31 on ICRP 51. Otherwise, recommend a library to purchase it.

R. Mould

Protection of the Patient in Nuclear Medicine (Annals of the ICRP, Publication 52). Ed. by H. Smith, pp. xii + 37, 1987 (Pergamon Press, Oxford), £15.50, $25.00.
ISBN 0-08-033188-2
ISSN 0146-6453

All physicians and physicists involved in the specialty of nuclear medicine ought to purchase this Publication, which includes a statement from the 1987 Como meeting of the ICRP. It has been prepared by a Task Group of Committee 3 of ICRP and contains six chapters whose titles and sections clearly define its scope.

For example, Chapter 2 is "Guidelines to Good Clinical Practice" with (2.1) Diagnosis and (2.2) Therapy. Chapter 3 is entitled "Education and Training" and includes information for the nuclear medicine physician, the medical physicist, the nuclear medicine technologist and the radiopharmacist radiochemist and nurses. In Chapter 4, "Estimates of Absorbed Dose", the topics include formalism for calculating mean absorbed dose in organs, uncertainties in biokinetic and dosimetric data and effective dose-equivalent. Chapter 5 is one of the longest, and deals with "Design of Facilities, Instrumentation, Quality Assurance and Control", covering many topics, such as laboratory design and storage areas for radioactive waste. The section on quality control has 13 sub-sections for all the useful instruments such as activity meters, probe systems and gamma cameras. In addition, SPECT is included, together with positron-emission tomography and data processing systems. The final chapter is on "Radiopharmaceuticals: Preparation and Quality Assurance".

There are some three pages of references, but with such a comprehensive list of contents, the bibliography is obviously far from being complete and up to date on all the topics covered. Indeed, with a total of only 37 pages, no more than brief statements can be included for some sections/sub-sections.

There are only four tables, but these are of interest: "Cancer mortality risk estimates by site" for red bone marrow, lung, breast, bone surfaces and for the thyroid; "Methods used for the reduction of organ doses in various nuclear medicine procedures" where the organ in question is either the bladder region, thyroid, bowel, kidney or gallbladder; "Illustration of dose-rates at various distances and times from a typical adult patient after administration of a radiopharmaceutical", for bone, liver and myocardial scintigraphies and for blood pool determination; and "Absorbed dose and effective dose-equivalent per unit administered activity in normal adults". This useful table contains the following function or organ examined: bone, renal, thyroid, liver (+gallbladder), brain, lung, heart, abscess, thrombi, pancreas, adrenals, spleen and gastrointestinal tract. ICRP 52 has only one illustration, a schematic representation of the value of diagnostic information as a function of amount of administered activity. It would be interesting to have a series of such figures for different investigations but with quantitative data. In summary, therefore, this is an essential item for your library of nuclear medicine books, reports and papers.

R. F. Mould

The Management of Bladder Cancer. Ed. by Derek Raghavan, pp. xiv + 338, 1988 (Edward Arnold, London), £29.50.
ISBN 0-7131-4528-5

This commendable compact volume is the 12th in the publishers' series of oncology-related titles. The editor has marshalled the contributions from 37 authors from seven countries and three continents to produce 17 chapters covering advances in the biology and pathology of bladder cancer, perspectives on current management as practised in Europe, North America and Australia, and an evaluation of the role of the newer combinations of cytotoxic chemotherapy and prospects for improved management in the future. In his preface the editor describes the management of bladder cancer as "evolving through a renaissance" and sets out to present a broad perspective of the innovations and approaches to the practical management of urothelial malignancy, to resolve some of the controversies about what constitutes "optimal management", and to provide the practising clinician with an overview to assist in the management of this group of neoplasms. It is clearly not possible in a book of this size to cover all topics in exhaustive detail, but references are comprehensive and up to date (all chapters are referenced until at least 1985) which allows ready access to further detail when this is required. It would have been inappropriate for the editor to try and reach a complete consensus on the optimal management of either superficial or invasive bladder cancer but he has balanced the contributions on the use of surgery, radiotherapy and chemotherapy without introducing undue bias and has achieved a consistent concise style to the text without undue repetition of content between the various contributions.

The first three chapters cover advances in the biology and pathology of urothelial cancer. Recent studies using electron microscopy, tumour markers including monoclonal antibodies, flow cytometry and cytogenetics are outlined and the developing role of oncogenes in bladder cancer is discussed, although in such a concise manner as to be difficult for the non-specialist to follow. This is a field of rapidly developing interest, and coverage of some of the basic techniques involved would have been helpful. Experimental models are essential for laboratory studies of bladder cancer as well as for chemosensitivity testing, and the various approaches using spontaneous or induced animal tumours, the growth of murine or human bladder cancer in tissue culture, and xenografted human tumours in nude mice are described.

Current clinical practice and the controversies surrounding the management of superficial or invasive bladder cancer are presented in six chapters. These are based soundly upon the extensive clinical experience of the contributing authors but serve to demonstrate the wide variation in current clinical practice. The natural history and prognostic factors relating to the progression of superficial bladder cancer are dealt with in detail. The use of intravesical chemotherapy is described (although the specialist chapter on this subject makes no mention of epodyl) and the results and limitations of clinical trials with these agents and of BCG are fully discussed. For invasive bladder cancer the surgical and radiotherapeutic management alternatives are described, with no attempt to disguise the difference of approach in Britain and North America. The history of radical cystectomy is documented, together with the marked improvement in morbidity and mortality that has occurred over the last two decades. Emphasis is given to advances in surgical technique and new approaches in potency-preserving procedures and continent urinary diversion.

In the section on innovative approaches, intraoperative radiation therapy, radiation sensitizers and chemotherapy/radiation combinations are mentioned, but the potential of altered fractionation techniques using either hyperfractionation or accelerated fractionation is ignored, which is unfortunate as improvements in tumour modelling may allow fruitful collaboration between the laboratory and the clinic in determining optimal radiation schedules.

A further six chapters document developments in cytotoxic chemotherapy. The mechanism of action, pharmacology and toxicity of individual agents are described, together with results of phase one and phase two studies. The exciting early experience from North America using combination chemotherapy in metastatic disease is presented, together with an excellent and timely reminder of the difficulties in assessment of response and importance of standardization of response criteria, which emphasizes the importance of clear design and evaluation of clinical trials. Chapters are devoted to the important issues of chemotherapy to the elderly patient and the development and validation of assessments of quality of life. The editor describes the rationale and initial experience of neo-adjuvant chemotherapy and the current EORTC trials are summarized.

Overall this is a well produced and enjoyable book to read, and sections will appeal to urologists, radiotherapists and oncologists, medical oncologists and laboratory workers wishing to get a feel for current clinical practice. At under £30 it represents good value and should find its way into many individual as well as institutional libraries.

D. P. Dearnaley

Management of Advanced Cancer of Prostate and Bladder. (Progress in Clinical & Biological Research Vol. 260; EORTC Genitourinary Group Monograph 4). Ed. by Philip H. Smith and Michele Pavone-Macaluso, pp. xxiii + 658, 1988 (Alan R. Liss, New York), $120.00.
ISBN 0-8451-5110-X

This volume is in two sections. The first and shorter part (134 pp.) is devoted mainly to the hormone treatment of advanced carcinoma of the prostate. The 12 chapters derive from presentations at an EORTC symposium held in Leeds in October 1986, and include reviews of total androgen blockade (Labrie et al), LHRH-analogues in Dutch studies (Debruyne et al) and a thoughtful interim analysis of MRC Trials (Kirk). Three EORTC trials are reviewed. The published comparative studies of cyproterone acetate (CPA), medroxyprogesterone acetate, estramustine phosphate and low-dose diethylstilboestrol (DES) are summarized by deVoogt et al, who also discuss response criteria though unfortunately not including prostate-specific antigen. A preliminary report on the trial comparing orchidectomy (O), O + CPA and DES (1 mg/day) is presented by Robinson. The cytotoxic chemotherapy of prostatic cancer is dealt with in only two pages, in contrast to two detailed and rather promotional chapters from pharmaceutical company laboratories on new hormonal agents. Wide-field radiotherapy and systemic radioisotopes are not discussed at all.

The second part of the volume is on bladder cancer (505 pp.) and derives from a course on urological oncology held in Sicily in December 1986. It starts strongly, with a lucid introduction to the cell and molecular biology of bladder cancer by Brosman. It was difficult to discern a common theme in the remainder of the sub-section entitled "Biology and Research", which also covers interferon and EORTC chemotherapy trials in superficial bladder cancer, and a presentation optimistically entitled "*In vitro* synergism of radiation and chemotherapy". Other sub-sections are: "Diagnosis in Staging", "Surgery—Radical Cystectomy", "Urinary Diversion, Surgery with Preservation of Sexual Function", "Radiotherapy", "Chemotherapy" and "Adjuvant and Neo-adjuvant Chemotherapy". These sections provide an excellent overview of the diverse approaches to management of local advanced T2–T4 bladder cancer. Though some highly topical subjects such as the use of M-VAC neo-adjuvant chemotherapy have already been updated in recent journal articles, the principles and data remain a useful and comprehensive compendium of trials in this important multi-modality area of oncology. The chemotherapy of metastatic disease is also well represented, with the exception of the CMV regimen.

The volume as a whole is a useful addition to the libraries of all clinicians involved in clinical research on invasive and metastatic bladder cancer or on the hormone treatment of advanced prostatic cancer. Cover of other subjects is often interesting but not comprehensive. The motif of individual chapters was more often a presentation of results of one group's approach than an attempt at balanced review of the relevant field. The volume is therefore a poor introduction for clinicians first entering urological oncology, but a valuable reference for those who already have a mature view of treatment alternatives. The breadth and variety of short presentations leads to an easily digestible and entertaining book; however, the brevity of some chapters was frustrating and there is no doubt that some would not have been acceptable in a peer-reviewed journal. The volume is up-to-date and good value for money and can be recommended both for individual purchase and for oncology libraries.

A. HORWICH

Mesothelioma. Diagnosis and Management. By C. Frederick Kittle, pp. xii + 106, 1987 (Year Book Medical Publishers, Chicago), £35.50.
ISBN 0-8151-5095-4

This short book concerning the diagnosis and management of mesothelioma is timely as the incidence of asbestos-related tumours is increasing. An initial chapter on epidemiology, pathogenesis and pathology describes the different types of asbestos and the relationship of this both to mesothelioma and carcinoma of the bronchus. This is followed by a chapter on the clinical presentation and diagnosis of mesothelioma and subsequently by one on the imaging of mesothelioma. It is perhaps a sad reflection on our ability to treat this disease that these three initial chapters take up more than two-thirds of the book and the treatment of mesothelioma is dealt within only 26 pages. There are separate chapters on the surgery of mesothelioma, the use of chemotherapy and the use of radiotherapy. In general all the chapters are concise and well referenced. The book would be of particular interest to both trainee physicians and oncologists.

PETER BLAKE

International Agency for Research on Cancer. Biennial report 1986/87, pp. x + 225, 1987, (IARC, Lyon, France).
ISBN 92-832-1087-5

The main interests of the IARC continue to be cancer aetiology and prevention, but within these fields the research undertaken at Lyon, and also in the international collaborative studies supported by the Agency, cover a very wide range of disciplines varying from descriptive epidemiology to molecular genetics. This report includes summaries of all the projects undertaken by the Agency during the last 2 years. Summaries are fairly concise, but in general they include all the most important data. They are grouped under three main headings: I—Studies on Etiology and Prevention, II—Studies on Mechanisms of Carcinogenesis, III—Data Collection and Research Methods.

The first section includes a number of geographical surveys of cancer incidence, some of which have led to the production of a new volume of the classic *Cancer Incidence in Five Continents*. For this work the Agency continues to help establish and support cancer registries in many developing countries throughout the world. Aetiological studies are both epidemiological and laboratory-based. Some are concerned with determining the risk factors for cancer associated with various environmental and occupational hazards. Others are site-oriented studies seeking to identify the important risk factors for many of the common epithelial cancers. Tissue samples collected from cases identified by some of the epidemiological surveys provide material to support experimental studies of genetic linkage, and also studies of the role of viruses and cytogenetic anomalies in the aetiology of cancer. Section II is concerned with experimental studies of DNA damage and repair, and mechanisms of cell transformation and of tumour initiation and promotion in mammalian cells. Section III discusses the work of the Agency in attempting to improve international data collection and analysis. It includes methods for cancer registration, methods for statistical analysis of epidemiological and screening studies, and mathematical modelling of carcinogenesis. Quite a large section on methods for the detection of environmental carcinogens is also included.

The report is very well written and presented. Because of the broad scope of the research conducted from Lyon there will be something of interest here for most scientists and clinicians involved in cancer research; however, much of the original work will be published elsewhere in greater detail. This book will therefore be of most value to epidemiologists and workers in the field of carcinogenesis as a catalogue of the many international studies in progress and of the data bases in use. Its purchase by the libraries of cancer research institutes is recommended.

JUDITH DEACON

1989, *The British Journal of Radiology*, 62, 107–113

VOLUME 62 NUMBER 734

FEBRUARY 1989

The British Journal of Radiology

Radiological evaluation of temporal bone disease: high-resolution computed tomography versus conventional X-ray diagnosis

By P. Fritz, MD, K. Rieden, MD, *T. Lenarz, MD, *J. Haels, MD, and K. zum Winkel, MD

Departments of Radiology and *Otolaryngology, University of Heidelberg, D-6900 Heidelberg, Federal Republic of Germany

(*Received April 1988 and in revised form July 1988*)

Abstract. Sixty-two patients with different temporal bone lesions were prospectively examined by high-resolution computed tomography (CT) and conventional plain radiography, including pluridirectional tomography. High-resolution CT enabled a clear diagnosis in 80% of cases, conventional radiology in 63%; 1.6-times more bone information was recorded by high-resolution CT which is clearly superior for imaging cholesteatomas, metatastases and inflammatory processes and for evaluating osseous destruction. With regard to pathological soft tissue or effusions filling the tympanic cavities, conventional radiology shows poor sensitivity (0.61). High-resolution CT is the most sensitive method for the imaging and classification of temporal bone fractures, including labyrinthine damage and ossicular chain injuries. Only in cases of atypical fractures with an unfavourable relationship to the CT planes, can carefully directed tomography be more effective. In most cases high-resolution CT replaces conventional radiology and should be the method of choice for comprehensive radiological examination of the temporal bone.

Radiological evaluation of the petrous bone is difficult owing to the complicated anatomical structure of the middle and inner ear. Because of different spatial arrangements of the anatomical structures, multiplanar views are required.

The topography as well as the smallness of many structures limit the imaging possibilities. Radiological imaging of the petrous bone must meet high standards of topographic representation and spatial resolution. In conventional radiological procedures, there exist a number of special projections for optimal representation of particular structures but they are often diagnostically insufficient and additional tomographs in one or more planes are necessary.

Thin-section, high-resolution computed tomography (CT) with modern equipment allows, by means of special algorithms, imaging of osseous structures up to a spatial resolution of 0.45–0.65 mm. However, without additional equipment, CT cannot reproduce the various projections of conventional radiological procedures. In routine diagnosis, CT is limited to standard axial and coronal images. However, high-resolution CT has the advantage of excellent topographic visualization, devoid of artefacts from superimposition of structures. All relevant parts of the petrous bone are represented with high sensitivity and there is considerably less skin and eye lens exposure than with conventional tomography (Chakeres & Spiegel, 1983; Köster & Ewen, 1986; Fritz et al, 1987).

Numerous CT studies deal with the identification of anatomical details and the appearance of various lesions of the petrous bone (Chakeres & Spiegel, 1983; Swartz et al, 1983a, b; Zonneveld, 1983; Zonneveld et al, 1983, 1984; Damsma et al, 1984; Köster et al, 1984; von König & Kurtz, 1984; De Groot et al, 1985; Mafee et al, 1985a, b; Köster & Straehler-Pohl, 1986; Welleschick & Salomonowitz, 1986; Fritz et al, 1987) but there are few published studies comparing conventional radiological procedures with CT. Brunner et al (1986) consider plain radiographs and tomographs sufficient for assessment of chronic otitis media, malformations and fractures. Imhof et al (1986) see the need for CT mainly in the investigation of malignant disease and in the pre-operative evaluation of cholesteatoma. In the case of petrous bone fractures, CT should be performed only if a complication is suspected. According to Virapongse et al (1983), bone destruction by cholesteatoma was more readily diagnosed by conventional tomography. The latter and CT were of equal value in diagnosing fractures with or without dislocation of the middle ear ossicles. There is agreement on the superiority of CT in the visualization of soft-tissue structures and of fluid collections.

Most studies regard the main role of CT as an adjunct to conventional radiology and the conflicting conclusions probably reflect the different techniques employed and the small number of patients examined.

This paper will contribute to the discussion of the value of conventional and computed tomographic procedures in middle and inner ear diagnosis.

Materials and methods

Sixty-two patients with different petrous bone lesions were prospectively examined (Table I). Only patients with a firm clinical diagnosis established through case history, otological examination and audiometry were

---

Address correspondence to: Dr P. Fritz, Radiologische Universitätsklinik, Kopfklinikum, Im Neuenheimer Feld 400, D-6900 Heidelberg, Federal Republic of Germany.

Table I. Number of patients and clinical diagnoses

Diagnosis		*n*
Fractures		23
Cholesteatoma		12
Metastases		12
Otosclerosis		7
Inflammatory processes		6
Chronic otitis media	(4)	
Chronic mastoiditis	(1)	
Labyrinthine osteomyelitis	(1)	
Dysplasia of the external auditory meatus		2
Total		62

tested by CT. Petrous bone fractures were most common, followed by metastatic deposits and cholesteatomas. High-resolution CT as well as conventional plain radiographs and tomograms were obtained in all patients.

Computed tomography

Computed tomography was performed in a standardized manner with a GE 8800 unit using 120 kV and 320 mA. To minimize the radiation exposure, no overlapping or contiguous slices were performed but all patients were examined in both axial and coronal planes. The distance between slices was 2 mm; the thickness of each slice was 1.5 mm. In the axial plane, an average of 12 slices was taken parallel to the orbitomeatal; in the coronal plane, an average of 13 sections was taken. To obtain coronal slices free of motion artefacts, we examined the patients prone with the head fully flexed by means of a special head support. Image reconstruction was done primarily with a 1.5 magnifying factor on the prospective target mode of the GE high-resolution bone algorithm. With this method the spatial resolution of the CT image is 0.65 mm. The images were recorded at a window of 4000 Hounsfield units (HU) and a level between 1000 and 2000 HU.

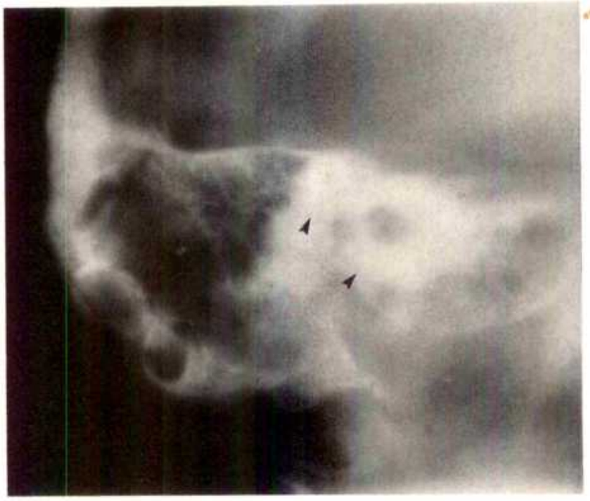

Figure 1. Stenvers' view of pluridirectional tomography. Atypical transverse fracture of the base of the temporal bone extending to the vestibule and the mastoid (arrowheads). Neither axial nor coronal CT planes demonstrated the fracture line.

Conventional X-ray diagnosis

In conventional imaging, at least two views, either Stenvers, Schüller or Mayer, were taken and, in addition, tomograms in lateral, modified lateral or antero-posterior (AP) projections (coronal plane). The above pluridirectional tomography was performed with hypocycloid technique using a 2 mm distance between layers at 65 kV and 75 mA.

The CT scans and conventional radiographs were examined separately by two independent observers.

Results

Fractures (Table II)

A fracture was diagnosed by CT in 18% more cases than by conventional radiology. Of the 16 conventionally diagnosed fractures, 15 were also

Table II. Fractures of the temporal bone ($n = 23$)

	CT	Conventional radiology	Reference methods[a]
Diagnosis of fracture	20/23 (87%) (1 fn)	16/23 (69%)	23/23
Classification of fracture	20/20 (100%)[b]	8/16 (50%) (1 f)	
Labyrinthine injury	8/7 (114%) (1 fp?)	3/7 (42%)	7/23
Ossicular disarticulation	1/2 (50%) (1 fn)	0/2 (0%) (2 fn)	2/23
Injury to facial canal	1/1 (100%)	1/1 (100%)	1/23
Haemotympanum ($n = 10$)/ cerebrospinal fluid leak ($n = 2$)	12/12 (100%)	13/12 (108%) (2 fp)	12/23

fn = false negative; fp = false positive; f = false classification when compared with CT and reference methods.

[a] Reference methods: case history, clinical findings, audiometry, surgery ($n = 4$). [b] CT findings: 12 longitudinal fractures, five transverse fractures, five combined fractures, one atypical fracture.

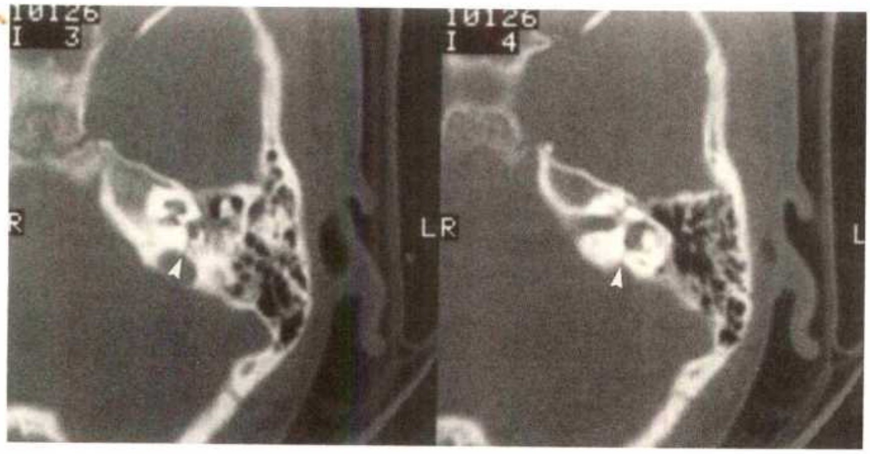

Figure 2. High-resolution CT scan shows a transverse fracture with labyrinthine damage (arrowheads). The fracture was not diagnosed by conventional means.

confirmed by CT. In one case, the fracture line was evident only in the Stenvers tomogram (Fig. 1). It was impossible to recognize the atypical fracture on either axial or coronal CT scans. Fractures diagnosed by CT were always clearly classifiable whereas by conventional means the fracture type could be clearly defined in only half of the diagnosed cases. The diagnosis of combined fractures was difficult by conventional techniques and one of the conventionally diagnosed fractures was incorrectly described when compared with the CT image.

Lesions of the labyrinth or ossicular chain were more clearly demonstrated by CT as shown by comparison with the audiometric findings (Fig. 2). Out of eight patients with labyrinth lesions demonstrated by CT, seven had audiometric findings (sensory impairment of hearing up to deafness and/or disturbance of vestibular function). This group included those patients whose labyrinth lesions were diagnosed by conventional radiology. In one case, CT showed a fracture line in the area of the anterior semicircular canal although there was no loss of vestibular function. A lesion of the ossicular chain was diagnosed by audiometry in two patients and later confirmed at operation. In another case, there was rupture of the ossicular chain articulations with dislocation of the incus, which had been correctly diagnosed by CT but not by conventional radiology (Fig. 3). In this case there was also a stapes fracture which was diagnosed neither by CT nor conventional radiology. In a case of primary, partial paralysis of the facial nerve, the fracture line running through the internal auditory meatus was recognized in the CT image as well as in the conventional tomogram.

An important advantage of CT is the correct representation of liquids and soft-tissue masses. Twelve patients presented clinically with haemotympanum, among these two patients with cerebrospinal fluid loss. The accumulated fluid was correctly identified by CT in all cases. By conventional means, fluid accumulation in the middle ear was diagnosed 13 times. However, two of the findings were false positive and six were false negative.

Cholesteatoma (Table III)

The low sensitivity of conventional radiology with regard to pathological fluid accumulations and soft-tissue structures limits the value of this procedure, especially in the case of cholesteatoma. In eight out of 12 cholesteatoma patients, the diagnosis was confirmed by surgery. The clinical findings were obvious in four of the patients. A typical, localized, soft-tissue lesion was

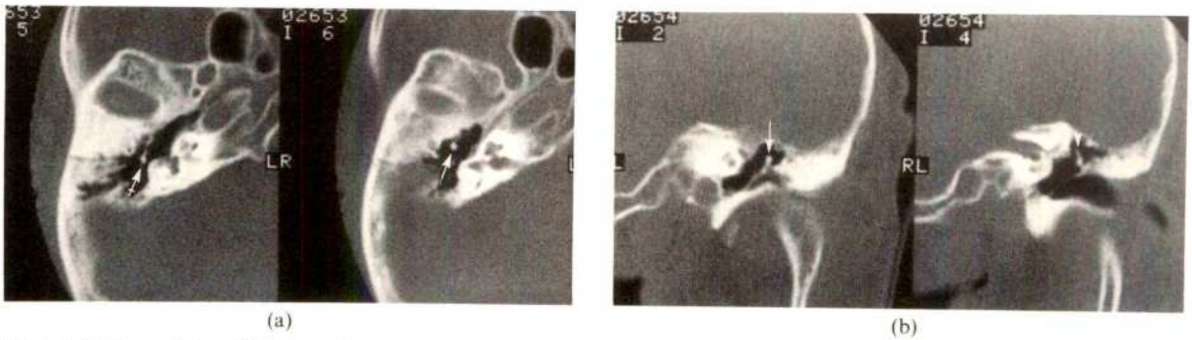

(a)

(b)

Figure 3. High-resolution CT scans, (a) transverse and (b) coronal planes, showing a transverse fracture with discontinuity of the ossicular chain and complete dislocation of the incus due to rupture of the incudomalleolar and incudostapedial joint. The long process of the incus is displaced into the epitympanum (arrowhead). Body of the malleus (←) and incus (↞).

Table III. Cholesteatomas (n = 12)

	CT	Conventional radiology	Reference methods[a]
Soft-tissue tumour	12/12 (100%)	7/12 (58%)	12/12 (100%)
Bony destruction	5/8 (62%)[b]	2/8 (25%) tp	8/8 (100%)[c]
Ossicular erosion	4/6 (66%)[b]	3/6 (50%) tp	6/8 (75%)[c]

[a] Reference methods: clinical findings, surgery. [b] True positive. [c] Surgical findings (n = 8).

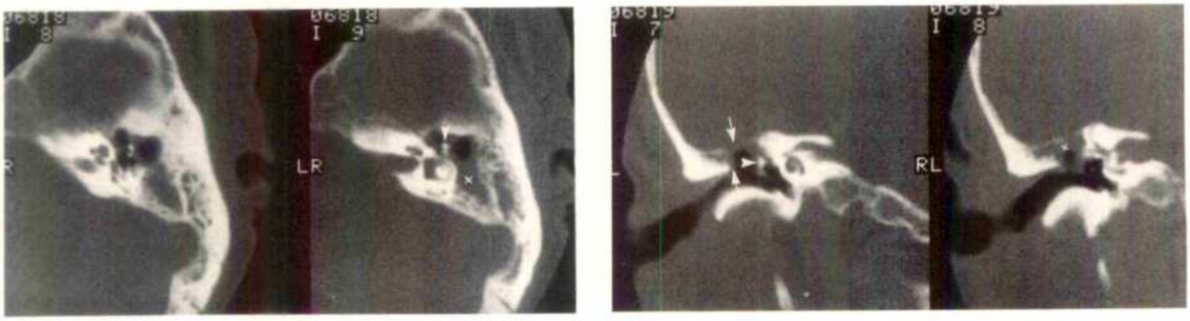

(a) (b)

Figure 4. High-resolution CT scans, (a) axial and (b) coronal planes, showing attic cholesteatoma (**X**), remnants of the ossicle walled in (◄) and erosion of the antrum and destruction of the external auditory canal and the tegmen tympani (←).

recognized by CT in all patients (Fig. 4). Five false negative diagnoses were made by conventional procedure.

Computed tomography was also superior in assessing bone erosions. Cholesteatoma masses next to the lateral semicircular canal may lead to a closed fistula of the canal, which may be opened during surgical procedures, leading to serious complications. The prediction of the possibility of a fistula of the lateral semicircular canal has a decisive influence on the choice of operative approach.

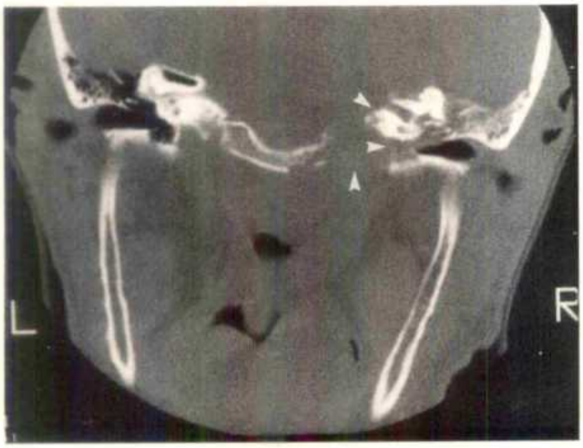

Figure 5. High-resolution CT scan (coronal plane) showing metastasis in the temporal bone from bronchial carcinoma and destruction of the clivus, internal auditory canal and the middle ear wall (arrowheads). Tumour masses are sealing the tympanic cavity.

Computed tomography is also able to visualize the spatial relationship to the lateral semicircular canal.

Petrous bone metastases

In metastatic osteolysis and sclerosis, CT showed a superior detection rate of 83% as opposed to 67% by conventional means (Fig. 5; Table IV).

Otosclerosis (Table V)

The possibility of otosclerosis was diagnosed conventionally more often than by CT, by virtue of increased opacification or of seeming resorption zones in the labyrinth area. Sclerosis in the area of the footplate of the stapes was diagnosed neither by conventional means nor by CT. In one case the radiological diagnosis was examined at operation, turning out to be false negative. The higher percentage of positive findings by pluridirectional tomography could be explained by artefacts. Conventional tomography is influenced by opacification artefacts and the centring of the X-ray beam. Faulty positioning of the apparatus which is not centred exactly can lead to a seeming difference in density of the petrous bone images.

Table IV. Metastases (n = 12)

	CT	Conventional radiology
Osteolytic/osteoblastic	10/12 (83%)	8/12 (67%)
Soft-tissue tumour	3/12 (25%)	4/12 (33%) (1 fp)

Reference methods: clinical findings, follow-up bone scan; fp = false positive when compared with CT.

Table V. Otosclerosis ($n = 7$)

	CT	Conventional radiology
Qualitative bone change (lucent/sclerotic areas)	1/7	3/7
Fenestral sclerosis	0/7 (1 fn)	0/7 (1 fn)*
Opacification (soft-tissue/effusion)	0/7	2/7 (2 fp)

Reference methods: case history, audiometry, *surgery ($n = 1$).
fn = false negative; fp = false positive when compared with CT.

Table VI. Inflammatory processes ($n = 6$)

	CT	Conventional radiology
Resorption zones/sclerosis	3/6	1/6
Opacification (soft-tissue/effusion)	5/6	3/6 (3 fp)

Reference methods: clinical findings, bone scan.
fp = false positive when compared with CT.

Inflammation

Computed tomography resulted in more diagnoses compared with conventional radiology, confirmed by clinical and nuclear medicine findings (Fig. 6; Table VI).

Stenosis of the external auditory meatus

Osseous stenosis was diagnosed by both CT and conventional radiography. An additional obstructive soft-tissue membrane in one of the two cases was diagnosed only by CT (Table VII).

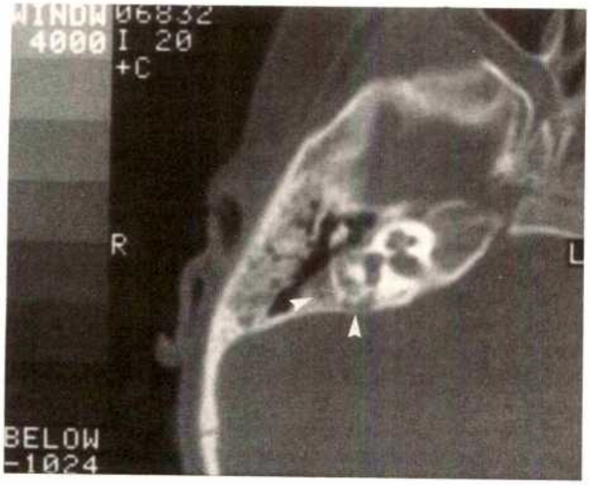

Figure 6. High-resolution CT scan (axial plane) showing osteomyelitis of the petrous bone; CT clearly shows areas of bone resorption in the lateral semicircular canal capsule (arrowheads). No abnormality was discovered on conventional tomography.

Table VII. Dysplasia of the external auditory canal ($n = 2$)

	CT	Conventional radiology	Reference methods
Osseous stenosis	2/2	2/2	2/2
Soft-tissue stenosis	1/2	0/2 (1 fn)	1/2

Reference methods: surgery ($n = 2$), clinical findings.

The value of conventional radiology to determine pathological soft-tissue structures or fluid accumulations in the external auditory meatus, tympanic cavity and the mastoid air cells was also investigated. Sealing of the air-filled cavities of the petrous bone can be diagnosed with certainty by CT. However, a clear differentiation between solid masses or liquids by means of density measurements is not always possible. The small dimensions of the air-filled cavities only allow for small regions of interest with correspondingly poor count statistics and high standard deviation. In addition, adjacent osseous structures lead to partial volume effects which can falsify density measurements considerably. However, it can always be determined whether the air-filled cavities are open or closed. Hence, CT can serve as a reference standard for conventionally diagnosed opacifications. In 29 out of 62 patients (47%), opacification was diagnosed by conventional radiology. Compared with CT, eight of these were false positive (27%). Thirteen of 33 negative diagnoses were false negative (39%). Sensitivity of conventional radiology with regard to soft tissue or effusions filling the tympanic cavities was 0.61, specificity 0.71 and accuracy 0.66.

Discussion

The majority of basic otological diagnoses can be made by clinical and audiometric testing. Radiological procedures are used to confirm the clinical diagnosis and to provide a more thorough pre-operative evaluation. An exact radiological diagnosis is of particular importance in the prediction of complications and the topographic representation of petrous bone lesions before surgery. Computed tomography is clearly superior in the imaging and classifying of temporal bone fractures. Only in cases of uncomplicated petrous bone fractures is conventional radiology sufficient, provided that the fracture can be identified on the plain radiograph.

Conventional tomography should be used as required if doubt still exists after CT. This can be the case with atypical fractures, where the spatial relationship is unfavourable to the CT imaging planes. In the case of cerebrospinal fluid loss, the exact identification of the fracture line determines the operative approach. In many cases it is possible to determine the location of the cerebrospinal fluid leak by CT cysternography (Valavanis et al, 1986).

The demonstration of a fracture through the facial canal facilitates the decision to undertake a decompression operation which might preserve function. If a post-traumatic conductive hearing loss of more than

30 dB persists longer than 2 months, damage to the middle ear bones must be considered (Bellucci, 1983; Swartz et al, 1985). Radiological evidence of such trauma will be the deciding factor in planning a reconstructive operation of the ossicular chain. Injury of this kind mostly involves the incus (Wright, 1974) and usually leads to rupture of the incudostapedial joint (Goodwin, 1983). Ossicular chain dislocation and injuries of the inner ear can be visualized better by CT than conventional tomography. Stapes fractures are mainly secondary to dislocation of the incus (Bellucci, 1983) and generally cannot be recognized by radiological means because anatomical details of the stapes normally cannot be determined by high-resolution CT (Miller et al, 1985; Fritz et al, 1987). Radiological evidence of labyrinthine damage determines the prognosis of post-traumatic sensorineural hearing loss (Zonneveld, 1983).

In cases of cholesteatoma, determination of the exact extent of the tumour mass, including bony erosions, is only possible through high-resolution CT. Cholesteatoma masses in contact with the lateral semicircular canal threaten the possibility of fistula and influence the operative approach. Similarly, CT is indispensable when there are metastases within the petrous bone. In these circumstances, CT is not only more sensitive but visualizes the extent of the tumour better than conventional radiology and also provides a basis for the planning of radiation therapy. Computed tomography is clearly superior in imaging pathological soft-tissue and tympanic effusions and therefore should be the method of choice for evaluation of obscure inflammatory processes.

The possibility of opacification and centring artefacts produced through conventional tomography should be taken into consideration if otosclerosis of the labyrinthine capsule is suspected. In fenestral otosclerosis, we believe that the spatial resolution of both high-resolution CT and conventional tomography is still too limited to give clear answers about the status of the footplate and the oval window niche. The above requirement makes clear the need for accurate and exact radiographic diagnosis. At present, CT is the most effective means. In our total series, 1.6-times more bone findings were recorded by high-resolution CT. When compared with CT, conventional radiology shows poor sensitivity for evaluation of soft-tissue processes and effusions. Computed tomography enabled a clear diagnosis in 80% of the cases, conventional radiology in 63% of the cases. Conventional radiological procedures, including pluridirectional tomography, were not only less informative but also often led to wrong interpretation.

Lower radiation exposure as well as the savings in time are additional advantages of CT. We believe high-resolution CT performed in a standardized manner with both axial and coronal planes and 2 mm increments at 1.5 mm thickness will be sufficient for the majority of clinical circumstances. Inaccuracy might occur with regard to very small, particular structures of the inner ear, like the stapes. In our opinion, contiguous or overlapping slices should be reserved for additional, very detailed examinations. We conclude that, if available, high-resolution CT is the method of choice for a comprehensive radiological examination of the temporal bone and should replace conventional X-ray diagnosis.

References

Bellucci, R. J., 1983. Traumatic injuries of the middle ear. *Otolaryngologic Clinics of North America, 16*, 633–650.

Brunner, E., Türk, R., Swoboda, H., Imhof, H. & Schratter, M., 1986. Die Bedeutung der Computertomographie für die Mittelohrdiagnose. *Laryngologie Rhinologie Otologie, 65*, 327–330.

Chakeres, D. W. & Spiegel, M. D., 1983. A systematic technique for comprehensive evaluation of the temporal bone by computed tomography. *Radiology, 146*, 97–106.

Damsma, H., de Groot, J. A. M., Zonneveld, F. W., van Waes, P. F. G. M. & Huizing, E. H., 1984. CT of cochlear otosclerosis (otospongiosis). *Radiologic Clinics of North America, 22*, 37–43.

Fritz, P., Lenarz, T., Haels, J. & Fehrentz, D., 1987. Feinstrukturanalyse des Felsenbeines mittels hochauflösender Dünnschicht-Computertomographie Teil 1: Sensitivität der Feinstrukturdarstellung bei einer standardisierten Untersuchungstechnik. *Fortschritte auf dem Gebiete der Röntgenstrahlen und der Nuklearmedizin, 147*, 266–271.

Goodwin, W. J., 1983. Temporal bone fractures. *Otolaryngologic Clinics of North America, 16*, 651–659.

de Groot, J. A. M., Huizing, E. H., Zonneveld, F. W., Damsma, H. & van Waes, P. F. G. M., 1985. Labyrinthine otosclerosis studied with a new computed tomography technique. *Annals of Otology, Rhinology and Laryngology, 94*, 223–225.

Imhof, H., Salomonowitz, E., Kumpan, W., Canigiani, G., Schratter, M., Zrunek, M. & Türk, G., 1986. CT und konventionelle Schläfenbeindiagnostik-Wertigkeit und Einsatzfolge. In *Digitale Bildgebende Verfahren. Integrierte Digitale Radiologie*, Grazer Radiologisches Symposium, 3–5 October, ed. by E. Vogler & G. H. Schneider (Schering, Berlin), pp. 270–277.

König, H. von & Kurtz, B., 1984. Hochauflösende Computertomographie der Felsenbeine. *Fortschritte auf dem Gebiete der Röntgenstrahlen und der Nuklearmedizin, 141*, 129–135.

Köster, O., Böckler, R., Lackner, K. & Koch, U., 1984. Die hochauflösende Computertomographie des Mittel-und Innenohrs. *Laryngologie Rhinologie Otolaryngologie, 63*, 488–493.

Köster, O. & Ewen, K., 1986. Zur Strahlenbelastung bei der hochauflösenden Computertomographie des Felsenbeines. *Digitale Bilddiagnostik, 6*, 176–180.

Köster, O. & Straehler-Pohl, H. J., 1986. Die hochauflösende Computertomographie in der Abklärung knochendestruierender Prozesse des äußeren Ohres. *Fortschritte auf dem Gebiete der Röntgenstrahlen und der Nuklearmedizin, 145*, 651–656.

Mafee, M. F., Valvassori, G. E., Deitch, R. L., Norouzi, P., Henrikson, G. C., Capek, V. & Applebaum, E. L., 1985a. Use of CT in the evaluation of cochlear otosclerosis. *Radiology, 156*, 703–708.

Mafee, M. F., Henrikson, G. C., Deitch, R. L., Norouzi, P., Kumar, A., Kriz, R. & Valvassori, G. E., 1985b. Use of CT in stapedial otosclerosis. *Radiology, 156*, 709–714.

Miller, D., Dawes, A. T. & Cowie, J. W., 1985. Routineuntersuchungen des Felsenbeines unter Verwendung hochauflösender multiplanarer Rekonstruktionsverfahren. *Electromedica, 53*, 12–15.

Swartz, J. D., Goodman, R. S., Russel, K. B., Ladenheim, S. E. & Wolfson, R. J., 1983a. High-resolution computed tomography of the middle ear and mastoid. Part III: Surgically altered anatomy and pathology. *Radiology, 148*, 461–464.

Swartz, J. D., Goodman, R. S., Russel, K. B., Marlowe, F. E. & Wolfson, R. F., 1983b. High-resolution computed tomography of the middle ear and mastoid. Part II: Tubotympanic disease. *Radiology, 148*, 455–459.

Swartz, J. D., Swartz, N. G., Hampel, A., Korsvik, H., Ronis, M. L., Wolfson, R. J. & Lowery, L. D., 1985. Computerized tomographic evaluation of the middle ear and mastoid for post-traumatic hearing loss. *Annals of Otology, Rhinology and Laryngology, 94*, 263–266.

Valavanis, A., Schubinger, O., Stuckmann, G. & Antonucci, F., 1986. CT-Diagnostik traumatischer Läsionen des Felsenbeines. *Radiologe, 26*, 85–90.

Virapongse, C., Sarwar, M., Kier, E. L., Sasaki, C. & Pillsbury, H., 1983. Temporal bone disease: a comparison between high resolution computed tomography and pluridirectional tomography. *Radiology, 147*, 743–748.

Welleschick, B. & Salomonowitz, E., 1986. Innenohrmißbildung. Otoliquorrhoe bei Stapedektomie. *Laryngologie Rhinologie Otologie, 65*, 688–690.

Wright, J. W., 1974. Trauma of the ear. *Radiologic Clinics of North America, 12*, 527–532.

Zonneveld, F. W., van Waes, P. F. G. M., Damsma, H., Rabischong, P. & Vignaud, J., 1983. Direct multiplanar computed tomography of the petrous bone. *Radiographics, 3*, 400–449.

Zonneveld, F. W., 1983. The value of non-reconstructive multiplanar CT for the evaluation of the petrous bone. *Neuroradiology, 25*, 1–10.

Zonneveld, F. W., de Groot, J. A. M., Damsma, H., van Waes, P. F. G. M. & Huizing, E. H., 1984. Die Anwendbarkeit der hochauflösenden CT zur Darstellung des Aquaeductus vestibuli (Ménière) und der Otospongiosis des Labyrinths. *Radiologe, 24*, 508–515.

1989, *The British Journal of Radiology*, *62*, 114–116

Basic concepts of femoral neck anteversion: comparison of two definitions

By *Arne Høiseth, MD, †Olav Reikerås, MD and ††Erik Fønstelien, MSc

Department of Diagnostic Radiology, †Department of Surgery, Orthopedic Section and ††Department of Clinical Physiology, University of Oslo, Ullevål Hospital, 0407 Oslo 4, Norway

(*Received June 1988 and in revised form October 1988*)

Abstract. Femoral neck anteversion is determined by the neck, shaft and knee axes. It is commonly assumed that the neck axis is a straight line connecting the centre of the femoral head, the centre of the femoral neck and the axis of the femoral shaft. However, the line through the centre of the femoral head and neck crosses anterior to the axis of the femoral shaft. A distinction has therefore to be made between two principal different definitions of anteversion, denoted ANTEV 1 and ANTEV 2 in this paper, depending on the precise definition of the neck axis. Previous studies have indicated substantial differences between these definitions. The present study, using precise measuring methods, shows that the definitions have a systematic but small spread of differences. The large individual variation previously found between the two definitions is therefore caused mainly by the measuring methods and to a lesser extent by real anatomical variations.

The femoral neck axis is traditionally considered to be a straight line connecting the centre of the femoral head and the centre of the femoral neck with the axis of the femoral shaft (Dunn, 1952; Dunlap et al, 1953; Magilligan, 1956; Weiner et al, 1978; Ruby et al, 1979). However, the line from the centre of the femoral head to the centre of the femoral neck, the head–neck axis, usually passes in front of the axis of the femoral shaft (Norman, 1969; Grote et al, 1980) and therefore differs in principle from the definition using the line from the centre of the femoral head to the intersection with the shaft axis (head–shaft axis) (Fig. 1). Two different definitions of anteversion can therefore be made, depending on whether the head–neck or the head–shaft axes are used.

In this work the first angle is denoted ANTEV 1 and the latter ANTEV 2 in accordance with Henriksson (1980). It has previously been shown that ANTEV 2 is larger than ANTEV 1 (Grote et al, 1980; Henriksson, 1980; Herrlin & Ekelund, 1983; Reikerås et al, 1985b). Previous studies have also shown a large spread of differences (Henriksson, 1980; Reikerås et al, 1985b).

In both practical and theoretical contexts, it is important to determine the anatomical and biomechanical implications of the two angles. In this context, it is the spread of the difference between the two definitions that is most relevant. A systematic difference can be dealt with by correcting the values and therefore has few clinical or biomechanical implications. The spread of the differences may, however, indicate differences of importance. Such a spread of the measured differences may, however, be due to poor precision of the measuring methods rather than to real anatomical variations.

Previous estimations of the difference between these two definitions have been performed with methods of unknown precision and with various definitions of the shaft axis. The data concerning the true differences between the two definitions of anteversion are therefore unreliable. The main purpose of this work is to estimate the differences between ANTEV 1 and ANTEV 2 by methods that contribute little to the variation. A secondary purpose is to draw attention to the real anatomical relationship of the axis of the femoral neck.

Materials and methods

The estimations were made on a total of 33 unpaired dissected femur specimens removed from adult corpses. ANTEV 1 and ANTEV 2 are defined by the respective neck axes described above, by the long shaft axis (the line from the centre of the trochanteric mass to the centre of the femoral condyles) and by the tangent to the back of the femoral condyles.

ANTEV 2 was first measured by a conventional method on 17 specimens (Norman, 1965). Two radiographs were obtained of the upper ends of the femora, one with vertical projection and one lateral. The shaft axis was constructed on both radiographs as the line from the middle of the trochanteric mass to the middle of the femoral condyles. The perpendicular distance from the centre of the femoral head to the shaft axis was measured and the anteversion was measured by a geometrical construction (Fig. 2). The precision of this method was determined as the standard deviation of the inter- and intrapersonal variation of four sets of measurements.

On all 33 specimens, ANTEV 2 was determined on EMI 5005 computed tomographic (CT) equipment. The CT slices were made at a right angle to the shaft axis. Superimpositions were made of a slice through the centre of the femoral head and one through the middle portion of the trochanteric mass. The shaft axis was marked as the point equidistant from the most anterior and

---

*Author for correspondence.

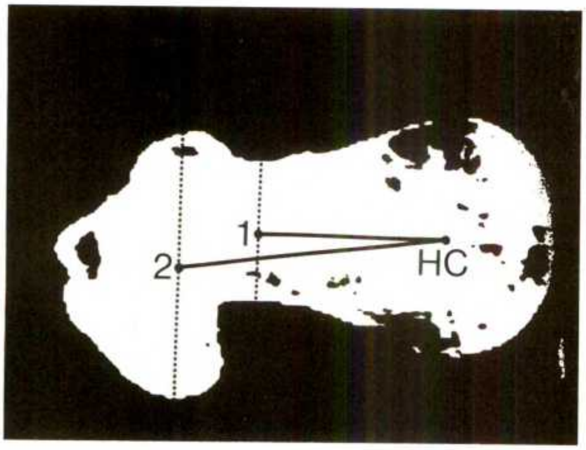

Figure 1. Superimposition of CT slices showing the construction of the neck axis according to ANTEV 2 definition (HC–2). On the same slice the principal difference between the definitions is shown by the neck axis according to ANTEV 1 (HC–1). The difference in inclination of the neck axes by the two definitions causes ANTEV 1 to be smaller than ANTEV 2. (HC = the head centre.) The lines from the head centre to points 1 and 2 are ANTEV 1 and ANTEV 2 neck axes, respectively, and points 1 and 2 are the midpoints of the respective dotted lines.

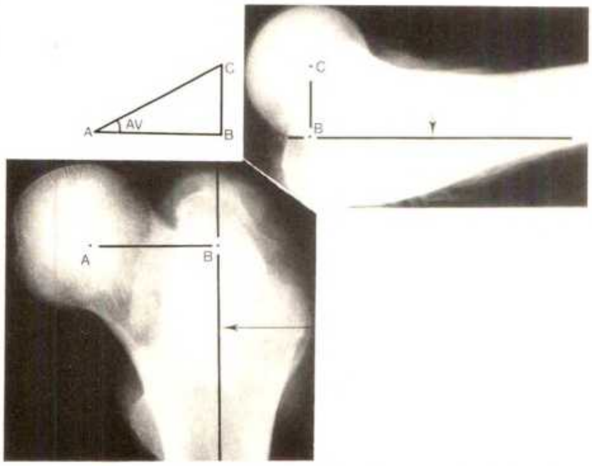

Figure 2. The geometrical construction for measurement of the femoral neck anteversion (angle CAB) by the conventional radiographic method. The shaft axis is marked in the shaft. The perpendicular distance from the head centre to the shaft axis is measured (lines AB and BC). The triangle ABC is constructed and the angle CAB, which is equal to the anteversion, is measured.

posterior points on the trochanteric mass (Fig. 1). ANTEV 2 was measured as the angle between the neck axis and a plane marking the dorsal aspects of the femoral condyles. The precision of the CT measurements was calculated by the following formula (Colquhoun, 1971):

$$\mathrm{var}(A-B)=\mathrm{var}\ A+\mathrm{var}\ B$$

The same equation is used to calculate the spread of the difference between ANTEV 1 and ANTEV 2 caused by the precision of the two definitions. In this equation $\mathrm{var}(A-B)$ is the variance (square of one standard deviation) of the paired differences between two sets of measurements; var A and var B are the variances of the precision of the two sets of measurements.

ANTEV 1 was determined on all 33 dissected, adult femur specimens by a near to direct anatomical projection of the angle as previously described (Reikerås et al, 1985a) without correcting the values. (This is identical to the projection used by Mesgarzadeh et al (1987).) The precision of this method was previously shown to have a standard deviation of 2.5°.

Results

The precision of the conventional method for determining ANTEV 2 had a standard deviation of 4.8° (mean of the standard deviations of inter- and intrapersonal paired differences which were 4.7, 5.4 and 4.3°). The paired differences between the values obtained by the conventional method and by CT had a standard deviation of 5.1°. The precision of CT was calculated to have a standard deviation of 1.7° ($\sqrt{(5.1^2-4.8^2)}$).

There was a close and linear relationship between the definition of ANTEV 1 and ANTEV 2 (Fig. 3). The mean paired difference was 4.2°, ANTEV 2 being larger than ANTEV 1. The standard deviation of the difference was 3.9°. The standard deviation of the difference accounted for by the precision of the two definitions was 3.1° ($\sqrt{(2.5^2+1.7^2)}$).

Discussion

Norman (1969) was the first to point out the anatomical difference between the head–neck and head–shaft axes of the femoral neck and thus the discrepancy between the theoretical definition and the design of measuring methods. Dunn (1952), Dunlap et al (1953), Magilligan (1956), Weiner et al (1978) and Ruby et al (1979) have all described methods using the head–neck axis and a definition implying a straight line between the head centre, neck centre and the shaft axis. Recently, Murphy et al (1987) and Mesgarzadeh et al (1987) evaluated CT as a method for measuring the anteversion by first using the head–neck axis definition. To overcome problems of variability in the neck anatomy, they defined the neck axis in accordance with the head–shaft axis without attending to the principal alteration in the definition of the anteversion. In the international literature, little attention has been given to the real anatomical relationship of the femoral neck and to the difference between the neck axis definitions. This may cause confusion and inadvertent use of the measured values.

To estimate the real anatomical variation or the real difference between the two definitions it is necessary to use measuring methods with known precision or with

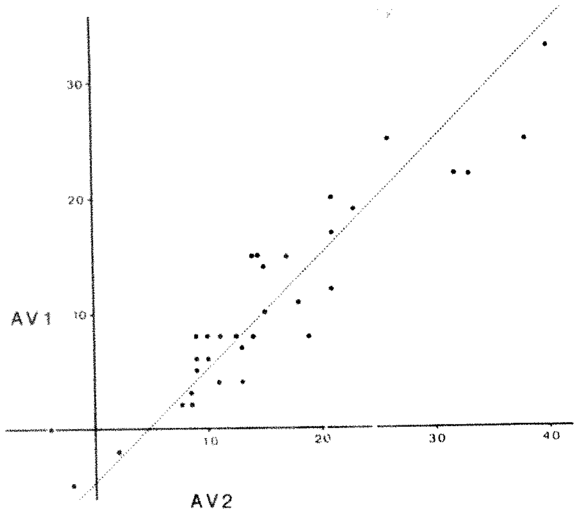

Figure 3. Scattergram between ANTEV 1 (AV1) and ANTEV 2 (AV2) showing the spread of the differences and the linear relationship between the definitions. The dotted line is drawn at 45° and intersects the base line at the mean of the paired differences.

very high precision. In the latter case the methods do not contribute substantially to the variation. We have previously determined the precision of a method for determining ANTEV 1 (Høiseth et al, 1989). However, the precision of methods for determining ANTEV 2 has always been unknown. Furthermore, while ANTEV 1 can be determined by a near to correct projection of the anteversion, no such simple and direct method is available for ANTEV 2.

We have determined the precision of a conventional approach previously described (Norman, 1965) and a CT method which we designed. We found the latter to have a high precision. Murphy et al (1987) have also described a very similar method for determination of ANTEV 2; this differs from ours in the location of the intersection between the neck and shaft axis. We have used Norman and Billing's definitions which locate this point in the middle of the trochanteric mass. Murphy et al (1987), however, located this point at the base of the femoral neck which is in the distal portion of the trochanteric mass at the junction with the shaft. Murphy et al (1987) found precision of the same order as in the present study. Computed tomography therefore seems suitable for our purpose.

Our findings confirm the principal anatomical difference between the two definitions of anteversion. Contrary to Henriksson (1980) and Reikerås et al (1985b), the present study showed a small spread of differences between the two definitions expressed by a small standard deviation. Furthermore, a substantial part of this variation was accounted for by the precision of the methods. Disregarding the systematic difference, a very good agreement was found between the two definitions. They must, therefore, be considered to have the same clinical and biomechanical implications and the previously found individual variations must be due to the error of the measuring methods. Provided correction is made for the systematic difference, the two definitions and corresponding measuring methods are comparable.

References

Colquhoun, D., 1971. *Lectures on Biostatistics* (Clarendon Press, Oxford), p. 37.

Dunlap, K., Shands, A. R. Jr, Hollister, L. C. Jr, Stuart Gaul, J. Jr & Streit, H. A., 1953. A new method for determination of torsion of the femur. *Journal of Bone and Joint Surgery, 35A*, 289–311.

Dunn, D. M., 1952. Anteversion of the neck of the femur. A method of measurement. *Journal of Bone and Joint Surgery, 34B*, 181–186.

Grote, R., Elgeti, H. & Saure, D., 1980. Bestimmung des Antetorsionswinkels am Femur mit der axialen Computertomographie. *Röntgenblatter, 33*, 31–42.

Henriksson, L., 1980. Measurement of femoral neck anteversion and inclination. A radiographic study in children. *Acta Orthopaedica Scandinavica Supplementum, 186*, 30.

Herrlin, K. & Ekelund, L., 1983. Radiographic measurement of the femoral neck anteversion. Comparison of two simplified procedures. *Acta Orthopaedica Scandinavica, 54*, 141–147.

Høiseth, A., Reikerås, O. & Fønstelien, E., 1989. Evaluation of three methods for the measurement of the femoral neck anteversion. *Acta Radiologica Scandinavica, 30*, in press.

Magilligan, D. J., 1956. Calculations of the angle of anteversion by means of horizontal lateral roentgenography. *Journal of Bone and Joint Surgery, 38A*, 1231–1246.

Mesgarzadeh, M., Revesz, G. & Bonakdarpour, A., 1987. Femoral neck torsion angle measurement by computed tomography. *Journal of Computer Assisted Tomography, 11*, 799–803.

Murphy, S. B., Simon, S. R., Kijewski, P. K., Wilkinson, R. H. & Griscom, N. T., 1987. Femoral anteversion. *Journal of Bone and Joint Surgery, 69A*, 1169–1176.

Norman, O., 1965. Beskrivande geometri som hjälpmedel vid bestämning av collum-anteversions-och—diafysvinkeln samt fracturvinkeln. *Nordisk Medicin, 73*, 446–447 (in Swedish).

——1969. Mätning av collumanteversionsvinkeln. En principiell diskusjon. *Nordisk Medicin, 82*, 991–992 (in Swedish).

Reikerås, O., Høiseth, A. & Reigstad, A., 1985a. Evaluation of the Dunlap/Rippstein method for determination of femoral neck angles. *Acta Radiologica Diagnosis, 26*, 177–179.

——1985b. Femoral anteversion measured by the Dunlap/Rippstein and Norman methods. *Acta Radiologica Diagnosis, 26*, 303–305.

Ruby, L., Mital, M. A., O'Connor, J. & Patel, U., 1979. Anteversion of the femoral neck. Comparison of methods of measurement in patients. *Journal of Bone and Joint Surgery, 61A*, 46–51.

Weiner, D. S., Cook, A. J., Hoyt, W. A. Jr & Oravec, C. E., 1978. Computed tomography in the measurement of femoral anteversion. *Computed Tomography, 1*, 299–306.

1989, *The British Journal of Radiology*, 62, 117–120

Intravenous digital subtraction angiography in non-specific aorto-arteritis

By Sanjiv Sharma, MD, Shashi Aggarwal, MD, *K. K. Talwar, MD, DM and Mira Rajani, MD

Divisions of Radiodiagnosis and *Cardiology, Cardiothoracic Centre, All India Institute of Medical Sciences, New Delhi, India

(*Received May 1988*)

Abstract. We have studied 40 patients with non-specific aorto-arteritis (Takayasu's disease) using intravenous digital subtraction angiography (DSA). The aorta, its major branches and (in 18 patients) pulmonary arteries were evaluated to determine the degree and extent of involvement. No complications related to the procedure were encountered. Good quality diagnostic images were obtained in 39 out of 43 instances. The unsuccessful examinations were in patients with congestive cardiac failure, and in one patient who would not co-operate. Aortic wall thickness and mild involvement of the descending aorta in the region of the diaphragm could not be assessed. Intravenous DSA is acceptable for the diagnosis and follow-up of aorto-arteritis in suitable patients.

Non-specific aorto-arteritis is a chronic and progressive disease of unknown aetiology, commonly involving the aorta, its major branches and the pulmonary arteries (Hachiya, 1970; Das et al, 1982; Yamato et al, 1986), and eponymously called Takayasu's disease. It results in stenosis, occlusion, dilatation or aneurysm formation in the involved blood vessels and the angiographic features are well documented (Liu, 1985). Conventional arteriography by direct arterial puncture is usually employed for evaluation of these patients (Gotsman et al, 1967; Lande & Rossi, 1975; Lupi et al, 1975).

The availability of intravenous digital subtraction angiography (IV-DSA) has provided an alternative means of imaging the arterial system. Various disorders of the cardiovascular system have been successfully evaluated by IV-DSA (Rosen et al, 1983; Wood et al, 1983; Chernin et al, 1984; Pond, 1985; Wilms et al, 1986). We have performed IV-DSA in 40 patients with aorto-arteritis and discuss the advantages and limitations of IV-DSA in the assessment of these patients.

Materials and methods

Forty patients with non-specific aorto-arteritis have been examined in the last 18 months using intravenous digital subtraction angiography. All examinations were performed on a commercially available Angiotron CMP (Siemens) unit. The diagnosis of aorto-arteritis was based on clinical and angiographic findings in all these patients.

A 5 F high-flow pigtail catheter was introduced from an antecubital or femoral vein and positioned in the mid-right atrium during deep inspiration. Twenty to thirty millilitres of Urografin 370 (Schering AG) were injected at a flow rate of 18–22 ml/s during each filming sequence. For evaluation of pulmonary arteries, 10–15 ml of Urografin 370 were used. Care was taken not to exceed a total contrast medium dose of 4 ml/kg body weight of the patient during one complete examination. An abdominal binder and intravenous injection of 20–60 mg Buscopan were used to control intestinal peristalsis during abdominal and pelvic studies.

The protocol for examination included an antero-posterior (AP) view for the abdomen and pelvis, left anterior oblique (LAO) view for the aortic arch, and right anterior oblique (RAO) view for the neck vessels in most patients, with AP and LAO views to show the pulmonary arteries in 18 patients. Further examinations were tailored according to the situation. All examinations were evaluated for the degree of arterial opacification, misregistration artefacts due to motion, swallowing or inadequate exposure, overlap of vessels and the extent and degree of involvement of various arteries by aorto-arteritis.

Results

A total of 43 IV-DSA studies were performed in 40 patients. Three patients underwent two examinations each, one for diagnostic purposes and the other two for assessing the response to immunosuppressive therapy. The age of the patients ranged from 10 to 57 years and there were 29 females. Good-quality diagnostic IV-DSA images of the aortic arch, abdominal, pelvic and neck vessels were obtained in 39 out of the 43 examinations.

The thoraco-abdominal aorta in the region of the diaphragm could not be successfully shown, because the difference in the exposure factors for the thoracic and abdominal aortas always produced misregistration artefacts. The evaluation of thoracic and abdominal aortas in separate filming sequences was more successful but resulted in an additional injection to show the descending thoracic aorta. However, even then, mild irregularity of contour involving the descending thoracic aorta could not confidently be diagnosed in this study.

Address correspondence to: Dr Sanjiv Sharma, Division of Radiodiagnosis, Cath Lab, Cardiothoracic Centre, All India Institute of Medical Sciences, Ansari Nagar, New Delhi 110029, India.

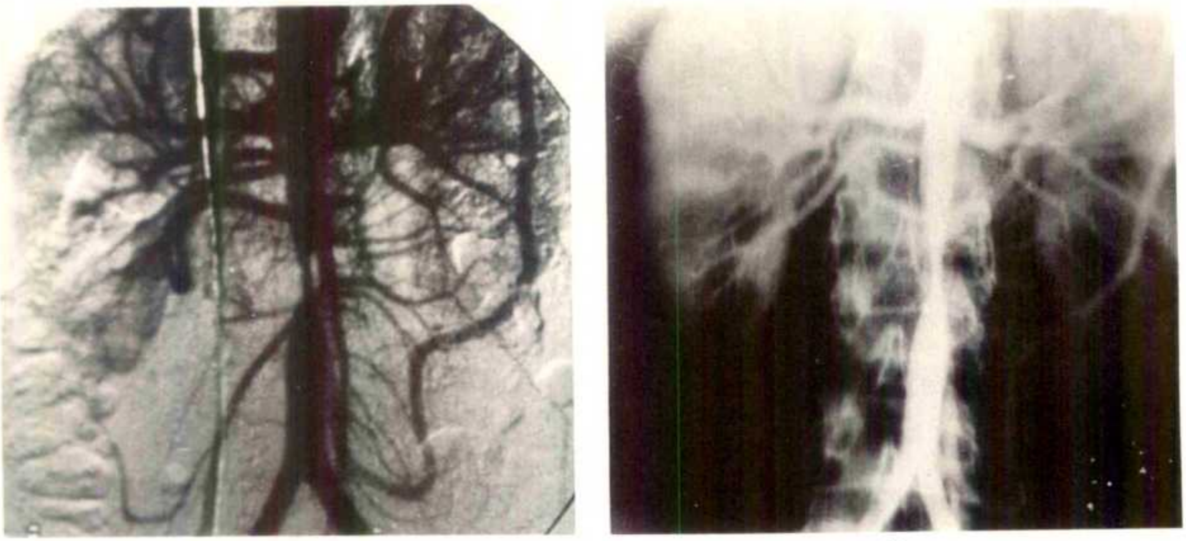

(a) (b)

Figure 1. (a) Intravenous digital subtraction angiogram showing severe stenosis of the infrarenal segment of the abdominal aorta. (b) Conventional angiogram showing the stenosed segment.

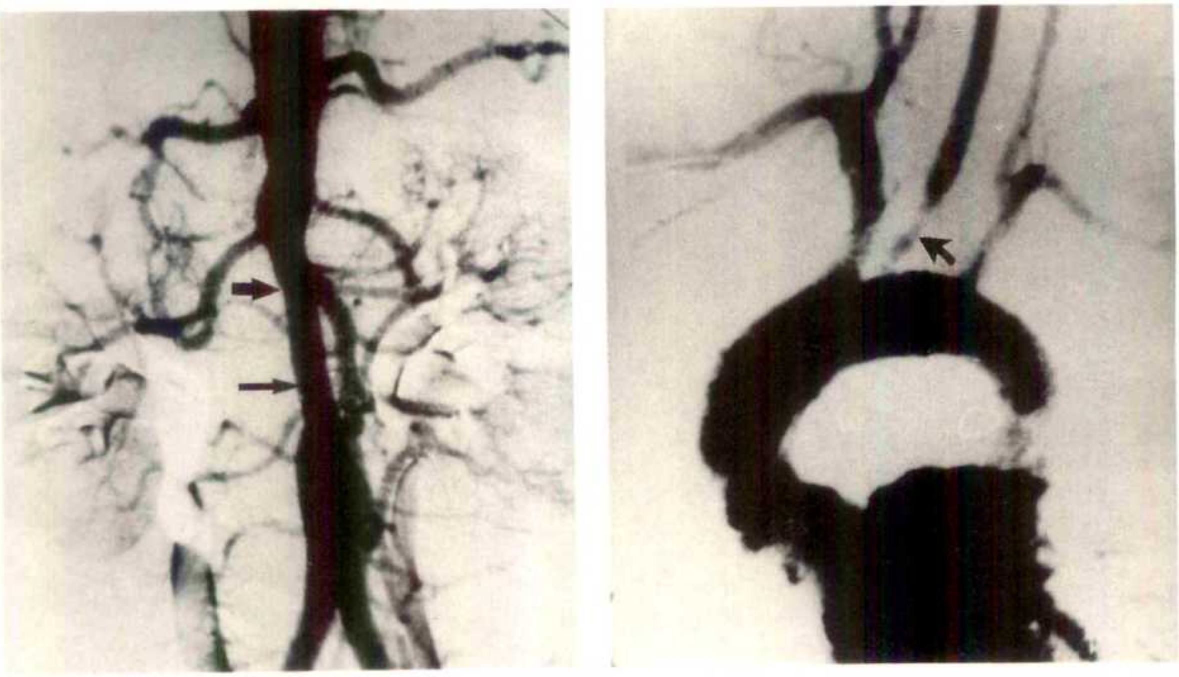

(a) (b)

Figure 2. Intravenous digital subtraction angiogram (a) showing long segment narrowing of the infrarenal segment of the abdominal aorta (arrows) and (b) for the aortic arch (LAO view) showing narrowing of the left carotid artery at the origin with post-stenotic dilatation (arrow).

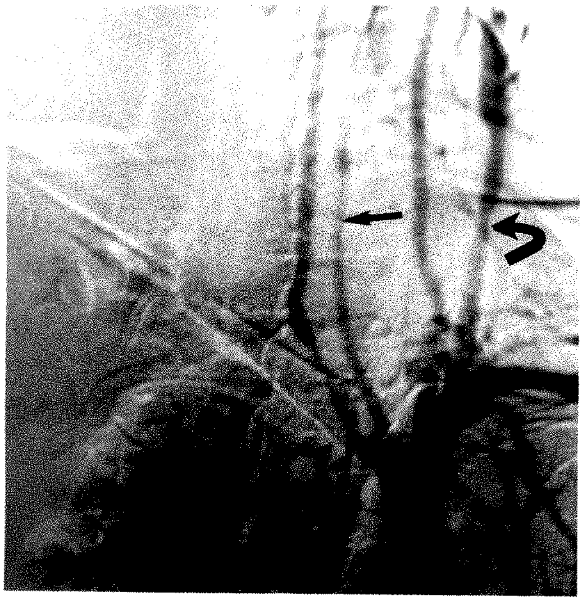

Figure 3. Intravenous DSA of neck vessels (RAO view) showing total occlusion of the right subclavian artery beyond the origin of the right vertebral artery. Left (curved arrow) and right (straight arrow) carotid arteries are also diseased.

The collateral flow in subclavian and mesenteric arterial occlusions and distal reconstitution beyond arterial occlusions was adequately shown.

Unsuccessful examinations were initially seen in four patients because of lack of patient co-operation (one patient) and congestive cardiac failure (three patients). The study in the first patient was successfully repeated at a later date. The three patients with congestive cardiac failure needed further evaluation by arteriography utilizing direct arterial puncture.

Conventional arteriograms were available for comparison in eight patients. Intravenous DSA showed the extent and degree of arterial involvement as well as the conventional arteriograms in all these patients and was found to be more accurate in one patient. In this patient, the overlying bone obscured the left subclavian artery in the arch aortogram and was wrongly interpreted as blocked. Intravenous DSA images showed a normal left subclavian artery.

The angiographic features were divided into four types (Table I) (Yamato et al, 1986). The abdominal aorta was frequently involved in our patients (26 out of 40), usually by a long stenosing lesion in its infrarenal segment (Figs 1, 2). The renal arteries were the most frequently involved branches of the aorta (25 patients) followed by the left subclavian artery (18 patients).

Table I. Angiographic features in 40 IV-DSA studies

Type	Features	No. of patients
1	Involvement of branches of aortic arch only	8
2	Involvement of thoracic aorta and its branches only	1
3	Involvement of abdominal aorta and its branches only	12
4	Extensive involvement of whole length of aorta and its branches	19

Lesions were frequently in the form of a proximally located severe narrowing or a total occlusion of the vessel and long segments of vessels were frequently involved (Fig. 3). Femoral artery involvement was seen in nine patients. Pulmonary arteries were evaluated in 18 patients and found to be abnormal in two, with obstruction of the right upper lobe branch in one and peripheral pruning of the pulmonary vessels in the second patient. The angiographic features are summarized (Table II).

Discussion

Total aorto-arteriography is necessary to establish the diagnosis and determine the extent of involvement before starting specific therapy in patients with aorto-arteritis. Conventional arteriography by direct arterial puncture utilizing any route (femoral, axillary or lumbar) is associated with a small but definite morbidity and mortality (Haunt & Amplatz, 1968; Gammill & Craighead, 1975; Hessel et al, 1981; Hoevels, 1983). Frequent involvement of the abdominal aorta and the subclavian arteries in patients of aorto-arteritis from this subcontinent pose a special problem for selecting the site for arterial catheterization. Catheter manipulation in severely diseased arteries constitutes an additional hazard.

The introduction of IV-DSA and subsequent improvements in the post-processing techniques have now resulted in the production of good-quality subtraction images of the arterial system (Carmody et al,

Table II. Angiographic involvement in 40 patients with aorto-arteritis

Aortic arch	Descending thoracic aorta	Abdominal aorta	Subclavian artery		Carotid artery		Renal artery			Other visceral arteries	Femoral arteries
			Right	Left	Right	Left	Right	Left	Bilateral		
3	9	26	12	18	6	12	9	4	12	9	9

1986). The advantages of IV-DSA are well documented (Pavlicek et al, 1982; Rosen et al, 1983; Wilms et al, 1986). Aorto-arteritis is particularly suited for evaluation by IV-DSA because the disease effectively neutralizes two important limitations of the IV-DSA technique. Panarteritis associated with aorto-arteritis frequently results in diminished movements of the aortic wall, which reduces motion artefacts and gives better images. The reduced spatial resolution of IV-DSA is less important when looking at the larger vessels affected by the disease. In general, IV-DSA images are comparable in quality to conventional arteriograms, although one technique may be better than the other on occasions.

Pulmonary arterial anatomy can also be demonstrated by IV-DSA and obstructive lesions in the major branches, pruning of the peripheral vessels and defects in the parenchymal phase were seen. Although pulmonary arterial involvement in aorto-arteritis is reported to be common (Lupi et al, 1975; Yamato et al, 1986), only two out of 18 patients in the present study showed evidence of pulmonary arterial involvement.

There are some limitations in the use of IV-DSA. Patient co-operation is essential as the patients are required to remain absolutely still for as long as 20 s. Those with congestive cardiac failure generally have low cardiac output and slow circulation time, and are not suitable for the technique. This is because of the dilution of contrast medium and frequent occurrence of motion artefacts as these patients are unable to hold their breath for long. All except one of the unsuccessful IV-DSA examinations in the present study were in patients with congestive cardiac failure. Careful screening of these patients to rule out congestive cardiac failure appears essential prior to selection for IV-DSA.

The limitations of IV-DSA interpretation of the aortic wall thickness and mild involvement of the descending aorta in the region of the diaphragm were noted and conventional arteriography may be a better alternative in these situations. Another important limitation of IV-DSA is caused by vessel overlap, especially in the evaluation of renal artery origins. By utilizing shallow anterior oblique views and off-line manipulation of IV-DSA images, it is possible to assess the origin of renal arteries in most patients (Smith et al, 1982). Oblique views are also essential for visualization of the common carotid artery bifurcation. We emphasize that although multiple views were frequently necessary, complete arterial evaluation within the maximum permissible contrast medium dose was possible in all our patients. The contrast medium load was well tolerated and no untoward effects were seen.

Matsunaga et al (1987) recently reported on digital subtraction angiography in the follow-up of 32 patients with aorto-arteritis. The present study suggests that IV-DSA could be the first choice for making the radiological diagnosis in patients suspected of having the disease. Aortic wall thickness and irregular outline of the descending thoracic aorta depict early stages of involvement in aorto-arteritis and cannot be detected by IV-DSA. However, in view of the frequent, severe and widespread arterial involvement in aorto-arteritis, these signs are rarely essential for establishing the diagnosis.

References

Carmody, R. F., Yang, P. J., Seeger, J. F. & Capp, M. P., 1986. Digital subtraction angiography update 1986. *Investigative Radiology, 21*, 899–905.

Chernin, M. M., Pond, G. D. & Sahn, D. J., 1984. Digital subtraction angiography of the aortic arch. *Cardiovascular and Interventional Radiology, 7*, 196–203.

Das, J. P., Padhee, B., Mishra, M., Basit, M. A., Nayak, C. R. & Swain, V., 1982. Non-specific aorto-arteritis. *Indian Heart Journal, 34*, 391–395.

Gammill, S. & Craighead, C., 1975. Translumbar aortography updated. *Surgery, Gynaecology and Obstetrics, 140*, 59–64.

Gotsman, M. S., Beck, W. & Schrire, V., 1967. Selective angiography in arteritis of the aorta and its major branches. *Radiology, 88*, 232–248.

Hachiya, J., 1970. Current concepts of Takayasu's arteritis. *Seminars in Roentgenology, 5*, 245–259.

Haunt, G. & Amplatz, K., 1968. Complication rates of transfemoral and transaortic catheterisation. *Surgery, 63*, 594–596.

Hessel, S. J., Adams, D. F. & Abrams, H. L., 1981. Complications of angiography. *Radiology, 138*, 273–281.

Hoevels, J., 1983. Single catheter technique for transaxillary aorto-femoral angiography. *Acta Radiologica (Diagnosis), 24*, 381–384.

Lande, A. & Rossi, P., 1975. The value of total aortography in the diagnosis of Takayasu's arteritis. *Radiology, 114*, 287–297.

Liu, Y. Q., 1985. Radiology of aorto-arteritis. *Radiologic Clinics of North America, 23*, 671–688.

Lupi, H. E., Sanchez, G., Horwitz, S. & Gutierrez, E., 1975. Pulmonary artery involvement in Takayasu's arteritis. *Chest, 67*, 69–74.

Matsunaga, N., Hayashi, K., Aikawa, H., Uetani, M., Matsuoka, Y., Hombo, A., Fukushima, T. & Maeda, H., 1987. Digital subtraction angiography in Takayasu arteritis. *Acta Radiologica (Diagnosis), 28*, 247–252.

Pavlicek, W., Weinstein, M., Modic, M. T., Buonocore, E. & Duchesneau, P. M., 1982. Patient doses during digital subtraction angiography of the carotid arteries: comparison with conventional angiography. *Radiology, 145*, 683–685.

Pond, G. D., 1985. Pulmonary digital subtraction angiography. *Radiologic Clinics of North America, 23*, 243–260.

Rosen, R. J., Roven, S. J., Taylor, R. F., Imparato, A. M. & Riles, T. S., 1983. Evaluation of aorto-iliac occlusive disease by intravenous digital subtraction angiography. *Radiology, 148*, 7–8.

Smith, C. W., Winfield, A. C., Price, R. R., Harding, D. R., Tucker, S. W., Witt, W. S. & Hollifield, J. W., 1982. Evaluation of digital venous angiography for the diagnosis of renovascular hypertension. *Radiology, 144*, 51–54.

Wilms, G. E., Baert, A. L., Staessen, J. A. & Amery, A. K., 1986. Renal artery stenosis: evaluation with intravenous digital subtraction angiography. *Radiology, 160*, 713–715.

Wood, G. W., Lukin, R. R., Tomsick, T. A. & Chambers, A. A., 1983. Digital subtraction angiography with intravenous injection: assessment of 1000 carotid bifurcations. *American Journal of Roentgenology, 140*, 855–859.

Yamato, M., Lecky, J. W., Hiramatsu, K. & Kohda, E., 1986. Takayasu's arteritis: radiographic and angiographic findings in 59 patients. *Radiology, 161*, 329–334.

1989, *The British Journal of Radiology*, 62, 121–126

Assessment of angioplasty balloon catheters: further studies*

By W. D. Jeans, FRCR, J. H. L. Henson, PhD, FRCR, †T. M. A. Holloway, BEng, †A. G. G. Forman, BEng and †A. Blakeborough, MA, PhD

Departments of Radiodiagnosis and †Civil Engineering, University of Bristol, Bristol

Abstract. Eight millimetre diameter angioplasty balloon catheters of both the Gruntzig and Olbert types from five manufacturers have been tested *in vitro* to establish bursting pressures and the changes in maximum and deflated diameters following repeated inflations, both when free and within a restraining sleeve. Maximum inflated diameters were within 10% of that stated and all types of balloon except one burst at a pressure greater than the recommended value. Deflated diameters were approximately 1 mm greater than insertion diameters, which are much smaller in the Olbert type. All balloons became a little larger with each of the first few distensions, and became stiffer. The maximum diameter was reached and remained constant after 10–15 distensions. Distension within a latex sleeve did not change bursting pressures, and it is considered that results from unconstrained testing can be extrapolated to behaviour *in vivo*. Computer modelling and calculation of maximum stress resultants also showed that calculated longitudinal and circumferential stresses are unaffected by applied restrictions. It is concluded that balloon technology is steadily improving and it is suggested that British Standards should be established for dilatation balloon catheters. Amongst other factors these Standards should include maximum recommended inflation pressures that are at least 2 atm less than bursting pressures, whilst the stated maximum diameter should be for fully extended balloons, and should have a tolerance of no more than ± 10%.

With the growth in the acceptance and application of percutaneous transluminal angioplasty has gone the technological development of balloon catheters and ancillary equipment. The earliest balloon catheters were made of rubber latex and these have been superseded by polymeric materials such as polyvinylchloride, polyethylene and polyurethane.

Balloon catheters exert a dilating force which has a linear relationship to the increase in pressure in the balloon and which is greater if the balloon material does not stretch (Abele, 1980). Modern catheters are said to fail less often and to cause less problems for the user (Hartz & McLean, 1986) and this has been attributed to changes both in the materials used and in construction. The precise materials used are trade secrets, and are affected by both the variations in amounts of polymer, stabilizer and plasticizer present, and the way in which the composite is treated.

We have previously described a technique for testing balloons, and found in the preliminary studies that some balloons burst at well below the maximum recommended pressure (MRP), and that inflated diameters reached up to twice the expected maximum diameter (Henson et al, 1988). There was a tendency for larger balloons to be less stable. We have therefore tested a range of 8 mm balloons from five manufacturers and have measured the change in diameter with repeated inflations and the effect of an external constriction on the balloon. We have also made a computer model of the stress distribution within some of the balloons so that behaviour can be predicted and designs improved.

Methods

Apparatus

This was essentially as previously described (Henson et al, 1988). The catheter under test is positioned between two mirrors positioned at 90° to each other in a water bath at 37°C. A camera positioned at a fixed distance vertically above the catheter is used to photograph the balloon and the measurements made from the photographs are corrected for magnification. Pressure is applied to the balloon from a threaded plunger and measured using a calibrated diaphragm pressure transducer.

Testing procedure

Unrestrained balloons. (i) The balloon was filled with water and pressure increased by regular steps up to the maximum recommended pressure, and then reduced by the same steps. At each step two photographs were taken, one focused on the balloon itself, and the other on the two reflected images. (ii) The balloon was then distended up to the MRP and deflated eight times. (iii) On the 10th cycle the steps in (i) were repeated. (iv) The cycle of distension and deflation was repeated with photographs being taken at the MRP on Cycles 15, 20, 30 and 40. (v) On the 50th cycle the balloon was photographed at MRP and the pressure increased until the balloon failed. A photograph was then taken and the type of failure recorded.

Restrained balloons. The balloon was surrounded by a latex sleeve. A circular neoprene ring with slight distensibility and of slightly smaller diameter than the maximum balloon diameter was positioned over the sleeve at the middle of the balloon. This was distended as in (i) above and photographed. It was then distended to failure and the pressure noted. A loose ring was placed over the balloon near the constricting ring to allow

---

*Parts of this paper were presented at Radiology '88 in Glasgow, 23–25 May, 1988.

Address correspondence to: Dr W. D. Jeans, Department of Radiodiagnosis, Bristol Royal Infirmary, Bristol BS2 8HW.

accurate measurement of magnification. The developed negatives from all tests were projected onto a screen and balloon sizes measured. For the restrained tests, measurements were of the latex sleeve at the constraining ring and at measured distances from it.

Computer modelling. The distension patterns of two of the balloon catheters were modelled using a commercial software package ANSYS (Swanson Analysis Systems, Houston, USA) which is a complex finite element program. This was used to calculate stress distribution in the catheters during distension.

Results

Eleven catheters supplied by five different manufacturers were studied.

Unrestrained tests

The Gruntzig-type balloons from three of the manufacturers have double lumens, with the two lumens running in parallel. The Olbert-type catheters (Olbert & Muzika, 1983) from the other two manufacturers are co-axial, with the inner catheter, through which guide wires and contrast medium enter the artery, passing through the outer catheter. The inner catheter has a movable proximal segment. The balloon shortens as it distends, moving the proximal segment away from the catheter assembly to accommodate the shortening. These catheters had a smaller initial balloon diameter which returned nearer to this after distension than did the Gruntzig type of balloons (Fig. 1).

The greatest increase in diameter in all makes was on the first distension, and the diameter after deflation was greater than it was initially. A graph of the first and 10th cycles of distension and deflation for one balloon is shown (Fig. 2). The maximum diameter of all balloons tested reached a plateau after 10 to 20 distensions and then remained relatively constant (Fig. 3). The final deflated diameter was approximately 1 mm greater than the initial insertion diameter for all balloons (Table I). The Schneider, Medi-Tech I, Cook and Meadox catheters all maintained a balanced shape with little buckling, and the first three failed with longitudinal tears. The Meadox balloon became aneurysmal prior to failure at 1.7 atmospheres above the MRP (Fig. 4), and the Eschmann balloon failed on its first distension at 13.6 atm, less than its maximum recommended pressure, when a small hole developed in the balloon. The Meadox and Eschmann balloons become shorter as they distend, the Meadox by 26%, and the Eschmann by 33%. The pressures at failure together with the maximum diameter achieved are shown in Table I.

Restrained balloon testing

The effect of changes in pressure up to MRP on the measured diameter at three positions along the length of the balloon is shown graphically for the Cook catheter (Fig. 5). Diameters are larger than in the unrestrained tests because measurements include the thickness of the sleeve of latex. The pressures at failure and the maximum diameters obtained adjacent to and away from the

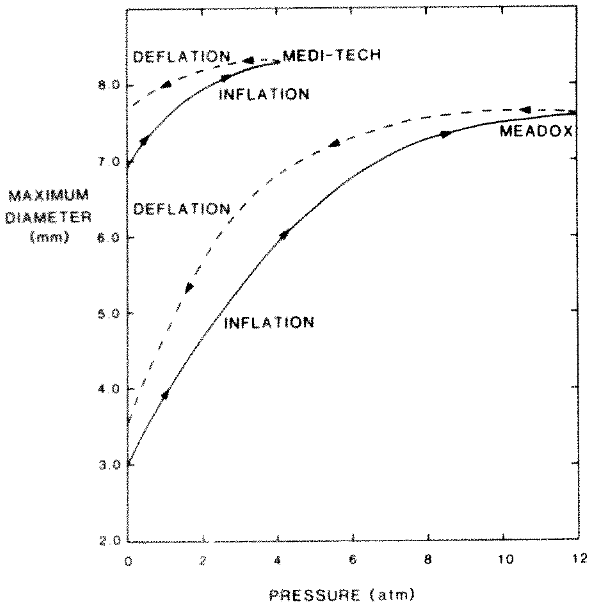

Figure 1. Comparison of inflation and deflation diameters of two balloons with different types of construction.

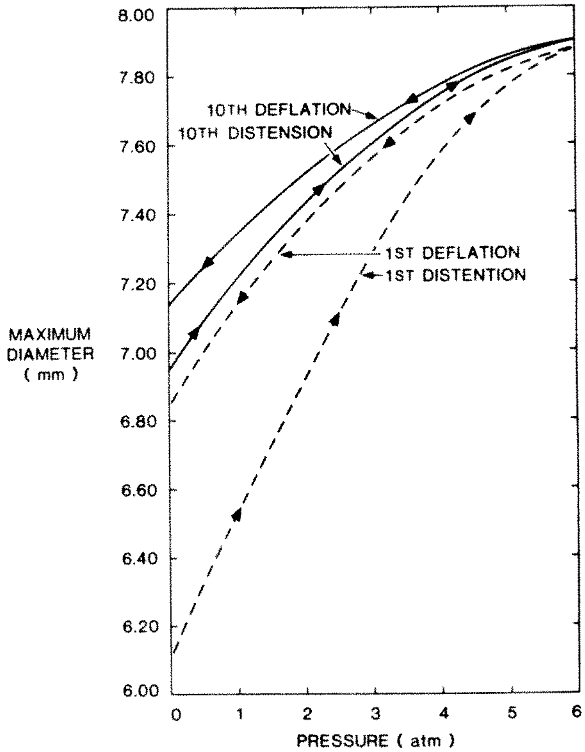

Figure 2. Graph showing the distended and deflated diameters of a Schneider catheter balloon on the 1st and 10th cycles.

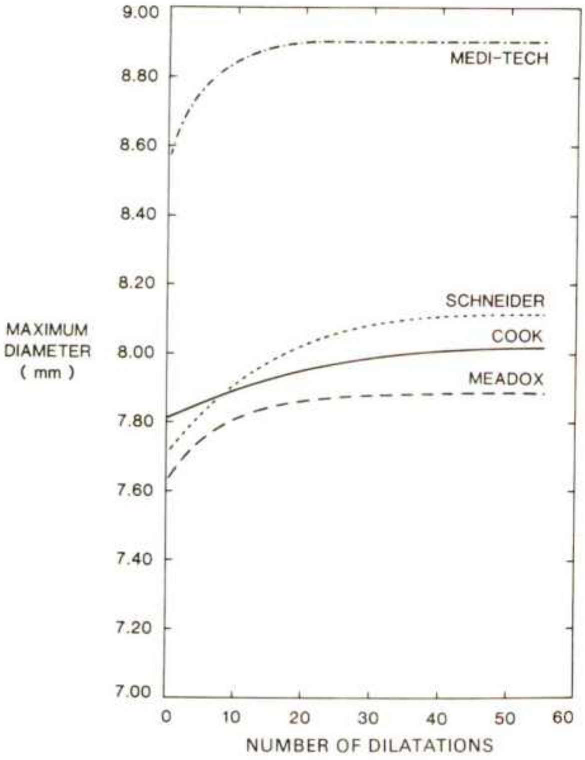

Figure 3. Graphs showing the change in maximum distended diameter of four makes of catheter over 50 cycles of distension.

constraining ring are shown in Table II. Results were very similar for all the catheters tested, and balloon behaviour in general was the same in the restrained and unrestrained tests with little significant change in the bursting pressures, except for the Medi-Tech I catheter which reached a greater pressure before failure when restrained. The buckling effect within the latex sleeve is shown for a Cook catheter (Fig. 6).

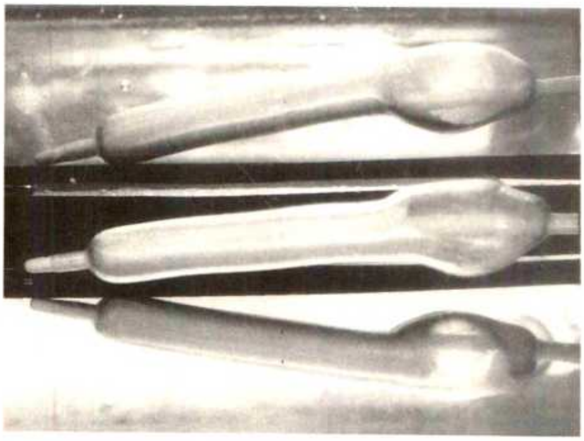

Figure 4. Photograph showing three views of a Meadox catheter balloon immediately prior to failure, with the development of an aneurysm at greater than the maximum recommended pressure.

Computer modelling results

From the finite element models the stiffness for the Schneider and Cook balloons was calculated at 3.9 and 18.5 N/mm, respectively. The maximum principal stress resultants for each load step were calculated for restrained and unrestrained dilatation (Figs 7, 8) and show that the calculated resultants are the same under both conditions. This offers a theoretical explanation for the experimental finding that burst pressures are unaffected by applied restrictions. The graphs also demonstrate that circumferential stresses are greater than longitudinal stresses in the two catheters modelled and this encourages tearing to occur along the length of the balloon rather than circumferentially. The Schneider catheter has a minimum safety factor between these stresses of 1.20 at the position of maximum change of shape on the balloon profile. If the value falls too close to 1.0 there is a high risk of circumferential tearing. The Cook balloon has a smoother profile and a much larger minimum safety factor of 1.44.

Table I. Diameter of balloon at insertion, with maximum diameter reached, final deflated diameter, recommended and bursting pressures for 8 mm diameter balloons from five manufacturers

Make	Type	Insertion diameter (mm)	Maximum diameter reached		Final deflated diameter (mm)	Recommended maximum pressure (atm)	Pressure at failure	
			(mm)	(%)			(atm)	(%)
Cook	(G)	6.7	7.8	98	7.5	12.0	13.7	114
Eschmann	(O)	2.2	7.4	93	—	17.0	13.6	80
Meadox	(O)	3.0	7.6	95	4.0	12.0	13.7	114
Medi-Tech I	(G)	6.9	8.8	110	8.0	4.1	6.4	156
Schneider	(G)	6.1	7.9	99	7.1	6.0	10.6	176

Type: G = Gruntzig double lumen, O = Olbert co-axial.
Measurements of diameter are ± 5%.

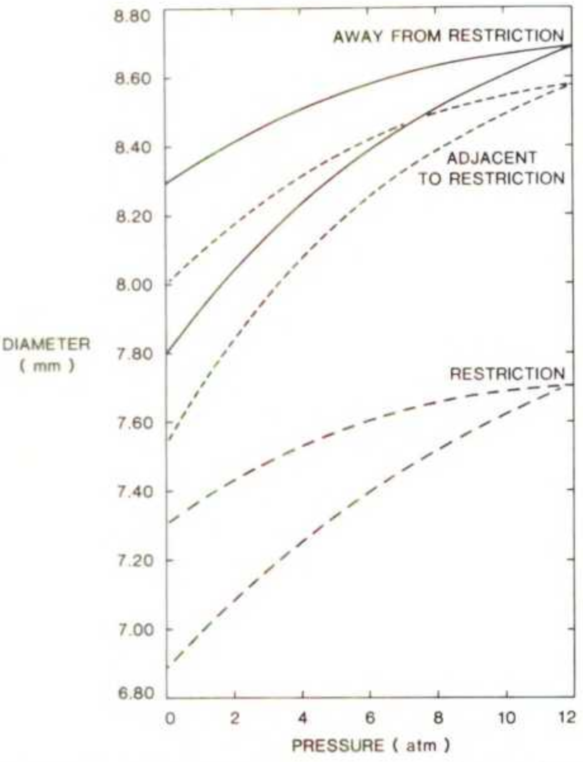

Figure 5. Graph of measured diameters of a Cook catheter balloon during distension and deflation at three points: beneath a restriction ring, adjacent to, and at 3.25 mm from the restriction.

Discussion

All of the balloons tested became a little larger with each of the first few distensions. This is to be expected from the known physical properties of the polymers used for balloons (Arridge, 1985). In extension they exhibit two types of behaviour. Initially, the molecules are pulled out straight and orientate themselves with the load; this also introduces a permanent set in the plastic. Once lined up along the principal load direction, the stiffness is much higher for subsequent loading. The inflation and deflation cycle then becomes fixed, and this was apparent from Fig. 3 where the plateau of maximum distension appears after some 10–15 distensions. Suggestions that multiple distensions may be responsible for balloon rupture (Yune & Klatte, 1980) are not borne out by these results and we have previously shown that if failure is going to occur it happens early in the cycle of distension and deflation (Henson et al, 1988). This was again seen in the one make of balloon that failed at less than the maximum recommended pressure in these tests.

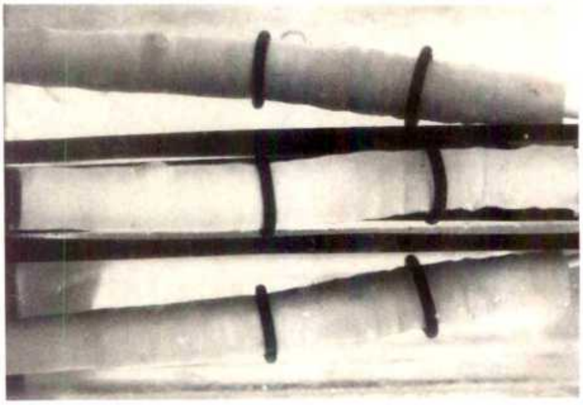

Figure 6. Photograph of a Cook catheter bending within the latex sleeve, showing the restriction ring and the ring used to estimate magnification.

It has been shown that the expansion characteristics of a balloon constrained in a rigid Teflon tube differ from those found when no constraint is applied (Zollikofer et al, 1986). Tests within rigid tubes resulted in higher bursting pressures, with rupture occurring at the unsupported ends. The results of our tests on constrained balloons in a latex tube able to distend produced different results, with an increased bursting pressure in only one balloon. The Teflon model is very different from the situation in an elastic artery, and it is probable that our results are closer to the real life situation. If this is accepted it appears that unconstrained tests give results that can be extrapolated to behaviour *in vivo*.

The diameter of a balloon catheter should be as small

Table II. Effect of restriction ring on maximum balloon diameters and bursting pressures for 8 mm balloons from five manufacturers

Make	Maximum diameter reached (mm)		Recommended maximum pressure (atm)	Pressure at failure (atm)
	Under restriction	3.25 mm from restriction		
Cook	7.7	8.7	12.0	13.7
Eschmann	7.4	8.4	17.0	13.6
Meadox	7.8	8.9	12.0	13.6
Medi-Tech I	7.1	7.8	4.1	9.8
Medi-Tech II	7.5	8.0	6.0	13.7
Schneider	7.3	8.2	6.0	10.6

Measurements include the thickness of the latex sleeve.

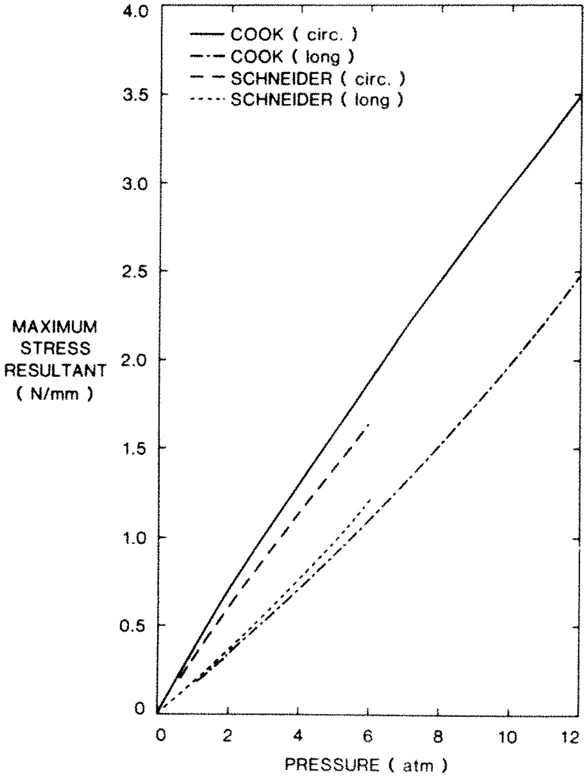

Figure 7. Graph of the maximum calculated circular and longitudinal stress resultants plotted against the distension pressures for a Cook and Schneider catheter.

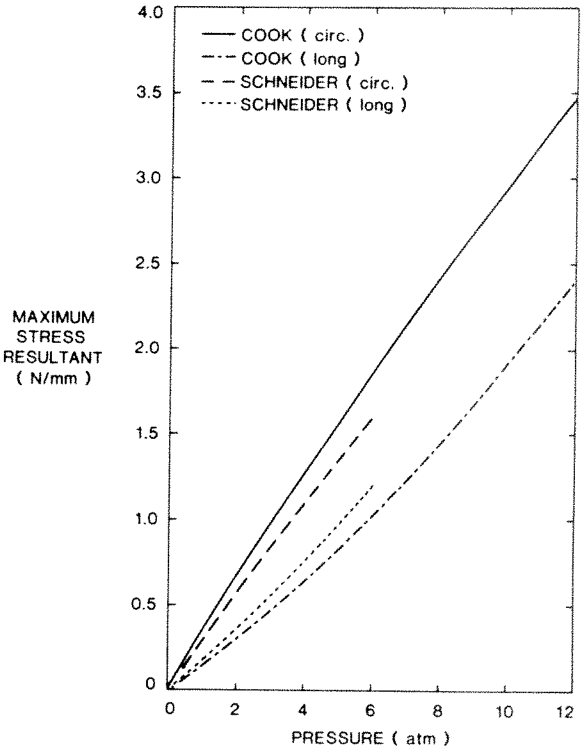

Figure 8. Graph of the maximum calculated circular and longitudinal stress resultants plotted against the distension pressures for a Cook and a Schneider catheter when in a latex sleeve with a restriction ring.

as possible on insertion or removal from the artery. The Meadox and Eschmann balloons both had initial diameters of less than 3 mm, and were still smaller after distension than the insertion diameter of the Gruntzig-type balloons. These balloons had initial diameters of over 6 mm and have to be wrapped around the shaft of the catheter to be inserted. Similarly, they often have to be rotated on removal to rewrap the balloon and reduce the diameter presented to the arterial wall.

All the balloons studied in this series distend to within ±0.8 mm of the stated diameter, apart from two which became aneurysmal prior to failure, and the bursting pressures were greater than the maximum recommended pressure in all makes except one. These results were better than those found in our earlier studies on balloon catheters and, although the numbers tested were small, suggest that catheter materials and design have improved in the 2-year interval between obtaining and testing the two sets of balloons.

It has been suggested that some of the complications described in angioplasty may in part be due to arterial damage caused by shear stress (Kinney et al, 1985). The shortening of about one-third in length during inflation of the Meadox and Eschmann balloons raises the theoretical possibility of this occurring. However, there is no suggestion that this occurs in practice and these balloons have the practical advantage of smaller insertion and removal diameters.

The early experience gained with computer modelling of balloon behaviour suggests that it may provide a good basis for future designs.

Conclusions

It appears from these tests that the majority of the currently available balloons tested can be expected to keep to the stated maximum inflated diameter, and burst at a greater than recommended maximum inflation pressure. Those of the Gruntzig type burst longitudinally, whilst one of the Olbert type burst through a hole between reinforcing fibres, and one became aneurysmal. The behaviour of the balloons is not affected by a circular constraint designed to mimic a localized ring stenosis, nor by restraint in a latex tube, suggesting that the results of *in vitro* tests can be extrapolated to the *in vivo* situation.

Despite clear improvements in compliance of balloon catheters with manufacturers' specifications, some balloons still do not meet these. Premature failure leads to prolongation of procedures, increased cost, and may be a factor in arterial rupture. We would therefore suggest that there should be a British Standard for balloon catheters with specifications that include (i) a recommended maximum inflation pressure which is at least 2 atm less than the bursting pressure; (ii) that the stated maximum diameter should allow for the plastic to become fully extended, and should be accurate within a 10% tolerance; (iii) that all Gruntzig-type balloons should be designed to burst longitudinally; and (iv) that in view of the deterioration in some polymers with time, a maximum shelf life should be stated on the packet.

Acknowledgments

We are grateful to all the manufacturers for donating catheters for testing, and for their co-operation and encouragement. We are also grateful to the Department of Medical Illustration of the Bristol Royal Infirmary for the illustrations.

References

Abele, J., 1980. Balloon catheters and transluminal dilatation: technical considerations. *American Journal of Roentgenology*, *135*, 901–906.

Arridge, R. G. C., 1985. *An Introduction to Polymer Mechanics* (Taylor and Francis, London).

Hartz, W. H. & McLean, G. K., 1986. In *Angioplasty*, ed. by G. D. Jang (McGraw-Hill, New York), p. 158.

Henson, J. H. L., Jeans, W. D., Newham, F. J., Paice, C. & Blakeborough, A., 1988. Assessment of angioplasty balloon catheters: preliminary studies. *British Journal of Radiology*, *61*, 1026–1031.

Kinney, T. B., Fan, M., Chin, A. J., Finn, J. C., Hayden, W. G. & Fogarty, T. J., 1985. Shear force in angioplasty: its relation to catheter design and function. *American Journal of Roentgenology*, *144*, 115–122.

Olbert, F. & Muzika, N. 1983. Dilatation and the expanding balloon catheter. Advantages of the expanding balloon catheter. In *Percutaneous Transluminal Angioplasty*, ed. by C. T. Dotter, A. R. Gruntzig, W. Schoop & E. Zeitler (Springer Verlag, Berlin), pp. 37–45.

Yune, Y. Y. & Klatte, E. C., 1980. Circumferential tear of percutaneous transluminal angioplasty catheter balloon. *American Journal of Roentgenology*, *135*, 395–396.

Zollikofer, C. L., Salomonowitz, E., Brühlmann, W. F., Castañeda-Zuniga, W. R. & Amplatz, K., 1986. Dehnungs- Verformungs- und Berstungscharakteristika häufig verwendeter Ballondilatationskatheter. *Fortschritte auf dem Gebiete der Roentgenstrahlen*, *144*, 40–46.

1989, *The British Journal of Radiology*, *62*, 127–133

Percutaneous drainage of subphrenic abscesses

By Daniel van Gansbeke, MD, Celso Matos, MD, *Michel Gelin, MD, Patrick Müller, MD, Marc Zalcman, MD, †Jacques Devière, MD and Julien Struyven, MD

Departments of Radiology, *Gastrointestinal Surgery and †Gastroenterology, Hôpital Erasme, Free University of Brussels, Belgium

(*Received July 1988*)

Abstract. Forty subphrenic abscesses were drained percutaneously in 37 patients. These abscesses were subsequent to abdominal surgery (28 patients), biliary obstruction and/or fistula (six patients), trauma (two patients) or acute pancreatitis (one patient). The procedures were usually monitored by duplex sonography and fluoroscopy (35 out of 40 cases), with an angled subcostal approach to the subphrenic space in over 85% of the cases. Forty-three drainage catheters were inserted using the Seldinger method; 37 (86%) had a size of 12 F or more, 21 were 16 F in size. Only two out of 43 catheters were double-lumen sump drains. The clinical condition improved after insertion of the catheter in all 37 patients. Definitive successful drainage, defined as hospital discharge without complementary surgery, was achieved in 32 patients (87%), without major complications. A temporizing effect was obtained in three additional patients (8%) who underwent curative surgery for the underlying process after complete drainage of the abscess. Two patients died from multiple organ failure before their abscess healed. Considerations for successful drainage of subphrenic abscesses include a good knowledge of the subphrenic space anatomy, the use of large-bore drainage catheters and the recognition and correct management of underlying enteric, biliary or pancreatic fistulas.

Percutaneous drainage has become the treatment of choice for the majority of intra-abdominal abscesses and fluid collections, regardless of aetiology (Mueller et al, 1984). The origin of the abscess, its relationship to the adjacent anatomical spaces, the nature of the liquid and the presence of digestive fistulas are the main factors that determine the outcome of percutaneous drainage. Until now, very few reports have stressed the specific factors that may determine the management, the results and the complications of percutaneous drainage of subphrenic abscesses. We report here a series of 40 subphrenic abscesses, associated with eight abscesses in other abdominal regions, that were percutaneously drained with radiological monitoring. A consecutive series of 143 percutaneous drainage procedures of abdominal fluid collections and abscesses in 112 patients was carried out.

Materials and methods

Patients

Forty subphrenic abscesses were percutaneously drained with radiological monitoring in 37 patients during a 4-year period. Patients ranged in age from 18 to 76 years (mean 58 years); nine out of 37 patients were aged at least 70 years.

The subphrenic collection was single in 26 out of 37 patients and coexisted in eight out of 37 patients with another abdominal abscess or fluid collection located in the subhepatic space (five cases), the iliac fossa (two cases) or the pancreatic region (one case). These collections were also drained percutaneously. One patient had bilateral subphrenic abscesses, one patient had two homolateral separate subphrenic abscesses and one patient had a recurrent left subphrenic abscess. These abscesses were located on the right in 27 out of 40 cases and on the left in 13 out of 40 cases.

Abscesses occurred subsequent to abdominal surgery in 28 patients: biliary surgery (five patients), hepatectomy (five patients), hepatic transplantation (one patient), gastric or colic surgery (nine patients), splenectomy alone or associated with gastrectomy, and oesophagectomy or pancreatectomy (eight patients). The other cases were related to biliary obstruction (five patients), abdominal trauma (two patients), acute pancreatitis (one patient) and perforated acute cholecystitis (one patient).

Twenty patients had a fistula (six enteric, 12 biliary and two pancreatic) (Fig. 1). All enteric and pancreatic fistulas were secondary to gastrointestinal surgery, while biliary fistulas were related to biliary obstruction or to hepato-biliary surgery.

Technique

Manipulations were monitored by duplex sonography and fluoroscopy in 35 cases, by ultrasound alone in two cases, by computed tomography (CT) alone in two cases and by CT and fluoroscopy in one case. The Seldinger method was used for the drainage of all 40 subphrenic collections as well as for the eight associated collections in the abdomen.

After identification of the subphrenic collection and determination of its relationship to the adjacent tissues, an 18 G needle angled in a caudal to cephalad direction was directed with ultrasound (35 cases) or CT (three cases), aiming toward the potential space between the liver/spleen and the abdominal wall. In two out of 40 cases, an exploratory puncture was first performed using a 22 G needle with duplex sonographic and fluoroscopic monitoring. An 18 G needle was then directed under

---

Address reprint requests to: Daniel van Gansbeke, MD, Department of Radiology, Hôpital Erasme, route de Lennick, 808, B-1070 Brussels, Belgium.

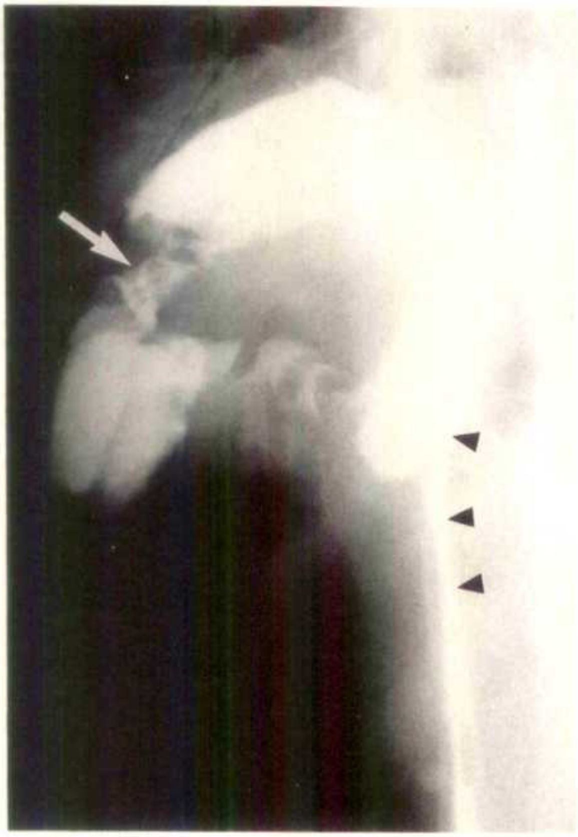

Figure 1. Left subphrenic abscess after gastrectomy and splenectomy drained percutaneously by a 16 F drain (arrowheads). A delayed sinogram shows a fistulous communication (arrow) between the abscess and the left flexure of the colon.

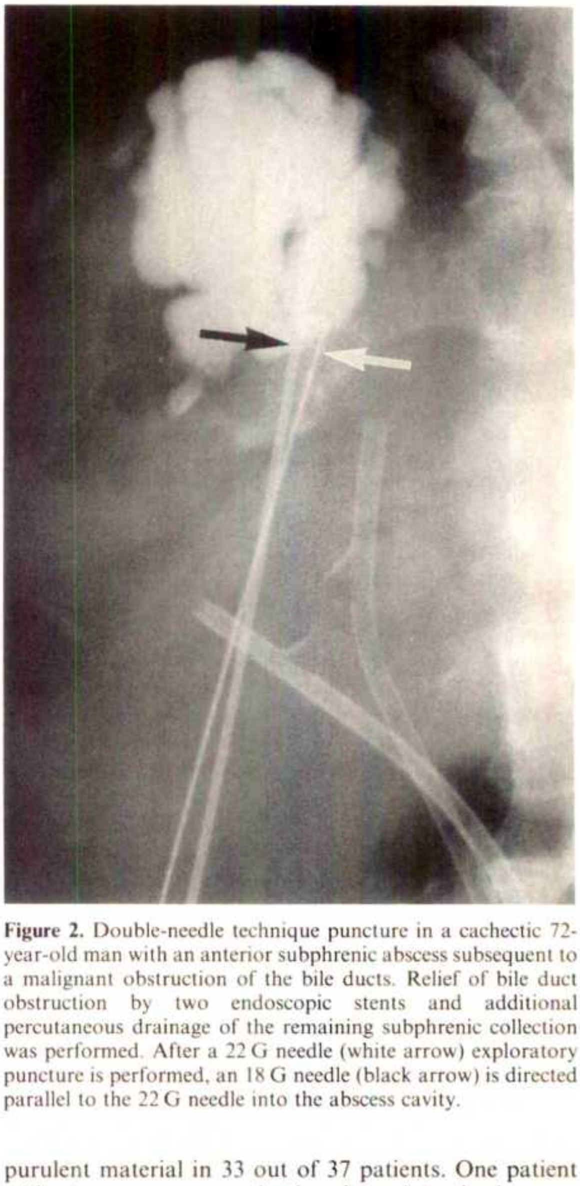

Figure 2. Double-needle technique puncture in a cachectic 72-year-old man with an anterior subphrenic abscess subsequent to a malignant obstruction of the bile ducts. Relief of bile duct obstruction by two endoscopic stents and additional percutaneous drainage of the remaining subphrenic collection was performed. After a 22 G needle (white arrow) exploratory puncture is performed, an 18 G needle (black arrow) is directed parallel to the 22 G needle into the abscess cavity.

fluoroscopic monitoring parallel to the 22 G needle (Fig. 2). This double-needle technique was used in cases where safe continuous sonographic monitoring of the puncture was impossible because of the patient's anatomy and/or the abscess location. A floppy-tip 0.038 J guidewire was then inserted through the cannula with fluoroscopic monitoring and the tract enlarged with increasing size dilators. Finally, the drain was positioned and fixed to the skin of the patient (Fig. 3). Catheter follow-up was done in the standard manner (vanSonnenberg et al, 1982a).

A total of 43 drains was used for drainage of the subphrenic collections. Forty-one were single-lumen catheters and two were double-lumen sump catheters. Thirty-seven drains (86%) had a size of 12 F or more; 21 drains (49%) had a bore of 16 F.

Results

Collapse of the abscess cavity and improvement of the clinical status were rapidly achieved after insertion of the drainage catheter in all 37 patients. The initial drainage procedure was adequate for complete evacuation of the purulent material in 33 out of 37 patients. One patient with two non-communicating homolateral abscesses underwent drainage of the second pouch 2 days after the initial procedure. In two patients, the initial catheter was exchanged for a larger 16 F catheter with multiple side holes, because of the thickness of pus and debris. One case of a large infected haematoma of the right subphrenic space required fluid lavage of the abscess cavity, and the initial single-lumen catheter was replaced by a double-lumen sump drain.

Definitive successful catheter drainage, defined as hospital discharge without complementary surgery, was achieved in 31 patients. One patient died of unrelated causes (cardiac stroke) after the abscess was healed and the drain removed. The definitive success rate was thus 87%. Three patients (8%) underwent delayed curative surgery for the underlying process that caused the

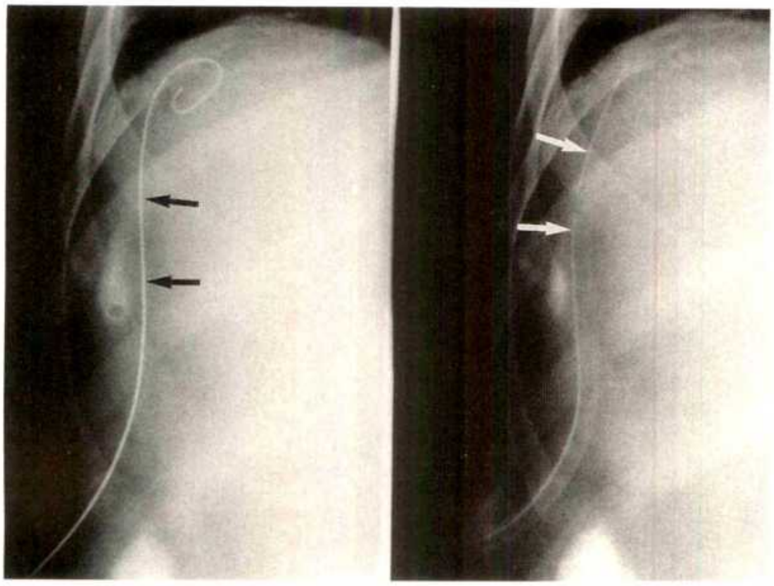

Figure 3. Common technique of percutaneous drainage of subphrenic abscess. After identification of the subphrenic collection, an 18 G needle angled in a caudal to cephalad direction is directed with sonographic monitoring. A floppy-tip 0.038 J guidewire (black arrows) is then inserted through the cannula with fluoroscopic monitoring, and the tract enlarged with increasing size dilators up to 18 F. Finally, a 16 F multiperforated single lumen drain (white arrows) is positioned and fixed to the skin of the patient.

subphrenic abscess (perforated acute cholecystitis, tumoral involvement of an hepatico-jejunostomy and pancreatic fistula after splenectomy), after the patient's condition improved owing to the percutaneous drainage. The overall success rate of percutaneous drainage, including definitive healing and temporizing drainage, was thus 95%. Two patients died from multiple organ failure, despite adequate drainage of the subphrenic abscess.

Patients with abscesses related to enteric, biliary or pancreatic fistulas were definitively cured by percutaneous procedures alone or by combined percutaneous and endoscopic procedures in 17 out of 20 cases (85%).

Complications of the drainage procedure were uncommon. Two patients had a germ-free pleural effusion that required aspiration in one case and thoracic drainage in the other. In these two cases, post-operative pleural adhesions had to be transgressed intentionally because of the absence of a more adequate route to the abscess cavity. Two patients developed a small pneumothorax immediately after manipulation, but these were asymptomatic and required no treatment. In one of these patients, the double-needle technique was used because of the position of the abscess and the patient's anatomy; in the other patient, post-operative pleural adhesions were intentionally crossed. Although no one developed septicaemia requiring intensive therapy, a few of the patients experienced transient worsening of fever during the hours following the manipulations.

Discussion

The selection of a safe route is perhaps the most crucial aspect of the entire procedure of percutaneous drainage of abdominal collections under radiological monitoring (vanSonnenberg et al, 1982a). The optimal drainage route should be as direct, short and dependent as possible, but it must also be absolutely free of any intervening organs or vital anatomical structures. Regarding percutaneous drainage of subphrenic abscesses, the most important technical consideration is to avoid transgression of the pleura and the lung. Infrequent but serious complications associated with transgression of the pleural space during percutaneous biliary drainage have been reported (Neff et al, 1984; Nichols et al, 1984).

The pleural reflection in the costophrenic sulcus stretches downward from its highest point anteriorly behind the xiphoid process, crossing the 8th rib at the costochondral junction, and reaching its lowest level at the 10th rib in the mid-axillary line. The reflection then passes posteriorly in a virtually horizontal manner, crosses the 11th and 12th ribs and ends medially at the level of L1 (Nichols et al, 1984). Therefore, we attempted whenever possible initially to insert the 18 G needle and the subsequent catheter below the 7th rib anteriorly or the 10th rib laterally.

An additional advantage of this low subcostal approach is that it allows the best dependent drainage. Such an approach was possible in up to 85% of our cases, as in over 90% of the cases in the series of Mueller et al (1986), because of the very frequent presence of a thin film of liquid in the potential space between the liver or spleen surface and the lateral abdominal wall (Fig. 4). When this approach is impractical because of the interposition of intestine, especially the right flexure of the colon after hepatectomy, a more direct approach must be used, with potential risk to the pleura. Frequently, the inferior margin of the pleural reflection is obliterated by inflammatory reaction caused by the operation or the abscess itself, permitting transgression of pleural adhesions without risk. However, it is difficult to decide in advance which patients will tolerate the

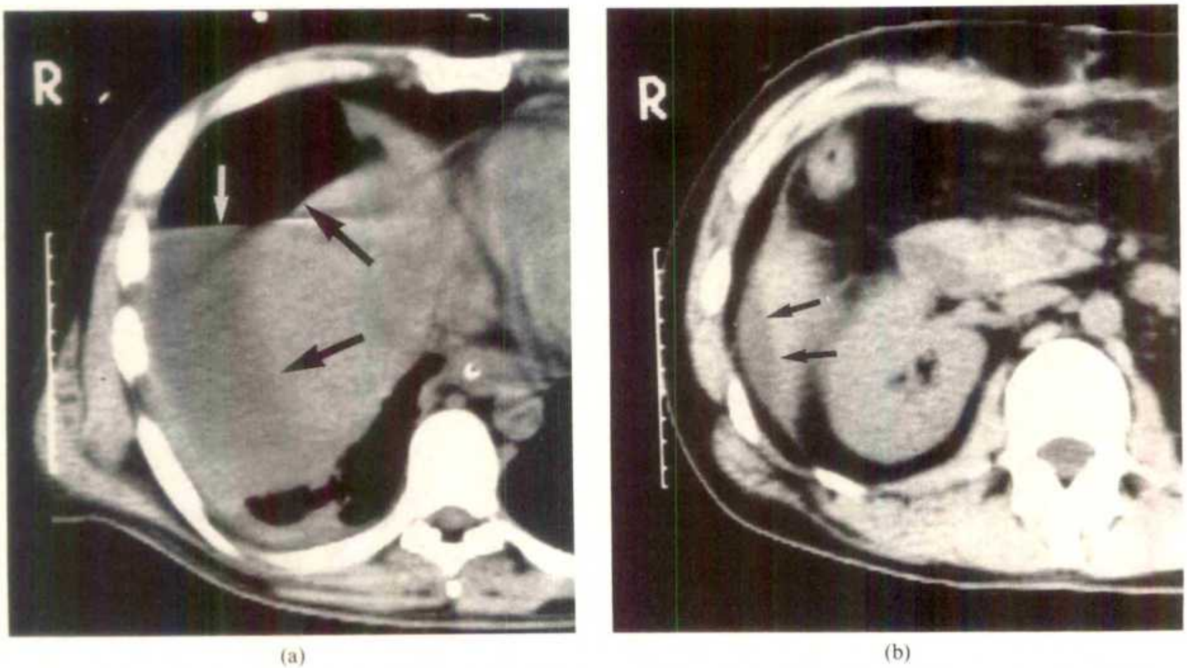

Figure 4. (a) CT scan of a right subphrenic abscess (black arrows) with a marked air–fluid level (white arrow) subsequent to a duodenal fistula. Although the fluid collection is maximal above the liver, a direct intercostal approach will transgress the pleural space, with a risk of complications. (b) The presence of a thin film of liquid (arrows) between the liver and the abdominal wall facilitates a more caudal approach to the subphrenic collection.

intercostal approach without pleural complications. Indeed, the two sterile pleural effusions and one of the two asymptomatic pneumothoraces were complications resulting from the intercostal approach with intentional transgression of pleural adhesions. So, if crossing the pleura cannot be avoided, the radiologist must be aware of possible pleural complications, and of the relative risk versus benefit ratio of the procedure (Neff et al, 1984).

The most important similarity between surgical and radiological drainage of abdominal abscesses is that the major therapeutic effect of both procedures occurs at the time of initial management. Rapid evacuation of purulent material by percutaneous drainage can result in recovery of a critically unstable patient within a matter of hours without the morbidity of surgery. Therefore, the use of large-bore drains has been recommended if the fluid volume exceeds 100 ml (Mueller et al, 1984). Large-bore 12–14 F double-lumen sump drains (vanSonnenberg, Meditech; Ring-McLean, Cook Inc) are well known. The second (sump) lumen allows circulation of room air at ambient pressure and theoretically prevents adherence of the side holes to the walls of the abscess. Irrigation of the abscess cavity to reduce pus viscosity for better evacuation may also be performed via the second lumen.

We, however, prefer the initial use of large-bore but single-lumen catheters for several reasons. Immediate irrigation prior to evacuation of most of the purulent material is dangerous because it increases the pressure inside the abscess cavity with the risk of blood stream contamination by infected detritus and bacterial toxins. Therefore, since lavage of the cavity must necessarily be delayed, the most important quality of a drain is its ability to evacuate rapidly the purulent material. Although the total size of a 12–14 F double-lumen sump drain is large, the effective lumen for drainage is reduced by the presence of the second channel. Moreover, double-lumen sump drains are more complex in shape and are consequently much more expensive than the simple single-lumen variety. The size of the single-lumen catheter we use is determined by the viscosity of the pus, by the shape of the collection and by the ability to dilate the tract adequately. The large lumen allows rapid evacuation of the thick pus and debris and the cavity is usually nearly collapsed at the end of the procedure. Such collapse minimizes the risks of contrast medium injection into the abscess cavity and permits a careful sinogram with minimal risk of bacteraemia and septicaemia. This early sinogram is used chiefly to determine the optimal position of the drain for maximally dependent drainage, but it may also identify a recess or poorly communicating pouch requiring specific drainage (Fig. 5), or gross fistulous communications. Insertion of a large-bore catheter during the initial procedure may also improve drainage enough to make septate fracture or other management of a multiseptated abscess unnecessary (Lieberman et al, 1986).

Catheters for percutaneous drainage of abdominal

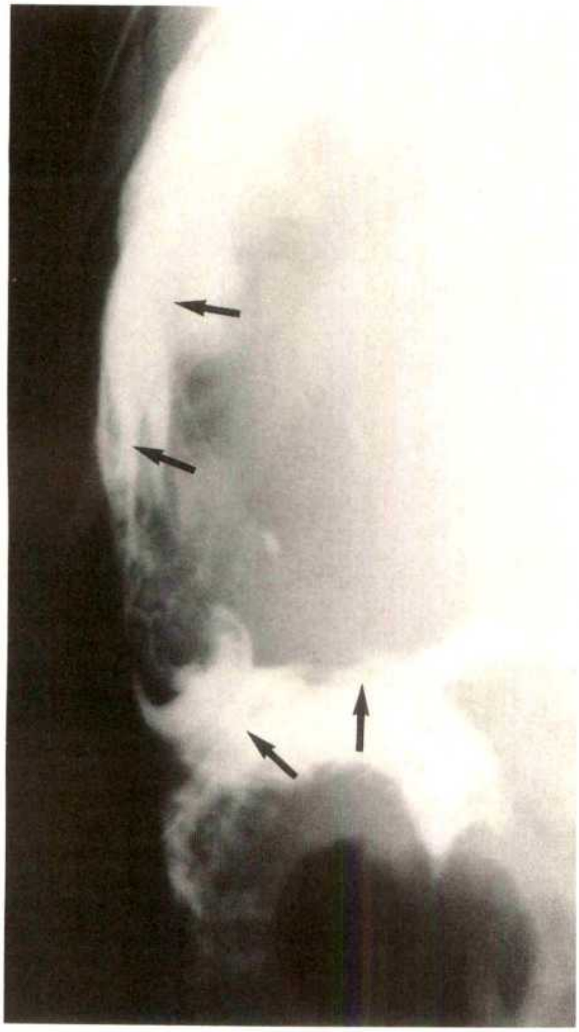

Figure 5. Right subphrenic abscess with extension to the right subhepatic space. The two pouches are poorly communicating and specific drainage of the pouches by two drains (arrows) is mandatory.

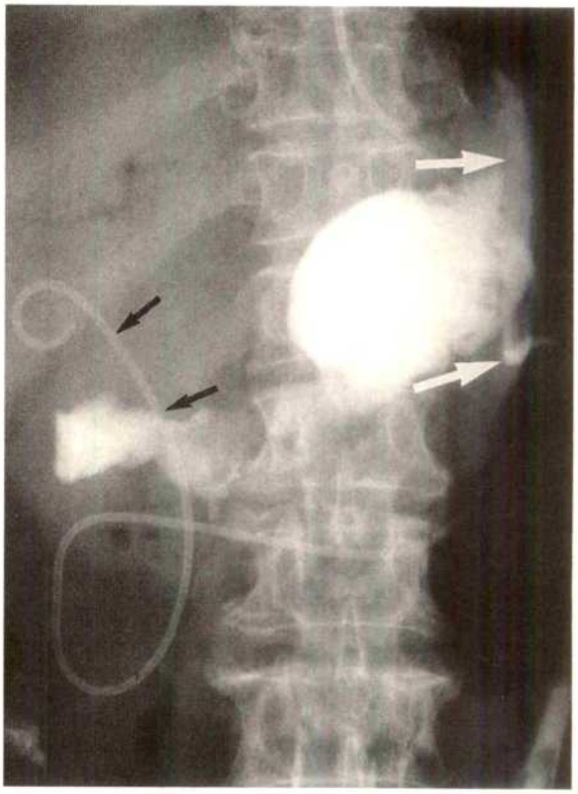

Figure 6. Left subhepatic abscess with extension to the subphrenic space due to a post-surgery common bile duct leak. Percutaneous drainage of the subphrenic abscess (white arrows) and biliary drainage of a naso-biliary catheter (black arrows) is shown.

abscesses can be placed by either the Seldinger or the trocar method. The Seldinger technique permits more operator control, both for initial puncture and for catheter positioning (Mueller et al, 1984). Moreover, the use of large-bore trocar catheters tends to favour a more direct approach to the abscess, posing a higher risk for the pleural recess. Also, the film of liquid which is frequently present between the abdominal wall and the liver or spleen surface, facilitating the low subcostal approach, is usually thin. Puncturing this small film of liquid with a large trocar and pushing the straight rigid trocar up to the top of the subphrenic space can be dangerous to the underlying liver or spleen (Fig. 4). For these reasons, the Seldinger technique appears to be preferable for insertion of large-bore catheters in subphrenic abscesses.

We prefer duplex sonography or fluoroscopy for monitoring the entire percutaneous drainage procedure. Sonography is widely available and permits adequate guidance of the needle insertion in most patients. The angled subcostal approach is also easier to perform with continuous sonographic monitoring rather than with discontinuous CT control. Fluoroscopic guidance is more accurate for the subsequent guidewire insertion and tract dilatation, as well as for the optimal positioning of the drainage catheter. Duplex sonography and fluoroscopy may also be useful for monitoring an initial sinogram. Indeed, unless sonography (or CT) is performed after initial aspiration of the abscess contents, it may be difficult to determine whether a complex abscess has been completely evacuated (Jeffrey et al, 1985). We used CT monitoring only in cases in which the sonographic monitoring was inadequate to guide the puncture safely. Sonographic monitoring alone was used for bedside percutaneous drainage as a lifesaving procedure (McGahan, 1985) in critically ill patients who could not be transported to a radiology unit.

Biliary, enteric or pancreatic fistulas were present in 20 patients of this series (54%). Although fistulous communications with abdominal abscesses are not infrequent if carefully sought (Kerlan et al, 1985), this high rate of abscess–fistula association may also be partially related to the selection of our cases; some of the patients were referred to our institution specifically because of a persisting abdominal fistula. Diagnosis of a fistulous communication following abscess drainage is important for three reasons. First, it may clarify the underlying aetiology of the abscess. Second, it may indicate the necessity of repositioning of the drainage catheter or of inserting an additional catheter to control the flow of drainage. Third, decisions regarding nasogastric suction, parenteral nutrition or biliary drainage may be altered accordingly.

The fistulous communication is often first recognized by careful follow-up and clinical evaluation, which reveals a change in the amount and character of the drainage. A complicating fistula should be suspected whenever drainage from an abscess exceeds 50 ml/24 h (Kerlan et al, 1985) to 75–100 ml/24 h (Papanicolaou et al, 1984) after initial evacuation of the cavity. On the other hand, detection of the fistula by retrograde injection of contrast medium may initially be missed, because the site of communication between the abscess cavity and the viscus may be clogged with debris and oedema at the time of the abscess drainage procedure (Papanicolaou et al, 1984).

Surgical experience has clearly established the mechanical principles affecting the healing of an internal fistula. Usually, a fistula will heal spontaneously unless there is a distal obstruction of the duct or the bowel. Jejunostomy or T-tubes are routinely removed without complications. Similar mechanics apply in successful fistula drainage: if there is obstruction of the distal bile duct or if there is intestinal obstruction distal to the leak, the system remains under high pressure and the fistula continues to drain externally (Edmunds et al, 1960; Papanicolaou et al, 1984; vanSonnenberg et al, 1984a). In this series, bile duct obstruction was managed by endoscopic procedures: endoscopic sphincterotomy, internal biliary drainage by nasobiliary catheter or removable endoprosthesis (Fig. 6) (Sauerbruch et al, 1986; Smith et al, 1986; Devière et al, 1987). Healing of the abscess cavity and the underlying fistula was achieved in 85% of the cases of this series. In the remaining cases, only surgery could remedy the underlying cause of the fistula, but the percutaneous drainage improved the patient's condition before operation. Therefore, even when not definitively curative, such temporizing percutaneous drainage offers significant therapeutic benefit, permitting a more limited and less time-consuming surgery with a lower rate of morbidity (vanSonnenberg et al, 1984b).

The duration of the catheter drainage was variable from several days to several weeks, and depended primarily on the presence of an underlying fistula. Indeed, although there may be improvement in the patient's condition because the purulent material has been removed, continuous drainage may be required for several weeks. Premature removal of the catheter is one of the well known causes of percutaneous drainage failure (Lang et al, 1986), particularly in cases of associated fistulas. So, as in all cases of abscess drainage, catheter removal should be determined by the quantity of drainage, and by the radiological assessment, especially by CT, of the resolution of the collection.

In conclusion, percutaneous drainage under radiological monitoring has become the technique of choice for initial treatment of subphrenic abscesses. Definitive drainage is achieved in over 85% of the cases with a very low rate of mortality and morbidity, while a temporizing effect permitting more limited surgery is obtained in an additional number of patients. In our opinion, immediate operation should be reserved for only those cases requiring prompt surgical treatment of the underlying process causing the abscess.

References

DEVIÈRE, J., VAN GANSBEKE, D., ANSAY, J., DE TOEUF, J. & CREMER, M., 1987. Endoscopic management of a post-traumatic biliary fistula. *Endoscopy, 19*, 136–139.

EDMUNDS, L. H. JR, WILLIAMS, G. M. & WELCH, C. E., 1960. External fistulas arising from the gastro-intestinal tract. *Annals of Surgery, 152*, 445–469.

JEFFREY, R. B., WING, V. W. & LAING, F. C., 1985. Real-time sonographic monitoring of percutaneous abscess drainage. *American Journal of Roentgenology, 144*, 469–470.

KERLAN, R. K. JR, JEFFREY, R. B. JR, POGANY, A. C. & RING, E. J., 1985. Abdominal abscess with low-output fistula: successful percutaneous drainage. *Radiology, 155*, 73–75.

LANG, E. K., SPRINGER, R. M., GLORIOSO, L. W. III & CAMMARATA, C. A., 1986. Abdominal abscess drainage under radiologic guidance: cause of failure. *Radiology, 159*, 329–336.

LIEBERMAN, R. P., HAHN, F. J., IMRAY, T. J. & PHALEN, J. T., 1986. Loculated abscesses: management by percutaneous fracture of septations. *Radiology, 161*, 827–828.

MCGAHAN, J. P., 1985. Aspiration and drainage procedures in the intensive care unit: percutaneous sonographic guidance. *Radiology, 154*, 531–532.

MUELLER, P. R., VANSONNENBERG E. & FERRUCCI, J. T. JR, 1984. Percutaneous drainage of 250 abdominal abscesses and fluid collections. Part II: current procedural concepts. *Radiology, 151*, 343–347.

MUELLER, P. R., SIMEONE, J. F., BUTCH, R. J., SAINI, S., STAFFORD, S. A., VICI, L. G., SOTO-RIVERA, C. & FERRUCCI, J. T. JR, 1986. Percutaneous drainage of subphrenic abscess: a review of 62 patients. *American Journal of Roentgenology, 147*, 1237–1240.

NEFF, C. C., MUELLER, P. R., FERRUCCI, J. T. JR, DAWSON, S. L., WITTENBERG, J., SIMEONE, J. F., BUTCH, R. J. & PAPANICOLAOU, N., 1984. Serious complications following transgression of the pleural space in drainage procedures. *Radiology, 152*, 335–341.

NICHOLS, D. M., COOPERBERG, P. L., GOLDING, R. H. & BURHENNE, H. J., 1984. The safe intercostal approach? Pleural complications in abdominal interventional radiology. *American Journal of Roentgenology, 141*, 1013–1018.

PAPANICOLAOU, N., MUELLER, P. R., FERRUCCI, J. T. JR, DAWSON, S. L., JOHNSON, J. F., SIMEONE, J. F., BUTCH, R. J. & WITTENBERG, J., 1984. Abscess-fistula association: radiologic recognition and percutaneous management. *American Journal of Roentgenology, 143*, 811–815.

SAUERBRUCH, T., WEINZIERL, M., HOLL, J. & PRATSCHKE, E., 1986. Treatment of postoperative bile fistulas by internal endoscopic biliary drainage. *Gastroenterology, 90*, 764–769.

Smith, A. C., Shapiro, R. H., Kelsey, P. B. & Warshaw, A. L., 1986. Successful treatment of nonhealing biliary-cutaneous fistulas with biliary stents. *Gastroenterology, 90*, 764–769.

vanSonnenberg, E., Ferrucci, J. T. Jr, Mueller, P. R., Wittenberg, J. & Simeone, J. F., 1982a. Percutaneous drainage of abscesses and fluid collections: technique, results, and applications. *Radiology, 142*, 1–10.

vanSonnenberg, E., Mueller, P. R., Ferrucci, J. T. Jr, Neff, C. C., Simeone, J. F. & Wittenberg, J., 1982b. Sump catheter for percutaneous abscess and fluid drainage by trocar or Seldinger technique. *American Journal of Roentgenology, 139*, 613–614.

vanSonnenberg, E., Mueller, P. R. & Ferrucci, J. T. Jr, 1984a. Percutaneous drainage of 250 abdominal abscesses and fluid collections. Part I. Results, failures, and complications. *Radiology, 151*, 337–341.

vanSonnenberg, E., Wing, V. W., Casola, G., Coons, H. G., Nakamoto, S. K., Mueller, P. R., Ferrucci, J. T., Jr, Halasz, N. A. & Simeone, J. F., 1984b. Temporizing effect of percutaneous drainage of complicated abscess in critically ill patients. *American Journal of Roentgenology, 142*, 821–826.

1989, *The British Journal of Radiology*, 62, 134–137

Experiences at the new magnetic resonance imaging centre at Bristol*

By J. L. G. Thomson, MD, FRCP, FRCR

MRI Centre, Frenchay Hospital, Bristol

(*Received June 1988 and in revised form August 1988*)

Abstract. The magnetic resonance imaging unit in Bristol has been housed in a new purpose-built centre, shared between three District Health Authorities, but operated entirely separate from the National Health Service. Inasmuch as this is thought to be a unique arrangement, the publication of its finances and statistics have been readily tabulated at the end of its first year's operation, and may be of interest to others planning a similar organization.

Magnetic resonance imaging (MRI) has now reached a level of detail and accuracy such that demand for its availability is becoming widespread in the UK. However, it is expensive to purchase and maintain, with the result that almost all centres in existence at the present time depend on private finance or public subscription for survival. The National Health Service (NHS) has been slow to recognize the benefits of this latest technology and its financial support has been small overall. This has been to the detriment of our patients at a clinical level, and to the country in a commercial sense. Our experiences in Bristol, therefore, where an MRI centre has been operational since June 1987, may be of interest to others who would like such installations, but find that finances are inadequate to meet the reality.

We were very fortunate in the first instance that a local Charitable Trust heard of, and responded to, our expressed radiological desire for MRI, with a magnificent gift of a £1 000 000 scanner to the three District Health Authorities (DHAs) that serve Bristol itself and the adjacent population, amounting to about 1 000 000 people.

An immediate approach to the South West Regional Health Authority for assistance in providing a suitable building in which to house the scanner proved unfruitful because of financial constraint at the time. However, an arrangement was agreed by which the NHS would take over the total running costs of the machine in Year 5 of its operation, with a gradual phasing in during the preceding 3 years.

As a result it was clearly incumbent on the recipients of the donation to go to public appeal to provide for the building and the running costs until this NHS arrangement had time to materialize. A group of four Trustees was therefore formed, comprising a radiologist from each DHA and a retired General Practitioner (GP) as Chairman. The appeal was launched in January 1986 and continues to this day, with an excellent response from the public in particular.

A neutral site for the building had to be chosen, which would allow equal access to each DHA at all times, and we were fortunate that Frenchay Health Authority was able to offer a splendid plot of ground at a peppercorn rent, to meet this requirement. A proper legal agreement was subsequently drawn up to satisfy all parties concerned.

In respect of a building, we were able to commission Messrs Picker International, the manufacturers of the MRI machine, on a turnkey basis, to organize and design a suitable lay-out, which they did with the employment of a local contractor. The appeal proved to be successful enough to pay for the cost of the building as it proceeded from start to finish as well as previous site clearance, thus saving the need for any loan. The whole enterprise was finished and ready to receive patients by June 1987, about 18 months from the date of the original donation.

As it is now a year since the service was commissioned, it seems appropriate for us to review our operational performance and the finances involved.

Results and discussion

Building

Inasmuch as three DHAs were to share the building, adequate space was necessary, and this has proved to have the additional benefit of comfort and relaxation, both for staff and patients. The high quality of the internal fittings and soft furnishings has produced praise from numerous sources. The total cost of the building with all contents, apart from the machine itself, has been estimated at £543 000. However, for many anticipated centres elsewhere, particularly if serving just one DHA, it should be noted that a corresponding cost would be proportionately less, commensurate with the size of the building erected, in comparison with ours which is admittedly high.

Staff and pay

The details of staffing arrangements are set out in Table I. We do not feel that extra medical staff are required. So many of the examinations performed are "instead of" traditional radiological techniques rather than "in addition", so that the medical officer concerned can concentrate his attention on MRI as the preferred

---

*Based on a presentation made at Radiology '88, Glasgow, 23–25 May, 1988.

Table I. Bristol MRI Centre staffing costs (June 1987/88)

Pay	WTE	£000s
Medical	—	—
Radiography		
Superintendent III radiographer	1.00	15.5
Senior I	1.00	14.0
Senior II (3 months)	1.00	3.5
Secretary/receptionist HCO	1.38	10.0
Nursing	—	—
Portering	—	—
Domestic	0.38	2.2
Total		45.2

WTE = Whole time equivalent. HCO = higher clerical officer.
All the above figures include employer's contributions.

technology. After a time, many of the examinations do indeed follow a routine programme, and the whole-time presence of a radiologist would be extravagant in these cases. A part-time presence with communication via telephone or IMTRAN appears to be adequate, although it would be agreed that any unusual requirement is certainly best monitored by a radiologist on the spot.

We started our year with a full-time Superintendent III radiographer, already experienced in MRI, and a full-time Senior I, with limited MRI experience, acted as number two. As we planned to work a longer day in Year 2, we have latterly employed a third full-time radiographer for the last 3 months, with the result that we now have three fully trained radiographers. Two part-time secretary-receptionists, who overlap at lunch-time to provide continuity, handle the office side of the centre under the supervision of the Superintendent radiographer. A part-time cleaner is employed each day, but we have not felt the need to employ a porter or nurse, although the hospital kindly collects our mail and carries out one or two other minor duties on a voluntary basis. Our pay costs have amounted to £45 200 in the first year, but will clearly be a little more in Year 2 because of pay rises and the third radiographer, by then full-time. Our day now extends from 8 a.m. to 6 p.m. with a research programme on one evening a week.

Non-pay items

Table II itemizes our expenses for the year, and is self-explanatory. We keep hard copy of all the cases that come through the centre and send out copies of our hard copies to the clinicians requesting the examination, at the discretion of the radiologist supervising the examination. Films and reports are thus usually included in the patient's ordinary radiograph envelope. The liquid helium and nitrogen (cryogens) are the most expensive items, with heat, light and power significant, mainly because of the size of the building with its heating and air conditioning. In Year 2, the service charge will become payable as the guarantee period will be over; the same may apply to the tapes which were gratuitous in our first year. These two items are thus added into Year 2's estimate.

Table II. Costing for non-pay items (1987/88)

Non-pay	£000s
Films and chemicals	14.5
Tapes	(2.5)
Cryogens	22.1
Heat, light and power	11.7
Oil	1.1
Rates	2.1
Peppercorn rent	0.001
Stationery	2.5
Printing and advertising	0.5
Postage	0.2
Telephones	0.5
Uniforms	0.2
Medical supplies	0.6
Insurance	2.5
Maintenance of MRI (service)	(65.0)
Maintenance of office	3.0
Maintenance of building	2.6
Miscellaneous	5.0
Total	69.101 (67.5)

Figures in parentheses are those covered by guarantee and donation.

Total costs

Adding pay and non-pay for the first year produces a total of £114 301 (Table III). In Year 2, however, the whole year's salary for the third radiographer, together with the two items mentioned above, pay awards, inflation, and possibly the purchase of new software, will produce a figure of around £220 000. Income from private patients, and other district health authorities sending patients, produces about a quarter of these totals.

Patient throughput

In Table IV it can be seen that 1604 patients have been examined in Year 1 and 6% of these had more than one area examined, which means more time in the machine. As expected, about 80% of this number attended on an

Table III. Total costs for Years 1 and 2 at the Bristol MRI Centre

Costs			
Building			£543 000
Pay Non-pay	£45 200 £69 101	Year 1	£114 301
Add £67 500		Year 2	£181 801
But allow for	Senior II radiographer Pay awards New software Inflation		£220 000

Table IV. Number of patients examined at Bristol MRI Centre (1987–88)

			Inpatients	Outpatients	GA
Hospital A	496	1604	336	1268	3
Hospital B	437				
Hospital C	402				
Others	269				

GA = General anaesthesia.
In addition 6% had a second region imaged, (*i.e.* extra time in the machine). All hospitals have CT facilities.

outpatient basis, supporting the contention that this is *par excellence* an outpatient technique, thereby saving hospital beds. Three patients were examined under general anaesthesia, and the procedure was carried out without any undue elaboration of technique. Eight babies and children were also sedated for the examination to be carried out. The majority of patients requiring general anaesthesia are probably better examined with computed tomography (CT), unless MRI is thought to be particularly advantageous. The rejection rate from claustrophobia has been less than 0.8%.

Cost per patient

Dividing the total cost for the first year by the number of patients examined (Table V) gives the cost per patient at £71, and for Year 2, this will probably be somewhat higher at £110. It must, however, be realized that these estimates are the absolute basic minimum, taking no account of the original purchase price of either the machine or the building, and excluding new software or machine replacement. Perhaps the figures should therefore be doubled to be more realistic.

Regions examined

The three DHAs together cover almost every medical and surgical specialty, so that patients may attend with a wide spectrum of disease. Nevertheless, the analysis of the regions examined shows that head and spine rank high in the list (Table VI) which confirms similar analysis in centres elsewhere. However, as clinical awareness and experience develop, it can be envisaged that examination of the cardiac and vascular, and the musculoskeletal systems, for example, will assume greater importance, and the figures may thus change.

Table V. Cost per scan

Year 1
£114 301/1604 = £71 per patient, minimum (excluding cost of building, machine, new software, etc.)
Year 2
£220 000/2000 = £110 per patient, minimum (excluding cost of building, machine, new software, etc.)

Table VI. Region of patients examined

Region	%
Head	35.0
Cervical spine	19.0
Lumbar spine	12.3
Pelvis	10.1
Hips, knees and legs	8.0
Dorsal spine	5.5
Abdomen	4.1
Chest	2.6
Heart	1.5
Shoulders and arms	1.4
Temporo-mandibular joints	0.2
Face	0.1
Miscellaneous	0.2
Total	100.0

Cost-effectiveness

The figures are not yet large enough to indicate significant savings in many areas of examination, but trends are already apparent. The most significant relates to the numbers of myelograms carried out in Bristol. In comparable 3-month periods before and after the introduction of MRI, a reduction of 77 myelograms is recorded, and in a comparable 8-month period, a reduction of 208 myelograms has occurred (Table VII). It is anticipated that as in certain cities in the USA and Canada, our myelography rate could soon be reduced to zero provided enough time on the machine is available. If one takes into account the lumbar puncture required for myelography, the amount of contrast medium used, the overnight admission of the patients and the subsequent morbidity in some, the total saving shown by MRI on an outpatient basis becomes not inconsiderable. A graph of the numbers of myelograms per month is included (Fig. 1), to show the gradual decline in demand from June 1986 onwards. The initial decline shown on the graph for the first year resulted from the improved facility of CT for lumbar spine examination throughout Bristol, and the introduction of MRI in June 1987 shows further decline in the numbers, following the new facility allowing the examination of the neck and dorsal spine as well. Some cases still need myelography out of hours when the Centre is closed, and in certain cases of brachialgia, myelography is still the preferred

Table VII. Myelography in Bristol

Period	Numbers	Saving
January–March, 1987	134	
January–March, 1988	57	77
May–December, 1986	387	
May–December, 1987	179	208
—	—	Time in hospital Contrast medium Morbidity

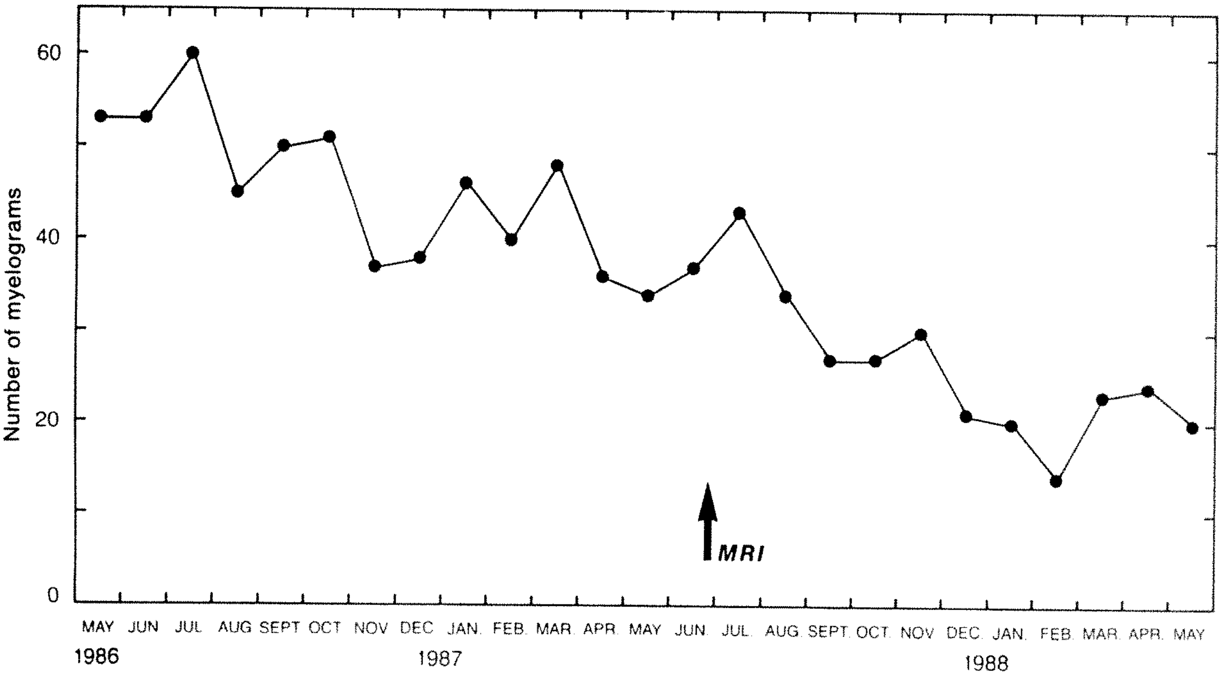

Figure 1. Effect of CT (1986) and MRI (1987) on the number of myelograms performed in Bristol from June 1986 to May 1988.

examination by some surgeons. In current investigations of the brain, any clinical assessment indicating a possible lesion in the posterior fossa, around the sellar region or at the cranio-cervical junction leads to MRI rather than CT, thus reducing significantly the demand for CT. Similarly, in oncology, MRI of the spine has already produced a significant reduction in lumbar puncture (with cerebrospinal studies) and overnight stay, as well as reduced nuclear medicine requirements for skeletal scans. Present studies of the musculoskeletal system and the heart confirm further areas where savings are likely to be made.

It is current fashion to relate the value of any new technology to its cost-effectiveness, and although this has instant financial appeal it tends to overlook other parameters which are also important, such as patient comfort, outpatient accessibility, accuracy of diagnosis and absence of morbidity. On all counts, MRI is far preferable to existing technology in many areas of traditional radiological investigation. Several articles have been published over the recent years in the American journals, outlining the virtues and cost-effectiveness of MRI but their findings cannot be reasonably transferred to the NHS. The sheer number of installations in the USA, about 700 at a recent count, compared with about 25 in the UK illustrates a difference of approach and application which arise from fundamental contrasts in medical financing. In the UK, very few opportunities have so far presented themselves which would allow an assessment of the impact of MRI on a local population. We believe that in Bristol we have one of the few centres able to present such an analysis. Meantime we feel that large neuroscience centres in particular will find MRI indispensable for the maintenance of proper clinical standards, and that the technology will be cost-effective when efficiently used.

Acknowledgments

I would like to express my thanks to my three fellow Trustees in this venture, Dr A. L. T. Beddoe, our Chairman, Dr Paul Goddard and Dr Clive Johnson, who have all accepted equal responsibility and shared enthusiasm. Thanks also to Sally Alden for typing the manuscript.

1989, *The British Journal of Radiology*, 62, 138–144

Patient doses from computed tomography in Manitoba from 1977 to 1987

By Walter Huda, PhD, George A. Sandison, PhD and *Ting Y. Lee, PhD

Department of Medical Physics, Manitoba Cancer Treatment and Research Foundation, 100 Olivia Street, Winnipeg, Manitoba, Canada R3E 0V9

(*Received July 1988*)

Abstract. The number of patients undergoing computed tomographic (CT) examinations in the province of Manitoba is reported for the period 1977–1987. The annual patient throughput has increased from 4.2 per 10^3 population in 1978 to 18.2 per 10^3 population in 1987. Over the same period, the per capita population dose from CT has increased from 4.2 to 81.0 μSv. This substantial rise has occurred because of an increase in patient throughput, higher radiation doses associated with modern CT scanners and an increasing proportion of (higher dose) body CT studies. The mean patient dose on a second generation (EMI 5005) scanner was about 1.4 mSv, whereas the corresponding doses on third generation scanners operating in Manitoba were 3.9 mSv (GE 9800) and 5.6 mSv (Siemens DRH).

Computed tomography (CT) was first introduced into clinical practice in 1973 (Hounsfield, 1973) and rapidly gained acceptance as a major advance in diagnostic imaging. By 1983, it was estimated that there were between 2000 and 2200 CT scanners in the USA alone, with an expansion rate of approximately 200 additional units per year (Evans, 1984). The radiation doses associated with CT scanners are generally at the higher end of the range of doses normally encountered in diagnostic radiology. A recent report estimated that CT doses in Great Britain contributed 2.9% of the collective effective dose from diagnostic imaging procedures, including dental radiography and nuclear medicine, but only accounted for 0.9% of all imaging procedures (Shrimpton & Wall, 1986; Wall et al, 1986). In general, data on the diagnostic use of CT, and the corresponding patient doses, are very limited. This situation has resulted in the United Nations Scientific Committee on Atomic Radiation (UNSCEAR, 1982) requesting additional data on the frequencies of X-ray examinations such as CT and on the absorbed doses in various organs and tissues. These latter data are intended to provide more precise estimates of collective effective dose equivalents, which UNSCEAR considers to be appropriate measures of collective patient doses from radiation exposure such as CT.

The province of Manitoba has a stable population of one million and had its first CT scanner installed in 1977. This paper reports on the diagnostic use of CT over the 11-year period from 1977 to 1987. The radiation doses to patients from the three types of scanners deployed in the province are evaluated in terms of the effective dose equivalent, H_E, and the collective effective dose equivalent, S_E.

Computed tomography in Manitoba

The province of Manitoba has two major cities which provide, or plan to provide, a diagnostic CT imaging service. Winnipeg, which also serves the eastern part of the province, has a total urban population of 600 000, and is the home of two tertiary care teaching hospitals, the Health Sciences Centre (HSC) and St Boniface General Hospital (StBGH). The western city of Brandon, with a population of 40 000, is served by one major non-teaching hospital, the Brandon General Hospital (BGH).

The HSC had an EMI 5005 CT scanner installed in September 1977 and for the next 7 years this was the only CT scanner in the province. In November 1986, a Siemens DRH scanner was added and, because of the marked superiority of its imaging performance *vis-à-vis* the EMI 5005, it performed the overwhelming majority of subsequent CT scans at this centre. A GE 9800Q is due to be installed in mid-1988, and when operational will result in the EMI 5005 being taken out of active clinical service.

A GE 9800 was installed in StBGH in April 1984 and a second GE 9800Q was added in October 1987. The hospital plans to operate these two CT scanners for the foreseeable future.

A GE 9800Q is due to be installed in BGH in early 1988 and is planned to service approximately 120 000 people who live in the western region of the province.

The pattern of deployment of CT scanners in the province of Manitoba has been characterized by a limited number of units in the initial phase, which operated for very long hours and achieved a correspondingly high patient throughput. The EMI 5005 at the HSC and the GE 9800 at StBGH both operated long day shifts (7.00 a.m. to 12.00 p.m.) and often worked weekends. The daily patient throughput was occasionally in excess of 40. During the period from 1982 to 1986, the typical annual patient throughput on each machine was in excess of 7000, which is considerably higher than the typical values of 2500 patients per CT scanner per year reported in the USA (Terhorst, 1984). In 1986, the provincial government authorized the purchase of an additional three CT scanners, and by the middle of 1988, the province will be served by a total of five state-of-the-art machines, *i.e.* 1 per 200 000 population.

---

*Present address: Department of Radiology, St Joseph's Hospital, London, Ontario, Canada.

Method

The number of patients undergoing CT examinations is collected on a regular (monthly) basis by each hospital for administrative and billing purposes. In addition to the total number of monthly CT procedures per hospital, it is useful to obtain a more detailed breakdown of the types of CT examinations performed, since this will have an important impact on the resultant patient doses. Specific data at each CT centre is available on the relative frequency of head examinations. The non-head CT scans were divided into three general categories of "chest", "abdomen" and "pelvis". The relative frequency of each non-head procedure was obtained from a 3-monthly sample obtained from each of the three CT scanners during the period 1986–1987 and involved a total patient case load of approximately 5000. The relative frequency of "chest", "abdomen" and "pelvis" examinations for each model of CT scanner was taken to be valid for the total period of operation of each CT scanner examined in this study.

The radiation dose delivered in a CT examination is non-uniform both within an individual CT scan slice and along the patient axis. Detailed experimental investigations of the radiation dose distributions associated with head and body scans in an EMI 5005 scanner have previously been performed (Huda & Sandison, 1985). The most convenient way of expressing these dose distributions is to compute the value of the effective dose equivalent, H_E, which is considered to be the most appropriate parameter of the relative risk of a diagnostic study which utilizes ionizing radiation. Values of H_E for typical head, chest, abdominal and pelvic CT examinations on the EMI 5005 scanner have been explicitly calculated and the advantages, and limitations, of these data discussed in detail elsewhere (Huda & Sandison, 1986). To obtain corresponding H_E values on the GE 9800 and Siemens DRH scanners, advantage is taken of the fact that for any given type of scan, such as a head scan, the relative risk is directly proportional to the total energy imparted in the examination (Huda, 1984). The relative values of energy imparted for differing scanners can be obtained by using measured (or published) values of the computed tomography dose index (CTDI). The method of obtaining CTDI values specified in the literature (Shope et al, 1981) and its measurement is a USA regulatory requirement of the Food and Drug Administration (FDA, 1984). It is important to note that CTDIs will generally be different for head and body scans, and will also depend on a range of operating parameters such as kVp, slice thickness, mAs and X-ray beam filtration.

For a given scanner, it is possible to specify a parameter, $R_{\mathrm{kVp,H/B}}$ (Scanner) which is defined as

$$R_{\mathrm{kVp,\,H/B}}\,(\text{Scanner}) = \frac{\overline{\mathrm{CTDI}}}{T \times \mathrm{mAs}} \qquad (1)$$

where $\overline{\mathrm{CTDI}}$ is the mean of the four circumferential and one central CTDI value, expressed in mGy, T is the slice thickness in mm and is normally restricted to the (maximum) slice thickness used in routine CT scanning and mAs is the total milliamp-seconds used in the scan

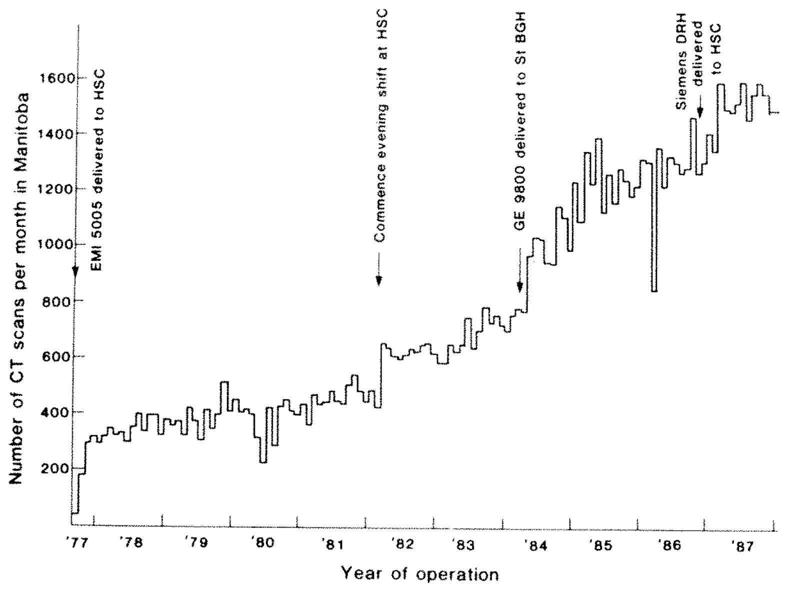

Figure 1. Total number of patients undergoing CT examinations each month in the province of Manitoba for the period September 1977 through to December 1987.

Table I. Percentage of head CT examinations

Year	HSC (EMI 5005 and/or Siemens DRH) (%)	StBGH (GE 9800) (%)
1977	99	—
1978	91	—
1979	91	—
1980	79	—
1981	75	—
1982	75	—
1983	75	—
1984	74	68
1985	68	63
1986	68	65
1987	61	66

Table III. Typical technique factors for CT examinations on the EMI 5005, GE 9800 and Siemens DRH

Scanner type	Examination	mAs	Number of slices
EMI 5005	Head	560	8
140 kVp; 13 mm slice thickness	Chest	560	12
	Abdomen	560	16
	Pelvis	560	10
GE 9800	Head	340	9
120 kVp; 10 mm slice thickness	Chest	340	20
	Abdomen	340	20
	Pelvis	340	16
Siemens DRH	Head	410	11
125 kVp; 8 mm slice thickness	Chest	210	25
	Abdomen	310	25
	Pelvis	410	20

procedure. The subscripts for the R parameter refer to the CT kVp setting and to the choice of head (H) or body (B) scan, and the bracket refers to the type of CT scanner, *i.e.* R(EMI), R(GE 9800) or R(DRH). For a given CT scanner X, the value of the H_E for the chosen CT examination can be obtained using the H_E values on an EMI scanner from the following expression:

$$H_E(\mathrm{X}) = H_E(\mathrm{EMI})\frac{R(\mathrm{X})}{R(\mathrm{EMI})} \times \frac{N(\mathrm{X})}{N(\mathrm{EMI})} \times \frac{T(\mathrm{X})}{T(\mathrm{EMI})} \times \frac{\mathrm{mAs(X)}}{\mathrm{mAs(EMI)}} \quad (2)$$

where the R(X) and R(EMI) values are obtained under the appropriate kVp and head (or body) conditions, N(X) and N(EMI) are the number of slices for this examination on scanners X and EMI, respectively, T(X) and T(EMI) the corresponding slice thicknesses and mAs(X) and mAs(EMI) are the corresponding milliamp-second values.

Results

The total number of patients undergoing CT examinations in Manitoba each month for the period 1977–1987 is shown in Fig. 1. Major events that affect patient throughput, such as the acquisition of a new CT scanner by the province or the commencement of evening shift work, are marked on the graph and show the expected discontinuities in patient throughput. The large drop in March 1986 occurred because of a prolonged breakdown of one of the two scanners which were in operation at that time.

Table I shows the total number of head CT examinations, expressed as a percentage of all CT examinations, at both the HSC and at StBGH for the period 1977–1987. Table II shows a breakdown of all CT examinations, for each CT scanner, into four separate categories: head and neck, chest, abdomen and pelvis. These data were obtained from a (continuous) 3-month sample of patient workload on each scanner and include data on the EMI scanner at the HSC both prior to the introduction of the Siemens DRH in November 1986 and after. These data show a very constant distribution, with head/neck examinations typically accounting for 65% of all CT scans, chest accounting for 5%, abdomen for 20% and pelvis for the remaining 10%. The EMI 5005 differed significantly from this general pattern in 1987 when its use was restricted to those (small number of) patients who did not require the relatively high-resolution performance available on the adjacent Siemens DRH. Table III shows a summary of the typical technique factors employed on each scanner for any given category of CT examination. All the subsequent radiation doses for specified scanners (and examination category) are based on the technique factors given in Table III. However, it is clearly straightforward to account for changes in H_E

Table II. Breakdown[a] of all CT examinations into differing body categories

Examination category	EMI 5005 1987 only (%)	EMI 5005 prior to Nov 1986 (%)	GE 9800 (1987) (%)	Siemens DRH (1987) (%)
Head and neck	66.6	66.5	64.5	64.2
Chest	0.7	4.1	4.6	4.8
Abdomen	31.2	22.1	19.1	21.2
Pelvis	1.5	7.3	11.8	9.8

[a] Based on analysis of a continuous 3-month sample in specified year.

Table IV. Values of R for the EMI 5005, GE 9800 and Siemens DRH

Scanner	kVp	$R(\mu\text{Gy mm}^{-1}\text{ mAs}^{-1})$	
		Head	Body
EMI 5005[a]	120	2.75	1.11
EMI 5005[a]	140	3.28	1.59
GE 9800[b]	80	5.68	2.01
GE 9800[b]	120	14.2	6.71
GE 9800[b]	140	19.9	9.39
Siemens DRH[c]	96	7.35	5.73
Siemens DRH[c]	125	14.2	11.1

[a] Slice thickness 13 mm. [b] Slice thickness 10 mm. [c] Slice thickness 8 mm.

values which will arise from changes in examination technique factors (mAs, slice thickness, number of slices, etc.) by use of Equation (2).

Values of R, expressed in μGy mm^{-1} mAs^{-1} for all three CT scanners, are shown in summary form in Table IV. The EMI 5005 data are based on direct measurements on the HSC scanner and have an estimated precision of $\sim 3\%$. Both the GE 9800 and Siemens DRH data in Table IV are based on the technical specification data published by both companies in 1987. These data were experimentally confirmed on both Winnipeg machines with typical differences between specification and experimental measurements being $< 10\%$. The resultant H_E values, for each type of CT scanner and examination type, are shown in Table V. These data were calculated using Equation (2), the EMI 5005 H_E values published by Huda and Sandison (1986) and the technique factors summarized in Table III.

Table VI shows the resultant annual values of the total number of patients undergoing CT examinations each year for the period 1977–1987. Also listed are the annual collective doses in Manitoba from CT, expressed in man-Sv, and the corresponding per capita dose, expressed in μSv. Table VII shows the average dose to a patient undergoing CT examinations as a function of year and as a function of CT scanner. The data for the years 1977–1987 were obtained by dividing the annual collective dose from CT by the total number of patients undergoing CT examinations. Scanner-specific average patient H_E were generated using the examination category breakdown for each scanner shown in Table II.

Table V. Average H_E values, in mSv, for the EMI 5005, GE 9800 and Siemens DRH

Scanner	Examination type			
	Head	Chest	Abdomen	Pelvis
EMI 5005	0.84	4.8	2.6	2.1
GE 9800	1.9	15.7	6.3	6.7
Siemens DRH	2.3	16.0	9.5	13.4

Table VI. Number of CT scans, collective dose and per capita dose in Manitoba

Year	Number of patients undergoing CT scans	Colletive dose[a] (man-Sv)
1977	845	0.7
1978	4158	4.2
1979	4670	4.7
1980	4645	5.8
1981	5534	7.3
1982	7208	9.5
1983	8188	10.8
1984	11 206	23.5
1985	14 802	40.8
1986	15 342	43.5
1987	18 189	81.0

[a] In the case of Manitoba which has a stable population of one million, this collective dose is also numerically equal to the per capita dose in μSv.

Discussion

The number of CT scanners per given population dose is not a very informative parameter since the utilization of a given CT scanner can vary considerably owing to local operational (and political) factors. It is therefore more appropriate to consider CT utilization in terms of patients scanned per year per 10^3 population base. The number of patients undergoing CT examinations in the province of Manitoba has increased by approximately a factor of 4 in the decade following the first full year of the availability of CT services in 1978. The general pattern of increase in patient throughput depicted in Table VI is similar to that of the province of Quebec (population 6.4 million) over the same time

Table VII. Average H_E values for patients undergoing CT scans in Manitoba

Year/Scanner	Average patient H_E (mSv)
1977	0.86
1978	1.0
1979	1.0
1980	1.3
1981	1.3
1982	1.3
1983	1.3
1984	2.1
1985	2.8
1986	2.8
1987	4.5
EMI 5005 (before Nov 1986)	1.4
EMI 5005 (1987)	1.5
GE 9800 (1987)	3.9
Siemens DRH	5.6

period. In quebec, the annual CT patient throughput was reported as being 1.4 per 10^3 in 1977–78, 5.1 per 10^3in 1980–81 and 9.9 per 10^3 in 1983–84 (Carrier, 1988, personal communicaton). In general, comprehensive data on CT usage are very limited, although UNSCEAR (1982) reported that CT usage in Sweden increased from 1.4 per 10^3 in 1977 to 3.0 per 10^3 in 1979 and that the value for Japan in 1979 was 0.68 per 10^3. Preliminary data from the UK suggest a value of 6.5 per 10^3 in 1983 (Wall et al, 1986), whereas in the same year in the USA, Evans and Mettler (1985) report a value of 22 per 10^3. Thus for CT utilization, Canadian provinces appear to fall between the higher values observed in the USA and the lower values found in Western Europe and Japan. This pattern of CT utilization in Canada relative to the rest of the world is very similar to the patterns observed for conventional radiological examinations (MacEwan et al, 1982; UNSCEAR, 1982) and for nuclear medicine (Huda & Gordon, 1988).

The data in Table I show that head CT examinations, as a percentage of all CT scans, have shown a steady decrease from 99% in 1977 to ~ 64% in 1987. This pattern is probably due to the increased use of CT for body scans given the availability of high-resolution CT scanners, with short scan times, such as the GE 9800 and Siemens DRH. The present percentage of head CT scans in Manitoba is comparable to the values reported in Sweden (1979) of 67%, in Japan (1979) of 65% (UNSCEAR, 1982) and in the USA (1983) of 63% (Evans & Mettler, 1985). For analysis of body scans, as summarized in Table II, three categories (chest, abdomen and pelvis) were chosen, as opposed to the simpler approach of specifying a "body" or a "spine" study. The rationale for the alternative approach developed in this study is that the resultant patient H_E values are primarily determined by the energy deposited from the CT X-ray beam and the specific region of this energy deposition. From this radiation dose perspective, thoracic spine examinations should clearly be classified together with other chest examinations. For similar reasons, neck studies were included with head examinations (see Table II). The data shown in Table II demonstrate a consistent pattern between scanners, with ~ 14% of all body scans involving the chest region, 57% the abdominal region and the remaining 28% the pelvis.

Specifying the radiation dose delivered to patients undergoing CT examinations has been widely acknowledged as being problematical (Mossman, 1982; UNSCEAR, 1982). By experimentally measuring the three-dimensional CT dose distributions in Rando phantoms, Huda and Sandison (1986) were able to generate H_E values for different CT examination categories for an EMI 5005 scanner. Unfortunately, this direct approach is clearly too time consuming to be used as a universal dosimetric tool. A convenient way of extending the usefulness of the (limited) EMI 5005 H_E data is to make use of the imparted energy concept, whilst limiting its application to a given body region such as the head or abdomen. For an EMI 5005 scanner, the measured H_E per unit energy imparted values were 10 μSv per mJ in the head, 27 μSv per mJ in the chest, 14 μSv per mJ in the abdomen and 17 μSv per mJ in the pelvis. These values can be compared directly with the value of 14 μSv per mJ for uniform whole body irradiation in a standard man of 70 kg (ICRP, 1975a, b). To obtain relative values of energy imparted from one scanner to another, the mean CTDI value is considered to be both appropriate and convenient, since values of this parameter are easily measured and readily available (*i.e.* are a regulatory requirement) for all CT machines currently sold in the USA. Using this energy imparted concept, and assuming the mean CTDI value is proportional to the energy imparted, involves a number of approximations which will affect the accuracy of the resultant H_E values. However, the errors associated with these approximations are considerably smaller than the uncertainties in the radiation risk estimates themselves, for which $H_E$values are ultimately used. It is possible to estimate the magnitude of the error associated when Equations (1) and (2) are used to generate CT H_E values by calculating the expected H_E for a head scan (EMI 5005) performed at 120 kVp. The predicted value, using the parameters given in Table III (except for change in kVp), is 0.70 mSv, whereas the experimentally determined value (Huda, 1984) was 0.61 mSv, a difference of only 13%. These limited data suggest that the overall accuracy of determining CT H_E using this method is likely to be in the range 10–20%. In this context, it is nevertheless worthwhile emphasizing that the relative H_E values for a given CT scanner (*e.g.* GE 9800) are likely to have a considerably higher precision.

The H_E values for the three scanner types and four examination categories (Tables V and VII) clearly show CT doses to be amongst the highest of all diagnostic procedures which utilize ionizing radiations (Shrimpton & Wall, 1986). It is of interest to note that these values are considerably higher than the 0.1 mSv values for H_E quoted in UNSCEAR (1982). Modern third-generation scanners (*i.e.* GE 9800 and Siemens DRH) typically result in patient (H_E) doses between two and three times those encountered in the older second-generation scanners (*i.e.* EMI 5005). An "average" CT scan is currently associated with a patient dose of ~ 4–5 mSv (Table VII). However, it is necessary to note that the H_E values of Table V are clearly dependent on the technique factors summarized in Table III, which were taken as being representative for current usage in Manitoba. Any individual scan which uses, for example, twice this mAs value and twice the number of slices will obviously result in an H_E value that is a factor of 4 higher than presented in Table V. The differences between the $H_E$values for the GE 9800 and Siemens DRH are of the order of 30%. This factor cannot be explained by any intrinsic difference between the two scanners, since both are very similar in basic design (third-generation systems) with the Siemens system employing more efficient solid state detectors as opposed to the Xenon gas detectors of the GE 9800. To perform a meaningful comparison, however, it is essential to include CT system performance parameters such as the spatial resolution, the noise and the low-contrast detectability. This important question of the choice of "optimal" CT scan parameters for any given patient examination is one that still remains to be tackled (McCrohan et al, 1987) and is likely to receive increasing attention from the medical physics community in the future. In these studies, the radiation dose to the patient will undoubtedly be expressed in terms of a single H_E parameter and thereby enable comparisons to be performed as technique factors such as kVp, mAs, filtration are systematically varied.

The annual per capita dose from CT in Manitoba has increased by a factor of 19.3 in the decade starting in 1978 and currently stands at a value of 81 μSv (1987). The principal reasons for this dramatic rise include more patients undergoing CT studies (×4.4), more radiation doses from modern scanners (×3.0) and an increase in the proportion of (higher dose) body studies (×1.5). This trend is likely to continue into the forseeable future, with the addition of two new scanners at the end of 1987 and replacement of the EMI 5005, scheduled for mid-1988. The projected number of CT scans in Manitoba, with five fully operational scanners, is estimated to be 28 000 per year. This would result in a per capita dose of about 120 μSv, assuming the constancy of the technique factors currently in use and the relative proportion of head scans. These data demonstrate that the CT per capita dose will be comparable to the nuclear medicine per capita dose in Manitoba where the latter has remained relatively constant over the period 1981–1985 at 120–130 μSv per year (Huda & Gordon, 1988). Thus CT is expected to join other high-dose and/or high-throughput procedures such as barium enemas, barium meals, IVPs and lumbar spines, which are the major contributors to the population dose from diagnostic medical X-ray examinations (MacEwan et al, 1982; Shrimpton et al, 1986).

Expressing CT doses in terms of H_E values is obviously useful for obtaining relative risk values in CT. Different scan procedures on a given machine can be readily intercompared, as can similar examination categories on different machines (see Table V). Furthermore, direct comparisons can also be made with any other modality which utilizes radiation, such as chest radiography (Shrimpton et al, 1986) and nuclear medicine scans (Johansson et al, 1984). In performing such comparisons, it is salutary to note that an implicit assumption is that the exposed population is an adult working population (ICRP, 1977). This use of the H_E in medicine is sometimes subject to criticism on the grounds that patients undergoing diagnosis frequently differ markedly in demographic terms from an adult working population. Although this is generally true, the criticism is based on the erroneous assumption that the ICRP (or other) radiation risks will be used directly to translate "radiation doses" into a corresponding "risk" or "detriment". Thus age and sex specific H_E have been suggested as being more appropriate for the quantification of medical radiation exposure. Adoption of this approach would invariably lead to confusion, since the exposed population obviously varies with hospital, X-ray clinic, province and country. Thus identical equipment, used with the same technique factors, could result in markedly differing patient (age/sex specific) H_E. A more rational approach is to evaluate relative risks using the standard (ICRP) adult population. To convert the relative risks into an absolute number (detriment), account would need to be taken of the age/sex distribution and general life expectancy of the exposed population. This would result in the generation of appropriate discount (or multiplier) factors for both the genetic and somatic components of the radiation risk expressed as an H_E, on the lines recently performed for CT (Huda & Sandison, 1985). Clearly these discount (or multiplier) factors for population H_E values will be population specific and vary from one area to another. The translation of population H_E values into detriment should be performed as a final step after collective H_E have been computed. This step will require careful attention to the demographic characteristics of the exposed population. However, this separate problem should not interfere with the major benefits to be gained from utilizing H_E for patients undergoing CT examinations as a relative risk parameter and used as such throughout this paper.

Acknowledgments

The authors gratefully acknowledge the assistance of J. Lundberg and D. Palahniuk in collecting the patient data, and Dr N. Donofrio in providing the body CT phantom.

References

Evans, R. G., 1984. Computed tomography—a controversy revisited. *New England Journal of Medicine, 310*, 1183–1184 (Editorial).

Evans, R. G. & Mettler, F. A., 1985. National CT use and radiation exposure: United States 1983. *American Journal of Roentgenology, 144*, 1077–1081.

FDA, 1984. *Diagnostic X-ray Systems and their Major Components. Amendments to Performance Standards, Final Rule.* Federal Register August 31, 1984, 34698–34714 (Washington DC)

Hounsfield, G. N., 1973. Computerized transverse axial scanning (tomography) Part I. Description of system. *British Journal of Radiology, 46*, 1016–1022.

Huda, W., 1984. Is energy imparted a good measure of the radiation risk associated with CT examinations? *Physics in Medicine and Biology, 29*, 1137–1142.

Huda, W. & Sandison, G. A., 1985. CT dosimetry and risk estimates. *Radiation Protection Dosimetry, 12*, 241–249.

Huda, W. & Sandison, G. A., 1986. The use of the effective dose equivalent, H_E as a risk parameter in computed tomography. *British Journal of Radiology, 59*, 1236–1238.

Huda, W. & Gordon, K., 1988. Nuclear Medicine staff and patient doses in Manitoba (1981–1985). *Health Physics*, in press.

ICRP, 1975a. *Report of the Task Group on Reference Man.* ICRP Publication 23 (Pergamon Press, Oxford).

ICRP, 1975b. *Recommendations of the International Commission on Radiological Protection.* ICRP Publication 26 (Pergamon Press, Oxford).

JOHANSSON, L., MATTSSON, S. & NOSSLIN, B., 1984. Effective dose equivalents from radiopharmaceuticals. *European Journal of Nuclear Medicine, 9,* 485–489.

MACEWAN, D. W., GELSKEY, D. E., LOCK, J. R., POPOFF, J. & SOURKES, A. M., 1982. 1979 diagnostic radiology services in the province of Manitoba. *Journal of the Canadian Association of Radiologists, 33,* 246–254.

MCCROHAN, J. L., PATTERSON, J. F., GAGNE, R. M. & GOLDSTEIN, H. A., 1987. Average radiation doses in a standard head examination for 250 CT systems. *Radiology, 163,* 263–268.

MOSSMAN, K. L., 1982. Analysis of risk in computed tomography and other diagnostic radiology procedures. *Computerized Radiology, 6,* 251–256 (Editorial).

SHOPE, T. B., GAGNE, R. M. & JOHNSON, G. C., 1981. A method for describing the doses delivered by transmission X-ray computed tomography. *Medical Physics, 8,* 488–495.

SHRIMPTON, P. C. & WALL, B. F., 1986. Doses to patients from medical radiological examinations in Great Britain. *Radiological Protection Bulletin, 77,* 10–14.

SHRIMPTON, P. C., WALL, B. F., JONES, D. G., FISHER, E. S., HILLIER, M. C. & KENDALL, G. M., 1986. *A National Survey of Doses to Patients Undergoing a Selection of Routine X-ray Examinations in English Hospitals* (National Radiological Protection Board, Chilton, Oxon).

TERHORST, L. L., 1984. National survey of computed tomography unit capacity: An update. *Radiology, 153,* 207–210.

UNSCEAR, 1982. *Ionizing Radiation: Sources and Biological Effects.* 1982 Report to the General Assembly (United Nations, New York).

WALL, B. F., HILLIER, M. C. & KENDALL, G. M., 1986. *An Update on the Frequency of Medical and Dental X-ray Examinations in Great Britain, 1983* (National Radiological Protection Board, Chilton, Oxon).

1989, *The British Journal of Radiology*, 62, 145–147

Radical radiotherapy for carcinoma of the vulva

By *N. J. Slevin, MRCP, FRCR and R. C. S Pointon, MA, FRCP, FRCR

Department of Radiotherapy and Oncology, Christie Hospital, Wilmslow Road, Withington, Manchester M20 9BX

(*Received May 1988 and in revised form July 1988*)

Abstract. A study was made of 58 patients with carcinoma of the vulva treated by radical radiotherapy between 1965 and 1982. The choice of treatment technique was influenced by site and extent of disease as well as the general condition of the patient. The crude 5-year survival was 26% (15/58). Local control was achieved in 40% of cases and was associated with tumour size of 4 cm or less. Radionecrosis occurred in nine cases but none of these required surgical intervention. Surgery remains the treatment of choice for carcinoma of the vulva. This report emphasizes that radical radiotherapy has a curative potential in those cases considered unsuitable for surgery and that the necrosis type and rate are within the limits of acceptable morbidity.

Carcinoma of the vulva is predominantly a disease of the elderly with 65% (Way, 1982) to 80% (Green, 1978) of cases occurring in patients over the age of 60, and up to 20% over the age of 80 (Green, 1978). In the overall context of gynaecological cancer, the incidence of carcinoma of the vulva in England and Wales is about one-fifth of that of carcinoma of the cervix or body of the uterus (Office of Population Censuses and Surveys, 1983). With rising longevity of the population the incidence is likely to increase.

The traditional surgical approach to treatment has been radical vulvectomy with wide excision of the primary cancer and contiguous pre-malignant tissue together with dissection of inguinal (Rutledge et al, 1970) and sometimes iliac nodes (Way, 1982). However, variation in the general condition of the patient and extent of disease lead in practice to considerable variation in surgical approach, from simple excision to total pelvic exenteration. From a large personal series reported by Way (1982), the crude 5-year survival from radical vulvectomy with node dissection was 63%; this procedure was undertaken in 60% of his patients. The histological nodal status was evidently an important prognostic factor with 5-year survival dropping from 84% for negative nodes to 52% for positive superficial nodes only and to 21% for deep nodal involvement.

If surgery is considered unsuitable for primary or locally recurrent disease, then radical radiotherapy may be used. Tod (1949) reported 71 non-metastatic cases, previously untreated because of general condition or site of disease, in which the 5-year survival was 33% using radium needles as the primary treatment. However, the vulva is considered a site susceptible to radionecrosis. Ellis (1949) cited a 32% necrosis rate in 103 patients, four-fifths of whom had received radiotherapy alone. Since these early reviews the role of radical radiotherapy as primary treatment has been seen as limited and is emphasized by the small numbers in recently reported series, with at most one case per year of study (Helgason et al, 1972; Pirtoli & Rottoli, 1982; Prempree & Amornmarn, 1983; Carlino et al, 1984; Fairey et al, 1984; Pao et al, 1988). We report 58 cases of carcinoma of the vulva treated by radical radiotherapy over an 18-year period at this centre and discuss its role as a primary treatment.

Patients and methods

There were 380 cases of carcinoma of the vulva registered at this centre between 1965 and 1982. A study was made of 58 patients accepted for radical radiotherapy during this 18-year period. Previous surgery was radical vulvectomy in 16, simple vulvectomy in 13, local excision in six and biopsy only in 23 cases. There was involvement of anus, urethra or vagina in 42 cases which were referred for radical radiotherapy in preference to major surgery. The remaining 16 cases were considered unfit for any surgery.

The median age of the patients at registration was 71.5 years (range 52–91 years) and 13 patients were aged 80 years or over. The tumour histology was squamous carcinoma in 54 cases, melanoma in two and single cases of Bartholin gland adenocarcinoma and basal cell carcinoma. Pre-invasive carcinoma and metastatic lesions from previously treated carcinoma of the cervix were excluded from the study. Radiotherapy used for patients with fixed nodal disease was given with palliative intent. Survival curves were calculated using the life table method and survival between groups compared using the log rank test (Peto et al, 1977). Survival was measured from the date of treatment. Peri-operative death occurred in three cases and these were included in the analysis. Of the 322 registered cases who did not receive radical radiotherapy, 74 were referred for surgery, 101 were not treated because of advanced disease and poor general condition and 137 had palliative radiotherapy, to primary and/or fixed nodes in 131 cases and to bone metastases in six cases; a further 10 cases received palliative chemotherapy.

---

*Author for correspondence.

Table I. Type of radical radiotherapy given in 58 cases

Single-plane needle implant	19
Two-plane needle implant	19
Gold seed implant	7
Single-plane implant and vaginal sorbo	1
Volume needle implant	1
External-beam therapy	11
Total	58

Radiotherapy considerations

Radical radiotherapy was considered for patients who were deemed unsuitable for surgery because of their general condition, the site or extent of disease. In view of the direct accessibility of the vulva and the propensity to necrosis from high-dose radiotherapy, interstitial techtechniques were generally considered preferable to external-beam treatments. The type of radiotherapy given is shown in Table I. The treatment was confined to patients without fixed nodal or distant metastatic disease. Block dissection was considered the treatment of choice for mobile inguinal lymphadenopathy; this was performed in one case.

The techniques of interstitial brachytherapy for carcinoma of the vulva have been described previously (Tod, 1949). The choice of technique was influenced by the extent of disease and the general condition of the patient. For the larger tumours, patients selected for external-beam treatment were generally younger (mean 64 years) than those who had a two-plane needle implant (mean 74 years). The desired dose was 5250–5500 cGy at 0.5 cm for single-plane needle and gold seed implants, 5250 cGy at 0.5 cm for the two-plane implant and 4500–5250 cGy in 15 or 16 daily fractions over 3 weeks for the external-beam treatments. The external-beam radiotherapy was given as a megavoltage rotation or fixed three-field technique, with field dimensions usually 7–10 cm. Radionecrosis was arbitrarily divided into minor and major, the latter requiring surgical intervention.

Results

The crude 5-year survival was 26% (15/58) with a median survival of 19 months. In 10 of the 15 long-term survivors the tumour had involved anus, vagina or urethra. The vital status of the patients at 5 years is shown in Table II. This shows that local control was achieved in 40% of cases (23/58). Local control was associated with tumour size of 4 cm or less. The 5-year survival for the different techniques was 7/19 for single plane, 2/7 for gold seed, 1/19 for two-plane implants and 4/11 for external-beam therapy. The patient treated by single-plane implant with sorbo was a further long-term survivor. Survival for newly diagnosed cases was 39% (9/23) compared with 17% (6/35) for post-operative recurrences. Ten of the 15 survivors were below the median age of 71.5 years.

Table II. Outcome of 58 cases 5 years after treatment by radical radiotherapy

Alive and well	14
Alive, recurrent disease	1
Dead, intercurrent	3
Dead with mets, primary well	6
Dead, primary residual/recurrent	34
Total	58

Minor necrosis occurred in nine cases. In eight of these cases this was noted 3–12 months post-radiotherapy whilst the other necrosis occurred 8 years after treatment. The necrosis healed within 1 year in seven cases. Urethral stenosis which required dilatation was seen in the case treated with single-plane implant and vaginal sorbo. Of the 15 patients who survived 5 years, seven developed minor necrosis. No major radionecrosis was seen. There were three peri-operative deaths, due to pulmonary emboli in two cases and acute hepatic failure in the third. The intercurrent deaths were at 1½, 3½ and 4½ years due to cerebrovascular accidents in two and pneumonia in the other; the patients died at ages 81, 84 and 93 years. The one patient who underwent subsequent block dissection of nodes died 18 months after radiotherapy.

Discussion

The crude 5-year survival was 26% (15/58). This compares unfavourably with the results from radical vulvectomy and node dissection of 60–65% (Green, 1982; Way, 1982). However, despite being a group selected for radical treatment, the majority of the 58 cases had poor prognostic features. Involvement of the anus, vagina or urethra is an adverse prognostic factor (UICC, 1982) and this was present in 72% (42/58) of the patients. Cases with post-operative recurrent disease appear to have a more aggressive course with a 5-year survival of 17% compared with 39% for newly diagnosed cases; recurrent cases accounted for 60% (35/58) of the series.

Local control of vulval disease was achieved in 40% of cases (23/58) and was associated with tumour size of 4 cm or less. It has been reported that recurrent disease of 5 cm or more is difficult to control with either surgery or radiotherapy (Buchler et al, 1979; Prempree & Amornmarn, 1983). For larger tumours treated by implant it is difficult to achieve precise geometric configuration of sources. Attempts have been made to increase accuracy using an afterloaded system with a perineal template (Branson et al, 1985) but it has not yet been demonstrated that the poor prognosis associated with these larger tumours can be improved.

Minor necrosis occurred in nine cases, within 12 months of treatment in eight of them. This necrosis rate is within the limits of acceptable morbidity. However, it should be noted that within 12 months of treatment 38% (22/58) of the patients had already died. It is perhaps surprising that eight of the nine necroses were in patients below the median age of 71.5 years. One reason for this could be the continuation of sexual activity in the younger patients.

The results from external-beam therapy (4/11) were better than for two-plane implants (1/19). However, the patients selected for external-beam therapy were generally younger than those treated by implant. Nevertheless with four of the 11 patients disease-free at 5 years, it seems that the use of external-beam therapy should not be too restricted.

The vulva is considered to have a poor tolerance to high-dose radiotherapy (Ellis, 1949). This is presumably because of its lack of collateral vascularity, the tendency to atrophy in the elderly, and its occlusive nature with moist surfaces prone to infection. However, none of the 58 treated cases developed major necrosis requiring surgical intervention.

Seven of the long-term survivors developed minor necrosis. This suggests that carcinoma of the vulva had a low therapeutic ratio. This is not due to radioresistance of the tumour, but rather to the limited normal tissue tolerance of the vulva to radiation.

Surgery remains the treatment of choice for carcinoma of the vulva, with its potential for wide margins of local tumour clearance as well as inguinal lymphadenectomy. This report shows that radiotherapy as primary treatment has a curative role, with 26% (15/58) of the patients alive at 5 years, with the advantage over surgery of preservation of sphincter function in some cases.

References

BRANSON, A. N., DUNN, P., KAM, K. C. & LAMBERT, H. E., 1985. A device for interstitial therapy of low pelvic tumours—the Hammersmith perineal hedgehog. *British Journal of Radiology, 58,* 537–542.

BUCHLER, D. A., KLINE, J. C., TUNCA, J. C. & CARR, W. F., 1979. Treatment of recurrent carcinoma of the vulva. *Gynecologic Oncology, 8,* 180–184.

CARLINO, G., PARISI, S., MONTEMAGGI, P. & PASTORE, G., 1984. Interstitial radiotherapy with ^{192}Ir in vulvar cancer. *European Journal of Gynaecological Oncology, 3,* 183–185.

ELLIS, F., 1949. Cancer of the vulva treated by radiation— an analysis of 127 cases. *British Journal of Radiology, 22,* 513–520.

FAIREY, R. N., MACKAY, P. A., BENEDET, J. L., BOYES, D. A. & TURKO, M., 1984. Radiation treatment of carcinoma of the vulva, 1950–1980. *American Journal of Obstetrics and Gynecology, 151,* 591–597.

GREEN, T. H., 1978. Carcinoma of the vulva—a reassessment. *Obstetrics and Gynecology, 52,* 462–469.

HELGASON, N. M., HASS, A. C. & LATOURETTE, H. B., 1972. Radiation therapy in carcinoma of the vulva. *Cancer, 30,* 997–1000.

OFFICE OF POPULATION CENSUSES AND SURVEYS, 1983. *Cancer Statistics Registrations.* England and Wales Series, MBI, No. 15, (HMSO, London).

PAO, W. M., PEREZ, C. A., KUSKE, R. R., SOMMERS, G. M., CAMEL, H. M. & GALAKATOS, A. E., 1988. Radiation therapy and conservative surgery for primary and recurrent carcinoma of the vulva: Report of 40 patients and a review of the literature. *International Journal of Radiation Oncology, Biology, Physics, 14,* 1123–1132.

PETO, R., PIKE, M. C., ARMITAGE, P., BRESLOW, N. E., COX, D. R., HOWARD, S. V., MANTEL, N., MCPHERSON, K., PETO, J. & SMITH, P. G., 1977. Design and analysis of randomized clinical trials, requiring prolonged observation of each patient. *British Journal of Cancer, 35,* 1–39.

PIRTOLI, L. & ROTTOLI, M. L., 1982. Results of radiation therapy for vulvar carcinoma. *Acta Radiologica Oncology, 21,* 45–48.

PREMPREE, T. & AMORNMARN, R., 1983. Radiation treatment of recurrent carcinoma of the vulva. *Cancer, 54,* 1943–1949.

RUTLEDGE, F., SMITH, J. P. & FRANKLIN, E. W., 1970. Carcinoma of the vulva. *American Journal of Obstetrics and Gynecology, 106,* 1117–1130.

TOD, M. C., 1949. Radium implantation treatment of carcinoma vulva. *British Journal of Radiology, 22,* 508–512.

UICC, TNM-ATLAS 1982. *Illustrated Guide to the Classification of Malignant Tumours,* ed. by B. Spiessl, O. Scheibe & G. Wagner (Springer-Verlag, Berlin), pp. 126–132.

WAY, S., 1982. In *Malignant Disease of the Vulva* (Churchill Livingstone, Edinburgh), pp. 6–33.

1989, *The British Journal of Radiology*, 62, 148–153

Possibility of retrospective dosimetry for persons accidentally exposed to ionizing radiation using electron spin resonance of sugar and mother-of-pearl

By Toshiyuki Nakajima

Division of Physics, National Institute of Radiological Sciences, Anagawa-4-chome, Chiba-shi 260, Japan

(*Received April 1988 and in revised form September 1988*)

Abstract. An electron spin resonance (ESR) dosemeter was used to measure ESR absorption spectra of sugar and shell buttons made of mother-of-pearl, for the purpose of evaluating the external dose to exposed inhibitants in the vicinity of a radiation accident. The ESR absorption intensity of sugar was proportional to dose in the range from about 30 mGy to $6x10^4$ Gy. The lifetime of the free radical created in both sugar and shell buttons by radiation was stable for at least 6 months after irradiation. If sugar and shell goods left in or around houses since the occurrence of the Chernobyl reactor and the Brazilian accidents were obtained, it would be possible to estimate from them the integrated external dose to exposed people.

Much effort has been devoted to studying both the effects of radiation accidents on the health of those exposed to radiation and the medical treatment of such people. An important parameter is the dose absorbed by those exposed, and this should be evaluated. However, methods for evaluating the dose absorbed by those accidentally exposed have not been established. For example, in the case of the evaluation of the γ-ray dose from the atomic bombs dropped on Hiroshima and Nagasaki, thermoluminescence from the roof tiles was used to evaluate the dose to people. However, roof tiles lack purity and uniformity in providing a sample of thermoluminescence dosemeter phosphor. Therefore, the reliability of the evaluated γ-ray dose is suspect. As a result, a reassessment of the atomic bomb radiation doses was recently carried out (Radiation Effects Research Foundation (RERF), 1983). Furthermore, such material is not distributed worldwide and so cannot be used for evaluating the absorbed dose to people in every country.

There is, however, the potential for accidental exposure of people worldwide as shown by the Chernobyl reactor accident and the incident which occurred in Brazil in 1987. Therefore, there is clearly a need for a dose estimation method and suitable substances that can be used worldwide.

Recently, an electron spin resonance (ESR) dosemeter using plastic (Nakajima & Watanabe, 1974; Nakajima, 1987) and alanine (Regulla & Deffner, 1982) has been studied. This method has some advantages in that common materials can be analysed, and it has good physical properties such as reliability, sensitivity and absorbed dose linearity.

We report here the application of this method to people accidentally exposed to radiation using the radiation properties of sugar and shell buttons made of mother-of-pearl (hereinafter referred to as "shell buttons"). Furthermore, from the ESR absorption intensity of such substances, the possibility of estimating the external dose to those exposed at the Chernobyl reactor accident will be discussed.

Experimental procedure

Free radicals and lattice defects in many natural and artificial goods are created by radiation, and the number of such free radicals is easily evaluated by ESR.

If suitable substances are available, they can be used to obtain an integrated external dose in a period from the date of the accident to the date of the ESR measurement. They should have the following properties.

1. Personal belongings or household goods including foods and seasoning that are common throughout the world.
2. Have ease of sample preparation without creating free radicals.
3. Have a simple ESR spectrum.
4. Have minimum detectable dose of 0.1 Gy or less for medical treatment.
5. The ESR spectrum should be linear in the range 0.1–30 Gy.
6. The free radicals should have a long lifetime.
7. There should be no background ESR signal from free radicals before irradiation.

Background ESR absorption and the decay of free radicals in some common substances collected from both inside and outside the house were studied. The decay of free radicals is shown in Table I. It was found that saccharides and shell buttons satisfy many of the above properties. On the other hand, many other substances did not satisfy many of the requirements, in particular, the decay of the free radicals and the background ESR signal. Sugar and other saccharides in both powder and crystalline forms, an amorphous body such as candy, and broken shell buttons were, therefore, used as samples for the ESR absorption measurements.

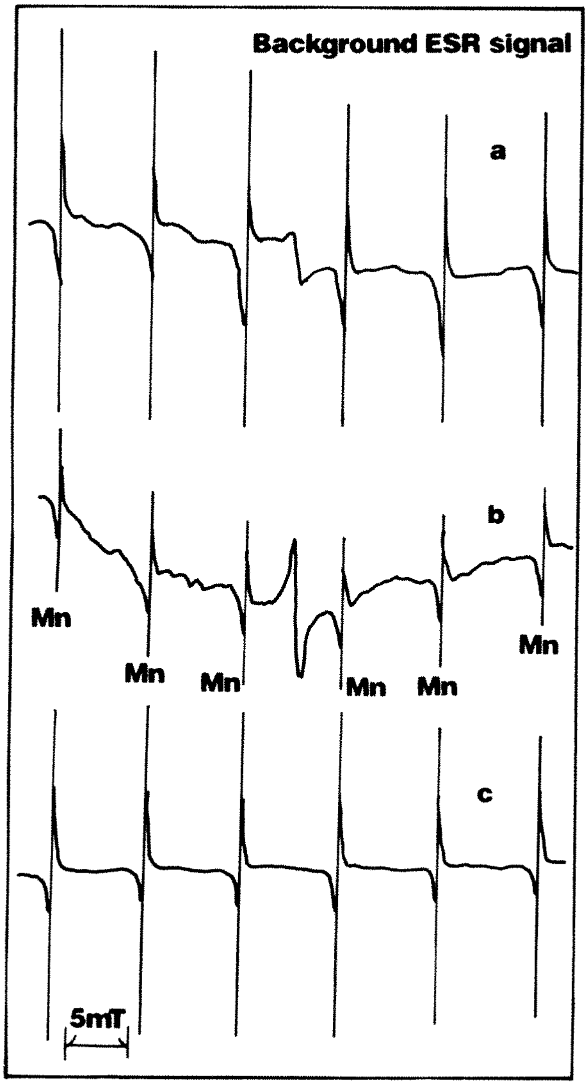

Figure 1. Background ESR spectra of (a) broken and (b) powdered shell buttons and (c) granulated sugar.

Table I. Decay of free radicals in some materials stored at room temperature 24 h after irradiation

Material	Decay coefficient
Old newspaper	0.52
Paper	0.52
Wood chips	0.59
Japan cedar	0.56
Wood in pencil	0.53
Nail	0.50
Salt	0.46
Hair	1.07[a]
Ivory	1.05
Sugar	1.04
Shell button (*Pinctada maxima* or *Pinctada margaritifera*)	1.00
Shell (*Meretrix meretrix lusori*)	0.97
Shell (*Venerupis japonica*)	0.99
Egg shell	0.86
Amber	0.92

[a] Strong background ESR absorption was observed.

The substances were put into a quartz sample tube of 3.5 mm inside diameter in order to obtain reproducible ESR measurements. Prior to irradiation of the sample, the ESR absorption spectra of the sample and quartz tube were observed. The ESR absorption intensity due to free radicals could hardly be obtained from sugar and other saccharides before irradiation. On the other hand, an ESR intensity was observed from the broken and powdered shell buttons before irradiation and that from the powdered sample was larger than from the broken one, as shown in Fig. 1. Thus, in the case of shell buttons, broken ones were used as the sample.

In the case of ^{60}Co γ-ray irradiation, the samples were irradiated at room temperature in air with the main beam from a ^{60}Co teletherapy unit, having been covered with a plate of tissue-equivalent material of 5 mm thickness. In the case of X-ray irradiation, the samples were wrapped in paper and irradiated at room temperature in air with the main X-ray beam from an X-ray machine. The effective energy of the X rays was determined from the half-value thickness. The dose was measured with a calibrated ionization chamber and samples were irradiated with doses from about 40 mGy to 30 Gy.

Electron spin resonance spectrometers were operated at room temperature with X band (Nakajima, 1987), *i.e.* about 9.5 MHz of the microwave frequency for the ESR resonance, with a microwave power level from 2 to 8 mW with a 100 kHz modulation unit, and the ESR absorption spectra of the free radicals were observed with 1.0 mT modulation width, a 25 mT magnetic field and 16 min canning period.

The samples in the fused quartz tube were left to reproduce the axial readout of the samples inside the microwave resonance cavity. The ESR measurements of all the samples were made at room temperature with a Mn^{2+} standard sample in the same resonance cavity. The mean intensity of six absorption peaks in the ESR spectra of the Mn^{2+} standard sample in each ESR measurement was used as a reference value. The ESR absorption intensity of the free radicals in the samples was determined relative to the reference value.

Result and discussion

Figures 2a and 2b show the typical ESR spectra of crushed shell buttons and granulated sugar irradiated with ^{60}Co γ rays with the Mn^{2+} standard sample.

As shown in Figs. 2a and 2b, the ESR absorption peaks from the irradiated samples appeared between the third and fourth peaks of the Mn^{2+} standard sample. The intensity of the ESR absorption edges fixed at the start of

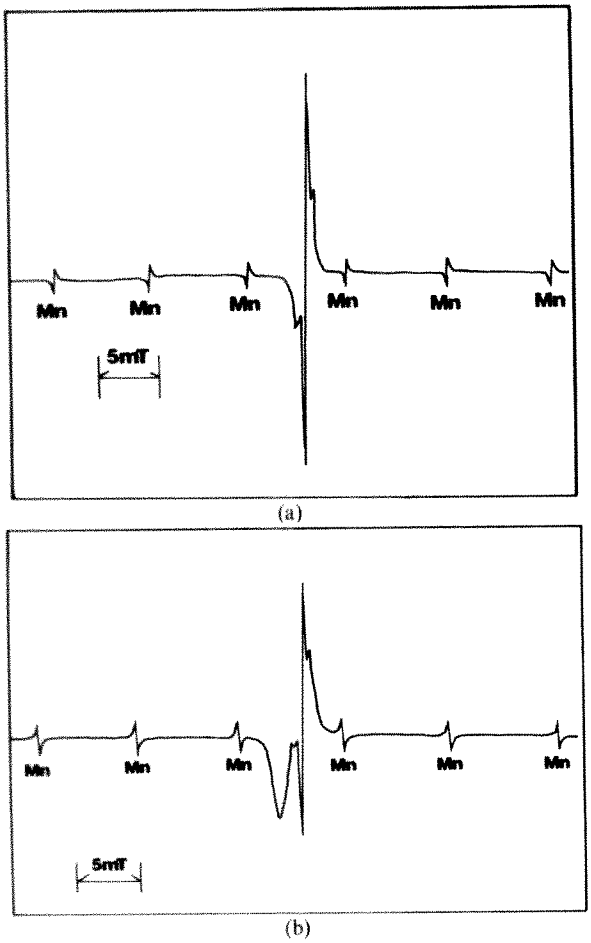

(a)

(b)

Figure 2. (a) The ESR spectrum of shell button irradiated at room temperature with about 80 Gy. Modulation width is 0.63 mT. (b) The ESR spectrum of granulated sugar irradiated at room temperature with about 27 Gy. Modulation width is 1 mT.

the experiments was used for dose evaluation throughout the experiment and was determined relative to the reference value of the Mn^{2+} standard sample.

Figure 3 shows the ESR spectra of oyster shell without irradiation. Some kinds of shell, such as oyster and scallop shells, reveal the ESR absorption spectra of manganese ions in the sample as background ESR absorption. Thus, such shells are difficult to use as dosimetric material because it is not easy to separate the ESR signal of the sample irradiated with a low dose of about 2 Gy or less from the background signal, and hence evaluate the dose.

The main purpose of this work is to ascertain the feasibility of the ESR method for emergency dosimetry. The dose linearity, the sensitivity and the fading behaviour of the substance chosen to serve as a monitor and dosemeter will be discussed.

Figures 4a, 4b and 4c show linearity of the ESR response of 600 mg of amorphous or granulated sugar and broken shell buttons relative to the absorbed dose. As shown in Fig. 4a, in the case of sugar, dose proportionality was obtained in the dose range 0.038–2.5 Gy and, indeed, up to about 6×10^4 Gy, as shown in Fig. 4b. Furthermore, the ESR absorption peaks due to free radicals were clearly observed from 600 mg of granulated sugar after 5 mGy using the RE-2X type ESR equipment with a data treatment system. The ability to detect the effect of such a small dose and the linearity of response with dose for sugar may make it satisfactory as a dosemeter for studying the health effects on, and the medical treatment of, exposed people. Sugar can be used as a highly sensitive material for an ESR dosemeter. The purity of the sugar could affect the number or density of free radicals created by radiation. However, their yield was essentially identical in all sugars, regardless of where they were produced, so that the ESR sensitivity (ESR response per unit dose) is scarcely affected by the type of sugar used.

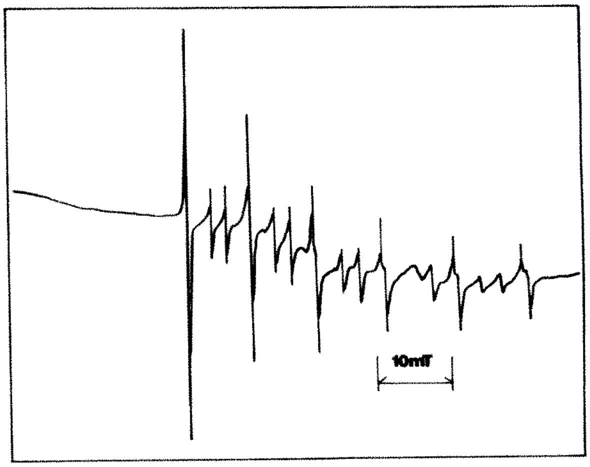

Figure 3. The ESR spectrum of oyster shell before irradiation.

On the other hand, many kinds of saccharide can be found, such as fructose, dextrose, maltose and lactose. For the purposes of comparison, the ESR sensitivity of these substances relative to that of amorphous sugar (sucrose) was obtained and is given in Table II. The relative sensitivity of the amorphous saccharide was nearly the same as sugar, but, in the case of the powder or crystalline form, the sensitivity was about half that of amorphous sugar. Such saccharides in both powder and amorphous form could be used as an emergency individual monitor for people.

Figure 4c shows the dose linearity of the ESR absorption intensity of the broken shell buttons. The sensitivity of shell buttons is lower than that of sugar and the minimum detectable dose was higher because of high ESR absorption intensity of the background. However, the minimum detectable dose of the shell buttons was about 0.5 Gy.

According to data on the ESR absorption of a plastic button exposed in Kiev, it was reported that the exact dose evaluation was not carried out because of a large

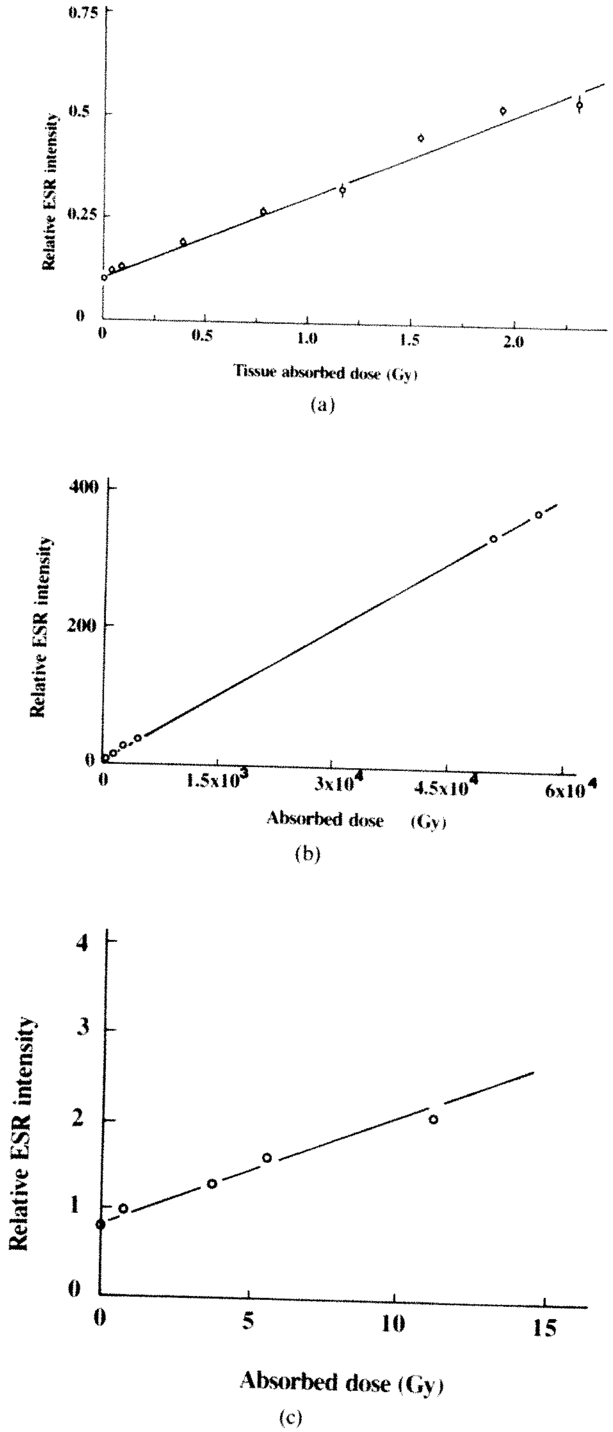

Figure 4. (a) The proportionality of ESR response of irradiated amorphous sugar to absorbed dose. Weight of the sample sugar was 600 mg. (b) The proportionality of ESR response of irradiated granulated sugar to absorbed dose. (c) The proportionality of ESR response of irradiated shell button to absorbed dose. Weight of the sample was 600 mg. The shell buttons were cut before irradiation.

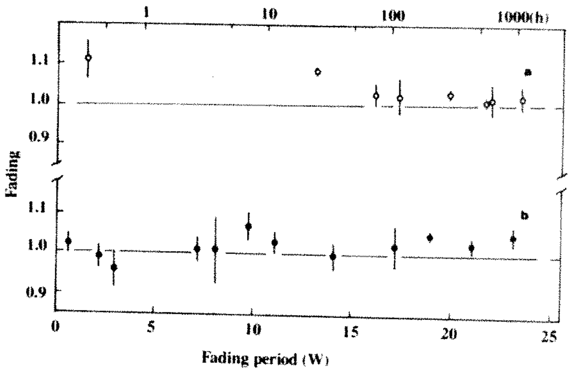

Figure 5. The fading of free radicals in (a) shell buttons and (b) sugar stored at room temperature after irradiation. "W" stands for weeks.

decreasing ratio of free radicals (Nakajima, 1987). Therefore, one of the most important dosimetric properties of a substance to be used as an emergency dosemeter is the decay time of the free radical or ESR response, as well as high sensitivity, because the dose absorbed by the exposed persons is measured and evaluated some days after the accident.

The decay is defined as a ratio $I(t)/I_0$ between the initial I_0 and residual $I(t)$ ESR responses of the same samples stored for a period t until measurement after irradiation. The fading of the ESR response of irradiated granulated sugar and shell stored at room temperature after irradiation is shown in Fig. 5. The result reveals that the ESR absorption intensity, especially of sugar, scarcely decreases during the 6-month period following irradiation.

Figure 6 shows the effect of storage temperature of the irradiated sugar and shell buttons on the ESR response. The vertical axis is the ratio between the ESR response of

Table II. Comparison of the relative ESR absorption intensity of some saccharides and amorphous sugar. The mean value and standard deviation were obtained from five samples

Substance	Z_{eff}	Form	Relative ESR intensity
Sucrose	6.92	Amorphous	1.000 ± 0.074
		Small crystal	0.453 ± 0.036
		Amorphous	1.187 ± 0.096
Fructose	6.95	Amorphous	1.123 ± 0.111
		Small crystal	0.571 ± 0.061
		Amorphous	1.296 ± 0.264
Dextrose	6.95	Amorphous	0.975 ± 0.096
		Powder	0.433 ± 0.038
		Amorphous	1.532 ± 0.405
Maltose	6.92	Amorphous	1.098 ± 0.008
		Powder	0.615 ± 0.008
		Amorphous	1.281 ± 0.126
Lactose	6.92	Powder	0.502 ± 0.004

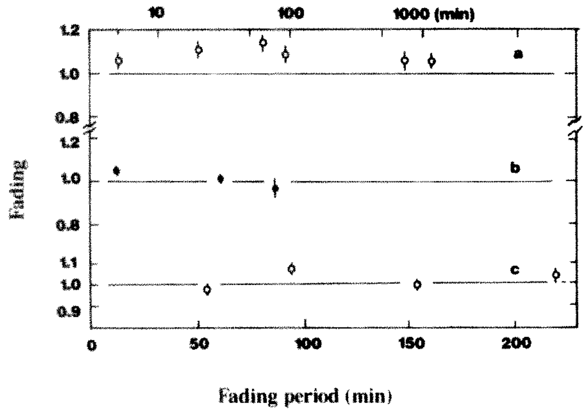

Figure 6. The thermal fading of free radicals in granulated sugar and shell buttons after irradiation at room temperature. Curves (a) and (b) are the fading of the irradiated sugar stored at 55 and 100°C, respectively, and curve (c) is that of the irradiated shell button stored at 100°C.

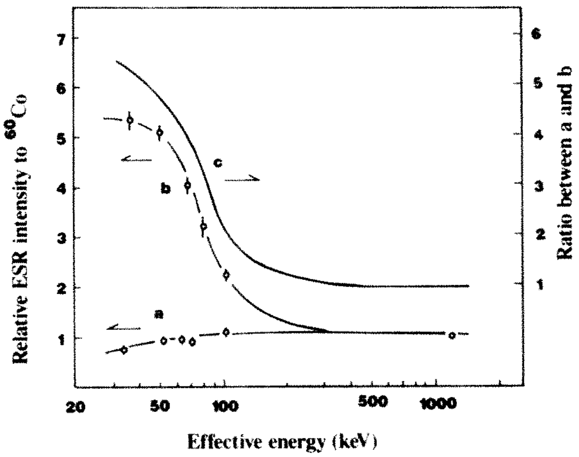

Figure 7. Energy dependence of ESR sensitivity of (a) sugar and (b) shell buttons and (c) the response ratio between them.

sugar and shell buttons measured immediately after irradiation at room temperature to that measured after storing for various periods at 55 and 100°C.

As shown in curve (a) of Fig. 6, at 55°C the ESR response of the sugar sample hardly decreased with storage period until about 1000 min. On the other hand, as can be seen in curves (b) and (c) of Fig. 6, when the irradiated sugar and shell buttons were stored at 100°C for about 80 and 220 min after irradiation at room temperature, they maintained their initial ESR response. These results on the thermal decay reveal that the number of free radicals or lattice defects created in the irradiated sugar or shell buttons scarcely changes over several years in the natural environment, even when the atmospheric temperature varies. Thus sugar and shell buttons can be used for radiation dosimetry such as personnel monitoring for accidental radiation and medical use.

It has been reported that, in the case of thermoluminescent dosimetry, the response or the sensitivity ratio between substances with different effective atomic numbers is a function of radiation energy (Gorbics & Attix, 1968). If both sugar and shell buttons or other shell goods are exposed at the same place at the same time, the radiation energy at the place will be estimated from the ratio between them and will facilitate the medical treatment. Therefore, if both substances are gathered from houses around or near the site of the accident, the radiation energy as well as the absorbed dose can be estimated from the ESR absorption intensities.

Figure 7 shows the energy dependence of the ESR signal of both the sugar and shell buttons in the energy range from 35 keV to 1.25 MeV. The ESR response was normalized to one for ^{60}Co γ rays.

As can be seen in Fig. 7, shell buttons show a dependence on the energy of the ionizing radiation, and the response for 35 keV was about 5.5 times that for ^{60}Co γ rays. This energy dependence is similar to that of $CaSO_4$ thermoluminescent dosemeter phosphors. If it is assumed that the shell material consists of $CaCO_3$, the effective atomic number of shell, calculated using the mass attenuation coefficient of Hine and Brownell (1956), is about 15, which is nearly the same as that of $CaSO_4$. This may explain the large energy dependence of shell buttons. On the other hand, sugar scarcely shows any dependence on the energy of the ionizing radiation in the range from 35 keV to 1.25 MeV, and the response for 35 keV was about 0.9 times that for 1.25 MeV. These results reveal that the ESR response of the irradiated material is dependent on the effective atomic number. If both the sugar and shell goods such as buttons and broochs, with differing effective atomic numbers, are collected from the same place, the effective energy of the radiation can be estimated from the ESR response ratio between these materials. Such information could contribute to the medical treatment of exposed persons.

Conclusions

The results presented in this paper indicate that it should be relatively simple to detect a dose of about 0.04 Gy using this ESR method and suitable substances. If saccharides such as sugar, sugarplum (*i.e.* candy or sweets), dextrose, fructose and maltose, or shell goods left in houses around or near the site of an accident, such as the Chernobyl reactor plant, are used as a dosimetric sample, the external dose at the accident can be estimated long after the accident. This evaluation of the external dose could contribute to the estimation of the effect on the health of people exposed even when the exposure is at a low dose-rate.

Acknowledgments

The author thanks Mrs Toshiko Ootuki for assistance and the Science and Technology Agency of the Japanese Government and the Association of Japanese Radiation Effect for support.

References

Gorbics, S. G. & Attix, F. H., 1968. LiF and CaF_2:Mn thermoluminescent dosemeters in tandem. *International Journal of Applied Radiation and Isotopes, 19,* 81–89.

Hine, G. J. & Brownell, G. L., 1956. *Radiation Dosimetry* (Academic Press Inc., Englewood Cliffs, NJ), chap. 1.

Nakajima, T. & Watanabe, S., 1974. New method for estimating γ-ray exposure sustained in radiation accidents. Possibilities of using organic substances as monitor. *Journal of Nuclear Science and Technology, 11,* 575–582.

Nakajima, T., 1982. The use of organic substances as emergency dosemeters. *International Journal of Applied Radiation and Isotopes, 33,* 1077–1084.

——1987. External dose to a Japanese tourist from the Chernobyl reactor accident. *Health Physics, 53,* 405–407.

Regulla, D. F. & Deffner, U., 1982. Dosimetry by ESR spectroscopy of alanine. *International Journal of Applied Radiation and Isotopes, 33,* 1101–1114.

RERF, 1983. *US–Japan Joint Workshop for Reassessment of Atomic Bomb Radiation Dosimetry in Hiroshima and Nagasaki* (Radiation Effects Research Foundation).

1989, *The British Journal of Radiology*, 62, 154–157

Interstitial iridium-192 implantation for malignant brain tumours

Part I: Techniques of dosimetry planning

By Andrew Wu, PhD, Mison Chun, MD, *D. Kasdon, MD, †D. Heros, MD, P. McKeough, MD and H. Chang, MD

Departments of Radiation Oncology, *Neurosurgery and †Neurology, New England Medical Center Hospital, Tufts University School of Medicine, Boston, Massachusetts 02111, USA

(Received May 1988)

Abstract. Interstitial implants for brain tumours with removable iridium-192 radioactive seeds have been performed using a Brown–Roberts–Wells stereotactic frame. A simple and accurate computed-tomography-guided dosimetry pre-planning technique and procedure prior to implant have been developed and are discussed.

Over a number of years, it has been recognized that aggressive de-bulking surgery followed by external-beam radiation treatment provides the best prognosis in terms of survival for patients with brain tumours (Scanlon & Taylor, 1979; Walker, 1979). Almost a decade ago, it was reported that increasing the radiation dose up to 70 Gy resulted in an improvement in survival (Salazar et al, 1979). However, radiation toxicity to normal surrounding brain parenchyma continues to be a limiting factor. Interstitial brachytherapy may be a logical choice (Gutin et al, 1984; Sewchand et al, 1984; Rossman et al, 1985; Salcman et al, 1986) because it restricts a much higher dose to the tumour site.

The potential success of such implants is primarily dependent on accurate knowledge of tumour volume and precise placement of catheters carrying radioactive seeds. In recent years, various stereotactic frames guided with computed tomographic (CT) scanners, such as the Leksell frame (Leksell, 1951), Marchosky–Moran system (Marchosky & Moran, 1983), and the Brown–Roberts–Wells (BRW) frame (Heilbrun et al, 1983), have been developed to help place a single or multiple catheter(s) carrying radioactive sources into brain tumours with remarkable accuracy.

In terms of target volume determination, while some investigators have tried to use high-power computers to re-construct three-dimensional tumour volumes for such implant procedures (Lansky et al, 1983), many procedures still oversimplify by assuming the brain tumour to be ellipsoid (Weaver et al, 1986). Also, while some have designed a template allowing the catheters to be inserted only parallel to the CT scan plane (Abrath et al, 1986), others have used the BRW stereotactic frame which allows catheters to be inserted from any direction for brain tumours (Mackay et al, 1982; Heilbrun et al, 1983).

In 1983, the neuro-oncology group at New England Medical Center developed a protocol using the CT-guided BRW stereotactic system for interstitial implants, as part of the treatment of malignant brain tumours. Patients with recurrent, primary or metastatic brain tumours of 5 cm or less in diameter were eligible. Iridium-192 radioactive seeds were used to deliver a dose rate of 80–100 cGy h^{-1} up to 100 Gy in total to the contrast-enhancing margin of the tumour. The advantages of the sharp dose drop-off because of the lower energy of iodine-125 as used by other investigators (Gutin et al, 1984; Eddy et al, 1986) is compromised by the expense of these high-activity sources.

In this paper, a simple but accurate CT-guided dosimetry planning technique and procedure to determine the target volume at the neurosurgeon's viewpoint and to place catheters with removable ^{192}Ir seeds is described.

Materials and methods

About a week prior to the scheduled implant procedure, the position must be determined of an entry point or burr hole on the patient's scalp, through which a catheter will be inserted. The path of the catheters to reach the tumour must avoid major vessels, motor strip, and midline ventricles of the brain. A small dot of radio-opaque barium is placed to mark the position so that it will show up on CT scans. A contrast-enhanced CT scan is performed on a Siemen's DR3 CT scanner with 4 mm slices from the base of skull to the vertex to cover the entire tumour volume as well as the barium dot.

The co-ordinates of the barium dot and a reference target in the tumour must be determined next. First, the scan with the barium dot indicating the entry point of the first catheter is identified. The cursor of the CT scanner is used to obtain the pixel position of the X and Y co-ordinates of the entry point. Secondly, a representative scan of the tumour is selected to provide its centre. Usually, it is the one with the largest dimension. Using this reference scan, the cursor is again used to determine the X and Y co-ordinates of the reference target at the centre of the tumour. It should be easily reproduced on the day of implant when the patient is scanned with the BRW stereotactic frame in place.

The tumour volume should be reconstructed from the

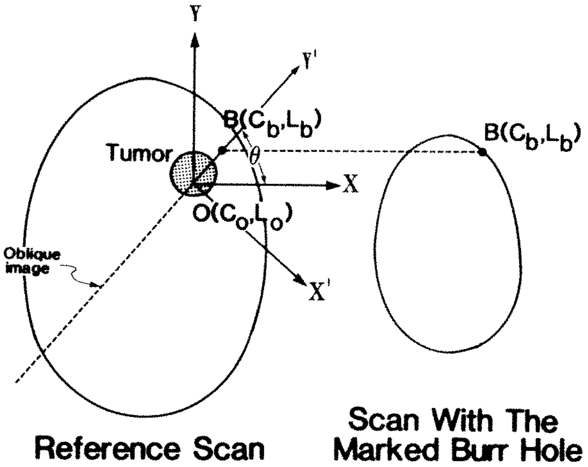

Figure 1. Schematic diagram of the reconstruction of an oblique CT image encompassing both burr hole, B, and target, O. The angle θ represents the angle of obliquity of the reconstructed image.

neurosurgeon's perspective. An oblique image is necessary to include both the barium dot (burr hole) and the reference target at the centre of the tumour in the same plane. The angle necessary to form this oblique image is obtained by connecting the X and Y co-ordinates of the entry point and the reference target with a straight line.

Figure 1 illustrates schematically what is described above. The origin, O, represents the reference target in the tumour and B represents the entry point on the skull. The angle, θ, represents the angle of the oblique reconstructed image. To obtain the neurosurgeon's viewpoint of the tumour, the frame of reference XYZ is rotated around the body axes, *i.e.* the Z axis, to become a new frame of reference X'Y'Z'. In this new frame, the Z' axis is the same as the Z axis and the entry point and the target are in the same Y'Z' plane. This simple approach reduces a potentially complicated three-dimensional problem to relatively easy two-dimensional geometry.

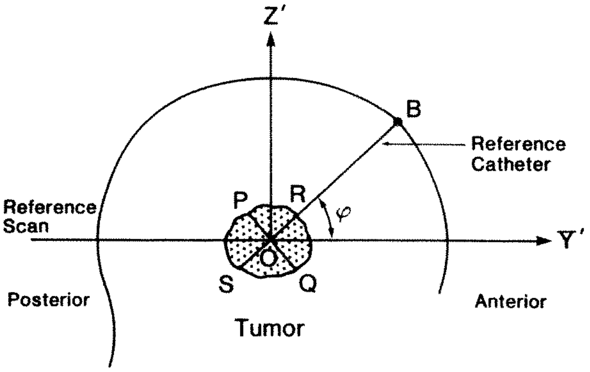

Figure 2. Schematic diagram of an oblique image which illustrates the trajectory pathway of the reference catheter, BO. The distances of PQ and RS, measured on the CT screen, represent the length and depth, respectively, of tumour from the neurosurgeon's viewpoint.

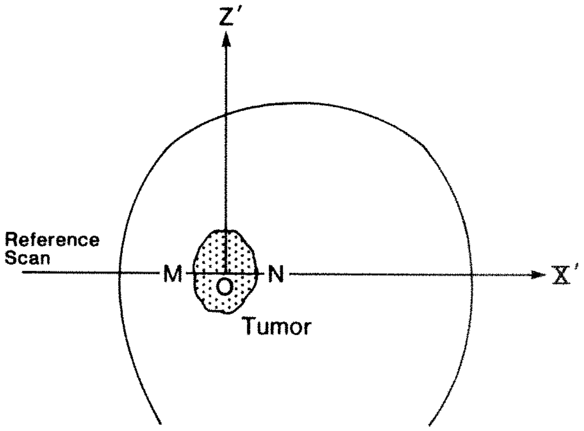

Figure 3. Schematic diagram of the oblique reconstructed image which is perpendicular to that described in Fig. 2. The measured distance, MN, represents the width of the tumour.

In the oblique CT reconstructed image shown schematically in Fig. 2, the line connecting the entry point, B, and the reference target, O, defines the trajectory or pathway of the first or reference catheter. Furthermore, many essential measurements, such as the depth of the reference target, BO, the angle of the catheter, φ, the over-shoot distance, OS, for the catheter to reach the distal margin of tumour, and the length of catheter, RS, within the tumour, are carefully determined using the distance-measuring cursor of the scanner.

From the length of tumour, PQ, measured from the neurosurgeon's viewpoint, more targets may be necessary to ensure an adequate dose coverage. In most cases, two more targets are chosen at either side of the reference target with appropriate spacings ranging from 0.7 to 1.7 cm. Similar measurements have to be made along the parallel trajectories using the distance-measuring cursor.

To determine the width of the tumour, another oblique CT image along the OX' axis with an angle perpendicular to the original oblique image is necessary (see Fig. 1). The width of the tumour, MN, is measured at the level of the reference scan, as shown in Fig. 3. Again, depending on the size of tumour, more catheters may be necessary. If more catheters are required for adequate dose coverage, basic measurements such as the depth, angle, over-shoot distance, and the length of catheter in the tumour may be reasonably assumed to be approximately the same as for the reference catheter. If one wishes to be more accurate in placing these catheters, more oblique CT images parallel to the first one (along OY') may be obtained at an appropriate spacing. One then proceeds using the same steps as before for determining the positions of the catheters.

With all three dimensions of tumour volume measured from the neurosurgeon's viewpoint, a simulated treatment plan is then created using the AECL Theraplan

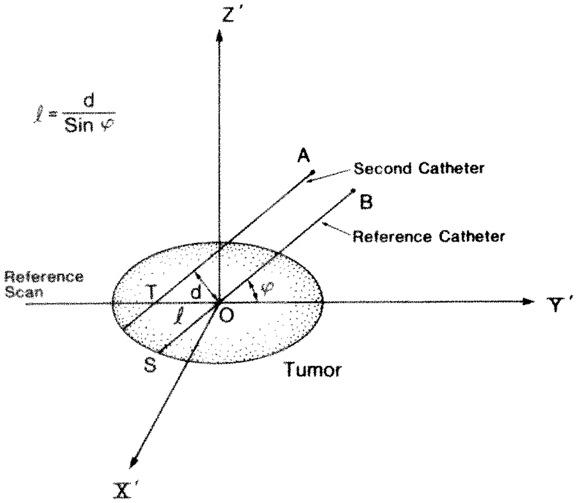

Figure 4. Schematic diagram showing the geometric rationales to determine the distance, l, between two targets on the reference scan. The distance, d, is the spacing between two catheters and φ is the angle of the reference catheter from the burr hole to the target.

treatment-planning computer. The optimal treatment plan determines the number and position of the catheters. Iridium-192 seeds of an activity of 1 mg(RaEq) each are used in this planning. Spacing between seeds in a catheter is 0.5 cm to avoid "ripple" effects in dose distribution at close range. According to our protocol, a total of 100 Gy will be delivered (in addition to 60 Gy from the external-beam treatment) to the margin of the contrast-enhanced region over 5 days. Consequently, the seed activity can be scaled up or down from 1 mg(RaEq) to achieve an appropriate dose rate, *i.e.* 80–100 cGy h^{-1}. Seeds with different activities are sometimes used in planning. They are ordered once the position of all the catheters and the number and activity of the seeds have been determined from an optimal computer-simulated plan.

On the day of implant 1 week later, another CT scan with a BRW stereotactic base frame and its localizer is performed on the patient. Care must be taken to ensure the CT gantry angle is the same as used for the planning CT scan. Once the same reference scan is selected, the reference target is also carefully reproduced on that scan.

Since catheters are not likely to be perpendicular to the reference scan, the distances of other targets with respect to the reference target on that scan must be determined. First, we orient ourselves to the new frame of reference, X′Y′Z′ co-ordinates, which is rotated with the same angle as the angle of the oblique image around the Z axis (see Fig. 1). In this new frame of reference, shown in Fig. 4, the distance, d, between two catheters situated on the Y′Z′ plane is not the same distance measured on the reference scan. Rather, the projected distance, OT or l, between these two catheters or targets on the CT scan is $d/\sin\varphi$, where φ is the angle of the trajectory of the catheters. Therefore, the Y′ co-ordinate of the second target, T, can be appropriately calculated and positioned on CT scan. Its pixel position, *i.e.* column and line, are also accurately recorded and input to another program also provided by the BRW stereotactic frame manufacturer. This program enables users to back-project the catheter pathways parallel to each other from the targets to the skull.

After repeating this procedure for all targets, a diagram can be created containing the configuration of all catheters including their spacing with respect to the reference catheter, the active source length in each catheter calculated from the length of catheter traversing through the tumour, and the over-shoot distance of the catheter to be pushed once it has reached its target. There are occasions when the "over-shoot" distance is negative, when the catheter is not inserted the complete distance to the target.

The implant procedure takes place in the operating room with the patient under local anesthaesia. With the guidance of the BRW arc system, a burr hole is drilled at the pre-determined position. A catheter with a steel stylet is inserted until its tip reaches the given depth which includes the depth from the skull to the target and the "over-shoot" distance. After all the catheters are in place, ribbons with dummy seeds are inserted and radiographic confirmation of catheter placement is obtained. If the catheter placement agrees with the plan, they are loaded with radioactive ^{192}Ir seeds. This afterloading technique reduces unnecessary exposure to the operating room personnel. An additional set of orthogonal radiographs are obtained after leaving the operating room for isodose calculations.

Discussion and conclusions

For a brain tumour implant to be successful, a technique for delivering adequate radiation dose to cover the tumour volume is essential. It should be comprehensive but not prohibitively complicated in its ability to cover the tumour volume and estimate dose delivery in treatment planning. The technique described in this paper demonstrates that a three-dimensional tumour volume can be simply reconstructed from the neurosurgeon's viewpoint using a CT scanner. It also comprehensively determines the number of necessary catheters, the position of these catheters, and the number of seeds and their activities, all prior to the implant. Furthermore, with good reproducibility of the treatment-planning CT scan and the scan with the BRW frame in place, this procedure also allows the catheters carrying the radioactive seeds to be guided accurately to their planned position.

In conclusion, virtually any institution using BRW stereotactic frames for brain implants is able to use the technique and procedure outlined in this paper to perform treatment planning with just a CT scanner, making a three-dimensional high-power treatment-planning computer unnecessary.

The clinical results in terms of complications and survivals are presented in the second part of this paper (Chun et al, 1989).

References

Abrath, F. G., Henderson, S. D., Simpson, J. R., Moran, C. J. & Marchosky, J. A., 1986. Dosimetry of CT-guided volumetric Ir-192 brain implant. *International Journal of Radiation Oncology, Biology, Physics, 12,* 359–363.

Chun, M., McKeough, P., Wu, A., Kasdon, D., Heros, D., & Chang, H., 1989. Interstitial iridium-192 implantation for malignant brain tumours. Part II: Clinical experience. *British Journal of Radiology, 62,* 158–162.

Eddy, M. S., Selker, R. G. & Anderson, L. L., 1986. On a method of dosimetry planning and implantation of I-125 for interstitial irradiation of malignant gliomas. *Journal of Neuro Oncology, 4,* 131–139.

Gutin, P. H., Phillips, T. L., Wara, W. M., Leibel, S. A., Hosobuchi, Y., Levin, V. A., Weaver, K. A. & Lamb, S. E., 1984. Brachytherapy of recurrent malignant brain tumors with removable high-activity iodine-125 sources. *Journal of Neurosurgery, 60,* 61–68.

Heilbrun, M. P., Roberts, T. S., Apuzzo, M. L. J., Wells Jr, T. H. & Sabshin, J. K., 1983. Prelimary experience with Brown-Roberts-Wells (BRW) computerized tomography stereotaxic guidance system. *Journal of Neurosurgery, 59,* 217–222.

Lansky, L. L., Batnitzky, S., Price, H. I., Cook, P. N. & Dwyer III, S. J., 1983. Application of three-dimension computer reconstruction from computerized tomograph to intracranial tumor in children. *Journal of Neuro Oncology, 1,* 347–356.

Leksell, L., 1951. The stereotaxic apparatus for intracerebral surgery. *Acta Chirurgica Scandinavica, 102,* 316–319.

Mackay, A. R., Gutin, P. H., Hosobuchi, Y. & Norman, D., 1982. Computerized tomography-directed stereotaxy for biopsy and interstitial irradiation of brain tumors. *Neurosurgery, 11,* 38–42.

Marchosky, J. A. & Moran, C. J., 1983. A simple stereotaxic CT controlled brain biopsy system for general neurosurgical use. *Contemporary Neurosurgery, 5,* 18.

Rossman, K. J., Shetter, A. G., Speiser, B. L. & Nehls, D., 1985. Stereotactic afterloading iridium implants in treatment of high-grade astrocytomas. *Endocurietherapy/Hyperthermia Oncology, 1,* 49–57.

Salazar, O. M., Rubin, P., Feldstein, M. L. & Pizzutiello, R., 1979. High dose radiation therapy in the treatment of malignant gliomas: Final report. *International Journal of Radiation Oncology, Biology, Physics, 5,* 1733–1740.

Salcman, M., Sewchand, W., Amin, P. P. & Bellis, E. H., 1986. Technique and preliminary results of interstitial irradiation for primary brain tumors. *Journal of Neuro Oncology, 4,* 141–149.

Sewchand, W., Amin, P. P., Drzymala, R. E., Salazar, O. M., Salcman, M., Samaras, G. M. & Botero, E., 1984. Removable high intensity iridium-192 brain implant. *Journal of Neuro Oncology, 2,* 177–185.

Scanlon, P. W. & Taylor, W. F., 1979. Radiotherapy of intracranial astrocytomas: Analysis of 417 cases treated from 1960 through 1969. *Neurosurgery, 5,* 301–308.

Walker, M. D., Strike, T. A. & Sheline, G. E., 1979. An analysis of dose effect relationship in the radiotherapy of malignant gliomas. *International Journal of Radiation Oncology, Biology, Physics, 5,* 1725–1731.

Weaver, K., Peksens, R. & Barnett, C., 1986. Special brachytherapy procedures and dosimetry for tumors of the brain, eye, head and neck, and perineum. In *Radiation Oncology Physics–1986,* ed. by J. G. Kereiakes, H. R. Elson & C. G. Born, Medical Physics Monograph no. 15 (American Association of Physicists in Medicine, New York).

1989, *The British Journal of Radiology*, 62, 158–162

Interstitial iridium-192 implantation for malignant brain tumours

Part II: Clinical experience

By M. Chun, MD, P. McKeough, MD, A. Wu, PhD, *D. Kasdon, MD, †D. Heros, MD and H. Chang, MD

Departments of Radiation Oncology, *Neurosurgery and †Neurology, New England Medical Center Hospitals and Tufts University School of Medicine, Boston, Massachusetts 02111, USA

(Received May 1988 and in revised form August 1988)

Abstract. The treatment results of 37 patients with malignant brain neoplasms treated with a computed-tomography-guided stereotactic iridium-192 implant are reviewed. Of these, 29 patients with high-grade gliomas (20 with glioblastoma multiforme (GBM), nine with anaplastic astrocytoma (AA)) received an implant as part of their initial management. The median survival was 14.5 and 15.5 months in the patients with previously untreated GBM and AA, respectively. In those patients with recurrent tumour after external-beam irradiation, durable local control over a year was achieved with implantation. Increasing the total tumour dose from 120 to 160 Gy did not improve survival or local control. Karnofsky Performance Status (KPS) was used as an indicator of quality of life and was seen to decrease with a median interval of 8.5 months following treatment. No severe complications were noted in the entire group of patients treated with this implant procedure.

The estimated incidence of primary brain tumours for the United States in 1987 is 14 700, with 10 200 deaths (Silverberg & Lubera, 1987). Of these, high-grade astrocytomas are the most common primary malignant brain tumours in adults.

Even with aggressive surgery and conventional external-beam radiation therapy, the overall survival is generally poor. Several retrospective analyses have demonstrated that the 5-year survival rates with surgery followed by radiation therapy for anaplastic astrocytoma (AA) and glioblastoma multiforme (GBM) are approximately 20% and 0%, respectively. A median survival of 24 months is reported for AA and 9 months for GBM (Marsa et al, 1975; Sheline et al, 1975; Rutten et al, 1981). Most deaths are due to persistent or recurrent disease at the primary tumour site. One post-mortem study demonstrated that 90% of tumour recurrences occur within 2 cm of the original tumour volume (Hochberg & Pruitt, 1980). A few studies comparing whole-brain irradiation and local or partial brain irradiation have not demonstrated a difference in survival (Ramsay & Brand, 1973; Descyryer et al, 1976; Burger et al, 1983).

The Brain Tumour Study Group has shown a dose–response relationship for malignant gliomas and demonstrated an increase in the median survival when total doses of 6000 cGy against 5000 cGy were used with conventional fractionation (Walker et al, 1979). Salazar et al (1979) demonstrated an increase in survival by increasing the total dose from 5000 cGy to 6000 and 7000 cGy (30 weeks against 42 and 52 weeks). Although a higher dose to the tumour bed appears to be warranted for longer survival, the toxicity of this high dose delivered by conventional external-beam radiation therapy can lead to severe complications including cerebral radionecrosis and death (Sheline et al, 1980; Marks et al, 1981).

As early as 1914, Frazier performed the first radioactive seed implant for a brain tumour with the intent of delivering a high local tumour dose. The technique has been improved since the development of the stereotactic frame in the mid-1950s (Leskell, 1951) with better accuracy of implant volume and dosimetry. Multiple reports are available regarding technique and preliminary results (Bouzaglou et al, 1985; Rossman et al, 1985; Abrath et al, 1986; Eddy et al, 1986). We have described our pre-planning and dosimetric technique in Part I (Wu et al, 1989) and report here our initial clinical results of 37 patients.

Materials and methods

On the day of surgery, 4 mm computed tomographic (CT) cuts are done on the patient with BRW localizer ring in place. On the same reference scan obtained at the time of tumour volume reconstruction, the X,Y co-ordinates for each catheter and of the nine rods of the localizer ring were required to determine the four angles and depth necessary for placement of the first catheter. The parallel trajectories of the other catheters can also be determined with another program at the same time. The implant procedure is performed under local anaesthesia in the operating room. The BRW arc frame is set according to the calculated and verified angles. The catheters are inserted and reach the target at a given depth according to the pre-plan (Wu et al, 1989). A set of orthogonal radiographs are taken to confirm the position of catheters and iridium-192 sources are inserted as a final step in the operating room. The entire implant procedure can be performed in 2–3 h.

Patients were carefully selected for this procedure.

Table I. Tumour characteristics

Histopathology	
Glioblastoma multiforme	24
Recurrent	(4)
Primary, untreated	(20)
Anaplastic astrocytoma, primary	9
Others	4
Location of tumour	
Frontal lobe	15
Parietal lobe	9
Temporal lobe	5
Occipital lobe	4
Thalamus	4

Primary malignant gliomas, recurrent metastatic tumour, or recurrent high-grade gliomas were included. Selection criteria included age less than 70 years old, Karnofsky Performance Status (KPS) over 70, maximum tumour diameter of 5 cm within the contrast-enhancing region, and tumours not in proximity to the motor strip.

Between April 1984 and June 1987, 37 patients were entered into this study. The characteristics of tumours are shown in Table I. A total of 29 patients (20 GBM and nine AA) received interstitial implantation as primary treatment and the other eight patients underwent implantation for local failure from previous external-beam treatment. Prior to the implant, most patients had a debulking procedure and five patients underwent stereotactic biopsy only for tissue diagnosis. The characteristics in patients with primary gliomas are described in Table II.

In primary untreated gliomas, patients started a course of external-beam irradiation on either a 4 or 6 MV linear accelerator with a 5 cm margin to 5000 cGy followed by a reduced field including the tumour with a 2 cm margin for another 1000 cGy (180 cGy/fraction). Initially, implantation was performed and delivered 6000 cGy within 2–3 weeks following the completion of external-beam irradiation (in seven patients with GBM and five patients with AA). In a few cases, tumour growth was noted on follow-up CT scans after the external-beam treatment prior to implantation.

Since November 1985, the treatment schedule has been modified and the implant performed halfway through the external-beam therapy. The tumour dose from the implant was increased to 10 000 cGy because of histologic evidence of persistent tumour cells in specimens from two patients who underwent re-operation. The total dose was adjusted to 16 000 cGy. Eleven patients with GBM and three patients with AA were treated in this manner. Since October 1986, implantation alone was considered as a primary treatment for tumours smaller than 3 cm in diameter, reserving external-beam treatment as a salvage modality. Two patients with GBM and one patient with AA were treated in this fashion.

Implant volume was determined by the area of contrast enhancement on the CT scan obtained 1–2 weeks prior to the scheduled implant procedure. The volume in 37 patients ranged from 4 to 175 cm^3 (average 54 cm^3) and average tumour volume in patients with GBM was larger than that in patients with AA (64 against 36 cm^3). A total of between three and eight catheters were placed to cover the volume with 1–1.5 cm separation between catheters as determined by pre-planned dosimetry. The activity of sources (average 52 MBq(1.4 mCi) per seed) was ordered to cover the tumour volume with 80–100 cGy h^{-1}.

Follow-up ranged from 2 to 50 months after the implant with a median follow-up of 27 months. Computed tomographic scans were obtained at 3-month intervals to assess tumour response. The time interval until the first decrease in KPS and the interval from the implant until the KPS was less than 50 were documented to assess quality of life. Survival was calculated using the Kaplan–Meier method for statistical analysis (Kaplan & Meier, 1958).

Results

The implant procedure was tolerated very well by all patients without catheter-induced haemorrhage or seizure. A total of eight patients had some kind of complication from the procedure itself (Table III). There were no infectious episodes after the institution of antibiotic prophylaxis while the catheters were in place. The three patients who experienced worsening neurological function immediately after the procedure had tumour located near the motor strip and regained their strength to the level of the pre-implant KPS with physical therapy.

Survival was analysed separately by grade, total tumour dose, age at presentation and tumour volume. The results are summarized in Table IV. There was no apparent difference in median survival by grade (14.5 months in patients with GBM and 15.5 months in patients with AA) and by tumour volume. The patients with recurrent GBM survived 8.8+, 9.9, 10 and 15.4+

Table II. Patient characteristics for 29 primary high-grade gliomas

	Average age (years)	Average tumour size (cm^3)	Sex	
			M	F
20 GBM	52 (24–70)	54 (4–175)	10	10
9 AA	43 (26–65)	36 (16–70)	6	3

Table III. Complications after implant procedure

Meningitis	2
Worsening neurological status	3[a]
Pustule at suture site	1
Temporary CSF leaks	2
Total	8

[a] All three patients had tumour near the motor strip and gained neurological function with physical therapy.

Table IV. Median survival from time of diagnosis in patients with primary gliomas

Overall survival in 20 primary GBM	14.5 months (4.5–27.2+)
Patients' age < 50 years	16
> 50 years	13
Tumour size < 40 cm^3	14.5
> 40 cm^3	14.5
Overall survival in 9 AA	15.5

months from the time of the implant after having recurred 11, 18, 18 and 4 months, respectively, after the completion of external-beam therapy. Median survival from the time of diagnosis for the patients less than 50 years of age was 16 months and for those older than 50 years, 13 months. Survival for the five patients younger than 40 years was 11.6, 14.4, 16+, 16+ and 21.3+ months.

Two patients with metastatic breast cancer survived 120+ and 76+ months from diagnosis of brain metastases and 22+ and 23+ months from the time of implant without evidence of recurrence. One patient with metastatic melanoma survived 9 months after the implant and expired with carcinomatous meningitis. A patient with a mixed oligodendroglioma died of progressive local disease at 96 months from initial diagnosis after having recurred 60 months following external-beam therapy.

The patterns of failure were documented by follow-up CT scans or by autopsy reports in 23 patients with malignant gliomas. Fourteen patients had local failure alone, six had local failure and sub-ependymal spread and two patients failed with both local and multicentric parenchymal disease. The last patient was locally controlled but failed with sub-ependymal spread.

The initial average KPS was 80 and was determined after the surgical procedure. The median time interval between implantation and the first decrease in KPS for all patients was 8.5 months (7.5 months in patients with primary GBM and 7 months in AA patients). This correlated well with the median interval until an increase in the contrast-enhanced region was identified by CT. All patients who demonstrated a decrease in KPS progressed to a KPS of less than 50 within 3 months.

Three patients underwent brain implantation as their initial therapy, reserving external-beam treatment for recurrence or tumour re-growth. One patient had near total resection of a left frontal GBM in October 1986 and implant at the tumour resection margin with two subsequent cycles of intra-arterial BCNU. He developed sub-coronal spread with local tumour growth in 3 months for which he received external-beam treatment. He died 6 months after the diagnosis. The second patient presented with a small tumour, 3 cm diameter, in the right frontal lobe which was implanted with four catheters in January 1987. Shortly after the first cycle of chemotherapy, he was found to have distant tumour growth with local control in the primary tumour bed. Subsequent irradiation had been given with stabilization of his KPS at 60. The last patient is a young female with a totally resected AA in the right frontal lobe. In her case, implant alone has been successful for local tumour control over 8 months without evidence of any complication.

Re-operation was performed in nine patients for clinical deterioration and increase in the contrast-enhanced region on the CT scan. Three patients, two with gliomas and one with metastatic tumour from breast cancer, had necrosis without tumour cells in the re-operation specimen. The two patients with high-grade gliomas died shortly after re-operation. The patient with breast cancer is still alive. The other five patients showed mostly necrosis and foci of tumour cells, but progressed locally and died soon after the surgery. Seven of these eight patients received chemotherapy after their irradiation. The patient with metastatic malignant melanoma showed tumour cells in the specimen and died of carcinomatous meningitis. The median survival after re-operation in all nine patients was 4.5 months.

Discussion

Interstitial brain implantation allows a high localized dose of radiation to be delivered to a defined target volume. The European experience with interstitial irradiation has focused on low-grade gliomas. Szikla et al (1984) performed implants with removable ^{192}Ir wires in patients with Grade III and Grade IV gliomas and achieved a 5-year survival of 55% and 2-year survival of 19%. The experience in patients with recurrent gliomas has demonstrated an overall response rate of 68% in those with recurrent neoplasms treated with 3000–12 000 cGy (Gutin et al, 1984). The updated results showed that the median survival for 18 recurrent GBM was 52 weeks after brachytherapy and 153 weeks for 23 recurrent AA (Gutin et al, 1987).

The Northern California Oncology Group has, since 1983, been carrying out a Phase II study combining external-beam irradiation with hydroxyurea as a radiosensitizer and multi-agent systemic chemotherapy utilizing interstitial irradiation as a "boost". Leibel et al (1987) reported a preliminary finding of a 3-year survival rate of 53% in patients with AA and 55% in patients with GBM. Rossman et al (1985) reported median survival of 23 months in three patients below the age of 40 years, and 11 and 12 months in four patients aged 40 to 60 years and those greater than age 60 years, respectively. The median survival for the patients with previously untreated GBM in this series of 14.5 months is a slight improvement from the data of other series using conventional radiation therapy with or without adjuvant chemotherapy (Sheline, 1975; Walker et al, 1980). However, the results are still disappointing.

Our own result is obviously an experience based on the selected group with an average KPS of 80 and with tumours less than 5 cm diameter. Even in this small patient group, there is a trend of better survival rate in younger patients aged less than 40 years. Similar observations were reported previously after the treatment of high-grade gliomas (Walker et al, 1980).

Surprisingly, the median survival of patients with AA was only 15.5 months, which is not different from the survival of patients with GBM. Similar findings have been reported by Leibel et al (1987).

We found that the sequencing of the external-beam irradiation and the implant had no influence on survival. It is not clear why there was decreased survival for the patients who received a higher dose. It is possible that necrosis or inclusion of patients who demonstrated tumour re-growth when the external-beam radiation is given during the first 6 weeks may have contributed to the decreased survival. It has been documented that there is tumour progression in 11% of patients when serial CT scans were taken after surgery and radiation therapy (Marks & Gado, 1977).

The number of patients who failed with distant spread of disease away from the primary tumour bed was more than expected. Other authors have demonstrated that there was no statistical difference between those patients with malignant gliomas who received an implant compared to those treated conventionally (Choucair et al, 1986).

The implant procedure did not adversely affect the quality of life in this group of patients. The median interval until the KPS decreased for all patients was 8.5 months, which is comparable to the overall survival of patients with GBM in most series. After the initial decrease in the KPS, the average time until the patients reached a KPS of less than 50 was 3 months. Patients generally died a short time after that.

Re-operation did not provide a significant benefit to patients in this series. Necrosis as the only pathological finding in the re-operation specimen was seen in only two patients with GBM and they both died within 4 months of the procedure. Patients with necrosis and tumour identified in the pathological specimen all died shortly after the re-operation.

Conclusions

In summary, interstitial irradiation can be performed as a boost treatment without major side-effects in the management of primary untreated high-grade gliomas. The appropriate dose from the implant is still not defined and those patients who received a total dose of 16 000 cGy appeared to do worse than those who received 12 000 cGy. A durable local control can be obtained in those patients with recurrent primary CNS neoplasm or selected patients with brain metastases.

References

Abrath, F. G., Sheri, D. H., Simpson, J. R., Moran, C. J. & Marchosky, A., 1986. Dosimetry of CT-guided volumetric iridium-192 brain implant. *International Journal of Radiation Oncology, Biology, Physics, 12*, 359–363.

Bouzaglou, A., Dyck, P., Solt-Bohman, L. G. & Gruskin, P., 1985. Stereotactic interstitial implantation of brain tumors. *Endocurietherapy/Hyperthermia Oncology, 1*, 99–112.

Burger, P. C., Dubois, P. C., Schold, S. C., Smith, K. R., Odom, G. L., Crafts, D. C. & Giangaspero, F., 1983. Computerized tomographic and pathologic studies of the untreated quiescent and recurrent glioblastoma multiforme. *Journal of Neurosurgery, 58*, 159–169.

Choucair, A. K., Levin, V. A., Gutin, P. H., Davis, R. L., Silver, P., Edwards, M. & Wilson, C. B., 1986. Development of multiple lesions during radiation therapy and chemotherapy in patients with gliomas. *Journal of Neurosurgery, 65*, 654–658.

Descyryver, A., Greitz, T. & Forsby, N., 1976. Localized shaped field radiotherapy of malignant glioblastoma multiforme. *International Journal of Radiation Oncology, Biology, Physics, 1*, 713–716.

Eddy, M. S., Selker, R. G. & Anderson, L. L., 1986. On a method of dosimetry planning and implantation of ^{125}I for interstitial irradiation of malignant gliomas. *Journal of Neuro-oncology, 4*, 131–139.

Gutin, P. H., Phillips, T. L., Wara, W. M., Leibel, S. A., Hosobuchi, Y., Levin, V. A., Weaver, K. A. & Lamb, S., 1984. Brachytherapy of recurrent malignant brain tumors with removable high activity iodine-125 sources. *Journal of Neurosurgery, 60*, 61–68.

Gutin, P. H., Leibel, S. A., Wara, W. A., Choucair, A., Levin, V. A., Philips, T. L., Silver, P., Da Silva, V., Edwards, M. S. B., Davis, R. L., Weaver, K. A. & Lamb, S., 1987. Recurrent malignant gliomas: survival following interstitial brachytherapy with high-activity iodine-125 sources. *Journal of Neurosurgery, 67*, 864–873.

Hochberg, F. H. & Pruitt, A., 1980. Assumptions in the radiotherapy of glioblastoma. *Neurology, 30*, 907–911.

Kaplan, E. L. & Meier, P., 1958. Nonparametric estimation from incomplete observations. *Journal of the American Statistics Association, 53*, 457–481.

Leibel, S., Gutin, P., Phillips, T., Wara, W., Levin, L., Hannigan, J., Silver, P. & Weaver, K., 1987. The integration of interstitial into the preliminary management of patients with malignant gliomas: results of Phase II Northern California Oncology Group Trial. *American Journal of Clinical Oncology, 10*, 102.

Leskell, L., 1951. The stereotaxic apparatus for intracerebral surgery. *Acta Chirurgica Scandinavica, 102*, 316–319.

Marks, J. E. & Gado, M., 1977. Serial computed tomography of primary brain tumors following surgery, irradiation and chemotherapy. *Radiology, 125*, 119–125.

Marks, J. E., Baglan, R. J., Prassad, S. C. & Blank, W. F., 1981. Cerebral radionecrosis: incidence and risk in relation to dose, time, fractionation and volume. *International Journal of Radiation Oncology, Biology, Physics, 7*, 243–252.

Marsa, G. W., Goffinet, D. R., Rubenstein, L. J. & Bagshaw, M. A., 1975. Megavoltage irradiation in the treatment of gliomas of the brain and spinal cord. *Cancer, 36*, 1681–1689.

Ramsay, R. G. & Brand, W. M., 1973. Radiotherapy of glioblastoma multiforme. *Journal of Neurosurgery, 39*, 197–202.

Rossman, K. G., Shetter, A. G., Speiser, B. L. & Nehls, D., 1985. Stereotactic afterloading iridium implants in treatment of high-grade astrocytomas. *Endocurietherapy/Hyperthermia Oncology, 1*, 49–57.

Rutten, E., Kazem, I., Sloof, J. & Walder, A. D. H., 1981. Post-operative radiation therapy in the management of brain astrocytomata: A retrospective study of 142 patients. *International Journal of Radiation Oncology, Biology, Physics, 7*, 191–195.

Salazar, O. M., Rubin, P., Feldstein, M. L. & Pizzutiello, R., 1979. High dose radiation therapy in the treatment of malignant gliomas: Final report. *International Journal of Radiation Oncology, Biology, Physics, 5*, 1733–1740.

Sheline, G. E., 1975. Conventional radiation therapy of gliomas. *Recent Results in Cancer Research, 51*, 125–134.

Sheline, G. E., Wara, W. M. & Smith, V., 1980. Therapeutic irradiation and brain injury. *International Journal of Radiation Oncology, Biology, Physics, 6*, 1215–1228.

Silverberg, E. & Lubera, J., 1987. Cancer statistics 1987. *Cancer Journal for Clinicians, 37*, 2–11.

Szikla, G., Schlienger, M., Blond, S., Daumas-Duport, C., Missir, O., Miyahara, S., Musolino, A. & Schaub, C., 1984. Interstitial and combined interstitial and external irradiation of supratentorial gliomas. Results in 61 cases treated 1973–1981. *Acta Neurochirurgica, Supplement, 33*, 355–362.

Walker, M. D., Strike, T. A. & Sheline, G. E., 1979. An analysis of dose-effect relationship in the radiotherapy of malignant gliomas. *International Journal of Radiation Oncology, Biology, Physics, 5*, 1725–1731.

Walker, M. D., Green, S. B., Byar, D. P., Alexander, E., Batzdorf, U., Brooks, W. H., Hunt, W. E., MacCarthy, C. S., Mahaley, M. S., Mealey, J., Owens, G., Ransohoff, J., Robertson, J. T., Shapiro, W. R., Smith, K. R., Wilson, C. B. & Strike, T. A., 1980. Randomized comparisons of radiotherapy and nitrosoureas for the treatment of malignant glioma after surgery. *New England Journal of Medicine, 303*, 1323–1329.

Wu, A., Chun, M., Kasdon, D., McKeough, P., Heros, D., Chang, H., 1989. Interstitial Iridium-192 implantation for malignant brain tumours. Part I: Technique of dosimetry planning and tolerance. *British Journal of Radiology, 62*, 154–157.

1989, *The British Journal of Radiology*, *62*, 163–167

Films, screens and cassettes for mammography

By J. Law, PhD, FInstP and *A. E. Kirkpatrick, FRCR, FRCS

Department of Medical Physics & Medical Engineering, Western General Hospital, Crewe Road, Edinburgh EH4 2XU and *Department of Radiology, Royal Infirmary, Edinburgh EH3 9YW

(*Received June 1988 and in revised form September 1988*)

Abstract. Various film–screen combinations intended for mammography have been compared for image quality and for dose. Image quality was assessed as in an earlier paper, using a test object having details which are both realistic and quantitative. Relative doses required to give film densities of 1.0 were measured. The Kodak MinR–MinR combination was taken as a standard against which others were compared, and in general a lower dose was accompanied by poorer image quality. The Fuji NH film with Fuji Hi-Mammo screen was the sole exception, giving slightly better image quality at about half the dose required by the MinR combination. A number of cassettes were also compared with each other and with evacuated envelopes. The Dupont Cronex cassette and three carbon-fibre fronted cassettes all performed well in image quality.

In an earlier paper (Kirkpatrick & Law, 1987), results were reported on comparisons of image quality and speed between various film–screen combinations used in mammography. That work was carried out in 1985–1986, and concluded that the Kodak MinR–MinR combination remained the best available for image quality, except for Agfa Medichrome Blue which is no longer available. Some other combinations required a lower dose, but the loss in image quality was considered to outweigh this advantage. At present dose levels, image quality and diagnostic accuracy are thought to be more important, even in a screening programme (Law, 1987). This view is supported by remarks made in leading articles elsewhere (Anon, 1985; Roebuck, 1986).

The MinR–MinR combination appeared then to have been the best black and white one for image quality since 1980, and it was surprising that no newer one had displaced it in this respect. The desirability of identifying a fresh combination which gave better image quality at lower dose was fully recognized. This paper reports further trials and provisionally identifies one such film–screen combination. The opportunity has also been taken to compare various cassettes with each other and with the Dupont evacuated plastic envelope system used previously.

Materials and methods

In general these have remained as close as practicable to those used in the previous study referred to. For a test object, the "Barts" phantom (White & Tucker, 1980) has again been used. At the time of this work, 1987–1988, it remained the only one available to us which was quantitative and contained "realistic" details, apart from the Wisconsin type, which was previously shown to give the same results as the Barts one but which is much more complex and time consuming in use.

Films and screens supplied to us by various manufacturers have been compared in the Dupont evacuated black plastic envelopes. As before, each film has been tried on screens of the same manufacture and on MinR screens, and each screen has been used with the corresponding film(s) and with MinR film. A few other combinations have also been tried. Cassettes have been compared with envelopes using films and screens of the same manufacture, or using MinR, and sometimes both.

All films were exposed on a CGR 500t X-ray set in the Royal Infirmary, Edinburgh, and processed on a Durr-Med Model 260 table-top processor. This X-ray set has a molybdenum target. The processor was the one adjacent to this X-ray set; the image quality obtained with it using MinR films and screens was found to be as good as on any of six others available to us (Law & Kirkpatrick, 1988). Kodak chemicals were used at 35°C, with a nominal processing time of 3.5 min which was close to 2.5 min when corrected for feed time.

For an ideal comparison of films, the processing chemicals should match the film in every case, and the same processor and of course the same X-ray set must be used for all films. This is quite impractical unless a processor with an adjacent X-ray set is available dedicated to research and development work. In practice, X-ray departments do not always choose their processing chemicals to match their film. Moreover, in informal discussion, two major X-ray film makers have said that processing chemicals should not affect image quality in films of different make provided processing instructions are strictly adhered to. In our experience, seven processors of various makes using various chemicals have given almost uniformly good image quality with MinR film (Law & Kirkpatrick, 1988).

Manual exposure control was used throughout, and the aim was to have a density of 1.0 under blank parts of the phantom near the centre of the field. For each combination of film and screen, whether in envelopes or cassettes, six radiographs were obtained under identical conditions. The density of each film was measured and the mAs used was noted; in this way the mean mAs required to achieve unit density was estimated.

All radiographs were obtained at a nominal 25 kV using molybdenum filtration (0.03 mm), and at 55 cm FFD. Measurements of tube kV by various techniques, including K-edge fluorescence detection and an RMI

Model 232 digital kV meter, suggest that the actual kV was probably about 24.

Results

Films and screens

Each radiograph was scored by each author independently, the number of details visible (out of a total of 78) being taken as the score. Allowance was made for details doubtfully visible, and the two scores combined as described in the previous paper. The quoted uncertainties are standard errors on the means of each set of six radiographs and represent 68% confidence levels. It will be noted that these scores are higher than those reported when Barts phantoms were first used (Fitzgerald et al, 1981). This is not surprising as in the intervening period X-ray sets have improved very considerably, there have been some improvements in films and screens, and there is greater recognition of the need for care in processing and for dedicated mammography processing.

Since the work was carried out over many months, the MinR–MinR combination was used at intervals throughout this period, which provided some check on the consistency of standards in processing, in scoring and in the quality of the MinR films and screens themselves. For the whole of the period concerned they were the type used clinically in this department.

Results from a number of Kodak films were reported in the previous paper, all used with MinR screens. Since then no new Kodak films or screens have been available to us. For convenience, results from each of the other main manufacturers are grouped in separate tables: Agfa products are shown in Table I, Dupont in Table II, Fuji in Table III and 3M in Table IV. Other products are grouped in Table V.

It is important to appreciate that a small change in score represents an appreciable change in image quality. For example, a score of 53.5 was found at a nominal 25 kV compared with 48 at a nominal 35 kV on the same X-ray set and processor. From past experience, a score of 55 is good, one of 52 is mediocre and below 50 is relatively poor. Results in this series of comparisons cannot be compared directly with those of the previous paper, as both the X-ray set and the processor are different.

Table I. Image scores and relative doses for Agfa products and Kodak MinR

	Film	Screen			
		MinR	Agfa Detail	Agfa Detail S	Agfa Detail (new)
Image scores	MinR	55.3 ± 0.4[a]	54.2 ± 0.5	49.5 ± 1.1	49.9 ± 0.7
	MR3	53.7 ± 0.6	51.2 ± 0.5	46.8 ± 0.6	47.6 ± 0.5
Relative doses	MinR	1.0	0.95	0.5	1.0
	MR3	0.45	0.45	0.25	0.45

[a] Mean of five sets of six radiographs.

Table II. Image scores and relative doses for Dupont products and Kodak MinR

	Film	Screen	
		MinR	Cronex Ortho-Micro
Image scores	MinR	55.3 ± 0.4[a]	54.5 ± 0.8
	Cronex Micro	52.9 ± 0.7	51.8 ± 1.0
	Cronex Micro Plus	51.9 ± 0.5	51.7 ± 0.9
	Cronex SP 150	52.3 ± 0.5	51.6 ± 1.0
Relative doses	MinR	1.0	1.0
	Cronex Micro	0.5	0.5
	Cronex Micro Plus	0.45	0.45
	Cronex SP 150	0.4	0.35

[a] Mean of five sets of six radiographs.

Table III. Image scores and relative doses for Fuji products and Kodak MinR

	Film	Screen	
		MinR	Fuji[a] HiMammo
Image scores	MinR	55.3 ± 0.4[b]	55.6 ± 0.5[c]
	Fuji NCII	53.9 ± 0.6	53.7 ± 0.8
	Fuji NH	53.8 ± 1.0	56.0 ± 0.5[d]
Relative doses	MinR	1.0	1.05
	Fuji NCII	0.85	0.85
	Fuji NH	0.5	0.55

[a] Further comparisons with this screen are shown in Table VII.
[b] Five sets of six radiographs each.
[c] Two sets of six radiographs each.
[d] Three sets of six radiographs each.

Table IV. Image scores and relative doses for 3M products and Kodak MinR

	Film	Screen		
		MinR	Trimax T1	Trimax T2
Image scores	MinR	55.3 ± 0.4[a]	53.4 ± 0.7	53.7 ± 0.5
	Trimax MS	52.5 ± 0.8	52.3 ± 1.0	52.8 ± 0.9
	SX315[b]	49.6 ± 0.5	48.8 ± 0.6	48.1 ± 0.6
Relative doses	MinR	1.0	1.6	0.9
	Trimax MS	0.5	0.7	0.45
	SX315[b]	0.25	0.35	0.2

[a] Five sets of six radiographs each.
[b] 3M have stated that this film was a pre-production batch of their FM film.

Relative doses, estimated as described above, have been normalized to 1.0 for MinR–MinR and rounded to 0.05. In assessing risks to patients, the total integrated dose to the breast should be employed, and this naturally

Table V. Image scores and relative doses for other screens and Kodak MinR

	Film	Screen		
		MinR	X-Ograph S-100	Toshiba[a] MM
Image scores	MinR	55.3 ± 0.4[b]	53.7 ± 0.6	54.5 ± 1.0
	Agfa MR3	53.7 ± 0.6	—	48.6 ± 1.0
	Fuji NH	53.8 ± 1.0	53.8 ± 0.5	—
Relative doses	MinR	1.0	1.1	0.7
	Agfa MR3	0.45	—	0.3
	Fuji NH	0.5	0.6	—

[a] It is understood that Toshiba no longer produce this screen.
[b] Mean of five sets of six radiographs each.

depends on many factors including beam quality and breast composition. Nevertheless, other things being equal, film speed is inversely proportional to patient dose, whether at the surface or integrated over depth. Therefore relative exposures as in Tables I–V should be proportional to relative risks (as far as film–screen combinations are concerned).

Envelopes and cassettes

Several cassettes have been made available by manufacturers. Some have plastic fronts while some others have carbon-fibre fronts. Each has been compared with evacuated envelopes on at least one and generally two film–screen combinations, in exactly the same way that the films and screens have been compared. The results have been summarized in Table VI. A few small differences between results in Table VI and in earlier tables may be noticed. This is because the result using a cassette has been compared with the envelope result obtained on the same day, rather than with the mean envelope result from more than one day.

Discussion

Films and screens

In Table I, the Agfa MR3 film is consistently poorer than MinR film on all four screens. The consistency of the difference is rather better than the uncertainties on the separate scores would lead one to expect. Of the three screens, none is as good as MinR, and the "Detail S" and the newer Detail screens are poorer than the older Detail screen (a further development of the Detail screen and a new film from Agfa are anticipated).

In Table II, the Cronex Ortho-Micro screen is nearly as good as the MinR screen, but with no significant gain in dose required, on all four films. As with results in Table I, the consistency of the difference on each film gives added confidence in the results reported. The three Cronex films appear very similar in image quality, and are distinctly poorer than MinR. They are not very different in speed, and although the new SP150 is considerably faster than MinR film, this is not considered to outweigh the poorer image quality. Cronex Micro Plus film is double sided but was used here with a single back screen as were the others.

In Table III, the Fuji Hi-Mammo screen appears on average very slightly superior to MinR screens, though with no dose advantage. Further evidence for this slight average superiority is provided by the results in Table VI from various cassettes. As soon as this possibility was realized a further six loose screens of this type were borrowed from Fuji, and these were used in obtaining the results in Table III, thus demonstrating that the advantage over MinR screens did not lie in one specimen only of this screen.

The performance of the two Fuji films on MinR screens was not outstanding, the NCII failing to match that reported in the earlier paper and performing no better on the Fuji screen. The NH film, however, did perform well on the Fuji screen, slightly better than MinR film and at only about half the dose.

Table VI. Results from various types of cassette

Film	Screen	Cassette type					
		Plastic			Carbon fibre		
		Kodak	Agfa Detail	Cronex	Toshiba	X-Ograph[a]	X-Ograph[b]
MinR	MinR	52.2 ± 1.0	—	—	55.4 ± 0.7	53.7 ± 1.0	53.8 ± 0.6
MinR	Fuji HiMammo	56.0 ± 1.0[c]	—	—	55.0 ± 0.6	55.0 ± 1.0	55.5 ± 0.6
MinR	Agfa Detail	—	52.4 ± 0.5[d]	—	—	—	—
MinR	Cronex Ortho-Micro	—	—	54.8 ± 1.0	—	—	—
Cronex Micro	Cronex Ortho-Micro	—	—	51.8 ± 0.9	—	—	—
MinR	Toshiba MM	—	—	—	53.9 ± 0.5	—	—
Mean difference envelope-cassette		3.1 ± 1.1	2.5 ± 0.7	−0.2 ± 1.0	0.4 ± 0.5	1.1 ± 0.8	0.8 ± 0.5

[a] Toshiba front, X-Ograph back.
[b] Daylight model.
[c] Fuji screen loose on top of Kodak screen.
[d] Dose ratio, cassette/envelope, about 1.4; all others between 0.9 and 1.0.

In Table IV, the Trimax T2 screen is faster than the T1, and slightly faster than MinR, but both give poorer image quality on all three films. The MS film is faster than MinR and the SX315 faster again, but in each case the image quality is correspondingly poorer. Once more, the consistency of the differences between each pair of films and between each pair of screens is noteworthy and encouraging.

In Table V, the results from a miscellaneous group of products are shown. The films have already been considered. Of the screens, the Toshiba MM performed nearly as well as MinR when each was used with MinR film and with some reduction in dose. This Toshiba screen had its name marked in black lettering; another Toshiba MM screen with the name in gold letters performed very poorly. Toshiba are now believed to have ceased supplying screens. The X-Ograph S-100 screen was not outstanding in these tests, but two MinR films taken at another department with another screen of this type and sent to us for comment did score slightly better than two MinR–MinR films from that department (Lawinski, personal communication). The S-100 screen appears very slightly slower than MinR screens.

To sum up this part of the work, the best film–screen combination for image quality appears to be Fuji NH on Fuji Hi-Mammo screens. This combination was then compared with MinR–MinR on the original X-ray set and processor again, using a fresh supply of NH film and six different loose Hi-Mammo screens, and then on two entirely different X-ray sets, using different processors and different chemicals (Table VII). In all cases the advantage in image quality, slight though it sometimes was, lay with the Fuji combination. The relative dose required was even lower than given in Table III, slightly less than half that for MinR–MinR.

If dose reduction were the prime consideration, and image quality were ignored, the best combinations would probably be Agfa MR3 on Agfa Detail S screens, or the 3M film SX315 on MinR or Trimax T2 screens. Of these three, the Agfa combination gave the lowest image score and SX315 on MinR the highest, but all were below 50 and none of them is in any way recommended here.

To underline the importance of image quality in relation to patient dose, the relative numbers of cancers detected, and cancers which may be induced, should be considered. For a screened population of 1 million aged 50–64 years, about 2000 cancers will be detected at repeat examinations and over 5000 at first examination (Law, 1987). In contrast, the numbers induced are likely to be in the range 10–20 (depending on number of films, whether grid is used, etc.). Therefore, if image quality falls to the extent that the detection rate falls by 10%, many more cancers will be missed than would be avoided by cutting the radiation dose to zero.

Envelopes and cassettes

A direct comparison of MinR films and screens in envelopes and in Kodak MinR cassettes was reported in the course of work with a grid (Kirkpatrick & Law, 1985), and this showed a quite pronounced advantage to envelopes. In the present work (Table VI), this comparison was repeated and showed an even greater advantage to envelopes. The Agfa Detail cassette was compared with envelopes using Agfa Detail screens and MinR film; not only did envelopes give better image quality but also the cassette required a dose greater by about 40%.

Table VII. Further comparisons of Kodak MinR–MinR and Fuji NH–HiMammo film–screen combination

X-ray set	Processor and chemicals	Image score		
		MinR–MinR	NH–HiMammo	Difference, Fuji – Kodak
CGR 500t	Durr-Med 260, Kodak	55.3 ± 0.4[a]	56.0 ± 0.5[a]	0.7 ± 0.7[a]
CGR 500t	Durr-Med 260, Kodak	54.4 ± 0.4	55.9 ± 0.6	1.5 ± 0.7
Siemens Mammomat B	Agfa Curix 242S, Agfa Curix	54.3 ± 0.7	55.1 ± 0.4	0.8 ± 0.8
Philips Mammodiagnost	Fuji FPM 2100 May & Baker	55.2 ± 0.3	55.6 ± 0.3	0.4 ± 0.4

[a] Results from Table III; others were obtained later with a fresh batch of film.

Of the plastic cassettes reported here, only the Dupont Cronex could match envelopes fully in image quality, and it did so at the same dose. All three carbon-fibre-fronted cassettes gave similar image quality, at a level only slightly below that of envelopes and at very similar doses. Where cassettes give poorer image quality than envelopes, this may be because more radiation is scattered by their front surfaces, or because film–screen contact is poorer.

The conclusion here seems to be that users with an envelope system which is working well have no cause to change to cassettes. At the same time, the Dupont envelope system is apparently not being kept readily available, and repairs and spares may become a problem. Some mammography X-ray sets are made with cassette holders and these will be used more with the increasing use of grids. Envelopes may be difficult to position reliably in cassette holders, although two manufacturers can supply envelope platforms which fit their cassette holders. Cassettes are therefore likely to remain in general use, but at present only the Cronex model and those with carbon-fibre fronts are acceptable on grounds of image quality. There are, of course, many other criteria on which to choose a cassette. If a higher kV were used, this increase in dose would be reduced, but it would still be higher than for envelopes.

Conclusions

At the time of writing (May, 1988) the Fuji NH film–HiMammo screen combination is the only one showing an advantage over MinR–MinR both in image quality and in dose. This advantage has been shown with three different makes of processing chemicals. Several manufacturers, including Fuji, are about to produce further products, which means that any conclusion on the best available combination has to be provisional. It is also important to recognize that at least some manufacturers frequently modify their products but do not always make this plain to the user, either by changing the product name or otherwise. This is one more reason why quality assurance is so important. The good results with Fuji HiMammo screens were obtained with screens supplied loose and not fitted in cassettes.

The conditions under which this comparison was conducted were closely controlled to ensure that all the results are indeed comparable, but this does not remove the desirability of similar checks by others, although the difficulties and time involved should not be underestimated.

These results are presented at this time because the promise of new products is never absent and the quantity of data is already considerable. For practical reasons the X-ray set and processor used to obtain these results is unlikely to remain available for such work, and all further comparisons will be carried out elsewhere and hence will not be directly comparable with these.

Acknowledgments

All manufacturers and suppliers are thanked for making samples of their products so freely available to us. We also thank Mrs Isobel Massie, the Senior Mammography Radiographer, in the Royal Infirmary, Edinburgh, for her co-operation and forebearance in many practical ways.

References

ANONYMOUS, 1985. Screening for breast cancer (editorial). *Lancet, i*, 851–852.

FITZGERALD, M., WHITE, D. R., WHITE, E. & YOUNG, J., 1981. Mammographic practice and dosimetry in Britain. *British Journal of Radiology, 54*, 212–220.

KIRKPATRICK, A. E. & LAW, J., 1985. The usefulness of a moving grid in mammography. *British Journal of Radiology, 58*, 257–258.

——1987. A comparative study of films and screens for mammography. *British Journal of Radiology, 60*, 73–78.

LAW, J., 1987. Cancers induced and cancers detected in a mammography screening programme. *British Journal of Radiology, 60*, 231–235.

LAW, J. & KIRKPATRICK, A. E., 1988. Film processing in mammography. *British Journal of Radiology, 61*, 939–942.

ROEBUCK, E. J., 1986. Mammography and screening for breast cancer. *British Medical Journal, 292*, 223–226.

WHITE, D. R. & TUCKER, A. K., 1980. A test object for assessing image quality in mammography. *British Journal of Radiology, 53*, 331–335.

1989, *The British Journal of Radiology*, 62, 168–171

Case reports

Unusual long bone changes in thalassaemia: findings on plain radiography and computed tomography

By T. Singcharoen, MD

Department of Radiology, Faculty of Medicine, Chiangmai University, Chiangmai 50000, Thailand

(*Received March 1988*)

Bone change is one of the most outstanding radiological manifestations of marrow hyperplasia in thalassaemia. The "hair-on-end" skull, a variety of radiological changes of the ribs and osteoporosis with coarse trabeculation of other bones have been well described (Moseley, 1974; Lawson et al, 1981). We have encountered three thalassaemic patients with unusual marrow proliferation in the long bones of the extremities.

Case reports

Case 1

An 8-year-old boy had β-thalassaemia major diagnosed in early childhood. Haemoglobin levels ranged from 3 to 7 g/100 ml. Splenectomy was performed at 7 years of age. The patient still suffers from severe anaemia and frequent episodes of congestive heart failure. A plain radiograph of the skull showed widening of the diploic space with "hair-on-end" appearance, typical of thalassaemia (Fig. 1a). A chest radiograph revealed osteoporosis with coarse trabeculation of the bony thorax. Rib widening and soft-tissue masses at the anterior ends of some ribs were also observed (Fig. 1b). Plain radiographs of the extremities demonstrated cortical erosion with periosteal reaction in the humeri, tibiae, fibulae, ulnae, radii and small bones of the hands (Fig. 2). Computed tomography (CT) of the legs confirmed evidence of breaks in the cortex, proliferation of hyperplastic marrow outside the bony cortex and "hair-on-end" periosteal reaction (Fig. 3). A technetium-99m bone marrow scan also showed a marked increase in activity of marrow tissue in the extremities.

Case 2

A 12-year-old girl had β-thalassaemia haemoglobin E diagnosed at the age of 2 years. Haemoglobin levels ranged from 3.5 to 8 g/100 ml. Splenectomy was performed when she was 4 years old. Plain radiographs of the skull, chest and extremities demonstrated thalassaemic bone changes. Computed tomography of the thighs and legs revealed cortical breaches of the femora, tibiae and fibulae with evidence of marrow proliferation outside the cortex (Fig. 4). A chest CT scan showed extramedullary haemopoiesis in both anterior and posterior rib ends. Breakage of bony cortex in the humerus was incidentally observed (Fig. 5).

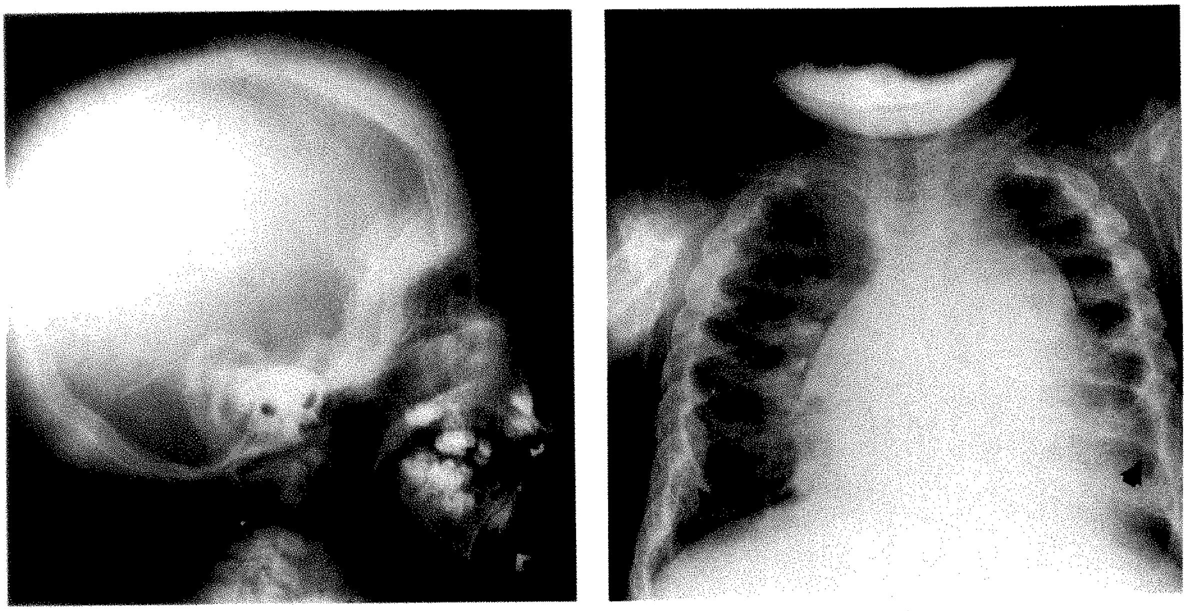

(a) (b)

Figure 1. (a) Lateral skull radiograph showing the "hair-on-end" appearance. (b) Chest radiograph showing thalassaemic changes in the bony thorax with extramedullary haemopoietic masses at the anterior ends of the ribs (arrows).

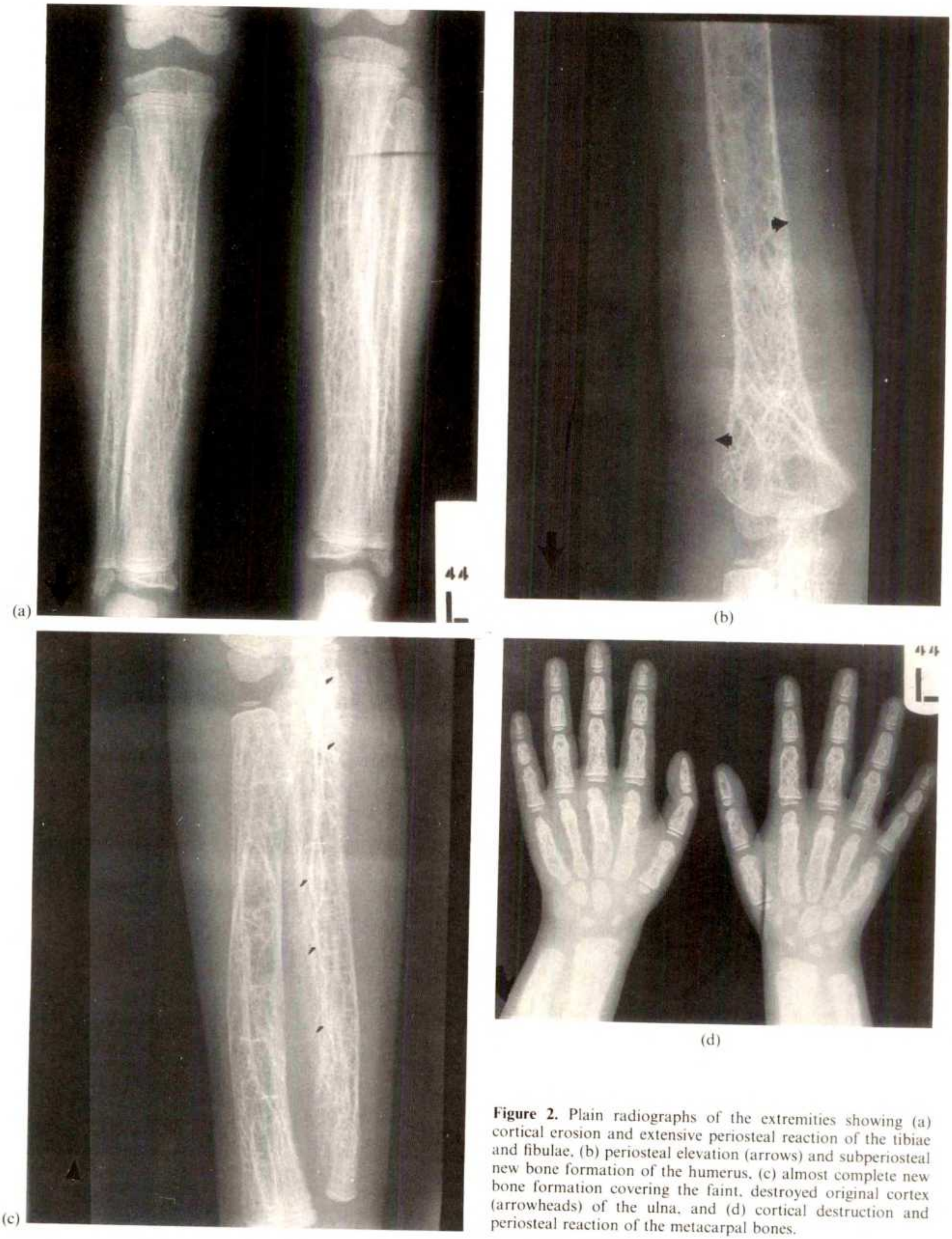

Figure 2. Plain radiographs of the extremities showing (a) cortical erosion and extensive periosteal reaction of the tibiae and fibulae, (b) periosteal elevation (arrows) and subperiosteal new bone formation of the humerus, (c) almost complete new bone formation covering the faint, destroyed original cortex (arrowheads) of the ulna, and (d) cortical destruction and periosteal reaction of the metacarpal bones.

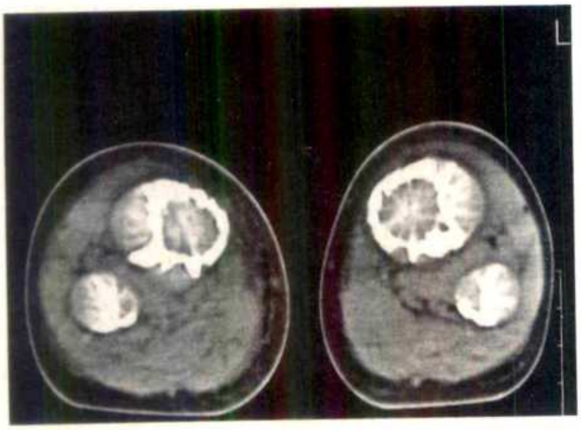

Figure 3. Computed tomographic scans of both legs demonstrate cortical destruction, extramedullary marrow proliferation and periosteal reaction of both tibiae and fibulae.

Case 3

An 11-year old boy was found to have β-thalassaemia major at the age of 3 years. Haemoglobin levels ranged from 3.2 to 7 g/100 ml. Splenectomy was performed when he was 11 years old. Plain radiographs of the skull, chest and extremities showed typical bone changes of thalassaemia and CT of the legs demonstrated early cortical breaks of the fibulae (Fig. 6).

Discussion

Thalassaemia is characterized by severe anaemia occurring early in life with bone changes and hepatosplenomegaly. The main problem is defective globin production, leading to ineffective erythropoiesis and anaemia. The bone changes occur as a result of bone marrow hyperplasia in response to anaemia.

In the skull, the diploic space is widened and the outer table thinned or obliterated. When the hyperplastic marrow perforates or destroys the outer table, it proliferates under the periosteum and new bone spicules are laid down perpendicular to the inner table, producing the "hair-on-end" skull (Moseley, 1974). A localized mass of intracranial extramedullary haemopoiesis with connection to the diploic space of the overlying skull has also been reported (Fucharoen et al, 1985).

In the thorax, marrow hyperplasia produces a wide spectrum of rib changes, including widening, osteoporosis, localized lucency, cortical erosions and "rib-within-a-rib" appearance (Lawson et al, 1981). Extramedullary haemopoietic masses can occur near both the posterior and anterior ends of the ribs; they are believed to represent an outgrowth or extrusion of the hyperplastic marrow from the medulla through the cortical defect, with subperiosteal proliferation (Long et al, 1980; Lawson et al, 1981; Papavasiliou et al, 1986).

In the extremities, the hyperplastic marrow destroys the finer bone trabeculae, thins the cortex and widens the medullary space. Cortical destruction and irregularity has been described only in the short tubular bones of the hands and feet (Moseley, 1974). In all of our cases, CT clearly demonstrates gross cortical destruction of major long bones. In Case 1, this is so obvious that it is well recognized on the plain radiograph but in the other two cases, the feature is shown only on the CT scan.

Proliferation of hyperplastic marrow outside the medullary cavity is demonstrated by CT in two cases. This marrow tissue appears to be confined to the area around the destroyed cortex, beneath a fat plane, suggestive of subperiosteal collection.

Although not a common feature in thalassaemia, in Case 1 several different patterns of periosteal reaction were observed. In the legs, extensive "hair-on-end" periosteal reaction was noted without a visible thin line of periosteum (Fig. 2a) whereas, in the humerus, there is

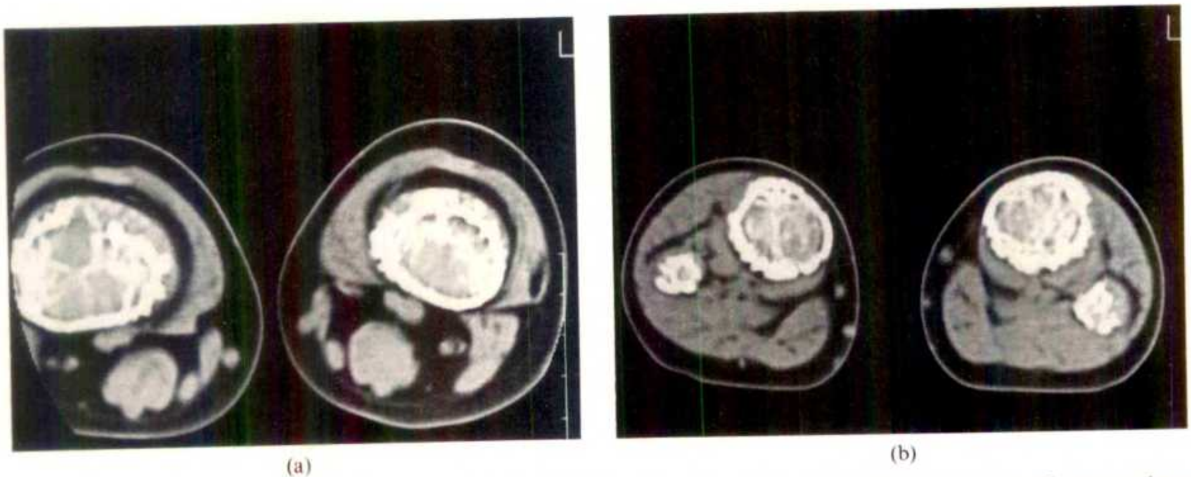

(a) (b)

Figure 4. Computed tomographic scans of the thighs and legs demonstrate cortical destruction and invasion of marrow tissue outside the medullary space in (a) femur and (b) tibia and fibula.

1989, *The British Journal of Radiology*, *62*, 171–173

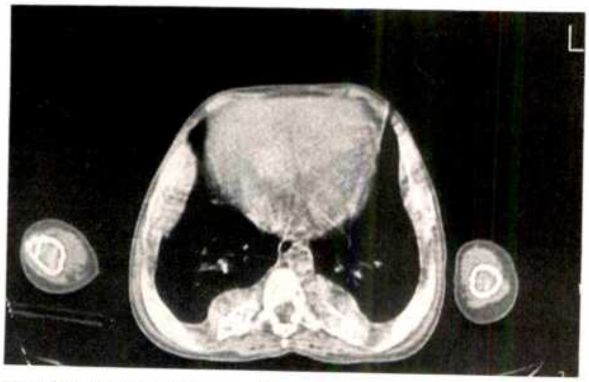

Figure 5. A chest CT scan shows extramedullary haemopoietic masses at both the anterior and posterior ends of the ribs. Early cortical erosion of the humerus was noted.

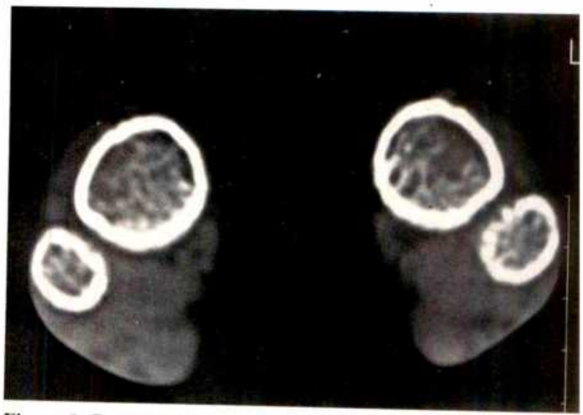

Figure 6. Computed tomographic scan of the legs showing early cortical erosion of the fibulae.

a white line of elevated periosteum bounding the subperiosteal new bone formation (Fig. 2b). Periosteal reaction is also seen around some metacarpal bones in the hands (Fig. 2d). In the forearm, the process appears to be at a more mature stage with a widened, newly formed cortex covering the faint original cortex (Fig. 2c).

Our findings indicate that, even in the major long bones, the hyperplastic marrow can erode the bony cortex and proliferate outside the medullary space causing periosteal elevation and reaction, similar to those observed in the skull and ribs. Widening of long bones in thalassaemia may be caused by extramedullary marrow proliferation with subperiosteal new bone formation as well as intramedullary marrow proliferation.

References

Fucharoen, S., Suthipongchai, S., Poungvarin, N., Ladpli, S., Sonakul, D. & Wasi, P., 1985. Intracranial extramedullary hematopoiesis inducing epilepsy in a patient with β-thalassemia-hemoglobin E. *Archives of Internal Medicine*, *145*, 739–742.

Lawson, J. P., Ablow, R. C. & Pearson, H. A., 1981. The ribs in thalassemia. II: The pathogenesis of the changes. *Radiology*, *140*, 673–679.

Long, J. A., Doppman, J. L. & Nienhuis, A. W., 1980. Computed tomographic studies of thoracic extramedullary hematopoiesis. *Journal of Computer Assisted Tomography*, *4*, 67–70.

Moseley, J. E., 1974. Skeletal changes in the anemias. *Seminars in Roentgenology*, *9*, 169–184.

Papavasiliou, C., Gouliamos, A. & Andreou, J., 1986. The marrow heteropia in thalassaemia. *European Journal of Radiology*, *6*, 92–96.

Sickle-shaped scapulae in a patient with the Pierre Robin syndrome

By Diran R. Bezirdjian, MD and Richard Szucs, MD

Medical College of Virginia Hospitals, Department of Radiology, Box 615, MCV Station, Richmond, Virginia 23298-0615, USA

(Received July 1988 and in revised form September 1988)

We report a patient with Pierre Robin syndrome who also has scapulae of an unusual appearance and speculate that this anomaly may represent yet another skeletal change to be associated with this syndrome. We reviewed the literature and did not find this association described previously.

Case report

A 5-year-old white girl was transferred to our institution after a 2-week hospitalization elsewhere for fever, cough, tachypnoea and wheezing. A chest radiograph on the day of admission to a community hospital showed infiltrates in the right middle and left lower lobes and the patient was started on antibiotics.

The diagnosis of Pierre Robin syndrome had been made at birth and there was a history of poor feeding and weight loss in early childhood. Surgical repair of a cleft palate was undertaken. She has also had several orthopaedic procedures to repair bilateral club foot deformity.

A chest radiograph on the day of transfer to our institution showed infiltrates in the right middle and both lower lobes. In addition, an unusual sickle-shaped deformity of both scapulae was noted (Figs 1, 2).

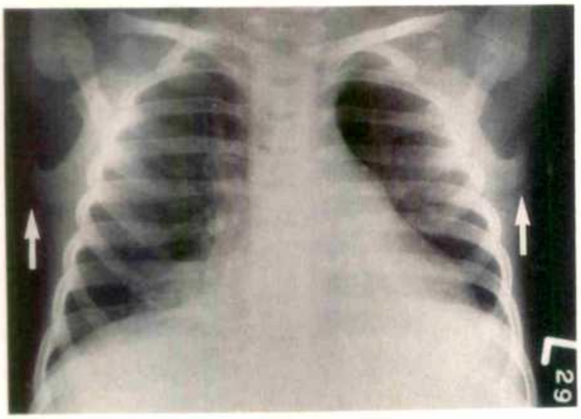

Figure 1. Chest radiograph showing infiltrates in the right middle and both lower lobes and hook-like processes arising from the inferior angle of both scapulae (arrows).

Discussion

The full-blown clinical picture of the Pierre Robin syndrome consists of the classical triad of micrognathia, cleft palate and glossoptosis (Randall et al, 1965). Hypoplasia of the mandible causes the tongue to drop backward against the posterior wall of the pharynx and predisposes to airway obstruction and feeding difficulties. The concern about these two problems was popularized by Pierre Robin himself. He postulated that this resulted in failure to gain weight and was the cause of death of several of his patients (Randall et al, 1965).

Although about 40% of children with this syndrome are free from skeletal defects, a wide variety of skeletal and developmental anomalies has been described in association with the Pierre Robin syndrome. Some of the skeletal changes have also been seen in patients who did not have all the manifestations of the syndrome but had isolated micrognathia or a cleft palate.

The skeletal abnormalities which have been reported in association with the Pierre Robin syndrome include a variety of limb anomalies ranging from a simple brachydactyly to femoral aplasia and amelia. Spondyloepiphyseal dysplasia congenita and diastrophic dwarfism have also been reported (Holthusen, 1972; Carey et al, 1982). In addition, more complex anomalies have been described including an association with cerebral maldevelopment and costal deficiency in the cerebro-costo-mandibular syndrome in which club foot deformity may be present (Silverman et al, 1980). Hyperphalangy and clinodactyly of the index finger have been linked together in the Catel-Manzke syndrome (Sundaram et al, 1982). A lethal X-linked syndrome of generalized dysostosis has been described (Carey et al, 1982). Non-skeletal deficiencies can also be present, most commonly mental retardation and cardiac anomalies.

There is a high association between the Pierre Robin syndrome and the Stickler syndrome, which includes, among other anomalies, cleft palate as well as arthropathy (Winter et al, 1983). Further association exists between the Pierre Robin syndrome and the Weissenbacher-Zweymuller and Marshall syndromes, which originally came under the Pierre Robin sequence defect because of the presence of micrognathia in addition to skeletal defects such as rhizomelic chondrodysplasia (Haller et al, 1975).

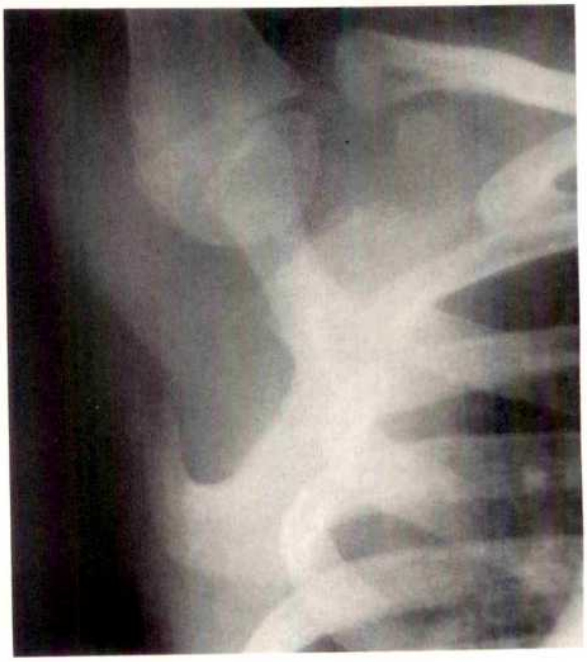

Figure 2. Close-up view of one scapula.

The patient described herein has features of the Pierre Robin syndrome with bilateral club foot deformity. In addition, there is a peculiar appearance of both scapulae, in the form of a hook-like process arising from their inferior angles, giving them the shape of a sickle.

To our knowledge such a scapular deformity has not been described previously. Whether this anomaly is related to the fact that the patient has Pierre Robin syndrome or merely represents a coincidental finding is unknown. However, this deformity is not thought to be of major clinical importance.

References

Carey, J. C., Fineman, R. M. & Ziter, F. A., 1982. The Robin sequence as a consequence of malformation, dysplasia and neuromuscular syndromes. *Journal of Pediatrics*, *101*, 858–864.

Haller, J. D., Berdon, W. E., Robinson, M., Slovis, T. L., Baker, D. H. & Johnson, G. F., 1975. The Weissenbacher-Zweymuller syndrome of micrognathia and rhizomelic chondrodysplasia at birth with subsequent normal growth. *American Journal of Roentgenology*, *125*, 936–943.

Holthusen, W., 1972. The Pierre Robin syndrome: unusual associated developmental defects. *Annales de Radiologie*, *15*, 253–262.

Randall, P., Krogman, W. M. & Jahina, S., 1965. Pierre

1989, *The British Journal of Radiology*, *62*, 173–174

Robin and the syndrome that bears his name. *Cleft Palate Journal*, *2*, 237–246.

Silverman, F. N., Strefling, A. M., Stevenson, D. K. & Lazarus, J., 1980. Cerebro-costo-mandibular syndrome. *Journal of Pediatrics*, *97*, 406–416.

Sundaram, V., Taysi, K., Hartmann, A. F., Shackelford, G. D. & Keating, J. P., 1982. Hyperphalangy and clinodactyly of the index finger with Pierre Robin anomaly: Catel-Manzke syndrome. A case report and review of the literature. *Clinical Genetics*, *21*, 407–410.

Winter, R. M., Baraitser, M., Laurence, K. M., Donnai, D. & Hall, C. M., 1983. The Weissenbacher-Zweymuller, Stickler, and Marshall syndromes: further evidence for their identity. *American Journal of Medical Genetics*, *16*, 189–199.

Re-irradiation of astrocytoma of the brain

By A. Y. Rostom, FRCR and K. Sunderland, FRCS

Regional Centre of Radiotherapy and Oncology, St Luke's Hospital, Warren Road, Guildford, Surrey GU1 3NT

(*Received June 1988 and in revised form July 1988*)

Astrocytoma of the brain in adults is invariably a fatal disease. The majority of cases present with inoperable, high-grade III or IV tumours. The place of radiotherapy in the management of such cases is of limited value. However, prolonged remission, and even occasional cures, have been reported (Sheline, 1977). Recurrence of high-grade astrocytoma long after surgery and/or radiotherapy is a rare event in clinical practice. Radical surgery has no place in such cases. Chemotherapy has also been tried with occasional transient success (Levin et al, 1980). Re-irradiation of selected cases has been tried in the past with occasional short remission in some patients (Dritschillo et al, 1981). We present the treatment result of a 36-year-old woman with recurrent Grade III astrocytoma, 9 years after initial biopsy and radiotherapy, who was given a second course of radiotherapy and chemotherapy.

Case report

In 1971, a 27-year-old woman presented with a 6-month history of episodes of black-outs lasting for up to 10 min at a time. Numb feeling on the left side of the face, arms and legs followed. She was occasionally incontinent of urine. She also had auditory hallucinations, repetitive speech and excessive lacrimation from the left eye. A few days earlier, she had had three episodes of left hemiparesis lasting for a few seconds. When examined there were no neurological signs. On isotope brain scan and carotid angiogram, a right temporal brain tumour was demonstrated. On 20 July 1971 partial excision of the tumour was carried out and a post-operative course of radiotherapy was given. A 250 kV machine (HVL 2.5 mm Cu) with a four-field technique was used, delivering a tumour dose of 4300 cGy in 23 fractions over 34 days. She remained well until 9 years later when she developed right temporal headaches of increasing severity, associated with dizziness. Clinically she had left upper motor facial weakness and left homonymous hemianopia. The power, tone and sensations were normal on the right with Grade 4+ weakness on the left side. There was impairment of the superficial sensations on the left and reflexes were brisk on that side also. The left plantars were equivocal on the right and extensor on the left. A computed tomography (CT) scan of the brain showed diffuse recurrence of the tumour in the right temporal lobe with deep infiltration and mid-line shift (Fig. 1). The clinical picture and the CT findings suggested chiasmal compression secondary to the right to left shift. The clinical picture and the radiological findings were consistent with recurrent astrocytoma. At this stage further radiotherapy was recommended and the patient subsequently received a further 5495 cGy tumour dose in 35 fractions over 58 days using two wedged fields, an anterior and right lateral on a cobalt machine. This was followed by six courses of chemotherapy using BCNU (100 mg) on Day 1 of

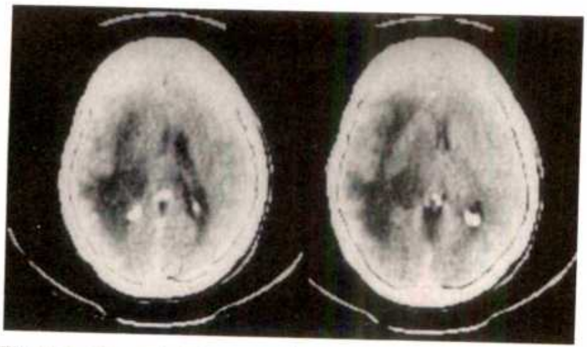

Figure 1. Computed tomography scan in 1981 shows diffuse recurrence of the right temporal lobe with deep infiltration and mid-line shift.

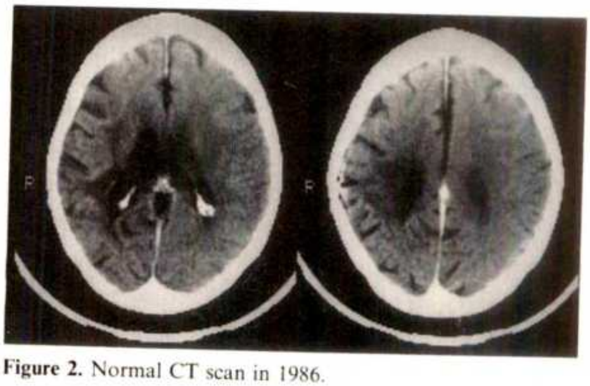

Figure 2. Normal CT scan in 1986.

each course, 2 mg vincristine Days 1 and 8, and procarbazine (50 mg) tds for 2 weeks. Courses were repeated every 6 weeks. Following the radiotherapy and chemotherapy the patient was completely symptom free and clinically there was only mild left-sided facial weakness. Figure 2 shows the CT scan appearance 5 years later. The patient remains well at the time of reporting, 7 years after the second treatment.

Discussion

Re-irradiation of recurrent brain tumours is very rarely used, but with high-grade astrocytoma it is often a palliative measure only, with patients living an average of 12 months following re-irradiation. Dritschilo et al (1981) reported 32 patients with various recurrent brain tumours who had undergone a second course of irradiation. Median survival for the entire group was 36 months from the completion of the second course of radiotherapy. Six patients in the group with Grade III and IV astrocytoma all died within 16 months. Horns and Webber (1967) reported 12 similar cases and half of these had significant palliation of symptoms but only two patients were alive at 3 years.

It appears from our case report and those reported in the literature that a second course of radiation can be given with reasonable chance of palliation and occasional prolonged survival. The addition of chemotherapy to radiation seems to be well tolerated, at least in the one patient reported here. To our knowledge, this is the longest surviving patient to be treated in this way, who remains well 7 years after the second treatment.

References

DRITSCHILO, A., BRUCKMAN, J. E., CASSADY, J. R. & BELLIA, J. A., 1981. Tolerance of brain to multiple courses of radiation therapy. Clinical experiences. *British Journal of Radiology*, *54*, 782–786.

HORNS, J. & WEBBER, M. M., 1967. Retreatment of brain tumours. *Radiology*, *88*, 322–325.

LE VIN, V. A., EDWARDS, M. S., WRIGHT, D. C., SEAGER, M. L., SCHIMBERG, T. P., TOWNSEND, J. J. & WILSON, C. B., 1980. Modified Procarbazine, CCNU & Vincristine combination chemotherapy in the treatment of malignant brain tumours. *Cancer Treatment Report*, *64*, 237–241.

SHELINE, G. E., 1977. Radiation therapy of brain tumours. *Cancer*, *39*, 873–881.

Autopsy assessment of the Gunther vena caval filter

By M. Mahendran, MB, MRCP, *D. J. Gwilt, DM, MRCP, FFARCS, O. P. Fitzgerald Finch, MB, FRCR and S. Jalloh, MB, MRCPath

Milton Keynes General Hospital, Standing Way, Milton Keynes, Buckinghamshire MK6 5LD

(Received April 1988 and in revised form July 1988)

The Gunther vena caval filter has been in clinical use for some years. Accounts of findings at post-mortem examination in animals are available (Gunther et al, 1985), but there are no detailed human autopsy reports.

We describe the findings at post-mortem examination of a patient who had a filter inserted 2 months prior to her death.

Case report

A 63-year-old lady had a history of recurrent deep venous thrombosis and pulmonary embolism, despite long-term anticoagulation therapy. She also had severe osteoarthritis of her hips, worse on the left, and needed a total hip replacement. Surgery had been deferred for 3 years because of concern about thromboembolism in the post-operative period, but it seemed reasonable to protect her with a Gunther vena caval filter and then proceed to surgery. A filter was inserted without difficulty and the patient discharged to await hip replacement.

Her anticoagulation therapy had to be withdrawn 6 weeks after this, as she developed a small spontaneous subdural haematoma. This was not evacuated, but was treated with dexamethasone and she recovered. However, 2 months after the filter was implanted the patient was admitted in severe respiratory distress. Because pulmonary embolism was possible, pulmonary angiography using digital subtraction techniques was performed. This showed no evidence of pulmonary emboli and it became clear that the patient had severe bronchopneumonia. She died a day after admission.

Pathology

Post-mortem examination revealed the following features.

(1) The filter was in position and firmly adherent to the wall of the inferior vena cava. There was no displacement and no gaps between filter and caval wall for emboli to pass through.

(2) Emboli were seen emerging from the common iliac veins extending up the inferior vena cava to the level of the filter. The clots were enmeshed within the filter, but there was no evidence of emboli proximal to the filter (Fig. 1).

(3) The caval wall was intact, with no evidence of perforation by the filter. However, there was complete destruction of the endothelial lining of the intima at the site of attachment of the anchoring limbs of the filter (Fig. 2).

(4) The pulmonary arteries appeared normal and extensive dissection of the pulmonary vessels demonstrated no emboli. There was severe pneumonia.

(5) There were no collaterals visible around the common iliac vein.

---

*Author for correspondence.

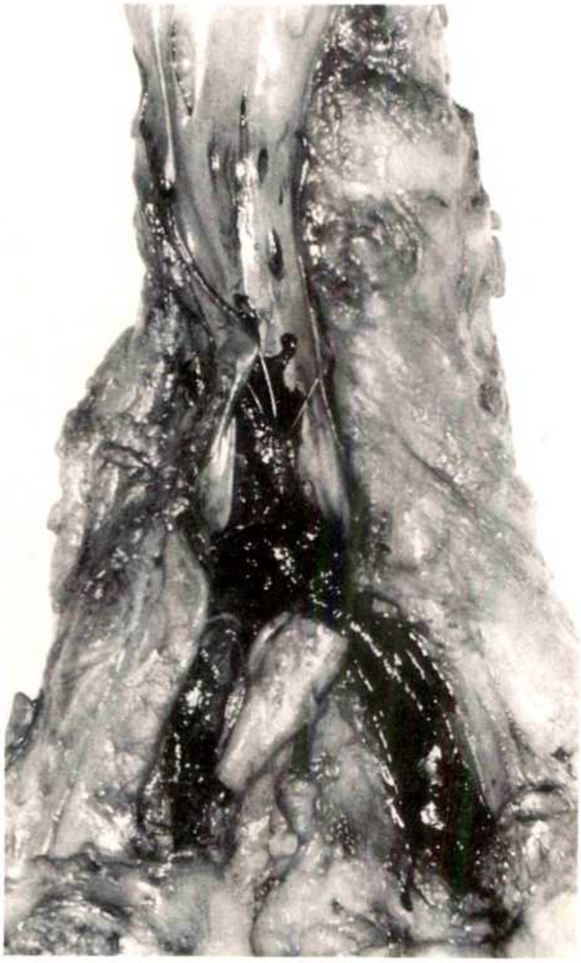

Figure 1. Photograph showing the two common iliac veins as they unite to form the inferior vena cava. In the lower portion of the vena cava is the basket filter with entrapped thrombi straddling the bifurcation and completely occluding the common iliac veins.

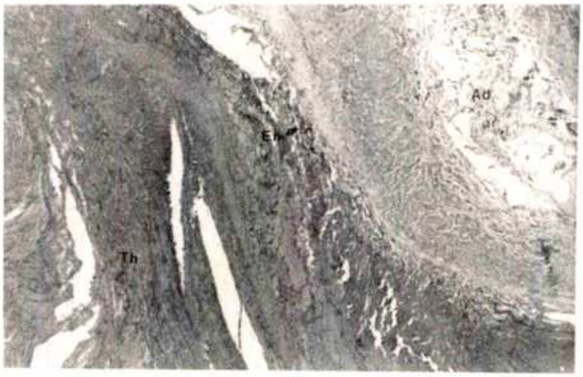

Figure 2. Photograph of a high-power view of the inferior vena caval wall shows complete destruction of the endothelial lining of the vein to which the thrombi are attached, and fragmentation of the elastic lamina in the wall of the vein. The adventitia remains intact. Th = thrombus; En = endothelium; Ad = adventitia.

Discussion

John Hunter tried to prevent pulmonary embolism by ligating the femoral vein in 1784. This was followed by caval ligation (Ochsner & DeBakey, 1943) and later by caval plication (De Weese & Hunter, 1958).

However, these procedures involved laparotomy and a search for less aggressive forms of treatment led to consideration of intravenous filters. The first permanent filter was devised by Mobin-Uddin et al (1969) and was followed by various devices, of which the Kimray-Greenfield filter is perhaps the most widely used (McCollum, 1987).

More recently, the Gunther caval filter has been used which has the advantages of easy insertion (Gunther et al, 1987), even by those with no previous experience of this type of filter (Mahendran et al, 1987). *In vitro* and animal studies have shown it to be an effective filter (Gunther et al, 1985), but there are no detailed human autopsy reports.

Our report highlights two important observations. First, it confirms the efficacy of the filter in clinical practice. Two months after implantation the filter was well positioned with no displacement, there were no gaps between the filter and the caval wall, and, although a major venous thrombus had formed and detached, all the thrombus was trapped in the filter with no angiographic or autopsy evidence of pulmonary embolism. Secondly, it shows that there was no serious damage to the vena caval wall. The anchoring legs were firmly adherent to the vessel wall and although there was marked intimal damage, there was no perforation or damage to the wall of the cava external to the intima.

This detailed autopsy analysis increases our confidence in this device.

References

De Weese, M. S. & Hunter, D. C., 1958. A vena caval filter for the prevention of pulmonary emboli. *Bulletin de la Société Internationale de Chirurgie*, *1*, 17–25.

Gunther, R. W., Schild, H., Fries, A. & Störkel, S., 1985. Vena caval filter to prevent pulmonary embolism: experimental study. *Radiology*, *156*, 315–320.

Gunther, R. W., Schild, H., Hollman, J. P. & Vorwerk, D., 1987. First clinical results with a new caval filter. *Cardiovascular and Interventional Radiology*, *10*, 104–108.

Mahendran, M., Fitzgerald Finch, O. P. & Gwilt, D. J., 1987. Pulmonary embolism, haematemesis and the Gunther vena caval filter. *British Journal of Radiology*, *60*, 595–596.

McCollum, C., 1987. Vena caval filters: keeping big clots down. *British Medical Journal*, *294*, 1566.

Mobin-Uddin, K., McLean, R. & Jude, J. R., 1969. A new catheter technique of interruption of inferior vena cava for prevention of pulmonary embolism. *American Surgeon*, *35*, 889–894.

Ochsner A. & DeBakey, M., 1943. Intravenous clotting and its sequelae. *Surgery*, *14*, 679–690.

1989, *The British Journal of Radiology*, 62, 176–177

Demonstration on computed tomography of tracheomalacia in tracheobronchomegaly (Mounier-Kuhn syndrome)

By Anthony James Doyle, MD

Department of Radiology, Medical University of South Carolina, 171 Ashley Avenue, Charleston, South Carolina 29425-0720, USA

(*Received June 1988 and in revised form August 1988*)

The appearances on computed tomography (CT) (Shin et al, 1988) and magnetic resonance imaging (MRI) (Rindsberg et al, 1987) in single cases of tracheobronchomegaly (TBM) have been described. These reports emphasize the tracheal and proximal bronchial dilatation with diverticulosis of the main bronchi. In a recent case examined by us, these features were also present but even more striking was extreme thinning and deformation of the tracheal wall and indentation anteriorly by the brachiocephalic artery. This finding reflects the tracheomalacia found in this condition. As in previously reported cases, TBM was first detected in this patient on CT after numerous negative chest radiographs.

Case report

A 27-year-old black man was seen for recurrent pneumonia. He had had five radiographically documented episodes over the past 4 years, all of which had been treated with antibiotics with prompt resolution. He had a 10-year history of cigarette smoking (one and a half packets per day). Chest radiographs showed right lower lobe consolidation.

Computed tomography revealed marked tracheobronchomegaly. The trachea measured 3.7 cm in transverse diameter at a point 2 cm above the aortic arch and 2.4 cm in antero-posterior (AP) diameter. The proximal right and left main bronchi measured 3 cm and 2.3 cm, respectively. Diverticulum formation was seen in the right main bronchus (Fig. 1a). The lobar bronchi were also slightly dilated, but the lung periphery showed no evidence of bronchiectasis. There was striking thinning of the tracheal wall with deformation and indentation by the brachiocephalic artery anterolaterally (Fig. 1b).

Discussion

Tracheobronchomegaly is best examined by cross-sectional imaging. The proximal airway dilatation and diverticulum formation described previously on plain radiographs and bronchography (Katz et al, 1962; Johnston & Green, 1965; Al-Mallah & Quantock, 1968; Himalstein & Gallagher, 1973; Bateson & Woo-Ming, 1973) can be demonstrated on CT and MRI (Rindsberg et al, 1987; Dunne & Reiner, 1988; Shin et al, 1988). Tracheomalacia as seen in this case correlates well with

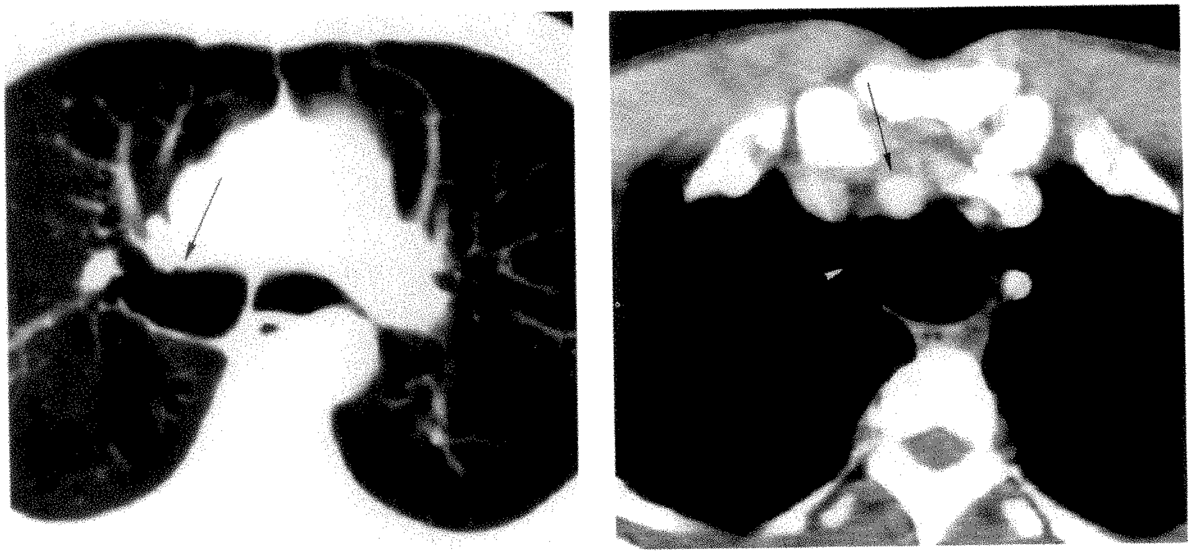
(a) (b)

Figure 1. (a) Contrast-enhanced CT scan of the chest just below the carina demonstrating the dilated right and left main bronchi with diverticulum formation on the right (arrow). (b) The greatly dilated trachea is seen just below the thoracic inlet with marked thinning of the wall (arrowhead) and considerable deformity caused by indentation of its anterior wall by the brachiocephalic artery (arrow).

the pathological data showing atrophy of the elastic and muscular tissue of the trachea and bronchi (Katz et al, 1962; Al-Mallah & Quantock, 1968; Gay & Dee, 1984).

Fundamental to the diagnosis of TBM is demonstration of a tracheal or central bronchial diameter exceeding that of the mean plus three standard deviations (Katz et al, 1962; Breatnach et al, 1984). This figure for the average of transverse and AP diameters of the trachea on CT is 2.18 cm (Vock et al, 1984). The average tracheal diameter in our case was 3.1 cm, easily meeting this criterion. No reliable figures are available for normal bronchial diameters on CT. Figures for right and left mainstem bronchi (mean + 3 SD) from bronchography are 2.40 and 2.30 cm, respectively (Katz et al, 1962). Other features of the syndrome are the abrupt transition from dilated to normal-size bronchi peripherally, the diverticulum formation in the bronchial walls and thinning and weakness of the tracheal wall pathologically reflected on bronchography by extreme deformability of the trachea (Katz et al, 1962; Al-Mallah & Quantock, 1968).

The aetiology and true incidence of TBM remain unknown and the natural history poorly understood. There is often a history of cigarette smoking (Katz et al, 1962; Dunne & Reiner, 1988; Shin et al, 1988) but this is by no means invariable and it seems likely that smoking and other irritants exacerbate the condition rather than cause it. There is an almost invariable history of chronic infection (Johnston & Green, 1965) but this could just as easily be the result as the cause of the widened airways, which clear secretions inefficiently (Al-Mallah & Quantock, 1968). A number of authors note the existence of TBM without clinical or pathological evidence of inflammation and point out that while chronic inflammatory lung disease is common, TBM is rare (Katz et al, 1962; Johnston & Green, 1965; Al-Mallah & Quantock, 1968; Himalstein & Gallagher, 1973). This further militates against TBM being an acquired disorder.

The consensus seems to be that there is a congenital anomaly, with or without overlying inflammatory changes (Katz et al, 1962; Johnston & Green, 1965; Al-Mallah & Quantock, 1968; Himalstein & Gallagher, 1973). Bateson and Woo-Ming (1973) argued against a congenital aetiology on the grounds that TBM tends to present in the third decade or later; however, so do other congenital lesions such as polycystic kidney and Huntington's chorea. Johnston and Green (1965) suggested an autosomal recessive pattern of inheritance, but family studies have been limited. An association with Ehlers-Danlos syndrome has been reported (Aaby & Blake, 1966; Wanderer et al, 1969). Use of CT in patients with unexplained recurrent pulmonary infection to search for anatomical abnormalities should lead to detection of more cases and a better understanding of TBM.

References

AABY, G. V. & BLAKE, H. A., 1966. Tracheobronchiomegaly. *Annals of Thoracic Surgery*, *2*, 64–70.

AL-MALLAH, Z. & QUANTOCK, O. P., 1968. Tracheobronchomegaly. *Thorax*, *23*, 320–324.

BATESON, E. M. & WOO-MING, M., 1973. Tracheobronchomegaly. *Clinical Radiology*, *23*, 354–358.

BREATNACH, E., ABBOTT, G. C. & FRASER, R. G., 1984. Dimensions of the normal human trachea. *American Journal of Roentgenology*, *141*, 903–906.

DUNNE, M. G. & REINER, B., 1988. CT features of tracheobronchomegaly. *Journal of Computer Assisted Tomography*, *12*, 388–391.

GAY, S. & DEE, P., 1984. Tracheobronchomegaly—the Mounier-Kuhn syndrome. *British Journal of Radiology*, *57*, 640–644.

HIMALSTEIN, M. R. & GALLAGHER, J. C., 1973. Tracheobronchiomegaly. *Annals of Otology, Rhinology, and Laryngology*, *82*, 223–227.

JOHNSTON, R. F. & GREEN, R. A., 1965. Tracheobronchiomegaly: report of five cases and demonstration of familial occurrence. *American Review of Respiratory Disease*, *91*, 35–50.

KATZ, I., LEVINE, M. & HERMAN, P., 1962. Tracheobronchiomegaly. The Mounier-Kuhn syndrome. *American Journal of Roentgenology*, *88*, 1084–1094.

RINDSBERG, S., FRIEDMAN, A. C., FIEL, S. B. & RADECKI, P. D., 1987. MRI of tracheobronchomegaly. *Journal of the Canadian Association of Radiologists*, *38*, 126–128.

SHIN, M. S., JACKSON, R. M. & HO, K. J., 1988. Tracheobronchomegaly (Mounier-Kuhn syndrome): CT diagnosis. *American Journal of Roentgenology*, *150*, 777–779.

VOCK, P., SPIEGEL, T., FRAM, E. K. & EFFMANN, E. L., 1984. CT assessment of the adult intrathoracic cross section of the trachea. *Journal of Computer Assisted Tomography*, *8*, 1076–1082.

WANDERER, A. A., ELLIS, E. F., GOLTZ, K. W. & COTTON, E. K., 1969. Tracheobronchiomegaly and acquired cutis laxa in a child. Physiologic and immunologic studies. *Pediatrics*, *44*, 709–715.

1989, *The British Journal of Radiology*, *62*, 178–180

Lipoma arborescens of the knee

By S. J. Armstrong, MRCP and I. Watt, MRCP, FRCR

Department of Radiodiagnosis, Bristol Royal Infirmary, Bristol BS2 8HW

(*Received August 1988 and in revised form October 1988*)

Lipoma arborescens is a rare intra-articular lesion, consisting of collections of fat beneath the synovial lining producing clusters of swollen villous projections. It macroscopically resembles pigmented villonodular synovitis, but is macroscopically and histologically different from a synovial lipoma. Histologically, lipoma arborescens is indistinguishable from other collections of subsynovial fat, the only differences being its large size and frond-like macroscopic appearance. The alternative name of "villous lipomatous proliferation of the synovial membrane" has been suggested (Hallel et al, 1988).

Case report

A 52-year-old man was seen in outpatients as a newly diagnosed diabetic. On examination he was found to have a swollen right knee joint (Fig. 1). The patient confirmed that his knee had been swollen for several years and he related this to an old twisting injury. He had declined investigation of the swelling in the past. The clinician diagnosed an effusion of the knee joint. Joint fluid was aspirated and sent for laboratory analysis. A radiograph of the knee and a rheumatological opinion were requested.

The radiograph of the knee (Fig. 2) showed a well defined soft-tissue mass in the region of the suprapatellar pouch. Degenerative changes in the patello-femoral joint were also noted. The joint aspirate revealed occasional lipid globules and white cells containing lipid globules. No crystals or organisms were found.

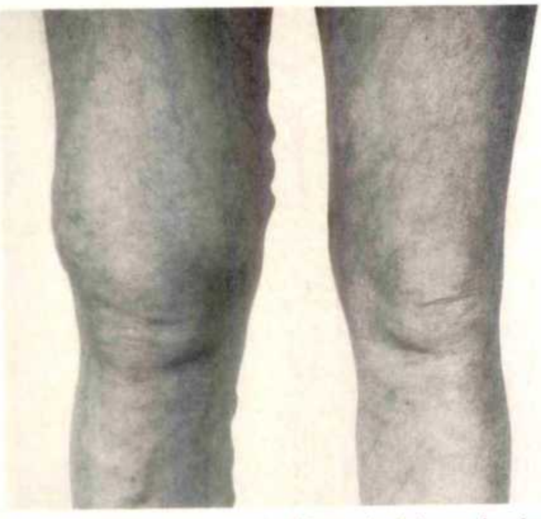

Figure 1. Clinical photograph of the patient's knees showing the degree of enlargement of the right knee.

A single-contrast arthrogram of the right knee (Fig. 3) demonstrated a frond-like mass of lipid density within the suprapatellar pouch. There was also a substantial popliteal cyst.

A computed tomographic (CT) scan (Fig. 4) confirmed a large joint effusion and the presence of lipoma arborescens in the suprapatellar pouch. The popliteal cyst was also demonstrated.

Discussion

Twelve cases of true lipoma arborescens have been described in the literature. The age range of these cases varied from 9 to 66 years, and 10 were male and two female. The joints involved included the knee joint in six cases unilaterally (Weitzman, 1965; Coventry et al, 1966; Hermann & Hockberg, 1980; Hallel et al, 1988) and

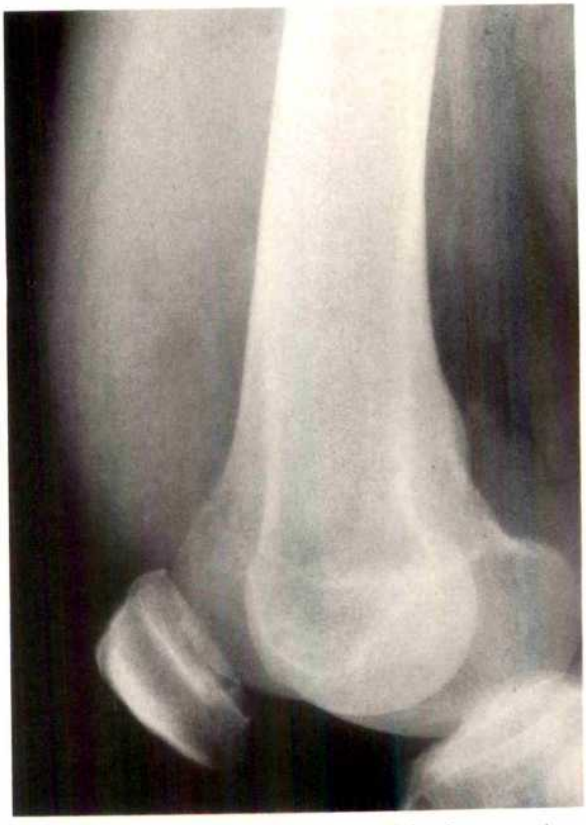

Figure 2. Lateral radiograph of right knee joint demonstrating a lobulated mass of low density in the suprapatellar pouch.

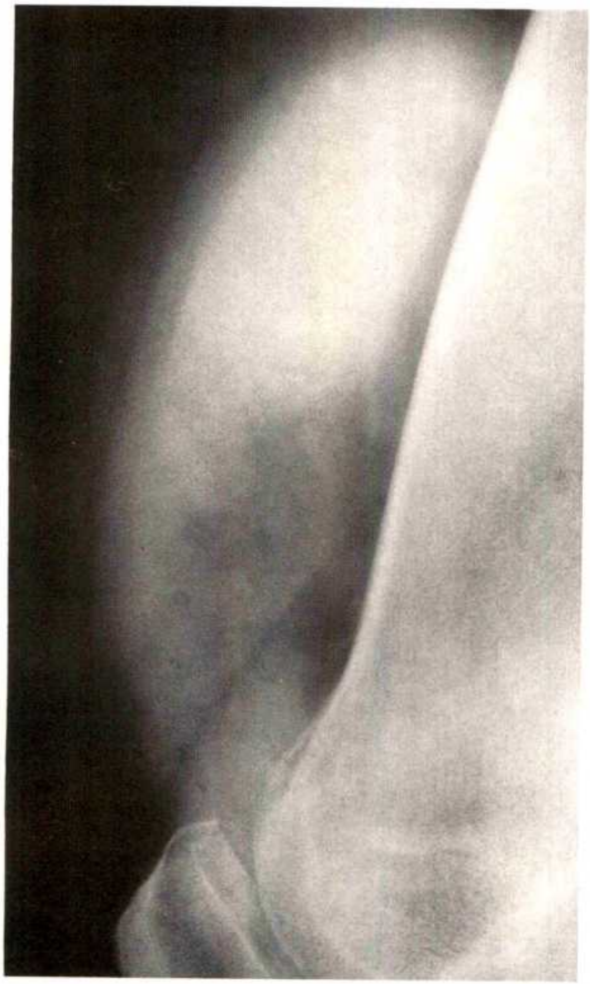

Figure 3. Single-contrast arthrogram of right knee showing contrast medium outlining the frond-like low-density lesion.

three bilaterally (Arzimanoglu, 1957; Hallel et al, 1988), the wrists bilaterally in one case (Napolitano, 1957), the hip unilaterally in another (Noel et al, 1987) and multiple joints in the final case (Gaede, 1961).

Lipoma arborescens is of unknown aetiology. Most appear to arise *de novo*, although there are associations with degenerative joint disease, chronic rheumatoid arthritis and trauma. It is generally regarded as benign and no malignant lesions have been reported.

The typical clinical presentation is of painless joint swelling over many years, accompanied by intermittent effusion. The knee joint is most commonly involved, with a predilection for the suprapatellar pouch. Laboratory tests, including erythrocyte sedimentation rate and serological tests for rheumatoid factor and serum uric acid, are normal. The joint aspirate does not show crystals or cells and culture is sterile. The recommended treatment is synovectomy.

One case showed recurrence following resection (Coventry et al, 1966). There was usually restriction of joint movement. At the time of diagnosis one case was suggested to be tuberculous infection, and in two cases (including that of multiple joint involvement) a generalized systemic chronic synovitis was postulated.

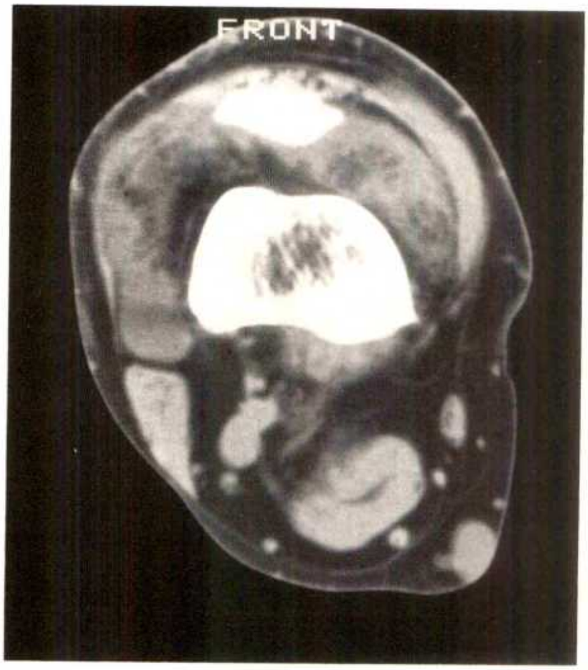

Figure 4. Computed tomographic scan of the right knee confirming the fatty nature of the mass and demonstrating its synovial origin. A joint effusion is also present.

Other lipomatous lesions within the knee joint have been described and given the name of lipoma arborescens, but these lack the characteristic macroscopic appearance and are likely to represent organized collections of synovial fat in association with meniscal injury or other trauma (Placeo & Tassi, 1953). These fatty collections are not related to true lipoma arborescens.

Computed tomography was not necessary to make the diagnosis in the present case as this had been made by plain radiography, but CT was of value in confirming the synovial site of origin of the lesion and in demonstrating its extent. The characteristic frond-like appearance was readily appreciated on CT. Another value of CT is in differentiating lipoma arborescens from pigmented villonodular synovitis. The former is of low attenuation value because of its fat content and would not be expected to enhance following intravenous injection of contrast medium. The latter is usually of high attenuation value because of its iron content, does not contain fat and enhances following injection of contrast medium. The differential diagnosis also includes synovial chondromatosis and synovial haemangiomatosis, both of which can cause painless effusion and synovial thickening without systemic involvement.

The suggested treatment of lipoma arborescens is synovectomy. This is successful in preventing the recurrence of effusions. Only one of the reported lesions (Coventry et al, 1966) recurred following synovectomy during a period of follow-up ranging from 1 to 11 years. This case was successfully treated by repeat synovectomy.

References

ARZIMANOGLU, A., 1957. Bilateral arborescent lipoma of the knee. A case report. *Journal of Bone and Joint Surgery, 39,* 976–977.

COVENTRY, M. B., HARRISON, E. G. & MARTIN, J. F., 1966. Benign synovial tumours of the knee: a diagnostic problem. *Journal of Bone and Joint Surgery, 7,* 1350–1358.

GAEDE, E. A., 1961. Ein fall von synovitis chronica villosa generalisata. *Archiv Orthopädic Unfallchirurgie, 53,* 315–319.

HALLEL, T., LEW, S. & BANSAL, M., 1988. Villous lipomatous proliferation of the synovial membrane (lipoma arborescens). *Journal of Bone and Joint Surgery, 70A,* 264–270.

HERMANN, G. & HOCHBERG, F., 1980. Lipoma arborescens: arthrographic findings. *Orthopedics, 3,* 19–21.

NAPOLITANO, A., 1957. Il lipoma arborescente della synoviale; contributo clinico di un caso a localizzazione nella synoviale. *Progresso Medico, 13,* 109–118.

NOEL, E. R., TEBIB, J. G., DUMONTET, CH., COLSON, F., CARRET, J. P., VAUZELLE, J. L. & BOUVIER, M., 1987. Synovial lipoma arborescens of the hip. *Clinical Rheumatology, 6,* 92–96.

PLACEO, F. & TASSI, D., 1953. Considerazioni cliniche su 62 osservazioni di lipoma arborescente posttraumatico del ginocchio come entita patologica a se stante ed associata a lesione meniscale. *Minerva Chirurgica, 8,* 316–322.

WEITZMAN, G., 1965. Lipoma arborescens of the knee. Report of a case. *Journal of Bone and Joint Surgery, 47A,* 1030.

Cystic haemangioma of the spleen: findings on ultrasound and computed tomography

By M. J. Duddy, FRCR and *C. J. Calder, MB, BS

Departments of Radiology and *Pathology, Walsgrave Hospital, Coventry CV2 2DX

(Received June 1988 and in revised form August 1988)

A case of cystic haemangioma of the spleen is reported. Although haemangioma is the commonest benign tumour of the spleen, the majority are of the small capillary type found incidentally at autopsy. Symptomatic cystic haemangioma is rare. Even less common is the diagnosis considered pre-operatively. This has been facilitated in recent years by non-invasive imaging modalities.

The appearances on computed tomography (CT) and ultrasound and the duplex ultrasound properties are described and correlated with the pathological findings. The use of duplex ultrasound has not previously been reported for this tumour.

Case report

A 27-year-old caucasian woman presented complaining of left hypochondrial pain on sexual intercourse. She also complained of gastric fullness and vomiting. She had had two normal deliveries, the most recent being 13 months previously. She was found clinically to have moderate splenomegaly.

Full blood count, biochemical profile and a chest radiograph were all normal. An ultrasound scan (Siemens Sonoline SL-2) showed an enlarged spleen containing many cystic spaces, the majority of which were anechoic (Fig. 1). Others were of mixed echogenicity or homogeneously echogenic (Fig. 2). Duplex Doppler ultrasound examination of the spleen was subsequently performed (Hewlett-Packard 77020) which showed a strong Doppler signal from the remaining splenic parenchyma but no detectable flow was recorded from any of the cystic spaces.

Computed tomography showed an enlarged spleen displacing the stomach and containing multiple, well defined, rounded, low-attenuation lesions (Fig. 3). A pre-operative diagnosis was made of cystic haemangioma or lymphangioma.

At splenectomy, a 1200 g, firm, irregular spleen was removed measuring 18 cm × 12 cm × 8 cm. The splenic parenchyma was almost completely replaced by multiple cysts (Fig. 4); these were thin-walled and measured up to 4 cm in diameter. Most contained a yellow, serous fluid and correlated with the

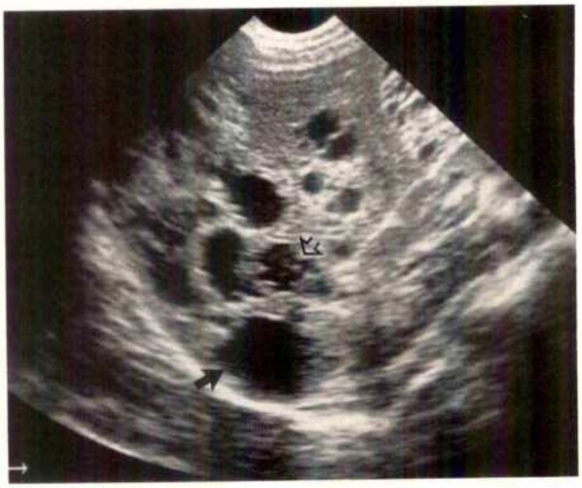

Figure 1. Longitudinal ultrasound scan of the spleen showing anechoic cysts (solid arrow) and lesions of mixed echogenicity (open arrow).

Correspondence address: Dr M. J. Duddy, Department of Radiology, Queen Elizabeth Hospital, Edgbaston, Birmingham.

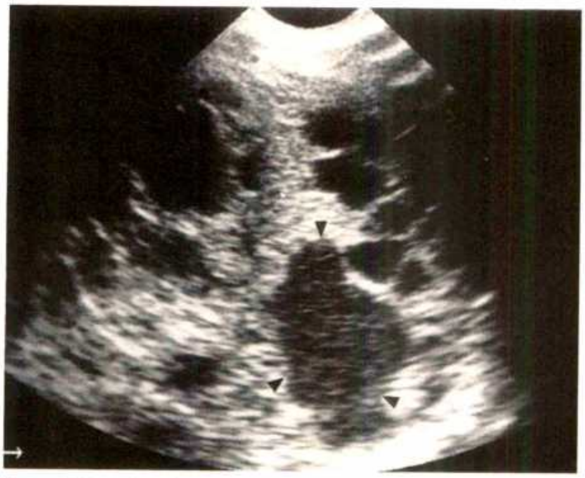

Figure 2. Longitudinal ultrasound scan of the spleen showing a homogeneously echogenic cavity (arrowheads).

anechoic lesions seen on ultrasound. Some cysts were loculated by fibrous septa, represented on ultrasound by lesions of mixed echogenicity. The homogeneously echogenic lesions seen represented cavities containing gelatinous material. There appeared to be no communication between these discrete cysts. Histology showed numerous cystic spaces lined by a flattened vascular endothelium. Many cysts contained abundant erythrocytes whilst others contained an eosinophilic proteinaceous material. The appearances were those of cystic haemangioma (Fig. 5).

Discussion

The spleen is the least common abdominal organ to develop cystic disease. The following causes should be considered.

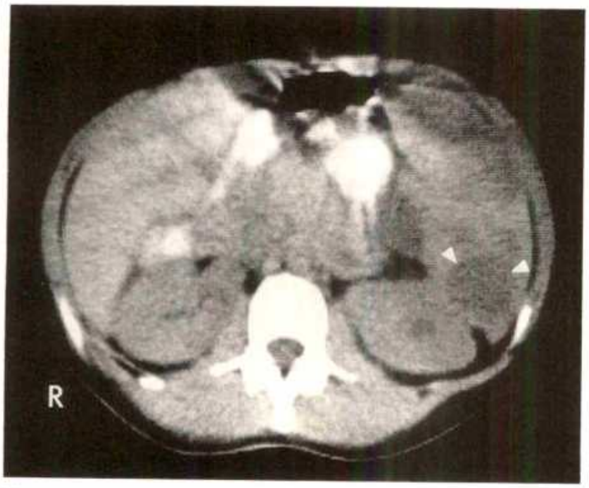

Figure 3. Computed tomographic scan of the upper abdomen showing an enlarged spleen containing rounded, well defined, low-attenuation defects (arrowheads).

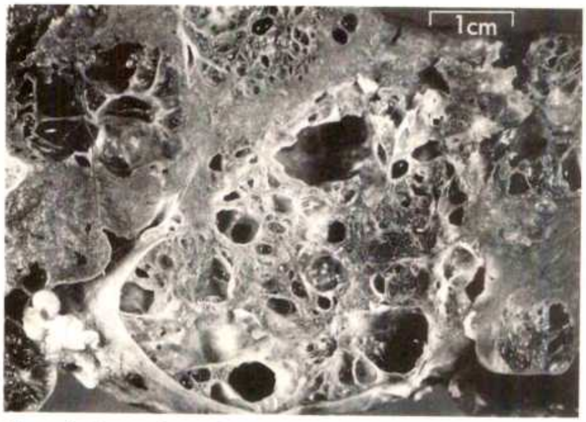

Figure 4. Cut surface of the spleen showing replacement of the parenchyma by cysts.

1. Hydatid.
2. Primary cysts: (a) endothelial lined (haemangioma, lymphangioma) or (b) epithelial lined (dermoid, epidermoid, transitional cell).
3. Post-traumatic.

The appearances on CT and ultrasound of the endothelial lined cysts have been previously reported. Computed tomography of cystic haemangioma (Moss et al, 1986) and cystic lymphangioma (Clark et al, 1983) may be indistinguishable. Dynamic CT has been reported of a splenic cavernous haemangioma (Päivänsalo & Siniluoto, 1985). The pattern of enhancement was similar to that described for hepatic cavernous haemangioma (Johnson et al, 1981). However, their tumour was not cystic on ultrasound and cystic haemangiomas are often avascular (Husni, 1961).

Manor et al (1984) described three types of lesion on ultrasound of a splenic cystic haemangioma: (a)

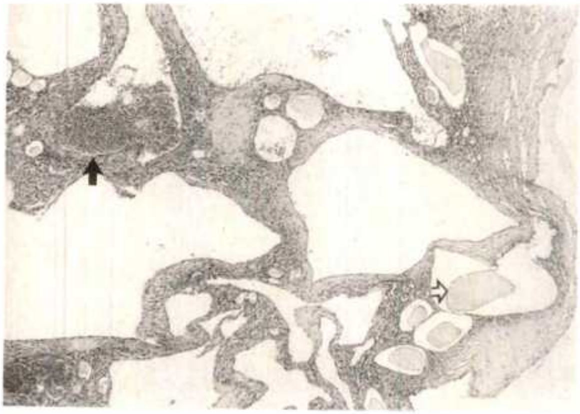

Figure 5. Photomicrograph (haematoxylin and eosin × 22) showing endothelial lined cysts. Some contain erythrocytes (solid arrow) and others contain an eosinophilic proteinaceous substance (open arrow).

sonolucent, representing serous, fluid-filled cysts, (b) echodense, representing capillary haemangiomas and (c) mixed, representing clot-filled cavities. Similar ultrasound appearances have been ascribed to cystic lymphangioma (Clark et al, 1983). Both cystic haemangioma (Manor et al, 1984) and cystic lymphangioma (Pearl & Nassar, 1979) often have cavities containing serous fluid and others containing gelatinous material. Lymphangiomas are said to develop in the subcapsular region of the spleen (Pearl & Nassar, 1979). However, its site of origin may be obscure when large and replacing much of the splenic substance.

The pathological distinction can also be difficult. Willis (1962) described cystic changes in splenic cavernous haemangioma thus emphasizing the similarity with cystic lymphangioma. Moreover, the two lesions may occur simultaneously (Stanley, 1966). In this case the finding of abundant erythrocytes in many of the cysts (Rappaport, 1966) and the lack of communication between the cysts (Kings, 1975) would strongly indicate that this is a haemangioma.

Although a benign tumour, the splenic haemangioma is associated with life-threatening complications. Husni (1961) reviewed the 56 cases reported up to that date and found that 25% had presented with an abdominal catastrophe due to spontaneous splenic rupture. Sarcomatous transformation has also been reported (Husni, 1961) but the incidence of this is not known.

Acknowledgments

The authors wish to thank Mr D. A. K. Woodward for granting permission to record the case report, Dr A. W. Robinson for his helpful comments and the medical photography staff at Coventry and Warwickshire hospital.

References

CLARK, M. A., GARVIN, D. F., PYATT, R. S. & MARSHALL, D. P., 1983. Multicystic lymphangioma of the spleen: case report. *Military Medicine, 148*, 54–55.

HUSNI, E. A., 1961. The clinical course of splenic hemangioma. *Archives of Surgery, 83*, 681–687.

JOHNSON, C. M., SHEEDY, P. F., STANSON, A. W. & STEPHENS, D. H., 1981. Computed tomography and angiography of cavernous hemangioma of the liver. *Radiology, 138*, 115–121.

KINGS, G. L. M., 1975. Multifocal haemangiomatous malformation: a case report. *Thorax, 30*, 485–488.

MANOR, A., STARINSKY, R., GARFINKEL, D., YONA, E. & MODAI, D., 1984. Ultrasound features of symptomatic splenic hemangioma *Journal of Clinical Ultrasound, 12*, 95–97.

MOSS, C. N., VAN DYKE, J. A., KOEHLER, R. E. & SMEDBERG, C. T., 1986. Multiple cavernous hemangiomas of the spleen: CT findings. *Journal of Computer Assisted Tomography, 10*, 338–340.

PÄIVÄNSALO, M. & SINILUOTO, T., 1985. Cavernous haemangioma of the spleen. *Fortschritte auf dem Gebiete der Röntgenstrahlen und der Nuklearmedizin, 142*, 228–230.

PEARL, G. S. & NASSAR, V. H., 1979. Cystic lymphangioma of the spleen. *Southern Medical Journal, 72*, 667–669.

RAPPAPORT, H., 1966. Tumours of the haemopoietic system. *Armed Forces Institute of Pathology, Section III*, fascile 8, 358–359.

STANLEY, K. E., 1966. Hemangioma-lymphangioma of the bladder in a child: report of a case with associated hemangioma of the external genitalia. *Journal of Urology, 96*, 51–54.

WILLIS, R. A., 1962. *The Borderland of Embryology and Pathology*, 2nd edn (Butterworth, London), pp. 354–355.

1989, *The British Journal of Radiology*, *62*, 183–184

Case of the month

The jockey with a mass in the thigh

By A. M. Davies, DMRD, FRCR, N. Evans, FRCR and R. J. Grimer, FRCS

Department of Radiology, Royal Orthopaedic Hospital, Birmingham

(*Received February 1988*)

A 40-year-old professional jockey presented with a 2-week history of severe pain in the right knee region which commenced whilst riding. Examination revealed a firm mass, 10 cm × 5 cm, within the soft tissues of the medial aspect of the right distal thigh. All laboratory investigations were normal. The radiological investigations of the right femur included plain radiography (Fig. 1) and computed tomography (CT) (Fig. 2). A bone scan revealed a solitary, non-homogeneous area of increased uptake in the right distal femur.

What is your diagnosis?

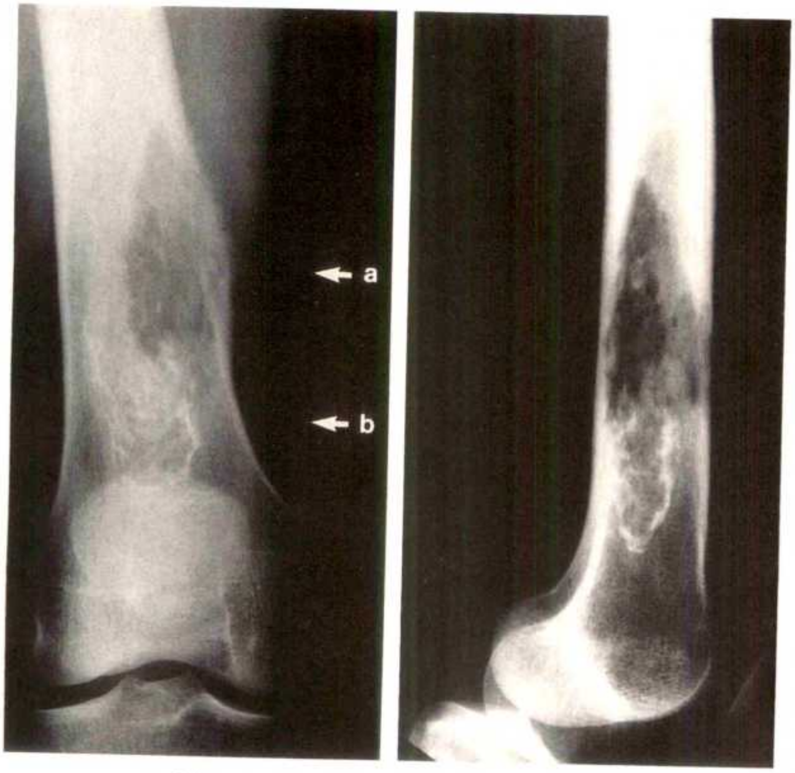

(a) (b)

Figure 1

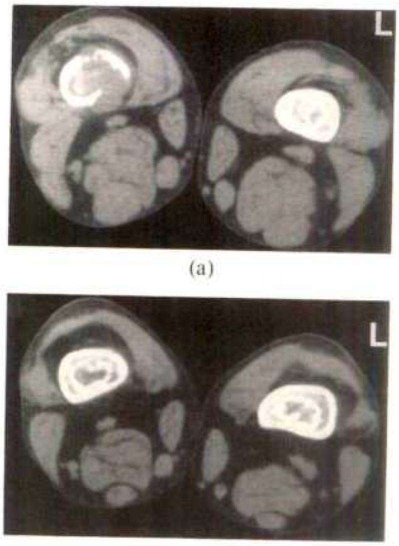

(a)

(b)

Figure 2

Figure 1. (a) Antero-posterior and (b) lateral radiographs of the right distal femur.

Figure 2. Two representative slices from the axial CT of the distal femora. The approximate levels of (a) and (b) are indicated by the arrows on Fig. 1a.

Address for correspondence: Dr A. M. Davies, Department of Radiology, Royal Orthopaedic Hospital, Woodlands, Northfield, Birmingham B31 2AP.

The plain radiographs (Fig. 1) show an extensive abnormality of the distal femoral meta-diaphysis. Superiorly there is a lytic, permeative lesion breaching the medial cortex with minimal periosteal reaction. The cortical defect is associated with a soft-tissue mass, confirmed by CT, which also shows soft tissue within the medullary canal (Fig. 2a).

The radiological features are those of a malignant lesion and the differential diagnosis includes malignant fibrous histiocytoma, fibrosarcoma, lytic osteosarcoma, reticulum cell sarcoma (primary malignant lymphoma) or metastasis. Inferiorly, however, the lesion consists of medullary calcification with a serpiginous margin typical of a long-standing medullary infarct. This latter observation effectively reduces the differential diagnosis down to one single probable entity and that is a malignant fibrous histiocytoma (MFH) arising in a bone infarct. This is a rare, but well recognized, complication of chronic medullary infarction and this was subsequently confirmed histologically by biopsy.

Another diagnosis that might be considered is malignant degeneration in a benign cartilage tumour but the medullary calcification would be expected to be central and punctate rather than peripheral and curvilinear as seen in a typical infarct. The presence of symmetrical lesions is also more in favour of infarction than chondroid tumours and the observant reader will have noted that on the CT scan the intramedullary calcification is also present on the left (Fig. 2). A plain radiograph of the left femur confirms that the infarcts are bilateral and symmetrical (Fig. 3).

Malignant fibrous histiocytoma, although a relatively common sarcoma of soft tissues, represents only about 5% of all primary malignant bone tumours (Boland & Huvos, 1986). Radiologically this highly aggressive tumour is indistinguishable from a fibrosarcoma and differentiation between the two relies on histological examination. Approximately 20–25% of MFHs have been shown to arise in pre-existing bone abnormalities (Capanna et al, 1984). These include bone infarction, irradiated bone, Paget's disease, enchondroma, fibrous dysplasia and tissue adjacent to prosthetic joint replacements (Mirra et al, 1974; Heselson et al, 1983; Capanna et al, 1984; Tait et al, 1988). Those patients with an MFH arising in a pre-existing bone abnormality tend to be older, aged over 40 years and have a poorer prognosis than those with an MFH arising in previously normal bone.

The majority of malignant tumours arising in bone infarcts are MFHs although other tumours such as fibrosarcoma and osteosarcoma have been described (Mirra et al, 1974). This rare association is not thought to be a coincidental occurrence but to be a true causal relationship. The generally accepted hypothesis is that the MFH arises from primitive mesenchymal cells in the chronic reparative tissue around the periphery of an area of bone infarction (Heselson et al, 1983). There is a long latent period before such malignant transformation may occur. Three former caisson workers who presented with this complication had all left their employment approximately 20 years before (Mirra et al, 1974).

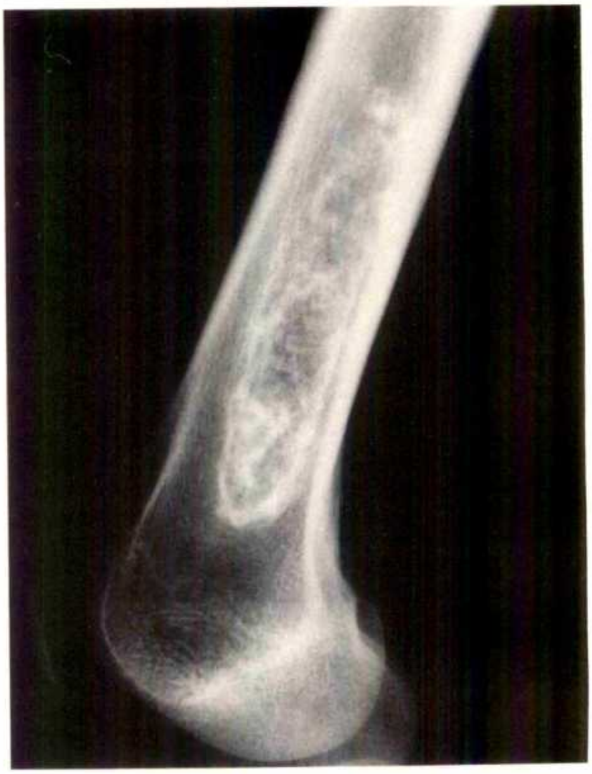

Figure 3. Lateral radiograph of the left distal femur showing a typical medullary infarct.

The aetiology of the bone infarction in the present case is unknown. Chest CT showed no evidence of metastases and treatment consisted of chemotherapy and endoprosthetic replacement of the distal femur. Currently, the patient remains disease free although the quoted 5-year survival for a patient with an MFH arising in a pre-existing bone abnormality is less than 25% (Capanna et al, 1984).

References

Boland, P. J. & Huvos, A. G., 1986. Malignant fibrous histiocytoma of bone. *Clinical Orthopaedics and Related Research, 204*, 130–134.

Capanna, R., Bertoni, F., Bacchini, P., Bacci, G., Guerra, A. & Campanacci, M., 1984. Malignant fibrous histiocytoma of bone. *Cancer, 54*, 177–187.

Heselson, N. G., Price, S. K., Mills, E. E. D., Conway, S. S. M. & Marks, R. K., 1983. Two malignant fibrous histiocytomas in bone infarcts. *Journal of Bone and Joint Surgery, 65A*, 1166–1171.

Mirra, J. M., Bullough, P. G., Marcove, R. C., Jacobs, B. & Huvos, A. G., 1974. Malignant fibrous histiocytoma and osteosarcoma in association with bone infarcts. *Journal of Bone and Joint Surgery, 56A*, 932–940.

Tait, N. P., Hacking, P. M. & Malcolm, A. J., 1988. Malignant fibrous histiocytoma occurring at the site of a previous total hip replacement. *British Journal of Radiology, 61*, 73–75.

1989, *The British Journal of Radiology*, 62, 185–187

Short communications

Radiation dose to urological surgeons during X-ray fluoroscopy for percutaneous stone extraction

By J. Law, *J. A. Inglis and *D. A. Tolley

Department of Medical Physics and Medical Engineering, Western General Hospital, Edinburgh and
*Department of Urology, Royal Infirmary, Edinburgh

(Received June 1988 and in revised form August 1988)

Radiation protection of staff using X rays in UK hospitals is generally acknowledged to be satisfactory. This is supported by the fact that relatively few need to be Classified Workers under the *Ionizing Radiations Regulations* (HMSO, 1985). This view is based on routine measures to protect the main body of the worker, *e.g.* with a lead apron, and the results of routine dose monitoring, generally with monitors underneath such aprons.

There remains the problem of dose to unshielded parts of the body from procedures such as fluoroscopy where protection depends mainly on lead aprons, and where some staff are very close to unshielded X-ray beams. Doses to heads and arms of radiologists were reported earlier (Law, 1985). This paper reports doses received by one surgeon conducting percutaneous nephrolithotomy using an overcouch system. This procedure requires the surgeon's fingers, head and neck to be very close to the X-ray beam, and monitors were therefore worn on two fingers of each hand, as well as over the thyroid. Satisfactory sterile conditions were maintained.

Under the *Ionizing Radiations Regulations* (HMSO, 1985) there is renewed emphasis on monitoring dose to staff, and under the 1988 Regulations (HMSO, 1988) on protection of the patient there is a requirement for adequate training of all staff using X-ray equipment, not only radiologists and radiographers. It seems desirable to avoid, if possible, the need for finger monitors on all staff using fluoroscopy at all times, though continuous monitoring of that kind is undoubtedly necessary if or where finger doses are significant, *e.g.* approaching three-tenths of the dose limit. The present work reports doses measured directly during a high-dose procedure, which included the use of an overcouch tube. Doses with such a system are well known to be higher than with undercouch tubes (International Commission on Radiological Protection (ICRP), 1985). Those implications which are mainly of concern to urologists are discussed more fully elsewhere (Inglis et al, 1989).

Urological procedures

This study concerned the procedures of percutaneous nephrolithotomy whereby endoscopic access to the collecting system of the kidney in an anaesthetized patient was obtained in order that renal calculi could either be removed intact or fragmented prior to removal in a single-stage operation. At the time of preliminary cystoscopy, a ureteric catheter was passed retrogradely in order that the renal collecting system could be subsequently opacified by injection of contrast medium into the catheter.

With the anaesthetized patient turned prone, fluoroscopy, by means of an overcouch X-ray source, allowed screening of the opacified system so that percutaneous access could be achieved by direct needle puncture of the renal collecting system. A flexible guide wire was passed by the same route and manipulated via the renal collecting system into the ureter under screening. Graduated dilators were then passed along the guide wire under fluoroscopic control so enlarging the tract, ultimately allowing the passage of a hollow Amplatz sheath into the kidney. The irrigating nephroscope was then passed directly into the kidney within this sheath so that the stone could be visualized and removed piecemeal or intact. During the procedure a maximally coned view was used at all times. As the screening pedal was controlled by the surgeon's foot, it was possible to ensure that the surgeon's hands were outside the direct beam prior to screening.

X-ray equipment and dose-monitoring procedures

The X-ray equipment consisted of a Siemens Polyphos generator and a Uroskop B table. Operating factors were generally 75–80 kV and about 1.5 mA.

Finger monitors in the form of thermoluminescent chips encased in plastic finger bands were obtained from the Regional Radiation Physics and Protection Service, Queen Elizabeth Medical Centre, Birmingham. These were renewed every 4 weeks and returned to Birmingham for assessment. This service is an Approved Dosimetry Service under the *Ionizing Radiations Regulations*. Monitors were worn on the dorsum of two fingers of each of the surgeon's hands, for eight periods of 4 weeks. In one period the monitors were mislaid, and in another only four procedures were carried out and the doses on two fingers were reported as less than 0.2 mSv. Results for the remaining six periods are given in Table I. For the last four dose-monitoring periods an additional monitor was worn over the thyroid.

Sterility procedures

When dose monitoring of surgeons' hands is recommended, objections are sometimes raised by the surgeons that adequate sterile conditions cannot be maintained during use or that the integrity of the monitors would not survive the necessary sterilizing procedures throughout the normal 4-week period. During this study the individually numbered monitors were simply placed in Cidex solution for 10 min prior to use, then rinsed and dried. They were then secured over the dorsum of the middle phalanges of the index and ring fingers of both hands of the surgeon using sterile adhesive "Band Aid"-type dressings before the donning of surgical gloves. No problems were encountered regarding sterility using the above practice. As the monitors were small and pliable the manual dexterity of the surgeon was not in any way impaired. The monitors were changed at 4-week intervals and the results matched with carefully recorded details of screening time and patient data for the relevant period. As the monitors were individually numbered it was possible to apply the same monitor to the

Table I. Numbers of cases, total screening time and doses recorded on fingers of a single surgeon in each of six monthly periods

Month	No. of procedures	Screening time (min)	Finger dose recorded (mSv)			
			L. middle	L. index	R. middle	R. index
1	12	38.6	1.8	2.3	0.7	1.0
2	9	37.6	1.5	1.5	1.0	1.7
3	10	42.4	2.1	3.4	0.9	1.4
4	9	57.7	3.8	6.3	1.6	3.3
5	7	27.2	1.6	2.7	0.6	1.2
6	8	38.3	1.6	2.6	0.7	1.8
Mean dose per procedure (mSv)			0.23	0.34	0.10	0.19
Mean dose per minute (mSv)			0.05	0.08	0.02	0.04

relevant finger on each occasion and therefore to assess the cumulative dose to each finger over the 4-week period.

Results

The results with the overcouch system are summarized in Table I. They demonstrate that for this surgeon performing such a high-dose procedure the dose received was well within the dose limit for extremities and comfortably below the three-tenths of that limit which would require him to be Classified under the *Ionizing Radiations Regulations*. Since the dose-rate within the primary beam on the patient entrance side is likely to be of the order of $10\,\mathrm{mSv\,min^{-1}}$, these low-dose results indicate that the surgeon's fingers were virtually never in the primary beam. (The monitors were worn near the finger tips.) Radiation dose limits do not, therefore, constitute any effective limit on the number of these procedures the surgeon can perform in a year. However, if a surgeon's fingers were to enter the primary beam for even half of the average screening time of 4.4 min which was required for these procedures, then a limit of around 25 procedures per year would be set, or seven procedures if classification were to be avoided.

The beam-on time for each case was recorded and hence the total beam-on time was calculated in each 4-week period for which the monitors were worn. Recorded doses from each set of monitors reflected the variation of beam-on time from one period to another. Results from individual monitors also showed a consistent variation between one finger and another, the index finger of the left hand receiving the highest dose. This is consistent with a right-handed surgeon using his left hand to steady instruments during screening and has been reported previously (Lowe, 1986).

The thyroid doses recorded were 0.3 mSv in one period during which seven procedures were performed, and less than 0.2 mSv in each of three other periods in which a total of 19 procedures were performed. These doses are, like the finger doses, quite low in relation to the dose limit of 150 mSv per year for eyes. These results show that this surgeon would reach the dose limit for hands before reaching that for eyes. Since any hazard to thyroid and eyes arises from scatter from an extended source, we assume that doses to each will be very similar.

Discussion

The results provide perhaps false reassurance that finger and head doses can, with reasonable care, be kept satisfactorily low without any need to modify surgical procedures. Our measured radiation doses are gratifyingly low simply because screening times are minimal. Other published series show that average screening times for this procedure of 20–30 min are the norm (Bush, 1984; Rao, 1987). Such a time would entail a six-fold increase in radiation exposure using this overcouch system with serious implications regarding safety and/or permissible number of procedures performed. The results also demonstrate that the surgeon's hands do not need to enter the primary beam. If this were not so, dose limits for 1 year would be exceeded within very few cases. The crucial importance of all operators keeping their fingers out of the primary beam cannot be overemphasized.

Urological surgeons seem, on the whole, to appreciate the disadvantage of overcouch screening very well, and this needs to be taken into account by radiologists and others concerned in X-ray equipment procurement. The ICRP have advised against overcouch fluoroscopy quite strongly, and it appears to be contrary to the ALARA (as low as reasonably acheivable) principle. If the user's fingers do enter the primary beam, the resulting dose is much higher with overcouch than with undercouch tubes, quite apart from the greater scatter outside the beam involved with overcouch systems.

Problems which might have been expected regarding sterility or manual dexterity while wearing the monitors have not arisen in practice.

Surgeons, radiologists and any others conducting fluoroscopy with their hands close to the beam should be involved in monitoring programmes to confirm that actual doses are satisfactory. Such programmes might be for a few months only to establish a satisfactory record and might concentrate on a minority of staff with a greater workload than their colleagues. Constant monitoring of all users is not necessarily justified, but repeat monitoring as procedures, equipment and staff change is desirable.

References

Bush, W., 1984. Radiation exposure to patient and urologist during percutaneous nephrolithotomy. *Journal of Urology, 132*, 1148–1152.

HMSO, 1985. *Ionizing Radiations Regulations 1985* (Her Majesty's Stationery Office, London).

—— 1988 *Ionizing Radiation (Protection of Persons Undergoing Medical Examination or Treatment) Regulations* (Her Majesty's Stationery Office, London).

ICRP, 1985. Statement from the 1985 Paris meeting of the International Commission on Radiological Protection. *British Journal of Radiology, 58*, 910.

Inglis, J. A., Tolley, D. A. & Law, J., 1989. Radiation safety during percutaneous nephrolithotomy. *British Journal of Urology*, *63*, in press.

LAW, J., 1985. Doses to heads and arms of radiologists and other staff during fluoroscopy. *British Journal of Radiology*, *58*, 187–188.

LOWE, F., 1986. Monitoring radiation exposure to medical personnel during percutaneous nephrolithotomy. *Urology*, *28*, *3*, 221–226.

RAO, P. N., 1987. Radiation dose to patient and staff during percutaneous nephrostolithotomy. *British Journal of Urology*, *59*, 508–512.

Intraoperative radioactive localization of an osteoid osteoma: a useful variation in technique

By *B. D. Todd, FRCS, L. W. Godfrey, FRCS and R. N. Bodley, FRCR

Stoke Mandeville Hospital, Aylesbury

(*Received September 1988*)

Only complete excision of the nidus of an osteoid osteoma can guarantee cure. Localization of the nidus by using a gamma camera in theatre (Rinsky et al, 1980) is cumbersome and inaccurate in delineating how much bone should be excised. The use of a sterilizable, portable scaler-ratemeter (Colton & Hardy, 1983) provides good results, but the equipment is expensive to buy and maintain. The use of a scintillation well counter outside theatre to measure counts from bone punch biopsy specimens in and around the suspect area has also been reported (O'Brien et al, 1984). However, up to 24 specimens were required and operative time must have been substantially prolonged.

When a patient presented to our hospital with a probable osteoid osteoma we devised a variation on the above techniques which is reasonably speedy and only requires the type of gamma camera found in most nuclear medicine departments.

Patient and methods

A 25-year-old man was referred to the orthopaedic department with a 4-year history of pain in the dorsal aspect of his wrist extending into his hand. The pain was eased by a non-steroidal, anti-inflammatory medication but still often woke him at night. He had previously been treated at another hospital. Radiographs of his wrist had been normal but a technetium bone scan had demonstrated an area of high uptake in the right capitate. Exploration had been carried out and a small quantity of bone with a sclerotic appearance had been removed. However, the bone was histologically normal and the patient's symptoms were unchanged post-operatively.

In our outpatient department more than 2 years after this operation, his wrist appeared normal to inspection apart from the surgical scar. He was tender dorsally in the area of the capitate. A radiograph (Fig. 1) showed no abnormality.

A bone scan was performed using 500 MBq of technetium-99m hydroxymethylene diphosphonate. A General Electric 400 gamma camera with a general-purpose, medium-resolution, parallel-hole collimator was used. Three hours after the intravenous injection, the palmar view of the right hand (Fig. 2) showed a solitary focus of increased activity in the capitate consistent with diagnosis of osteoid osteoma.

It was decided to proceed with a second exploration. Two hours pre-operatively, the same dose of technetium 99m was given. En route to theatre, further views of the hand were taken and a lateral scan (Fig. 3) demonstrated the lesion toward the dorsum of the capitate.

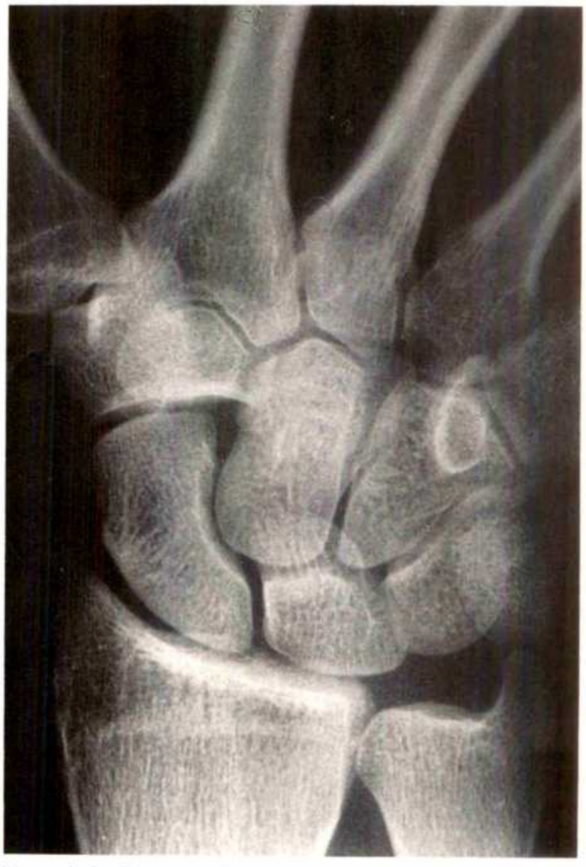

Figure 1. Radiograph of the wrist showing no abnormality.

---

*Address for correspondence: Department of Orthopaedics, St Thomas' Hospital, London SE1 7EH.

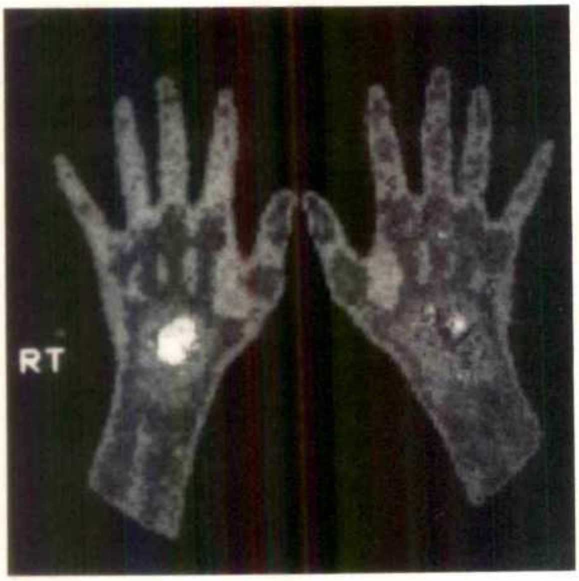

Figure 2. Bone scan (anterior) showing a solitary focus of increased activity in the right capitate, consistent with the diagnosis of osteoid osteoma.

After preparation of the hand, the capitate was localized fluoroscopically and the dorsal skin incision was sited appropriately. The capitate was exposed and appeared macroscopically normal. The central portion of the dorsal cortex was carefully excised with a small osteotome. The pieces of bone were laid in an agar-containing petri dish, the agar being used to maintain the relative position of the fragments, and hence their location within the capitate. Each collection of fragments was numbered to allow later correlation of fragments with histological findings.

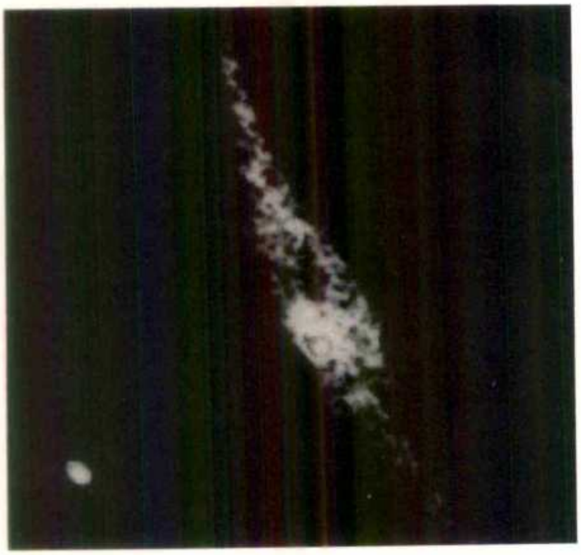

Figure 3. Lateral view scan of the wrist showing increased activity in the dorsal aspect.

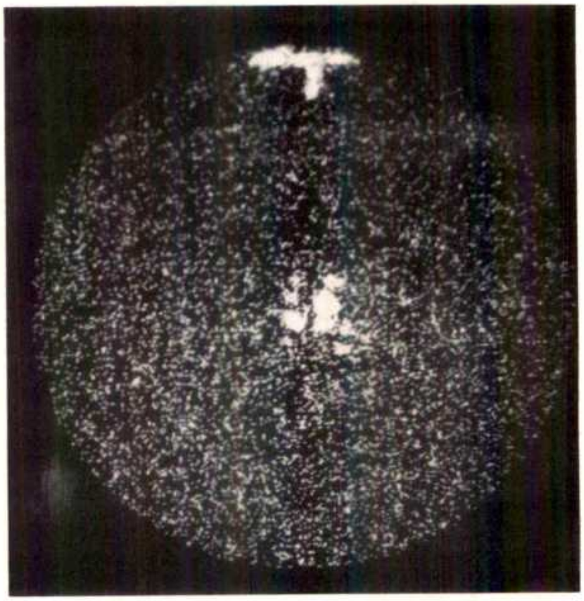

Figure 4. Scan appearance of the second collection of fragments. High activity is present in four of the six bone fragments on the agar plate.

The petri dish with its embedded fragments was then transported to the Nuclear Medicine department and imaged on the gamma camera. The fragments showed minimal activity suggesting the nidus had not been removed. Six more fragments were then removed from an adjacent area on the dorsum of the capitate. These fragments also appeared macroscopically normal but on scanning four of the six showed much higher activity than the original fragments (Fig. 4). A third collection of fragments was made from around the periphery of the positive area and this collection had a similar low activity to the first group.

On histological examination the typical appearances of osteoid osteoma were found in the second collection of fragments. The other two collections showed normal bone. The patient was symptom-free post-operatively and remained so at his final review at 6 weeks.

Discussion

We used this simple technique to aid in the localization of an osteoid osteoma. As all removed bone appeared macroscopically normal we feel that a second operative failure may well have been avoided.

The technique has a potential use in any hospital which has a gamma camera. In our hospital the Nuclear Medicine department is situated close to the theatre block and delay in transport of the three sets of bone fragments did not add appreciably to operating time.

Although the count rate from each fragment was not quantified we feel that the difference in scan appearance between hot and cold fragments was so substantial that quantification is not necessary to achieve a reasonable chance of success.

References

COLTON, C. L. & HARDY, J. G., 1983. Evaluation of a sterilizable radiation probe as an aid to the surgical treatment of osteoid osteoma: technical note. *Journal of Bone and Joint Surgery*, *65A*, 1019–1022.

O'Brien, T. M., Murray, T. E., Malone, L. A., Dervan, P., Walsh, W., McManus, F. & Ennis, J. T., 1984. Osteoid osteoma: excision with scintimetric guidance. *Radiology*, *153*, 543–544.

Rinsky, L. A., Goris, M., Bleck, E. E., Halpern, A. & Hirshmann, P., 1980. Intra-operative skeletal scintigraphy for localization of osteoid osteoma in the spine: case report. *Journal of Bone and Joint Surgery*, *62A*, 143–144.

Alteration of cardiac myosin isozymes after whole-body irradiation

By *R. Z. Litten, T. L. Walden, G. T. Gainey and †R. Nagai

Departments of Physiology and Biochemistry, Armed Forces Radiobiology and Research Institute, Bethesda, Maryland 20814-5145 and †Department of Physiology and Biophysics, University of Vermont, Burlington, Vermont 05405, USA

(Received March 1988 and in revised form July 1988)

Three myosin isozymes (V_1, V_2, V_3) have been shown to exist in the heart. V_1 isozyme, containing two α heavy chains, has relatively higher actin- and calcium-stimulated myosin adenosine triphophatase (ATPase) activities than does V_3, which is composed of two β heavy chains (Hoh et al, 1978; Martin et al, 1982; Litten et al, 1983). V_2 isozyme appears to be a heterodimer composed of one α and one β heavy chain (Hoh et al, 1979; Everett et al, 1983a).

The proportions of myosin isozymes are altered under various conditions of stress. During pressure-overload-induced hypertrophy, there is a shift toward the V_3 isozyme (Mercadier et al, 1981; Litten et al, 1982). The amount of V_3 isozyme is also increased with hypothyroidism and age and is decreased by hyperthyroidism and exercise (Litten et al, 1982; Everett et al, 1983b).

Changes in the relative amounts of V_1 and V_3 isozymes are believed to be responsible, in part, for altered cardiac performance. A high proportion of V_3 isozyme is associated with relatively slow, economic tension development within the heart, whereas a high proportion of V_1 isozyme is associated with a faster, but less economical force development (Schwartz et al, 1981; Alpert et al, 1983).

In this study, measurements of cardiac myosin isozymes were carried out in rats subjected to acute sublethal whole-body irradiation. The studies showed, for the first time, that there is a shift in the pattern of myosin isozymes 9 days after irradiation. This change may result in functional alterations of the heart following whole-body irradiation.

Methods

Animal model

Three-month-old male Sprague Dawley rats were obtained from Taconic Farms (Germantown, NY). Rats were quarantined for a period of 2–3 weeks and examined for pathological and serological indications of illness or infection. The rats were housed three to a cage in Micro-isolator cages on hardwood-chip bedding, maintained in conventional animal holding rooms on a 12-h light–dark cycle. The rooms were maintained at 21 ± 1°C with 50% relative humidity and 12 room changes of 100% conditioned fresh air per hour. Wayne Rodent Blox dietary pellets and acidified water (pH 2.4) were provided *ad libitum*.

For whole-body irradiation, rats were placed in individual plastic rectangular cages and irradiated with a total dose of 5 Gy or 10 Gy using a bilateral cobalt-60 source at a dose-rate of 1 Gy/min. Aged-matched rats were used as controls.

At euthanasia, rats were anaesthetized with menthoxyflurane. The heart was immediately removed and weighed. Portions of the heart tissue were fixed in 10% formalin for histological examination and the remainder of the heart was frozen at −80°C. Tissue samples for histological examination were embedded in paraffin, sections cut and stained with either haematoxylin and eosin or Masson's stain.

Pyrophosphate gel electrophoresis

Cardiac myosin was extracted by homogenization of the frozen left ventricular apex in 100 mM sodium pyrophosphate (pH 8.8) 5 mM EDTA, 2 mM 2-mercaptoethanol and 0.2 mM dichlorvous. Pyrophosphate gel electrophoresis was carried out as previously described (Litten et al, 1985). The gels were then scanned with an LKB Ultrascan laser densitometer (Fig. 1) and quantitated as described previously (Litten et al, 1985). The amount of the heterodimer V_2, which is a minor component, was divided equally between V_1 and V_3.

Results and discussion

Radiation exposure induced an alteration in the relative amounts of cardiac myosin isozymes at 9 days and 1 month after irradiation (Figs 1, 2). The percentage of the V_3 isozyme was significantly increased from 26 ± 4% in age-matched control rats, to 40 ± 5% at 9 days after irradiation, and from 19 ± 4% in controls to 36 ± 5% at 1 month after irradiation (Fig. 2). There was no significant difference in the percentage of V_3 composition 3–12 months after irradiation in comparison with age-matched controls. During this period, V_3 comprised ~ 55% of the myosin. If the radiation dose to the rat was increased from 5 to 10 Gy, 100% lethality resulted by approximately 12 days after the radiation exposure. The percentage of the V_3 isozyme observed at 9 days after 10 Gy increased to values similar to that observed after 5 Gy, suggesting that higher radiation doses do not produce a greater effect. However, it is possible that the shift to the V_3 isozyme occurred at an earlier time after 10 Gy. Future experiments which examine earlier post-irradiation time points will test this possibility.

Although a shift in the cardiac myosin isozymes was observed after whole-body irradiation, there was no histo-

---

*Author for correspondence.

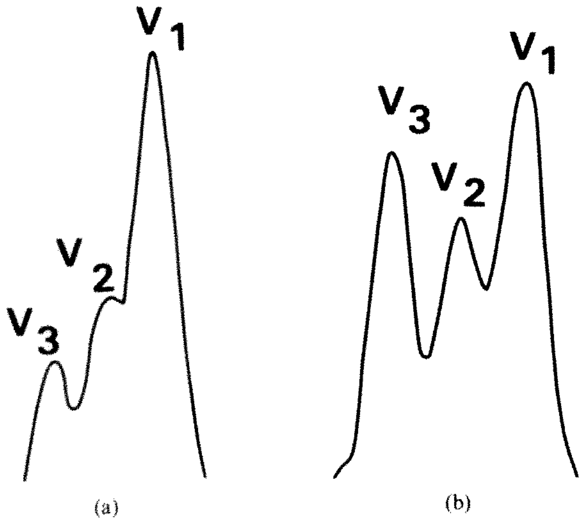

Figure 1. Densitometric traces from a pyrophosphate gel of samples from (a) an age-matched control and (b) a rat 9 days after irradiation (5 Gy). Similar separations were obtained for all samples in this study. Details regarding quantifications of the myosin isozymes are provided in the Methods section.

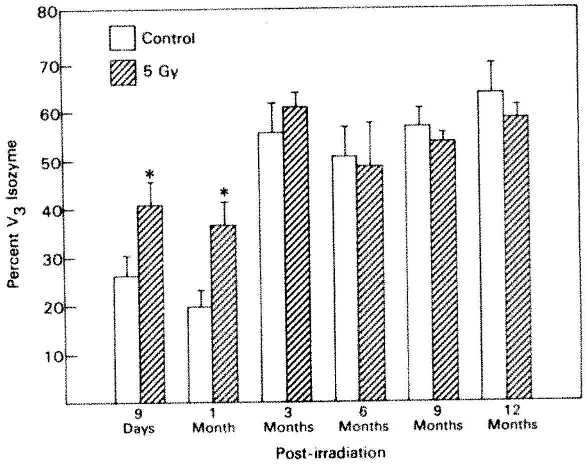

Figure 2. Percentage of V_3 myosin isozyme against time after irradiation in irradiated (5 Gy) as compared with age-matched control rats. Values are mean ± SE, four to seven hearts per group. *Indicates a significant difference from age-matched controls ($p \leqslant 0.05$).

logical evidence of heart damage. There was no radiation-induced increase in fibrosis or any apparent changes in the structure of the myocardial cells. In addition, there was no increase in the ventricular weights.

This increase in the V_3 isozyme following whole-body irradiation has been observed under various conditions. One condition responsible for an increase in the V_3 isozyme is hypothyroidism (Litten et al, 1982; Everett et al, 1983b). Gray et al (1980) have previously demonstrated that whole-body irradiation with 7.5 Gy reduced the level of the serum thyroid hormones in rats. Studies are in progress to examine the possible relationship between the increase in V_3 isozyme and the thyroid state of the rat after irradiation.

Semi-starvation of rats also increases the amount of cardiac V_3 isozyme (Dillman et al, 1983). Since the rats consume very little food for several days following whole-body irradiation with 5 and 10 Gy, this may be responsible in part for the increase in the V_3 isozyme. However, Dillman et al (1983) also demonstrated a decrease in the plasma thyroid hormone level in semi-starved rats. Thus the shift toward the V_3 isozyme in the semi-starved rats may simply be caused by the hypothyroid state of the animals.

Finally, an increase in age has been associated with an increase in the V_3 isozyme (Lompre et al, 1981; Litten et al, 1985). Several investigators have postulated that radiation causes an acceleration of aging in various tissues (Alexander, 1957; Alderman & Britton, 1975; De et al, 1983). Thus the increase in percentage of V_3 following whole-body irradiation may be interpreted as an acceleration of aging. Further experiments are needed to support this suggestion.

Changes in myosin isozymes result in changes in actin-activated myosin ATPase activity (Litten et al, 1983). An increase in the proportion of V_3 isozyme has occurred at Day 9 and 1 month after irradiation, resulting in the heart having less myosin ATPase activity. A decrease in the velocity of muscle shortening, a decrease in the rate of isometric force development and an increase in the economy of force development within the heart are the functional cardiac changes that have been associated with an increase in the V_3 isozyme (Schwartz et al, 1981; Alpert et al, 1983). It has been postulated that the effect of an increase in the V_3 isozyme on cardiac function is caused by a decrease in the crossbridge cycling rate between actin and myosin due, in part, to an increase in the time of actin and myosin attachment during crossbridge cycling (Alpert et al, 1984).

The mechanisms causing changes in cardiac myosin isozymes after whole-body irradiation are unknown. It has previously been shown that the change in the β and α myosin heavy chains (V_3 and V_1, respectively) is a pre-translational event during pressure-overload-induced hypertrophy of the right ventricle (Nagai et al, 1987). Others have postulated a similar conclusion using hypo- and hyperthyroid states to induce changes in cardiac myosin isozymes (Everett et al, 1984; Mahdavi et al, 1987). Recently, Umeda et al (1987) have demonstrated that regulation of the β and α myosin heavy chain mRNA levels by thyroid hormone occurs at the level of transcription.

In summary, it has been shown that doses of radiation (sublethal and lethal) cause changes in cardiac myosin isozymes which may lead to functional changes in the heart. This shift in myosin isozyme pattern is similar to that caused by hypothyroidism, semi-starvation and aging. These changes in cardiac myosin isozymes occur without evidence of myocardial damage. Thus, the results here raise the following important questions; first, how much of a functional change occurs in the heart following radiation-induced changes in the myosin isozymes and secondly, what is the mechanism of signal causing the myosin isozymes to change? Future experiments will be directed toward answering these questions.

Acknowledgments

The authors would like to thank Dr James E. Rogers for the histology studies, June Egan for technical assistance and Mila Ly for secretarial assistance.

This work was supported by the Armed Forces Radiobiology Research Institute, Defense Nuclear Agency, under

Research Work Units B2152 and 0169. The views presented in this paper are those of the authors. No endorsement by the Defense Nuclear Agency has been given or should be inferred. Research was conducted according to the principles enunciated in the *Guide for the Care and Use of Laboratory Animals*, prepared by the Institute of Laboratory Animal Resources, National Research Council.

References

ALDERMAN, R. C. & BRETTON, G. W., 1975. The impaired capability for biochemical adaptation during aging. *Bioscience, 25*, 639–643.

ALEXANDER, P., 1957. Accelerated aging: a long-term effect of exposure to ionizing radiation. *Gerontologia, 1*, 174.

ALPERT, N. R., MULIERI, L. A. & LITTEN, R. Z., 1983. Isoenzyme contribution to economy of contraction and relaxation in normal and hypertrophied hearts. In *Cardiac Adaptation to Hemodynamic Overload, Training, and Stress*, ed. by R. Jacob, R. W. Gulch & G. Kissling (Steinkopff Verlag, Dormstadt), pp. 147–157.

ALPERT, N. R., MULIERI, L. A., LITTEN, R. Z. & HOLUBARSCH, C., 1984. A myothermal analysis of the myosin crossbridge cycling rate during isometric tetanus in normal and hyperthyroid rat hearts. *European Heart Journal, 5* (Suppl. F), 3–11.

DE, A. K., CHIPALKOTTI, S. & AIYAR, A. S., 1983. Effects of chronic irradiation on age-related biochemical changes in mice. *Radiation Research, 95*, 637–645.

DILLMAN, W. H., BERRY, S. & ALEXANDER, N. M., 1983. A physiological dose of triiodothyronine normalizes cardiac myosin adenosine triphosphatase activity and changes myosin isoenzyme distribution in semistarved rats. *Endocrinology, 112*, 2081–2087.

EVERETT, A. W., CHIZZONITE, R. A., CLARK, W. A. & ZAK, R., 1983a. Relationship of changes in molecular forms of myosin heavy chains to endogenous level of thyroid hormone during postnatal growth. In *Perspectives in Cardiovascular Research. Cardiac Hypertrophy in Hypertension*, ed. by R. C. Tarazi & J. B. Dunbar (Raven Press, New York), Vol. 8, pp. 83–92.

EVERETT, A. W., CLARK, W. A., CHIZZONITE, R. A. & ZAK, R., 1983b. Change in synthesis rates of α- and β-myosin heavy chains in rabbit heart after treatment with thyroid hormone. *Journal of Biological Chemistry, 258*, 2421–2425.

EVERETT, A. W., SINHA, A. M., UMEDA, P. K., JAKOVCIC, S., RABINOWITZ, M. & ZAK, R., 1984. Regulation of myosin synthesis by thyroid hormone: relative change in the α- and β- myosin heavy chain mRNA levels in rabbit heart. *Biochemistry, 23*, 1596–1599.

GRAY, W. M., ORR, J. S. & RATCLIFFE, W. A., 1980. The effects of whole-body irradiation on the serum levels and kinetics of thyroid hormones in rats. *International Journal of Radiation Biology, 37*, 653–666.

HOH, J. F. Y., MCGRATH, P. A. & HALE, P. T., 1978. Electrophoretic analysis of multiple forms of rat cardiac myosin: effects of hypophysectomy and thyroxine replacement. *Journal of Molecular and Cellular Cardiology, 10*, 1053–1076.

HOH, J. F. Y., YEOH, G. P. S., THOMAS, M. A. W. & HIGGINBOTTOM, L., 1979. Structural differences in the heavy chains of rat ventricular myosin isozymes. *FEBS Letters, 97*, 330–334.

LITTEN, R. Z., MARTIN, B. J., LOW, R. B. & ALPERT, N. R., 1982. Altered myosin isozyme patterns from pressure-overloaded and thyrotoxic hypertrophied rabbit heart. *Circulation Research, 50*, 856–864.

LITTEN, R. Z., MARTIN, B. J., LOW, R. B., SOLARO, R. J. & ALPERT, N. R., 1983. Structural alterations in contractile proteins from thyrotoxic and pressure-overloaded hypertrophic rabbit hearts. In *Perspectives in Cardiovascular Research: Myocardial Hypertrophy and Failure*, ed. by N. R. Alpert (Raven Press, New York), Vol. 7, pp. 405–425.

LITTEN, R. Z., MARTIN, B. J., BUCHTHAL, R. H., NAGAI, R., LOW, R. B. & ALPERT, N. R., 1985. Heterogeneity of myosin isozyme content of rabbit heart. *Circulation Research, 57*, 406–414.

LOMPRE, A. A., MERCADIER, J. J., WISNEWSKY, C., BOUVERET, P., PANTALONI, C., D'ALBIS, A. & SCHWARTZ, K., 1981. Species- and age-dependent changes in the relative amounts of cardiac myosin isozymes in mammals. *Developmental Biology, 84*, 286–290.

MAHDAVI, V. M., IZUMO, S. & NADAL-GINARD, B., 1987. Developmental and hormonal regulation of sarcomeric myosin heavy chain gene family. *Circulation Research, 60*, 804–814.

MARTIN, A. F., PAGANI, E. D. & SOLANO, R. J., 1982. Thyroxine induced re-distribution of isoenzymes of rabbit ventricular myosin. *Circulation Research, 50*, 117–124.

MERCADIER, J. J., LOMPRE, A. M., WISNEWSKY, C., SAMUEL, J. L., BERCOVICI, J., SWYNGHEDAUW, B. & SCHWARTZ, K., 1981. Myosin isoenzymic changes in several models of rat cardiac hypertrophy. *Circulation Research, 49*, 525–532.

NAGAI, R., PRITZL, N., LOW, R. B., STIREWALT, W. S., ZAK, R., ALPERT, N. R. & LITTEN, R. Z., 1987. Myosin isozyme synthesis and mRNA levels in pressure-overloaded rabbit hearts. *Circulation Research, 60*, 692–699.

SCHWARTZ, K., LECARPENTIER, Y., MARTIN, J. L., LOMPRE, A. M., MERCADIER, J. J. & SWYNGHEDAUW, B., 1981. Myosin isoenzymatic distribution correlates with speed of myocardial contraction. *Journal of Molecular Cellular Cardiology, 13*, 1071–1075.

UMEDA, P. K., DARLING, D. S., KENNEDY, J. M., JAKOVCIC, S. & ZAK, R., 1987. Control of myosin heavy chain expression in cardiac hypertrophy. *American Journal of Cardiology, 59*, 49A–55A.

1989, *The British Journal of Radiology*, *62*, 192

Correspondence

(The Editors do not hold themselves responsible for opinions expressed by correspondents)

Variation of image quality with X-ray tube potential in mammography

THE EDITOR—SIR,

It has long been accepted in general radiology that decreasing tube potential (kV) leads to increased contrast. With tungsten target tubes there has been no cause to question this in the mammography region down to 25 kV or even below. With molybdenum targets and filters, X-ray spectra are a little more complex, owing to the molybdenum characteristic radiation. Any difference in behaviour, if it exists, will arise from this radiation, but the same broad conclusion is likely to apply here also. A further possible point of interest could be the rate at which contrast varies with kV. Most clinical experience seems to support the view that contrast does increase as kV falls, and experimental confirmation has been reported (Stanton et al, 1979) on a Mo/Mo tube assembly. Yet in private discussion the point is still sometimes questioned. This letter reports some direct experimental evidence that the conventional view is correct.

An objective measure of contrast was obtained from radiographs of a "Barts" phantom (White & Tucker, 1980) taken at different kVs. The difference in density was measured under the thickest steps of two step wedges, one of water equivalent and one of adipose equivalent tissue. Five radiographs were taken at each of 5 kV settings on a CGR 500t X-ray set, using MinR films and screens. The mean contrast obtained from the five radiographs at each kV value, with the standard error of the mean, is given in Table I. The actual kV values were estimated from absolute measurements by the fluorescence method, using the silver and tin K-edges at 25.5 and 29.2 keV, supported by measurements with a digital kV meter from a nominal 25 to 35 kV.

The measured contrast increases fairly steadily throughout the kV range studied, *i.e.* down to about 23.5 kV.

Further evidence is provided by scoring the same radiographs of the Barts phantom, *i.e.* by counting the number of details visible in each radiograph. Four persons scored each radiograph, half-scores being given for details doubtfully distinguished, and the mean count from each group of five radiographs was taken as an index of image quality. The results appear in Table I. This method of scoring, with four persons, is slightly simpler than the one used by Kirkpatrick and Law (1987) with two persons scoring. Other scoring methods are, of course, possible, but the essential requirement is consistency within each set of results.

Table I. Image scores from "Barts" phantom at different tube potentials with a molybdenum target and four radiograph scorers. The tube potential was checked by fluorescence, Adran-Crookes penetrameter, and digital kV meter

Indicated kV	Measured kV	Filter (mm Mo)	Image score	Contrast (see text)
25	23.5	0.03	53.5 ± 0.8	0.289 ± 0.009
28	27.5	0.03	52.1 ± 1.0	0.282 ± 0.012
30	29.5	0.03	50.2 ± 0.9	0.257 ± 0.010
32	31.5	0.03	49.1 ± 0.3	0.234 ± 0.010
35	34.5	0.03	48.1 ± 0.4	0.228 ± 0.006

Table II. Image scores from "Barts" phantom at different tube potentials with a tungsten target and two scorers. The tube potential was checked by an Adran-Crookes penetrameter

Indicated kV	Measured kV	Filter (mm Al)	Image score
22	24	0.45	51.4 ± 0.6
25	27	0.45	47.8 ± 0.3
30	31.5	0.45	43.9 ± 0.3
31	32	0.58	44.0 ± 0.3
40	41	0.58	38.3 ± 0.4
49	50	0.58	37.8 ± 1.2
50	51	1.62	35.4 ± 0.5
60	61	1.62	31.8 ± 0.4

The same technique, involving sets of radiographs of the same Barts phantom, had earlier been applied to another mammography X-ray set having a tungsten target and aluminium filters of three different thicknesses. On this set the kV had been checked with an Ardran-Crookes penetrameter, which had been calibrated at the NPL using a tungsten target tube. This calibration should be valid for the mammography tube with a tungsten target.

The results are given in Table II and show that there is no essential difference in the variation of image score with tube kV between tubes with Mo targets and filters and tubes with tungsten targets and aluminium filtration.

We thank Dr A. E. Kirkpatrick for joining us in the scoring of the radiographs.

Yours, etc.,

J. LAW
*K. FAULKNER
*S. SMITH

Department of Medical Physics and
Medical Engineering,
Western General Hospital,
Edinburgh EH4 2XU and
*Regional Medical Physics Department,
Newcastle General Hospital,
Newcastle upon Tyne NE4 6BE

(*Received June 1988 and in revised form August 1988*)

References

KIRKPATRICK, A. E. & LAW, J., 1987. A comparative study of films and screens for mammography. *British Journal of Radiology*, *60*, 73–78.

STANTON, L., VILLAFANA, T., DAY, J. L., LIGHTFOOT, D. A. & STANTON, R. E., 1979. A study of mammographic exposure and detail visibility using three systems: Xerox 125, Min-R and Xonics XERG. *Radiology*, *132*, 455–462.

WHITE, D. R. & TUCKER, A. K., 1980. A test object for assessing image quality in mammography. *British Journal of Radiology*, *53*, 331–335.

1989, *The British Journal of Radiology*, *62*, 193

Aid to localization for computed tomographic biopsy and aspiration procedures

THE EDITOR—SIR,

In computed tomography (CT)-guided biopsy and aspiration procedures, various methods of precise localization have been described (vanSonnenberg et al, 1981; Frederick et al, 1985; Onik et al, 1986). When such refined methods are not available, the scanner's registration scale is normally used but the first attempt at a slice through a desired level may miss its target. When this happens, it is often difficult to know the amount of correction required, and whether this should be cranial or caudal.

We have found it useful to tape two hypodermic 21G 4 cm (currently green) needles to the skin surface to extend about 2 cm above and below the required level. One needle is aligned cranio-caudally and the other placed beside it at an angle so that the distal ends of the needles are 1 cm apart and their proximal ends 3 cm (Fig. 1). The needles may be left in their sterile containers. When the trial slice has been taken the separation of the needles is measured (Fig. 2). From this is deduced the amount of correction necessary and whether it should be cranial or caudal. This reduces the overall number of false levels scanned and speeds procedures.

Yours, etc.,
M. J. TURNER
P. BALL

X-ray Department,
The London Hospital,
Whitechapel,
London E1 1BB

(*Received August 1988*)

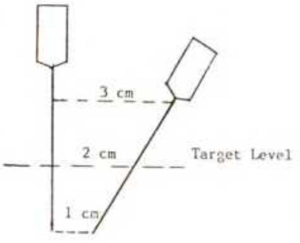

Figure 1. Schematic diagram showing the arrangement of the needles.

References

VANSONNENBERG, E., WITTENBERG, J., FERRUCCI, J. T. & MUELLER, P. R., 1981. Triangulation method for percutaneous needle guidance. *American Journal of Roentgenology*, *137*, 757–761.

FREDERICK, P. R., BROWN, T. H., MILLER, M. H., BAHR, A. L. & TAYLOR, K. H., 1985. A light-guidance system to be used for CT-guided biopsy. *Radiology*, *154*, 535–536.

ONIK, G., COSTELLO, P., COSMAN, E., WELLS, T., GOLDBERG, H., MOSS, A., KANE, R., CLOUSE, M. E., HODDICK, W., MOORE, S. & DEMAS, B., 1986. CT body stereotaxis: an aid for CT-guided biopsies. *American Journal of Roentgenology*, *146*, 163–168.

(*Dr J. E. Husband writes*: I learnt an even easier way to determine the precise position of the needle from Dr Michael Bernardino at Emony University. All you need to do is take a scout view with the needle in the patient. This shows the position of the needle tip and a slice is then taken right through it.)

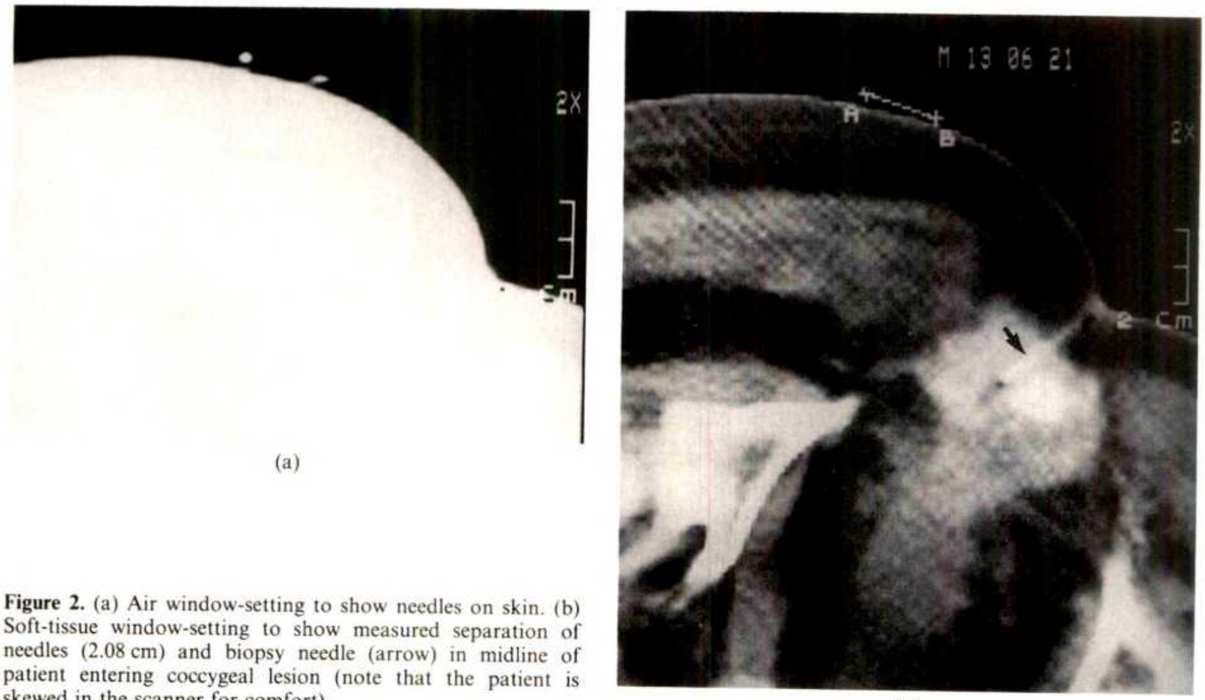

(a)

(b)

Figure 2. (a) Air window-setting to show needles on skin. (b) Soft-tissue window-setting to show measured separation of needles (2.08 cm) and biopsy needle (arrow) in midline of patient entering coccygeal lesion (note that the patient is skewed in the scanner for comfort).

Stress changes of the wrist in adolescent gymnasts

The Editor—Sir,

I note the bilateral nature of the lesions presented in the paper by Carter et al (1988) but I think it important to point out the original lesions that I wrote up were in fact unilateral. All of the bilateral lesions presented here are in males where as mine were originally only in girls. However, since then I have now seen some boys with unilateral lesions. In a personal communication with Mr Aldridge we wondered if male gymnasts' lesions stemmed from the work on the pommel horse whilst unilateral lesions stemmed from the rotational vaults or rotational manoeuvres on the floor. Certainly clinically, I feel that tenderness over the volar surface of the radius must be followed-up by a radiograph to exclude stress fracture and indeed by following this very rule on one occasion with a male gymnast I confirmed the stress fracture to be present.

Yours, etc.,
M. R. T. F. Read

60 Woodbridge Road,
Guildford,
Surrey GU1 4RF

(*Received August 1988*)

Reference

Carter, S. R., Aldridge, M. J., Fitzgerald, R. & Davies, A. M., 1988. Stress changes of the wrist in adolescent gymnasts. *British Journal of Radiology*, *61*, 109–112.

The cost of imaging procedures

The Editor—Sir,

I was interested to see the letter by Dr Russell (1989) on attempts to cost the harm resulting from radiation used in diagnostic radiology. If we started allowing for these costs it would of course be necessary to start allowing for the costs of the benefits of diagnostic radiology, and as Dr Russell is a diagnostic radiologist he probably feels that radiology is of some positive use in diagnosing the causes of disease, and occasionally in treating them using interventional techniques.

I would be most interested if Dr Russell could produce some figures on the credit side of the equation.

Yours, etc.,
W. D. Jeans

Department of Radiodiagnosis,
Bristol Royal Infirmary,
Bristol BS2 8HW

(*Received August 1988*)

Reference

Russell, J. G. B., 1989. Costing imaging procedures. *British Journal of Radiology*, *62*, 94.

1989, *The British Journal of Radiology*, *62*, 195–200

Book reviews

Radiation Dose to Patients from Radiopharmaceuticals: A Report of a Task Group of Committee 2 of the ICRP (Annals of the ICRP—ICRP Publication 53), pp. ix + 377, 1988 (Pergamon Press, Oxford), £62.00.
ISBN 0–08–035591–9

This important publication from the International Commission on Radiological Protection has been long awaited by those involved in making and using estimates of radiation dose to nuclear medicine patients. The earlier "blue book", ICRP Publication 17, has been available since 1971 and has become out of date, partly because of substantial changes in the range and usage of radiopharmaceuticals. Furthermore, ICRP 17 comprised a compilation of inconsistent results from various authors who had used a variety of biological models to calculate doses to a variety of target organs, generally for adult patients only. Comparisons of radiation dose within and between modalities were very difficult to make; the work pre-dated the emergence of the concept of the effective dose-equivalent.

ICRP 17 has now been replaced by two publications which overcome these limitations: ICRP 52, *Protection of the Patient in Nuclear Medicine* appeared last year and contains the philosophy and principles of good practice. For details of absorbed dose calculations it refers to ICRP 53, the subject of this review.

The book comprises two parts. The first part, 37 pages, describes the principles of biokinetics and dosimetry which have been adopted; the second part, 340 pages, gives tables of input and output data for individual radiopharmaceuticals.

The first part is a very welcome integration, albeit in summary form, of current thinking on radiation dose estimation. It describes the use of the "MIRD" methodology (as developed by the Medical Internal Radiation Dose committee of the US Society of Nuclear Medicine) and the selection of appropriate biokinetic models. It explains how weighted sums of doses to different target organs may be used to derive the *effective dose equivalent*, an extremely useful quantity whose estimation is required by bodies such as the UK ARSAC Committee. General biokinetic models are described for 11 physiological systems.

The second part includes data on more than 100 pharmaceuticals, involving 71 radionuclides of 34 elements. For each pharmaceutical a biokinetic model is described and the relevant biokinetic data are tabulated. A particular strength of this work is the clarity of presentation of these input data, and the consistency of approach adopted for all the calculations. A consistent list of target organs is adopted for all radiopharmaceuticals and for each one a computer print-out tabulates the absorbed dose per unit activity administered in units of mGy/MBq. The effective dose-equivalent is derived in units of mSv/MBq with an indication of which organs were used for the calculation. Data are tabulated for adult patients, and for 15-year-, 10-year-, 5-year- and 1-year-olds. In some cases the calculations have been repeated for different levels of organ function.

An attraction of the inclusion of such complete input data is that the reader may be able to extend the calculations to new materials or different conditions. The work is very well referenced and it seems a pity to have to report a small but significant gap in the literature: the "S factors", essential to all the calculations, have been published by MIRD only for adult patients—the values for children have not been published. Another question of continual interest which is not fully treated here is the estimation of dose to embryo or fetus. The reader is advised to quote the dose to the uterus which is included in all the tables.

It is difficult to keep up to date in nuclear medicine. Neither ^{99}Tc^{m}-HMPAO nor ^{99}Tc^{m}-isonitriles have been included—perhaps anticipating the next edition! Meanwhile this immensely valuable compilation will be welcomed with enthusiasm by the nuclear medicine community. The members of ICRP Committee 2 and its task groups deserve our thanks and congratulations.

R. A. SHIELDS

Non-ionising Radiation: Microwaves, Ultraviolet and Laser Radiation (Medical Physics Handbooks 18). By H. Moseley, pp. x + 293, 1988 (Adam Hilger, Bristol), £37.50.
ISBN 0–85274–166–9

As the title states, the book covers three topics: microwave radiation, light derived from sources other than lasers, and finally, lasers and their applications. The book is written by a medical physicist and the text is specifically directed towards those who work or have concerns in this area.

For each of the above topics, the underlying physics of the radiation and its means of generation are discussed. The detail given is adequate for an intelligent awareness of the fundamental processes involved. There are also succinct descriptions of the properties of the various radiations together with extended accounts of applications in biological and medical areas. Safety and protection are assigned separate chapters in each of the classes of radiation mentioned. Much useful detail is provided in these latter sections, and the author draws upon an extensive knowledge of these aspects.

The subject matter covered by the book is very broad and it could be argued that there is a strong case for two books, one dealing with microwaves and the other with light-related phenomena. In less than 300 pages, microwaves take up just over 100, ultraviolet, visible or infrared take 110, leaving only about 40 pages allocated to lasers. In view of the increasing uses of lasers in medicine, industry and commerce, more information could have been provided on all aspects. The overall treatment given by the author, however, is such that both newcomers and experienced workers can learn from the text and follow their own interests by making use of the selected references and short bibliography provided. The chapters which deal with safety matters seems to me particularly useful, and their careful study is to be recommended.

The editorial standards of the text are high and I was impressed by the excellent tables which feature in the various chapters. Together with many of the figures, these provide the reader with applicable data on the properties of the various radiations and the performance of equipment used in the laboratory and clinic.

In these days, the price for a book of this type is probably not excessive and should not deter its acquisition by biologists and clinicians who use non-ionizing radiation. The author is to be complimented on producing a text which is comprehensive, up to date, readable and interesting. It forms a very useful volume to have at hand for reference.

B. CUNDALL

Quality Assurance and Image Artifacts in Magnetic Resonance Imaging. By R. James, R. Knowles and John A. Markisz, pp. xiii + 149, 1988 (Little, Brown & Co., Boston), £16.50.
ISBN 0-316-49974-9

In general, this is a well presented text concerned with the logistics for obtaining good-quality images in MRI. The authors assume a basic knowledge of the physics of MRI and a greater awareness for the formation of MRI images. Overall the text will appeal to those professionals who are actively involved in MRI, both medical and scientific.

The book has 14 chapters which develop the theme of quality assurance and the important factors affecting the quality of MR images. The chapter headings are helpful in describing the range of information in the book: "Introduction to quality assurance", "The MR image", "Operator-adjustable parameters", "General imaging measurements", "Electronic measurements", "NMR measurements", "Archival QA", "QA conclusions", "Introduction to image artifacts", "Reducing image artifacts by patient screening and preparation", "Reducing patient motion artifacts", "Instrumental artifacts", "Artifacts from the microscopic environment" and "Image artifact conclusions". The chapters examining "measurements" are divided into fundamental sections (*e.g.* "Signal and noise", "Duty cycle effects", etc) and then subdivided, presenting the underlying factors, tests, and follow-up procedures that may be undertaken. Although this type of presentation is repetitive, it does allow efficient reading of the salient information. I imagine that some physicists will disagree with some of the test procedures, but this should be expected in the infancy of a new imaging modality.

My only adverse criticisms are directed towards the publishers. Firstly, the use of plastic ring binding might enable a less costly production but it does not aid durability in a book which is likely to be referred to more than once! Secondly, it would have made reading much more pleasant if the legends to figures and tables had been in a different typeface or somehow distinguished from the text. Invariably a legend appears at the beginning of each page, thus leading the reader to search for the next relevant phrase or sentence. Perhaps this feature is a product of computer-aided typesetting!

Overall this is a very useful book, particularly for the technically orientated professional, and quite affordable. The clinical images may not be state-of-the-art always, but they do represent a useful compendium of potential artefacts that may occur on current equipment. I believe this book is unique in its approach to the technicalities of MRI and should prove a justified purchase by individuals, libraries and MRI centres.

P. C. Jackson

Clinimetrics. By Alvan R. Feinstein, pp. xii + 272, 1987 (Yale University Press), £25.00, $35.00.
ISBN 0-300-03806-2

The introduction to this book is a succinct and seductive justification for establishing a code for clinimetric measurement. The already widespread adoption of clinimetric ratings and indices underlines an acceptance of the science in principle, but the author emphasizes the science's lack of principles. The aim of this book, therefore, is to structure a system for rating clinical information, such that observation of human phenomena can produce scientifically credible data.

The objective having been stated, this book goes on to describe a set of methods, strategies, and principles for constructing and evaluating clinimetric indices. In effect, an attempt is made to establish clinical standards.

The book is aimed at all those seeking precision in clinical assessment, particularly those involved in the construction of studies and the collection of data. Chapters 2 to 7 are concerned with the precise structuring of clinimetric indices, their component variables, and the organization of output scales, and provides a consistent reminder of the necessity to define goals when attempting clinical measurement. There are useful chapters (8 and 9) which draw attention to the necessity for compatibility of these clinical goals with the goals of statistical and psychosocial methods. There are then a group of chapters which address the problems of validating the chosen clinimetric index. As the author says, "the validation process is complex", and at times the terminology is overwhelming. The final chapter of this book provides a useful summary to each of the constituent chapters, and helps consolidate the extensive terminology and complex principles introduced throughout the book.

The principles encapsulated in this book are refreshingly expressed and invigorating. It should provide interest, information and inspiration for clinicians involved in any area of investigation. Although the vastness of the terminology is at times cumbersome and daunting, the author has made an admirable attempt to structure a system. The reader's task is lightened by illustrating the principles with familiar clinical indices, such as the APGAR score, and by frequent reference to specific clinical questions. More liberal use of illustrations might have aided general comprehension and made the text more approachable.

Diana Tait

Nuclear and Atomic Data for Radiotherapy and Related Radiobiology. Proceedings of a meeting at Rijswijk 16–20 September, 1985, pp. x + 454, 1987 (International Atomic Energy Agency, Vienna), Austrian Schillings 950.
ISBN 92-0-131087-0

This is the proceedings of the meeting of the Advisory Group on Nuclear and Atomic Data for Radiotherapy and Related Radiobiology held in Rijswijk, Netherlands, 1985. The meeting was organized by the International Atomic Energy Agency and attended by 35 scientists from several countries with the following objectives: to make an inventory of available knowledge on nuclear and atomic data relevant to radiotherapy and related radiobiology; to identify and specify further needs for nuclear and atomic data and their accuracies; to stimulate new experimental and theoretical work to fill the identified gaps in nuclear reaction, decay and atomic data; and to formulate specific technical recommendations for further work.

The six chapters address topics on the physical and chemical bases for biological effects in DNA targets; neutron beam production and application; neutron, pion and charged particle interaction; and charged particle track structure. The book has a wide scope, giving up-to-date information on radiation physics and chemistry related to radiobiology and radiotherapy protocols, and there are some very good articles among the 27 papers. The book has a wide appeal to those involved in fundamental radiation effect research in radiobiology and radiotherapy and is particularly useful for identifying new research projects.

The most valuable part is the final section, on the report of the three working groups: beam production and field specification; dosimetry; interpretation and optimization of biological effects. This section gives details of specific requirements and critical parameters in the field and identifies the gaps in the present available data. It seems that data on cross-sections are the most needed at the present time. My criticism is reserved for the first objective of the meeting (an inventory of the available data), in which a better presentation could have been made.

H. Nikjoo

Physical Aspects of Brachytherapy (Medical Physics Handbooks 19). By T. J. Godden, pp. ix + 291, 1988 (Adam Hilger, Bristol), £37.50.
ISBN 0–85274–511–7

This is a useful and interesting book for any physicists and radiotherapists dealing with brachytherapy treatments. It is well written and up to date in the techniques and developments it describes, and is a good reference book for those people already involved in brachytherapy techniques, since there is sufficient detail on purchase, testing, calculation and safe handling of sources. All necessary subject areas are covered and therefore each topic is dealt with fairly concisely, but there are sufficient references for further study.

The chapters on sealed source dosimetry and the localization of radioactive sources *in situ* are, of necessity, theoretical; but most, if not all, chapters are interesting and informative reading for anyone requiring an introduction to the subject. The illustrations are clear and appropriate to the text, and the tables of constants and source specifications draw together the most recent data available.

The first chapter begins with a historical background to sealed source therapy and goes on to describe the radiation units required, in both the SI and more historical format. The latest definitions and tables of constants for most sealed sources in brachytherapy use are well set out and easy to find. The biological effects of radiation are discussed briefly and models for calculating dose–time relationships are reviewed. Chapter 2 describes the production and construction of all the sealed sources in common use. There is a comprehensive review of calculation methods in Chapter 3, and considerations of absorption, attenuation and scatter.

Any confusion over specification of source strength is cleared up in Chapter 4 and quality assurance checks are described. There is a brief review of dosemeters suitable for absolute and relative dose measurement and a comprehensive list of references for further study. Line and point source distributions are described, but there are no diagrams, which would have been helpful here.

External applicators and moulds, interstitial and intracavitary therapies are described in detail in Chapters 5–7. The relevant dose calculation methods and the limitations of each are presented. Worked examples are helpful and relevant to clinically-encountered situations. Interstitial and intracavitary therapy using neutrons completes these chapters. Chapter 8 reviews current techniques of *in vivo* source localization in some detail, and the computer algorithms available for point sources, straight and curved line sources. The last chapter is concerned with the safe use of sealed sources from the protection requirements, storage and custody of sources to the routine source checks and source handling and transport.

The book fulfils the aim set out in the preface of "providing the reader with an overall view of historical and current brachytherapy practice and sources available and to give an insight into the associated dosimetry and a practical guide to the use of dosage systems in clinical situations". It forms a complete, cost-effective guide to modern brachytherapy techniques. It appears rather brief in some aspects, but covers all the necessary topics and provides a basis for further research. It is useful for intercomparison of properties of currently available brachytherapy sources. The editorial standard is reasonably high and the price reflects the quality and quantity of information presented. I would definitely recommend its purchase as a reference book by anyone involved, now or in the future, with brachytherapy treatments.

ELIZABETH M. DEAN

Pediatric Tumors of the Genitourinary Tract. Ed. by Bruce H. Broecker and Frederick A. Klein, pp. ix + 336, 1988 (Alan R. Liss, New York), $72.00.
ISBN 0–8451–4244–5

Pediatric Tumors of the Genitourinary Tract is intended to be a clinical reference text collating the most current information available on management of this group of rare tumours. This volume is edited by Bruce Broecker, MD and Frederick Klein, MD who are both specialists in surgery, the former being in paediatrics and the latter in urology. However, contributions have been gathered from a number of specialties so that this volume brings together current views from pathologists, haematologists, medical oncologists, paediatricians and radiotherapists, in addition to some major contributions from surgical specialists. The contributors are mainly American, with some input from Europe giving a balance of opinion from both sides of the Atlantic. With this varied input, the book provides and excellent source of reference for diagnosticians, pathologists, clinicians and scientists who may be involved in the management of, or research activities associated with, these tumours.

This is a well presented book, which is easy to read, informative and up-to-date. In addition to the obvious clinical requirements of the subject, the authors have had the foresight to include chapters such as the "genetics of paediatric genitourinary tumours" and "coping with cancer in childhood".

It is hard to pick out particular chapters for praise, as the general standard of contributions is high, but to this reviewer, the most interesting were the "Genetics of paediatric genitourinary tumours" by Vincent Riccardi and "Adverse effects and sequelae of paediatric genitourinary cancer therapy" by Frederick Klein. These two chapters contain information of newly recognized significance and highlight the importance of the aspects of cancer biology and management beyond the traditional application of surgery, radiotherapy and chemotherapy.

This is an excellent reference book, which will be useful both to medical libraries and to individuals concerned with the management of childhood tumours.

DIANA TAIT

Essentials of Clinical MRI. Ed. by Theo H. M. Falke, pp. x + 235, 1988 (Martinus Nijhoff, Dordrecht), £49.50; US $79.00; Dfl.160.00.
ISBN 0–89838–353–6

The stated aim of this book is to provide an introduction to the essentials of magnetic resonance imaging. There are a number of articles under the headings of General Principles, Neuro Imaging, Abdominal Imaging and Musculoskeletal Imaging. Most of the contributors are Dutch, the majority being from Leiden, with a few from the United Kingdom and United States.

The book is not comprehensive in its coverage of the subject and there are some important deficiencies. Useful features include summaries on potential hazards, high-speed imaging of the heart and magnetic resonance imaging of the abdomen. The standard of contribution varies in regard to the scientific content and language. Firmer editing would have been beneficial for these reasons, as well as preventing the substantial amount of repetition. The expert is unlikely to find little new information here, while the beginner in magnetic resonance imaging would be better advised to consult one of the larger text books for either detailed reference or for wider coverage of the subject.

G. H. WHITEHOUSE

MRI: A Teaching File Approach. By John H. Bisese, pp. xiv + 300, 1987 (McGraw-Hill, New York), £59.95.
ISBN 0–07–005403–7

This book consists of the magnetic resonance images of 250 cases (249 when one realises that the same case is used as an example of retroperitoneal fibrosis on p. 282 and carcinoma of the prostate on p. 283!). Each set of images is accompanied by a short description under the headings Examination, Clinical Information, Technique, Findings, Impression, Confirmation, Discussion and Reference. The most serious criticism is that only a small minority of the cases illustrated have any confirmation at all. The majority have been labelled as examples of a particular disease on the basis of the radiologist's 'impression' and unfortunately only an impression not even a diagnosis.

Once one begins to look for faults they are all too numerous. The overall quality of the illustrations, obtained at 0.6 T, is good but the images appear to have been taken directly from the monitor without deleting distracting scan details. It is especially distracting when the sequence data on the images contradicts the information given under "Technique" in the main text. For example, in Case 4 the text states that axial and coronal images were obtained at a TR of 2000 with TE of 40 and 80 and yet the coronal images show a TR of 1800 and there is one sagittal image with TR 500 and TE 32 clearly visible. Similar errors are repeated throughout. No attempt is made to label the individual images as T_1, T_2 or spin-density weighted and the terms are used inconsistently. Arrows are employed liberally but without labels or notes in the text to determine what is arrowed. The discussion section of each case is usually short — five to 10 lines — and makes one or two general points on MRI. When it becomes more specific there are problems. The attempt to explain the appearance of haemorrhage on MR on p. 42 is so garbled that I wondered if it had been translated.

The book is expensive at nearly £60 and I am unsure for whom it is intended. The errors and inconsistencies referred to above make it unsuitable for the trainee and anyone who can work out which image is which will be able to arrive at their own 'impressions' of the pathology demonstrated.

MICHAEL WILLIAMS

MRI of the Brain, Head, Neck and Spine. A Teaching Atlas of Clinical Applications. By Jaap Valk, pp. xiv + 576, 1987 (Martinus Nijhoff, Dordrecht), D.fl 350.00, $175, £110.00.
ISBN 0–89838–957–7

This book is based on the author's personal experience of more than 5000 documented cases studied with a 0.6 T superconducting MRI system in Amsterdam.

A very brief summary of the basic physical principles of MRI is followed by a useful description of various technical considerations such as pulse sequences; some anatomical structures displayed by them; tissue differentiation; artefacts; flow phenomena and surface coils. A short section on MRI studies of special regions such as the pituitary follows. The 14 subsequent chapters cover all the major disease processes and include affections of the brain, orbit, larynx, neck and temporomandibular joints. Spinal disorders and the use of contrast agents are also covered.

The range of pathology and MRI appearances covered is comprehensive. The text is profusely illustrated with half-tone illustrations (more than 1500), mostly of the highest quality, although some are too dark and many could have been larger. It is most gratifying to see frequent and intelligent use of inversion recovery sequences. The closing pages of the book include an extensive and up-to-date list of references and a useful index.

The style and content of the book assumes an extensive knowledge of anatomy and pathology amongst its readers. Indeed, there is no formal section of normal anatomy. Furthermore, the section on basic physical principles, though very brief, is almost certainly too complex for those who do not already have a basic understanding of the subject.

Each of the sections covering disease processes is preceded by a short introduction to the pathology involved and the role of MRI in that anatomical area or clinical problem. This is followed by a series of case presentations displaying the pathology as studied by MRI. A total of more than 250 cases is presented. In keeping with the concept of an atlas, the text provides very little coverage of the interface between MRI and other imaging modalities. These case presentations form the core of the book (about 500 pages) and are of a high standard. The approach and the information are up-to-date. This reviewer would have appreciated some cross-referencing between cases, however, and felt that the balance of content could have been improved with, for example, less emphasis on "gliomatosis cerebri" (seven cases) and more on intracranial meningiomas (four cases). The non-specificity of many abnormal MRI signal characteristics could have been emphasized. Many readers would probably have found it useful in a book at this level to have the references cited in the text.

While the printing and binding are of high quality, other aspects of the publication and editing unfortunately are not. The text is peppered with minor spelling errors and there are many unusual expressions. Although most of the latter are the charming consequence of language differences, others are irritatingly inconsistent. For example the "Circle of Willis" is also referred to as the "Circulus Willisi" in other parts of the text. Broadly, however, the style is lucid and easily followed. Half the "T" entries in the index are misplaced and initially misled me into believing that a number of important topics were not covered. Reference to images in the text is often unclear and several appear to be out of place. In other cases it is unclear which images have been enhanced or which pulse sequence has been used, although in most instances unhelpful data on excitations and matrix are provided to the detriment of clarity. The order in which topics are presented does not follow any obvious logic, with spinal lesions and contrast agents lying between intracranial tumours and infections. As one progressed through the book one gradually became increasingly frustrated by these errors, which should not be so evident in a book at this price.

In the foreward the author quite rightly states "MR images . . . may cause confusion and uncertainty about their diagnostic content. This will sometimes lead to an unecessary retreat to other diagnostic modalities." The author sets out to correct this situation and overall, he fulfills his aims. Despite the criticisms outlined above, I believe the book is fair value at today's prices. However, its purchase will be largely confined to those individuals and institutions performing MRI, or using an MRI service regularly.

JOHN R. BRADSHAW

Magnetic Resonance Imaging of the Brain, Head and Neck. A Text Atlas. By William G. Bradley Jr, W. Ross Adey and Anton N. Hasso, pp. ix + 130, 1985 (Aspen Systems, Maryland), £82.80.
ISBN 0–87189–094–1

This book is basically in two parts. The first 35 pages present a discussion of the physics of NMR, while the following 90 pages comprise an atlas of head and neck images. The book is handsomely presented, but the images, which are produced from a 0.35T superconductive system, whilst of reasonable standard, are not of the highest quality currently available. They are exclusively spin-echo sequences, and tissue contrast could have been increased with alternative sequences.

Dr Bradley's introductory chapter, "Fundamentals of Magnetic Resonance Image Interpretation", is an excellent, concise yet comprehensible, account of the nature of nuclear resonance, explaining the major concepts of T_1 and T_2 weighting and effects of flow in the image. The second chapter, dealing with interaction of cells and electromagnetic fields, is a much more esoteric contribution, and probably superfluous to this text atlas, which is obviously intended for readers at a very early stage of their exposure to NMR imaging.

The head and neck images include axial, sagittal and coronal display. The anatomical features in the images are clearly and directly labelled, but occasionally the eye of faith is required, as for example in specific naming of seventh and eighth nerves when the internal auditory canal is indicated, and of the optic chiasma when the suprasellar region is indicated. There is only one image per page, and this only occupies about 60% of its area. The other 40% is expensive blank paper!

The information contained in this book is available elsewhere but presented here in a very convenient format. Radiologists in training, clinical neuroscientists and even medical students could all find it useful, but it represents a fairly expensive investment for readers who will rapidly assimilate its contents and want to proceed to a text including pathological material.

A. R. VALENTINE

Cranial and Spinal Magnetic Resonance Imaging. An Atlas and Guide. By David L. Daniels, Victor M. Haughton and Thomas P. Naidich, pp. xvi + 315, 1987 (Raven Press, New York), $150.00.

ISBN 0-88167-185-1

This book commences with a presentation of the principles of magnetic resonance imaging and its application in the recognition of normal and pathological conditions. Neuroanatomy is then described on a regional basis, and beautifully illustrated with cryomicrotome sections juxtaposed to almost identical magnetic resonance sections. These are supplemented, as necessary, in the more complex regions such as the deep grey matter and the limbic system, with helpful diagrams. The commoner manifestations of the diseases affecting the particular regions are also illustrated and briefly described.

The cranial section does not include orbits, sinuses, facial structures, pharynx or larynx, and the spinal section does not include the musculature. Otherwise, all regions are well covered, and the presentation is simple and lucid, and suitable as an introduction to the subject for people at all levels of knowledge from medical students to neuroradiologists. The complex anatomy of the deep cerebral structures and of the limbic system are particularly well demonstrated in an easily assimilated manner.

There is virtually no repetition. All the magnetic resonance images are of good quality and the anatomical colour plates excellent. The latter obviously contribute considerably to the cost of the well produced volume which is rather expensive for individual purchase. It is recommended for departmental and hospital libraries as an excellent introduction to the subject. The references are contemporary and there is a good index, making it useful for reference purposes also.

BRIAN KENDALL

Atlas of Axial, Sagittal and Coronal Anatomy (with CT and MRI). Ed. by A. John Christoforidis, pp. xii + 563, 1988 (W B Saunders, Philadelphia), £95.00.

ISBN 0-7216-1278-4

A really good atlas of sectional anatomy with radiological correlation is a long awaited product. So many are good up to a point. Others omit key areas of the body. Wagner and Lawson's *Segmental Anatomy* is one of the best to date. But now comes this tome from Ohio which poses a real challenge. The driving force emanates from Dr Christoforidis who has stimulated his colleagues into sharing the production of a really worthwhile book. To create this work while being Chairman of a Department is an exceptional task, but maybe Chairmen have hidden powers of persuasion!

The whole body is covered. Sections on Head and Neck, Spine, Thorax, Abdomen, Pelvis and Extremities ensure that there are no lacunae. That there are more illustrations in the axial plane is hardly surprising, given the ever-increasing role of computed tomography in modern medicine. But approximately 40% of the book is devoted to sagittal and coronal MR images. There is roughly one cadaver photograph (several in colour) for every four radiological images. Wherever possible the authors have tried to marry a photograph of a section of a cadaver with counterpart images both from a cadaver and from patients. From personal experience I know how difficult this is; it might have been easier had CT been performed with the cadaver frozen, although this does cause some curious artefacts. Nevertheless the correlation is quite good and more than illustrates the use of cross-sectional images in displaying and teaching topographical anatomy.

This book is aimed at students, anatomists, radiologists and physicians. All would benefit from close acquaintance with the contents. The editorial style is good with very few inconsistencies (*e.g.* azygous admixed with the correct azygos). The book is up-to-date and I suppose that it represents realistic value for money. It is probably the most comprehensive work of its kind and will therefore become a necessary string to the bow of each imaging department.

But there are several features on the debit side. First is that the tonal range of many of the images is deficient. Whether this is due to the chosen window widths and levels on the original images, the subsequent photography or the final printing is hard to say, but in several illustrations the labelled structures are hard to identify. It might have been better to have had a few unlabelled images/line drawings alongside for comparison. Occasionally detail is insufficient. For example, the segmental bronchi are now well delineated; similarly, hepatic segmentation is not considered. On this latter topic, the quadrate lobe is given too much prominence and even incorrectly labelled (it should be the posterior convexity of the medial segment of the left lobe). Finally, in this era where we strive for universal uniformity in the display of images, I ask what is the correct method of displaying sagittal images? I prefer them viewed from the patient's right, as in ultrasound. We have won the war for axial images which should now universally be viewed from below. Surely as a profession we should aim for similar uniformity elsewhere? The clinician has long examined the patient from the right of the bed. Thus, in our MR unit, images are displayed as viewed from the patient's right; but not in this book.

Despite these reservations, this work deserves and will receive wide success.

ADRIAN K. DIXON

Magnetic Resonance Imaging of the Knee. By Jerrold H. Mink, Murray A. Reicher and John V. Crues III, pp. xiii + 178, 347 figs, 1987 (Raven Press, New York), $95.50.
ISBN 0–88167–332–3

This book is outstanding. It introduces the complex subject of magnetic resonance imaging (MRI) of the knee in an authoritative fashion based on the experience gained from over 2000 such examinations. I was particularly impressed by the views stated in the preface, where Dr Mink expresses his initial doubts about the technique and his slight reluctance to change from arthrography; the honest account of his subsequent conversion to MRI makes compelling reading. Much of the book represents an expanded version of the many scientific papers on this subject which have emanated from these workers. It also provides what must be the largest available collection of up-to-date references pertinent to knee MRI.

A good account of the necessary physics is provided at the outset. The section on technique is sound, with good practical advice as to projection and sequence selection. The authors admit that thinner slices may be helpful in the future; at the time of writing they were limited to 5 mm slices. An excellent description of the anatomy of the knee follows. This chapter contains extensive correlative gross specimen/MRI images which are well arranged and easy to interpret (the cadaveric photographs are in colour). Many second MB and FRCS candidates might find their understanding of the anatomy of the knee improved after acquaintance with this chapter. I certainly did! The description of meniscal and cruciate tears is, as expected from these distinguished workers, excellent. The authors nobly accepted menisci with abnormal MRI appearances, shown to be normal at arthroscopy, as false positives, although they do describe patients in whom subsequent probing of apparently normal menisci revealed defects. They also emphasize how the arthroscopist can only see the surfaces of certain parts of the menisci. Rupture of the cruciate ligaments is well described; I think I now understand why it is so much more difficult to identify the anterior cruciate ligament than its posterior counterpart. There are good accounts of osteonecrosis and allied disorders as well as descriptions of other common clinical disorders. The closing chapter on pitfalls brings the reader back to earth with a bump. As ever with new techniques, there is a wealth of interpretive problems for the uninitiated. I predict that many of these images will turn up in future editions of "Keats".

There are virtually no negative features in this book, which will be of help to anyone involved in knee imaging. There are very few errors. The price is about par for such a volume nowadays, but in this instance the book does provide value for money. On the subject of cost, the authors even point out some possible savings if MRI replaced diagnostic arthroscopy!

ADRIAN K. DIXON

Clinical Applications of Doppler Ultrasound. Ed. by Kenneth J. W. Taylor, Peter N. Burns and Peter N. T. Wells, pp. xii + 371, 1988 (Raven Press, New York), $86.50.
ISBN 0–88167–355–2

Until very recently it would have gone without saying that angiography was exclusively an X-ray based technique. The development of flow-sensitive NMR imaging sequences has been one factor in altering that perception but what now seems likely to be a much more powerful and versatile tool in the investigation of the vascular system is being provided by ultrasound. The use of the Doppler frequency shift for observing blood flow is an old trick, but two comparatively recent developments have enabled that phenomenon to be exploited in a manner that is clinically practicable in a wide range of applications. The first of these developments was to marry, in so-called "duplex" systems, a real-time ultrasonic imager with Doppler analysis of flow characteristics at a chosen region of interest in the observed image. The present book provides a thorough and systematic account of the principles and practice of this approach and its value should be in no way diminished by its having been effectively overtaken by the most recent phase of technical development, that of so-called "colour flow mapping", in which real-time display of presence and direction of flow can be overlaid, as an additional image parameter, on the conventional B-scan image. Indeed, this development (which is here only briefly described and illustrated) will simply strengthen the value and practicability of what the book has to offer.

A major strength of Doppler is that it provides information on vascular dynamics. The detailed principles by which such information is derived will be unfamiliar to many of the radiologists, clinicians and sonographers for whom this book is intended and it opens therefore with four introductory chapters that give a clear but reasonably detailed account both of the haemodynamic parameters that are accessible to study and also of the method and instrumentation employed. The remaining two-thirds of the book provides a series of systematic accounts of the clinical role of what might well be termed "ultrasonic angiology" (with the connotation of a study that is not merely graphical but also analytical) in eight different areas of application: carotid, gastrointestinal, renal, pelvic, obstetric and paediatric, together with arterial and venous aspects of vascular disease of the lower extremities. Each chapter gives a well illustrated account of the relevant normal vascular characteristics, contrasts this with a variety of pathological appearances and discusses the relative place of ultrasound and complementary alternative techniques. Although a minor criticism of some of the clinical chapters is that neither their authors nor the editors have succeeded in properly relating the practice described there with the principles set out in the introductory chapters, they nonetheless provide abundant illustration of the practical use of various accessible haemodynamic parameters, such as bulk flow, flow velocity, flow turbulence, and vascular bed impedance.

This is a well conceived and timely book on a subject that is on the way to having an important place in the practice of radiology. The chapters are all of good standard, well set out and illustrated, and without an undue degree of repetition. The coverage is quite comprehensive although, for a book with strong intellectual origins in Bristol, it is perhaps surprising to see no reference to study of blood flow in the breast. It should have a useful place in any departmental library and anyone with access to a duplex or colour-flow imaging system is likely to benefit from having a reference copy on their own shelf.

C. R. HILL

1989, *The British Journal of Radiology*, 62, 201–208

MARCH 1989

VOLUME 62 NUMBER 735

The British Journal of Radiology

A new high-definition microfocal X-ray unit

By J. C. Buckland-Wright, PhD

Macroradiographic Research Unit, Anatomy Department, United Medical and Dental Schools of Guy's and St Thomas' Hospitals, London Bridge, London SE1 9RT

(Received July 1988 and in revised form September 1988)

Abstract. A new microfocal unit is described with an operating range up to 170 kVp (limited to 125 kVp for medical use), 0–1 mA and a maximum output of 75–80 W. The unit comprises a lanthanum hexaboride (LaB_6) cathode, a single electromagnetic lens and a stationary oil-cooled multifaced tungsten target. The estimated source size ranges from 6 to 20 μm between 14 and 77 W. The tube's output is ×3 to ×3.5 greater than that of a conventional X-ray unit. The use of fast rare-earth film–screen systems permits exposures of most views of the patient within 1 s. The spatial resolution within these film–screen systems is 40–30 μm diameter at magnifications of ×5–10. The tube is fixed so as to project a horizontal beam and the patient table is designed to position the patient close to the source (20–30 cm) with the film placed at a focus–film distance of 1–3 m. Stereopair macroradiographs permit greater accuracy in the identification and location of radiographic features. The large magnification and resolution of macroradiographs allow direct and accurate measurement of radiographic features.

Microfocal X-ray units are characterized by an X-ray source of between 100 and 10 μm diameter, and in terms of the tubes described here of the order of < 20 μm. The principal advantage of the point source of X rays is the production of high-resolution macroradiographs with a geometric magnification of ×5 or more obtained by placing the object close to the source and the recording emulsion or detector at some distance away. For these instruments the production of a micron-sized X-ray source through the focusing of an electron beam by one or two electromagnetic lenses was first suggested in 1939 (Ardenne, 1939; Marton, 1939). The first tubes were designed and made at the Cavendish Laboratories, Cambridge by Cosslett and Nixon (1951; 1952a, b; 1960; Nixon, 1961). The low energy of these units restricted their application to the study of insects and thin biological samples (Cosslett & Nixon, 1960). Wider application of the microfocus X-ray units followed the modifications introduced by Ely (1980). These included the isolation of the electron gun from its outer casing and the replacement of the foil transmission by a solid cylindrical target (Ely, 1960; 1980).

These modifications were incorporated in not only the electromagnetic but also an electrostatically focused X-ray unit known as E12. In the latter, the electron beam is focused by a shaped bias cup onto the side of the solid target (Sharpe, 1979; Parish, 1986). The normal operational range is 30–80 kV, with a maximum tube current of 0.5 mA at 80 kV and 1.0 mA at 50 kV or less. The effective focal spot size was 10–20 μm. These units were most successfully applied in industry for both investigation and quality control (Sharpe & Parish, 1980). One such unit was placed at the Orthopaedic Centre, Oswestry, where its application to patient investigation was severely restricted by the low tube current.

The introduction of the same modifications to the electromagnetically focused units ultimately resulted in a two-coiled electromagnetically focused unit with an operating range of 20–60 kV (Buckland-Wright, 1980a). The maximum tube current was 1.0 mA at 60 kV with an effective focal spot of 6–8 μm. The electromagnetic lenses overcame the difficulties in retaining the very small X-ray source with the increased accelerating voltage and beam current.

The low power, characteristic of microfocus X-ray units, would have restricted their application to the study of human and animal post-mortem material, had it not been for the parallel development in the rare-earth film–screen combinations. Although these systems are inherently noisy, the advantages of projection magnification of ×3 or more has been found to overcome this limitation (Doi & Imhoff, 1977). Using 3M's Trimax T16 and T8 screens and XD film, studies have been carried out successfully on the examination of the wrist and hands of patients with rheumatoid and osteoarthritis using the electromagnetically focused microfocal unit at 60 kV, 1 mA with exposures of < 1 s (Buckland-Wright, 1983a, b; 1984; Buckland-Wright et al, 1987a, b).

The high magnification and spatial resolution obtained with ×5 macroradiographs of the wrist and hand permitted the early detection of bony lesions in the joints, as well as their alteration in size within as short an interval as 3 months (Buckland-Wright, 1983a). The low output of this X-ray unit (XM 60G) restricted its application to the study of small joints such as found in the wrist and hand. This paper describes the recent

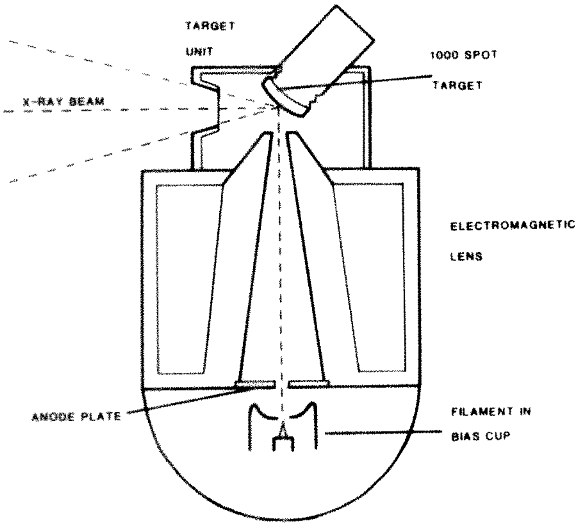

Figure 1. Schematic diagram of the microfocal X-ray unit HF200M illustrating the arrangement of the cathode, electromagnetic lens and target assembly.

Table I. Output measurements at different kVp for the microfocus tube HF200M compared with a three-phase 0.6 mm focal-spot conventional tube (Siemens, Megalix with Polydoras generator). Measurements were carried out at an FOD of 75 cm with an MDH 1015 ionization chamber and 2.4 mm Al filtration

kVp	Output (μGy/mAs)		
	Microfocus HF200M	Siemens Megalix	Difference
60	187.0	52.2	× 3.5
70	245.3	72.2	× 3.4
80	297.5	98.3	× 3.0
90	389.8	119.2	× 3.3
100	475.9	151.4	× 3.1
110	519.4	171.4	× 3.0

advances in microfocal radiography permitting the routine examination of large joints at magnifications of up to × 15. The advance has been possible through the development and manufacture of a new type of microfocal X-ray tube (HF200M) combined with the advances in the performance of rare-earth film–screen systems.

The new microfocal X-ray unit

HF200M

The HF200M was designed by Harwell and Oxford Applied Research Ltd and manufactured by Pantak Ltd (now Astrophysics Research Ltd). Although the design specifications were for an instrument for industrial use, modifications were incorporated, in collaboration with the author, for medical use. The result is a compact system for high-definition radiography over the range 20–170 kV, 0–1 mA (measured at the target) with a maximum output of 75–80 W (Fig. 1). For medical applications the maximum accelerating voltage is set to 125 kVp. The combination of autofocus and the absence of mechanical adjustments renders the tube particularly easy to operate. A small ion pump maintains the requisite operating vacuum (10 Torr) thus avoiding use of auxillary pumping units characteristic of earlier microfocus units (Ely, 1980).

The design of the electron gun incorporates a lanthanum hexaboride (LaB_6) cathode (Mulvey & Newman, 1975; Rockett & Parish, 1985; Parish, 1986). The greater electron emissivity of this cathode reduces the exposure of the cathode surface to the extraction field and the lower operating temperature greatly improves the mechanical stability. Because of the small virtual source, a single electromagnetic lens was considered sufficient to meet the specified focal conditions. The extended pole shape of the lens (Mulvey & Newman, 1975; Rockett & Parish, 1985; Parish, 1986) means that the focus occurs well clear of the lens face thus increasing the usable X-ray beam solid angle. The tungsten target or anti-cathode is stationary and oil cooled. The results of tests on the pre-production unit revealed that the electron beam eventually pitted the target surface and subsequent units have been fitted with a multifaceted anti-cathode. The first 1000-spot target unit was placed at this hospital. It has been estimated by Pantak Ltd that each spot would last 10 W hours. In practice it has been found that the spot life is between 20 and 25 W hours. Deterioration of the condition of the target is noted by both a drop in output and a loss in focus quality. In general a new focus position is selected at the start of each day.

The output characteristics of the tube, measured with an ionization chamber (MDH 1015), were compared with that of a three-phase 0.6 mm focal spot conventional tube (Megalix, Siemens) (Table I). The microfocal unit was found to have an output between × 3.0 and × 3.5 greater than the conventional unit over the range 60–110 kVp. The greater emissivity of the microfocal tube is due to a number of factors, including the efficiency of the electromagnetic lens in delivering the electron beam to the target, the different methods in which the tube current is measured (at the target in the HF200M and at the filament in the conventional unit), and the highly polished surface of the target in the microfocal tube.

The selection and maintenance of the optimal, *i.e.* smallest, focal spot is essential for achieving high magnification and spatial resolution in the macroradiographs. Accurate focusing of the X-ray tube is initially obtained by altering the lens control so as to obtain a sharp image of fine-wire meshes (400 and 300 lines cm^{-1}) placed at the tube window. The shadow image of the meshes are detected using a TV camera with a phosphor-coated fibre-optic-faced vidicon tube (Buckland-Wright, 1976; 1977). Figure 2 is a photograph of these meshes recorded on fine-grain X-ray film.

Once the optimum lens control position has been selected no further adjustment is required in view of the autofocus facility. The sizes of the fine meshes recorded

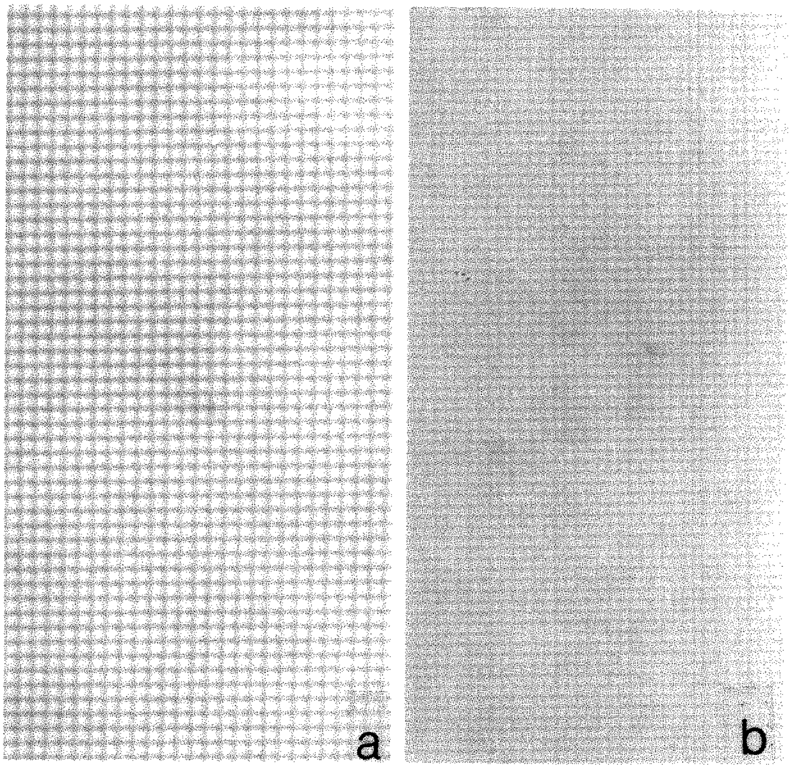

Figure 2. (a) 300 and (b) 400 lines cm^{-1} resolution meshes recorded on fine-grained industrial film (Cronex NDT55, Dupont) with the X-ray unit operating at 70 kV, 0.7 mA. The width of the bars are clearly defined as 12 and 6 μm diameter, respectively. Magnification of (a) × 50 and (b) × 57.

determined the dimensions of the smallest objects detectable by the X-ray apparatus and, in consequence, are an expression of the X-ray source size (Cosslett, 1957). At energy levels of 14–49 W (*i.e.* 20–70 kV at 0.7 mA) and 50–77 W (*i.e.* 80–110 kV at 0.7 mA) the diameter of the objects recorded ranged from 6 to 10 μm and from 12 to 20 μm, respectively. The high-resolution performance of the HF200M X-ray tube is thus similar to previous microfocal tubes designed by Ely (Ely, 1980; Buckland-Wright, 1980a).

The arrangement of the X-ray tube, control panel and unit is illustrated in Fig. 3. The tube is housed in lead casing and mounted on a column fixed to the floor to avoid any mechanical vibration to the tube head. The tube is placed at one end of the room to provide a horizontal X-ray beam (1 m above the floor) with sufficient source-to-film distance to permit the preparation of large magnification radiographs. A shutter, filter and collimator unit is mounted in front of the X-ray port. It is designed to be as narrow as possible so as to permit the object to be brought close to the source. This enables a large projection magnification to be achieved within both a short focus–film distance (FFD) and exposure time. A motor-driven shutter provides controlled exposures in 0.1 s incremental steps. In general, exposure duration is within 1 s for most parts of the body examined. The operation of the shutter separate from the X-ray tube permits the tube's autofocus to track and focus the electron beam prior to exposure of the film. This ensures that the image resolution is not lost through unfocused X rays at the commencement of the exposure. In front of the shutter, the filter carrier comprises a series of ports or windows for a number of filters; 2.4 mm aluminium filtration is normally used. Alternative filtration can be selected by sliding the filter carrier horizontally. The X-ray beam is finally defined by a series of lead apertures. These are of different dimensions providing collimation of the X-ray beam for the different sized X-ray plates at various distances from the source.

Patient table

As the X-ray source is fixed at a height of 1 m from the floor, patients are moved relative to the source both for positioning and for taking stereopair radiographs. The patient table, designed by the author and made in collaboration with Ciba Geigy and Fraser Nash Ltd, is illustrated in Figs 3 and 4. The table displaces the patient, relative to the source, in three planes. Vertical displacement is obtained through the hydraulics of the platform. Movement in the two horizontal planes is achieved by a guided wheel and track arrangement. Millimetre scales along the axes of movement permit the position of the patient on the platform to be recorded. The displacement required for the preparation of stereopair radiographs can be measured. Positioning of the patient relative to the centre of the X-ray beam is achieved with a cross-optic laser (Varian TM) mounted in front of the image intensifier (Fig. 4) with the light beam directed along the central axis of the X-ray beam

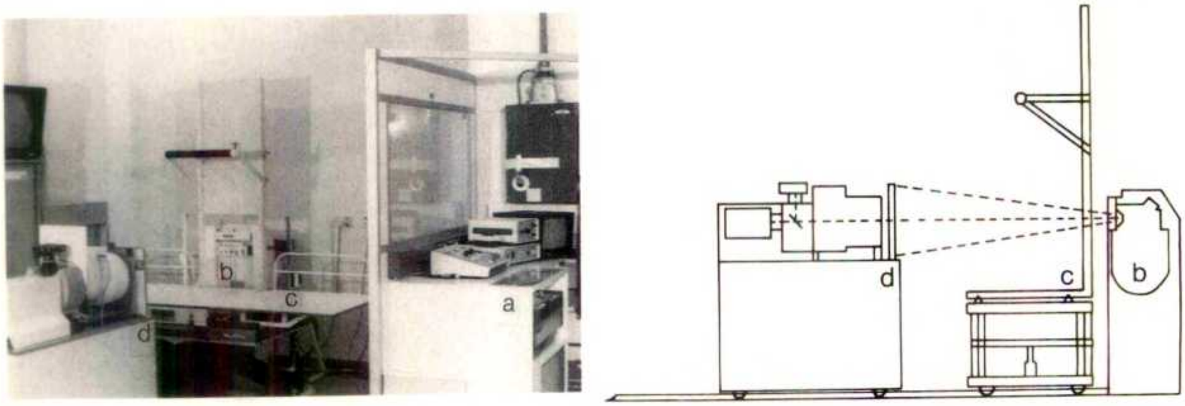

Figure 3. Photograph and schematic diagram showing the general arrangement of the equipment: (a) control panel, (b) X-ray tube, (c) patient table and (d) position of the film cassette in front of the image intensifier and camera assembly.

towards the X-ray port hole. When required, precise positioning of the area of interest is obtained by screening.

The image intensifier and camera system are mounted on a track. A motor drive allows the intensifier-to-object distance to be altered during screening, in order to select the required magnification with the FFD lying between 1 and 3 m. Restraining straps or foam wedges are applied to the patient to restrict movement during the X-ray procedure as the slightest patient movement is increased by the magnification factor when recorded on the film. For this reason the patient is brought close to the source, focus–object distance (FOD) between 20 and 30 cm, to achieve as short an exposure time for the required magnification as possible. The arrangement for taking radiographs of the wrist and hand, knee, hip, a modified tunnel view and knee arthrogram are shown in Figs 4 and 5.

Film–screen combinations

The selection of the fast rare-earth film–screen combinations required to obtain exposures of 1 s or less in the examination of large joints was obtained from an evaluation of 14 different combinations of commercially available film–screen systems (Table II). Plastic-faced

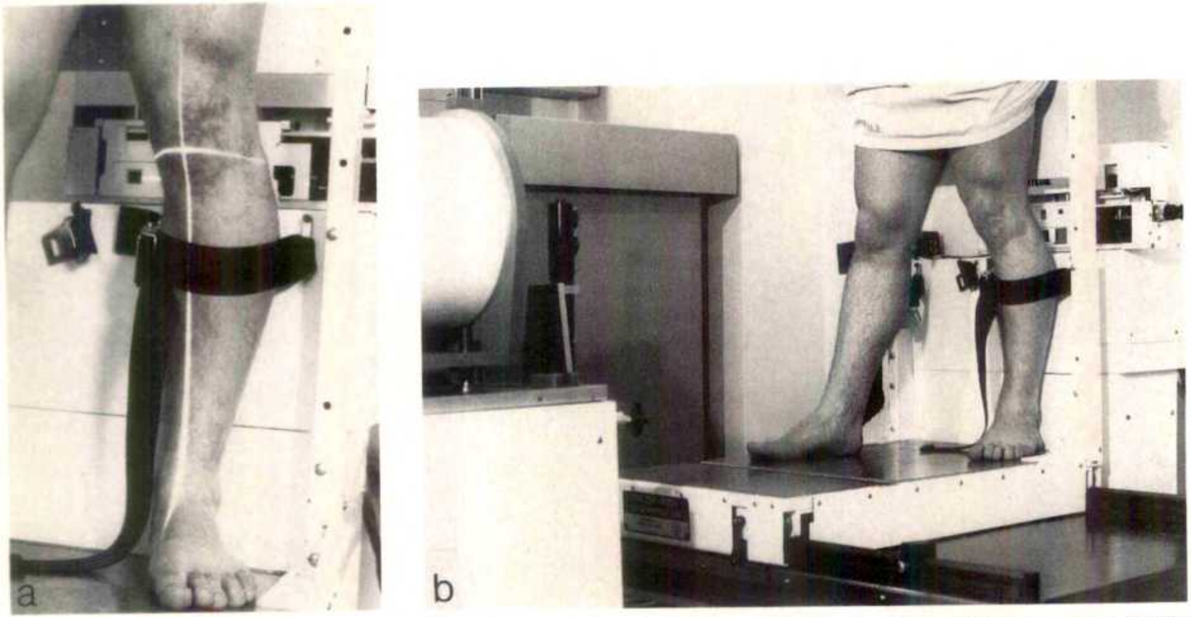

Figure 4. (a) Using the cross-optic laser to position the part of the patient to be examined in the centre of the X-ray beam. (b) The position of the laser in front of the image intensifier. Prior to making an exposure, the laser is dropped out of view. The postero-anterior view of the knee is preferred as in the antero-posterior position the patella is enlarged and overlies most of the tibio-femoral joint.

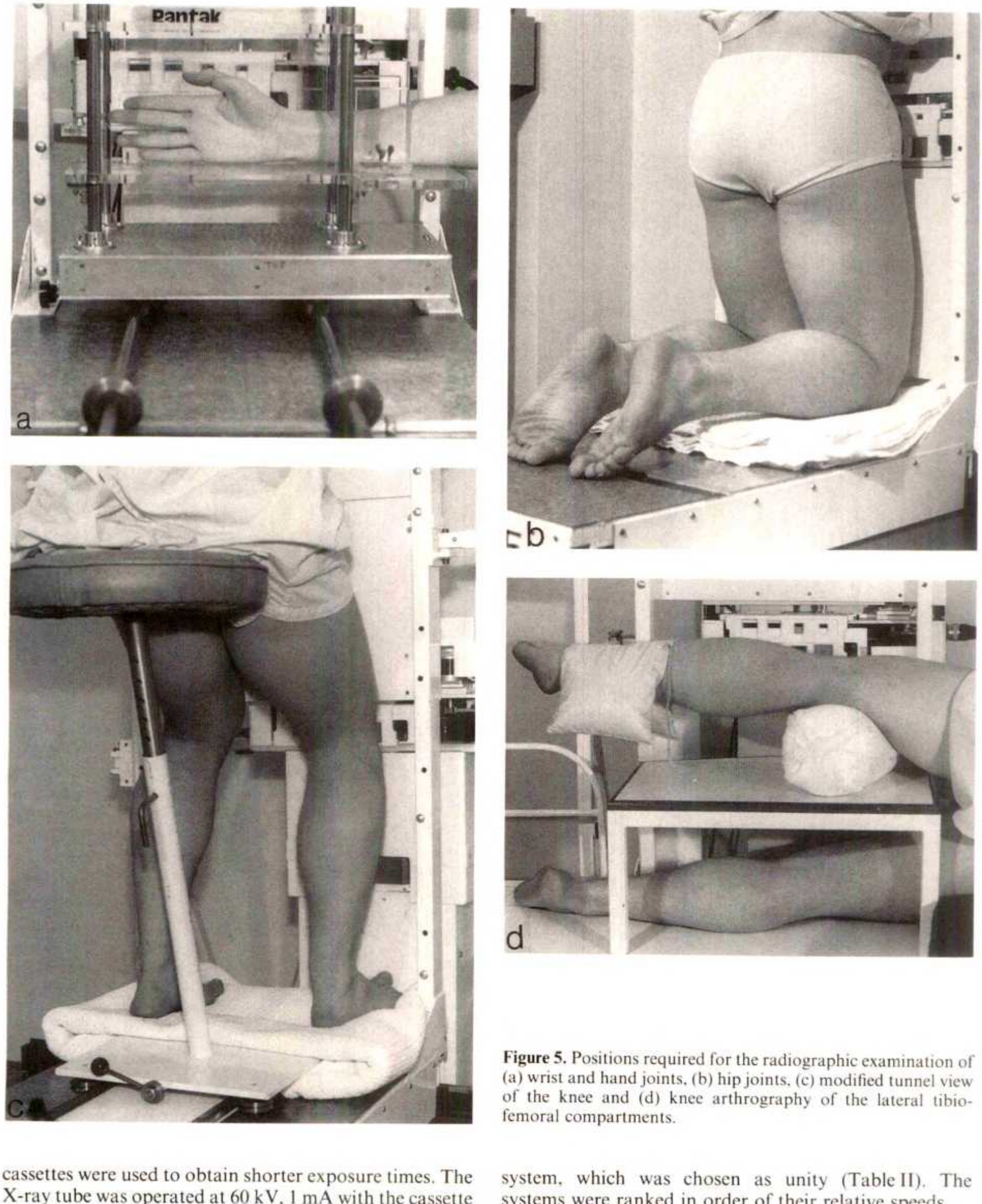

Figure 5. Positions required for the radiographic examination of (a) wrist and hand joints, (b) hip joints, (c) modified tunnel view of the knee and (d) knee arthrography of the lateral tibio-femoral compartments.

cassettes were used to obtain shorter exposure times. The X-ray tube was operated at 60 kV, 1 mA with the cassette at an FFD of 150 cm. All exposed film was processed in a 90 s automatic processor. The exposure times were recorded for each film with an optical density of 1 above fogging. The speeds of the different systems were expressed in increments of mAs relative to the fastest system, which was chosen as unity (Table II). The systems were ranked in order of their relative speeds.

The spatial resolution of the fastest film–screen system (Table II) when used with the microfocal X-ray unit was evaluated using test grids ranging from 12 lines cm^{-1} (bar width 270 μm) to 200 lines cm^{-1} (bar width 25 μm). The cassette was placed at an FFD of 150 cm and the FOD

Table II. Relative speeds in mAs of different film–screen systems tested to determine the fastest commercially available system. The reference to metal or plastic cassettes refers to the nature of the cassette's face plate

Cassette	Screen	Film	Relative mAs
Ilford Protex, metal	High definition	Rapid R	70.0
Trimax, metal	T8	XUD	11.2
Trimax, metal	T8	XD	8.0
Trimax, metal	T16 (front & back)	XD	4.2
Dupont, metal	Quanta III	3M.L	4.2
Trimax, plastic	T16 (front & back)	XD	2.5
Trimax, plastic	T16 (front & back)	3M.L	2.5
Kodak, plastic	Super Rapid	S4	2.5
Agfa Gevaert, plastic	MR800	RPI	2.5
Kodak, plastic	Super Rapid	XS24	1.7
Agfa Gevaert, plastic	MR800	3M.XM	1.7
Trimax, plastic	Siemens, Titan	Kodak XS24	1.7
Trimax, plastic	Siemens, Titan	3M.XM	1.7
Trimax, plastic	T16 (front & back)	XM	1.0

was altered to provide a range of magnifications at a constant exposure. These results were compared with the film–screen combinations already in use with the microfocal X-ray units (Buckland-Wright, 1984), *i.e.* Trimax T8 and T16 screens (T16 = T12 USA coding) with XD film in metal-faced cassettes (3M UK), and with the spatial resolution obtained using mammography film (Kodak Min R in a vacupak) in combination with a small source (0.3 mm) X-ray tube (Orbix, Elema-Schonander, Sweden) operating at 60 kV.

The results of the tests showed that the Trimax T16 front and back screens, XM film in a plastic cassette (Table II), had a spatial resolution not significantly different from that obtained for the finer-grained film–screen systems of T8 and T16 with XD film. The smallest object detected by the double T16 screens and XM films were 40 and 30 μm diameter at × 5 and × 10 magnification, respectively. Compared with the results using mammography film, the rare-earth film–screen systems and microfocal X-ray unit were better by a factor of 2. The smallest object detected in the mammography film when examined with a × 10 optical lens was 70 μm diameter. Furthermore, secondary X-ray scatter was present in the latter, whereas the air gap present in microfocal radiography improved the contrast in the macroradiographs.

Stereoscopy and measurement

One of the advantages of the point source in microfocal radiography is that all planes of the object in the film are in focus (Ely, 1972; Buckland-Wright, 1980a, b). Three-dimensional assessment of the radiographic features under investigation is possible through the preparation of stereopair radiographs. Either the whole or a part of the patient is displaced between successive exposures by up to 10 mm. The displacement is either vertical or horizontal depending on the region examined. The stereo-macroradiographs are examined under a large Format Stereoscope (Ross Instruments, UK). The increased visual information provided by stereopsis considerably improves the identification of lesions, their extent and position, either within the tissue or organ or relative to surrounding structures (Buckland-Wright, 1980b; 1983a, b).

The large magnification and high spatial resolution within the macroradiographs permit the direct measurement of the incidence and the change in the size of radiographic features associated with either the progression of a disease or its response to treatment. These features can be quantified using the computerized image analyser attached to the stereoscope (Buckland-Wright, 1983a; Buckland-Wright et al, 1986). This equipment is designed to provide quantitative evaluation of the change in the number or size of radiographic features between subsequent macroradiographic examinations. It has been shown to have a high degree of accuracy in quantifying disease progression (Buckland-Wright et al, 1986).

Discussion

The new microfocal X-ray unit (HF200M) incorporates a number of major advances in point-source X-ray technology. These include improvements in the design of the electron gun incorporating a lanthanum hexaboride (LaB_6) cathode, a single electromagnetic lens with automatic focus tracking and multifacet (1000 spot) stationary tungsten target. The result is a compact tube for high-definition radiography operating over the range 20–125 kV, 0–1 mA with a maximum output of 75–80 W. The X-ray source size of the unit at outputs up to 49 W is comparable to that of the existing lower-energy microfocal units in resolving objects as small as 6–8 μm (Buckland-Wright, 1980a). With increased output of 50–77 W, the HF200M focal spot size increases permitting the detection of objects as small as 12–20 μm diameter.

The X-ray tube is floor mounted with the beam directed horizontally along the room. The patient table is designed to move the patient relative to the X-ray source both for positioning and for taking stereopair macroradiographs. Where necessary, movement by the patient is restricted through the use of foam wedges or restraining straps. The precise positioning of the part of the body to be examined within the centre of the X-ray beam is achieved using a cross-optic laser and where necessary by screening with an image-intensifier assembly.

The examination of patients using microfocal radiography is possible through a combination of two factors: the output characteristics of the microfocal tube and the use of rare-earth film–screen combinations. The X-ray emissivity of the tube appears to be between × 3 and × 3.5 greater than a conventional tube (Table I). This is probably due to a number of factors including the highly focused electron beam, measurement of the tube current at the target as opposed to the filament, and the superior surface finish to the target material. Of the range of film–screen combinations tested (Table II), the fastest (Trimax 16 front and back screens, with XM film in a plastic-faced cassette) had a relative speed some 70 times faster than that of a calcium tungstate system (Ilford high-definition screens with Rapid R film in a metal-faced cassette). Projection magnifications of × 3 and above overcame the limitation of the large signal-to-noise ratio inherent in the fast film–screen combinations (Doi & Imhof, 1977). The object resolution within the film was found to be 40 to 30 μm at magnifications of × 5 and × 10. The object resolution in these systems was found to be two times better than that obtained using a × 10 optical lens on test grids recorded on mammography film using a 0.3 mm focal-spot X-ray unit.

The following are characteristic of point-source projection radiology and these advantages contribute towards the greater spatial resolution: minimal penumbral blurring (Cosslett & Nixon, 1960), reduced secondary X-ray scatter because of the air gap effect and enhanced object resolution because of the longitudinal magnification (Doi & Rossman, 1975). The preparation of stereopair macroradiographs is achieved by the displacement of the patient between successive exposures. A perspective as in normal vision is achieved when the stereopair are examined under a stereoscope. This is due to the geometrical magnification within the object which occurs when an object is placed close to a point source. Stereoscopy facilitates the identification and determination of the position of lesions within the part of the body examined.

The distinctive advantage of microfocal radiography is in providing macroradiographs from which it is possible to make accurate measurements (Buckland-Wright, 1980a; Buckland-Wright et al, 1986). This provides a method of quantifying the frequency and dimension of radiographic features characteristic of a disease (Buckland-Wright et al, 1987a) and also determining their alteration with disease (Buckland-Wright et al, 1987b; 1989) and their response to therapy. By obtaining radiographic images of changes in tissues at a level approximating to that of histology, greater information is obtained of the disease process as well as the mechanisms of tissue response to therapeutic intervention.

Acknowledgments

I wish to acknowledge my gratitude to the late R. V. Ely, the microfocal X-ray unit designer, without whose support and encouragement this work would not have been possible. The development of the microfocal unit at this school and hospital has been due to the support of Professors T. Clark, M. Berry and M. Maisey and Dr H. Saxton. Many have provided advice and encouragement and of these I thank in particular Messrs R. Sharpe and R. Parish of Harwell AERE and Drs M. K. Jasani and J. T. Patton; the following companies for their support: Astrophysics Research Ltd, Ciba Geigy, Thompson CSF, Grant and Taylor and Eltron Technical Products; and the following for their assistance: Mrs H. Rees, Mrs A. Robins, Miss M. Arnold, Mrs B. Clark for typing the manuscript and Mr K. Fitzpatrick and Miss Sarah Smith for preparing the photos.

References

Ardenne, M. von, 1939. Zur Leistungsfähigkeit des Elektronen-Schatten-mikroskopes und über ein Rontgenstrahlen-Schattenmikroskope. *Naturwissenschaften, 27*, 485–486.

Buckland-Wright, J. C., 1976. The microfocal X-ray unit and its application to bio-medical research. *Experientia, 32*, 1613–1615.

—— 1977. The microfocal X-ray unit: a demonstration of its potential. *Medical and Biological Illustration, 27*, 163–168.

—— 1980a. Qualitative and quantitative assessment of tissue organisation in normal and diseased organs. In *Microfocal Radiography*, ed. by R. V. Ely (Academic Press, London), pp. 147–195.

—— 1980b. Stereo-projection radiography in the study of the structural organisation of cat skull bones. *Journal of Anatomy, 130*, 487–498.

—— 1983a. X-ray assessment of activity in rheumatoid disease. *British Journal of Rheumatology, 22*, 3–10.

—— 1983b. Advances in the radiological assessment of rheumatoid arthritis. *British Journal of Rheumatology, 22 (Suppl.)*, 34–43.

—— 1984. Microfocal radiographic examination of erosions in the wrist and hand of patients with rheumatoid arthritis. *Annals of the Rheumatic Diseases, 43*, 160–171.

Buckland-Wright, J. C., Carmichael, I. & Walker, S. R., 1986. Quantitative microfocal radiography accurately detects joint changes in rheumatoid arthritis. *Annals of the Rheumatic Diseases, 45*, 379–383.

Buckland-Wright, J. C., Clarke, G. S. & Walker, S. R., 1989. Erosion number and area progression in the wrist and hand of rheumatoid arthritis patients: a quantitative microfocal radiographic study. *Annals of the Rheumatic Diseases, 48*, 25–29.

Buckland-Wright, J. C., Macfarlane, D. G. & Clark, B., 1987b. Quantitative microfocal radiography of disease progression in generalised nodal osteoarthritis (GOA) of the hand. *British Journal Rheumatology, 26 (Suppl. 2)*, 46.

Buckland-Wright, J. C. & Walker, S. R., 1987a. Incidence and size of erosions in the wrist and hand of rheumatoid patients: a quantitative microfocal radiographic study. *Annals of the Rheumatic Diseases, 46*, 463–467.

Cosslett, V. E., 1957. Optimum conditions of magnification and contrast in projection X-ray microscopy. In *X-ray Microscopy and Microradiography*, ed. by V. E. Cossett, A. Engstrome & H. H. Pattee (Academic Press, New York), pp. 321–328.

Cosslett, V. E. & Nixon, W. C., 1951. X-ray shadow microscope. *Nature, 168*, 24–25.

—— 1952a. X-ray shadow microscope. *Nature, 170*, 436–438.

—— 1952b. An experimental X-ray shadow microscope. *Proceedings of the Royal Society, Series B 140*, 422–431.

—— 1960. *X-ray Microscopy* (Cambridge University Press, Cambridge).

Doi, K. & Imhof, H., 1977. Noise reduction by radiographic magnification. *Radiology, 122*, 479–487.

Doi, K. & Rossman, K., 1975. Longitudinal magnification in radiographic images of thick objects: a new concept in magnification radiography. *Radiology, 114*, 443–447.

Ely, R. V., 1960. A high output rotating anode shock-proof tube (demountable) for X-ray microscopy. In *X-ray Microscopy and X-ray Microanalysis. Proceedings of the Second International Symposium*, ed. by A. Engstrom, V. E. Cossett & H. Pattee (Elsevier, Amsterdam), pp. 47–50.

—— 1972. X-ray microscopy. In *Physical Methods of Chemistry*, Part III, ed. by A. Weissberger & W. B. Rossiter (Wiley & Sons, New York), pp. 715–779.

—— 1980. The evolution of microfocal X-ray equipment. In *Microfocal Radiography*, ed. by R. V. Ely (Academic Press, London), pp. 1–41.

MARTON, L., 1939. Internal Report, RCA Laboratories, Princetown.

MULVEY, T. & NEWMAN, C. D., 1975. New electron-optical system for SEM and STEM scanning electron microscopy systems and applications. *Institute of Physics, Conference Series, 16*, 21.

NIXON, W. C., 1961. X-ray microscopy. *Contemporary Physics, 2*, 183–197.

PARISH, R. W., 1986. Microfocus X-ray technology—a review of developments and application. In *Review of Progress in Quantitative Nondestructive Evaluation*, Vol. 5A, ed. by D. O. Thompson & D. E. Chimenti (Plenum, New York), pp. 1–20.

ROCKETT, P. & PARISH, R. W., 1985. A wide energy range, high resolution microfocal X-ray source. *Harwell Report AERE R11742*, 1–9.

SHARPE, R. S., 1979. Projection microradiography. *Journal of Microscopy, 117*, 123–143.

SHARPE, R. S. & PARISH, R. W., 1980. Engineering applications of microfocal radiography. In *Microfocal Radiography*, ed. by R. V. Ely (Academic Press, London), pp. 43–81.

1989, *The British Journal of Radiology*, 62, 209–217

Clinical applications of high-definition microfocal radiography

By J. C. Buckland-Wright, PhD and C. R. Bradshaw, MB, BS, FRCR

Macroradiography Research Unit, Departments of Anatomy and Diagnostic Radiology, United Medical and Dental Schools of Guy's and St Thomas', Guy's Campus, London SE1 9RT

(Received July 1988)

Abstract. Recent advances in technology have lead to the development of a high-definition microfocal X-ray unit allowing macroradiographic examination of different parts of the body at × 5 to × 10 magnification and with a high spatial resolution. Its applications in the study of a number of arthritides, metabolic and some other bone diseases are described in terms of early detection of diagnostic features. Emphasis is placed on the advantages of direct accurate measurement of these features, providing a precise evaluation of disease progression and response to therapy.

Magnification techniques in bone radiography have been applied using × 2 magnification in conjunction with a 0.3 mm focal spot by Calenoff and Norfray (1973) and Genant et al (1975), who found the images to be either inferior or similar to contact exposures. Direct radiographic magnification, using microfocus tubes with an estimated 50 μm focal-spot size, has been well described (Genant et al, 1975; Takahashi & Sakuma, 1975), and it has been shown that the advantages of direct magnification are increased resolution, decrease in noise and the improved visual effect of image enlargement. The inherent air-gap of magnification reduces scatter without impeding the primary beam. Direct magnification is superior to conventional contact radiography with respect to the overall image quality (Genant et al, 1977). The magnifications used ranged between × 3 and × 4 and at most × 6 (Ishigaki, 1973; Genant et al, 1975, 1977; Takahashi & Sakuma, 1975). The images obtained with thick objects was found to be superior to other methods (Genant et al, 1975; Doi et al, 1976). Takahashi and Sakuma (1975) concluded that "the merit of magnification radiography lay in its ability to reveal new findings based on the minute X-ray images which can not be seen by normal roentgenography". In many instances, the magnification achieved by these investigators was not sufficient to have fulfilled these expectations entirely. The advantages of magnification radiography stated above depend on the smallness of the point source of X rays. With very small X-ray sources ($< 20\,\mu$m) the larger magnification (from × 5 to × 10) resolves very small details permitting the identification of features virtually at the histological level. This paper demonstrates the advantages of higher magnification obtained with the microfocal X-ray unit (HF200M) (Rockett & Parish, 1985; Parish, 1986; Buckland-Wright, 1989). This unit has an estimated source size (corresponding to the diameter of the smallest clearly detectable object) of 6–20 μm over an output range of 14–77 W (Buckland-Wright, 1989). The spatial resolution with the fast rare-earth screen–film systems ranges from 100 lines cm^{-1} (or an object diameter of 40 μm) to 200 lines cm^{-1} (or an object diameter of 25 μm) at magnifications of × 5 to × 10, respectively (Buckland-Wright, 1989).

Stereopair macroradiographs are prepared and examined under a large format stereoscope (Buckland-Wright, 1980, 1983a, 1989). Stereopsis helps considerably in the identification and location of features within the object and the large magnification and high spatial resolution enables accurate direct measurement of the radiographic features (Buckland-Wright, 1980, 1983a, 1989). The application of the technique in the quantitative evaluation of disease progression in the arthritides is outlined.

Methods

The radiographic magnifications ranged from × 5 to × 10. Exposures at × 15 have been taken but in these circumstances patient movement became more of a problem. The positioning of the patient and the preparation of the steropair macroradiographs have been previously described (Buckland-Wright, 1989). A large film format (35 cm × 42 cm) was used and the size of the part of the body recorded in the macroradiograph corresponded to approximately one-fifth to one-tenth of that normally recorded on the standard radiographic exposure. It is necessary to emphasize that the illustrations reproduced here are taken from part of the macroradiograph (Fig. 1). The different rare-earth screen–film systems used and their exposures for the different regions examined are listed in Table I. All films were processed in a 90 s automatic processor. The radiation dose to the skin was calculated for the different exposures and also appears in Table I.

Results

Table I lists the different regions examined to date. The list is incomplete as work is in progress on the exposures required for other regions of the body. The settings for the hip joint indicate a long exposure time because the output of the tube is limited to 75–80 W.

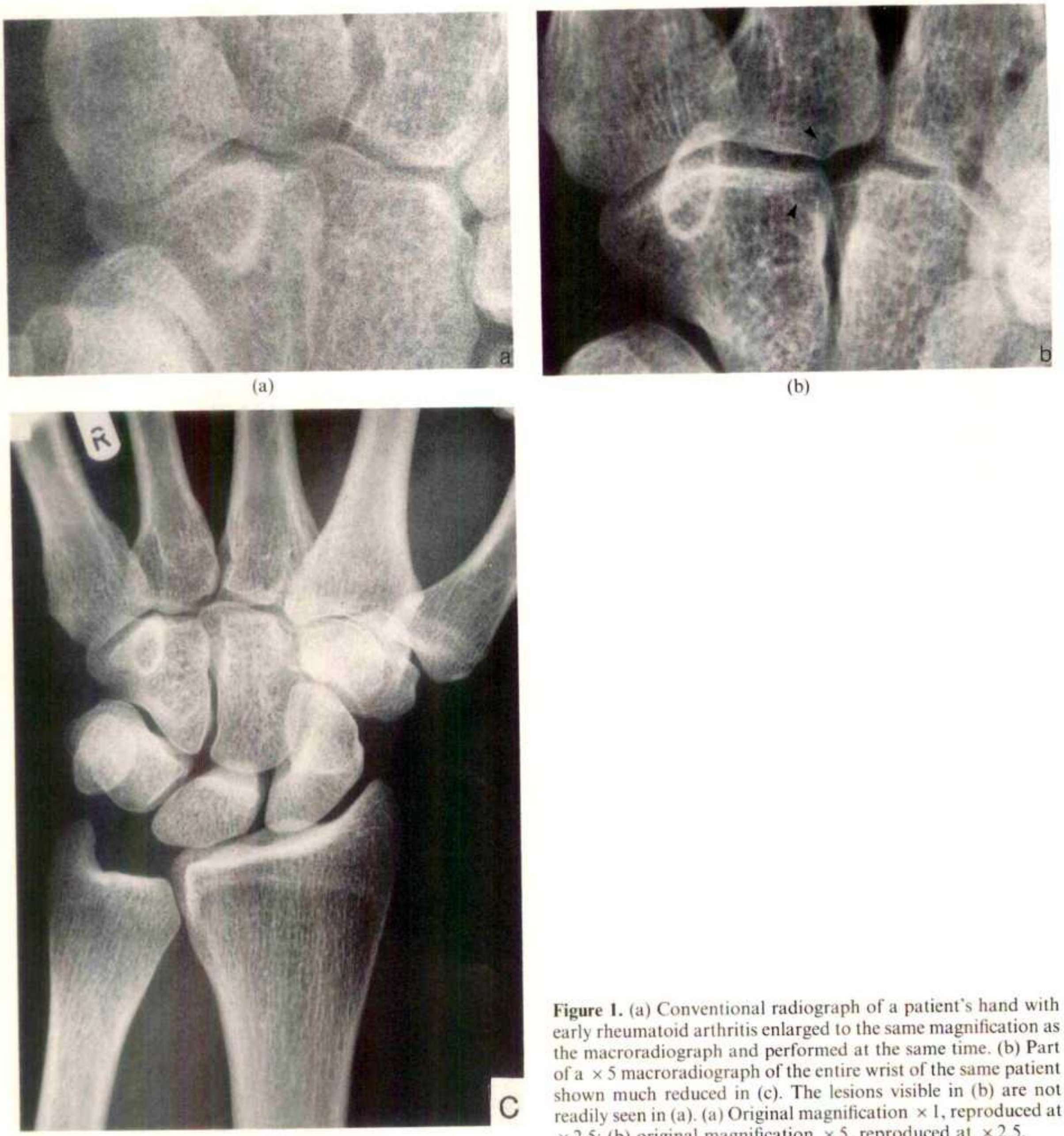

(a)

(b)

(c)

Figure 1. (a) Conventional radiograph of a patient's hand with early rheumatoid arthritis enlarged to the same magnification as the macroradiograph and performed at the same time. (b) Part of a × 5 macroradiograph of the entire wrist of the same patient shown much reduced in (c). The lesions visible in (b) are not readily seen in (a). (a) Original magnification × 1, reproduced at × 2.5; (b) original magnification × 5, reproduced at × 2.5.

The manufacturers indicate that it is possible to increase the beam current, the consequence of which would be an increased rate of target pitting leading to a shorter target spot life. This can be overcome by selecting a new target facet within a shorter number of exposures than at present.

Preliminary dosimetry indicates that the better image quality of the macroradiographs is at the expense of slightly increased radiation exposure to the patient (Table I). Comparison with conventional techniques indicates that skin dose using microfocal techniques for the hand and knee are between 3 and 5 times greater, and for the shoulder and hip between 1 and 2.5 times greater. However, it must be emphasized that with magnification the well collimated field size is reduced to approximately one-fifth (for hand and knee) and to one-tenth (for shoulder and hip) of that of the conventional technique. Thus, the skin doses with the conventional and microfocal techniques are comparable in terms of total-body radiation exposure. For the thicker regions the

Table I. List of the different regions of the body examined to date with the different settings for the microfocal unit, the film and patient distances, the magnification and film–screen combinations used. The skin dose was calculated from air kerma without a backscatter factor and for 2.4 mm Al filtration

Region	kV	mA	Time (s)	FOD (cm)	FFD (cm)	Magnification	Screen (3M UK)	Film	Skin dose (mGy)
Wrist	60	0.9	0.9				T16	XDA	1.2
MCP	60	0.9	0.9	27	135	× 5	T8/16	XDA	1.2
IP	60	0.7	0.9				T8	XDA	0.9
Scaphoid	60	0.9	0.9	17	135	× 8	T6	XDA	2.6
Knee									
Post ant	70	0.9	1.0	25	125	× 5	T16[a]	XM	1.9
Lateral	70	0.9	1.0	25	125	× 5	T16	XM	1.9
Tunnel	72	0.9	1.0	20	125	× 6.25	T16	XM	3.5
Arthogram	73	0.9	1.0	15	150	× 10	T16	XM	6.4
	73	0.9	1.0	20	150	× 7.5	T16	XM	3.6
Elbow	63	0.95	1.0	23	128	× 5.5	T16	XDA	2.3
Shoulder	70	0.9	1.0	24	140	× 7	T16	XM	3.0
Hip	115	0.66	2.5	20	125	× 5	T16	XM	8.6
Chest									
Lung fields	60	0.7	1.0	20	140	× 7	T16	XM	2.3
Skull[b]									
Pituitary fossa	85	0.85	1.4	23	115	× 5	T16	XM	4.8
Modified Stenvers	85	0.85	1.5	23	115	× 5	T16	XM	5.1

[a] These systems had both front and back T16 screens in plastic-faced cassettes.
[b] Figures obtained from a skull phantom.

total-body radiation exposure is lower in the macroradiographs relative to the conventional techniques. However, the radiation exposure is doubled where stereopair radiographs are prepared and is again further increased where fluoroscopy is required for positioning the thick regions of the body. Although there is an increase in the skin dose to the patient during this procedure, the advantage is that it prevents repeat exposures caused by bad positioning.

Clinical studies

The results of the clinical assessments are described below. The cases largely concern patients with arthritic and metabolic disorders.

Rheumatoid arthritis. Microfocal radiography enables the detection of small, early lesions which are not always visible in conventional radiographs (Fig. 2). These include regions of juxta-articular radiolucency (JAR)

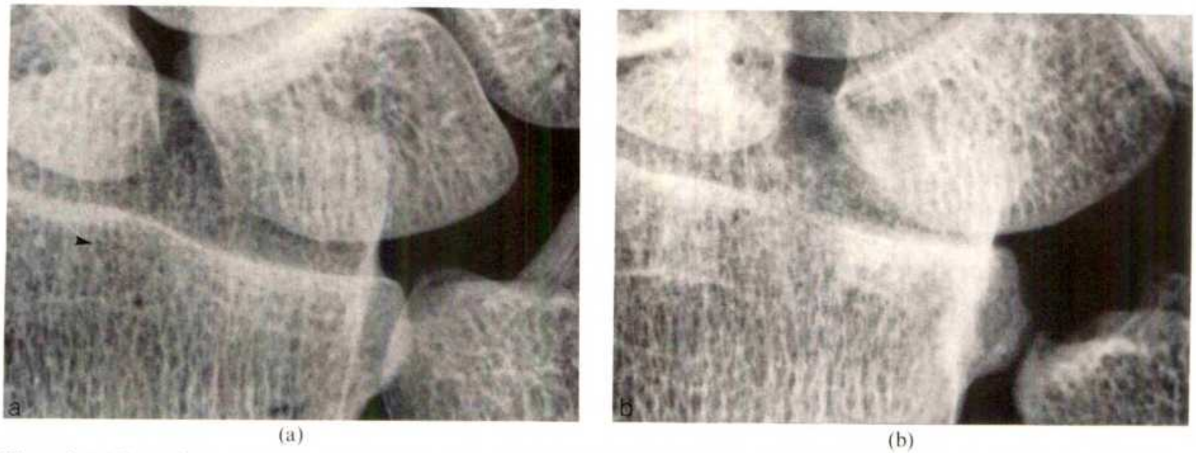

(a) (b)

Figure 2. (a) Part of a macroradiograph of the wrist of a patient with early rheumatoid arthritis. The juxta-articular radiolucency (JAR) at the distal end of the volar surface of the radius has increased in size 21 months later (b), to form a clearly defined erosive cavity with loss of cortex. Breaks in the cortex associated with JAR formation are seen at the ulnar margin of the lunate in (b). Other changes include erosions at the ulnar margin of the scaphoid, the distal end of the ulna and joint space narrowing. Original magnification × 5, reproduced at × 2.5.

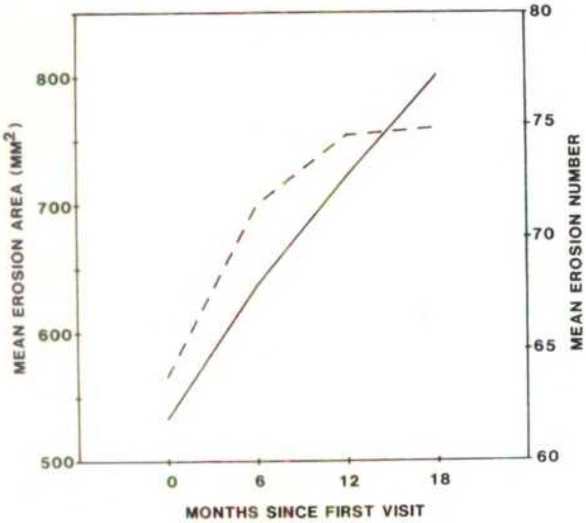

Figure 3. Graph of the change, over an 18-month period, in the mean total erosion number (— — —) and mean total erosion area (———) in the wrist and hands of a group of patients with early to moderately advanced rheumatoid arthritis. Erosion area continues to increase after erosion number progression has ceased (reproduced by permission from Buckland-Wright et al (1989)).

where the trabeculae are thin and of reduced density. The endosteal margin is clearly defined by relatively thicker trabeculae. Breaks in the cortex are small, narrow and occur subperiosteally becoming evident earliest in the bare areas of bone not covered by articular cartilage. Detection of cortical ruptures depends on their position relative to the X-ray beam and are not readily seen *en face*. Changes in the size of these lesions can be detected within a 3-month period (Buckland-Wright, 1983a, b, 1984). Figure 2 illustrates the progression of the JARs into the characteristic rheumatoid erosions. In addition, the appearance of JARs in the wrist and hand of affected patients has provided confirmation of the presence of an inflammatory arthropathy in patients with palindromic rheumatoid disease and, contrary to published reports (Beighton et al, 1983), macroradiography has demonstrated the presence of small erosions in patients with hypermobility syndrome.

Measurement of the number and size of erosions in the rheumatoid wrist and hand has shown where these features occur most frequently and at which sites the lesions are largest (Buckland-Wright & Walker, 1987). The size of erosions was found to correspond to the size of the bones. The most frequent sites were the radiocarpal, medial carpo-metacarpal and the second and third metacarpophalangeal joints.

The number and size of rheumatoid lesions can be measured directly and accurately (Buckland-Wright et al, 1986). The changes in the total number and area of erosions in a group of patients with early to moderately advanced rheumatoid disease is shown in Fig. 3. The mean total erosion number reached a constant of 75 erosions for each wrist and hand by the third X-ray visit, corresponding to a mean disease duration, for the group of patients, of 48 months from onset of symptoms. This constant of 75 erosions was due to a combination of patients, the majority of whom showed no change in erosion number; the rest were approximately evenly distributed between those showing an increase and those showing a decrease in erosion number (Fig. 4) (Buckland-Wright et al, 1989). By contrast, mean total erosion area continued to increase significantly. The change in erosion area better expressed the disease progression in rheumatoid arthritis than number alone. Erosion repair in rheumatoid patients took two forms, depending on the extent of bone destruction. Where this had been extensive a sclerotic margin formed around the erosion (Fig. 4, scaphoid). With less damage, there was either a reformation of the decalcified matrix at either the endosteal or cortical margins (Fig. 4, ulna and lunate), or both types of repair occurred together (Fig. 4, radius).

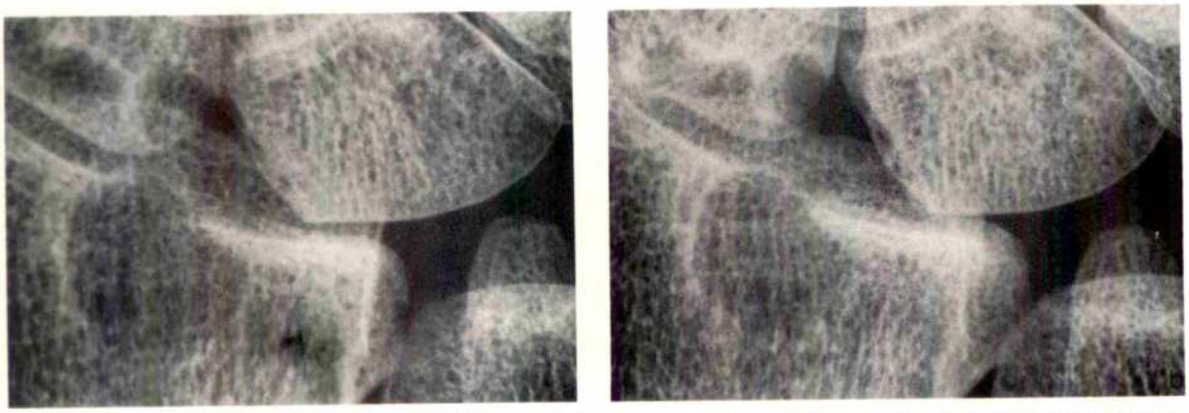

Figure 4. Part of a macroradiograph of the wrist of a patient with moderately advanced rheumatoid arthritis taken 7 months apart illustrating the repair to both erosions (radius and scaphoid) and their precursors, the juxta-articular radiolucencies (ulna and lunate). Original magnification × 5, reproduced at × 2.5.

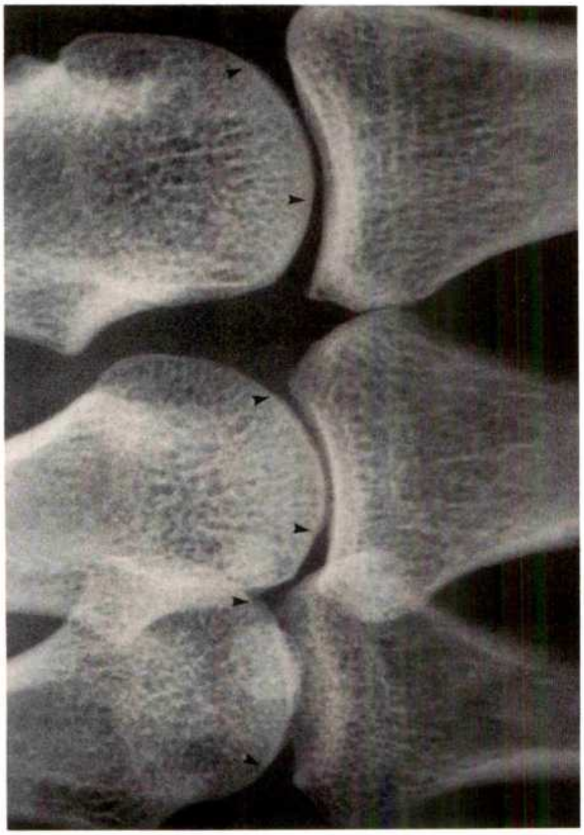

Figure 5. Part of a macroradiograph of the metacarpophalangeal joints of a patient with generalized nodal osteoarthritis showing the advance of the mineralized cartilage into the existing articular cartilage, contributing to the narrowing of the joint space. Original magnification × 5, reproduced at × 2.5.

Osteoarthritis. Features associated with this disease are well shown with conventional radiography. However, high-definition microfocal radiography reveals detail of changes more familiar to the histopathologist. Early changes, such as the advance of the edge of mineralized cartilage into the existing articular cartilage, are recorded in the small joints of the hand (Fig. 5), having been described previously in large joints only (Bullough et al, 1968; Lane et al, 1977; Duncan, 1983). This mineralization remains within the confines of the normal cartilage thickness and, radiographically, such encroachment produces joint space narrowing. Juxta-articular radiolucencies at the joint margins (Fig. 6) were recorded in the wrist and hand of all patients examined with generalized nodal osteoarthritis (GOA). In position and general appearance the JARs were similar to the early rheumatoid lesions. They differed in that they were smaller and the surrounding bone was less osteopenic. Their presence confirms the existence of low-grade inflammatory episodes associated with this disease (Swanson & Swanson, 1985).

Radiographic assessment of disease progression in GOA of the hand is not studied longitudinally as it is extremely slow using standard radiographic methods. However, precise measurements taken from macroradiographs of the joint space width (interbone distance) and subchondral cortical thickness showed significant change in their dimensions within a period of 12 months. By 18 months the pattern of disease progression was clearly defined (Buckland-Wright et al, 1987a, b) and showed that subchondral sclerosis appeared prior to the destruction of articular cartilage as measured by the joint space narrowing.

Studies of the degenerative changes in the knee. In this study particular attention is paid to determining the alteration in articular cartilage thickness from accurate

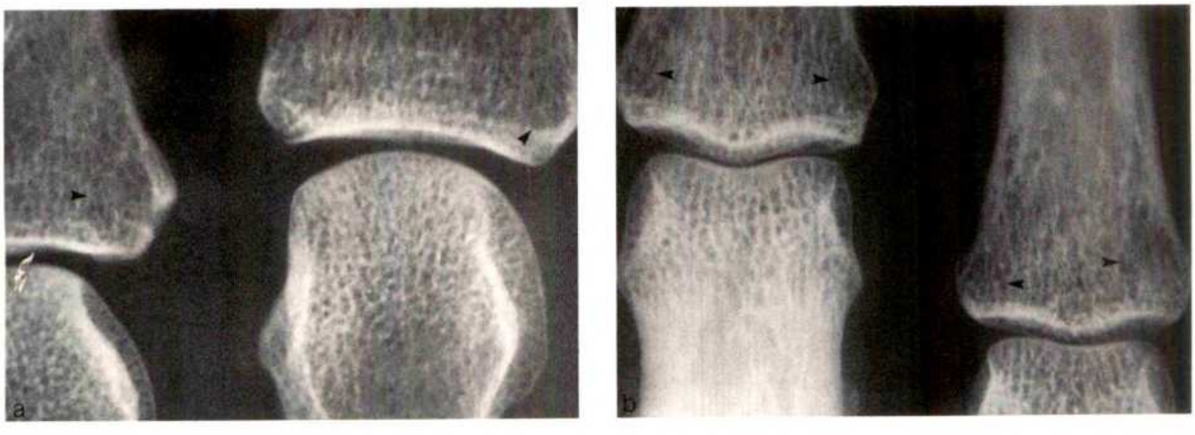

Figure 6. Part of a macroradiograph of (a) the metacarpophalangeal and (b) proximal interphalangeal joints of patients with generalized nodal osteoarthritis showing the juxta-articular radiolucencies and the cortical breaks at the "bare area" of the bone connecting the lesions with the joint space. Original magnification × 5, reproduced at × 2.5.

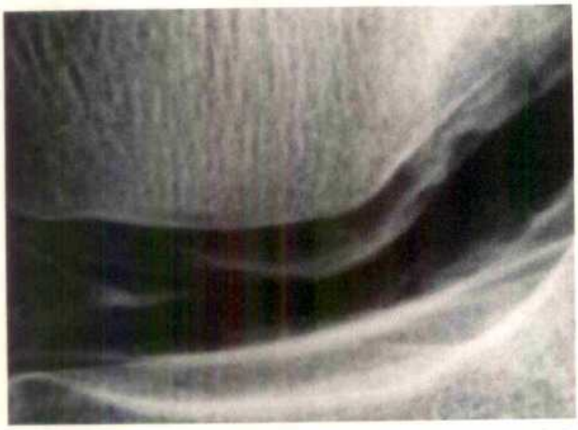

Figure 7. Part of a double-contrast macro-arthrogram of the medial tibio-femoral compartment of a knee with early osteoarthritis. There is increased imbibition of the contrast agent into the areas of damaged cartilage of the femur, tibia and meniscus. The grid is used to assess the degree of magnification. Original magnification × 7, reproduced at × 3.5.

measurements of the joint space width (interbone distance). In addition, the use of double-contrast arthrography has revealed sites of damaged articular cartilage by the imbibition of contrast agent (Stoker, 1980; Fujikawa, 1981) (Fig. 7). With hyaline cartilage destruction, the presence of fibrous tissue overlying the exposed bony surface of the femoral condyle can be readily seen (Fig. 8). Here the contrast agent has also penetrated into the subchondral bone through breaks in the cortex.

Pyrophosphate crystal deposition. Crystal deposition in joint tissue produces an inflammatory form of osteoarthritis (OA) (Gordon et al, 1984), leading to a far greater destruction of the bone than that present in joints with moderate OA (Figs 9, 10). Large subchondral cysts communicate with the joint space via breaks in the subchondral cortex. The collapse of the distal end of the third metacarpal has led to its shortening and crystals outline the articular margins (Fig. 9). In the radio-carpal and radio-ulnar joints there is marked disorganization of the trabeculae associated with the formation of a number of small erosions (Fig. 10). The extent of the articular

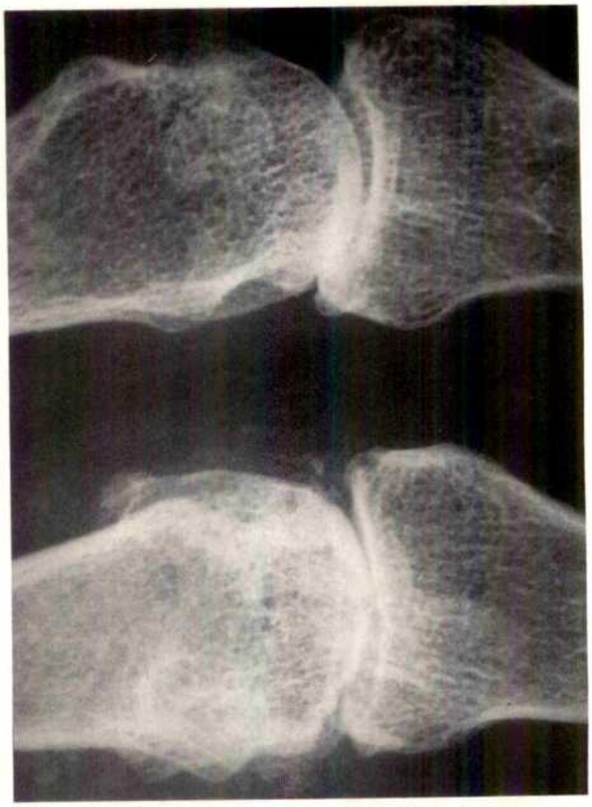

Figure 9. Part of a macroradiograph of the metacarpophalangeal joints of a patient with generalized nodal osteoarthritis showing crystal deposition in the third MCP joint compared with the more typical changes associated with osteoarthritis in the second MCP jointly. Original magnification × 5, reproduced at × 2.5.

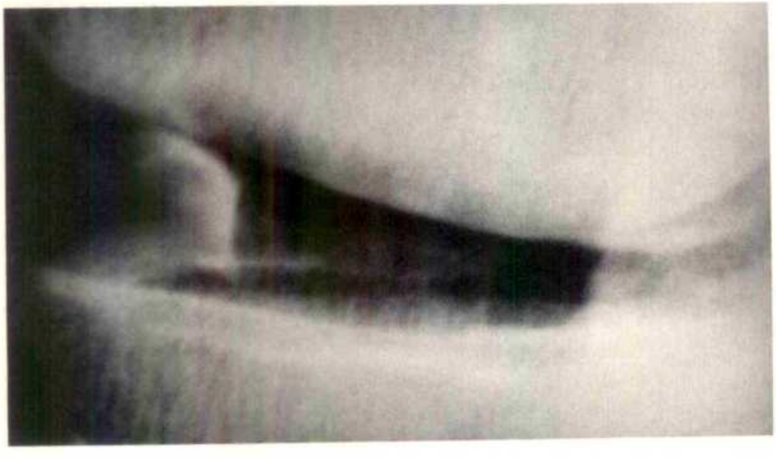

Figure 8. Part of a double-contrast macro-arthrogram of the medial tibio-femoral compartment of a patient with advanced osteoarthritis. The contrast agent highlights the fibrous tissue overlying the remaining articular cartilage, close to the femoral notch and the exposed bony femoral surface. The penetration of the contrast agent into the subchondral bone is associated with the loss of cortex. The medial meniscus is badly damaged. Patient motion has resulted in loss of image sharpness. Original magnification × 10, reproduced at × 5.

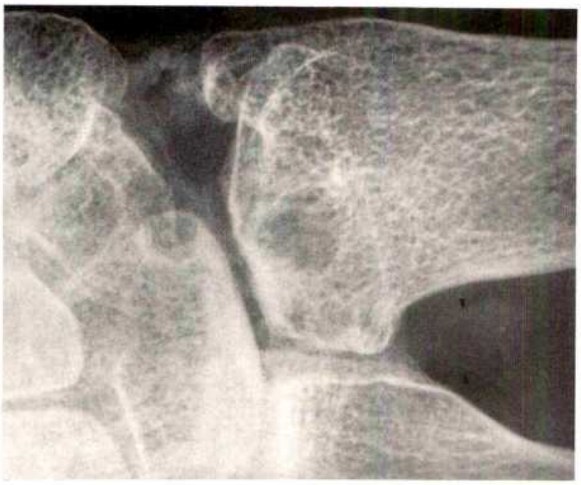

Figure 10. Part of a macroradiograph of the wrist of a patient with pyrophosphate crystal deposition in the radio-carpal and radio-ulnar joints. Note, in particular, the crystals filling the *recessus sacciformis*. Original magnification × 5, reproduced at × 2.5.

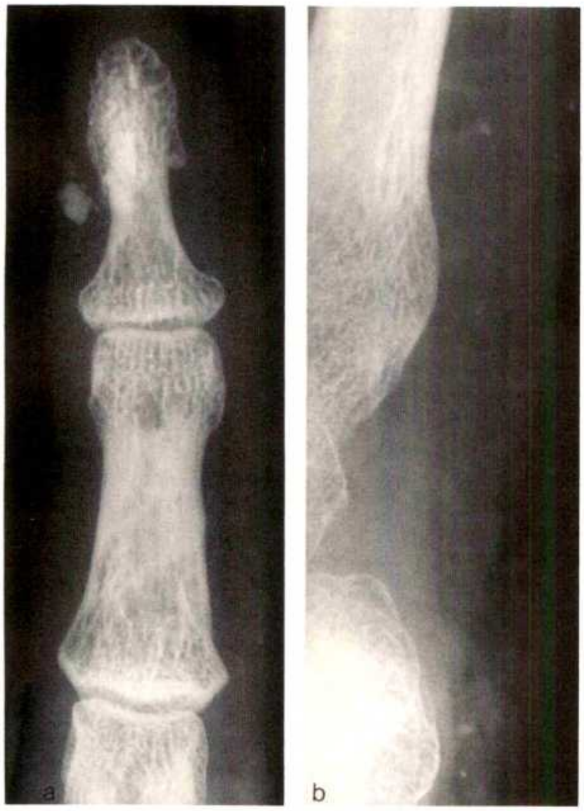

Figure 11. Part of the macroradiograph of the wrist and interphalangeal joints of a patient with scleroderma. The calcium deposits in (a), the TIP joint, were seen by conventional radiography, whereas those in (b), the ulnar side of the wrist, were not. Original magnification × 5, reproduced at × 2.5.

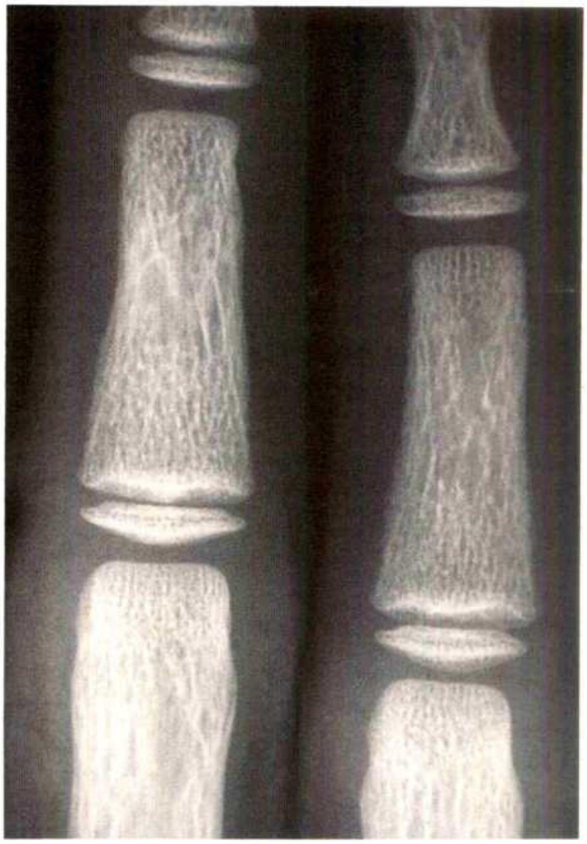

Figure 12. Part of the macroradiograph of the interphalangeal joints of a 10-year-old boy with renal osteodystrophy. The extent of subperiosteal resorption in the middle phalanges and the degree of cortical striation both within the shafts and the cortex are clearly defined. Original magnification × 5, reproduced at × 2.5.

cartilage damage is shown by the degree of joint space narrowing, subchondral sclerosis and attrition. Crystals within the distal radio-ulnar joint (Fig. 10) define the extent of the joint capsule, *i.e.* the *recessus sacciformis*. Macroradiography of OA patients has revealed, in a number of cases, low levels of crystal deposits within the joints. No inflammatory reaction was observed in these instances, which suggests that an inflammatory response may depend upon the concentration of the crystal exceeding a critical level.

Scleroderma. The facility with which microfocal radiography detects small calcifications is illustrated in patients with scleroderma (Fig. 11).

Hyperparathyroidism. With metabolic bone disease it is difficult to assess disease progression quantitatively by non-invasive methods. The problem is compounded in children, such as those with renal osteodystrophy, where the method of measurement has to be independent of growth (Wilson & Genant, 1979). In children with secondary hyperparathyroidism (Fig. 12) cortical striations, used by many investigators, are clearly shown. Subperiosteal erosions are well displayed (Fig. 12) and have been found to correspond well with the clinical disease. The extent of subperiosteal resorption along the phalangeal shafts has been measured and expressed as a percentage of the total subperiosteal length of the bone. Between successive visits, the change in the percentage length of subperiosteal resorption has been found to express the clinical progression of the disease. In those children who responded to treatment with oral phosphate binders, there was marked reduction in the extent of subperiosteal resorption. This method has the advantage of being independent of growth. The importance of changes at the ungual tufts as indications of early renal osteodystrophy (Eastwood et al, 1973; Parfitt, 1977; Sundaram et al, 1979) is supported by our observations on 18 children. However, contrary to Sundaram et al (1980), this feature was not found to be sensitive in the evaluation of disease progression. It showed no correspondence with either changes in the extent of subperiosteal erosion or clinical progression of the disease. The difference between our results and those of Sundaram et al (1980) may be due to differences in either the ages of the patients in the two studies or to type of treatment.

Discussion

The results of macroradiographic examination of the changes associated with the different diseases described here support the statements of Takahashi and Sakuma (1975) and Genant et al (1977) on the merit of the magnification technique revealing small, subtle changes of clinical importance. The difference between the results described here and those obtained by the earlier investigators is in the performance of the new microfocal X-ray unit. Here, the macroradiographs have a larger magnification and a higher spatial resolution, so that the detail recorded in the film approximates to that of features observed histologically. This advantage not only assists in diagnosis but also contributes to the understanding of the disease mechanism (Buckland-Wright, 1984).

The suggestion that "magnification radiography should open up a new radiodiagnostic field and promote the establishment of much more accurate diagnosis" (Takahashi & Sakuma, 1975), underestimates the full potential of the technique. The significant advantage of taking direct accurate measurements of radiographic features provides indisputable evidence of the extent of the disease process (Buckland-Wright et al, 1986; Buckland-Wright & Walker, 1987). In addition, the quantitative evaluation of disease progression obtained from serial macroradiographic examinations (Buckland-Wright et al, 1989) or the quantification of the response to therapeutic regimens (Buckland-Wright, unpublished findings) is far more precise than any method dependent on a system of scoring currently employed in conventional radiology. It is in this aspect of quantitative radiology that the magnification technique is proving to have an advantage over other radiographic techniques.

From the preliminary dosimetry measurements, it is apparent that the magnification technique results in relatively high skin dose, though total-body irradiation appears either similar or only slightly greater than conventional radiography. It is for this reason that magnification radiography, despite its slightly greater technical difficulty in positioning and the need for stereopairs, is recommended as a selective procedure. At present, microfocal radiography is proving to be important in the study of skeletal disease. Its application in other areas awaits investigation but preliminary work is currently being performed on the lung fields in patients with fibrosing alveolitis.

Acknowledgments

We wish to acknowledge our gratitude to the late R. V. Ely, microfocal X-ray unit designer, without whose support and encouragement this work would not have been possible. The development of the microfocal unit at this school and hospital has been due to the support of Professors T. Clark, M. Berry and M. Maisey and Dr H. Saxton. We wish to thank our colleagues in the Departments of Diagnostic Radiology, Rheumatology and Paediatrics, in particular Drs H. Saxton, R. Graham and D. Macfarlane and Professors C. Chantler and G. Panayi as well as Drs M. K. Jasani and J. T. Patton; the following companies for their support, Astrophysics Research Ltd and Ciba Geigy; and the following for their assistance, Mrs H. Rees, Mrs A. Robins, Miss M. Arnold, Mr G. Clarke, Mr J. A. Lynch, Mrs B. Clark for typing the manuscript and Mr K. Fitzpatrick and Miss Sarah Smith for preparing the photographs.

References

BEIGHTON, P., GRAHAME, R. & BIRD, H., 1983. *Hypermobility of Joints* (Springer Verlag, Berlin).

BULLOUGH, P. G. & GOODFELLOW, J. W., 1968. Incongruent surfaces in the hip joint. *Nature, 217*, 1290.

BUCKLAND-WRIGHT, J. C., 1980. Qualitative and quantitative assessment of tissue organisation in normal and diseased organs. In *Microfocal Radiography*, ed. by R. V. Ely (Academic Press, London), pp. 147–195.

—— 1983a. X-ray assessment of activity in rheumatoid disease. *British Journal of Rheumatology, 22*, 3–10.

—— 1983b. Advances in the radiological assessment of rheumatoid arthritis. *British Journal of Rheumatology, 22 (Suppl.)*, 34–43.

—— 1984. Microfocal radiographic examination of erosions in the wrist and hand of patients with rheumatoid arthritis. *Annals of the Rheumatic Diseases, 43*, 160–171.

—— 1989. A new high-definition microfocal X-ray unit. *British Journal of Radiology, 62*, 201–208.

BUCKLAND-WRIGHT, J. C., CARMICHAEL, I. & WALKER, S. R., 1986. Quantitative microfocal radiography accurately detects joint changes in rheumatoid arthritis. *Annals of the Rheumatic Diseases, 45*, 463–467.

BUCKLAND-WRIGHT, J. C., CLARKE, G. S. & WALKER, S. R., 1989. Erosion number and area progression in the wrist and hand of rheumatoid patients: a quantitative microfocal radiographic study. *Annals of the Rheumatic Diseases, 48*, 25–29.

BUCKLAND-WRIGHT, J. C., MACFARLANE, D. G., CARMICHAEL, I. & CLARK, B., 1987a. Relationship between soft and hard tissue changes in nodal GOA; a clinical and microfocal radiographic study. *British Journal of Rheumatology, 26 (Suppl. 1)*, 13.

BUCKLAND-WRIGHT, J. C., MACFARLANE, D. G. & CLARK, B., 1987b. Quantitative microfocal radiography of disease progression in generalised nodal osteoarthritis (GOA) of the hand. *British Journal of Rheumatology, 26 (Suppl. 2)*, 46.

BUCKLAND-WRIGHT, J. C. & WALKER, S. R. 1987. Incidence and size of erosions in the hand of rheumatoid patients: a quantitative microfocal radiographic study. *Annals of the Rheumatic Diseases, 46*, 463–467.

CALENOFF, L. & NORFRAY, J., 1973. Magnification digital roentgenography: a method for evaluating renal osteodystrophy in hemodialised patients. *American Journal of Roentgenology, 118*, 282–292.

DOI, K., GENANT, H. K. & ROSSMAN, K., 1976. Comparison of image quality obtained with optical and radiographic magnification techniques in fine detailed skeletal radiography: effect of object thickness. *Radiology, 118*, 189–195.

DUNCAN, H., 1983. Cellular mechanisms of bone damage and repair in the arthritic joint. *Journal of Rheumatology, 10 (Suppl. 11)*, 29–37.

EASTWOOD, J. B., BORDIER, P. H. J. & DE WARDENER, H. E., 1973. Some biochemical, histological, radiological and clinical features of renal osteodystrophy. *Kidney International, 4*, 128–140.

FUJIKAWA, K., 1981. Arthrographic study of the rheumatoid knee, part 2. Articular cartilage and menisci. *Annals of the Rheumatic Diseases, 40*, 344–349.

GENANT, H. K., DOI, K. & MALL, J. C., 1975. Optical versus radiographic magnification for fine-detail skeletal radiography. *Investigative Radiology, 10*, 160–172.

GENANT, H. K., DOI, K., MALL, J. C. & SICKLES, E. A., 1977. Direct radiographic magnification for skeletal radiology. *Radiology, 123*, 47–55.

GORDON, G. V., VILLANUEVA, T., SCHUMACHER, H. R. & GOHEL, V., 1984. Autopsy study correlating degree of osteoarthritis, synovitis and evidence of articular calcification. *Journal of Rheumatology, 11*, 681–686.

ISHIGAKI, T., 1973. First metatarsal-phalangeal joint of gout-macroroentgenographic examination in 6 times magnification. *Nippon Acta Radiologica, 48*, 839–854.

LANE, L. B., VILLACIN, A. & BULLOUGH, P. G., 1977. The vascularity and remodelling of subchondral bone and calcified cartilage in adult human femoral and humeral heads. *Journal of Bone and Joint Surgery, 59B*, 272–278.

PARFITT, A. M., 1977. Clinical and radiographic manifestations of renal osteodystrophy. In *Calcium Metabolism in Renal Failure and Nephrolithiasis*, ed. by D. S. David (John Wiley, New York), p. 167.

PARISH, R. W., 1986. Microfocus X-ray technology—a review of developments and applications. In *Review of Progress in Quantitative Non-destructive Evaluation*, vol 5a, ed. by D. O. Thompson & D. E. Chimenti (Plenum, New York), pp. 1–20.

ROCKETT, P. & PARISH, R. W., 1985. A wide energy range, high resolution microfocus X-ray source. *Harwell Report AERE, R11742*, 1–9.

STOKER, D. J., 1980. *Knee Arthrography* (Chapman & Hall, London).

SUNDARAM, M., JOYCE, P. F., SHEILDS, J. B., RIAZ, M. A. & SAGAR, S., 1979. Terminal phalangeal tufts—earliest site of renal osteodystrophy findings in hemodialysis patients. *American Journal of Roentgenology, 133*, 25–29.

SUNDARAM, M., PHILLIP, S. R., WOLVERSON, M. K., RIAZ, M. A. & RAO, B. J., 1980. Ungual tufts in the follow-up on patients on maintenance hemodialysis. *Skeletal Radiology, 5*, 247–249.

SWANSON, A. B. & SWANSON, G. de G., 1985. Osteoarthritis in the hand. *Clinics in Rheumatic Diseases, 11*, 393–420.

TAKAHASHI, S. & SAKUMA, S., 1975. *Magnification Radiography* (Springer-Verlag, Berlin).

WILSON, J. S. & GENANT, H. K., 1979. *In vivo* assessment of bone metabolism using the cortical striation index. *Investigative Radiology, 14*, 131–136.

1989, *The British Journal of Radiology*, *62*, 218–222

Paediatric brachytherapy

I. The role of brachytherapy in the multidisciplinary therapy of localized cancers

By *†P. N. Plowman, MD, FRCR, *D. Doughty, MSc and *‡A. N. Harnett, MRCP, FRCR

Departments of Radiotherapy, *St Bartholomew's Hospital and the †Hospital for Sick Children, London

(*Received July 1988*)

Abstract. Paediatric brachytherapy is rarely practised but has definite benefit in certain situations. Case reports illustrate the role of current brachytherapy strategies both as radical and salvage procedures and in the multidisciplinary management of childhood cancers.

The major advantage of brachytherapy is the ability to deliver a high radiation dose locally and yet, taking advantage of the natural inverse square law fall-off characteristics, to reduce the dose to the adjacent structures. Nowhere in radiotherapy should this be more important than in paediatric treatments, where surrounding normal tissues are most susceptible to growth retardation and other sequelae. However, it appears from the published literature, with the exception of France (Gerbaulet et al, 1985), and except for plaque therapy of retinoblastoma, that paediatric brachytherapy is practised relatively rarely. This is partly because of the extensive nature of many paediatric tumours and partly because of the current widespread availability of electron beam facilities, coupled with the relative lack of paediatric brachytherapy experience by radiotherapists.

There are undoubtedly instances, however, where brachytherapy has an important role in paediatric oncology. Of the eight (non-cerebral) cases (three vaginal, three bladder, one orbital rhabdomyosarcoma and one carcinoma of tongue) so treated at these hospitals over the last 5 years, we have chosen to describe the treatments of four patients with different disease presentations. As will be discussed below the treatment strategies of modern paediatric brachytherapy often vary from the radical brachytherapy treatments of "times-gone-by".

Case reports

Case 1

This 3½-year-old child presented with a 6-month history of intermittent vaginal discharge latterly streaked with blood. Just prior to medical referral, the mother noted a mass (described as a "bunch of grapes") at the introitus. There were no other features in the history. Examination under anaesthesia disclosed a polypoid, botryoid tumour confined to the vaginal walls. The histology disclosed the classical appearance of sarcoma botryoides; staging for systemic metastases was negative.

Chemotherapy with pulsed vincristine and actinomycin was commenced with good regression. At 8 weeks from commencement of therapy, a laparotomy with repositioning of both ovaries to the upper abdomen was performed (Fig. 1). The vaginoscopy at this time showed excellent regression of the primary tumour and the laparotomy findings were normal.

A 15 mm diameter Perspex applicator (Fig. 2) was inserted into the vagina and afterloaded centrally with iridium wire (^{192}Ir). At a depth of 5 mm from the applicator surface, a dose of 45 Gy over 4 days was prescribed. The relative dose distribution, seen superimposed upon the antero-posterior (AP) radiograph (Fig. 1), shows the rapid dose gradient delivering a maximum mucosal contribution of 188% and yet less than 2% of the prescribed dose to the translocated ovaries.

The child has returned to the adjuvant chemotherapy regime and remains well with no complications. Examination under anaesthesia at 6 months showed no vaginal lesion.

Case 2

This 14-year-old boy presented with a 2-month history of an enlarging lesion on the left side of his tongue. It had ulcerated and had become painful such that mastication was only possible on the right side of the mouth. There had been no bleeding. He had noted left-sided pharyngeal discomfort on swallowing and pain in the left ear.

The patient had been previously fit with no relevant past medical history. On examination, he was a fit-looking boy with no abnormal signs outside the mouth; in particular, there was no palpable cervical lymphadenopathy.

In the mouth there was obvious foetor. There was a craggy 4 cm ulcer on the left side of the tongue extending up to at least the midline. Although there was no obvious

---

‡Present address: Beatson Oncology Centre, Western Infirmary, Glasgow G11 6NT. Address reprint requests to: Dr P. N. Plowman, Department of Radiotherapy, St Bartholomew's Hospital, West Smithfield, London EC1.

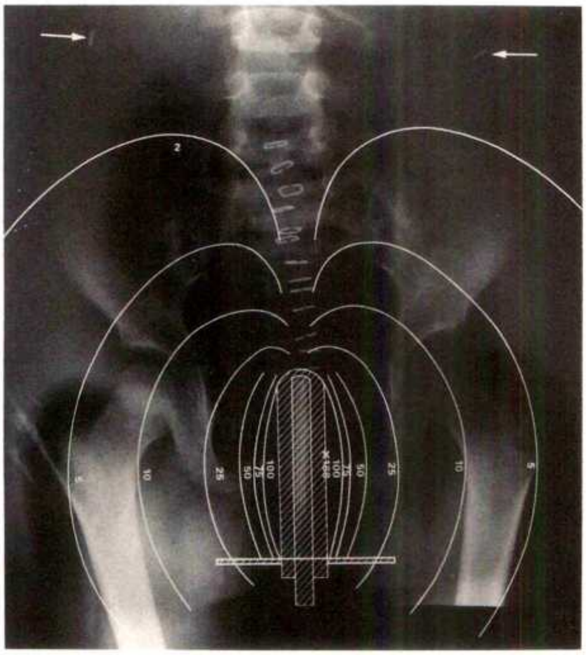

Figure 1. *Case 1.* Plain abdominal radiograph to demonstrate the repositioned ovaries, marked by radio-opaque clips (arrows), and the normalized dose gradient from the intravaginal iridium-wire-loaded applicator.

induration palpable bimanually in the floor of the mouth, the patient was unable to "put out his tongue" suggesting invasion as deep as the floor of mouth. The lesion was staged $T_3N_0M_0$. The histology revealed squamous carcinoma.

The patient received two courses of intravenous *cis*-platinum and bleomycin, with an interval of 3 weeks between courses. The lesion regressed and the pain disappeared following this chemotherapy.

The patient then received external-beam radiotherapy (parallel opposed, lateral, compensated, 6 MV X-ray portals to 43 Gy midpoint in 24 fractions over 31 days, the upper neck nodes receiving 40 Gy). Fifteen days elapsed between the last chemotherapy dose and the first radiotherapy fraction. There was good regression.

Nineteen days following completion of external-beam radiotherapy an iridium wire (double plane/hairpins) implant was performed of the midline tongue region. The objective of this procedure was to boost the dose to the medial perimeter of the tumour. Hairpins (5 cm × 4 cm) and a single pin (1 cm × 4 cm) were implanted through the dorsal surface of the fixed tongue (Fig. 3). A dose of 40 Gy was prescribed on the basal 85% isodose over 75 hours.

Following removal of the implant and regression of the radiation reaction, the patient proceeded to formal left hemiglossectomy. There was residual tumour on the lateral border but the resection margins were clear.

The patient remains disease-free at 3 years.

Case 3

This 5-year-old girl presented with a 1-month history of progressive swelling of the right eyelid. She was a previously fit child and there were no abnormal signs outside the right orbit. There was proptosis and the eye was displaced downwards with limited elevation. Fundi and acuity were normal. Computed tomography (CT) of the orbit showed the presence of a large mass superomedial to the right globe, which was displaced forwards, downwards and laterally. The mass appeared to be within the muscle cone and was causing displacement of the optic nerve. A biopsy showed

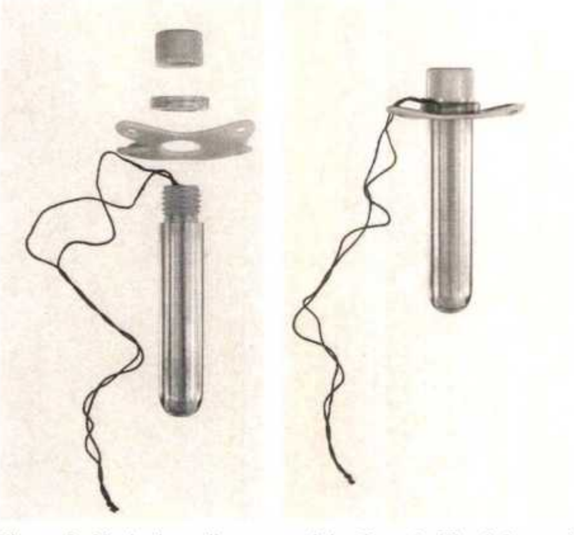

Figure 2. Vaginal applicator used in Case 1. The left panel demonstrates the components and the right panel the assembled device.

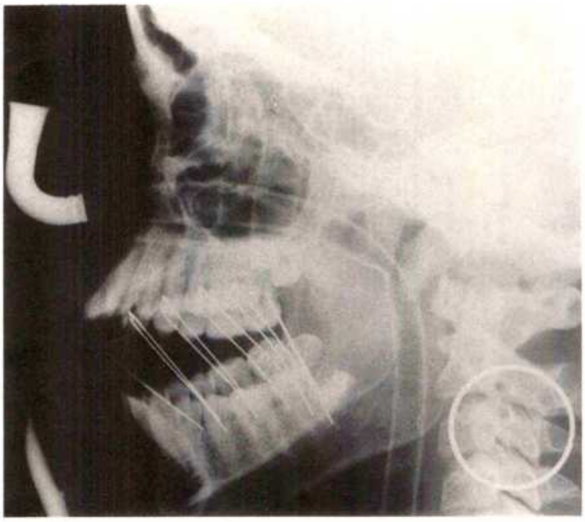

Figure 3. *Case 2.* Iridium wire implant of the tongue is shown in the lateral radiograph.

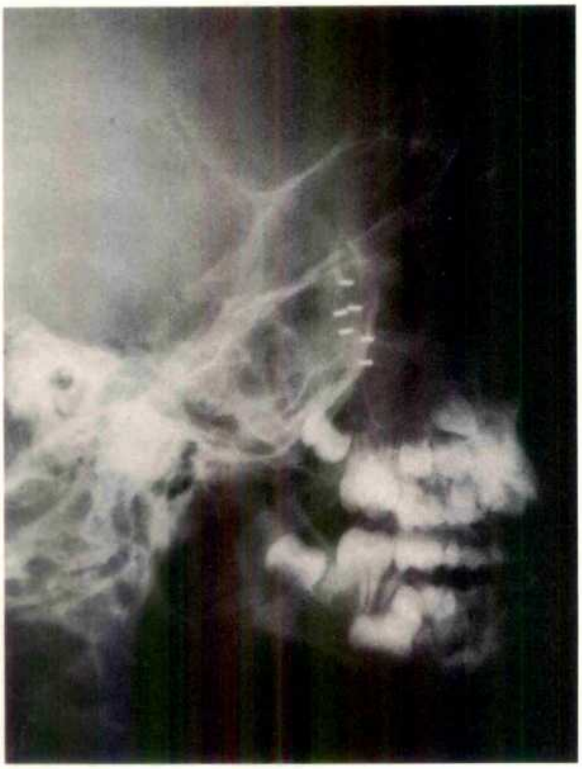

Figure 4. *Case 3.* Lateral skull radiograph showing the gold grain implant of the posterior orbit.

pleomorphic rhabdomyosarcoma. Staging for metastases was negative.

The child received four courses of combination chemotherapy (iphosphamide, vincristine, actinomycin) followed by orbital radiotherapy at another hospital closer to the child's home. Using a 6 MV wedged pair technique, a dose of 45 Gy was delivered in 25 fractions over 34 days. Adjuvant chemotherapy followed radiotherapy. Four and a half months later the child represented with headaches and right proptosis. Computed tomography showed a large intra- and extraconal mass. Chemotherapy (adriamycin, VP16, *cis*-platinum) was reintroduced with no substantial response by 4 weeks. At this juncture, a radical orbital clearance was performed (Professor D. Harrison). At operation, there was no evidence of erosion of the floor of the orbit or the lamina paparacea of the ethmoid. The periosteum was, however, unusually attached in this region. There was macroscopic tumour at the orbital apex. The histological analysis disclosed tumour-free margins except posteromedially where the viable tumour had been transected.

At a later operative session, the orbital apex was implanted with six permanent gold grains (^{198}Au) in a single plane of approximately 1.5 cm diameter (Fig. 4). The minimum dose delivered within this volume was 50 Gy.

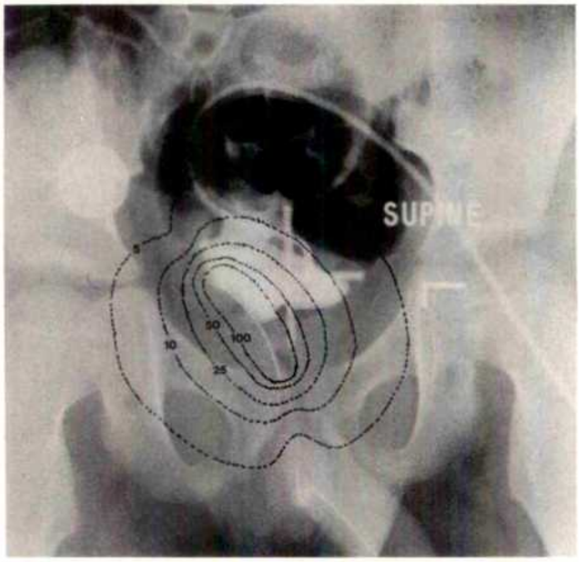

Figure 5. *Case 4.* Iridium wire afterloaded into a Foley urinary catheter with isodosimetry superimposed onto the pelvic radiograph.

The child remains disease-free at 28 months from the implant.

Case 4

This 5-year-old boy presented with a short history of difficulty in micturition and haematuria. He was a previously fit child. Investigations disclosed an abdominal mass which ultrasound demonstrated to be 11.0 cm × 6.5 cm × 6.5 cm and within the bladder. A CT scan did not show any evidence of extravesical spread of this large bladder tumour.

At cystoscopy the bladder was found to be full of tumour which was soft and frond-like with mucosal bubbles. The histology confirmed embryonal rhabdomyosarcoma. Other staging procedures were negative.

Combination chemotherapy (iphosphamide, vincristine, actinomycin D) was commenced with good initial response. As was the policy on that protocol (now discontinued), no external-beam radiotherapy was advised. The follow-up cystoscopy at 7 months demonstrated tumour (biopsy positive) in and around the bladder base and urethra. External-beam radiotherapy was delivered (through parallel opposed, anterior and posterior 6 MV X-ray portals, a midpoint dose of 40 Gy was delivered in 23 fractions over 29 days). However, 7 months later the biopsy from the urethral/bladder junction region was once again positive.

Under general anaesthesia and using a modern radiotherapy simulator, an ^{192}Ir wire was afterloaded into a 14-gauge urethral catheter and located in the correct position using fluoroscopic screening. A 4 cm long active wire was used, leaving at least 1 cm of active length protruding into the bladder. A dose of 40 Gy at 5 mm from the surface of the urethral catheter was delivered in 3.5 days (Fig. 5). A suprapubic catheter maintained urinary drainage during this period.

The child remains well with a negative cystoscopy at 6 months.

Discussion

Classic radiation brachytherapy aims to produce a radical treatment of the tumour, unassisted by external-beam therapy. This was achieved in the case of vaginal rhabdomyosarcoma described here (Case 1). However, the case is worthy of further comment as the design of treatment was to cure with minimum morbidity. Two points should be emphasized which influenced management: first, botryoid rhabdomyosarcoma of the vagina is classically a localized disease of high curability; and second, the Intergroup Rhabdomyosarcoma Study results suggest strongly that for such "good risk cases", the double drug combination of vincristine and actinomycin is comparable in activity to the triplet of these two drugs plus cyclophosphamide (with its sterilizing properties). Therefore ovarian function after therapy is possible if the ovarian radiation dose is minimized and cyclophosphamide omitted. The transposition of the ovaries to the upper abdomen may be performed owing to the derivation of the blood supply from the midabdominal aorta. The intravaginal brachytherapy then minimizes the dose to remaining pelvic organs and the hips. The sequelae envisaged for this child should be reduced to possible corpus uteri and vaginal maldevelopment. The technique of ovarian transposition is not new but had lost its relevance in this disease until the recent validated omission of cyclophosphamide became standard practice. The technique described here can therefore be recommended as an advance over previously described methods (Flamant et al, 1979; Hays et al, 1985).

In the other three cases described here, brachytherapy was not the whole radiation treatment nor was it to the entire tumour volume. In one case (Case 2) brachytherapy was directed specifically to the tumour's medial perimeter; it followed a moderate dose of external-beam radiation to the entire tongue and preceded a formal and pre-planned hemiglossectomy. It is worth stressing that with standard brachytherapy for carcinoma of the lateral border of the tongue, the aim is to implant the whole lesion and to give a radical dose. In our case, this 14-year-old boy had tumour to at least the midline, fixing the tongue to the floor of the month. Given the poor cure rate for a T_3 carcinoma of the tongue in young people (Fletcher, 1980), it was elected to give radiation prior to surgical resection. The late morbidity of surgery more extensive than hemiglossectomy is very severe, and so it was not desirable to excise beyond the midline of the tongue. As the tumour was known to extend beyond the midline at presentation, it was suggested (Professor G. Westbury) that the midline and adjacent contralateral tongue should be implanted. A double plane implant was effected with iridium hairpins as described. Given the difficulty with multiple plane implants in the mouths of children, this treatment scheme was, we believe, particularly desirable and has effected cure with a useful tongue. Indeed, the facility with which this boy has adapted to his disability is remarkable; he speaks well with a slight lisp and eats normally.

Cases 3 and 4 illustrate the usefulness of brachytherapy in the relapse situation. In the case of the orbital rhabdomyosarcoma, the original radical, wedged-pair, photon portal plan had already delivered near tolerance radiation dosage to the optic chiasm, hypothalamus and pituitary, and yet at the surgical orbital clearance there was disease at the resection margins posteromedially. Considering the absent medial wall of the orbit post-operatively, and the proximity of the cavernous sinus, the implant was not an initially attractive proposition. The implant that was achieved has effected cure with little extra morbidity. Such radioactive seed or grain implant salvage therapy has been previously documented in this type of situation (Mameghan et al, 1985; Knight et al, 1986; Curran et al, 1988).

Bladder rhabdomyosarcoma (Case 4) is a recurring problem in that these tumours most commonly occur in the bladder base (such that partial cystectomy is not an option), and since the discovery of their good response to chemotherapy and radiotherapy, bladder conserving chemoradiation protocols are universally practised in the first instance (Hays et al, 1982a, b). However, it is not uncommon for residual tumour to persist in the bladder base and it is now our policy that if this is proven at any of the follow-up cystoscopies, and there is no evidence of spread further afield, then a urethral intraluminal brachytherapy source is placed as described for Case 4. In the three similar cases so treated in the last 5 years at this centre we have not encountered late sequelae (in particular no urethral stenosis); this is in accordance with the observations of Middleton et al (1981).

In conclusion, modern brachytherapy has a definite place in the salvage of patients relapsing locally after chemoradiation and is optimal treatment as either the primary radiation treatment (Case 1) or the salvage radiation (Cases 3 and 4) where normal tissue radiation tolerance is critical. It also has a role as one part of primary multimodality radical treatment of occasional tumours (Case 2).

Acknowledgments

It is with great pleasure that we gratefully acknowledge the surgical skills of Professor D. Harrison, Mr J. Hungerford, Mr P. Ransley, Mr J. Shepherd and Professor G. Westbury. Miss T. Cocks kindly typed the manuscript.

References

CURRAN, W., LITTMAN, P. & RANEY, R. B., 1988. Interstitial radiation therapy in the treatment of childhood soft tissue sarcomas. *International Journal of Radiation Oncology, Biology, Physics, 14*, 169–174.

FLAMANT, F., CHASSAGNE, D., COSSET, J. M., GERBAULET, A. & LEMERLE, J., 1979. Embryonal rhabdomyosarcoma of the vagina in children. *European Journal of Cancer, 15*, 527–532.

FLETCHER, G., 1980. *Textbook of Radiotherapy* (Lea and Febiger, Philadelphia, USA).

GERBAULET, A., PANIS, X., FLAMANT, F. & CHASSAGNE, D., 1985. Iridium afterloading curietherapy in the treatment of pediatric malignancies. *Cancer, 56,* 1274–1279.

HAYS, D. M., RANEY, R. B., LAWRENCE, W., SOULE, E. H., GEHAN, E. A. & TEFFT, M., 1982a. Bladder and prostatic tumors in the intergroup rhabdomyosarcoma study (IRS I). *Cancer, 50,* 1472–1482.

HAYS, D. M., RANEY, B., LAWRENCE, W., TEFFT, M., SOULE, E. H., CRIST, W. M., FOULKES, M. & MAURER, H. M., 1982b. Primary chemotherapy in the treatment of children with bladder-prostate tumors in the intergroup rhabdomyosarcoma study (IRS II). *Journal of Pediatric Surgery, 17,* 812–819.

HAYS, D. M., SHIMADA, H., RANEY, R. B., CRIST, W. M., LAWRENCE, W., MAURER, H. M., NEWTON, W., GEHAN, E. A. & TEFFT, M., 1985. Vaginal-uterine rhabdomyosarcomas in the intergroup rhabdomyosarcoma study (IRS). *Proceedings of ASCO, 4,* 244, Abstr. C-949.

KNIGHT, P. J., DOORNBOS, F., ROSEN, D., LIN, J. J. & FARHA, G. J., 1986. The use of interstitial radiation therapy in the treatment of persistent, localised and unresectable cancer in children. *Cancer, 57,* 951–954.

MAMEGHAN, H., KAROLIS, C., KERN, I., TOBIAS, V. & VOWELS, M., 1985. Tumour control with ^{125}I seeds in childhood pelvic yolk sac tumour. *International Journal of Radiation Oncology, Biology, Physics, 11,* 1227–1228.

MIDDLETON, A. W., ELMAN, A. J., STEWART, J. R., O'BRIEN, R. T. & JOHNSON, D. G., 1981. Combined modality therapy with conservation of organ function in childhood genitourinary rhabdomyosarcoma. *Urology, 18,* 42–46.

1989, *The British Journal of Radiology*, 62, 223–229

Paediatric brachytherapy

II. Brain implantation

By E. S. Thomson, BSc, MSc, *F. Afshar, BSc, MD, FRCS and †‡P. N. Plowman, MD, FRCR

Departments of Radiation Physics, *Neurosurgery and †Radiotherapy, St Bartholomew's Hospital, London

(*Received July 1988 and in revised form October 1988*)

Abstract. The case histories of four children with brain tumours, for whom stereotactic brachytherapy was indicated, are presented from the St Bartholomew's Hospital intracranial brachytherapy programme. The recent evolution of the computed-tomography-directed stereotactic technique is described and the uses of different radionuclides (^{198}Au, ^{192}Ir) are discussed. The future of brachytherapy for paediatric brain tumours is debated.

Although attended by better survival results than adult brain tumours, the current management of many paediatric brain tumours is suboptimal. Radiotherapy maintains a cardinal role in therapy but the radiation tolerance of the paediatric nervous system often restricts the dose prescription for external-beam radiotherapy. There is great scope for brachytherapy in this situation, particularly as local failure is the cause of death in the vast majority of patients. In 1987, the paediatric brain tumour service of St Bartholomew's Hospital commenced a stereotactic brain brachytherapy service.

Four cases are presented to illustrate the scope and potential of the technique. Two different radionuclides and two stereotactic frame systems have been used in this programme and their differences, together with their relative advantages and disadvantages, are discussed.

Materials and methods

The philosophy at St Bartholomew's Hospital has been to use as few source-holding catheters as possible but still to attempt to obtain an isodose pattern shaped to fit the treatment volume. This requires careful planning and for each patient a treatment strategy is prepared approximately 1 week before the implant takes place. Such a strategy has the advantage that it avoids the necessity for complicated calculations on the day of the implant.

The radiation sources used were either ^{198}Au grains or ^{192}Ir wire. The choice of radionuclide was based on the particular treatment strategy to be adopted and this is illustrated in the sections describing the implant procedures of the four patients.

Planning

In order to plan a treatment, a contrast-enhanced computed tomographic (CT) scan of the patient is obtained. The position, size and shape of the volume to be treated are then assessed and a pattern of sources is chosen which produces isodose curves of the required dimensions. This is a subjective procedure and a number of options may be available. The final choice of a particular source arrangement is based on a compromise between its therapeutic efficacy and the difficulties associated with its surgical implementation.

The planned position of each source is reproduced at the time of implant using the pre-calculated relationship between tumour centre and source centre. This is also explained in more detail in the sections describing the implant procedures of the four patients. When using line sources, a specific trajectory needs to be calculated to ensure correct orientation of the source within the tumour. This is achieved through calculation of the geometrical relationship between the source and the tumour centre in two CT images. The two points used for calculation are generally the two ends of the source.

Cross-sections through the final acceptable isodose pattern are plotted on a standard radiotherapy planning system (IGE Target) and superimposed on the original CT images.

Implant procedure

The patient is anaesthetized before the surgical procedure begins and remains anaesthetized until all the catheters are in place and their correct position has been verified.

The first step in a stereotactic brain implant is the attachment of the base plate of the stereotactic frame to the patient. The plate forms a constant plane of reference and is fixed in place on the patient with four steel-tipped plastic screws. Once the base plate is in place, the patient has a contrast-enhanced CT scan in order to locate the target site. As the technique adopted to find the target site is different for the two stereotactic frame systems, each will be discussed separately.

For Case 1, the Bennett stereotactic frame was employed, having been modified for use with CT as described by Thomson et al (1984). With this system, the base plate is fixed to the CT couch, parallel to the image plane, and the centre of the base plate is brought into position on the axis of rotation of the scanner. This axis corresponds to $x=0$ and $y=0$ of the co-ordinate system of the CT image and with the base plate in this position, the x and y co-ordinates of a chosen point in a CT image correspond to the x and y co-ordinates of the stereotactic frame. The third co-ordinate, z, is found from the "scout view" and is the distance between the image containing the chosen point and the base plate. The Bennett system was found adequate for simple arrangements of parallel catheters (Case 1), but for more complicated arrays the calculation of specific trajectories and depths is more complex and the alternative stereotactic frame was felt to be more accurate.

---

‡Author for reprint requests.

Cases 2, 3 and 4 made use of the Brown–Robert–Wells (BRW) stereotactic system (Findlay et al, 1985; Apuzzo et al, 1987; Gutin et al, 1987) shown in Fig. 1. In contrast to the Bennett system, the frame does not attach to the couch. Instead, a localizing assembly is fixed to the base ring, consisting of two aluminium rings separated by nine carbon fibre posts. The posts fit around the patient's head and their relative positions on a CT image allows conversion of CT co-ordinates to frame co-ordinates (Lamb & Gutin, 1985).

A pre-programmed Epson HZ-20 microcomputer is provided to perform the co-ordinate conversion calculation. For line sources, use was made of the computer's facility to calculate the frame settings necessary to guide a cannula along a chosen trajectory. When performing a biopsy or implanting a point source the trajectory would normally be specified by the co-ordinates of the target point and an entry point. To correctly implant a line source, however, the co-ordinates used are those representing the required position of the two source ends (Fig. 2). It is important to note that, as a result of this procedure, the actual entry point cannot be changed. Its position should therefore be predicted at the planning stage in case the trajectory is surgically impractical (Case 2).

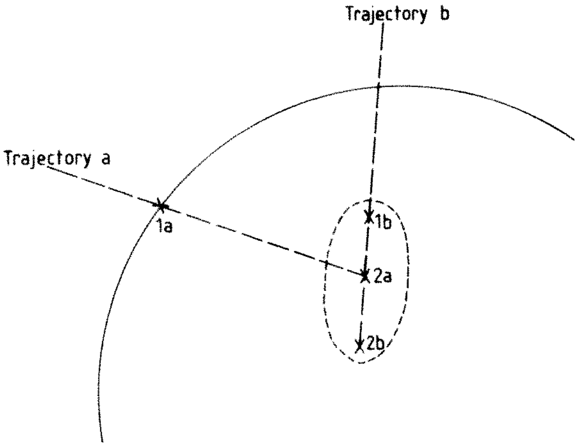

Figure 2. The technique for computing a trajectory along the longest tumour axis. When performing a biopsy or implanting a point source (trajectory a), the target point (2a) is found from a CT scan and the entry point (1a) is any chosen point on the surface. When computing a trajectory for a line source (trajectory b), both points (1b and 2b) are found from CT data and the entry point is therefore pre-determined.

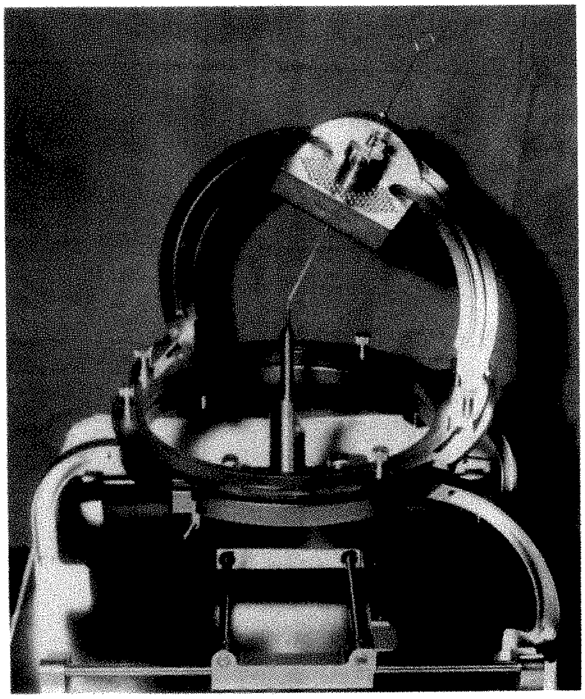

Figure 1. The Brown–Robert–Wells stereotactic frame and guide block assembly.

For multiple, parallel arrays of sources (Case 3), the BRW-NIHA NIH guide block assembly has been used. The guide block has a 37-hole matrix with optional separations of 7 mm or 10 mm between hole centres. Each hole is 6.3 mm in diameter and accepts the BRW guide tubes. The advantage of using the guide block assembly is that a large target volume can be encompassed from a single arc setting. This saves time and simplifies the surgical procedure considerably.

Following CT scanning, the patient is returned to theatre and coaxial silastic catheters (Gutin & Dormandy, 1982), suitable for holding iridium wire (Cases 1 and 3) or gold grains (Cases 2 and 4), are implanted. The catheters are inserted through burr holes or after re-opening a previous craniotomy scar, where multiple incision may jeopardize the scalp flap. The use of multiple twist-drill holes (Apuzzo et al, 1987) has not been favoured as this increases the risk of arterial and venous damage on the cortical surface. Each catheter is secured to the scalp surface using a silastic collar which is sutured to the scalp and then fixed to the catheter with biological adhesive.

Once the catheters are in place, dummy sources are loaded into them and the arc system is removed. The localizing assembly is once more attached to the base ring and the patient has another CT scan to verify that the position of the catheters within the tumour is correct.

The active sources are afterloaded several hours later when the patient is fully recovered and they remain in place for 4–5 days. Sutures are removed after 8 days.

Case histories

Case 1

This female presented at age 16 years with a headache, double vision and right facial weakness. Computed tomography demonstrated a left fronto-temporal enhancing mass. A left temporal craniotomy disclosed a 3 cm tumour and excision appeared macroscopically complete. The histology demonstrated a primitive neurectodermal tumour (PNET). There was no evidence of metastatic disease. The patient received post-operative radiotherapy using a three-field X-ray technique on a 4 MV unit. The prescribed tumour dose was 45 Gy in 26 fractions over 37 days.

Seventeen months later, right facial weakness and headaches recurred; CT suggested, and a second craniotomy confirmed, a cystic recurrence which was decompressed. The patient received post-operative chemotherapy (vincristine, VM26, *cis*-platinum, cyclophosphamide, *i.e.* "OPEC") resulting in some reduction in size of the persisting enhancing tumour on a CT scan. Following six courses of OPEC, a wedged pair of X-ray beams from an 8 MV unit were used to deliver 25 Gy in 15 fractions over 23 days to the tumour.

Sixteen months following the end of retreatment radiotherapy, the patient, who had been in full-time work, again complained of right facial weakness. The CT scan showed an increase in size of the cystic component and an aspiration decompression was performed followed by a re-exploration and excision of a tumour nodule in the cyst wall. No adjunctive medical therapy was given.

Twelve months later the patient presented again with weakness of the right side. Computed tomography demonstrated a further recurrence. A fourth left temporal craniotomy was performed and once again resectable tumour was removed.

Six months later the patient re-presented with mild motor dysphasia, some short-term memory impairment and mild right hemiparesis. She was, however, holding down an office job at this time. The CT scan showed a large recurrence, again in the primary site (Fig. 3a) and single-agent carboplatin (175 mg/m^2/week intravenously) was delivered as described by Allen et al (1987). The patient received six courses with dramatic effect (Fig. 3b). Eight weeks after the sixth course of chemotherapy, an iridium wire implant was performed.

Implant technique. For this patient the Bennett stereotactic frame was used. Three catheters were implanted, 1.5 cm apart, and afterloaded with three 3 cm long iridium wires. To ensure a parallel trajectory and an equal spacing between catheters, the electrode carrier on the arc system was used. This, in a similar way to the guide block on the BRW frame, allowed placement of all three catheters from a single arc setting.

Case 1 was early in our series and as a result lacked some of the sophistication of the later cases. A simple source trajectory was used, orthogonal to the plane of the CT images, which avoided complicated calculations of angles. The frame was adjusted such that the central hole of the electrode carrier guided the middle catheter towards the tumour centre. The depth stop on the catheter was set to allow the catheter tip to pass 1.5 cm beyond this point (*i.e.* half the source length). The remaining catheters were then inserted to the same depth, equally spaced on either side of the tumour centre.

The final source arrangement and resulting isodose pattern are shown in Fig. 4. The isodose curves are normalized to the average dose-rate at the mid-points between the sources, and the prescribed dose was 25 Gy to the 50% isodose.

The patient relapsed in the region of the sphenoidal wings at 4 months.

Case 2

This female presented aged 17 months with a 2-week history of vomiting, drowsiness and unsteadiness. On examination she was an irritable infant with a bulging anterior fontanelle, dilated pupils not reactive to light and no other localizing signs. A CT scan showed hydrocephalus and a mass obstructing the foramen of Munro. The ventriculogram and carotid arteriography showed dilatation of the right lateral ventricle and the appearances of a tumour occupying the anterior part of the third ventricle and obstructing the foramen of Munro. Bilateral ventriculo-peritoneal shunts were inserted but the neurosurgical opinion at that time was against biopsy. The child's condition improved and she received radiotherapy. Using parallel, opposed lateral beams from a cobalt unit, a mid-plane dose of 37.5 Gy was delivered in 18 fractions over 40 days, ketamine anaesthesia being administered on each occasion. The

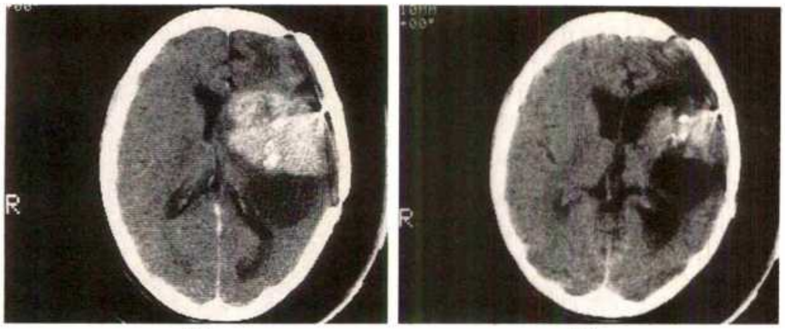

(a) (b)

Figure 3. The effect of carboplatin on a childhood PNET that has recurred after receiving *cis*-platinum-based chemotherapy. Figure 3a represents a transaxial CT scan (enhanced) before chemotherapy and Fig. 3b shows a similar scan following carboplatin (Case 1).

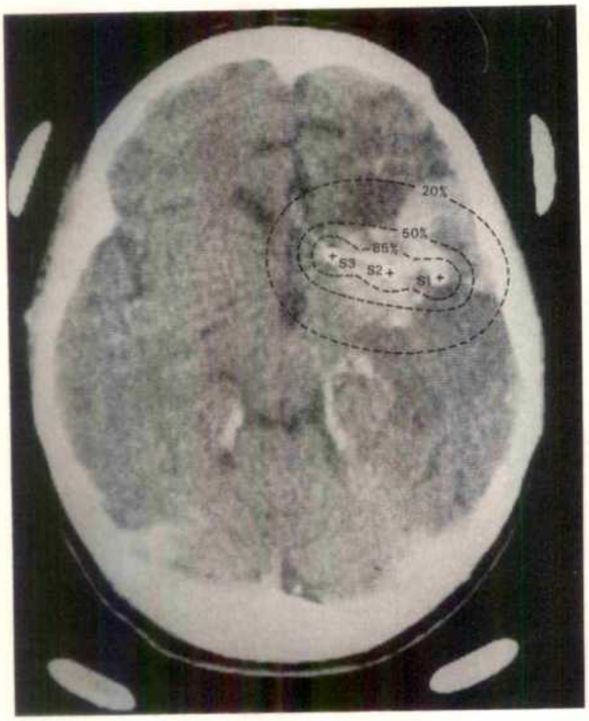

Figure 4. *Case 1.* Transaxial CT scan of the brain. The implanted source array is seen with the isodose curves superimposed.

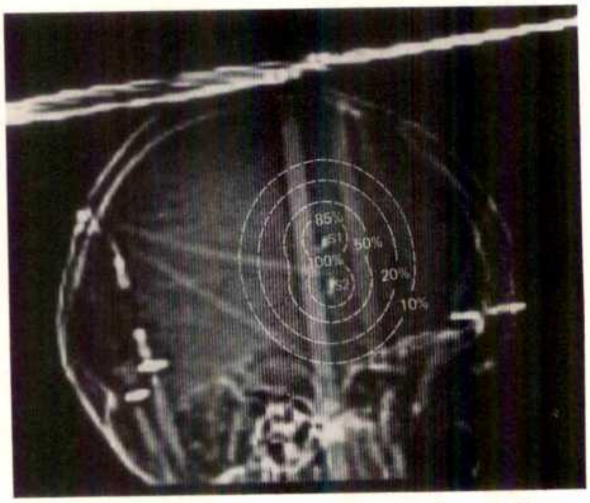

Figure 5. *Case 2.* Lateral skull reconstruction from a CT scan. The implanted sources are seen within the tumour and the resulting isodose curves are superimposed.

child made excellent progress and returned to normal development and later normal schooling.

Eleven years later, the child re-presented with headaches and vomiting but no focal neurological signs. Computed tomography demonstrated a small, discrete, ovoid enhancing lesion in the same situation as the original primary tumour. A stereotactic needle biopsy from the lower pole of the tumour demonstrated histologically a low-grade astrocytoma. Through the same biopsy channel, a brachytherapy catheter was placed in the lower pole of the tumour, and through another channel a second catheter was placed in the upper pole.

Implant technique. The optimum treatment for Case 2, a single line source along the tumour axis, was not possible as the implant trajectory would have passed dangerously close to the sagittal sinus. The alternative approach, two gold grains 1.2 cm apart, was therefore adopted.

At the CT session, with the base ring and localizing assembly in place, the patient was scanned using a 0.3 cm slice thickness. The images were then viewed and the slice containing the tumour centre was found. To locate the first target point, the image recorded 0.6 cm superior to the tumour centre was displayed. On this image, the x and y co-ordinates of the tumour mid-point and the nine carbon fibre rods were determined and the corresponding frame co-ordinates calculated. This procedure was then repeated using the image recorded 0.6 cm inferior to the tumour centre. The sources were considered point sources and so specific trajectories were not pre-planned.

The final source separation was found to be 1.3 cm and the isodose pattern is shown in Fig. 5. The prescribed dose was 40 Gy to the tumour perimeter (the 50% isodose). This was delivered in approximately 4 days giving an average dose-rate of 10 Gy per day.

The patient remains in remission 10 months after the implant.

Case 3

This previously fit child presented at age 12 years with a 1-month history of headache, vomiting, drowsiness and blurred vision. On examination she had bilateral papilloedema, left lower quadrantic homonymous visual field defects and very mild left upper motor neurone signs. A CT brain scan demonstrated a large, right parieto-occipital mass. A right parieto-occipital craniotomy and excision of tumour was performed. The histology demonstrated ependymoma. Wide-field (but not neuraxis) external-beam radiotherapy was delivered (50 Gy in 27 fractions over 30 days using parallel, opposed X-ray beams from a 6 MV unit). The patient remained well, albeit with a left homonymous hemianopia, for 1 year. She then re-presented with a worsening homonymous hemianopia. Computed tomography of the brain showed a large cystic and solid recurrence in the occipital region. Two cycles of chemotherapy were delivered (vincristine, etoposide, cis-platinum) with minimal response. A formal right occipital lobectomy was performed through 7 cm anterior to the occipital pole. Some residual tumour existed, a post-operative CT scan showing an enhancing tumour perimeter. A stereotactic implant was performed.

Implant technique. As a result of the large size and asymmetric shape of the volume to be treated, a larger number of sources were required than had previously been used. The final chosen arrangement was five 4 cm long iridium wires, placed 2 cm apart in an irregular pattern, designed to follow the tumour outline. The required co-ordinate of each source centre was found on the CT scan prior to implant. To ensure the catheters were implanted parallel and to simplify the surgical procedure, the BRW guide block system was used. The trajectory was calculated for one of the central sources and the arc assembly was set up accordingly. The phantom base unit was then adjusted to indicate the required position of the centre of each of the other sources, in turn. Catheters were inserted through various holes in the guide block, and for each source position the hole was found which guided the catheter closest to the indicated point. These holes were marked and with the frame attached to the patient, they were used to guide catheters to the genuine target sites. This technique avoided the need for repeated removal and readjustment of the arc system.

The final pattern of sources and the resulting dose distribution are shown in Fig. 6. The isodose curves are normalized to the average dose-rate at the points midway between consecutive sources. The prescribed dose was 40 Gy to the 50% isodose and this was delivered in 5 days. The patient remains in remission at 3 months.

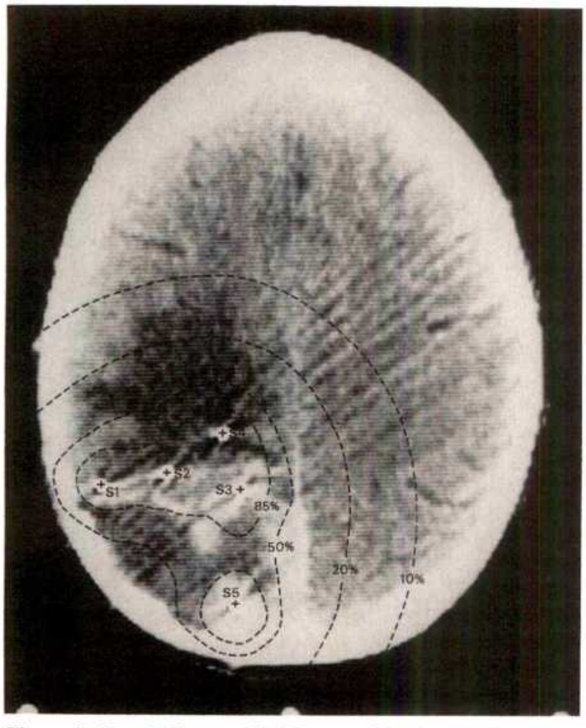

Figure 6. *Case 3*. Transaxial CT scan of brain. The implanted source array is seen, with the resulting isodose curves superimposed.

Case 4

This child aged 3 years 9 months presented first at 2 months of age with bilateral retinoblastoma. The tumours in the right eye were treated by xenon photocoagulation but the disease in the left eye was too extensive. The left eye was therefore given a dose of 40 Gy in 20 fractions over 28 days via an anterior beam from a cobalt unit. At follow-up, the disease in the left eye proved inert but further photocoagulation to new tumours in the right eye was required. At the age of 8 months, because of progressive disease in this eye, external-beam radiotherapy was delivered. Using an anterior beam from a cobalt unit, a dose of 42.5 Gy was delivered in 22 fractions over 44 days. Further follow-up showed inert disease in both eyes.

At the age of 3 years, the child presented with listlessness and an ataxic gait. The CT scan showed gross hydrocephalus with an enhancing midline mass in the region of the pineal, characteristic of ectopic intracranial retinoblastoma.

A ventriculo-peritoneal shunt was inserted. Cerebrospinal fluid cytology and myelography was negative. Systemic chemotherapy (vincristine, etoposide, carboplatin) and intrathecal chemotherapy (methotrexate, cytosine arabinoside and hydrocortisone) was commenced followed by neuraxis irradiation. Using a 6 MV linear accelerator, the neuraxis received 24 Gy in 15 fractions before a planned three-field boost to the pineal region gave a further 16 Gy in nine fractions, bringing the total dose to the pineal tumour to 40 Gy. A higher external-beam dose was not considered safe, bearing in mind the exit contributions from the previous two ocular cobalt portals.

Five months later the CT scan showed a small CT-enhancing lesion in the region of the pineal and a removable stereotactic gold grain implant was planned.

Implant technique. The tumour was assessed as a spherical lesion, 2.5 cm in diameter. Because of its relatively small size, it was felt adequate to implant a single source at the tumour centre. This had the added advantage, as in Case 2, that any trajectory could be chosen, the source being effectively a point source located at the tip of the catheter. The prescribed dose was 40 Gy to the tumour periphery and this was delivered in approximately 4 days. The patient remains in remission at 2 months.

Discussion

In recent years, there has been much interest in brain brachytherapy (Mundinger et al, 1980; Gutin & Bernstein, 1984; Findlay et al, 1985; Mantell et al, 1986; Gutin et al, 1987; Karlsson, 1987). Good results have been claimed for low-grade tumours recurring locally after conventional external-beam radiotherapy, and recently the San Francisco group have published promising data on high-grade tumours (Gutin et al, 1987).

In this report we describe the stereotactic techniques used for paediatric brain brachytherapy at St Bartholomew's Hospital. With the first patients treated, the Bennett stereotactic frame was used and was found adequate for relatively simple implant procedures. It was considered less adaptable, however, for the more complicated trajectories dictated by irregularly shaped tumours, particularly when considering normal anatomical structures that must not be traversed or penetrated during the implant. Our subsequent adoption of the BRW frame together with the NIH guide block assembly has advanced the programme's versatility and sophistication (Case 3). The choice of gold grains was made for small spherical implant volumes (Case 4) or cases where it was impractical to implant a line source along the longest tumour axis (Case 2). Where large or irregular volumes are to be implanted, the choice of iridium wire is more appropriate and reduces the number of sources necessary. We have not employed ^{125}I as an implant radionuclide although this is popular in the USA (Findlay et al, 1985; Gutin et al, 1987). However, the average dose-rate on the perimeter of the tumour volume has been similar to that of the San Francisco group (Gutin et al, 1987) at approximately 10 Gy per day.

The chosen brachytherapy dose in the cases reported here was 25 Gy for the patient who had twice received external-beam radiotherapy to this brain area (a total of 70 Gy), and 40 Gy for the other three cases. This dose was prescribed to the 50% isodose which was planned to correspond to the imageable tumour perimeter. We do not yet know how to calculate brain tolerance doses in children from mixed external-beam and brachytherapy prescriptions or whether lower dose-rate brachytherapy might be advantageous with regard to paediatric normal brain tolerance in a pre-treated patient (Findlay et al, 1985). Certainly, radiotherapy retreatment of recurrent brain tumours has been safely performed previously (Dritschilo et al, 1981).

In standard fractionated radiotherapy, it is now well established that there is a high weighting on the fraction size exponent in the isoeffect formulae for brain tolerance to radiation (Sheline et al, 1980; Wigg et al, 1981). This supports the argument for prescription of small daily fractions in order to best respect central nervous system radiation tolerance. Whether this also applies to low-dose-rate brachytherapy prescriptions, however, is unknown. As a result, our prescriptions to date have been empirical and conservative. We have not seen evidence of radiation necrosis although, from the experience of others, we may expect to encounter this in the central tumour areas. Later in the programme we may elect to increase the total dose prescribed in selected patients, based on the morbidity experienced with previous patients in our series.

The patients described in this report exemplify some important modern concepts in brain tumour management and salvage. Case 1, with multiple local recurrences of a supratentorial PNET, had twice received external-beam radiotherapy and combination chemotherapy (including *cis*-platinum). Although not the main objective of this publication, the dramatic response of the tumour recurrence to carboplatin (Fig. 3) provides support for the use of systemic chemotherapy in this situation (Allen et al, 1987). Following six carboplatin courses, the tumour was of implantable proportions and an array of iridium wires, parallel to the long axis of the tumour allowed a re-irradiation of the tumour volume. Because of the steep dose gradients around the volume, the surrounding fronto-temporo-parietal areas were not significantly re-irradiated.

Case 3 presented the problem of a post-radiation, locally recurrent ependymoma in the non-dominant parieto-occipital region. Radical neurosurgical resection had not been possible and there had been no meaningful response to chemotherapy. It seemed logical to implant the CT-enhancing tumour margins post-decompression. This was achieved by a sophisticated CT-directed iridium wire technique.

Case 2 perhaps exemplifies the ideal situation for brain brachytherapy. The case is most unusual in that a hypothalamic/third ventricular low-grade astrocytoma recurred as a small, discrete, midline mass, 11 years after radical external-beam radiotherapy. It is worth noting the good quality survival and development of this child following a radiation dose of 37.5 Gy at the age of 17 months. It is our belief that following this external-beam radiotherapy in infancy, further external-beam radiotherapy of the surrounding normal brain tissue would have been hazardous, risking severe late radiation morbidity. The recurrent mass was small, oval, midline and at the site of the primary tumour; stereotactic biopsy showed it to be a low-grade astrocytoma. We believe that a small discrete recurrence of a low-grade glioma occurring some years after radical external-beam therapy is the most appropriate indication for brain brachytherapy. This child is fully active and in complete remission.

Case 4 provides a fascinating dilemma. Although pineoblastomas are radiocurable growths (Sung et al, 1978; Bloom, 1983), local recurrence is a problem. This is particularly true in "trilateral retinoblastoma" patients (Kingston et al, 1985), and a conventionally fractionated dose of 50 Gy is recommended in older patients. The child described here was young and had received previous treatment to each eye with direct anterior photon beams. A subsequent external-beam treatment of the pineal tumour delivered a further dose to the pineal region of 40 Gy, a limited dose for reasons of normal tissue tolerance. The follow-up CT scan demonstrated a persisting, albeit very small, enhancing pineal lesion. Case 4 was therefore felt to represent another clearly advantageous situation for brain brachytherapy.

In conclusion, intracranial brachytherapy has an established place in the management of selected cases of paediatric brain tumours, either as part of the primary treatment programme (Case 4) or as a "salvage" radiation procedure (Cases 1–3). It is a procedure that requires a highly specialized and dedicated unit.

Acknowledgments

It is with great pleasure that we gratefully acknowledge the contributions to this project of Mr D. Doughty (radiation physics), Dr A. Bristow (neuro-anaesthesia), Mr P. Ward and

Mr P. Hamlyn (neurosurgery), Dr J. Kingston (paediatric oncology) and the staff of the Bart's neurosurgical theatre. Miss T. Cocks kindly typed the manuscript.

We are grateful to the Imperial Cancer Research Fund for their support in both the Radiation Physics and Neurosurgery departments.

References

Allen, J., Walker, R., Luks, E., Jennings, M., Barfoot, S. & Tan, C., 1987. Carboplatin and recurrent childhood brain tumours. *Journal of Clinical Oncology*, *5*, 459–463.

Apuzzo, M. L. J., Petrovich, Z., Luxton, G., Jepson, J. H., Cohen, D. & Breeze, R. E., 1987. Interstitial radiobrachytherapy of malignant cerebral neoplasms: rationale, methodology, prospects. *Neurological Research*, *9*, 91–100.

Bloom, H. J. G., 1983. Primary intracranial germ cell tumours. In *Clinics in Oncology: Germ Cell Tumours*, ed. by K. D. Bagshawe, E. S. Newlands & R. H. J. Begent (WB Saunders, London), pp. 233–257.

Dritschilo, A., Bruckman, J. E., Cassady, J. R. & Belli, J. A., 1981. Tolerance of brain to multiple courses of radiation therapy. 1. Clinical experiences. *British Journal of Radiology*, *54*, 782–786.

Findlay, P. A., Wright, D. C., Rusenow, U., Harrington, F. S. & Miller, R. W., 1985. ^{125}I interstitial brachytherapy for primary malignant brain tumours: technical aspects of treatment planning and implantation methods. *International Journal of Radiation Oncology, Biology, Physics*, *11*, 2021–2026.

Gutin, P. H. & Bernstein, M., 1984. Stereotactic interstitial brachytherapy for malignant brain tumors. *Progress in Experimental Tumor Research*, *28*, 166–182.

Gutin, P. H. & Dormandy, R. H., 1982. A coaxial catheter system for afterloading radioactive sources for the interstitial irradiation of brain tumors. *Journal of Neurosurgery*, *56*, 734–735.

Gutin, P. H., Leibel, S. A., Wara, W. M., Choucair, A., Levin, V. A., Philips, T. L., Silver, P., Da Silva, V., Edwards, M. S. B., Davis, R. L., Weaver, K. A. & Lamb, S., 1987. Recurrent malignant gliomas: survival following interstitial brachytherapy with high activity iodine-125 sources. *Journal of Neurosurgery*, *67*, 864–873.

Karlsson, U. L., 1987. Interstitial stereotactic irradiation of astrocytomas. *American Journal of Clinical Oncology*, *10*, 296–298.

Kingston, J. E., Plowman, P. N., Hungerford, J. L. & Bedford, M. A., 1985. Ectopic intracranial retinoblastoma in childhood. *British Journal of Ophthalmology*, *69*, 742–748.

Lamb, S. & Gutin, P. H., 1985. Interstitial radiation for treatment of primary brain tumors using the Brown–Roberts–Wells stereotactic system. *Journal of Neurosurgical Nursing*, *17*, 22–29.

Mantell, B. S., Klevenhagen, S. C. & Afshar, F., 1986. An afterloaded applicator for the interstitial irradiation of brain tumours. *Clinical Radiology*, *37*, 35–38.

Mundinger, F., Osterag, Ch. B., Birg, W. & Weigel, K., 1980. Stereotactic treatment of brain lesions. *Applied Neurophysiology*, *43*, 198–204.

Sheline, G. E., Wara, W. M. & Smith, V., 1980. Therapeutic irradiation and brain injury. *International Journal of Radiation Oncology, Biology, Physics*, *6*, 1215–1228.

Sung, D. I., Harisiadis, L. & Chang, C. H., 1978. Midline pineal tumours and suprasellar germinomas: highly curable by irradiation. *Radiology*, *128*, 745–751.

Thomson, G. S. M., Kingsley, D. P. E., Afshar, F. & Wylie, I. G., 1984. Stereotactic brain biopsy using a narrow aperture computed tomography scanner. *Clinical Radiology*, *35*, 209–214.

Wigg, D. R., Koschel, K. & Hodgson, G. S., 1981. Tolerance of the mature human central nervous system to photon irradiation. *British Journal of Radiology*, *54*, 787–798.

1989, *The British Journal of Radiology*, *62*, 230–233

Radiation dose to neonates on a Special Care Baby Unit

By *K. Faulkner, BSc, MSc, PhD, ‡J. L. Barry, DCR and †P. Smalley, DCR

Regional Department of Medical Physics and Bioengineering, Christie Hospital and Holt Radium Institute, Wilmslow Road, Manchester M20 9BX

(*Received February 1988 and in revised form August 1988*)

Abstract. Neonates on a Special Care Baby Unit often require radiography to monitor the progress of their treatment and as a result can have a large number of radiographs taken during their stay in hospital. The skin entrance dose was estimated from a knowledge of the technique factors, X-ray tube output and backscatter factors. Normalized organ dose data were employed to estimate the radiation dose to a number of critical organs. A number of methods of reducing the radiation dose to neonates were investigated. Initially, this involved changing the radiographic technique factors and introducing a lead rubber adjustable collimator, placed on top of the incubator, in addition to the light beam diaphragms on the X-ray tube. It was deduced from the results of calculations that these modifications to the radiographic examination technique had reduced the average entrance dose per radiograph from 92 μGy to 58 μGy, a reduction of 37%. Later, a rare-earth film–screen combination was introduced to replace the existing fast calcium tungstate screens. This enabled the average entrance dose per radiograph to be reduced to 39 μGy, a further reduction of 33%. The mean radiation dose to a neonate is mainly determined by the number of radiographs taken and this is dependent on the clinical symptoms.

Radiology is one of the main methods of assessing the progress of treatment of neonates on a Special Care Baby Unit (SCBU). Consequently, very ill neonates may have a large number of radiographic examinations during their stay in hospital. Despite the radiographic technique factors being lower than for older patients, it is still very important to monitor the radiation dose to neonates because of the high patient doses associated with the relatively large number of radiographs taken. In addition, certain somatic risk factors are considered to be higher for neonates than for adults (National Radiological Protection Board (NRPB), 1984).

It is therefore of interest to investigate various means of reducing the radiation dose to neonates and to estimate the reduction achieved by each method. Three methods of dose reduction were studied: (i) changing radiographic technique factors, (ii) improving the X-ray beam collimation by the introduction of a lead rubber adjustable collimator (Appleton & Carr, 1984) and (iii) the introduction of a rare-earth film–screen combination.

Materials and methods

All radiographic investigations were performed on a capacitor discharge mobile X-ray unit. The radiation output of the mobile X-ray set was measured using a Victoreen 660 digital survey meter and a previously calibrated ionization chamber. Radiation output measurements were made across the range of radiographic technique factors routinely used on the Special Care Baby Unit.

The entrance dose to each neonate was estimated retrospectively from a knowledge of the radiographic technique factors, using a previously published method of calculation (Harrison et al, 1983). Backscatter factor values were taken from a previous publication (Harrison, 1982). An allowance was made for the attenuation of X rays in the Perspex top of the incubator.

Radiation doses to a number of organs were estimated using the method of Rosenstein et al (1979). The normalization quantity for this data is the entrance exposure (free in air). The entrance exposure (free in air) was deduced from the entrance dose for each neonate.

The radiation dose to the breasts was estimated using a different method to that for the other organs, as normalized organ dose data for the breasts is not tabulated by Rosenstein et al (1979). When the breasts were in the primary beam, for example during chest radiography, the breast dose was taken to be equal to the entrance dose. Occasionally, an abdominal radiograph was taken on some of the neonates included in this study. For these radiographs, where the breasts were not in the primary beam, it was assumed that the scattered radiation dose to the breast was similar to that to the lungs. This was considered to be a reasonable approximation which would not have a large effect on the breast dose, as abdominal radiographs were very infrequent when compared with the number of radiographs taken where the breasts were in the primary beam.

Two methods of dose reduction were initially investigated: a lead rubber adjustable collimator was introduced and the radiographic technique factors were altered. The lead rubber adjustable collimator was based on an earlier design (Appleton & Carr, 1984) and is placed on the Perspex top of the incubator (Fig. 1). The use of the lead rubber collimator ensures the X-ray beam is tightly collimated to the area of interest, thereby decreasing the penumbra and the effect of any

---

Present addresses: *Regional Medical Physics Department, Newcastle General Hospital, Westgate Road, Newcastle upon Tyne NE4 6BE; †X-ray Department, Hope Hospital, Eccles Old Road, Salford; ‡X-ray Department, Dumfries and Galloway Infirmary, Galloway.

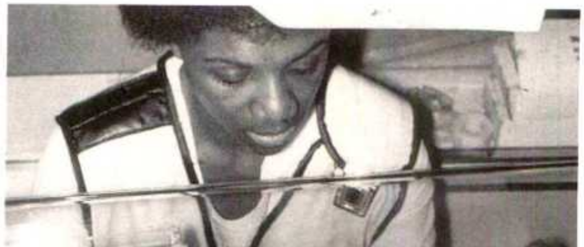

Figure 1. Adjustable collimator in position.

inaccuracies in the light beam alignment. It may be deduced from Figs 2 and 3 that the lead rubber collimator is very effective at reducing the size of the X-ray beam to the area of interest. Technique factors were changed by using a slightly higher tube potential and therefore lower mAs to decrease the entrance dose whilst keeping the same dose to the film. Increasing the tube potential will decrease the radiographic contrast, consequently a compromise has to be made between decreasing the entrance dose and therefore the dose to other organs and the radiographic contrast. Neonates radiographed before and after the introduction of these dose reduction techniques were in Groups 1 and 2, respectively.

An allowance was made for the effect of the difference in field size on organ doses when the lead rubber adjustable collimator was used based on the data of Rosenstein et al (1979). It is anticipated that the organ doses for the patients will be slightly overestimated as the radiographers, in general, will be able to collimate the X-ray field to an area smaller than the respective field sizes given by Rosenstein et al (1979). The normalized organ dose data of Rosenstein et al (1979) assumes that the X-ray field is collimated to the size of the body part using a rectangular field, whereas the adjustable collimator should reduce the field size even further. However, in practice the adjustable collimator could only be used in 66% of all examinations.

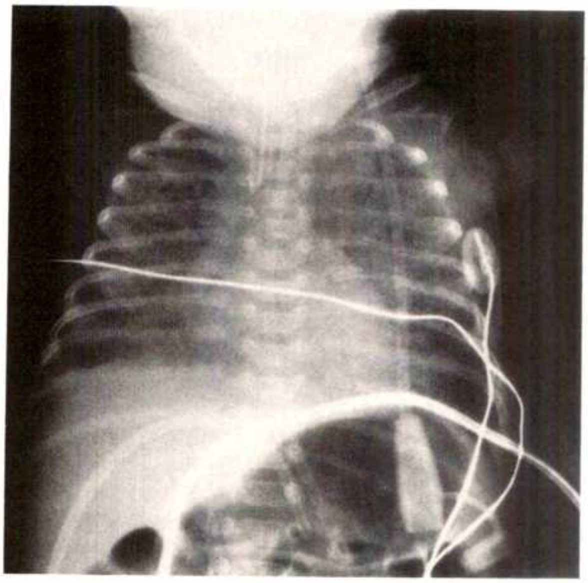

Figure 2. Radiograph with no extra collimation.

Later, a rare-earth film-screen combination (Agfa Curix MR400, Agfa RP film) was introduced to replace the existing fast conventional screens (Siemens Diamante Super Voderfolie). This constituted the third group of neonates. The lead rubber adjustable collimator was still used whilst radiographing this group.

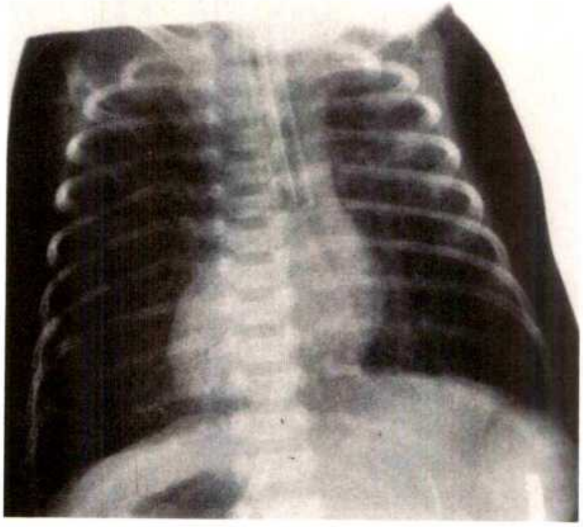

Figure 3. Radiograph with collimator in position.

Table I. Estimated mean radiation dose to a number of organs (mGy) for the three groups of neonates

Organ	Group		
	1	2	3
Breast	2.32 (2.66)	0.61 (0.41)	0.61 (0.77)
Testes	0.25 (0.21)	0.04 (0.04)	0.08 (0.10)
Ovaries	0.19 (0.14)	0.04 (0.05)	0.06 (0.07)
Thyroid	1.28 (1.35)	0.30 (0.22)	0.31 (0.39)
Active bone marrow	0.28 (0.29)	0.06 (0.04)	0.05 (0.07)
Lungs	1.02 (1.02)	0.23 (0.17)	0.24 (0.30)
Total body	0.84 (0.84)	0.18 (0.14)	0.14 (0.17)

Standard deviation in parentheses.

Results

Table I is a summary of the estimated mean radiation dose to different organs of the three groups of neonates. The first group comprised 10 neonates who were examined prior to the instigation of dose reduction techniques, whose radiation doses were calculated retrospectively. Typical radiographic technique factors were 46 kV, 5 mAs. The second group of seven neonates were those examined at a slightly higher tube potential (52 kV, 2 mAs) and after the introduction of the lead rubber adjustable collimator. The eight neonates in Group 3 were radiographed using a rare-earth film–screen combination. Radiographic technique factors for neonates in this third group were typically 46 kV and 2 mAs. Note that the radiographic technique factors have been rounded to the nearest integer value.

Discussion

As may be deduced from Table I, radiation doses to a typical neonate in Group 2 were considerably lower than in Group 1. For instance, the mean total body dose fell from 0.84 mGy for neonates in Group 1 to 0.18 mGy for neonates in Group 2. The main cause of this dose reduction was the lower average number of radiographs of each neonate in Group 2 (10.8) compared with Group 1 (28.5). The decrease in the number of radiographs is consistent with the neonates in Group 2 having slightly different clinical problems which required fewer radiographs.

The reduction in the number of radiographs taken accounts for most, but not all, of the reduction in dose to neonates in Group 2 compared with Group 1. One way of assessing the effect of the dose reduction techniques on the dose received by neonates in the three groups is to compare the average entrance dose per radiograph. This quantity is independent of the average number of radiographs taken on the neonates in the three groups. Because of changes in technique factors, the average entrance dose per radiograph was lower for neonates in Group 2 (58 μGy compared with 92 μGy for those in Group 1), a reduction of 37%.

The radiation dose to neonates in Group 3 was similar to those in Group 2 (Table I). This is despite the neonates in Group 3 having on average a larger number of radiographs (15.3) when compared with Group 2. The use of a rare-earth film–screen combination has reduced the average entrance dose per radiograph to neonates in Group 3 from 58 to 39 μGy, a reduction of 33%. Note that the rare-earth film–screen combination is not being used to its fullest advantage in this particular imaging task. The peak tube potential is too low to make full use of the greater attenuation of the screen caused by the K-edge of the rare-earth materials, as the majority of the X-ray spectra lies below the K-edge of the materials used (Birch et al, 1979). The increased light output of the rare-earth fluorescent screens is being utilized, however, to reduce radiation doses.

Radiation doses could be reduced even further by increasing the tube potential. However, this was not possible on this particular mobile X-ray set, because of the limited minimum tube current and exposure time which could be selected. Adding extra filtration to the beam by the introduction of a rare-earth metal filter (Webster, 1984) would solve this problem and would also reduce radiation doses as a result of the harder X-ray beam.

Values of entrance dose per radiograph given here for the neonates radiographed with a rare-earth film–screen combination (*i.e.* Group 3) are slightly lower than those reported by Robinson and Dellagrammaticas (1983) for chest and abdominal examinations, whereas the entrance dose per radiograph to neonates in Group 2 is similar.

Fletcher et al (1986) studied the risk of diagnostic radiation to the newborn. In their paper the skin dose for a single exposure (or radiograph) was given as 0.07 mGy (70 μGy), which may be compared to data on entrance dose per radiograph given here. The average entrance dose per radiograph to neonates in Group 1 was slightly higher than that quoted by Fletcher et al (1986). The introduction of rare-earth screens and changes in radiographic technique reduced the average dose per radiograph to 39 μGy for neonates in Group 3, somewhat lower than given by Fletcher et al (1986).

In the paper by Fletcher et al (1986), the various sources of data on carcinogenic and genetic risks were discussed. A value of 51 cases of malignant disease per 1000 Gy was given as a reasonable upper estimate of the risk of radiation to neonates. This somatic risk value has been used here in order to directly compare our findings with those of Fletcher et al (1986). Using our estimates of total body dose (Table I), the risk of radiation to the neonates is 43, 9 and 7 $(\times 10^{-6})$ for the neonates in Groups 1 to 3, respectively. It should be anticipated that the radiation risk to the neonates studied here is lower than that given by Fletcher et al (1986) as mean total body dose has been used in the calculation rather than entrance dose. However, the estimated risk of radiation to neonates in Group 1 is somewhat higher, due mainly to differences in the number of radiographs taken.

Conclusions

As anticipated, changing the radiographic technique factors by using a more penetrative beam and a lower mAs reduced the average entrance dose per radiograph by 37%. The introduction of a rare-earth film–screen combination produced a further reduction of 33%. However, the main influence on the estimated typical total body dose was the number of radiographs taken, which is related to the clinical problems of the neonates.

The lead rubber adjustable collimator which was used to tightly collimate the X-ray beam to the area of interest was very successful at reducing the radiation dose to certain organs and tissues. In practice, the dose reductions will be slightly less as the adjustable collimator could only be used in 66% of all examinations.

Acknowledgments

We would like to thank Drs Robinson and Hambleton for their assistance with the dosimetry measurements and Dr H. Mamtora for his encouragement and support.

References

APPLETON, M. B. & CARR, R. S., 1984. Radiation protection in a neonatal intensive care unit: a practical approach. *Radiography, 50,* 137–141.

BIRCH, R., MARSHALL, M. & ARDRAN, G. M., 1979. *Catalogue of Spectral Data for Diagnostic X-rays* (Institute of Physical Sciences in Medicine, York).

FLETCHER, E. W. L., BAUM, J. D. & DRAPER, G., 1986. The risk of diagnostic radiation of the newborn. *British Journal of Radiology, 59,* 165–170.

HARRISON, R. M., 1982. Backscatter factors for diagnostic radiology. *Physics in Medicine and Biology, 27,* 1465–1474.

HARRISON, R. M., CLAYTON, C. B., DAY, M. J., OWEN, J. P. & YORK, M. F., 1983. A survey of radiation doses to patients in five common diagnostic examinations. I. Principle and techniques for dose evaluation by indirect examinations. II. Survey results. *British Journal of Radiology, 56,* 383–395.

NRPB, 1984. *The Risks of Leukaemia and other Cancers in Seascale from Radiation Exposure,* R171 (Her Majesty's Stationery Office, London).

ROBINSON, A. & DELLAGRAMMATICAS H. D., 1983. Radiation doses to neonates requiring intensive care. *British Journal of Radiology, 56,* 397–400.

ROSENSTEIN, H., BECK, T. J. & WARNER, G. G., 1979. *Handbook of Selected Organ Doses for Projections Common in Paediatric Radiology, (Publication (FDA) 79-8079,* US Department of Health, Education and Welfare, Rockville, Maryland).

WEBSTER, D. J., 1984. An evaluation of the use of the k-edge filtration for dose reduction in paediatric radiology. In Hospital Physicists' Association CRS 42, *Dose Reduction in Diagnostic Radiology* (Institute of Physical Sciences in Medicine, York), pp. 15–20.

1989, *The British Journal of Radiology*, 62, 234–236

Experimental intra-arterial administration of SR-2508 in the rabbit V2 carcinoma model

By Douglas M. Coldwell, MD, PhD, *James Huff, RT, *Harvey Marcellus, PA and †Susan G. Coldwell, PhD

Department of Radiology, University of Washington, Seattle, Washington 98104, USA, *Department of Radiology, George Washington University Medical Center, Washington, DC 20037, USA and †Georgetown University, Washington, DC 20030, USA

(*Received March 1988 and in revised form August 1988*)

Abstract. The use of the nitroimidazole radiation sensitizers, misonidazole and SR-2508, has been limited by a variety of side-effects, principally peripheral neuropathies. In order to increase the effectiveness of radiosensitization and thereby reduce the administered dose of the sensitizers, intra-arterial delivery of SR-2508 was performed and followed with 10 Gy of 4 MeV photon beam radiotherapy in the rabbit V2 carcinoma tumour model. Comparison was made with rabbits treated with an identical dose of SR-2508 given intravenously prior to photon beam radiotherapy. Control animals were treated with radiation therapy only, intra-arterial SR-2508 only, or had no treatment. Neither the radiation therapy alone nor the SR-2508 alone had any effect on tumour growth. In the intra-arterial group, the tumour growth was slower and the size was significantly smaller than all other groups. The results suggest that the intra-arterial infusion of the radiation sensitizer produces greater response of the tumour than intravenous infusion when each is combined with radiation therapy.

Recently, interest has been generated in the radiation sensitizer SR-2508 because of a higher degree of sensitization than its predecessor, misonidazole, as well as reduction in side-effects (White et al, 1980). However, peripheral neuropathies are still seen with this drug and are dose dependent (Coleman et al, 1984). Since sensitizer effectiveness is concentration dependent and toxicity is total-dose dependent, a reduction in toxicity without loss of effectiveness could be achieved by administering a lower dose of sensitizer intra-arterially directly to the tumour. A comparison of intra-arterial and peripheral intravenous administration of radiosensitizer is reported, using the rabbit V2 carcinoma tumour model.

Materials and methods

Animals

Fifty-nine adult New Zealand white male rabbits of 3 to 4 kg body weight were divided into seven groups. Group I (12 rabbits) received intra-arterial SR-2508 and radiation therapy. Group II (12 rabbits) received intravenous SR-2508 and radiation therapy (RT). Group III (eight rabbits) received no treatment. Group IV (eight rabbits) received intra-arterial SR-2508 only. Group V (eight rabbits) received radiation therapy only. Group VI (three rabbits) were tumour donor animals. Group VII contained eight rabbits who did not have a tumour placed in the thigh and received intra-arterial SR-2508 and radiation therapy.

Tumour

Frozen rabbit V2 carcinoma fragments which are syngeneic in the New Zealand white rabbit were obtained from the Breast Cancer Animal and Human Tumor Bank, National Cancer Institute (Bethesda, Maryland) and were implanted intramuscularly into the thighs of donor animals. After 14 days growth, the tumour masses measured 1–2 cm diameter. At this time the donor animals were sacrificed and the tumour removed from the thigh. The tumour was then minced and 0.2 cm^3 of tumour fragments suspended in 0.3 ml Minimum Essential medium. These fragments were then implanted in the thighs of the experimental animals. Before intramuscular injection of the tumour fragments, the animals were anaesthetized with an intramuscular injection of 2.5 mg kg^{-1} acepromazine maleate (Ayerst Laboratory, New York) and 44 mg kg^{-1} ketamine hydrochloride (Bristol Myers Co., Syracuse).

Drug delivery

Intra-arterial delivery of the SR-2508 was performed by placing a 3 French single-lumen polyethylene catheter selectively in the common femoral artery of the leg containing the tumour. The arterial system was accessed by a surgical cut-down on a carotid artery and the catheter placed with fluoroscopic guidance. Before radiation therapy was begun, the catheter was removed, the carotid artery tied off, and the surgical site sutured. During the procedure, adequate anaesthesia in all groups was maintained by administration of 0.5–1.0 ml boluses of intravenous thiamylal sodium (Parke-Davis & Co., Detroit) via an ear vein every 15–20 min. Intravenous delivery of SR-2508 was via a marginal ear vein. SR-2508 was administered 15–20 min prior to radiation therapy. No sham operations were performed in groups which were not treated.

Radiation therapy

A total of 10 Gy of 4 MeV photon radiation therapy was administered to Groups I, II, V and VII at a rate of 1 Gy min^{-1}. A single lateral treatment field on the thigh, measuring 4 cm × 5 cm, was used.

Drugs

SR-2508 was supplied by the Drug Synthesis and Chemistry Branch of the National Cancer Institute. The dose was 20 mg kg^{-1}, which was dissolved in 50 ml of 0.9 N saline. This dose will give approximately 0.3 mg ml^{-1} in circulating blood.

Evaluation

Tumours were measured in two perpendicular directions at weekly intervals for 12 weeks after inoculation. Treatment was performed 2 weeks after implantation when the diameter of the tumour was 1–2 cm. After the animals recovered from anaesthesia, they were examined daily for food intake, state of consciousness and motor activity. Euthanasia, using 5 ml of intravenous T-61 solution (Taylor Pharmaceutical, Decatur), was performed 12 weeks after implantation or earlier if an animal became incapacitated. Necropsies were performed on all animals. Statistical analysis using the Mann-Whitney U-test compared the cross-sectional areas of the measured tumour on a weekly basis. Percentage growth was calculated from the difference of cross-sectional areas between two consecutive weeks divided by the earlier area. The level of significance was selected as 5%.

Results

The mean values of the cross-sectional areas of the tumour in Groups III, IV and V are shown in Fig. 1 with mean survivals of 52, 48 and 49 days, respectively. Cross-sectional areas were compared as they could be measured more easily than volumes and with a higher degree of reproducibility and because the tumour grew as a flat plate rather than a spheroid. No statistically significant difference was present among these groups. These rabbits died from lung metastases or were sacrificed. No rabbits showed any evidence of subsequent immunorejection of the tumour. In contrast, all animals in Groups I and II survived for the duration of the experiment and, at the time of sacrifice, animals in Group I showed no evidence of metastases while five of 12 rabbits in Group II demonstrated metastases in either lung or abdomen. The results of Groups I and II are shown in Fig. 1. Eight of 12 animals receiving intra-arterial SR-2508 with radiation had no detectable tumour on palpation of the leg 5 weeks after treatment. At necropsy, none of these animals had tumour present. No animals in any other group showed evidence of cure.

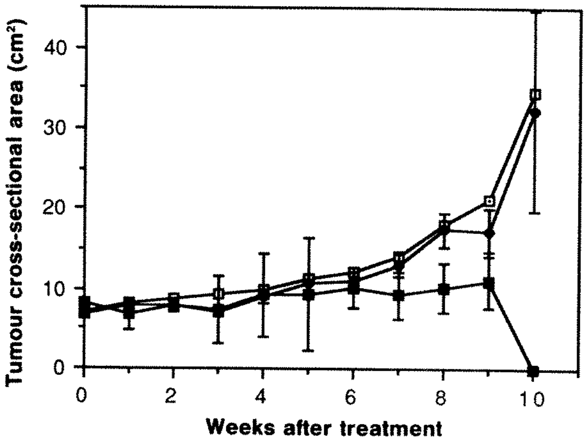

Figure 1. Cross-sectional area of the tumour as a function of time after treatment. Group I is intra-arterial SR-2508 plus radiation (■) and Group II is intravenous SR-2508 plus radiation (◆). Error bars represent one standard error of the mean. Control groups are collectively represented by the no treatment group cross-sectional area variation with time (□).

Since two-thirds of the animals treated with intra-arterial SR-2508 with radiation were cured of their tumour, a tumour regrowth delay assay would have been inaccurate (Fowler et al, 1980). Consequently, since the comparison between the experimental groups that had received intravenous and intra-arterial SR-2508 with radiation was of primary interest, a statistical comparison of the groups was performed on a weekly basis using non-parametric statistics because the groups were not necessarily Gaussian in distribution.

The cross-sectional tumour areas of Groups I and II were significantly different ($p<0.001$) from the 8th through the 12th week following implantation (6–10 weeks after treatment) with Group I tumours smaller than Group II. However, interval growth, defined as the percentage change between tumour cross-sectional areas in successive weeks, was statistically significant only during the first week after treatment; Group I interval growth was negative while Group II growth consistently increased.

No animals showed any evidence of neurological changes as evidenced by impaired mobility. However, the animals which received SR-2508 and radiotherapy, regardless of the method of administration, showed a higher sensitivity to intravenous anaesthetics than animals that did not receive SR-2508, such that only half of the usual dose of anaesthetics was required to place the animals under adequate analgesia to perform the radiotherapy.

Discussion

The radiation resistance of hypoxic tumours is well demonstrated. The use of radiation sensitizers to solve this problem in treatment was initially proposed in the 1960s and testing of the 2-nitroimidazoles, *e.g.* misonidazole, was begun. Second-generation sensitizers such as SR-2508 have been developed which are derivatives of misonidazole. The lack of adequate sensitization of the tumour as well as the development of toxicities, notably peripheral neuropathies, limits the use of misonidazole and SR-2508. However, because of the lower lipophilicity of SR-2508, neurotoxicity is not as great a problem (Brown et al, 1981).

In the past, the radiation sensitizers have been administered orally and intravenously. As with chemotherapeutic agents, the dose–response curve of radiation sensitizers is steep, and thus the actions should be enhanced by selectively delivering the drug intra-arterially to the tumour. Side-effects should also be diminished for two reasons: (a) it is likely that an intra-arterial dose to the tumour will produce adequate sensitization at a lower systemic dose because of the steep concentration gradient between the arterial system and the tumour, which will produce more diffusion of the sensitizer into the tumour, and (b) there may be a first pass extraction effect also resulting in a lower systemic dose.

The administered dose of SR-2508 was based on prior research with the rabbit VX2 carcinoma and murine fibrosarcoma models using misonidazole as the sensitizer (Milas et al, 1983; Coldwell et al, 1984; Newman et al, 1986a). The 10 Gy radiation dose was selected because previous work demonstrated that the V2 carcinoma was unresponsive to this dose of radiation (Muckle & Dickson, 1973). This lack of response to the administered dose of radiation only was again noted in the current study. A demonstrable change in the tumour was produced only when both SR-2508 and radiation were present. While 20–30 min elapsed between the administration of SR-2508 and radiotherapy, prior research has shown that peak tumour concentrations of SR-2508 are maintained for at least 20 min (Brown & Yu, 1980; Newman et al, 1986a).

The V2 tumour is a hypoxic tumour with a low pH and develops necrotic areas 3 weeks after implantation. The tumour is sensitive to the combination of intra-arterial SR-2508 and radiation therapy. This sensitivity to the method of delivery is underscored by the statistically significant difference between the groups of animals whose only variation in treatment was intra-arterial or intravenous drug delivery. The tumour was exposed to two different SR-2508 concentrations producing gradients that promoted diffusion of more SR-2508 into the tumour when it was given intra-arterially. These results are consistent with previous work which demonstrated a greater amount of misonidazole absorbed in tumours when it was administered intra-arterially rather than intravenously (Wright, 1986, personal communication). While tumour drug levels were not measured, prior work has demonstrated at least 60–100% of the serum level within the tumour (White et al, 1980; Newman et al, 1986b). Because the local serum concentration is higher in the intra-arterial infusion, the tumour levels should be higher than when it was given intravenously. This difference in tumour uptake is demonstrated empirically by the difference in tumour reactivity to the administered radiation since no other factors are different between the two groups.

This is a pilot study and has shown a very fruitful area for further research. Variation in drug and radiation doses are planned, as well as investigation into the pharmacokinetics and quantification of the tumour uptake of the sensitizer.

Acknowledgments

This research was supported by a Basic Science Research Grant from the National Institutes of Health grant 2-S07-RR-05359-24. The authors are indebted to Carolyn McCray and Myrna Anderson for their assistance with manuscript preparation.

References

BROWN, J. M. & YU, N. Y., 1980. The optimum time for irradiation relative to tumour concentration of hypoxic cell sensitizers. *British Journal of Radiology*, *53*, 915–916.

BROWN, J. M., YU, N. Y., BROWN, D. M. & LEE, W. W., 1981. SR-2508: a 2-nitroimidazole amide which should be superior to misonidazole as a radiosensitizer for clinical use. *International Journal of Radiation Oncology, Biology, Physics*, *7*, 695–703.

COLDWELL, D., WRIGHT, K., WALLACE, S. et al, 1984. The comparative efficacy of intra-arterial administration of misonidazole in the treatment of rabbit V2 carcinoma. Presented at the RSNA meeting, November 1984.

COLEMAN, C. N., URTASUN, R. C., WASSERMAN, T. H., HANCOCK, S., HARRIS, J. W., HALSEY, J. & HIRST, V. K., 1984. Initial report of the phase I trial of the hypoxic cell radiosensitizer SR-2508. *International Journal of Radiation Oncology, Biology, Physics*, *10*, 1749–1753.

FOWLER, J. F., HILL, S. A. & SHELDON, P. W., 1980. Comparison of tumour cure (local control) with regrowth delay in mice. *British Journal of Cancer*, *41*, Suppl. IV, 102.

MILAS, L., ITO, H. & HUNTER, N., 1983. Effect of tumor size on S-2-(3-amino-propylamine) ethylphosphorothioic acid and misonidazole alteration of tumour response to cyclophosphamide. *Cancer Research*, *43*, 3050–3056.

MUCKLE, D. S. & DICKSON, J. A., 1973. Hyperthermia (42°) as an adjuvant to radiotherapy in the treatment of allogenic V2 carcinoma in the rabbit. *British Journal of Cancer*, *27*, 307–315.

NEWMAN, H. F. V., BLEEHEN, N. M. & WORKMAN, P., 1986a. A phase I study of the combined hypoxic cell radiosensitizers Ro 03-8799 and SR 2508: a preliminary report of single-dose toxicity, pharmacokinetics and tumour concentrations. *British Journal of Radiology*, *59*, 423–425.

—— 1986b. A phase I study of two hypoxic cell radiosensitizers Ro 03-8799 and SR-2508: toxicity and pharmacokinetics. *International Journal of Radiation Oncology, Biology, Physics*, *12*, 1113–1116.

WHITE, R. A. S., WORKMAN, P. & BROWN, J. M., 1980. The pharmacokinetics and tumour and neural tissue penetrating properties of SR-2508 and SR-2555 in the dog — hydrophilic radiosensitizers potentially less toxic than misonidazole. *Radiation Research*, *84*, 542–561.

1989, *The British Journal of Radiology*, *62*, 237–240

A comparison of two different T-grain films in rare-earth screens with a standard film–screen combination for intravenous pyelography and bone examinations

By Hugh Logan, Lesley Daly and James Masterson

Department of Radiology, St Vincents Hospital, Elm Park, Dublin 4, Ireland

(*Received July 1988*)

Abstract. T-grain film is claimed to give significantly improved image quality, allowing the use of faster screens without loss of quality and thus reducing radiation dose. We tested this claim for two systems. In each case comparison was made with our usual screen–film combination, Agfa Curix RP1 film with Kodak Xomatic Regular screens (a nominally 200 speed system). The systems tested were Kodak TMatG in Kodak Lanex Medium screens (300 speed) and Agfa STG in Kodak Lanex Regular screens (400 speed). The Agfa STG–Lanex Regular system performed less well than the standard system for intravenous pyelograms (IVPs), bones and soft-tissue detail. Its speed advantage was not apparent below 70 kV. The Kodak TMatG–Lanex Medium system was better than the standard system for IVPs but not as good for bones. It gave virtually no speed advantage below 90 kV. Kodak T-grain film in a medium-speed, rare-earth screen was found to be better than the standard system for IVPs. Agfa T-grain film in a fast rare-earth screeen was unsatisfactory for IVPs. Neither combination was as good as the standard system for bones.

The search for ways of reducing X-ray exposure to patients in diagnostic radiology continues. There have been many reports of the use of rare-earth screens especially for intravenous pyelography (Stables et al, 1977; Segal et al, 1982; Picus et al, 1984). However, in practice their use is not widespread, as there is felt to be an unavoidable loss of quality in return for the reduced X-ray dose. Recently, research into silver grain technology has led to the introduction of T-grain film, which is claimed to give an improvement in quality over standard film. The manufacturers claim that its use with fast screens should allow a substantial reduction in exposure without loss of quality, because of reduced cross-over.

A major cause of unsharpness in film–screen systems is "cross-over", which is the exposure of the emulsion on one side of the film by light from the intensifying screen on the other side. The novel feature of T-grain film is that the silver grains are flat rather than round and orientated at right angles to the incident light. This is combined with new developments in dye technology and is claimed to reduce cross-over significantly.

We investigated the systems by comparing their performance with our existing film–screen combination, Agfa Curix RP1 film in Kodak Xomatic Regular screens, a nominally 200 speed system. We used each of the two films according to their manufacturers recommendations. In the case of the Kodak film this was Kodak TMatG film in Kodak Lanex Medium screens, a nominally 300 speed system. The Agfa film, STG, was used with Kodak Lanex Regular screens, a nominally 400 speed system.

Patients and methods

Two types of examination were used for the study: (a) excretion urography and (b) plain skeletal radiography of larger body parts.

For excretion urography, 50 consecutive patients had one radiograph of their examination duplicated, the order of study radiograph/standard radiograph being randomized. In all cases both exposures were made within 1 min of each other. In total, 10 control radiographs, 10 immediate post-injection radiographs, 10 after 5 min, 10 after 10 min, and 10 after 15 min full-length radiographs were repeated.

For the bone studies, large and medium-sized bones were selected, 10 each of pelvis, lateral lumbar spine, lateral cervical spine, antero-posterior knees or shoulder, and lateral skull.

The exposures were adjusted by changing the mAs to achieve similar film densities, keeping the kVp constant to preserve soft-tissue contrast. This gave satisfactory exposure matching in the majority of cases. Whenever an exposure mismatch was considered significant, that film pair was excluded. The two radiographs, T-grain and standard film, were kept as a pair. They were attached to a questionnaire and submitted to one of the two assessing radiologists. Assessments were made twice by one radiologist and once by the other. At least 1 month, and usually several months, separated the two assessments by Reader 1. No attempt was made to "blind" the assessments, as the two films are recognizable by their different coloured base material.

Intravenous pyelograms were assessed for clarity of renal outline and collecting systems. Soft-tissue detail was assessed overall and on the clarity of the psoas shadow. Bone margins and bone trabeculae were compared for sharpness.

Address for correspondence: Dr J. Masterson, X-ray Department, St Vincents Hospital, Elm Park, Dublin 4, Ireland.

Finally, the relative speeds of the two systems were compared with the standard system over a range of kV. This was done because we were impressed by how little exposure reduction was possible at low kV using the rare-earth screens. This was done with step-wedges.

Processing of all films was done in Kodak chemicals at 34°C in a Kodak RP XOMat processor whose performance is monitored daily. Agfa Curix RP1 is our departmental general purpose film and is normally processed in this machine. To assess the effect of different processing conditions, especially on the Agfa films, step-wedge exposures were made using the cassettes side-by-side and the step-wedge recorded on both simultaneously with the same exposure. Test exposures were also made using a line-pair phantom and a gallbladder phantom. One of each pair was developed in Agfa chemicals at 32°C.

The Agfa processing reduced the film–screen speed by approximately 30% for the Agfa T-grain and 10% for the RP1, both measured at a middle-density step, but made no measurable difference to contrast, base fog levels, line-pair resolution, or contrast resolution on the gallbladder phantom.

One interesting observation on the line-pair measurements is that the fastest system, Agfa STG–Lanex Regular, resolved 3.5 line-pairs per millimetre, compared with 2.9 for Agfa RP1–XOMatic Regular, though this may not reflect their relative performances at normal operating kVp levels.

The numbers in the Kodak study were less than originally planned because of difficulties with the supply of test film. Thirty IVPs and 35 bone examinations were done rather than the planned 50 of each. Bone assessments were done on the IVPs as well as the pure bone examinations, making 65 bone examinations in all.

Statistical analysis was performed using the Sign test.

Results

The results quoted in Tables I and II are the first readings by Radiologist 1. The other two readings were used for assessing his consistency and interobserver consistency.

The Agfa STG–Lanex Regular system (Table I) was found inferior in all aspects. The difference in all parameters reached significance.

Table I. Renal and bone assessment of the Agfa T-grain film

	Better shown on (no. of patients):		*p*
	Agfa STG–Lanex Regular (T-grain)	Agfa RP1–XOMatic Regular (standard)	
Renal outline	16	34	0.02
Collecting systems	9	21	NS
Soft tissues	21	66	0.01
Psoas shadow	11	36	0.01
Bone margins	12	87	0.001
Bone trabeculae	12	87	0.001

NS = non-significant.

Table II. Renal and bone assessment of the Kodak T-grain film

	Better shown on (no. of patients):		*p*
	Kodak TMatG–Lanex Medium (T-grain)	Agfa RP1–XOMatic Regular (standard)	
Renal outline	22	7	0.02
Collecting systems	12	9	NS
Soft tissues	32	10	0.01
Psoas shadow	23	6	0.01
Bone margins	27	37	NS
Bone trabeculae	23	41	NS

NS = non-significant.

The Kodak TMatG–Lanex Medium (Table II) was superior to the standard system in a significant number of cases for renal outline clarity, overall soft-tissue detail and clarity of the psoas shadow. Renal collecting systems were also better shown on a majority, although the difference was not significant. The bones were visualized better on a majority of the radiographs using standard films, though the difference did not reach significance.

Reader 1 (J.M.) was highly consistent in his assessment of the radiographs. Reader 2 (H.L.) scored the T-grain radiographs as better, but with the exception of overall soft-tissue detail on the Agfa T-grain radiograph, in no case were his conclusions different from Reader 1, although the margins of difference were smaller.

These results are all of the comparison of each of the T-grain films with the standard system. The two T-grain-based systems were not compared with each other directly.

Discussion

The factors that limit the applicability of fast screen–film combinations to general radiography are loss of resolving power and increasing mottle with the higher speeds (Doi et al, 1982). Intensifying screens become less sharp as their speed is increased because the increase is achieved mainly by increasing the thickness of the crystal layer and the crystal size. Rare-earth screens are faster than conventional screens in their ideal operating range because the gadolinium and lanthanum oxybromides trap a higher proportion of incident X rays than conventional screen materials and also emit more light. Lateral diffusion of light in the screens and cross-over of light from one screen to the opposite emulsion layer are the major causes of unsharpness. The manufacturers add dyes to the screens, the emulsions and the film base to reduce cross-over, but the density of the final image may be 30% because of cross-over exposure (Ovitt et al, 1975). Green-light-emitting rare-earth screens and their green-sensitive films have suffered more from cross-over than conventional systems, with typical cross-over levels of 30%, compared with 20% for the best conventional

Table III. Ratio of speed assessments at different kVp for film–screen combinations

kVp	Agfa STG (T-grain)–Kodak Lanex Regular	Kodak TMatG (T-grain)–Kodak Lanex Medium	Agfa Curix RP1 (standard)–Kodak XOMatic Regular
50	—	1.25	1
55	1.25	—	1
60	—	1.15	1
66	1.6	—	1
70	—	1.25	1
77	2.0	—	1
80	—	1.25	1
85	2.6	—	1
90	—	1.25–1.5	1

blue-light systems. It is now claimed that with the use of T-grain film, cross-over in the rare-earth systems has been reduced to 20% (Castel, Y., 1987, personal communication). This is claimed to reduce the unsharpness problems of these faster systems.

The response of film–screen combinations to radiation of different energies is complex and depends on the filtration of the beam, the peak energy of the beam and the position of K-absorption edges of the compounds in the screen (Venema, 1979). Calcium tungstate screens have a nearly flat response over the range 50–120 kVp. Barium strontium sulphate screens increase in speed as kV rises from 50 to 80 kVp and then fall off slightly. Below 65 kVp they can be slower than tungstate screens (Reynolds et al, 1976). Rare-earth screens increase speed rapidly with increasing kV from 50 to 120 kVp. Below 60 kVp they may have no speed advantage over tungstate or barium strontium sulphate (Reynolds et al, 1976).

We compared two new films in rare-earth screens with Agfa Curix RPI in Kodak Xomatic Regular, a barium strontium sulphate screen that has been shown to have excellent resolving power (Ovitt et al, 1975). The Xomatic Regular is a medium-speed screen (nominal speed 200) with a peak efficiency around 70–80 kVp.

The resolving power of the Agfa test system was found to be disappointing. Its performance on bone detail especially was significantly inferior to the standard system. There was no appreciable mottle. The film had a "broad-latitude" look, but on detailed examination its soft-tissue detail was also inferior.

The Kodak T-grain film was used with Lanex Medium screens and performed better than the Agfa STG–Lanex Regular combination. It was better than the standard system for IVP work, and especially for soft tissues, but a little worse for bones, although the difference in bone detail did not reach statistical significance.

The speed of the rare-earth systems is of interest. Table III shows their speeds relative to the standard system at a range of kVs. For this comparison, the speed of the standard system is taken as 1. It is seen that in the 55–66 kVp range the Agfa STG–Lanex Regular combination had minimal speed advantage over the standard system. It is in this range that most of our IVP work and a substantial part of our skeletal work is done. It achieved a 2:1 speed advantage at 77 kVp, which means that its speed advantage is substantial in the range where barium work, angiography and chest radiography are performed. However, for the bulk of general radiography it has little speed advantage over a system based on barium strontium sulphate screens, and this combined with its rather poor detail performance means that the fastest system proved unsatisfactory from every point of view.

The Kodak TMatG–Lanex Medium combination also failed to deliver a significant speed advantage over the standard system. It did, however, perform better on IVP work and in particular on soft-tissue detail. It was not quite as good on bone detail. Although the difference here did not reach statistical significance, the standard system was preferred by both readers in a majority of cases.

We have limited scope to comment on the possible influence of varying kilovoltage or processing conditions on our conclusions. Kilovoltage is chosen to suit the examination rather than the imaging system. In intravenous pyelography a low kilovoltage is used to maximize soft-tissue detail and to suit the special absorption characteristics of the iodine-containing contrast media. If an imaging system is to be useful in IVP work it must work at low kVp. The Lanex Medium screen clearly does work well at low kVp, although it brings no real speed advantage in this range. The Lanex Regular-based system does not work well in the kVp range we used, and we are unable to comment on how it would perform in its ideal operating range above 80 kVp.

In processing there are more potential variables than a clinical study like this can address. Both manufacturers were satisfied with the processing conditions in use in the department. Test films developed in Agfa chemicals showed a slight speed change but no detectable change in image quality.

In conclusion, our tests were on two film–screen combinations, and not on the film in isolation. We cannot recommend the Agfa STG–Lanex Regular combination. Its performance was poor and there was little speed advantage at lower kVs. The Kodak T-grain film in Lanex Medium screens can be recommended for IVP work. However, we do not yet feel justified in recommending this combination for general purpose use because of our reservations about its performance in bone work.

Acknowledgments

We wish to thank Ms Kate Mathews, radiographer, for her invaluable help and Ms Ismay O'Gorman for her help in preparing the manuscript.

References

DOI, K., HOLJE, G., LOO, L. N. & CHAN, H. P., 1982. *MFTs and Weiner Spectra of Radiographic Screen–Film Systems*, HHS Publication FDA 82–8187 (US Department of Health and Human Services, Washington DC).

OVITT, T., MOORE, R. & AMPLATZ, K., 1975. The evaluation of high-speed screen–film combinations in angiography. *Radiology*, *114*, 449–452.

PICUS, D., MCALISTER, W., SMITH, E., ROCKWALD, S., JOST, R. & EVANS, R., 1984. Plain radiography with a rare-earth screen: comparison with a calcium tungstate screen. *American Journal of Roentgenology*, *143*, 1335–1338.

REYNOLDS, J., SKUCAS, J. & GORSKI, J., 1976. An evaluation of screen–film speed characteristics. *Radiology*, *118*, 711–713.

SEGAL, A., MAILLIE, H. & LAMKIN, J., 1982. Uroradiographic dosimetry using a rare-earth screen–film system. *American Journal of Roentgenology*, *139*, 923–926.

STABLES, D., ROSSI, R., CARUTHERS, S., JR & ANDERSON, N., 1977. The application of fast screen–film systems to excretory urography. *American Journal of Roentgenology*, *128*, 617–619.

VENEMA, H. W., 1979. X-ray absorption, speed and luminescent efficiency of rare-earth and other intensifying screens. *Radiology*, *130*, 765–771.

1989, *The British Journal of Radiology*, *62*, 241–244

Radiobiological assessment of permanent implants using tumour repopulation factors in the linear-quadratic model

By R. G. Dale, PhD, FInstP

Department of Radiation Physics, Charing Cross Hospital, London W6 8RF

(Received August 1988 and in revised form October 1988)

Abstract. By combining existing linear-quadratic equations relating to decaying-source therapy with an assumed tumour repopulation factor, it has been possible to devise a method for the radiobiological assessment of permanent implants. For calculation purposes there is a time after which an implant can no longer be considered effective in sterilizing tumour cells. This "effective" treatment time for a permanent implant can be approximately defined in terms of the radionuclide decay constant, the potential doubling time, the initial dose-rate and the value of α in the tumour α/β ratio. The analytical technique has been applied to a specific intercomparison of commonly encountered implants using ^{125}I and ^{198}Au, and suggests that, even in the most favourable cases, the former radionuclide offers few radiobiological advantages. Although not specifically discussed here, the method can also be applied to the assessment of various forms of biologically targeted radiotherapy.

Radiotherapy treatment with permanently implanted decaying sources has been performed for many years, especially with nuclides such as ^{198}Au and ^{222}Rn. More recent interest in the technique has been generated by the advent of implantable sources with much longer half-lives, particularly ^{125}I. A number of authors have drawn attention to the apparently good local control which is achievable by treating with ^{125}I, but it remains a fact that the radiobiology of such treatments is very poorly understood, and indeed has been questioned (Giles & Brady, 1986).

A method for assessing falling dose-rate treatments in terms of the linear-quadratic (LQ) formalism has been presented in an earlier article (Dale, 1985). That analysis showed that therapeutic benefit is generally to be expected by protracting treatment, since the effect of low dose-rate is similar to the effect of small dose/fraction in fractionated therapy, *i.e.* there is greater opportunity for the late-reacting tissues (those with low α/β ratios) to repair during the course of the whole treatment. In principle therefore, ultra-low dose-rate can be expected to give the best therapeutic ratio, but this generalization will only hold if tumour repopulation is small during the course of the treatment. For nuclides such as ^{125}I (half-life 60 days) the period over which the whole dose is given is of the order of several months, during which time even tumours which are slowly dividing can be expected to exhibit considerable growth.

It therefore follows that an adequate radiobiological description of the effects of treatment with such sources must take account of concurrent tumour repopulation. The aim of this paper is to demonstrate how this might be accomplished within the formalism of the LQ method, and to discuss the implications of the findings.

Method

A possible way of incorporating a time factor in the fractionated LQ model has been discussed in general terms by a number of authors (Thames et al, 1983; Travis & Tucker, 1987; Wheldon & Amin, 1988). This approach has recently been examined in rather more detail (Dale, 1988) and applied to low-dose-rate continuous therapy as well as the various forms of fractionated therapy. Although the case of falling dose-rate was not specifically examined, it was shown that, for any type of treatment, the tumour extrapolated response dose (ERD), as defined by Barendsen (1982) in terms of the relative effectiveness per unit dose (RE), could be calculated from the relationship

$$\text{ERD} = \text{total dose} \times \text{relative effectiveness} - \text{repopulation factor}$$

i.e.

$$\text{ERD} = \text{TD} \times \text{RE} - \text{RF} \qquad (1)$$

Since ERD is related to the logarithm of the surviving fraction of cells, the tumour ERD should be as high as is allowable without exceeding the late-tissue tolerance.

The expression to use for the RE is dependent on the type of therapy involved. The repopulation factor, which in this context is expressed in the form of the dose which is "wasted" in combatting concurrent repopulation, may be calculated on the basis that exponential growth of the tumour takes place during the treatment, and may be obtained from: repopulation factor (in Gy) = KT, where

$$K = 0.693/(\alpha\Phi) \qquad (2)$$

α is the numerator (in Gy^{-1}) of the α/β ratio, Φ is the clonogenic cell doubling time (days) and T is the overall time of the treatment (days). Note that the relationship between K, α and Φ takes the form of Equation 2 because of the particular definition of ERD used in the LQ formalism (Dale, 1988); no mechanistic relationship between these variables is implied.

Since cell loss factors (Steel, 1977) may not be known with any certainty, it is not unrealistic to use potential doubling times for Φ. Potential doubling times can be very short (Denekamp, 1988; Wilson et al, 1988), and figures of less than 5 days are not uncommon. Similarly, Marchese et al (1987) and Steel et al (1987) have reviewed α values for tumours and found them to cover a wide spread of values, although a value of 0.25 Gy^{-1} is a reasonably representative value for some applications. Because of the uncertainties in both α and Φ it is clear that K itself can take a wide range of values. However, by taking various combinations of α and Φ and calculating K, it is apparent that a K value of around 2 Gy day^{-1} corresponds to a particularly fast growing and/or insensitive tumour, whilst K values of around 0.2 or less correspond to more sensitive and/or slow growing tumours.

The first question to be addressed when considering a permanent implant is: what is the effective treatment time? We can approach this by calculating the dose-rate below which the treatment ceases to sterilize tumour cells. Since the LQ tumour regrowth rate is given by K Gy day^{-1} (Equation 2), the treatment effectively ends when the rate of change of the product (TD × RE) is equal to K. The full mathematical expression for this factor is extremely complex, but for the purpose of the following we may assume that its value at any time is approximately equal to the instantaneous dose-rate.

For an exponentially decaying implant the dose-rate (R_t) at time t is given in terms of the initial dose-rate R_0 by

$$R_t = R_0 \exp(-\lambda t) \qquad (3)$$

where λ is the radioactive decay constant of the particular nuclide used. By combining Equations 2 and 3 we can calculate the effective treatment time (t_{eff}) as being the time at which R_t falls to K, *i.e.*

$$t_{\text{eff}} = -[\ln(K/R_0)]/\lambda \qquad (4)$$

If there are any cells left unsterilized at time t_{eff} then it must be assumed that the treatment has failed. Thus the efficacy of the treatment should be judged by calculating the tumour ERD given in time t_{eff}, irrespective of how much more dose is delivered by the implant after this time. Also, since repopulation is occuring during the effective treatment time, the repopulation correction to subtract is given by Kt_{eff}.

The total dose (TD) delivered in time t_{eff} is given by:

$$\text{TD} = (R_0/\lambda)\,[1-\exp(\lambda t_{\text{eff}})] \qquad (5)$$

and the RE is given by an equation derived by Dale (1985), *viz.*

$$\text{RE} = 1+[2R_0\lambda/(\mu-\lambda)(\alpha/\beta)] \times A \times (B-C) \qquad (6)$$

where

$$A = 1/[1-\exp(-\lambda t_{\text{eff}})]$$
$$B = [1-\exp(-2\lambda t_{\text{eff}})]/2\lambda$$
$$C = \{1-\exp[-t_{\text{eff}}(\mu+\lambda)]\}/(\mu+\lambda)$$

In the above equations μ is the tumour damage recovery constant, related to the recovery half-life ($T_{1/2}$) by $\mu = 0.693/T_{1/2}$.

Table I. Calculated values of t_{eff} and tumour ERD for varying repopulation factors (expressed as Gy day^{-1})

K (Gy day^{-1})	t_{eff} (days)		ERD (Gy)	
	^{125}I	^{198}Au	^{125}I	^{198}Au
0	∞	∞	162.7 (100%)	81.1 (100%)
0.05	312	22.9	142.7 (87.7%)	79.8 (98.4%)
0.1	253	20.2	128.8 (79.2%)	78.7 (97.0%)
0.25	173	16.7	97.7 (60.0%)	76.0 (93.7%)
0.5	113	14.0	62.6 (38.4%)	72.2 (89.0%)
1	53.2	11.3	22.1 (13.6%)	65.9 (81.3%)
1.5	18.1	9.7	3.9 (2.4%)	60.7 (74.8%)
3	—	7.0	—	48.2 (59.4%)

For ^{125}I the assumed target dose is 160 Gy, corresponding to an initial dose rate of 1.848 Gy day^{-1}. For ^{198}Au the assumed target dose is 70 Gy, corresponding to an initial dose rate of 17.97 Gy day^{-1}. The figures in parentheses are the ERDs expressed as percentages of those which would be obtained if there were zero tumour repopulation.

Assuming respective α/β and $T_{1/2}$ values of 10 Gy and 1.5 h for tumour, and a range of K values between 0 and 3 Gy day^{-1}, values of ERD have been calculated (via Equation 1) for two practical cases:

(a) An ^{125}I implant designed to give a total dose of 160 Gy.
(b) An ^{198}Au treatment designed to give a total dose of 70 Gy.

Table I shows the calculated values of t_{eff} and ERD. It is clear that ^{198}Au delivers a higher ERD than ^{125}I for all tumours with a K value greater than about 0.4 Gy day^{-1}. It is also clear that, even where ^{125}I delivers the higher ERD, a greater fraction of the dose is wasted than is ever the case with ^{198}Au. After t_{eff} is passed, the residual activity in the implant continues to irradiate tissues both within and outside the treatment volume, and normal tissues are thus being irradiated unnecessarily. This is particularly the case with ^{125}I, even for the more sensitive, slowly growing tumours. Furthermore, in these examples, it has been assumed that there is no time delay before the onset of clonogenic tumour proliferation. If relatively short delays do occur after the initiation of treatment then they will tend to push the balance even more in favour of ^{198}Au, since a smaller number of tumour cells would need to be sterilized within the effective treatment time of the nuclide.

It is possible that a lower $T_{1/2}$ might be more appropriate for tumours (Dale, 1987; Steel, 1987), and Table I has therefore been re-assessed with $T_{1/2} = 0.5$ h. The ERD values for ^{125}I are almost unaltered, whilst those for ^{198}Au are around 9–14% lower. The general conclusions relating to these particular treatments are therefore not substantially dependent on the selected value of $T_{1/2}$.

Discussion

The increasingly widespread use of permanent implants of ^{125}I poses an interesting radiobiological challenge since more physical and biological factors have to be included in an assessment of the technique than is the case in most other clinical treatments. By combining existing LQ equations for analysing falling-dose-rate treatments with a mathematical description of the dose equivalent of repopulation during treatment, it has been possible to assess the particular areas where ^{125}I might be expected to show a clear clinical advantage.

In the light of the above analysis it does appear that the general clinical practice of delivering high doses with this nuclide (typically 140–200 Gy) goes some way towards offsetting what might otherwise be considered disadvantageous properties of the nuclide. In radiobiological terms the long protraction associated with an ^{125}I implant does not appear to offer many advantages over shorter-lived nuclides, and the proportion of the dose given which is wasted on the tumour, but which nevertheless continues to irradiate closely adjacent normal tissues, will often be substantial. However, there will be a sharper fall-off in dose at greater distances from an ^{125}I implant, which might be of some advantage if supplementary external irradiation is to be given.

Since ^{125}I gained much of its initial clinical popularity in prostatic implants (Hilaris et al, 1977), special consideration should be given to that case. Trott and Kummermehr (1985) have reported a potential doubling time for prostatic tumours of 30 days. Assuming an α value of between 0.1 and 0.25 Gy^{-1} we have a "working" K value of around 0.2 Gy day^{-1}. From Table I this corresponds to an ^{125}I tumour ERD of approximately 100 Gy. Assuming for the moment that there is no significant repopulation of late-reacting tissues over the course of the entire treatment (*i.e.* that t_{eff} is very large for such tissues) and that they receive the full 160 Gy, we can calculate the late ERD (with $\alpha/\beta = 3$ Gy) from

$$\text{ERD}_{\text{late}} = 160 \times [1 + R_0/(\mu+\lambda)\ (\alpha/\beta)]$$

where the expression in brackets is the RE after complete decay of the sources (Dale, 1985) and is obtainable from Equation 6 by letting t_{eff} go to infinity. Substituting the above values we have $\text{ERD}_{\text{late}} = 169$ Gy.

It is easy to calculate that, for $K = 0.2$ Gy day^{-1}, a tumour ERD of around 100 Gy is achievable with ^{198}Au with only a modest increase in total dose, *i.e.* from 70 to 87 Gy. [The ERD increases more than might be expected from the *pro rata* increase in dose on account of the increase in RE associated with the higher initial dose-rate (Equation 6).] The late-reacting ERD with the gold implant can then be calculated and is 145 Gy, *i.e.* still less than the 169 Gy associated with the ^{125}I implant. It therefore appears that 87 Gy delivered with an ^{198}Au implant is capable of achieving similar effects on prostate tumours as 160 Gy from ^{125}I, and yet with the probability of less damage to nearby late-reacting tissues. The case for ^{125}I is thus by no means clear-cut, even for a relatively slowly dividing tumour where the nuclide might be expected to show a clear advantage. [It is interesting to note that ^{131}Cs (Henschke & Lawrence, 1965), which emits photons of similar energy to ^{125}I, appears to be radiobiologically superior to the latter on account of its shorter half-life of 9.7 days. The advantages of using a soft X-ray emitter are therefore retained with ^{131}Cs without incurring such large radiation wastage problems caused by tumour repopulation (Dale, 1985).]

Obviously much of the numerical basis of the argument presented in this paper must remain speculative at present, even though the general observations relating to long-term irradiation might seem reasonable. In addition to the uncertainties associated with individual patient parameters and the way in which they change with the degree of hypoxia (Cohen & Creditor, 1983), there remains the possibility that the LQ formalism itself is an inadequate description of the processes involved. Moreover, there is always a real difficulty in defining the dose in interstitial implants, since dose gradients are very large and are not easily allowed for within analytical models. The availability of more experimental data will enable some of these questions to be answered and, in addition to shedding more light on the efficacy of ^{125}I implantation, will assist in determining whether the method described here has broader validity in examining the analytically similar problem of targeted antibody therapy.

References

Barendsen, G. W., 1982. Dose fractionation, dose rate and iso-effect relationships for normal tissue response. *International Journal of Radiation Oncology, Biology, Physics, 8,* 1981–1997.

Cohen, L. & Creditor, M., 1983. Iso-effect tables for therapeutic ratios for epidermoid cancer and normal tissue stroma. *International Journal of Radiation Oncology, Biology, Physics, 9,* 1065–1071.

Dale, R. G., 1985. The application of the linear-quadratic dose-effect equation to fractionated and protracted radiotherapy. *British Journal of Radiology, 58,* 515–528.

—— 1987. Radiobiology of changes in dose-rate. In *High-dose-rate Afterloading in the Treatment of Cancer of the Uterus, Breast and Rectum,* ed. by H. Vahrson & G. Rauthe (Urban and Schwarzenberg), pp. 24–29.

—— 1988. Time-dependent tumour repopulation factors in linear-quadratic equations—implications for treatment strategies. *Radiotherapy and Oncology,* in press.

Denekamp, J., 1988. Normal tissue response to radiation. In *Radiobiology in Radiotherapy,* ed. by N. Bleehan (Springer-Verlag, Berlin), pp. 17–29.

Giles, G. M. & Brady, L. W., 1986. ^{125}Iodine implantation after lymphadenectomy in early carcinoma of the prostate. *International Journal of Radiation Oncology, Biology, Physics, 12,* 2117–2125.

Henschke, U. K. & Lawrence, D. C., 1965. Caesium-131 seeds for permanent implants. *Radiology, 85,* 1117–1119.

Hilaris, B. S., Whitmore, W. F., Batata, M. A. & Barzell, W., 1977. Behavioural patterns of prostate adenocarcinoma following an ^{125}I implant and pelvic node dissection. *International Journal of Radiation Oncology, Biology, Physics, 2,* 631–635.

Marchese, M. J., Zaider, M. & Hall, E. J., 1987. Dose-rate effects in normal and malignant cells of human origin. *British Journal of Radiology, 60,* 573–576.

van Rongen, E. & Kal, H. B., 1987. Combined interstitial and external X-irradiation on a rat rhabdomyosarcoma. *Radiotherapy and Oncology, 9,* 319–327.

Steel, G. G., 1977. *Growth Kinetics of Tumours* (Cavendish Press, Oxford).

THAMES, H. D., PETERS, L. J., WITHERS, H. R. & FLETCHER, G. H., 1983. Accelerated fractionation vs hyperfractionation: Rationales for several treatments per day. *International Journal of Radiation Oncology, Biology, Physics, 9,* 127–138.

TRAVIS, E. L. & TUCKER, S. L., 1987. Isoeffect models and fractionated radiation therapy. *International Journal of Radiation Oncology, Biology, Physics, 13,* 283–287.

TROTT, K. R. & KUMMERMEHR, 1985. What is known about tumour proliferation rates to choose between accelerated fractionation and hyperfractionation. *Radiotherapy and Oncology, 3,* 1–9.

WHELDON, T. E. & AMIN, A. E., 1988. The linear-quadratic model (letter). *British Journal of Radiology, 61,* 700–702.

WILSON, G. D., MCNALLY, N. J., DISCHE, S. & BENNETT, M. H., 1988. Cell proliferation in human tumours measured by *in vivo* labelling with bromodeoxyuridine. *British Journal of Radiology, 61,* 419–422.

1989, *The British Journal of Radiology*, 62, 245–247

Evaluation of response following irradiation of juvenile angiofibromas

By Anne C. R. Robinson, MRCPI, FRCR, G. G. Khoury, MRCP, FRCR, *D. V. Ash, MRCP, FRCR and †B. D. Daly, MRCPI, FRCR, FFR(RCSI)

University Department of Radiotherapy and *Regional Radiotherapy Centre, Cookridge Hospital, Leeds LS16 6QB and †Department of Radiology, The General Infirmary at Leeds, Leeds LS1 3EX

(*Received July 1988*)

Abstract. Ten cases of angiofibroma treated by irradiation are reported. Relief of symptoms occurred by the end of treatment in eight patients. Objective regression was much slower, six having visible disease for greater than 6 months and four for at least 1 year. Only one was symptomatic. Radiological resolution lagged behind clinical improvement and was complete in only one of three asymptomatic patients evaluated by computed tomography (CT) at between 2 and 3 years after treatment. The significance of these residual masses seen on CT is unclear.

Angiofibromas are uncommon, accounting for between one in 5000 and one in 6000 ear, nose and throat admissions (Hora & Brown, 1962). They are highly vascular, locally invasive, non-encapsulated tumours, with a marked male predilection (Patterson & Durham, 1965). Their management is controversial. Observation with expectation of spontaneous resolution at puberty and hormone manipulation have been tried, but only anecdotal responses reported (Jafek et al, 1973). Surgery may be accompanied by significant bleeding and local recurrence rates vary from 25% to 50% (Biller et al, 1984). Irradiation has been successfully used in intra- and extracranial disease (Briant et al, 1978).

Patients and methods

This retrospective review includes all patients with angiofibroma treated at Cookridge Hospital between 1 January, 1975 and 30 June, 1987. The analysis was undertaken to assess the effectiveness of irradiation, the rate of tumour regression, both clinically and radiologically, and the morbidity of treatment.

Patients

Ten patients were referred to Cookridge Hospital. They were all male with a median age of 15 years (range 9–16 years). Epistaxis and nasal obstruction were the commonest presenting features (Table I). In seven patients there was a delay greater than 12 months between first symptoms and presentation to hospital. Three had had polypectomy prior to referral for irradiation, one a grommet insertion and one external carotid artery ligation. Nine patients had computed tomography (CT) scanning (seven pre-irradiation) and four had arteriography. Biopsy was obtained in six cases. In four patients, there was evidence of intracranial spread and three had orbital involvement. Nine patients had bone destruction and more than one bone was eroded in seven.

Table I. Symptoms

Symptom	No. of patients
Nasal obstruction	7
Epistaxis	6
Cheek swelling	3
Impaired hearing	2
Mouth breathing	1
Nasal discharge	1
Headache	1
Double vision	1

Treatment

Treatment using either a telecobalt source or megavoltage X rays (6 or 8 MV) was given using a beam direction shell. The volumes covered all tumour extensions with generous margins and uninvolved sensitive structures, *e.g.* eye and brain stem, were shielded. Check radiographs of the irradiation fields and measurements of eye doses were carried out. Doses used ranged from 30 Gy in 15 fractions over 21 days to 40 Gy in 20 fractions over 28 days. All patients were followed up regularly and seven had post-treatment CT scans.

Results

The treatment was well tolerated, a short break being necessary in only one patient. Relief of symptoms was usually achieved during the course of irradiation (eight cases). Symptomatic improvement did not occur until 3 and 6 months after treatment in the remaining two cases. Objective regression was delayed for up to 20 months in four patients and visible disease was present in six at 6 months, although only one was symptomatic (Table II). Regression of the tumour radiologically was much slower. Six patients had CT scans within the first 9 months of completing treatment and disease was present

---

Address for correspondence: Dr A. C. R. Robinson, Christie Hospital, Withington, Manchester M20 9BS.

Table II. Regression time

Clinical	No. of patients	
≤6 months	4	
>6 months, ≤12 months	2	
>12 months, ≤20 months	4	
Radiological (CT)	No. scanned	Persistent abnormality
≤6 months	3	3
>6 months, ≤12 months	3	3
>12 months, ≤24 months	4	4
>24 months, ≤36 months	3	2

in all. Only one was symptomatic. Four of these patients were rescanned between 1 and 2 years after irradiation. All, although asymptomatic, showed an abnormality. This was persistent in one patient at 28 months (Fig. 1) and in another at 34 months. A repeat scan was not performed in the remaining two cases. One patient had only one follow-up scan at 30 months, which was negative. Median follow-up was 46 months with a range of 8–141 months. The only treatment complication encountered was the development in one patient of unilateral cataract which required surgery; in another a posterior lens opacity was detected. Both had involvement of the orbit by tumour and no eye shielding was employed.

Discussion

The results reported in this series of patients confirm the effectiveness of irradiation in the treatment of angiofibromas. Careful planning of irradiation fields to include all sites of tumour extension with shielding of critical structures where possible is essential to achieve optimal control. The lowest radiation dose is unclear. Doyle et al (1977) used 15 Gy without effect. Sinha and Aziz (1978) described local control in six out of seven patients following 30–36 Gy in 15 fractions in 3 weeks and Cummings et al (1984) found 30–35 Gy in 14–16 fractions in 3 weeks to be effective. Our data also suggest that only moderate doses are required. Acute toxicity in our series was minimal. On follow-up, one patient has developed cataract requiring surgery. No second malignancies or endocrine complications have been noted but longer evaluation is needed. Experience with patients reviewed for up to 26 years has shown no significant impairment of growth or endocrine function (Cummings et al, 1984).

Despite rapid symptomatic relief, the majority of our patients had clinical evidence of disease for at least 6 months following treatment. Persistence of residual abnormality on CT for greater than 1 year occurred in all five cases evaluated at this time, but all remained asymptomatic. Cummings et al (1984) reported six patients with soft-tissue masses on CT at intervals of from 3 to 15 years after irradiation. Biopsy of one lesion showed fibrous tissue only and these authors recommended a watching policy for asymptomatic residual disease. We agree with this. Bryan et al (1981) have noted similar soft-tissue masses on CT in a group of five patients monitored for up to 5 years following irradiation. The findings of both of these studies and our own results indicate that the true significance of the residual tumour masses seen on CT following irradiation is as yet unclear.

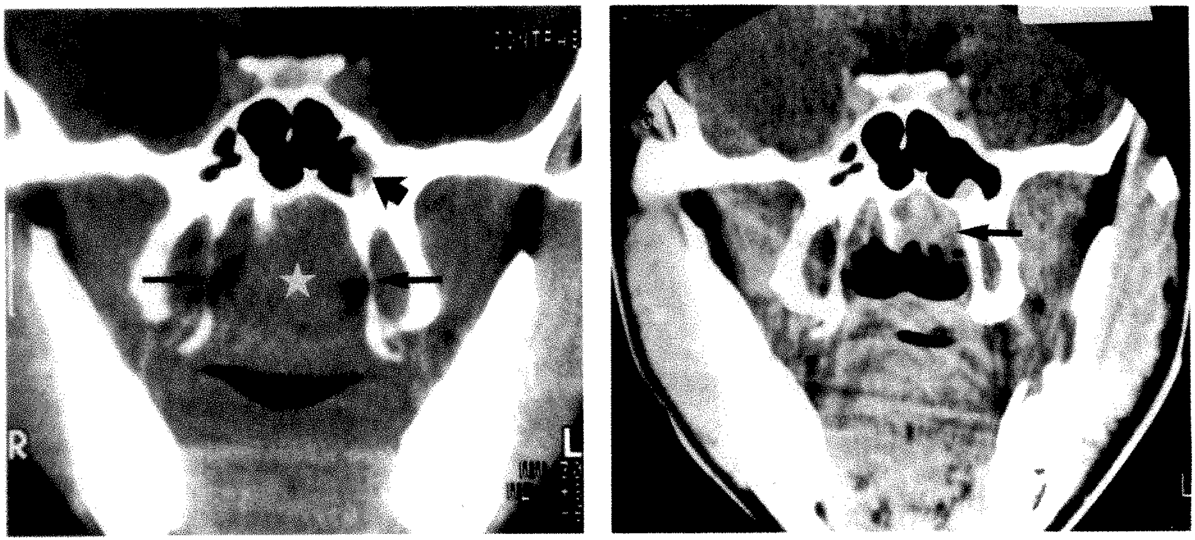

(a) (b)

Figure 1. (a) Post-contrast coronal computed tomogram prior to treatment. The nasopharynx is completely filled with tumour (star) with erosion of the medial pterygoid plate bilaterally (small arrows) and extension into the sphenoid sinus (large arrow). (b) Post-contrast coronal computed tomogram 1 year after irradiation. Considerable improvement has occurred although a tumour mass persists in the nasopharynx (arrow). The medial pterygoid plates now appear normal.

Conclusions

Treatment with irradiation is effective for both intra- and extracranial angiofibromas and is associated with minimal morbidity. It should be considered for initial management of these patients. Computed tomography is of value in defining disease extent but its role in the follow-up is unclear and is best reserved for those with persistent symptoms.

Acknowledgments

We are grateful to Dr S. Cartwright, Dr T. S. Worthy, Dr H. G. Frank and Mr Campbell Robson for permission to include their patients.

References

BILLER, H. R., SESSIONS, D. G. & OGURA, J. H., 1974. Angiofibroma: a treatment approach. *Laryngoscope*, *84*, 695–706.

BRIANT, T. D. R., FITZPATRICK, P. J. & BERMAN, J., 1978. Nasopharyngeal angiofibroma: a twenty year study. *Laryngoscope*, *88*, 1247–1251.

BRYAN, R. N., SESSIONS, R. B. & HOROWITZ, B. L., 1981. Radiographic management of juvenile angiofibromas. *American Journal of Neuroradiology*, *2*, 157–166.

CUMMINGS, B. J., BLEND, R., FITZPATRICK, P., CLARK, R., HARWOOD, A., KEANE, T., BEALE, F., GARRETT, P., PAYNE, D. & RIDER, W., 1984. Primary radiation therapy for juvenile nasopharyngeal angiofibroma. *Laryngoscope*, *94*, 1599–1605.

DOYLE, P. J., RIDING, K. & KAHN, K., 1977. Management of nasopharyngeal angiofibroma. *Journal of Otolaryngology*, *6*, 224–232.

HORA, J. F. & BROWN, A. L., 1962. Paranasal juvenile angiofibroma. *Archives of Otolaryngology*, *76*, 457.

JAFEK, B. W., NAHUM, A. M., BUTLER, R. M. & WARD, P. H., 1973. Surgical treatment of juvenile nasopharyngeal angiofibroma. *Laryngoscope*, *83*, 707–720.

PATTERSON, C. N. & DURHAM, N. C., 1965. Juvenile nasopharyngeal angiofibroma. *Archives of Otolaryngology*, *81*, 270–277.

SINHA, P. P. & AZIZ, H. I., 1978. Juvenile nasopharyngeal angiofibroma. *Radiology*, *127*, 501–505.

1989, *The British Journal of Radiology*, 62, 248–252

Contribution of computed tomography in the aetiology and prognosis of cerebral palsy in children

By E. Schouman-Claeys, MD, *A. Picard, MD, †G. Lalande, MD, †G. Kalifa, MD, *P. Lacert, MD, *E. Brentanos, MD and G. Frija, MD

Service de Radiologie and *Service de Rééducation Neurologique Infantile, Hôpital Raymond Poincaré, Garches, France and †Service de Radiologie, Hôpital Saint Vincent de Paul, Paris, France

(*Received July 1988 and in revised form October 1988*)

Abstract. Retrospective analysis of computed tomographic (CT) examinations in 76 children with cerebral palsy without any severe intellectual handicap has revealed abnormalities in 63% of these children; abnormalities were present in 88% of former pre-term infants. This study highlights the significant pathogenic role of periventricular leucomalacia in cerebral palsy, since in 45% of the cases of this series this diagnosis had been reached as a result of a characteristic CT appearance associated with a history of premature birth and very specific clinical deficits. The CT abnormalities, mostly posterior and generally bilateral and symmetrical, affect the contours of the lateral ventricles, which become straight and angular, and often involve ventriculomegaly (85%). Localized juxtaventricular hypodensities were only found in a few cases (6%). The cognitive and intellectual sequelae in these children were more severe than in those children whose CT examination was normal, and were also more pronounced when the longitudinal fissure of the cerebrum was enlarged.

This retrospective study was carried out to evaluate the abnormalities on computed tomography (CT) observed in cerebral palsy in children. The description and analysis of the underlying lesions have practical implications in that an improvement in prognosis can be expected through earlier rehabilitation adapted to the anatomical lesions. Computed tomographic investigations were carried out in children aged 7 months to 15 years with cerebral palsy but without severe mental retardation. The findings were correlated with possible prematurity, cognitive function and clinical deficits in an attempt to relate the CT appearances to the extent of psychomotor and intellectual impairment.

Material and methods

The study population of 76 children included 32 girls and 44 boys who were being followed in a Paediatric Department of Neurological Rehabilitation from the age of at least 2 years. Computed tomographic scans had been obtained for all patients between 1980 and 1985 when their ages ranged from 7 months to 15 years.

These children with cerebral palsy by definition presented non-progressive motor handicap subsequent to neurological injury occurring in the first year of life and, more particularly in this series, during the perinatal period. Only those children with no or moderate intellectual handicap were studied, since they were suitable for "interactive" rehabilitation. The criterion for inclusion was an IQ–DQ (intelligence quotient or development quotient) equal to or greater than 60. Three groups were defined with IQ–DQ values of 60–75, 76–90 and >90.

The motor handicap of these children was spastic in 73, mixed in two and athetotic in one. This handicap was classified according to the usual manner as follows: four limbs (tetraplegia), paresis of all four limbs but more severe in the legs (diplegia), lower limbs (paraplegia) and one half of the body (hemiplegia). The extent of the handicap was classified by Hansen's method: slight (A) moderate (B) and severe (C).

Forty-one of these children (53.9%) were born prematurely at between 28 and 36 weeks.

The children were evaluated by a standard neurological examination with a horizontal ocular motility test, speech tests and exploration of co-ordination and visual gnosia. Intellectual and cognitive functions were evaluated in infants up to 3 years of age according to the Brunet–Lezine scale, from 3 to 5 years with the Termann–Merill test and over 4½ years against the Wechsler scale.

The CT investigations were assessed by a team of four radiologists including two paediatric radiologists. Two successive analyses were made with random presentation of the cases, first without and then with knowledge of the clinical data. Interobserver variations were not taken into account, but in the event of significant differences, a consensus was reached after review.

The following basic abnormalities were sought.

1. Subtentorial level: parenchymatous abnormalities with direct signs of atrophy or hypodensity, enlargement of the cisternae, dilatation of the fourth ventricle.
2. Supratentorial level: abnormalities in the density of the white or grey matter, enlargement of the cortical sulci or the longitudinal fissure of the cerebrum or of the Sylvian fissures, abnormalities in the size or shape of the ventricles.

The size of the lateral ventricles was rated on a scale from 0 (normal) to 3 (extensive dilatation). The thickness of the periventricular white matter was not taken into

---

Reprint requests to Dr E. Schouman-Claeys, MD, Hôpital Raymond Poincare, F-92380 Garches, France.

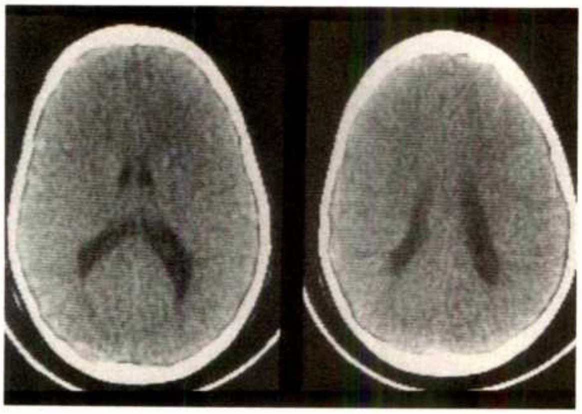

Figure 1. Characteristic abnormal pattern of the lateral ventricles resulting from periventricular leucomalacia in a 4-year-old child showing moderate enlargement of the ventricles in the posterior part of the ventricular body and in the atrium, which is stretched and angular.

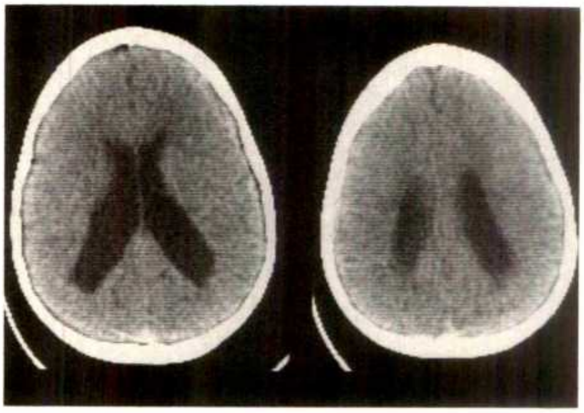

Figure 2. Characteristic abnormal pattern of the lateral ventricles resulting from periventricular leucomalacia in a 3-year-old child showing extensive dilatation of the lateral ventricles predominating in posterior regions and angular contours of the ventricular walls.

account since it was often quite difficult to assess it accurately.

Correlations between radiological findings and clinical data were statistically analysed using variance calculations or the χ^2 test and Scheffe's *S*-method for comparing paired means, with a first-order error of 5%.

Results

The CT investigations were normal (Group 1) in 28 cases (36.8%) and abnormal in 48 cases (63.2%). Almost all the abnormalities detected were located in the supratentorial area and could be divided into two groups: Group 2 (34 cases) were stereotype abnormalities and Group 3 (14 cases) included miscellaneous abnormalities.

Group 2 was noteworthy for abnormalities of the lateral ventricles with characteristic changes generally associated with ventriculomegaly (Figs 1, 2). The contours of the external walls of the ventricles had lost their normal curvilinear appearance to become straight and rectilinear. The abnormalities were more prevalent in the posterior part of the ventricular bodies and in the atria, which had a stretched, angular appearance.

Table I. Distribution and extent of ventricular dilatation for Group 2

Region	No. of ventricles dilated and extent		
	Slight	Moderate	Severe
Frontal	12	2	—
Anterior part of the ventricular body	31	14	—
Posterior part of the ventricular body	18	35	2
Atrium	24	21	6
Occipital horn	19	16	2
Temporal horn	4	—	2

Ventricular dilatation was assessed in 68 hemispheres as being absent (15%), minimal (23%) moderate (41%) or severe (21%). Ventricular dilatation, generally bilateral (91%) and generally symmetrical (83%), predominated in the posterior part of the ventricular body (100%) and the atrium (93%) (Table I).

In 14 (41%) of the patients, alterations in the ventricles were accompanied by enlargement of the longitudinal fissure. In addition, two children presented a limited, unilateral hypodensity abutting the external or superior wall of the lateral ventricle in the posterior parietal area (Fig. 3). Finally, three children from this group also presented an extensive hypodensity in the white matter around the entire periphery of the lateral ventricles (Fig. 4). These children were considerably younger than the average age in Group 2 (13 months versus 61 months).

Unlike the monomorphic appearance of Group 2, Group 3 (14 cases) included cases of miscellaneous abnormalities such as localized hypodensity of superficial or deep vascular topography, such as those found in Sylvian ischaemia (eight cases of which four shared hypodensity of the basal ganglia), bilateral subcortical-cortical atrophy (two cases), isolated cortical atrophy (one case), and isolated dilatation of the lateral ventricles (three cases, two minimal and one major).

Premature birth in relation to the general population in the study (54%) was significantly lower in Group 1 (5/28 = 18%) and in Group 3 (3/14 = 21%) than in Group 2 (33/34 = 97%).

A specific clinical picture was determined for the 34 children in Group 2 as well as for one of the 28 children in Group 1. This included spastic motor deficiency generally of the diplegic form (Table II), horizontal ocular motor disorders basically in the pursuit disorders, spatial agnosia, constructive dyspraxia and a particularly

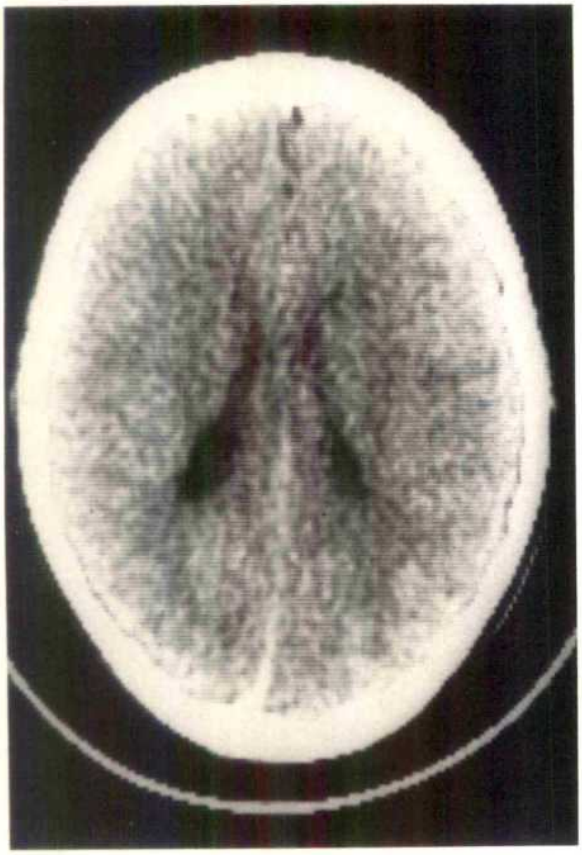

Figure 3. Irregular outlines of the posterior part of the ventricular bodies resulting from periventricular leucomalacia in a 9-year-old child.

frequent dissociation between verbal IQ, which was normal, and that of performance. These last abnormalities correspond to the clinical picture of child dyspraxia described by Ajuriaguerra (Stambak et al, 1964).

The average IQ–DQ (Table III) of the children in Group 2 was significantly less than that of those in Group 1 ($p \leq 0.05$).

Table II. Distribution of the type of cerebral palsy by groups

	Group			Total (76 cases)
	I 28 cases (37%)	II 34 cases (45%)	III 14 cases (18%)	
Spastic				
tetraplegic	4	—	3	7
diplegic	6	21	5	32
paraplegic	7	8	1	16
hemiplegic	9	5	4	18
Athetosis	1	—	—	1
Mixed form	1	—	1	2

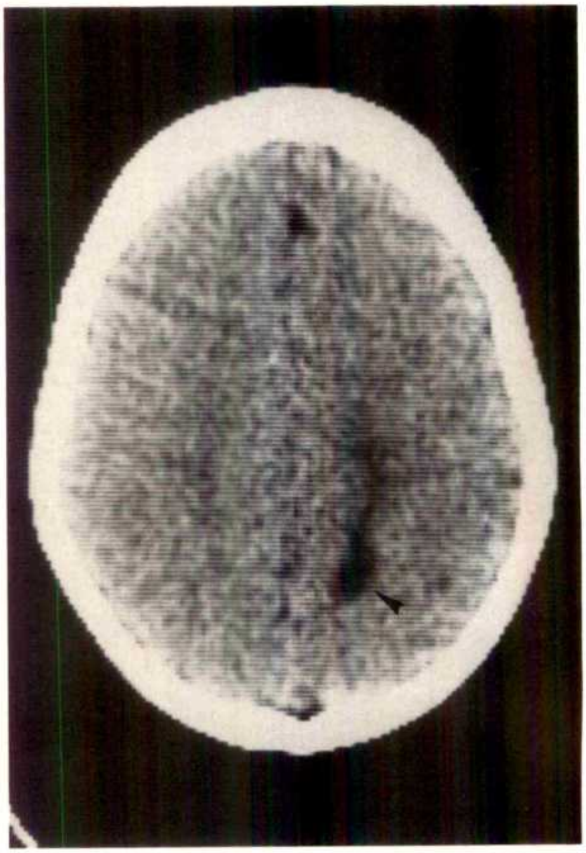

Figure 4. Well delineated hypodensity (arrow) abutting the roof of the posterior part of the ventricular body, associated with modifications in the pattern of the lateral ventricles, resulting from periventricular leucomalacia in an 8-year-old child. Note the decrease in the thickness of the white matter in the centrum semiovale.

The extent of the motor handicap did not appear to differ significantly from one group to another (Table IV). However, there was no case of any major handicap in any child. It should be noted that a certain experimental bias due to patient selection was present in this study, since IQ–DQ values for these children were equal to at least 65.

Given the homogeneity of Group 2, we sought to determine prognosis from the CT appearance. It appears

Table III. Distribution IQ–DQ values by groups

	Group		
	I 28 cases	II 34 cases	III 14 cases
IQ–DQ 60–75	7	22	8
IQ–DQ 76–90	15	7	3
IQ–DQ >90	6	5	3
Average IQ–DQ	85 ± 15	76 ± 13	78 ± 14

Table IV. Distribution of the extent of cerebral palsy by groups

Extent of deficit	Group		
	I 28 cases	II 34 cases	III 14 cases
Slight	9	5	4
Moderate	19	29	10
Severe	0	0	0

Table V. Relation between enlargement of the longitudinal fissure of the cerebrum and the IQ–DQ values for Group 2

IQ–DQ value	No. of cases	
	Enlarged fissure	Unenlarged fissure
60–75	13	9
76–90	1	6
>90	—	5

from Table V that the majority ($13/14 = 92.9\%$) of the children whose longitudinal cerebral fissure was enlarged (that is who presented a frontoparietal atrophy) belonged to the class with the lowest IQ–DQ values. These values were no higher than 80 for any of these children. On the other hand, the children whose longitudinal fissure was normal were less likely to have low IQ–QD values ($9/20 = 45\%$) and children with a high IQ–QD were only found in this group (corrected χ^2 test: $p \leqslant 0.02$ with a threshold IQ–QD value of 75.5).

No significant relation could be determined between the extent of ventricular dilatation and the IQ–QD values nor between the size of the ventricles and that of the longitudinal fissure of the cerebrum.

Discussion

The overall sensitivity of CT in the retrospective aetiological diagnosis of cerebral palsy proved to be fairly poor, since only 63% of the 76 children presented CT abnormalities. These results are very similar to those reported by Taudorf et al (1984), who found an overall sensitivity of 67% out of 83 cases of spastic cerebral palsy.

However, the rate of abnormalities that can be detected by CT is much higher (88%) if the examinations of former pre-term children only are considered. In this sub-group, 33/36 (92%) of the examinations presented a stereotype appearance forming a single entity (Group 2). It is possible to formulate a series of arguments to relate these abnormalities to the sequelae of periventricular leucomalacia (PVL), corresponding to neonatal periventricular white matter ischaemia, as follows.

(1) Children in Group 2 were, in the vast majority of cases (97%), former premature births (23 born before 34 weeks and 10 between 35 and 36 weeks). Periventricular leucomalacia is basically a condition of the pre-term infant (Banker & Laroche, 1962) whose immature haemodynamic regulatory system provides insufficient encephalic protection (De Reuck et al, 1972).

(2) These children all have a handicap for which analytic semiology (Picard & Lacert, 1985; Picard et al, 1987) corresponds precisely to the topography of the lesions described in PVL, *i.e.* the superoexternal angles of the lateral ventricles (Banker & Laroche, 1962). This area is extremely vulnerable in pre-term infants as it is vascularized by a terminal irrigation system, as a result of the immature development of the anastomotic network between the ventriculopetal and ventriculofugal arterial branches (De Reuck, 1972, 1984; Takashima & Tanaka, 1978).

(3) The CT scan abnormalities seem to be consistent with the anatomical evolution of PVL, with gliosis and thinning of the periventricular white matter in the posterior regions resulting in the dilatation of the adjacent lateral ventricles (Banker & Laroche, 1962). Periventricular cavities are rarely visible at this stage and we only found them in two children in the form of localized periventricular hypodensity. This can be explained by the unsuitability of transverse CT sections for visualizing the lesion topography, and also by the natural tendency of cavities to collapse (De Reuck et al, 1972).

Similar CT findings in PVL have been reported previously in more limited series (Schellinger et al, 1984; Taudorf et al, 1984; Flodmark et al, 1987). In the study carried out by Schellinger et al (1984), ultrasound correlation provided confirmation of the reliability of CT findings. Confirmation of PVL with previous ultrasound was possible in only two of our patients because neurosonography was not available for most of these children when they were neonates. The CT scan findings reported by Flodmark et al (1987) in a series of 15 children with clinical evidence of PVL also concur with ours, and, moreover, emphasize two interesting additional patterns: reduction in quantity of periventricular white matter and deep and prominent sulci abutting the ventricles.

(4) Additionally, three of the youngest children in the series also presented extensive periventricular hypodensity, which has also been reported in the literature in early CT investigation of PVL (Di Chiro et al, 1978; Estrada et al, 1980; Flodmark et al, 1980; Taboada et al, 1980; Martin et al, 1983; Schellinger et al, 1984; Chow et al, 1985; Bejar et al, 1986).

(5) Finally, 10 patients in this group, presenting with various severe deficiencies, underwent magnetic resonance examination. These are included in a larger series to be published. Inversion–recovery coronal sequences revealed thinning of superoexternal periventricular white matter with hypointense localized areas abutting the ventricular walls. These findings constitute convincing evidence to support the hypothesis that Group 2 patients actually exhibited sequelae of PVL.

This study highlights the significant role of PVL in the genesis of cerebral palsy. Among the 76 cases in this series, 35 appear to have lesions resulting from PVL on the basis of past medical history and clinical deficiencies, and 34 show both clinical and CT evidence of this disorder (Group 2). Computed tomographic examination was normal in only one case. These findings are consistent with the results of studies on the future of pre-term infants initially examined by ultrasound. Graziani et al (1986) found that for 15 premature birth infants who later developed cerebral palsy, 13 initially showed sonographic signs of PVL.

Conclusions

In a population of children with cerebral palsy without severe intellectual handicap (IQ–QD$\geqslant$60), CT examination can contribute significantly to retrospective aetiological diagnosis. The rate of abnormalities is significantly higher (88% versus 63%) for former pre-term infants. It is in this group of patients that periventricular leucomalacia occurs, and it would appear that in this series nearly half of the cases of cerebral palsy may be attributable to this disorder. Correlation of radiological findings with the clincial data also reveals that the IQ–DQ values of these same infants are lower than those of children with a normal CT examination. In addition, among those children suffering sequelae of periventricular leucomalacia, an enlarged inter-hemispheric fissure carries a poor prognosis for intellectual and cognitive handicaps.

References

BANKER, B. Q. & LAROCHE, J. C., 1962. Periventricular leukomalacia of infancy. A form of neonatal anoxic encephalopathy. *Archives of Neurology, 7*, 386–410.

BEJAR, R., COEN, R. W., MERITT, T. A., VAUCHER, Y., TRICE, J., CENTENO, R. & GILLES, F., 1986. Focal necrosis of the white matter (periventricular leukomalacia): sonographic, pathologic, and electro-encephalographic features. *American Journal of Neuroradiology, 7*, 1073–1080.

CHOW, P. P., HORGAN, J. J. & TAYLOR, K. J. W., 1985. Neonatal periventricular leukomalacia: real-time sonographic diagnosis with CT correlation. *American Journal of Neuroradiology, 6*, 383–388.

DI CHIRO, G., ARIMITSU, T., PELLOCK, J. M. & LANDES, R. D., 1978. Periventricular leukomalacia related to neonatal anoxia: recognition by computed tomography. *Journal of Computer Assisted Tomography, 2*, 352–355.

ESTRADA, M., EL GAMMAL, T. & DYKEN, P. R., 1980. Periventricular low attenuation. A normal finding in computerized tomographic scans of neonates? *Archives of Neurology, 37*, 754–756.

FLODMARK, O., FITZ, C. R. & HARWOOD-NASH, D. C., 1980. CT diagnosis and short-term prognosis of intracranial hemorrhage and hypoxic/ischemic brain damage in neonates. *Journal of Computer Assisted Tomography, 4*, 775–787.

FLODMARK, O., ROLAND, E. H., HILL, A. & WHITFIELD, M. F., 1987. Periventricular leukomalacia: radiologic diagnosis. *Radiology, 162*, 119–124.

GRAZIANI, L. J., PASTO, H. & STANLEY, C., 1986. Neonatal neurosonographic correlates of cerebral palsy in preterm infants. *Pediatrics, 78*, 88–94.

MARTIN, D. J., HILL, A., FITZ, C. R., DANEMAN, A., HAVILL, D. A. & BECKER, L. E., 1983. Hypoxic/ischaemic cerebral injury in the neonatal brain. A report of sonographic features with computed tomographic correlation. *Pediatric Radiology, 13*, 307–312.

PICARD, A., BRENTANOS, E., SCHOUMAN, E. & LACERT, PH., 1987. Séquelles motrices et intellectuelles tardives chez 34 enfants infirmes moteurs cérébraux ayant un aspect tomodensitométrique de leucomalacie périventriculaire. *Annales de Pédiatrie, 34*, 613–621.

PICARD, A. & LACERT, PH., 1985. Les dyspraxies constructives de l'infirme moteur cérébral. *Annales de Réadaptation et de Médecine Physique, 28*, 105–110.

DE REUCK, J., 1984. Cerebral angioarchitecture and perinatal brain lesions in premature and full term infants. *Acta Neurologica Scandinavica, 70*, 391–395.

DE REUCK, J., CHATTHA, A. S. & RICHARDSON, E. P., 1972. Pathogenesis and evolution of periventricular leukomalacia in infancy. *Archives of Neurology, 27*, 229–236.

SCHELLINGER, D., GRANT, E. G. & RICHARDSON, J. D., 1984. Cystic periventricular leukomalacia: sonographic and CT findings. *American Journal of Neuroradiology, 5*, 439–445.

STAMBAK, M., L'HERITEAU, D., AUZIAS, M., BERGES, J. & DE ADJURIAGUERA, J., 1964. Les dyspraxies de l'enfant. *La Psychiatrie de l'Enfant, 7*, 381–497.

TABOADA, D., ALONSO, A., OLAGUE, R., MULAS, F. & ANDRES, V., 1980. Radiological diagnosis of periventricular and subcortical leukomalacia. *Neuroradiology, 20*, 33–41.

TAKASHIMA, S. & TANAKA, K., 1978. Development of cerebrovascular architecture and its relationship to periventricular leukomalacia. *Archives of Neurology, 35*, 11–16.

TAUDORF, K., MELCHIOR, J. C. & PEDERSEN, H., 1984. CT findings in spastic cerebral palsy. Clinical, aetiological and prognostic aspects. *Neuropediatrics, 15*, 120–124.

1989, *The British Journal of Radiology*, 62, 253–255

Outpatient myelography: an acceptable and cost-effective technique

By A. H. Choudhri, MRCP, FRCR, P. C. Rowlands, BMedSci, MRCP, C. J. Barber, FRCS, FRCR, *J. Johnson, FRCS and J. M. Stevens, DRACR, FRCR

Departments of Radiology and *Orthopaedic Surgery, St Mary's Hospital, London W2 1NY

(*Received August 1988*)

Abstract. Sixty-five patients with stable low back pain had their lumbar myelography performed as outpatients, staying in the department for 1 h after the examination. The incidence of post-myelogram headache was similar to that reported for inpatients. No serious after-effects occurred in the study group. The vast majority of patients preferred to be at home following the study. It is concluded that outpatient myelography is safe, less expensive and preferred by the patients.

We were requested by the orthopaedic department to consider carrying out outpatient myelography, because of bed shortages and difficulty in admitting patients overnight following their myelogram. A prospective study of the tolerability of the outpatient examination was carried out on 65 patients.

There have been two previous studies of outpatient water-soluble myelography (Kostiner & Krook, 1985; Badami et al, 1986). Each was prospective and included thoracic and cervical myelography as well as lumbar studies, although the latter predominated. The groups used metrizamide as the contrast agent and the protocols required patients to be observed in a day-case unit for 3–7 h following the study. The results from these studies indicated that minor symptoms such as headache and nausea were common (28% and 15%, respectively, in Kostiner's and Krook's study paper, and 57% and 36%, respectively, in Badami et al's study). Major symptoms such as diplopia and photophobia occurred in less than 1% of cases and no patient having lumbar myelography experienced a grand mal seizure.

Materials and methods

The patients were selected from those attending orthopaedic outpatients' clinics at St Mary's Hospital, the majority being referred by a single surgeon. Patients were considered if they were mobile and had stable symptoms and signs. Patients excluded from the study were those whose symptoms were not referrable to the L4/5 or L5/S1 area; other categories of patients which were excluded were alcoholics, epileptics, patients on tricyclic/MAOI drugs, patients with known contrast agent allergy and patients with poor comprehension.

Sixty-five patients entered the study. Average age was 38 years (range 23–70 years). There were 30 males and 35 females.

Patients attended the department in the early morning following a light breakfast and plentiful fluid. The procedure was discussed with them by the radiologist. The puncture was made with a 22G spinal needle and a maximum of 12 ml of iohexol (240 mg ml^{-1}) was injected with the patient tilted feet down. The contrast medium was kept below the L1 level. A normal series of antero-posterior, lateral and oblique radiographs was taken but no radiographs of the conus or dorsal cord were made.

Immediately after the study the patient was seated for

Did you find the myelogram
not unpleasant
mildly unpleasant
moderately unpleasant
very unpleasant

Following the myelogram did you have any headache?
Yes
No

If so, was it
mild
moderate
severe

Following the myelogram did you have any nausea or sickness?
Yes
No

If so, was it
mild
moderate
severe

Following the myelogram did you have any back pain?
Yes
No

If so, was it
mild
moderate
severe

Did you have any leg pain following the myelogram?
Yes
No

Would you have preferred to stay overnight in hospital?
Yes
No

Do you have any other comments regarding your myelogram?

Name______________________________

Figure 1. Patient questionnaire.

Correspondence and requests for reprints to Dr Rowlands.

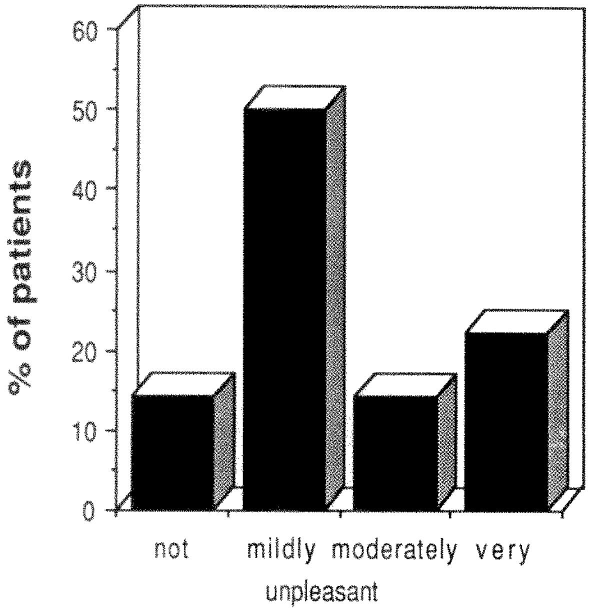

Figure 2. Tolerability of myelogram.

1 h in the department. They were then re-interviewed by the radiologist who noted their symptoms at that time. They were given a questionnaire (Fig. 1) and allowed to go home, with an escort. They were instructed to sit or stand for 8 h following the procedure and to remain well hydrated. They were requested to return their symptom questionnaire 4 days after the myelogram.

The patients were given a form, stating what procedure had been done and explaining the symptoms that might be expected following the myelogram. The form also gave a contact telephone number for further advice.

The questionnaire

Simple everyday language was employed, and subjective responses from the patients were encouraged. Certain direct questions pertaining to the known common side-effects were included and the patient was asked to give an overall reaction to the experience.

Results

Sixty-three patients (97%) returned their questionnaires. The results are shown in Figs 2–5. In addition, 36 patients (55%) experienced leg pain following myelography and 60 patients (93%) said they preferred to go home rather than stay overnight in the hospital.

Discussion

The majority of our patients found the myelography procedure itself tolerable. A minority of patients reported unpleasant post-study symptoms. The age, sex and preceding symptoms of the patient did not make any statistically significant difference to the post-study symptoms, nor did the radiological findings (analysis by Wilcoxson's rank sums test). The overwhelming majority of patients preferred to go home rather than to be admitted following their myelogram. In relation to this it was reassuring for the patients that the myelogram was, unlike hospital admission, certain to take place on the date specified.

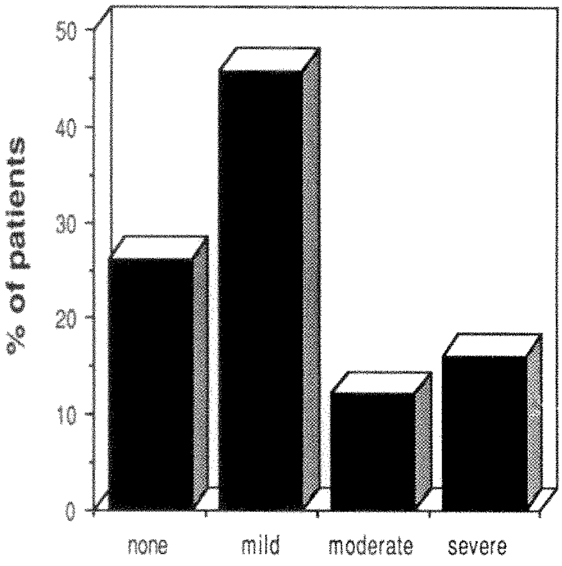

Figure 3. Incidence of headache following myelogram.

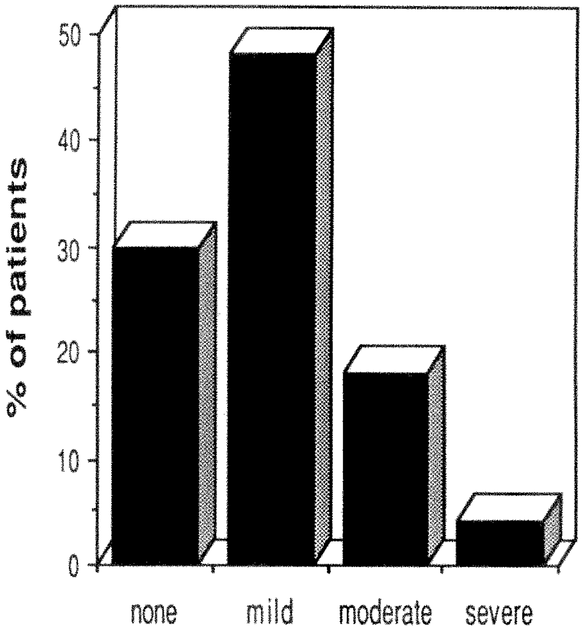

Figure 4. Incidence of back pain following myelogram.

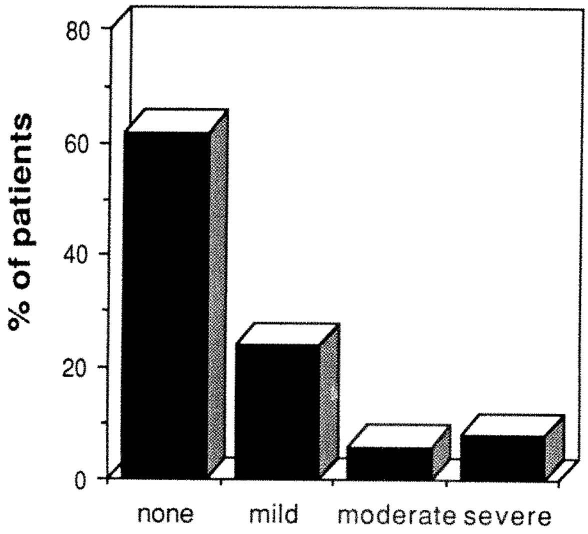

Figure 5. Incidence of nausea following myelogram.

The results from our study are not directly comparable with the previous studies as follow-up information in those was obtained via a telephone call. We feel that this is more likely to lead to under-reporting than over-reporting of symptoms. Despite this, the rates of post-myelogram symptoms were similar to the previous studies and also to reported rates for inpatient myelography. No serious side-effect occurred in any of our patients. No patient had to be detained in hospital following the myelogram.

Our protocol precluded inclusion of the spinal cord in the examination on the grounds that this significantly increases the incidence of adverse reactions (Badami et al, 1986). We acknowledge that back pain, leg pain or both is very rarely caused by spinal cord compression, especially from a neurofibroma in the lower thoracic region, and it is our practice with inpatients to include at least the thoracic region in myelograms that fail to show a relevant abnormality in the lower lumbar region. The limitation of the outpatient study to the lumbar region only was therefore clearly stated when no abnormality was found.

The financial implications of outpatient myelography are significant. One night's stay at this hospital costs £125 and there are various added administrative costs. This department carries out several hundred lumbar myelograms per annum and so, the potential savings are of the order of £40 000–£50 000 per annum. We feel that outpatient myelography is both acceptable to patients and cost-effective.

References

Badami, J. P., Baker, R. A., Scholz, F. J. & McLaughlin, M., 1986. Outpatient Metrizamide myelography: prospective evaluation of safety and cost effectiveness. *Radiology*, *158*, 175–177.

Kostiner, A. I. & Krook, P. M., 1985. Outpatient lumbar myelography with Metrizamide. *Radiology*, *155*, 383–385.

1989, *The British Journal of Radiology*, 62, 256–259

Radiological appearances of colonic ring staple anastomoses

By *B. D. Daly, MRCPI, FRCR, FFR(RCSI) and †B. M. Crowley, MB, FRCSI

Department of Radiology, St James's University Hospital, Beckett Street, Leeds LS9 7TF and †University Department of Surgery, Regional Hospital, Wilton, Cork

(*Received August 1988 and in revised form November 1988*)

Abstract. The radiographic appearances of colonic staple ring anastomoses are presented. Staple ring disruption on plain abdominal radiographs in the early post-operative period suggests dehiscence of the bowel anastomosis and is an indication for urgent water-soluble contrast medium enema to confirm the diagnosis. Rectal stenosis can develop as a late complication of staple anastomosis and may be detected on barium enema.

Circular ring stapling devices were first introduced by Russian surgeons in 1960 but have only become widely used since the introduction of more modern stapling "guns" in 1977. These devices allow lower rectal anastomosis than is possible with hand-sewn sutures and may thus avoid the need for permanent colostomy. Stapling guns can reduce operation time considerably and are also used for higher anastomoses in the recto-sigmoid colon for this reason. The staple gun technique requires considerable expertise, however, and the poor vascular supply to the rectum results in significant leakage rates in the early post-operative period. A temporary defunctioning colostomy is sometimes employed to protect the anastomosis, especially if its integrity is suspect. Animal studies suggest that the intact staple ring (Figs 1, 2) should remain unchanged for at least 4 weeks, and that migration of staples may occur after that time as a result of healing and fibrous tissue formation (Fain et al, 1975). Case reports of seven patients who demonstrate interesting radiological features and complications of ring staple anastomoses are presented.

Case reports

Case 1

An 80-year-old woman had an end-to-end staple anastomosis of the sigmoid colon following excision of a diverticular mass. The anastomosis was judged "airtight" at surgery. A supine abdominal radiograph was obtained 8 days after operation because of prolonged ileus and, while otherwise unremarkable, did show a disrupted staple ring (Fig. 3). The patient developed septicaemia 5 days later and a barium enema (Urografin, Schering AG) subsequently demonstrated dehiscence of the anastomosis. At laparotomy a pelvic abscess was drained and a permanent colostomy fashioned.

Case 2

A 74-year-old man had an end-to-end staple anastomosis for resection of a rectal villous adenoma. The anastomosis was considered "airtight" at surgery. A supine abdominal radiograph obtained for unrelated reasons 4 days after operation showed an intact staple ring (Fig. 4). A further supine radiograph performed 11 days later, because of abdominal pain and pyrexia, showed disruption of the staples (Fig. 5). Leakage at the anastomosis site was confirmed by Urografin enema 5 days later (Fig. 6). The patient recovered on intravenous feeding and antibiotic therapy.

Case 3

A 77-year-old woman had an end-to-end staple anastomosis following excision of a diverticular abscess. The anastomosis was satisfactory at operation. She became pyrexial 9 days after operation and a supine abdominal radiograph showed staple disruption. A Urografin enema 1 day later confirmed dehiscence of the anastomosis with a large leak of contrast medium into

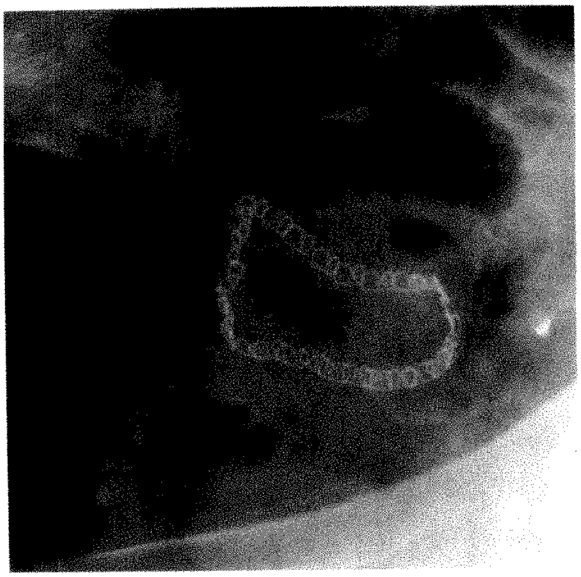

Figure 1. Plain radiograph showing a typical intact staple ring anastomosis.

---

*Author for correspondence.

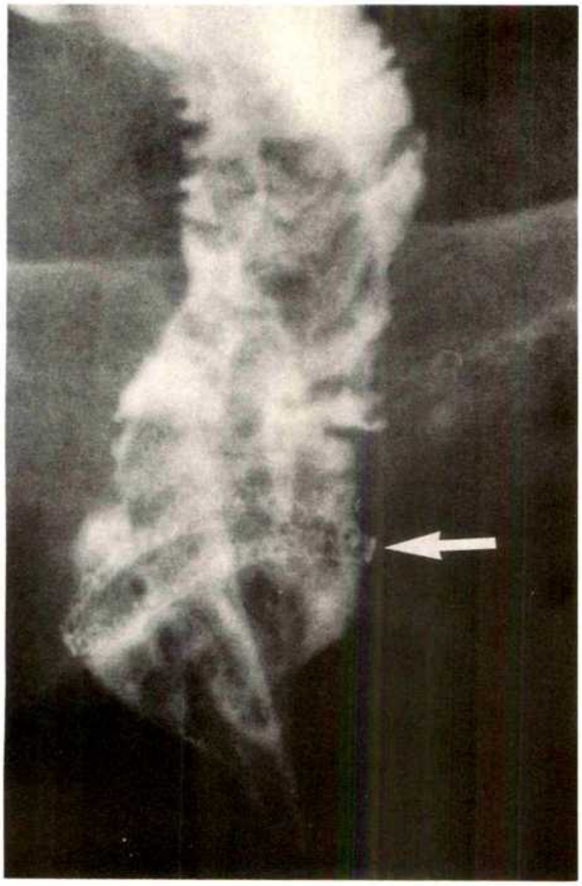

Figure 2. An intact staple ring is demonstrated on water-soluble contrast medium enema (arrow).

the pelvis. The patient required abscess drainage and a temporary colostomy.

Case 4

A 70-year-old woman had a very low end-to-end recto-anal anastomosis following excision of a villous adenoma. The anastomosis was satisfactory at surgery. Six days later she developed abdominal pain. Disruption of the staple ring was noted during a contrast enema (Hypaque, Winthrop) 14 days after operation which confirmed dehiscence of the anastomosis. Abscess drainage and a temporary colostomy were necessary.

Case 5

An 82-year-old man had excision of a rectal tubulo-villous adenoma with an end-to-end staple anastomosis. The integrity of the anastomosis was suspect at operation and a defunctioning colostomy was fashioned. Staple disruption was noted during Hypaque enema which demonstrated anastomotic leakage 10 days later.

Case 6

A 52-year-old man had an end-to-end recto-sigmoid staple anastomosis following excision of a diverticular abscess. The anastomosis was considered inadequate at operation and hand sutures were added. A supine radiograph of the abdomen on the 10th day after operation showed staple disruption. Unaware of the presence of additional hand sutures, the radiologist suggested a diagnosis of anastomotic dehiscence. A subsequent Urografin enema was normal.

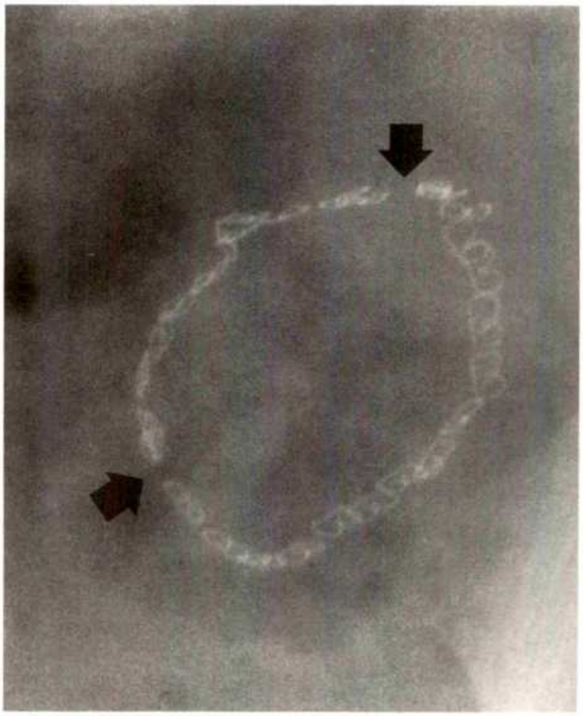

Figure 3. *Case 1.* Disrupted staple ring 8 days after recto-sigmoid anastomosis (arrow).

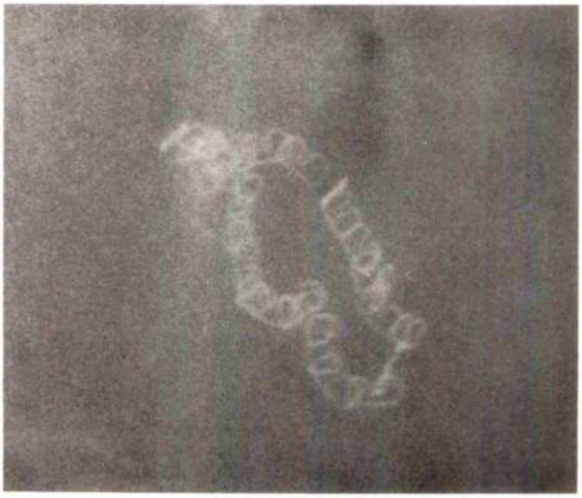

Figure 4. *Case 2.* An intact staple ring 4 days after recto-sigmoid anastomosis.

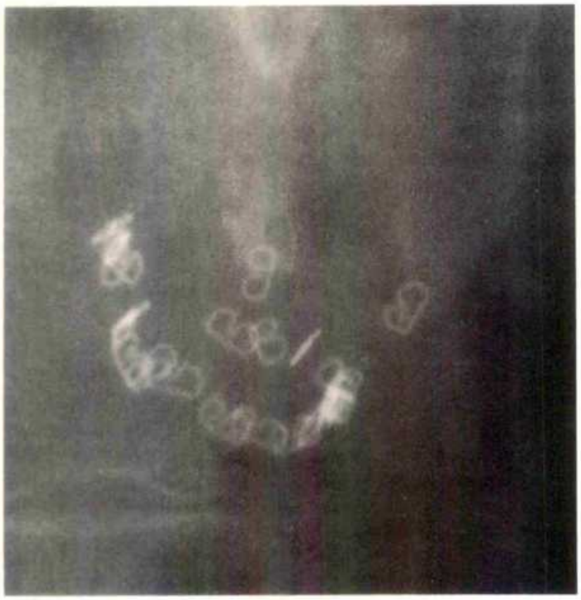

Figure 5. *Case 2.* The previously intact staple ring has now become disrupted 15 days after surgery.

Case 7

A 66-year-old man had excision of rectal carcinoma with an end-to-end staple anastomosis. A barium enema 2 months after operation showed stenosis of the rectum at the operation site (Fig. 7). Sigmoidoscopy, biopsy and computed tomography (CT) at the level of the stenosis showed this to be due to fibrous tissue reaction.

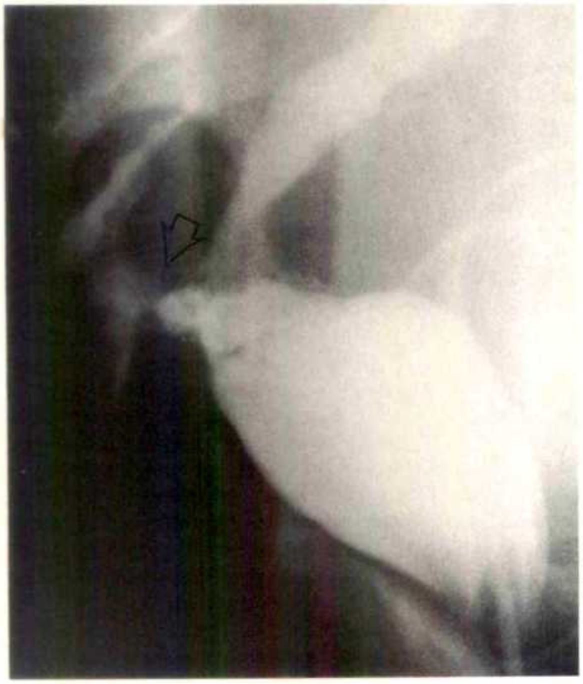

Figure 6. *Case 2.* Water-soluble contrast medium enema performed 5 days later (20 days after surgery) confirms leakage of contrast medium from the anastomosis site (arrow).

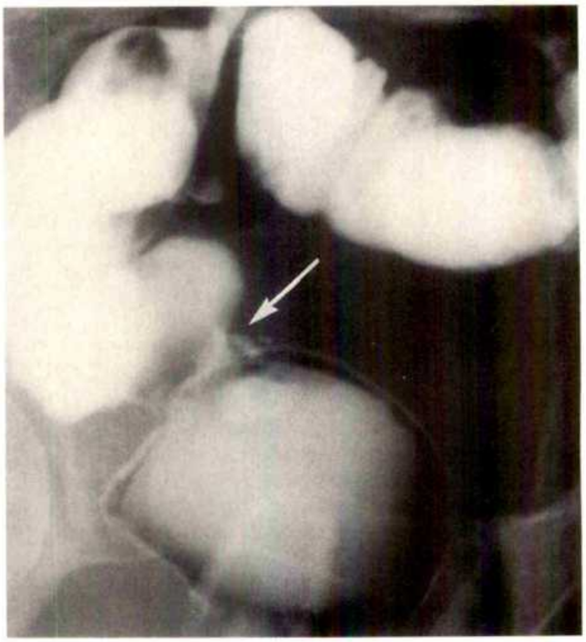

Figure 7. *Case 7.* Barium enema 2 months after rectal anastomosis demonstrates early stenosis at the anastomosis site (arrow).

Discussion

Plain abdominal radiographs are often requested when post-operative complications develop following rectal or sigmoid anastomosis. Leakage, as detected by water-soluble contrast medium enema, occurs in approximately 20% of all stapled rectal anastomoses (Kirwan, 1981; Doricott et al, 1982). Clinical leakage, *e.g.* pelvic abscess or fistula formation, varies in incidence between 6 and 9% in different studies (Waxman, 1983). In our series, four patients (Cases 1, 2, 3 and 6) had obvious disruption of staple rings on plain abdominal radiographs in the early post-operative phase. In three patients (Cases 1–3) the staple disruption was a sign of anastomotic dehiscence, although this diagnosis was only made in each case by water-soluble contrast medium enema after a delay of up to 5 days. In Case 2 an initially normal ring (Fig. 4) became disrupted on a subsequent plain radiograph (Fig. 5). Doricott et al (1982) have described the correlation of a disrupted staple ring with leakage from the anastomosis site on water-soluble contrast medium enema performed routinely 9 or 10 days after operation. Two further cases in our series (Cases 4 and 5) also demonstrated obvious ring disruption at the time of water-soluble contrast medium enema. However, the early detection of possible breakdown of the anastomosis on plain abdominal radiographs alone does not appear to have been previously described. While such a diagnosis was possible in Cases 1–3 of our series, this was only noted in retrospect after considerable delay. Case 6 demonstrates that a disrupted staple ring in the early post-operative phase is not invariably associated with anastomotic breakdown. In this patient the addition of hand sutures to an incomplete staple ring resulted in a satisfactory anastomosis on Urografin enema. We feel, nevertheless, that the presence of a disrupted staple ring on plain abdominal radiographs in the early post-operative period is suggestive of anastomotic dehiscence and, in the appropriate clinical setting, is an indication for urgent water-soluble contrast medium enema. It would therefore seem reasonable to recommend that a plain abdominal radiograph be obtained in the early post-operative phase in all cases of rectal or recto-sigmoid ring staple anastomosis, and especially when an unsatisfactory anastomosis is suspected at the time of surgery. A base-line appearance may thus be obtained for comparison with subsequent radiographs if dehiscence and infection are suspected.

A plain radiograph of the staple ring is also useful prior to the water-soluble contrast medium enema which many surgeons request routinely at 7–10 days following surgery. Some surgeons do not favour this procedure and one anecdotal reason for this is the potential risk of traumatic damage to the low rectal anastomosis by an enema tube. The presence of a disrupted staple ring on an initial plain radiograph prior to tube insertion excludes a traumatic cause if a leak is subsequently demonstrated at the anastomosis.

Rectal stenosis is a later complication of colonic or rectal staple anastomosis and occurs in up to 9% of all cases (Smith, 1981). The stenosis may be progressive and in extreme cases a rectal web may develop (Brain et al, 1981). When stenosis occurs at the anastomosis site following resection for carcinoma, it must be differentiated from local recurrence. Stenosis can usually be treated by sigmoidoscopic dilatation with re-operation rarely being necessary. Case 7 demonstrates early rectal stenosis 2 months following staple anastomosis (Fig. 7).

In conclusion we feel that a considerable amount of information may be obtained from the appearances of the early post-operative abdominal radiograph in patients who have had a rectal or recto-sigmoid ring staple anastomosis. This information can be very helpful in the post-operative management of these patients, especially when early complications develop.

Acknowledgments

We would like to thank Professor W. O. Kirwan for use of clinical cases, and Mrs June Wakefield for preparation of the manuscript.

References

Brain, J., Lorber, M. & Fiddian-Greene, R. G., 1981. Rectal membrane: an unusual complication following the use of the circular stapling instrument for colo-rectal anastomosis. *Surgery, 89,* 271–274.

Doricott, M. J., Baddeley, R. M., Keighley, M. R. B., Lee, J., Oates, D. G. & Alexander-Williams, J., 1982. Complications of rectal anastomoses with end-to-end anastomosis (EEA) stapling instrument. *Annals of the Royal College of Surgeons of England, 64,* 171–174.

Fain, F. M., Patin, E. S. & Morgenstern, L., 1975. Use of mechanical suturing apparatus in low colo-rectal anastomosis. *Archives of Surgery, 110,* 1079–1082.

Kirwan, W. O., 1981. Integrity of low colo-rectal EEA-stapled anastomosis. *British Journal of Surgery, 68,* 539–540.

Smith, L. E., 1981. Anastomosis with EEA-stapler after anterior colonic resection. *Diseases of the Colon and Rectum, 24,* 236–242.

Waxman, B. P., 1983. Large bowel anastomoses: the circular staplers. *British Journal of Surgery, 70,* 64–67.

1989, *The British Journal of Radiology*, 62, 260–265

A large trial of intravenous Conray 325 and Niopam 300 to assess immediate and delayed reactions

By Mark McCullough, MB, BS, FRCR, Peter Davies, DM, FRCR and *Ros Richardson, MSc, ARCS

Departments of Radiology and *Medical Physics, City Hospital, Hucknall Road, Nottingham

(*Received March 1988 and in revised form October 1988*)

Abstract. The trial was designed as an investigation into the incidence of both immediate and delayed reactions to the intravenous administration of Conray 325 (sodium iothalamate) (844 patients) and Niopam 300 (iopamidol) (855 patients) for urographic examination. Information was obtained from questionnaires returned by patients about a week after their examination, with a response rate of 81%. Significant differences were found in the incidences of both types of reactions to the two media with respect to nausea and vomiting, arm pain, and taste in the mouth, which was commoner in patients receiving Conray 325, whereas the incidence of delayed skin rashes and parotid swelling was commoner with Niopam 300. The occurrence of a flu-like illness, so-called "iodism", was found to be equal for the two contrast media.

A recently published study into the incidence of various types of both immediate and delayed reactions to intravenous urographic contrast media (Panto & Davies, 1986) concluded that delayed reactions, particularly skin rashes, were not uncommon after urography. The present trial was instituted specifically to compare the types and incidences of both immediate and delayed reactions to an ionic medium sodium iothalamate (Conray 325, May & Baker) and a non-ionic medium iopamidol (Niopam 300, Bracco).

Patients, materials and methods

All patients aged over 18 years referred to our department for non-emergency urography over a 15-month period were included in the study, the aim being to have 1000 patients examined with each medium. Fifty millilitres of the selected medium was given rapidly (in approximately 30 s) into an ante-cubital vein. Each examination was supervised by a radiologist, who explained the nature of both the examination and the questionnaire to the patient. The two types of contrast medium were assigned at random; this was not influenced by a history of previous reaction.

Prior to the injection a brief medical history was taken. Specifically, patients were questioned about a history of cardiac disease, a history of atopy (hay fever, asthma or eczema), and a drug history was also recorded, including any sensitivities. The clinical indications for the examinations were recorded. An assessment was also made of the patient's mental state: calm, reasonable anxiety or excessive anxiety. If a patient required a second injection of contrast medium because of suboptimal demonstration of the upper tracts, the alternate medium on the trial was used. At the end of the examination the patients were questioned about any reactions or side-effects they had noticed after the injection. These were divided into the following categories.

(1) Minor reactions: discomfort at the injection site or in the injected limb, a sensation of warmth or heat, flushing, a perineal sensation, taste in the mouth, coughing or sneezing, nausea and/or vomiting and faintness.
(2) Intermediate reactions: dyspnoea, dizziness, palpitations, shivering, parotid swelling and abdominal or chest pain.
(3) Sensitivity reactions: swelling of the face, urticaria, conjunctivitis, rhinitis and skin rash.

The time between the injection and any reaction was recorded, as was any reaction to abdominal compression. The patients were also asked whether they found the examination generally unpleasant. If a second injection was required, answers were recorded on a separate sheet.

Each patient was then given a questionnaire with a pre-paid reply envelope, and asked to complete and return it after a period of about a week. The questionnaire consisted of the following questions:

(1) Did you have any pain in the arm after the examination?
(2) If so, was it where the injection was made, or above this site?
(3) How many days after the examination did it come?
(4) How many days did it last?
(5) Did you have a "flu-like" illness after the examination—if so, please give brief details.
(6) Did you have any swelling of the face or pain after eating? If so, please give brief details.
(7) Are there any other comments you wish to make?

The answers both to the questions asked in the department and on the returned questionnaires were analysed manually and on computer.

Table I. Immediate reactions in the single-injection group

Reactions	Conray 325 (n = 844)	Niopam 300 (n = 855)	p
Arm pain at or above injection site	46 (5.45%)	28 (3.3%)	$0.05 > p > 0.01$
Sensation of warmth or heat	737 (87%)	626 (73%)	$p < 0.001$
Observed flushing	382 (45%)	242 (28%)	$p < 0.001$
Perineal sensation	194 (23%)	184 (21.5%)	NS
Taste in mouth	378 (45%)	204 (24%)	$p < 0.001$
Nausea	109 (12.9%)	31 (3.6%)	$p < 0.001$
Sensitivity reactions	11 (1.3%)	4 (0.47%)	NS
Intermediate reactions	27 (3.2%)	10 (1.2%)	$0.01 > p > 0.001$

NS = not significant.
The time from injection to acute reaction was the same for both media and both sexes at a mean of 1.1 min with a standard deviation of 1.6 min. The distribution was different for different reactions and rashes occurred later than the sensations of heat, nausea, etc.

Results

A total of 1699 patients received a single injection, Conray in 844 patients and Niopam in 855. The distribution of male and female patients was the same, as was the age and weight distribution.

Single-injection group

Table I summarizes the incidence and distribution of immediate reactions with percentages in parentheses.

Immediate reactions

Minor reactions. Arm pain at or above the injection site was more common with Conray, this result being statistically significant ($0.05>p>0.01$). There was a statistically significant difference in the sensation of warmth or heat between the two media occurring in 87% of those given Conray and 73% of those given Niopam ($p<0.001$). Although perineal sensations were equally common for each contrast medium, these reactions were commoner in women (33%) than men (13%). Statistically significant differences were found between the incidences of taste in the mouth, nausea and vomiting, these reactions being commoner with Conray. There was no significant difference in the incidence of cough or sneezing.

Intermediate reactions. Table II summarizes the intermediate reactions. There were 27 cases of intermediate reactions to Conray and 10 to Niopam. There was a significant excess in patients receiving Conray ($0.01>p>0.001$). These reactions were mostly of patients complaining of dizziness and palpitations, with only a small number of patients experiencing chest pain (2 Conray, 1 Niopam), abdominal pain (4 Conray), dyspnoea (3 Conray, 1 Niopam), shivering attacks (2 Conray, 2 Niopam) and pallor/sweating (5 Conray, 1 Niopam). Most patients only experienced one or two symptoms in this category, with only one patient experiencing three symptoms (shivering, dyspnoea and chest pain after Niopam). Only one of the patients in this category, who experienced abdominal pain, experienced a concomitant sensitivity reaction. All reactions were transient and self-limiting and required no treatment beyond reassurance.

Sensitivity reactions (including urticaria). A total of 15 patients experienced sensitivity reactions, 11 after Conray and four after Niopam. Although this difference is not statistically significant ($0.1>p>0.05$), it does indicate a definite trend towards more reactions to Conray. Most of these reactions involved urticaria of the

Table II. Intermediate reactions in the single-injection group

Reactions	Conray 325 (n = 844)	Niopam 300 (n = 855)	p
Shivering attack	3 (0.4%)	2 (0.2%)	NS
Hiccup	0	0	NS
Dizziness	11 (1.3%)	3 (0.35%)	$0.05 > p > 0.01$
Dyspnoea	2 (0.2%)	1 (0.1%)	NS
Palpitations	5 (0.6%)	4 (0.5%)	NS
Facial swelling	0	0	NS
Pallor and sweating	4 (0.5%)	1 (0.1%)	$p = 0.18$
Abdominal pain	2 (0.2%)	0	$p = 0.25$
Chest pain	1 (0.1%)	1 (0.1%)	NS
Other	3 (0.4%)	0	$p = 0.12$
Total	31 reactions 27 patients	12 reactions 10 patients	

Table III. Common delayed reactions in the single-injection group

Reactions	Conray 325 ($n = 687$)	Niopam 300 ($n = 694$)	p
Arm pain	100 (14.5%)	73 (10.5%)	$0.05 > p > 0.01$
Skin rash	20 (2.9%)	38 (5.5%)	$0.05 > p > 0.01$
Flu-like illness	101 (14.7%)	88 (12.7%)	NS
Parotitis	6 (0.87%)	12 (1.7%)	NS
Back/flank pain	18 (2.6%)	24 (3.5%)	NS
Nausea/vomiting/abdominal pain	33 (4.8%)	37 (5.3%)	NS
Headache	20 (2.9%)	18 (2.6%)	NS

Excluding arm pain, a total of 372 patients (26.9%) (184 Conray, 188 Niopam) reported delayed reactions. The sex incidence was equal.

face, neck and trunk, often associated with itchiness. One patient developed oedema of the eyelids (Conray) and one oedema of the lips (Conray); neither of these patients developed urticaria. The patient with labial oedema was the only patient given any treatment for the sensitivity reaction (oral Piriton), the other reactions resolved spontaneously during the course of the examination.

Delayed reactions

There were 1381 completed and returned questionnaires available for analysis, which represented a response rate of 81%. The results are summarized in Table III.

One hundred (14.5%) patients had pain in the arm after Conray and 73 (10.5%) after Niopam, this being a significant difference ($0.05 > p > 0.01$). However, for patients having pain at the injection site (presumably due to extravasation) the numbers were 72 (10.5%) and 54 (7.8%) (χ^2 test not significant). For those patients experiencing pain above the injection site (presumably due to thromboplebitis) 54 had Conray (7.9%) and 41 were given Niopam (5.9%); (χ^2 test again not significant).

A delayed skin rash was reported by 20 patients (2.9%) given Conray and 38 (5.5%) given Niopam, with a significant excess of delayed rashes for Niopam. Most patients described the rash as being on the trunk, although some had rashes on the face and neck. A few patients described the rash as being like measles. One patient described dryness and peeling of the skin on the palms of the hands (Niopam) and another the development of hard itchy lumps around the hairline (Niopam). Four patients reported irritation and itchiness of the forearms and backs of the hands (3 Niopam, 1 Conray). Only one patient given Conray and two given Niopam had both an immediate and delayed rash.

Mouth ulcers were also reported by six patients (4 Conray and 2 Niopam). Most of these patients also complained of a sore throat. The development of a flu-like illness was relatively common, occurring in 101 patients receiving Conray and 88 patients receiving Niopam. Patients described feeling generally unwell with lassitude, lethargy, dizziness, sore throat, sore and runny eyes, sneezing, generalized aches, hot and cold flushes, shivers, catarrh and runny nose in various combinations. Several patients spent a day or two in bed because of this.

Twenty patients (2.9%) given Conray and 38 (5.6%) given Niopam answered "yes" to the question "Did you experience any swelling of the face or pain after eating?" However, analysis of the additional comments showed that many of these patients in fact experienced either generalized facial swelling or abdominal pain after eating, whereas some patients provided no comments additional to the "yes" answer.

Analysis of those comments available showed that six patients given Conray (three male, three female) and 12 given Niopam (six male, six female) described a reaction which could be ascribed to parotitis, with pain and swelling under the ear (unilateral in all but two cases), usually with a strange sensation or clicking in the jaw on eating, and often with earache. Six patients given Conray and five given Niopam reported a prolonged unpleasant taste in the mouth, usually for 3–4 days. None of these experienced this taste as an immediate reaction, and none of these patients had mouth ulcers or parotitis. None of the patients with mouth ulcers had parotitis.

A number of other delayed reactions emerged from analysis of the free text comments. A relatively common problem seemed to be low back and flank pain (unrelated to any presenting complaint). This was specifically mentioned by 18 patients given Conray and 24 given Niopam. Unless specifically contra-indicated, all patients had abdominal compression during the urogram, and this phenomenon might be related to this, combined with the 30 min or so lying on the X-ray table. Several patients spontaneously suggested that this might indeed be the cause.

Delayed symptoms of nausea, vomiting and abdominal pain were also not uncommon. This was reported by 33 patients given Conray (21 females) and 37 given Niopam (25 females). It emerged from the question concerning facial swelling that five patients given Conray and 11 given Niopam specifically mentioned abdominal pain on eating. Again this may possibly be related to compression. Seven of these patients also remarked on the symptom of heartburn, and gastro-oesophageal reflux may have been provoked or exacerbated by the compression. Headache was another symptom mentioned by 20 patients given Conray and 18 given Niopam. Diarrhoea was experienced by eight patients given

Conray and two given Niopam. Leg cramps were reported by 10 patients (5 Conray, 5 Niopam). Five patients given Conray and 17 given Niopam reported swelling of the face, hands and ankles.

Other reported delayed reactions included excessive perspiration (1 Conray, 2 Niopam), excessive thirst (2 Niopam), passing more urine than normal (2 Conray), visual blurring (4 Conray, 1 Niopam), stiffness and pain in the shoulders (2 Conray), numbness of the lower face, numbness of the left side of the body, teeth aching on eating, cold extremities and pain at the site of a BCG injection (1 each Conray), loss of voice and pins and needles in the neck and chest (1 each Niopam). One patient given Niopam reported that his pulse was normally slow (46) due to heart block, but this had speeded up to 70–80 since the injection and had remained at that rate ever since. One patient had a myocardial infarction 1 week after injection of Conray; he had no past history of heart disease. Ten per cent of the returned questionnaires contained favourable comments, usually complimenting and expressing gratitude to the staff.

2nd injection

Two hundred and eighty patients were given two injections, 135 (13.8%) being given Conray first and Niopam second (C1 N2) and 145 (14.5%) *vice versa* (N1 C2).

There was no significant difference in the number of patients experiencing a sensation of heat after the first injection (114 Conray (84.4%) and 109 Niopam (75.2%)); χ^2 test 3.71, *i.e.* not significant. However, after the crossover injection the numbers experiencing a sensation of heat were 86 (64%) (C1 N2) and 130 (90%) (N1 C2), giving a significant difference ($p < 0.001$).

Four patients receiving Conray first and Niopam second spontaneously commented on the difference between the two injections, recording the experience of side-effects such as heat and flushing with the first injection and not the second. Conversely, four patients receiving Niopam first and Conray second specifically mentioned that the second injection was unpleasant whereas the first was not. Thus eight patients preferred the Niopam injection and none preferred the Conray injection.

Pain in the arm occurred in nine patients (6.7%) (C1 N2) and 17 (11.72%) (N1 C2); this was not a significant difference, and approximately the same as after a single injection. There were two cases of intermediate reactions, one of chest pain and one of dyspnoea, both occurring in patients given Conray as a second injection. Four cases of sensitivity reactions occurred, all in patients given Conray as a second injection. Delayed rashes occurred in three (C1 N2) and four (N1 C2) patients, an incidence of approximately 2.5%, approximately the same as for a single injection of Conray. A flu-like illness occurred in 16 patients given Niopam first and in nine given Conray first (12% and 6%, respectively), approximately the same as for a single injection. Excluding arm pain, a total of 29 patients (18 male, 11 female) (10.4%) reported delayed reactions.

Risk factors and previous history

The total percentage of patients with so-called risk factors was 32.2%. There was, however, no excess of severe or sensitivity reactions in this group, nor was there any such excess amongst the 240 (12.1%) patients over the age of 70 years.

No difference was detected in reaction incidence in patients having had previous urography, except for nausea, which was more common the more urograms the patient had undergone. A history of sensitivity to aspirin, penicillin, Septrin, topical iodine and Elastoplast was sought, but this did not affect the incidence of any reaction.

Twelve patients experienced immediate rashes, four of these having a history of asthma, eczema or hayfever (out of a total of 145 with such a history). Therefore, eight out of 1554 with a negative history experienced an immediate rash. This difference is significant ($0.01 > p > 0.001$). However, there was no statistical difference in delayed rashes between the two groups: 49 of 1554 patients who had no history of atopy (3.2%) and nine of 145 patients with a history of allergy (6.2%). A χ^2 test was 3.75, p lying between 0.10 and 0.05.

Current medication appeared to have no effect on the incidence of reactions nor did a history of previous reactions. The same was true of a history of cardiac symptoms or disease. A total of 351 patients (17.7%) had had a previous contrast medium reaction, were sensitive to some applied agent or had a history of asthma, eczema or hayfever. Two hundred and eighty-six patients (14.5%) had a history of heart disease of whom 113 had symptoms.

We were unable to demonstrate any relationship between the incidence of any type of reaction and signs or symptoms of anxiety as recorded at the time of the examination.

We calculated the sample size necessary to achieve a p value of 0.05 with the percentage difference we found. This necessary sample size is in excess of 4000, *i.e.* four times the size of the present study. Such a study would need to last some 5 years in our hospital.

Discussion

This study has provided the opportunity to investigate the nature and incidence of both immediate and delayed reactions following the administration of a high-osmolar and a low-osmolar intravenous contrast medium in a large number of patients. It was not possible to study the intensity of the side-effects in such a large group of patients.

Immediate reactions to both types of media are well documented, although less attention has been paid to delayed reactions, despite the fact that these are relatively common (Panto & Davies, 1986). Much has been written concerning the safety of the newer, non-ionic, low-osmolality contrast media, although there are actually few clinical trials concerned with direct comparison of a high-osmolar and low-osmolar medium. One such trial (Dalla Palma et al, 1982) reached the conclusion that there was no justification for routine use of non-ionic contrast media in urography, both on the basis of radiographic quality and on the incidence of side-effects. Similar conclusions were reached by two more recent trials (Davies et al, 1985; Panto & Davies, 1986), iothalamate and iopamidol being studied in all three trials.

There is no doubt that, with low-osmolar contrast media, there is a reduction in both the incidence and intensity of many of the acute effects, particularly arm pain, sensation of heat, nausea and vomiting. The lower-osmolality medium has proved of great benefit in the field of angiography, reducing pain to such a degree that it allows examinations to be performed without general anaesthesia. Patients in our intravenous trial tended to find the examination with the non-ionic medium more agreeable.

Several patients who received both types of media were able to tell the difference between the two because of the difference in intensity of the sensations: the crossover method was particularly chosen to study this as scoring a sensation for intensity is notoriously inaccurate, especially with the large numbers of patients and injectors in this study.

The high-osmolar medium gave a significantly higher incidence of intermediate type reactions, and a definite trend towards increased sensitivity reactions. However, those reactions which did occur were transient and self-limiting, and there were no instances of severe or life-threatening reactions with either agent.

Our observations on acute effects of intravenous contrast media agree with the observations of others. Other authors (White & Halden, 1986) have concluded that a distinction should be made between statistically significant effects, such as nausea, vomiting and heat sensation (commoner with high-osmolar agents) and clinically significant effects, such as sustained ventricular fibrillation, renal failure and anaphylaxis, which are not proven to be reduced with low-osmolar media. Likewise, urticaria, hypotension and bronchospasm have so far not been proven statistically to be significantly less common with non-ionic agents in our series. Many authors recommend use of low-osmolar media for "high-risk groups" (Grainger, 1984; Wolf, 1986). These groups include infants, the elderly, patients with heart disease or a history of allergy, and a history of previous reactions.

We found in our study that a history of cardiac disease or symptoms and a history of a previous contrast reaction was not of high predictive value for acute reactions. There was, however, an increased incidence of acute rashes in those patients with an atopic history. The question of the value of an "allergic" history appears unresolved. It has been stated (Ansell et al, 1980) that a history of allergy is linked with an increased incidence of severe reactions. However, this view has been questioned (Lieberman et al, 1986) and the true relevance of such a history still appears open to debate. Low-osmolar non-ionic contrast media are believed to cause less reactivity in the complement activation, histamine release and coagulopathy systems (Spartaro, 1984), although the relation of this to significant reactions is unclear, and we would agree with other workers that it would be clinically prudent to use low-osmolar contrast media in patients judged to be at high risk.

Delayed reactions to intravenous contrast media are much more common than has previously been recognized. Whilst these reactions could not be termed medically serious or life-threatening, many patients found them quite unpleasant, some having to take time off work.

Panto and Davies (1986) found that symptoms of headaches, weakness, malaise, nausea, taste disturbance, diarrhoea, stomach pains, aching joints and upper respiratory symptoms occurred quite commonly after injection of contrast media and referred to this syndrome as "iodism". This label was attached as it corresponds with the dictionary definition. However, this may indicate to some people that the term indicates that the precise causation is known or at least that there is a coherent theory of the aetiology. No such aetiology is implied and the use of the term merely indicates a clinical observation. It may be better to refer to it as the "flu-like illness" or the post-intravenous-contrast-medium syndrome.

Parotitis, which may be part of this syndrome, may well be commoner with Niopam. Although parotitis is difficult to evaluate from the results of a written questionnaire, there were fairly classical descriptions of parotitis by 18 patients, 12 of whom had received Niopam. These appear to be the first cases of parotitis reported with non-ionic contrast media. In contrast to other reports (Sussman & Miller, 1956; Koch et al, 1969; Harris et al, 1970; Talner et al, 1971; Navani et al, 1972; Kohri et al, 1977; Cohen et al, 1980; Goldberg et al, 1984), most of our cases were unilateral. We also found that delayed rashes were commoner with Niopam.

Non-selective use of low-osmolar contrast media for all cases of urography in our department would add approximately an extra £20 000 per annum to the departmental budget. Our results do not justify such usage. Low-osmolar agents could be used in patients who had had a previous non-trivial reaction to contrast medium. In cases where there had been a severe reaction, the patient must freely consent to the procedure after explanation of the risks. If the previous reaction had truly been life-threatening it seems unlikely that such consent could be obtained whatever medium was used, as it is not possible to state that low-osmolar agents are completely safe; indeed deaths have occurred after their use. It would also seem appropriate to warn patients of the possibility of delayed effects, whatever contrast agent they receive.

It is usual to assume that a decreased incidence of certain types of non-fatal reactions indicates that a contrast medium is safer and less likely to cause death. The present results pose a dilemma for those holding such a view as acute trivial reactions were more common with Conray while many delayed reactions were more common with Niopam.

While many patients given both types of contrast media can tell the difference and prefer non-ionic injections, these agents are not free from side-effects and urography performed with them can still be an unpleasant experience. Our evaluation of so-called risk factors indicates they are poor predictors of an increase in reactions, except in the case of atopic individuals who experience more immediate rashes, though these are trivial and self-limiting. To evaluate these risk factors adequately, sample sizes of about 4000 for each medium are required. We believe the real risk factors are poor clinical condition, disease in more than one organ system, advanced disease, and cardiovascular instability, none of which is open to study in a controlled trial. These should be recognized clinically and the need for an intravenous urogram reviewed very carefully.

Conclusions

After a study of 1979 patients given 50 ml of either Niopam 300 (non-ionic/low osmolar) (855 patients) or Conray 325 (ionic/high osmolar) (844 patients) or both (280 patients), the following conclusions were reached.

(1) Patients seem to prefer non-ionic media, which gives them a more comfortable examination.

(2) Intermediate and sensitivity reactions are commoner with Conray.

(3) Delayed reactions are very common with both types of media, particularly arm pain, a flu-like illness and rashes. Delayed rashes and perhaps parotitis are commoner with non-ionic media.

(4) Routine use of non-ionic contrast media for urography does not appear justified.

Acknowledgments

We wish to acknowledge the secretarial assistance of Miss A Till, and we would also like to thank Professor Ronald Grainger for his help, encouragement and literary advice.

References

ANSELL, G. M., TWEEDIE, M. C., WEST, C. R., PRICE EVANS, D. A. & COUCH, L., 1980. The current status of reactions to intravenous contrast media. *Investigative Radiology, 15* (Suppl.), S32–39.

COHEN, J. C., ROXE, D. M., SAID, R. & CUMMINS, G., 1980. Iodine mumps after repeated exposure to iodinated contrast media. *Lancet, i*, 762–763.

DALLA PALMA, L., ROSSI, M., STACUL, F. & AGOSTINI, R., 1982. Iopamidol in urography. *Urologic Radiology, 4*, 1–3.

DAVIES, P., PANTO, P. N., BUCKLEY, J. & RICHARDSON, R. E., 1985. The old and the new: a study of five contrast media for urography. *British Journal of Radiology, 58*, 593–597.

GOLDBERG, R., GROSMAN, H., ST LOUIS, E. L. & GRAY, R. R., 1984. Contrast-induced sialadenitis—a case report. *Journal of Otolaryngology, 13*, 331–332.

GRAINGER, R. G., 1984. The clinical and financial implications of the low osmolar radiological contrast media. *Clinical Radiology, 35*, 251–252.

HARRIS, P. F., SANCHEZ, J. F. & MODE, D. G., 1970. Iodide Mumps. *Journal of the American Medical Association, 213*, 2271–2272.

KOCH, R. L., BYL, F. M. & FIRPO, J. J., 1969. Parotid swelling with facial paralysis, a complication of intravenous urography. *Radiology, 92*, 1043–1044.

KOHRI, K., MYOSHI, S., NAGAHARA, A. & OHTANI, M., 1977. Bilateral parotid enlargement (iodide mumps) following excretion urography. *Radiology, 122*, 654.

LIEBERMAN, P., SIEGLE, L. & TREADWELL, G., 1986. Radiocontrast reactions. *Clinical Reviews in Allergy, 4*, 229–245.

NAVANI, S., TAYLOR, C. E., KAUFMAN, S. A. & PARLEE, R. H., 1972. Evanescent enlargement of salivary glands following tri-iodinated salts used for intravenous urography. *British Journal of Radiology, 45*, 19–20.

PANTO, P. N. & DAVIES, P., 1986. Delayed reactions to urographic contrast media. *British Journal of Radiology, 59*, 41–44.

SPARTARO, R. F., 1984. Newer contrast agents for urography. *Radiological Clinics of North America, 22*, 365–380.

SUSSMAN, R. M. & MILLER, J., 1956. Iodide "mumps" after intravenous urography. *New England Journal of Medicine, 255*, 433–434.

TALNER, L. B., LANG, J. H., BRASCH, R. C. & LASSER, E. C., 1971. Elevated salivary iodine and salivary gland enlargement due to iodinated contrast media. *American Journal of Roentgenology, 112*, 380–382.

WHITE, R. I. & HALDEN, W. J., 1986. Liquid gold: low osmolality contrast media. *Radiology, 159*, 559–560.

WOLF, G. L., 1986. Safer, more expensive iodinated contrast agents: how do we decide? *Radiology, 159*, 557–558.

1989, *The British Journal of Radiology*, 62, 266–268

Technical note

An iodine-125 applicator designed for irradiating blood vessels growing into the cornea of the eye

By E. R. Hering, PhD, *R. Sealy, FRCR, J. B. Korrubel, HTS and †J. Hill, FRCS

Departments of Medical Physics, *Radiotherapy and †Ophthalmology, Groote Schuur Hospital and University of Cape Town, South Africa

(*Received December 1987 and in revised form November 1988*)

The invasion of the traumatized cornea by blood vessels is a well known complication and is often associated with graft rejection. Graft acceptance may be improved by the induction of endarteritis with β radiation but the corneal stroma may be so changed by the necessary dose of radiation (commonly 4500–5000 cGy in three or four fractions) as to significantly increase the risk of sloughing (Macfaul & Bedford, 1970). To overcome this problem, we have designed and made an ^{125}I eye applicator to produce an extremely narrow radiation field for treating the vascularization at the base of the cornea only. The anterior part of the cornea receives a very small dose of about 11% of that given to the base and is sufficiently large to receive a 6 mm corneal transplant.

Applicator design

The use of ^{125}I seeds in gold applicators for treating malignant conditions of the eye has been well documented (Sealy et al, 1980). Our applicator is designed to achieve a field width of 0.4 mm at the base of the cornea. Seeds were positioned in a gold applicator, a cross-section of which is shown schematically in Fig. 1. Beam divergence was minimized by having the ring of sources 3 mm from the surface of the cornea. This narrow field of radiation avoids a significant dose to the lens, ciliary body and the anterior cornea.

The applicator was manufactured in two halves which, when fitted together in a "pill box"-like manner, resulted in a closed, hollow, round container with an aperture in the middle containing a reproducible slit of 0.4 mm (Fig. 1). The slit width can be easily checked with a stainless steel wire of 0.4 mm diameter (Fig. 2). After fixing the sources in position with "Tensol" (Fig. 2), and fitting the two halves together (Fig. 3), the applicator is filled with isotonic saline solution to provide a tissue-equivalent medium. Two holes in the upper "lid" are used for this purpose (Figs 2, 3). The slit width is checked before filling the applicator with saline by inserting the stainless steel wire into it. The holes as well as the slit on the inside of the aperture are then sealed with a thin layer of bone wax to avoid evaporation.

The applicator is mounted on a stainless steel or gold base moulded to fit snugly onto the eye-ball (Figs 1–3). Four pairs of holes in the base are used for four silk stitching sutures round the four rectus muscles. If the applicator is stitched onto the eye in this way any movement of the eyeball will result in the applicator moving with it. Consequently, there will be no displacement of the slit during treatment. Since the single treatment could last a day or two (fractionation is not intended), any drying of the cornea is prevented by a thin plastic cap (Figs 1–3), which fits snugly onto the applicator. This can be filled with saline or an antibiotic ointment.

Dosimetry

The isodose-rate distribution in the plane of the slit as calculated on our TP-11 planning computer is shown in Fig. 4. Each of the 111 MBq seeds (11 in all) on the applicator was of the resin bead type without X-ray marker, *i.e.* code 6702 supplied by 3M. For the dose-rate calculation each seed was considered to consist of three point sources, one for each resin bead inside the seed. Because of the position of the seeds in the applicator, the dose-rate distribution is not affected by anisotropic radiation emission and unknown seed orientation (Ling et al, 1985; Prasad et al, 1987).

The calculated dose was checked with lithium fluoride thermoluminescent dosemeters placed at positions A to F in Fig. 1. A phantom eye was made using muscle equivalent material M3 (Markus, 1956) into which holes were accurately machined to take the LiF Ti, Mg chips of 4.8 mm diameter and 0.9 mm

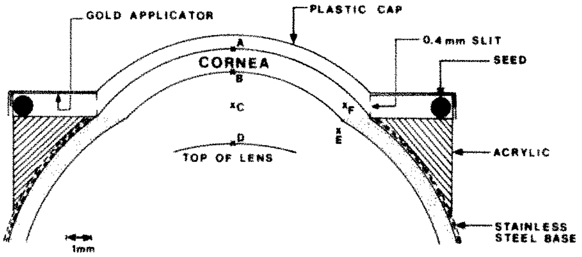

Figure 1. Schematic diagram of a cross-section through the corneal irradiator in position on the eye. A to F represent points at which the dose has been measured with lithium fluoride thermoluminescent dosemeters.

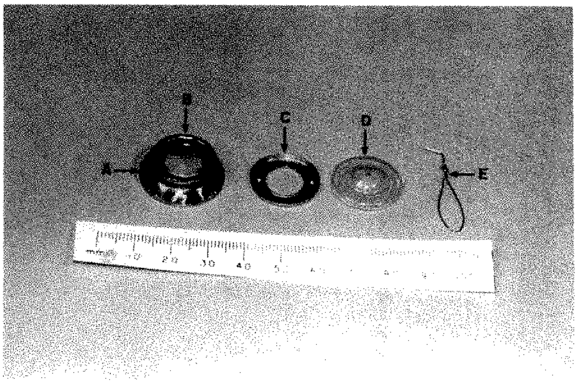

Figure 2. The various components of the irradiator. A, stainless steel base with holes for the sutures; B, bottom half of the gold applicator with seeds in position; C, top half of the gold applicator showing the holes for filling the applicator with saline; D, plastic cap; E, stainless steel wire for checking the width of the slit.

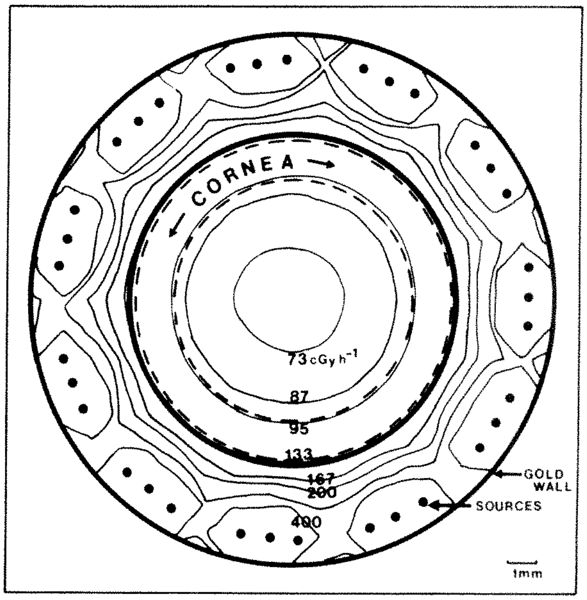

Figure 4. The dose-rate distribution calculated for a source activity of 111 MBq. Each source or seed consists of three resin beads with the activity adsorbed onto them.

thickness. For positions A to D the chips were stacked such that each of the individual points of measurement corresponded to the centre of a chip. For points E and F the chips were positioned vertically with the centre of the bottom and top end of each of the chips corresponding to points E and F, respectively. The applicator plus chip-loaded phantom was immersed in water during irradiation. The results of these measurements are shown in Table I for an irradiation time of 1 h. Because of limitations on our computer, comparisons with calculated doses could only be made for points C and F in the plane of the sources. It should also be noted that the measured doses extend over a region rather than a single point.

Iodine 125 has a half-life of 60 days, which means that the same applicator can be re-used on several patients during a period of about 2 months. Reloading of the applicator is a simple procedure. The applicator (without the plastic cap) is immersed in chloroform inside a stainless steel container for about 24 h, after which the loosened seeds can be easily replaced by new ones. The total dose to the finger tips for the seed change was measured with thermoluminescent dosemeters supplied by the South African Bureau of Standards. The maximum dose of 0.1 mSv was received by the right forefinger for a single source change.

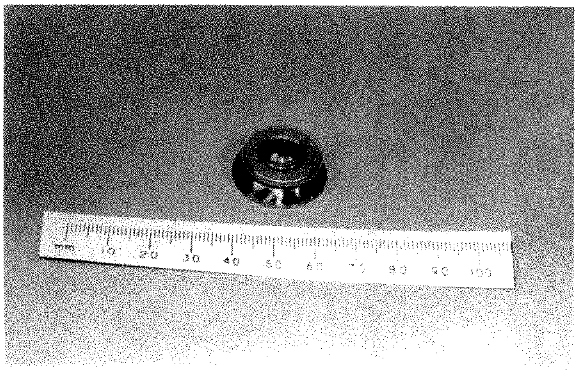

Figure 3. The assembled irradiator.

Radiobiology

Ultra-thin fields in themselves present interesting radiobiological questions regarding tolerance dose levels and the migration of cells across the field (Schoefl, 1963). None of the previous studies on the irradiation of the cornea (Gillette et al, 1975), on small skin fields (Peel et al, 1984) and on the canine brain (Fike et al, 1985), can be used to predict the radiation response in this new radiobiological situation.

We are therefore proceeding with radiobiological studies on rabbit cornea and the skin and blood vessels of the mouse tail for which a similar applicator has been made.

Table I. Results of dose-checking measurements

Dosemeter position	Measured dose ±(SEM) (cGy/h)	Calculated dose (cGy/h)
A	13.2 ± 2.1	—
B	15.6 ± 3.0	—
C	60.3 ± 6.1	72.5
D	10.0 ± 1.8	—
E	40.1 ± 7.2	—
F	117.6 ± 15.3	133.4

Acknowledgment

This work is supported by a grant from the South African Medical Research Council, the Ethics and Research Committee of the University of Cape Town, and the Teaching Hospitals Board (Cape Town).

References

Fike, J. R., Cann, C. E., Phillips, T. L., Bernstein, M., Gutin, P. H., Turowski, K., Weaver, K. A., Davis, R. L., Higgins, R. J. & DaSilva, V., 1985. Radiation brain damage induced by interstitial ^{125}I sources: a canine model evaluated by quantitative computed tomography. *Neurosurgery*, *16*, 530–537.

Gillette, E. L., Maurer, G. D. & Severin, G. A., 1975. Endothelial repair of radiation damage following beta irradiation. *Radiology*, *116*, 175–177.

Ling, C. C., Schell, M. C., York, E. D., Palos, B. B. & Kubiatowicz, D., 1985. Two-dimensional dose distribution of I-125 seeds. *Medical Physics*, *12*, 652–655.

Macfaul, P. A. & Bedford, M. A., 1970. Ocular complications after therapeutic irradiation. *British Journal of Ophthalmology*, *54*, 237–247.

Markus, B., 1956. Über den Begriff der Gewebeäquivalenz und einige "wasserähnliche" Phantomsubstanzen für Quanten von 10 keV bis 100 MeV sowie schnelle Elektronen. *Strahlentherapie*, *101*, 111–131.

Peel, D. M., Hopewell, J. W., Wells, J. & Charles, M. W., 1984. Nonstochastic effects of different energy beta emitters on pig skin. *Radiation Research*, *99*, 372–382.

Prasad, S. C., Bassano, D. A. & Fear, P. I., 1987. Dose distribution for ^{125}I implants due to anisotropic radiation emission and unknown seed orientation. *Medical Physics*, *14*, 296–298.

Schoefl, G. I., 1963. Studies on inflammation. III. Growing capillaries: their structure and permeability. *Virchow Archiv A, Pathological Anatomy and Histopathology*, *337*, 97–141.

Sealy, R., Buret, E., Cleminshaw, H., Stannard, C., Hering, E., Shackleton, D., Korrubel, J., le Roux, P. L. M. & Sevel, D., 1980. Progress in the use of iodine therapy for tumours of the eye. *British Journal of Radiology*, *53*, 1052–1060.

1989, *The British Journal of Radiology*, 62, 269–272

Case reports

Value of bone scanning and computed tomography in fibrodysplasia ossificans progressiva

By S. R. Carter, FRCS, *A. M. Davies, DMRD, FRCR, *N. Evans, FRCR and R. J. Grimer, FRCS

Bone Tumour Service and *Department of Radiology, Royal Orthopaedic Hospital, Birmingham

(*Received June 1988 and in revised form September 1988*)

Fibrodysplasia ossificans progressiva (FOP) (synonym: myositis ossificans progressiva) is an extremely rare congenital disorder characterized by unremitting heterotopic ossification associated with typical skeletal abnormalities (Rogers & Geho, 1979; Connor & Evans, 1982; Thickman et al, 1982). The prevalence in the UK population has been estimated to be less than 0.1 per million (Wynne-Davies et al, 1985) but despite this, or possibly because of it, there have been in excess of 700 publications worldwide on the subject (Illingworth, 1971) since the first description in 1692 (Patin, 1692).

We report a case of FOP presenting as a suspected soft-tissue neoplasm and discuss the value of bone scanning and computed tomography (CT) in the diagnosis and evaluation of this rare condition.

Case report

An 11-year-old boy first presented to his local Accident and Emergency department when his father noticed a large mass over the child's right scapula. The swelling was not tender and there was no history of trauma. Plain radiographs of the shoulder showed no abnormality and a clinical diagnosis of a haematoma was made. The swelling decreased in size over the next month but a further hot, tense mass developed over the left shoulder.

Biopsy of both masses was reported as showing muscle infiltrated with slender spindle cells in a myxoid stroma, and a pathological diagnosis of fibromatosis was made with the recommendation that total excision should be performed because of the risks of local recurrence. At referral to the Bone Tumour Service two further swellings had developed, one over the right sternomastoid muscle and the second on the left chest wall. These were associated with painless limitation of movement of the neck and both shoulder girdles.

Relevant past medical history included the fact that as an infant the patient had been noted to have minor congenital anomalies of both great toes for which no treatment was considered necessary. Clinically, his mother has a similar deformity of the feet but no radiographs were available. Seven years previously the patient had undergone tonsillectomy, adenoidectomy and bilateral myringotomies, since when he had been followed for low-tone deafness.

Apart from slight elevation of the serum calcium, alkaline phosphatase and C-reactive protein, all other laboratory investigations, including the erythrocyte sedimentation rate and creatine kinase levels were normal. The rheumatoid factor was negative and nerve conduction studies showed no evidence of a myositis.

Prior to referral, all the plain radiographs of the chest and shoulders were normal. On admission a bone scan and CT were obtained as part of the routine musculoskeletal tumour work-up. The bone scan revealed ectopic areas of increased activity with a nodular and linear bilateral distribution over the chest wall and in the paravertebral tissues (Fig. 1). No focus of abnormal uptake was evident overlying the lesion in the neck (Fig. 1a). Computed tomography demonstrated diffuse, hypodense swelling of the anterolateral muscles of the right side of the neck with swelling of the fascial planes (Fig. 2a). Focal calcification and linear ossification surrounded by hypodense oedema was identified within the soft tissues of the chest wall (Fig. 2b, c).

Following the bone scan and CT a limited skeletal survey was obtained which now confirmed the presence of ectopic ossification within the chest wall (Fig. 3) and lumbar paravertebral tissues. There was hypoplasia of the first metacarpals and first metatarsals (Fig. 4) with large plantar spurs (Fig. 5b). The cervical spine showed shortening of the antero-posterior diameter of the vertebral bodies with relative enlargement of the posterior arches and fusion of the arches of C3 and C4 (Fig. 5a). The diagnosis of FOP was therefore established in this case and surgical treatment of the lesions considered inadvisable.

Discussion

Fibrodysplasia ossificans progressiva is inherited as an autosomal dominant condition although most cases arise sporadically (Wynne-Davies et al, 1985). Similar deformities of the feet clinically apparent in the mother of this patient suggest that there may be variable genetic penetrance. The age of presentation with soft-tissue swellings is unusual in this case as the majority present within the first few years of life (Thickman et al, 1982). Although the clinical and radiological features are characteristic, a delay in reaching the correct diagnosis is common (Smith, 1975; Rogers & Geho, 1979; Connor & Evans, 1982). This is usually caused by a failure to appreciate the significance of the congenital abnormalities of the great toes (Connor & Evans, 1982) as had been the situation in this child when first seen almost a decade ago. This highlights the importance of recognizing the association, albeit uncommon, between congenital anomalies of the first rays of the hands and feet and various complex malformation syndromes (Poznanski, 1984). Similarly, the significance of deafness, detected 7 years before in this patient, and reported in

---

Address for correspondence: Dr A. M. Davies, Department of Radiology, Royal Orthopaedic Hospital, Woodlands, Northfield, Birmingham B31 2AP.

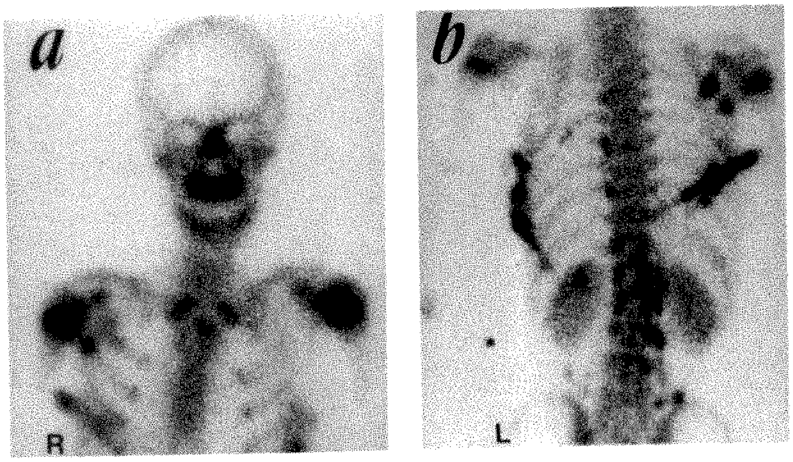

Figure 1. Bone scans. (a) Anterior image of the skull, neck and upper thorax showing ectopic activity over the right chest wall. (b) Posterior image of the thorax and spine showing linear and nodular activity over the chest wall and right paravertebral tissues.

almost one-quarter of all patients with FOP (Ludman et al, 1968; Rogers & Geho, 1979; Connor & Evans, 1982) may be overlooked.

The typical plain radiographic features of FOP as they affect the hands and feet (Fig. 4) are well documented (Rogers & Geho, 1979; Schroeder & Zasloff, 1980; Connor & Evans, 1982; Thickman et al, 1982). Within the spectrum of FOP a high proportion of patients also exhibit abnormalities of the cervical spine (Fig. 5a) consisting of small vertebral bodies with relative enlargement of the posterior arches. Progressive fusion can occur (Hall & Sutcliffe, 1979; Cremin et al, 1982) which may mimic the changes of Still's disease or the Klippel Feil syndrome (Connor & Smith, 1982).

Ossification of ligamentous insertions may produce pseudo-exostosis formation particularly from the proximal tibiae (Hall & Sutcliffe, 1979; Cremin et al, 1982). A prominent example is the calcaneal spur at the insertion of the plantar fascia (Fig. 5b) (Fairbank, 1950; Lutwak, 1964; Thickman et al, 1982) which is more florid than would be expected in an inflammatory enthesopathy due to a rheumatological disorder.

If the presence and significance of the underlying skeletal anomalies are not appreciated, the differential diagnosis at presentation with a soft-tissue mass includes soft-tissue sarcoma and fibromatosis. Once the ossification becomes apparent on the plain radiographs (Fig. 3) the differential diagnosis will then include post-traumatic myositis ossificans, dermatomyositis and the rare primary extraskeletal osteosarcoma.

The possibility of malignancy means that many of these patients undergo biopsy of the nodules. This is not to be recommended for two reasons. First, the histological appearances may be confusing and lead to misdiagnosis such as fibrosarcoma (Rogers & Geho, 1979) or fibromatosis as in this case. Secondly, it has long been recognized that trauma, including operation, may aggravate FOP and induce more rapid ossification (Rosenstirn, 1918; Rogers & Geho, 1979; Connor & Evans, 1982). The onus is therefore on the radiologist to play a preventative role in suggesting the correct diagnosis and thereby limiting the exposure of these patients to unnecessary invasive procedures (Thickman et al, 1982). In this respect both bone scanning and CT

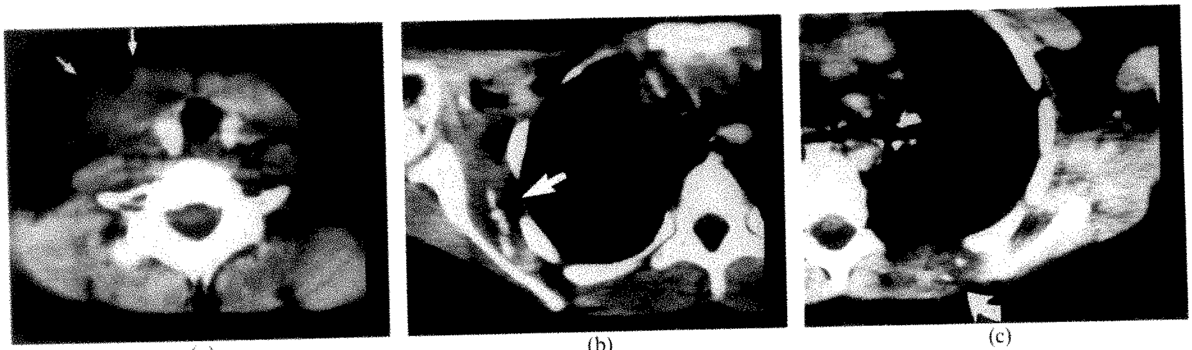
(a) (b) (c)

Figure 2. (a) Computed tomographic scan through the base of the neck showing a hypodense swelling of the right anterolateral musculature (small arrows) (sternomastoid, sternothyroid and sternohyoid muscles). (b) CT of right hemithorax showing linear ossification surrounded by oedema (arrow) deep to the subscapularis muscle. Small focus of calcification anteriorly in the axilla. (c) CT of left hemithorax caudal to Fig. 2b showing two small foci of calcification in the posterior muscles of the back (curved arrow), also surrounded by oedema.

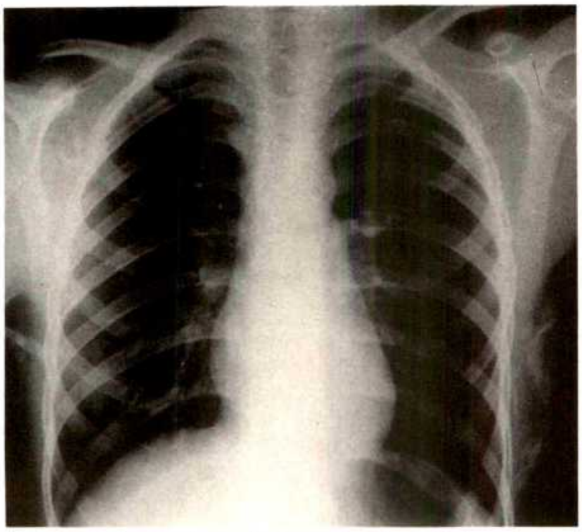

Figure 3. Chest radiograph 1 month after CT demonstrated ossification within the soft tissues of the chest wall bilaterally and underlying the scapula.

have a role to play in that both will reveal abnormalities before such changes are apparent on the plain radiographs (Lindhout et al, 1985; Fang et al, 1986; Reinig et al, 1986).

On a bone scan the increased uptake of the scanning agent is a sensitive indicator of active ossification and is known to produce positive scans in diverse conditions affecting the soft tissues such as post-traumatic myositis ossificans, dermatomyositis, scleroderma, diffuse pulmonary calcification and osteosarcoma metastases to the lungs and soft tissues (Choy & Murray, 1980). In both post-traumatic myositis ossificans and FOP, bone scans have been shown to demonstrate areas of soft-tissue activity prior to the appearance of changes on the plain radiographs (Suzuki et al, 1974; Fang et al, 1986)

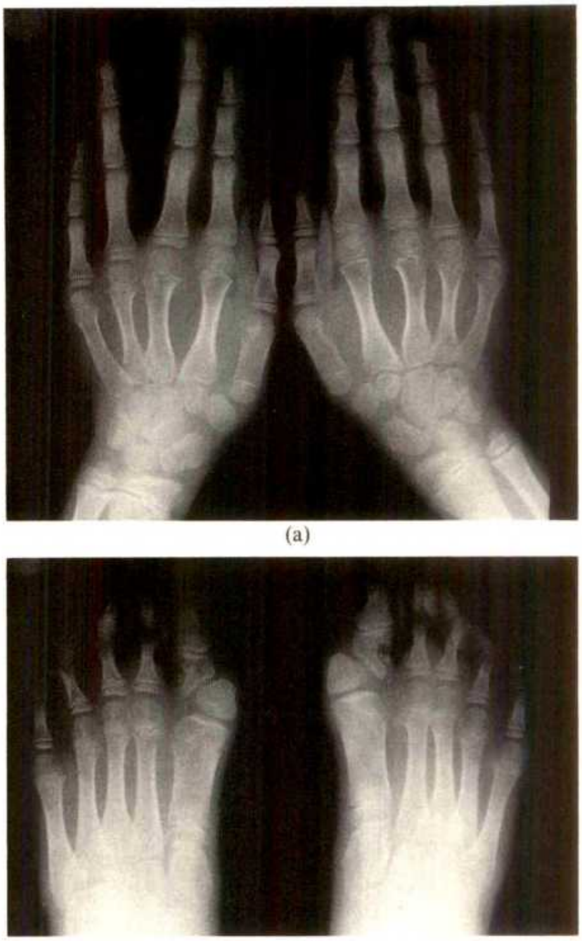

(a)

(b)

Figure 4. (a) Radiograph of the hands showing bilateral hypoplasia of the first metacarpals. (b) Radiograph of the feet showing bilateral valgus deformities and malformations of the phalanges of the great toes.

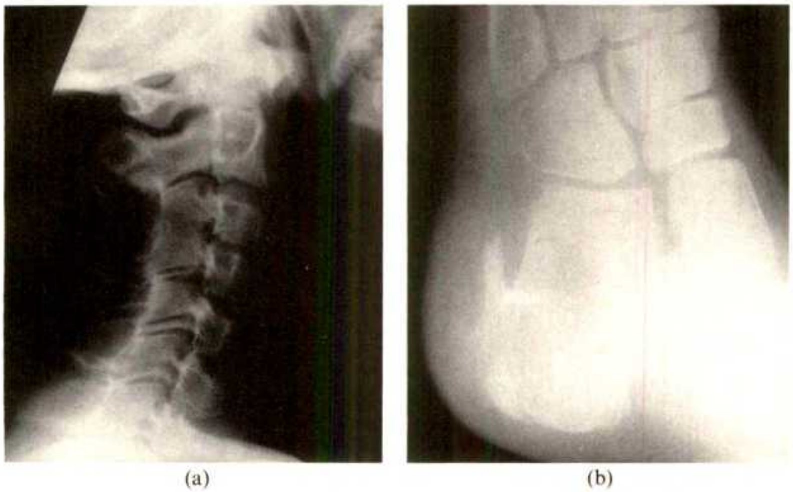

(a)

(b)

Figure 5. (a) Lateral cervical spine showing small vertebral bodies, relative enlargement of the posterior arches and fusion of the arches of C3 and C4. (b) Oblique radiograph of the left hindfoot showing a large plantar spur.

and in the current case the bone scan was the first examination to indicate the presence of heterotopic ossification (Fig. 1). Computed tomography will elegantly demonstrate small foci of calcification lying within the connective tissue between the muscles (Fig. 2c) and progressing to flattened sheets of ossification (Fig. 2b) which may extend partially or totally around the muscle (Reinig et al, 1986).

Prior to the onset of ossification the bone scan will not demonstrate the most acute lesions of FOP as shown by the absence of increased uptake in the neck of this patient at the site of the most recent swelling (Fig. 1a). Computed tomography, however, will demonstrate the early lesions of FOP by showing hypodense, oedematous swelling of the affected muscles and widening of the fascial planes (Fig. 2a) (Lindhout et al, 1985; Reinig et al, 1986).

Conclusion

Fibrodysplasia ossificans progressiva is an extremely rare congenital disorder but awareness of the associated skeletal abnormalities will enable the alert radiologist to suggest the correct diagnosis years before the onset of disability. Once there is soft-tissue involvement the bone scan is more sensitive than plain radiography in monitoring the extent of involvement (Fang et al, 1986). Although CT can fulfil this role, its most practical use is in revealing the nature and extent of the acute lesions which cannot be demonstrated by either plain radiography or bone scanning.

References

Choy, D. & Murray, I. P. C., 1980. Metastatic visceral calcification identified by bone scanning. *Skeletal Radiology, 5*, 151–159.

Connor, J. M. & Evans, D. A. P., 1982. Fibrodysplasia ossificans progressiva: the clinical features and natural history of 34 patients. *Journal of Bone & Joint Surgery, 64B*, 76–83.

Connor, J. M. & Smith, R., 1982. The cervical spine in fibrodysplasia ossificans progressiva. *British Journal of Radiology, 55*, 492–496.

Cremin, B., Connor, J. M. & Beighton, P., 1982. The radiological spectrum of fibrodysplasia ossificans progressiva. *Clinical Radiology, 33*, 499–508.

Fairbank, H. A. T., 1950. Myositis ossificans progressiva. *Journal of Bone & Joint Surgery, 32B*, 108–116.

Fang, M. A., Reinig, J. W., Hill, S. C., Marini, J. & Zasloff, M. A., 1986. Technetium-99m MDP demonstration of heterotopic ossification in fibrodysplasia ossificans progressiva. *Clinical Nuclear Medicine, 11*, 8–9.

Hall, C. M. & Sutcliffe, J., 1979. Fibrodysplasia ossificans progressiva. *Annales de Radiologie, 22*, 119–123.

Illingworth, R. S., 1971. Myositis ossificans progressiva (Munchmeyer's disease). Brief review with report of 2 cases treated with corticosteroids and observed for 16 years. *Archives of Diseases in Childhood, 46*, 264–268.

Lindhout, D., Golding, R. P. & Taets van Amerongen, A. H. M., 1985. Fibrodysplasia ossificans progressiva: current concepts and the role of CT in acute changes. *Paediatric Radiology, 15*, 211–213.

Ludman, H., Hamilton, E. B. D. & Eade, A. W. T., 1968. Deafness in myositis ossificans progressiva. *Journal of Laryngology and Otology, 82*, 57–63.

Lutwak, L., 1964. Myositis ossificans progressiva: mineral, metabolic and radioactive calcium studies of the effects of hormones. *American Journal of Medicine, 37*, 269–293.

Patin, G., 1692. In *Lettres Choisis de Feu M. Guy Patin.* Letter of August 27th, 1648 to A. F. (P. du Laurens, Cologne). Tome 1, vol. 5, p. 28.

Poznanski, A. K., 1984. *The Hand in Radiologic Diagnosis*, 2nd edn (W. B. Saunders, Philadelphia), pp. 244–248.

Reinig, J. W., Suvimol, C. H., Fang, M., Marini, J. & Zasloff, M. A., 1986. Fibrodysplasia ossificans progressiva: CT appearance. *Radiology, 159*, 153–157.

Rogers, J. G. & Geho, W. B., 1979. Fibrodysplasia ossificans progressiva: a survey of 42 cases. *Journal of Bone & Joint Surgery, 61A*, 909–914.

Rosenstirn, J. A., 1918. A contribution to the study of myositis ossificans progressiva. *Annals of Surgery, 68*, 591–637.

Schroeder, H. W. & Zasloff, M. A., 1980. The hand and foot malformations in fibrodysplasia ossificans progressiva. *John Hopkins Medical Journal, 147*, 73–78.

Smith, R., 1975. Myositis ossificans progressiva: a review of current problems. *Seminars in Arthritis and Rheumatism, 4*, 369–380.

Suzuki, Y., Hisada, K. & Takeda, M., 1974. Demonstration of myositis ossificans by Tc-99m pyrophosphate bone scanning. *Radiology, 111*, 663–664.

Thickman, D., Bonakdapour, A., Clancy, M., Orden, J. V. & Steel, H., 1982. Fibrodysplasia ossificans progressiva. *American Journal of Roentgenology, 139*, 935–941.

Wynne-Davies, R., Hall, C. M. & Apley, A. G., 1985. *Atlas of Skeletal Dysplasias* (Churchill Livingstone, Edinburgh), p. 547.

1989, *The British Journal of Radiology*, *62*, 273–274

Case reports

Ultrasound diagnosis of gallbladder perforation in a case of xanthogranulomatous cholecystitis

By J. P. Houston, MB, ChB, M. A. Sampson, MB, ChB, MRCP and
M. C. Collins, MB, ChB, FRCR

Department of Radiology, Royal Hallamshire Hospital, Glossop Road, Sheffield S10 2JF

(*Received May 1988*)

Cholelithiasis is a common disease and perforation and carcinoma of the gallbladder are well recognized complications. Xanthogranulomatous cholecystitis is an uncommon form of cholecystitis which is being recognized with increasing frequency. We report a case in which gallbladder perforation was diagnosed by ultrasound in a patient in whom all four conditions coexisted.

Case report

A 73-year-old woman presented with a 1-month history of rapidly worsening dementia following an episode of abdominal pain. Nine days before admission to hospital an abdominal swelling had been noticed. On examination she was pyrexial with a neutrophilia; there was a large, tender, fluctuant epigastric mass, pointing through erythematous skin.

Real-time ultrasound, using a 5 MHz sector probe, showed the gallbladder to be filled with calculi (Fig. 1). Medially, a well defined hypoechoic area characteristic of an abnormal fluid collection was identified around the anterior and inferior surfaces of the left lobe of the liver. Several 1–2 cm "bright" areas typical of calculi were seen layered in the dependent part of the collection moving appropriately with patient position (Fig. 2). No masses were seen. A diagnosis was made of perihepatic abscess secondary to gallbladder perforation and this was confirmed at laparotomy, 3 h later, when a perforated gallbladder was found with a perihepatic abscess containing calculi. The common bile duct, although dilated, was not obstructed.

Histological examination of the gallbladder revealed extensive xanthogranulomatous inflammation with fundal perforation. An adenocarcinoma was found in the wall, almost totally occluding the cystic duct. The gallbladder contained several stones of mixed composition.

Following surgery, the patient's condition deteriorated and she died 2 weeks later.

Discussion

We believe that in this patient gallbladder rupture resulted from the combination of an acute exacerbation of xanthogranulomatous cholecystitis associated with obstructed biliary drainage resulting from tumour occluding the cystic duct. Rupture led to the formation of a localized perihepatic abscess containing calculi.

Perforation of the gallbladder is a recognized complication of acute cholecystitis; it tends to occur at the relatively avascular fundus and carries a high mortality (Sherlock, 1985). The perforation is most commonly sub-acute and is walled off by peritoneal adhesions (Neimeier, 1934).

Findings on ultrasound in subacute gallbladder perforation have been previously described as hypoechoic areas of variable sonolucency (Bergman et al, 1979; Kane, 1980), but only one case has been described where the collection contained calculi (Madrazo et al, 1982).

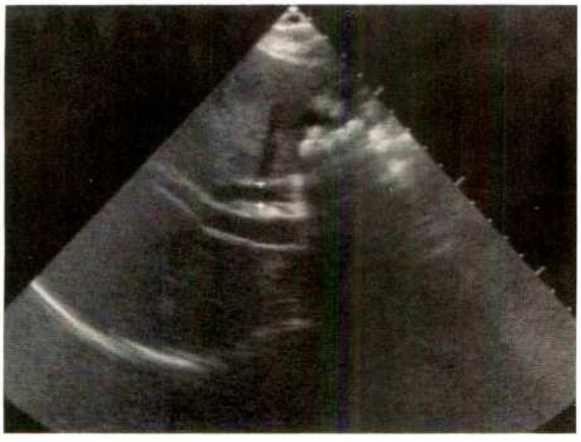

Figure 1. Oblique section through the right hypochondrium showing the gallbladder, containing numerous calculi, with the dilated common hepatic duct.

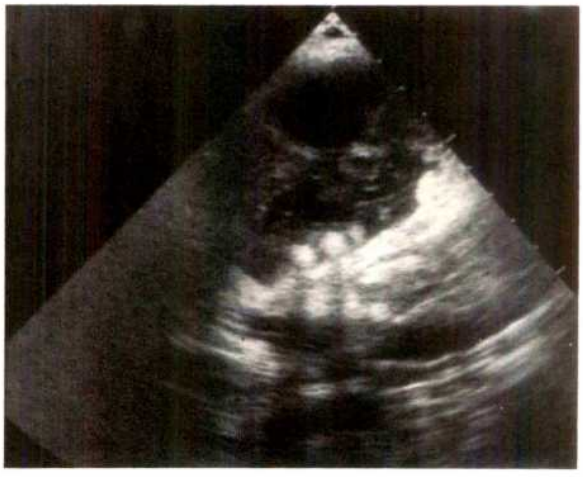

Figure 2. Longitudinal section through the epigastrium showing the hypoechoic area surrounding the left lobe of liver and containing low-level echoes and three calculi.

Xanthogranulomatous cholecystitis is an uncommon inflammatory disease of the gallbladder. It may present as acute, acute-on-chronic or chronic cholecystitis, with or without a right hypochondrial mass. It is characterized by yellow nodules in a thickened gallbladder wall and is morphologically similar to xanthogranulomatous pyelonephritis. The xanthogranulomatous tissue often extends to adjacent structures and fistulae may form. Recurrent infections in the presence of calculi are thought to be significant aetiological factors (Roberts & Parsons, 1987). An association with adenocarcinoma of the gallbladder has been noted (Goodman & Ishak, 1981).

In reports of the appearances on ultrasound in 23 cases of xanthogranulomatous cholecystitis (Bluth et al, 1979; Düber et al, 1984; Hanada et al, 1987; Lichtman & Varma, 1987; Roberts & Parsons, 1987), calculi were present in 96%. The gallbladder wall was thickened in 70%, appearing irregular in some and raising the suspicion of carcinoma. In four cases the disease appeared as a gallbladder mass. In a single case, gas in the biliary tree was found secondary to an enterobiliary fistula. To our knowledge there have been no previous reports of gallbladder perforation in xanthogranulomatous cholecystitis leading to abscess formation.

Adenocarcinoma of the gallbladder is an uncommon neoplasm whose association with gallstones is well established (Sherlock, 1985). In our case, although perforation was correctly diagnosed on ultrasound, neither xanthogranulomatous cholecystitis nor carcinoma was suspected pre-operatively.

In conclusion, the presence of calculi in a perihepatic collection in association with an obstructed biliary tree indicates that gallbladder rupture has occurred and urgent surgery is required. Recognition of such complex, multiple pathology pre-operatively may significantly affect the prognosis.

References

BERGMAN, A. B., NEIMAN, H. L. & KRAUT, B., 1979. Ultrasonographic evaluation of pericholecystic abscesses. *American Journal of Roentgenology*, *132*, 201–203.

BLUTH, E. I., KATZ, M. M., MERRITT, C. R. B., SULLIVAN, M. A. & MITCHELL, W. T., 1979. Echographic findings in xanthogranulomatous cholecystitis. *Journal of Clinical Ultrasound*, *7*, 213–214.

DÜBER, C., STÖRKEL, S., WAGNER, P. K. & MÜLLER, J., 1984. Xanthogranulomatous cholecystitis mimicking carcinoma of the gall bladder: CT findings. *Journal of Computer Assisted Tomography*, *8*, 1195–1198.

GOODMAN, Z. D. & ISHAK, K. G., 1981. Xanthogranulomatous cholecystitis. *American Journal of Surgical Pathology*, *5*, 653–659.

HANADA, K., NAKATA, H., NAKAYAMA, T., TSUKAMOTO, Y., TERASHIMA, H., KURODA, Y. & OKUMA, R., 1987. Radiologic findings in xanthogranulomatous cholecystitis. *American Journal of Roentgenology*, *148*, 727–730.

KANE, R. A., 1980. Ultrasonographic diagnosis of gangrenous cholecystitis and empyema of the gall bladder. *Radiology*, *134*, 191–194.

LICHTMAN, J. B. & VARMA, V. A., 1987. Ultrasound demonstration of xanthogranulomatous cholecystitis. *Journal of Clinical Ultrasound*, *15*, 342–345.

MADRAZO, B. L., FRANCIS, I., HRICAK, H., SANDLER, M. A., HUDAK, S. & GITSCHLAG, K., 1982. Sonographic findings in perforation of the gall bladder. *American Journal of Roentgenology*, *139*, 491–496.

NEIMEIER, O. W., 1934. Acute free perforation of the gall bladder. *Annals of Surgery*, *99*, 922–924.

ROBERTS, K. M. & PARSONS, M. A., 1987. Xanthogranulomatous cholecystitis: clinico-pathological study of 13 cases. *Journal of Clinical Pathology*, *40*, 412–417.

SHERLOCK, S., 1985. *Diseases of the Liver and Biliary System*, 7th edn. (Blackwell, Oxford), pp. 515–516, 543–544.

Giant central disc prolapse: a pitfall in computed tomographic diagnosis

By G. Buirski, MRCP, FRCR

Royal Melbourne Hospital, Melbourne 3050, Australia

(*Received July 1988 and in revised form October 1988*)

The diagnosis of lumbar disc prolapse by computed tomography (CT) is now well established and is often the initial investigation in patients with sciatica (Buirski, 1987). Myelography, however, is still necessary when the CT findings do not correlate with the clinical features or when an intrathecal abnormality is suspected. Occasionally, giant extruded disc fragments may lie within the central spinal canal either above or below the adjacent disc level. If the central canal is totally occupied by the disc then the characteristic CT appearances of an extradural mass may not be readily apparent. The case reported below illustrates this problem and a useful radiological sign on CT is discussed.

Case report

A 26-year-old woman initially presented in April 1987 with back pain associated with walking. This was treated conservatively with anti-inflammatory drugs and physiotherapy with good symptomatic relief. In October she noted paraesthesiae in both feet and shortly after developed pain

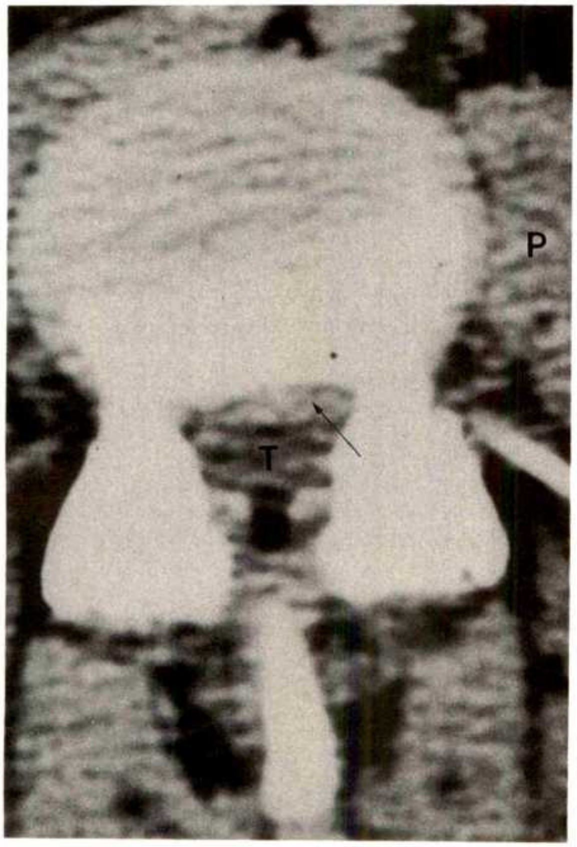

Figure 1. Coaxial CT scan through the L4/5 disc space showing only a mild central disc bulge slightly to the left of the midline (arrow). Note that the thecal sac (T) has an attenuation visibly lower than the psoas muscle (P).

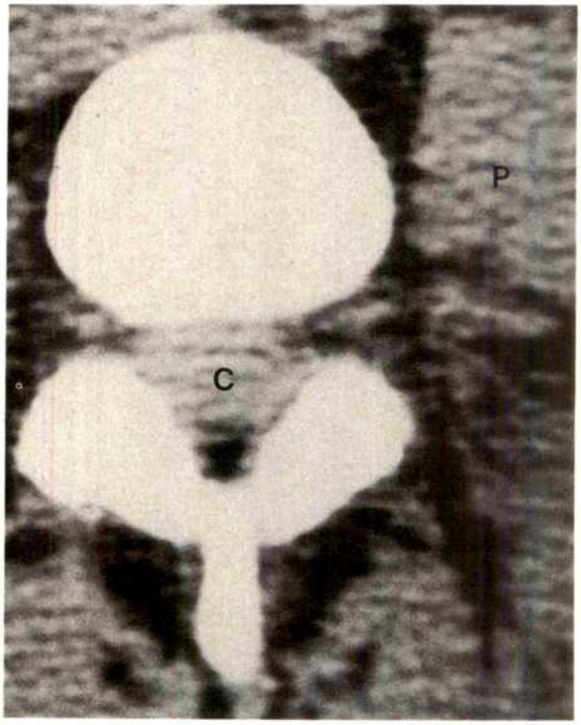

Figure 2. A coaxial CT scan showing that the central canal (C) just below the level of the pedicles of L4 has a higher attenuation than the adjacent psoas muscle (P). The thecal sac is totally obliterated.

down the right thigh. Following a minor fall 1 month later her symptoms worsened and she had some difficulty in walking. At no stage was there bladder or bowel dysfunction. Neurological examination revealed decreased muscle power in both legs with loss of the normal ankle reflexes; no other abnormality was demonstrated. The clinical diagnosis was a cauda equina lesion, possibly disc or tumour.

Routine haematological and biochemical estimations were normal. A CT examination of the lumbar spine was performed using a GE 9800 scanner. The scan protocol consisted of a stacked sequence of 5 mm contiguous images from L3 to S1, including angled coaxial scans through each of all the lumbar discs. Computed tomography showed no significant discrete disc prolapse at any adjacent disc level except for a mild postero-lateral bulge at L4/L5 (Fig. 1). However, the apparent thecal sac within the central canal above the L4/5 disc had a visibly higher attenuation than the theca at comparative levels (Fig. 2). This suggested the presence of an extradural mass within the canal, possibly a large sequestrated disc fragment causing complete obliteration of the normal thecal sac. A myelogram was recommended and confirmed the presence of an extradural mass, later proven to be disc material at surgery (Fig. 3).

Since this example, a further two patients with the "dense thecal sac" sign have been seen. The provisional radiological diagnosis of a sequestrated disc was confirmed by CT myelography studies in both cases.

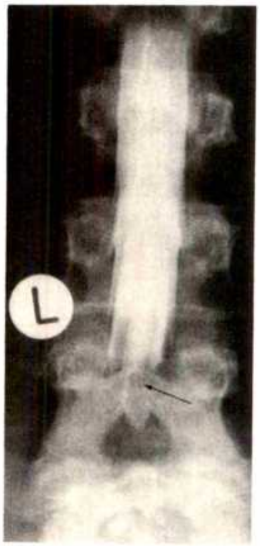

Figure 3. The myelogram demonstrates a complete extradural spinal block at the interpedicular level of L4 (arrow). This was proven to be disc material at surgery.

Discussion

Disc prolapse at an adjacent disc level is often easily recognized on CT: the presence of a high-attenuating mass, compression of the thecal sac and displacement of the associated nerve root are all features suggesting the diagnosis. The presence of epidural fat around the thecal sac and nerve roots allows these structures to be identified and any asymmetry may indicate pathology. Sequestration of a disc fragment into other parts of the spinal canal may be missed when scanning only the disc spaces but should be identified when contiguous scans are available. If the fragment is large and lies in the central canal, the thecal sac may be so compressed that the differences in the CT attenuation between the thecal sac and disc cannot be appreciated. In addition, the absence of nerve roots and epidural fat in this region eliminates the other radiological signs that may be helpful.

The importance of the density of the thecal sac has not been stressed previously. Normally the attenuation of the thecal sac is less than that of the surrounding muscles. This can best be confirmed by comparison with the adjacent psoas muscle. If the central canal has an attenuation higher than or equal to the psoas then a giant central disc protrusion or other extradural mass must be excluded. If necessary, measurements of CT attenuation numbers may be helpful. In the case presented, the difference in density was visibly apparent on the images (Figs 1, 2) and attenuation values were not required. Magnetic resonance imaging, myelography or a CT myelogram should be the next investigation of choice.

The "dense thecal sac" sign should be recognized by radiologists as it may be the only clue to significant pathology in the lumbar spine. This case illustrates another pitfall of CT interpretation in lumbar spine disease (Braun et al, 1984).

References

BRAUN, I. F., LIN, J. P., GEORGE, A. E., KRICHEFF, I. I. & HOFFMAN, J. C., 1984. Pitfalls in the computed tomographic evaluation of the lumbar spine in disc disease. *Neuroradiology*, *26*, 15–20.

BUIRSKI, G., 1987. The investigation of sciatica and low back pain syndromes: current trends. *Clinical Radiology*, *38*, 151–155.

Submarine escape training, lung cysts and tension pneumothorax

By W. R. Saywell, MA, FRCR

Royal Naval Hospital, Haslar, Gosport, Hampshire

(*Received July 1988*)

Submariners in the Royal Navy are required to undergo escape training, which is performed in a water-filled tower. Entry is gained via air-locks at depths of 9, 18 and 27 m. The subjects ascend to the surface exhaling continuously to compensate for the increased gas volume in the lungs as the pressure decreases. Divers are in the water as safety attendants, and a medical team including a doctor is on standby. Prior to escape training, chest radiography is performed in full inspiration and full expiration. Particular attention is paid to areas of reduced compliance (*e.g.* scarring) and evidence of air-trapping, either of which may pre-dispose to pulmonary barotrauma (Liebow et al, 1959; Campbell-Golding et al, 1960; Calder, 1985).

Case report

The subject of this report is a 21-year-old man who had an apparently normal chest radiograph (Fig. 1) and no significant previous medical history. He made an initial ascent from 9 m, during which he experienced transient right-sided chest pain. Examination by the Medical Officer revealed no abnormality and a further ascent from 9 m was made. On completion of this ascent he emerged from the water pale and unsteady, complaining of dizziness and diplopia, but with no evidence of chest pain or dyspnoea. He was immediately recompressed to 50 m. A Medical Officer entered the compression chamber and found evidence of barotrauma to the ears, but no other abnormalities. The subject was given intravenous dexamethasone and decompressed in accordance with a standard therapeutic table, RN Table 63 in *The Royal Navy Diving Manual* (HMSO, 1972). During the final 9 m slow ascent he complained of pain in the ears and right side of the chest. Examination on emerging from the chamber revealed evidence of a right-sided pneumothorax, and the patient was transferred to hospital.

The chest radiographs on admission (Fig. 2) confirmed the presence of a right-sided pneumothorax and showed curvilinear shadowing around the right hilum. A chest drain was immediately inserted and a further chest radiograph on the same day showed the right lung to have re-expanded revealing a number of well defined cystic lesions of varying sizes in the right mid and lower zones.

Over the next 2 weeks there were a number of recurrences of the pneumothorax, and the cystic lesions were seen gradually to fill with fluid (Fig. 3). It became apparent that a broncho-pleural connection had developed and that the right lung would not remain inflated. The patient was then transferred to a specialist thoracic unit where right thoracotomy was performed. This revealed that the pleural space was free, with a small serous effusion. All three lobes of the lung contained multiple cysts ranging in size from 2 mm to 5 cm and superficial blebs. The cyst walls were extremely friable and burst on the slightest touch. The cysts were shown to consist of normal lung tissue, with pulmonary vessels running unsupported within the wall. Partial pleurectomy and full pleurodesis were performed and the patient made an uneventful post-operative recovery.

Computed tomography was performed to assess the right lung, and to establish whether there were corresponding

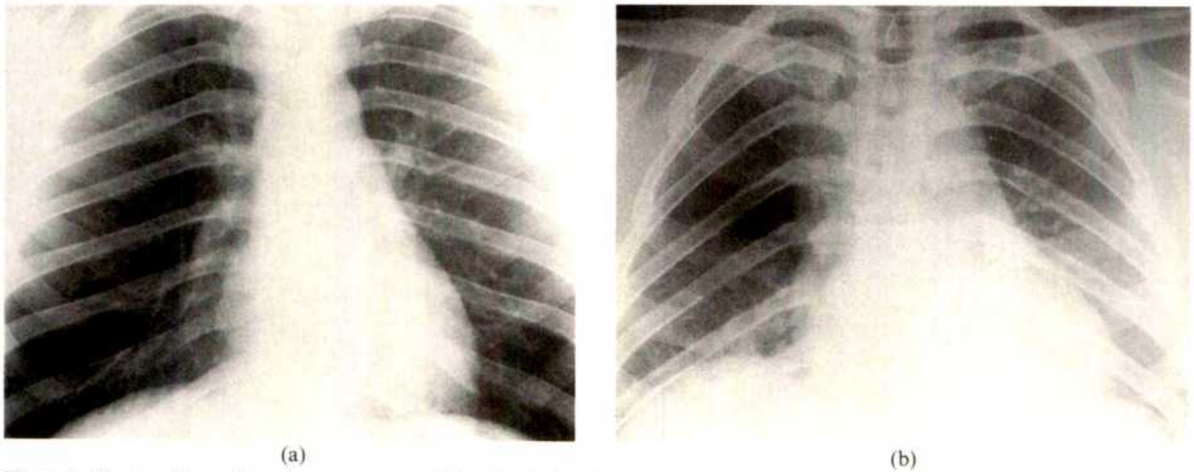

(a) (b)

Figure 1. Chest radiographs prior to escape training: (a) inspiration and (b) expiration.

abnormalities in the left lung (Fig. 4). Multiple cysts of varying sizes were shown throughout all three lobes of the right lung, but the left lung was of normal appearance.

Discussion

A computerized literature search has been unable to locate any other cases of pneumothorax following pressure changes in subjects with intrapulmonary lung cysts. There are reports of superficial blebs or bullae in association with pneumothorax or other barotrauma, but it has not been possible to ascertain whether these bullae or blebs have been the cause or effect of the barotrauma (Liebow et al, 1959; Collins, 1966; Okalyi, 1969; Calder, 1985). Campbell-Golding et al (1960)

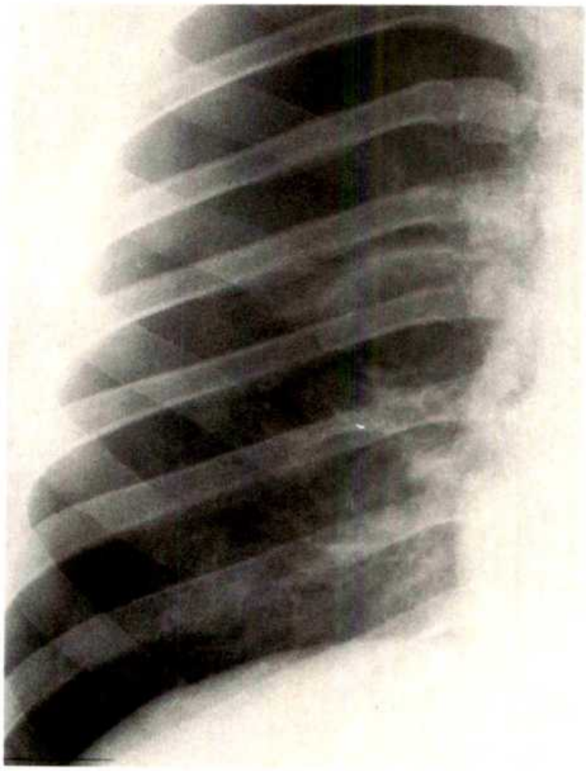

Figure 2. Chest radiograph on admission. Right pneumothorax and large air-filled cysts are clearly visible.

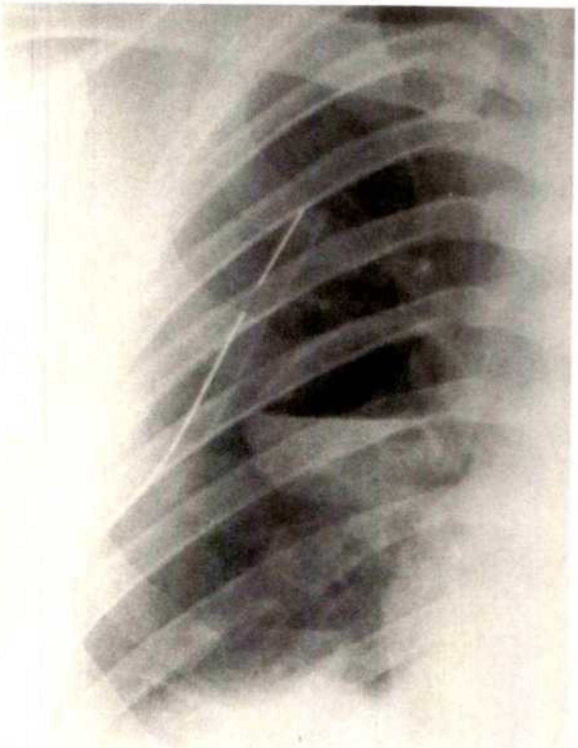

Figure 3. Chest radiograph 12 days after admission. The largest cyst is almost half-filled with fluid. The lung remains inflated with the chest drain *in situ*.

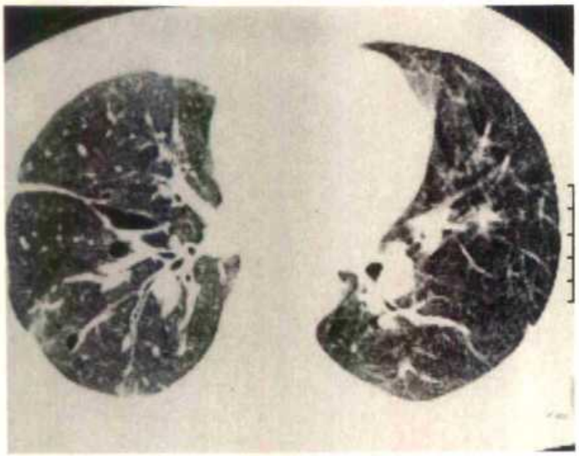

Figure 4. Computed tomographic scan 6 weeks after admission. The patient has made a good recovery from surgery. Intrapulmonary as well as superficial cysts are demonstrated. An air–fluid level is seen in the right main fissure. The left lung is of normal appearance.

report two cases of intrapulmonary cysts, but these were in cases of "bends" rather than pneumothoraces, and there were no previous radiographs, making the establishment of cause or effect impossible. In the current case, pre-morbid chest radiography taken only days before the incident are available (Fig. 1). Whilst initially reported as normal, retrospective assessment shows distinct areas of low attenuation corresponding to the sites of some of the larger of the subsequently demonstrated cysts. In particular, the area adjacent to the right hilum is of lower attenuation than the corresponding area on the left. These differences are slightly more apparent in the expiratory radiograph (Fig. 1b), as would be expected in the presence of a cyst.

Computed tomography shows a number of intrapulmonary cysts, in addition to the subpleural blebs seen at operation. Previously these have been attributed to the barotrauma. In this case there is radiographic evidence of pre-existing intrapulmonary cysts.

Although few radiologists are required to report chest radiographs for submarine escape training, similar pressure changes may occur during hyperbaric therapy (Unsworth, 1973), commercial diving, sport (scuba) diving and compressed air (caisson) construction working. Breath-hold diving does not have this risk, as the lung volume at the surface is reduced on descending, and merely returns to its original volume on ascending. It should be borne in mind that the dive does not have to be very deep to produce a risk of barotrauma. Gas within the lungs expands in accordance with Boyle's law, and in shallow water a relatively small change in depth can lead to a large change in volume.

Evidence of lung cysts or other causes of air trapping should be considered a contra-indication to the occupations listed above.

Acknowledgment

I am grateful to Surgeon Commander O. M. Howard, MRCP, Royal Navy, Consultant Physician, for permission to report his patient.

References

Calder, I. M., 1983. Autopsy and experimental observations on factors leading to barotrauma in man. *Undersea Biomedical Research, 12*, 165–182.

Cambell-Golding, F., Griffiths, P., Hempleman, H. V., Paton, W. D. M. & Walder, D. N., 1960. Decompression sickness during construction of the Dartford Tunnel. *British Journal of Industrial Medicine, 17*, 167–180.

Collins, J. J., 1966. An unusual case of air embolism precipitated by decompression. *New England Journal of Medicine, 266*, 595–598.

HMSO, 1972. *The Royal Navy Diving Manual* (Her Majesty's Stationery Office, London).

Liebow, A. A., Stark, J. E., Vogel, J. & Schaeffer, K. E., 1959. Intra-pulmonary air trapping in submarine escape training casualties. *United States Armed Forces Medical Journal, 10*, 265–289.

Okalyi, Z., 1969. Occupational mortality and morbidity among divers in the Torres Straits. *The Medical Journal of Australia, 1*, 1239–1242.

Unsworth, I. P., 1973. Pulmonary barotrauma in a hyperbaric chamber. *Anaesthesia, 28*, 675–678.

1989, *The British Journal of Radiology*, 62, 279–280

Case of the month

The misleading pre-operative chest radiograph

By *Janet Ipinyomi and Iain Watt

Department of Radiology, Bristol Royal Infirmary, Bristol BS2 8HW

(*Received September 1987 and in revised form June 1988*)

A 66-year-old man presented to the Accident and Emergency Department with pain in the right hip and difficulty in weight bearing after falling in the street that morning. He smoked about 15 cigarettes a day and had a wheeze which was relieved by Salbutamol. No other relevant history was elicited, apart from a vague story of ill defined upper chest pain in the past.

On examination he was observed to walk with a limp. His right hip was externally rotated, with limitation of movement because of pain. His right lower limb was 2 cm shorter than the left. Radiographs of the pelvis and chest and an apical view are shown in Figs 1 and 2 and frontal tomography of the chest was subsequently performed (Fig. 3).

What are the abnormalities demonstrated? What differential diagnosis should be considered and what might skeletal scintigraphy reveal?

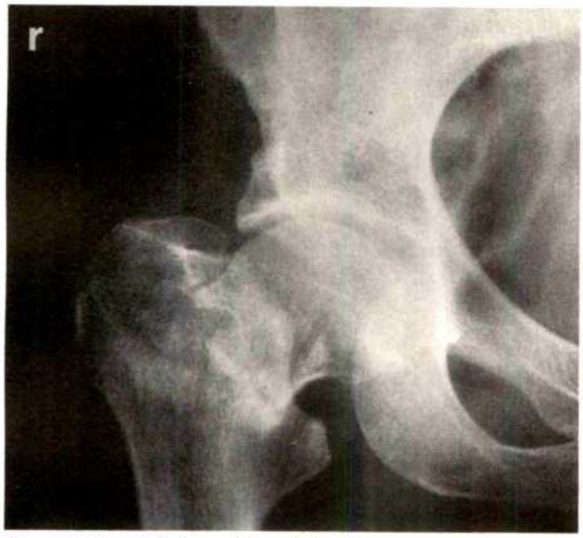

Figure 1. Frontal view of the right hip at presentation to the Casualty Department.

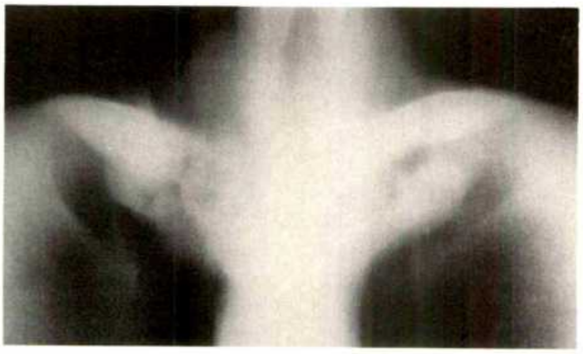

Figure 3. Frontal tomogram of the upper chest.

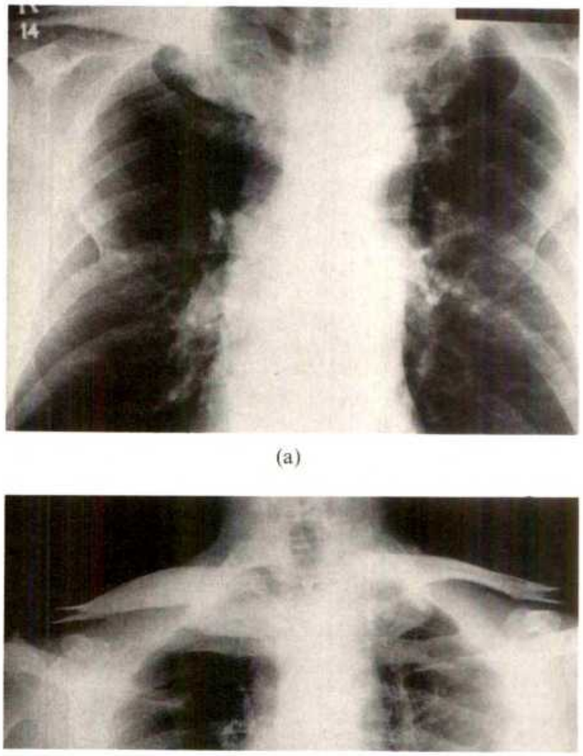

(a)

(b)

Figure 2. (a) Frontal and (b) apical views of the chest.

---

*Current address: X-ray Department, Kwara State Specialist Hospital, PMB 1452, Sobi-Ilorin, Kwara State, Nigeria.

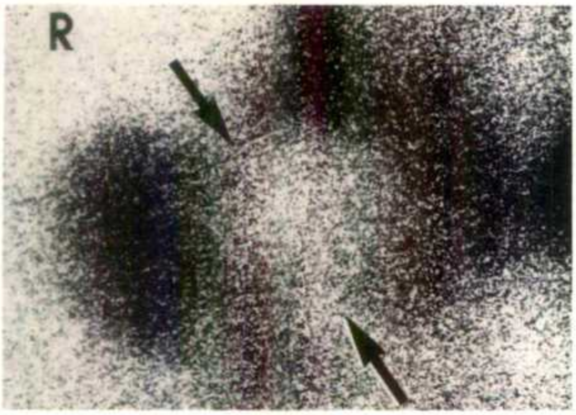

Figure 4. Late phase of an HDP bone scintigram, centred over the right upper femur and hip.

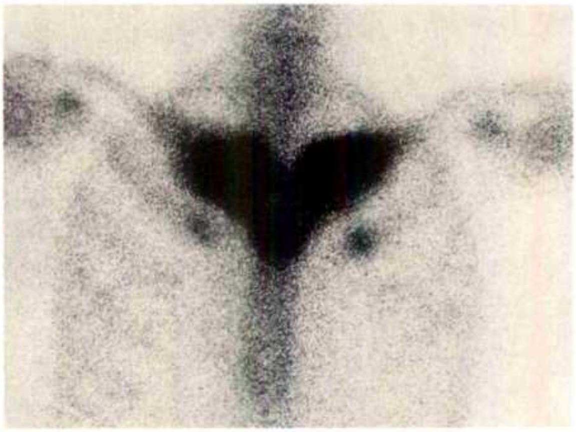

Figure 5. Late phase scintigram centred over the upper anterior chest.

A bone scintigram was performed a few days after admission to hospital. The right femoral head was imaged to assess vascularity (Fig. 4). Increased activity was shown at the fracture site but the femoral head was photon deficient. Delayed views of the upper thorax demonstrated marked activity in both clavicles medially, the manubrium and anterior upper ribs (Fig. 5). What is the diagnosis?

Discussion

Post-traumatic avascular necrosis and sternocostoclavicular hyperostosis were diagnosed. The pelvic radiograph reveals a transcervical fracture of the femur. The chest radiograph demonstrated no lung or mediastinal lesions but an ill defined opacity overlying the apices. An apical lordotic view confirmed that the apices were normal, the opacities being shown to be bony, corresponding to considerable sclerosis of the clavicles, first ribs and first costal cartilages. This was confirmed tomographically (Fig. 3). An initial impression of an apparent apical abnormality raised the possibility of a Pancoast tumour with, possibly, a pathological fracture of the femur, but the subsequent demonstration of sclerotic clavicles opened up a further differential diagnosis, including Paget's disease and prostatic metastases. No abnormality of blood chemistry was found, apart from a slight increase in serum alkaline phosphatase to 15 (normal range 3–13) KA units, consistent with a recent fracture.

The bone scan shows increased activity over the upper chest confirming considerably increased bone activity in the abnormal areas shown on plain radiography. Avascular necrosis of the right femoral head was also shown. Histological examination of the femoral head and neck at subsequent total hip replacement confirmed recent avascular necrosis and revealed no evidence of any other pathology.

The sclerotic clavicles, sternum and first ribs result from a disorder known as sternocostoclavicular hyperostosis with no known relevance to the fracture of the femoral neck. Sternocostoclavicular hyperostosis is a benign disorder characterized by hyperostosis and soft-tissue ossification between the clavicles, anterior portions of upper ribs and sternum. It was first reported in 1974 (Sonozaki et al, 1974) and over 50 cases have been described, mainly in the Japanese literature. The aetiology is unknown, but the condition may be more common than presently recognized. Males are affected more than females and patients are usually middle-aged (30–50 years), presenting with chronic upper chest pain of several years duration, local bullous eruptions and some with pustulosis palmaris et plantaris. Similar skin lesions are also described in chronic recurrent multifocal osteomyelitis which affects a younger age group (Cyrlak & Pais, 1986). A few reported cases had psoriasis for several years (Colhoun et al, 1987). The current patient did not present with any of the above symptoms, apart, perhaps, from his vague history of chest pain.

Local complications include bony overgrowth which may lead to a wide, thick sternum and occlusion of subclavian veins. Other associated skeletal disorders have included sacroiliitis and abnormalities of the spine similar to diffuse idiopathic skeletal hyperostosis (DISH), ankylosing spondylitis and peripheral inflammatory arthritis (Sartoris et al, 1986). Laboratory findings include raised erythrocyte sedimentation rate, positive C-reactive protein, and elevated α2 globulin. Rheumatoid factors are characteristically absent.

Differential diagnosis includes other sclerosing conditions of the clavicles, in particular osteoblastic metastasis, Paget's disease, chronic sclerosing osteomyelitis and condensing osteitis of the clavicles (Franquet et al, 1985). Osteoblastic metastases are rarely isolated to the clavicles. Paget's disease may affect the clavicles, but other bones are typically involved; the clavicles are usually expanded and bony fusion with the ribs and sternum is unlikely. Chronic sclerosing osteomyelitis may have similar appearances but is seldom symmetrical. Very early stages of sternocostoclavicular hyperostosis may simulate condensing osteitis of the clavicles. The latter, however, tends to affect a younger age group and is not progressive.

References

COLHOUN, E. N., HAYWARD C. & EVANS, K. T., 1987. Inter-sterno-costo-clavicular ossifications. *Clinical Radiology*, *38*, 33–38.

CYRLAK, D. & PAIS, M. J., 1986. Chronic recurrent multifocal osteomyelitis (CRMO). *Skeletal Radiology*, *15*, 32–39.

FRANQUET, T., LECUMBERRI, F., RIVAS, A., INARAJA, L. & IDOATE, M. A., 1985. Condensing osteitis of the clavicle. *Skeletal Radiology*, *14*, 184–187.

SARTORIS, D. J., SCHREIMAN, J. S., KERR, R., RESNICK, C. S. & RESNICK, D., 1986. Sternocostoclavicular hyperostosis: a review and report of eleven cases. *Radiology*, *158*, 125–128.

SONOZAKI, H., FURUSAWA, S., SEKI, H., KUROKAWA, T., TATEISHI, A. & KABATA, K., 1974. Four cases with symmetrical ossifications between the clavicles and the first ribs of both sides. *Kanto Journal of Orthopedics and Trauma*, *5*, 244–247.

1989, *The British Journal of Radiology*, 62, 281–282

Short communications

Effects of inhibition of intercellular communication on repair of damage induced by ionizing radiation

By J. Madhoo, BSc and *G. Blekkenhorst, PhD

Department of Radiotherapy, Groote Schuur Hospital and University of Cape Town, Observatory, 7925, South Africa

(*Received September 1988*)

It has been suggested that intercellular contact enhances cellular repair after radiation damage (Durand, 1984). One form of intercellular communication is mediated by intercellular gap junctions (Gilula et al, 1972). These are specialized cell–cell contacts that allow the direct passage of small molecules from the cytoplasmic compartments of one cell to that of a neighbouring cell. Intercellular junctional communication can be inhibited to varying degrees with tumour-promoting phorbol esters, retinoids (Davidson et al, 1985a), organochlorine pesticides (Davidson et al, 1985b), and α-glycyrrhetinic acid (AGA) (Davidson et al, 1986). The question posed in the present study was whether the junctional inhibitor AGA could be used to modify repair of radiation damage.

Materials and methods

All experiments were performed using murine B16 melanoma cells grown as monolayers in McCoy's 5A medium supplemented with 10% fetal calf serum. Cells were used in the plateau phase, *i.e.* grown to confluence. Since AGA binds to albumin, exposure of the confluent cells to irradiation or AGA was performed in serum-free medium. The AGA was added 30 min before irradiation in all experiments. Cells were maintained in this medium until they were plated out for clonogenic assay. Suspensions of cells were prepared by trypsinization and 400 cells were seeded into plastic tissue culture flasks (Falcon 25 cm^3) together with serum-containing medium. A minimum of four replicate flasks were used at each irradiation dose level.

Flasks were incubated at 37°C in a humidified atmosphere consisting of 5% CO_2 and 95% air for 13 days. Colonies were fixed and stained with 1% gentian violet and counted to ascertain cell survival. Each experiment using different conditions was performed at least four times, and data from the separate experiments was pooled. Survival curves were fitted by eye.

Irradiations were performed using an Eldorado 6 ^{60}Co Unit (Atomic Energy of Canada).

Results

Toxicity of AGA to the cells was determined by exposure of confluent monolayers of cells in serum-free medium to increasing concentrations of the compound for 48 h. A clonogenic assay revealed that up to 5 μM there was no decrease in cell survival over cells not exposed to AGA. In all subsequent experiments AGA at a concentration of 4 μM was used.

A shift of the survival curve to higher doses was observed when cells were irradiated and maintained in serum-free medium for 48 h before plating out compared with the curve obtained when cells were plated out immediately following irradiation (Fig. 1a).

When cells were exposed to 4 µM AGA and irradiated, and exposure to the compound was maintained for 48 h before cells were plated out, there appeared to be an inhibition of repair. This was evidenced by the reduction of the shoulder in the survival curve, as well as the shift of the survival curve to lower doses when compared with the survival curve obtained following 48 h delayed plating in the absence of AGA (Fig. 1b).

Figure 1d shows survival curves obtained when cells in the plateau phase of growth were irradiated with ^{60}Co γ-rays in the presence or absence of 4 µM AGA, followed by immediate plating. There was no difference in the curves up to 6 Gy, although an increase in survival was noted in cells irradiated by 8 Gy in the presence of AGA.

Discussion

We have observed an inhibition of repair of damage induced by ionizing radiation when B16 cells in culture were exposed to AGA for 48 h (Fig. 1b). The compound does not appear to act as a "classical" radiosensitizer, as indicated by our observations that up to 6 Gy the survival curves obtained when cells were plated out immediately after irradiation in the presence or absence of AGA were virtually superimposable (Fig. 1d). Indeed, it appeared that at 8 Gy the AGA acted to diminish the effect of irradiation (Fig. 1d).

A comparison of the immediate and delayed plating survival curves in the presence of AGA (Fig. 1c) is also of interest. When cells were exposed to AGA for 48 h following irradiation, there was an almost complete abolition of the shoulder although at the higher doses, *viz.* 6 and 8 Gy, survival levels were not significantly different from those obtained in the case of cells plated immediately. The compound AGA has previously been shown to inhibit intercellular junctional communication (Davidson et al, 1986).

We suggest that our findings are consistent with the concept that inhibition of intercellular communication adversely affects cellular repair following ionizing radiation. It is quite likely that this is not the only mechanism involved, and further studies are indicated. We believe that inhibition of cellular repair represents

---

*Address for correspondence: G. Blekkenhorst, Department of Radiotherapy, Groote Schuur Hospital, Observatory, 7925, South Africa.

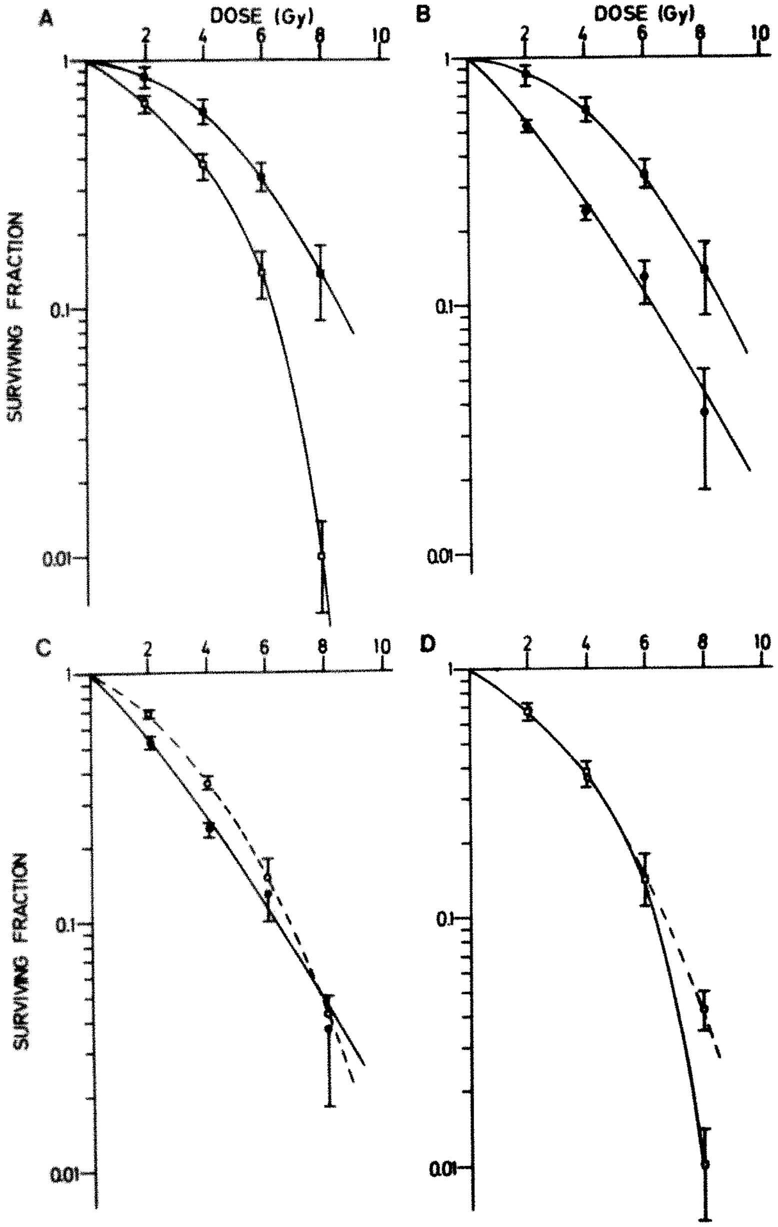

Figure 1. (a–d) Graphs comparing the survival of B16 mouse melanoma cells irradiated with ^{60}Co γ rays under various conditions: □, immediate plating after irradiation; ■, plating 48 h after irradiation; ●, plating 48 h after irradiation, but cells kept in presence of 4 μM AGA; ○, plating immediately after irradiation in the presence of 4 μM AGA. Points represent the mean ± the standard error of at least four experiments.

a novel approach to increasing radiosensitivity, and the junctional inhibitors warrant further investigation in this regard.

Acknowledgments

We thank the Cancer Trust Fund of the University of Cape Town for financial assistance and Dr J. Davidson for stimulating discussion.

References

Davidson, J. S., Baumgarten, I. M. & Harley, E. H., 1985a. Effect of TPA and retinoids on intercellular junctional communication measured with a citrulline incorporation assay. *Carcinogenesis, 6,* 645–650.

Davidson, J. S., Baumgarten, I. M. & Harley, E. H., 1985b. Use of new citrulline incorporation assay to investigate the inhibition of intercellular junctional communication by DDT in human fibroblasts. *Cancer Research, 45,* 515–519.

Davidson, J. S., Baumgarten, I. M. & Harley, E. H., 1986. Reversible inhibition of intercellular junctional communication by glycyrrhetinic acid. *Biochemical and Biophysical Research Communications, 134,* 29–36.

Durand, R. E., 1984. Repair during multifraction exposures: Spheroids versus monolayers. *British Journal of Cancer, 49, Supplement VI,* 203–206.

Gilula, N. B., Reeves, O. R. & Steinbach, A., 1972. Metabolic coupling, ionic coupling and cell contacts. *Nature, 235,* 262–265.

1989, *The British Journal of Radiology*, 62, 283–285

Short communications

Precipitation of radiation injury in kidney epithelium reveals a low fractionation sensitivity ($\alpha/\beta = 12.5$ Gy)

By *C. Ewen and †J. H. Hendry

Paterson Institute for Cancer Research, Christie Hospital and Holt Radium Institute, Wilmslow Road, Manchester M20 9BX

(*Received June 1988 and in revised form August 1988*)

The α/β ratio can be used to quantify the sensitivity to change in dose per fraction of tissues. It has been shown that late-responding tissues are more sensitive to these changes than are early-responding tissues, *i.e.* the former apparently have more repair capacity at low doses per fraction (Thames et al, 1982). For early responses in tissues the α/β ratio is generally between 5 and 20 Gy, and for late reactions it is usually 2–5 Gy (Fowler, 1984; Thames & Hendry, 1987). Of the various reasons currently considered most likely to explain this general difference, the cycling status of the target cells during the fractionation schedule may play a role. A greater initial or radiation-induced heterogeneity in sensitivity among the target cells in early-responding tissues, associated with differences in cell-cycle-phase distributions, could lead to a lesser overall fractionation effect (Zeman & Bedford, 1984; Schultheiss et al, 1987). However, the contribution of this effect for different tissues is difficult to quantify because of the difficulties in defining the target-cell populations and their cycling and sensitivity characteristics (Hendry & Potten, 1988).

Another reason relates to the times available for cellular repair among tissues prior to fixation of potentially lethal lesions consequent on movement in the division cycle (Thames, 1985; Curtis, 1987). Longer repair times will be available for the more slowly cycling target-cell populations in late-responding tissues. Post-irradiation repair of potentially lethal damage may affect the shoulder more than the final slope (Phillips & Tolmach, 1966; Gould & Clifton, 1979), and if the fractionation effect reflects the shape of the single-dose survival curve, lower α/β ratios would result for slowly cycling target cells in late-responding tissues. Correspondingly, higher α/β ratios should result if the target cells are stimulated to proliferate soon after irradiation (p. 119 in Thames & Hendry, 1987). The latter was tested using the liver by stimulating hepatocytes at various times after irradiation to grow and form colonies. For this system, the α/β ratio was low (1–2 Gy) for all delay periods and tended to increase with increasing delays (Fisher & Hendry, 1988). This may relate to the fact that for these cells there was little shoulder to the single-dose survival curve, in contrast to the high fractionation sensitivity, and that post-irradiation delays decreased the slope but did not decrease the shoulder. The α/β ratio for the kidney, measured acutely by precipitating injury in the epithelium, is now reported.

Materials and methods

Groups of five adult male B6D2F$_1$ mice were irradiated to both kidneys using a range of single or fractionated (up to 16) doses of 300 kVp X rays (1 Gy/min) with 8 h between doses. The maximum single dose given was 16 Gy and in the 16 fraction group the maximum total dose given was 48 Gy. One hour after the last fraction 16 mg kg^{-1} uranyl nitrate (UN) was injected intravenously followed by a second injection 7 days later. After a further 7 days the mice were killed. Longitudinal sections of the kidney were cut at 5 μm and stained with haematoxylin and eosin for counting tubular cross-sections (Withers et al, 1986). The UN produces acute tubular necrosis, principally in the straight portion of the proximal convoluted tubule. This is followed by a burst of compensatory proliferation which expresses the radiation injury through mitotic failure. This technique has been developed into a colony assay and has been used to measure the acute radiosensitivity of the colony-forming cells. It is described in detail elsewhere (Ewen, 1987; Ewen & Hendry, 1989).

Direct analysis of the raw data was performed to obtain the fractionation-sensitivity parameters for the colony-forming cells, using the equation:

$$\text{Probability of no colony formation} = \exp\left[-\exp\left(\ln K - n[\alpha d + \beta d^2]\right)\right]$$

where n fractions of dose d are delivered and K is a constant (Thames et al,1986a).

Results and discussion

The tubule cross-section data for the fractionated doses in two experiments are shown in Fig. 1. The parameter values in

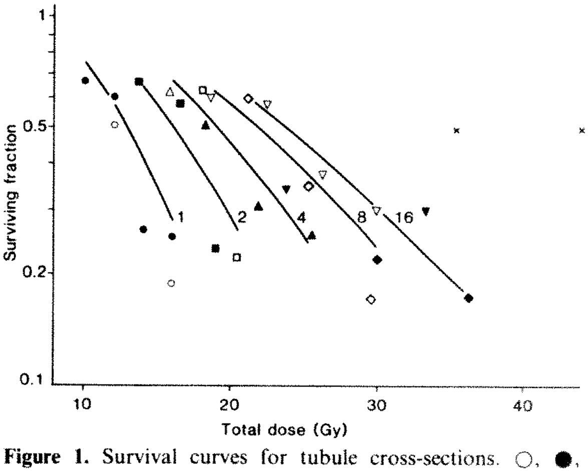

Figure 1. Survival curves for tubule cross-sections. ○, ●, single doses; □, ■, two fractions; △, ▲, four fractions; ▽, ▼, eight fractions; ◇, ◆, 16 fractions. Open and closed symbols represent two experiments. Standard errors are approximately 10% of the mean values. Left-hand cross, expected total dose in 16 fractions (see text) if $\alpha/\beta = 4.2$ Gy; right-hand cross, expected total dose in 16 fractions (see text) if $\alpha/\beta = 1.6$ Gy.

---

*Present address: Beecham Pharmaceuticals Human Pharmacology Unit, Medicinal Research Centre, Coldharbour Rd, Harlow, Essex CM19 5AD.
†Author for correspondence.

Table I. Direct analysis of kidney fractionation data from raw colony counts

	ln$K$	10 α(Gy^{-1})	100 β(Gy^{-2})	α/β (Gy)
Experiment 1	1.49 (1.41–1.57)	0.77 (0.74–0.80)	0.53 (0.49–0.57)	14.5 (13.3–15.9)
Experiment 2	2.00 (1.91–2.10)	0.88 (0.84–0.92)	0.65 (0.62–0.67)	13.6 (12.8–14.5)
Experiments 1 + 2	1.74 (1.69–1.80)	0.79 (0.77–0.81)	0.63 (0.61–0.65)	12.5 (12.0–13.1)
Experiments 1 + 2 excluding 16 fractions	1.54 (1.48–1.60)	0.60 (0.57–0.62)	0.71 (0.69–0.74)	8.4 (7.8–8.9)

Table I show that the α/β ratio was consistently in the range 12–16 Gy, much higher than values of 0.4–4.0 Gy reported for long-term functional assessments of kidney injury (reviewed by Thames & Hendry, 1987). The raw data for 16 fractions showed no clear separation from those after 8 fractions (Fig. 1), but even when the 16-fraction data were excluded from the calculation the α/β ratio was still high at 8.4 Gy (Table I). For interest, the doses calculated for 16 fractions resulting in 50% tubule survival, on the basis of a single dose of 13 Gy, are shown in Fig. 1 using an α/β ratio of 1.6 Gy (determined for weight loss and urination frequency; right-hand cross, Fig. 1) and 4.1 Gy (determined for ^{51}Cr-EDTA clearance; left-hand cross, Fig. 1) (Williams & Denekamp, 1984). Also, the values of α and β are higher than the reported range of 0.15–0.22 Gy^{-1} (α) and $\sim$0.02 Gy^{-2} (β) for the fractionation response of early-responding tissues using colony techniques (Thames & Hendry, 1987). This is due largely to the presence of a residual colony number at single doses above 20 Gy, which has the effect of reducing the rate of decline of colony number with increasing dose after lower single doses (Ewen & Hendry, 1988). The reason for this is not known but may relate to the UN not reaching part of the tubule which then does not proliferate in response to cell death in other regions, or to the presence of cells incapable of division in some parts of the tubules.

This is the first report of a fractionation response for a normally late-responding tissue being characteristic of that for early-responding tissues, when assayed acutely by precipitating the radiation injury. Unfortunately it was not found possible to perform this assay in the same way on mice at long times after irradiation because of their much lower tolerance of the UN treatment. The reasons for the different fractionation responses may relate to (a) the uncertain number of cell divisions accomplished in this short-term assay (Ewen & Hendry, 1988) and the possibility of differences in the number of post-irradiation divisions of cells depending on the dose/fraction (Wheldon et al, 1982; Thames et al, 1986b; McBride & Withers, 1986); (b) the type of target tissue being assessed (proximal tubule epithelium in the present studies and possibly vascular tissue in many of the functional assessments (Williams, 1986)) or (c) the fact that expression time and post-irradiation recovery phenomena *do* influence the sensitivity of tissues to fractionation. These data suggest that the kidney may respond much more severely than expected to cytotoxic trauma given shortly after multifractionated irradiation, because of the greater amount of injury yet to be repaired at these early times after low than after high dose-per-fraction regimens. Also, this effect may be relevant to the interpretation of the response of tissues in general to dose fractionation.

Acknowledgments

This work was supported by the Cancer Research Campaign. We thank Howard Thames for computing the values of the fractionation parameters.

References

Curtis, S. B., 1987. The cellular consequences of binary misrepair and linear fixation of initial biophysical damage. In *Radiation Research – Proceedings of the 8th International Congress of Radiation Research*, ed. by E. M. Fielden, J. F. Fowler, J. H. Hendry & D. Scott (Taylor and Francis, London), pp. 312–317.

Ewen, C., 1987. *The Effects of Radiation and Chemotherapy on Late Responding Tissues*, PhD Thesis (University of Manchester).

Ewen, C. & Hendry, J. H., 1989. The radiosensitivity of kidney colony-forming cells: a short-term assay *in situ* in the mouse. *Radiation Research*, in press.

Fisher, D. R. & Hendry, J. H., 1988. Dose-fractionation and hepatocyte clonogens: $\alpha/\beta \sim 1$–2 Gy and β decreases with increasing delay before assay. *Radiation Research, 113*, 51–57.

Fowler, J. F., 1984. What next in fractionated radiotherapy? *British Journal of Cancer, 49, Supplement VI*, 285–300.

Gould, M. N. & Clifton, K. H., 1979. Evidence for a unique in situ component of the repair of radiation damage. *Radiation Research, 77*, 149–155.

Hendry, J. H. & Potten, C. S., 1988. α/β Ratios and the cycling status of tissue target cells. *Radiotherapy and Oncology, 11*, 79–83.

McBride, W. H. & Withers, H. R., 1986. *In vitro* studies of *ante-mortem* proliferation kinetics. *British Journal of Cancer, 53, Supplement VII*, 386–388.

Phillips, R. A. & Tolmach, L. J., 1966. Repair of potentially lethal damage in X-irradiated HeLa cells. *Radiation Research, 29*, 413–427.

Schultheiss, T. D., Zagars, G. K. & Peters, L. G., 1987. An explanatory hypothesis for early and late-effect parameter values in the LQ model. *Radiotherapy and Oncology, 9*, 241–248.

Thames, H. D., 1985. An "incomplete-repair" model for survival after fractionated and continuous irradiations. *International Journal of Radiation Biology, 47*, 319–339.

Thames, H. D. & Hendry, J. H., 1987. *Fractionation in Radiotherapy* (Taylor and Francis, London).

Thames, H. D., Withers, H. R., Peters, L. J. & Fletcher, G. H., 1982. Changes in early and late radiation responses with altered dose fractionation: implications for dose-survival

1989, *The British Journal of Radiology*, *62*, 285–287

relationships. *International Journal of Radiation Oncology, Biology, Physics*, *8*, 219–226.

THAMES, H. D., ROZELL, M. E., TUCKER, S. L., ANG, K. K., FISHER, D. R. & TRAVIS, E. L., 1986a. Direct analysis of quantal radiation response data. *International Journal of Radiation Biology*, *49*, 999–1009.

THAMES, H. D., BROCK, W. A., BOCK, S. P. & DIXON, D. O., 1986b. Effect of dose per fraction on the division potential of lethally irradiated plateau-phase CHO cells exposed to isoeffective fractionation regimens. *British Journal of Cancer*, *53, Supplement VII*, 376–381.

WHELDON, T. E., MICHALOWSKI, A. & KIRK, J., 1982. The effect of irradiation in self-renewing normal tissues with differing proliferative organisation. *British Journal of Radiology*, *55*, 759–766.

WILLIAMS, M. V., 1986. The cellular basis of renal injury. *British Journal of Cancer*, *53, Supplement VII*, 257–264.

WILLIAMS, M. V. & DENEKAMP, J., 1984. Radiation induced renal damage in mice: influence of fraction size. *International Journal of Radiation Oncology, Biology, Physics*, *10*, 885–894.

WITHERS, H. R., MASON, K. A. & THAMES, H. D., 1986. Late radiation response of kidney assayed by tubule cell survival. *British Journal of Radiology*, *59*, 587–595.

ZEMAN, E. M. & BEDFORD, J. S., 1984. Changes in early and late effects with dose per fraction: alpha, beta, redistribution and repair. *International Journal of Radiation Oncology, Biology, Physics*, *10*, 1039–1047.

Autoradiographic imaging of pion stopping distribution utilizing scanning laser stimulated luminescence

By *H. Shirato, C. C. Gaffney and G. B. Goodman

Cancer Control Agency of British Columbia, 600 West 10th Avenue, Vancouver, Canada V5Z 4E6

(*Received July 1988 and in revised form October 1988*)

A new type of detector using scanning laser stimulated luminescence (SLSL system) (Sonoda et al, 1983) makes it possible to visualize small amounts of radiation exposure more efficiently than with conventional X-ray film. An autoradiographic technique using this system has the potential to image radioactivity when previously this was not possible. We have applied the system to the detection of radioactivity induced in aluminium foil by negative pion irradiation. The distribution of the trace of activity was well demonstrated, especially in the pion stopping region.

The new radiation area detector was developed for use in medical diagnostic radiography (Sonoda et al, 1983). The system (CR201) consists of a phosphor screen imaging plate, an image reader, an image processor, and an image writer (Fig. 1). The imaging plate (IP) is a 1 mm thick flexible plastic plate coated with a 0.15 mm thick layer of fine photostimulated phosphor crystals, $BaFBr:Eu^{2+}$. These crystals act as energy traps when exposed to ionizing radiation, thus producing a stored image that is subsequently released by illuminating the phosphor with red light from a helium–neon laser. The surface is scanned by this laser and emitted light is collected by a photomultiplier tube. The tube output is amplified and then digitized on a pixel by pixel basis (8 bits/pixel). The resulting digital data are manipulated by the image processor and finally converted back into analogue signals that modulate the intensity of another helium–neon laser beam scanning a photographic film to record the image.

The spatial resolution of the image has been reported to be less than two pixels (one pixel = 0.15 mm × 0.15 mm) at full width at half maximum (FWHM) in two orthogonal directions (Ameriya et al, 1983; Miyahara et al, 1986). The detector quantum efficiency and dynamic range are several orders of

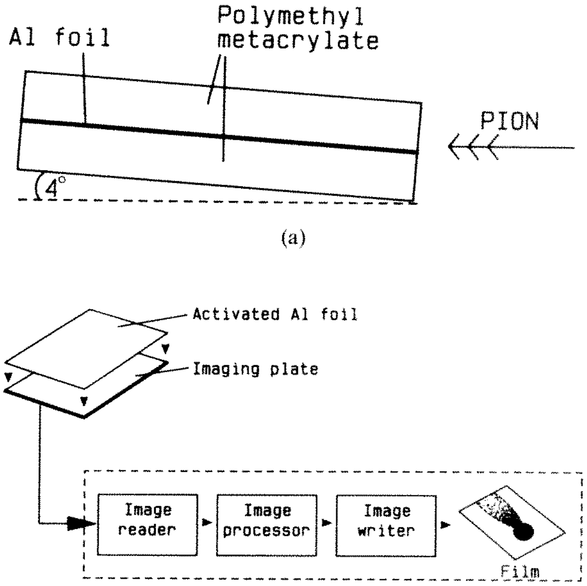

Figure 1. (a) Pion irradiation arrangement, showing horizontal static pion beam and aluminium foil sandwiched between PMMA blocks. The surface of the aluminium foil was inclined toward the beam axis at an angle of 4° so that pion stops in the foil with almost the same range as pions in PMMA. (b) Process for recording an autoradiographic image of pion-induced radioactivity in aluminium foil with an imaging plate and image developing installation, consisting of an image reader, processor and writer.

---

*Address correspondence to: H. Shirato, MD, Section of Radiotherapy, Department of Radiology, Hokkaido University Hospital, North-15, West-7, Kita-ku, Sapporo, Japan 060.

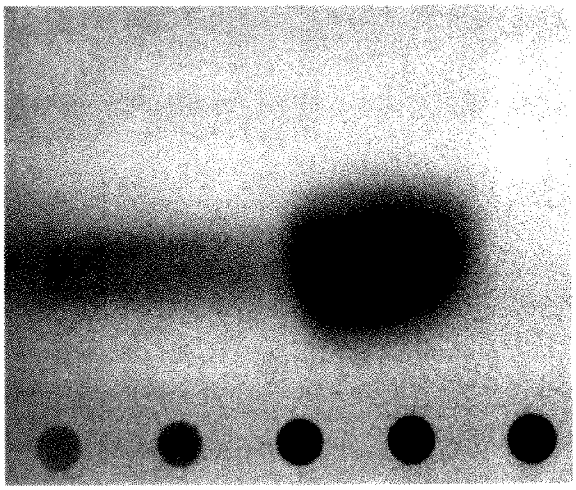

Figure 2. Autoradiographic image of pion-induced radioactivity in aluminium foil. The circles are autoradiographic images of a β-ray emitter corresponding to exposures of approximately 5, 10, 20, 30, 50×10^{-5} R (1 R = 258×10^{-6} C kg^{-1}).

magnitude greater than for conventional high-sensitivity photographic film. These characteristics make it possible to image extremely low radiation exposures without excessive background interference.

Beams of negative pions are being used for cancer radiotherapy at TRIUMF (Goodman et al, 1985). The "star" formation of the pion-capture reaction produces a localized region of dense ionization resulting in a greater biological effect than with conventional therapy using X-rays (Fowler & Perkins, 1961). Precise estimation of the pion-stopping distribution is necessary to ensure that they come to rest in the tumour region. This can be achieved by measuring the activity of the radioisotopes produced by pion-capture reactions. A model for this is the irradiation of aluminium pellets buried in tissue-equivalent plastic. Measurement of the resulting activity provides a profile of stopping intensity with depth (Hogstrom & Amols, 1980). Similarly, aluminium foil may be used to produce a two-dimensional pion-stopping distribution (Salzmann et al, 1982). Conventional X-ray film is not sufficiently sensitive to produce an autoradiographic image because of the very low level of activity, but this can be achieved by using the SLSL imaging system.

Methods

Horizontal pion beams were used to bombard an aluminium foil sandwiched between two thick polymethylmetacrylate (PMMA) blocks (Fig. 1). About 10 h after completing irradiation the activated foil was removed from the PMMA blocks and placed on an imaging plate for autoradiography. A calibration curve of relative exposure against optical density was determined for each imaging plate by exposing it to a circular ^{238}U β-ray source for different lengths of time.

To determine whether this technique can accurately define the pion stopping distribution the results were compared with aluminium pellet activation measurements. A similar irradiation set up was used for each technique. The pellets were irradiated in a PMMA block and the induced activity was counted in a NaI well counter with a single channel centred on the 1.37 MeV γ-ray full energy peak from the ^{24}Na produced by the ^{27}Al (π^-, π^-X) ^{24}Na reaction.

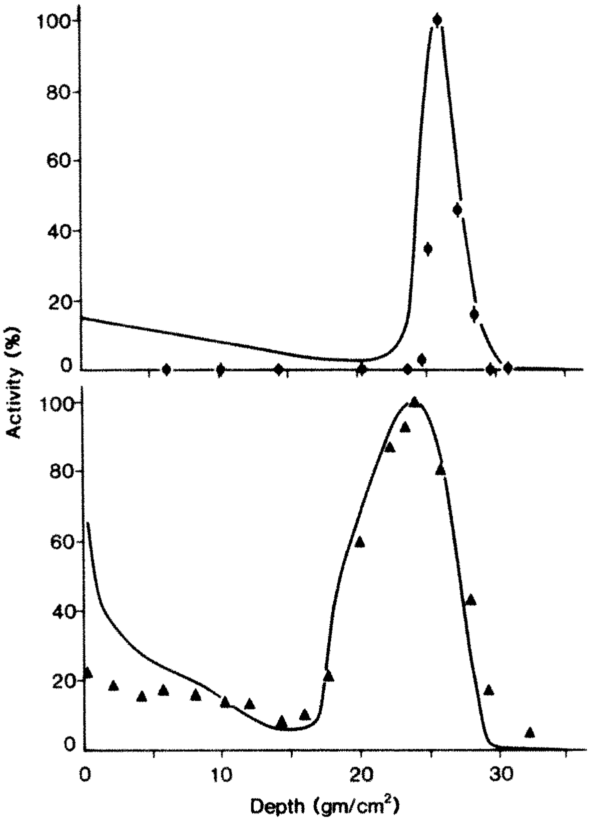

Figure 3. Comparison of relative depth–activity profiles along the beam axis measured with the aluminium pellet activation method (●, ▲) and autoradiography (———) in (upper) narrow and (lower) broad momentum spread beam.

Results and discussion

A typical autoradiograph obtained from the imaging plates is shown in Fig. 2. Prominent radioactivity was demonstrated in the pion-stopping region, the distribution of activity agreeing with that measured by aluminium pellet activation (Fig. 3). Units to accompany the autoradiographic curves in Fig. 3 are exposures estimated from aluminium foil using the calibration curve mentioned above, normalized at 100% to fit the activity peak. The depth of peak activity was 26 and 22–24 g cm^{-2} for the narrow and broad momentum spread beams used, corresponding to average pion kinetic energies of 100 and 88–92 MeV, respectively. There is a small amount of exposure from radioactivity in the pion entrance region which is relatively larger than with the aluminium pellet measurement.

The residual activity in the foil at the pion stopping region is due to the primary nuclear product from the pion-capture reactions and secondary products created when the lighter fragments (neutrons, protons, α particles etc.) from the pion stars in PMMA blocks and foil themselves undergo nuclear reactions with the aluminium atoms (Hogstrom & Amols, 1980). The activity at the pion entrance region can be attributed mainly to nuclear interactions by pions in flight. The discrepancy between autoradiographic and pellet measurement may be due to radioisotopes other than ^{24}Na formed in the foil.

Exposure density calibration curves from the β-ray emitter series fitted reasonably well to quadratic equations between 5×10^{-5} and 5×10^{-4} R.

Pion beam bombardment provides an appropriate starting point for the application of autoradiography using the SLSL system. The agreement between the SLSL system and aluminium pellet activation suggests that this could be a breakthrough in measurement of low-radioactivity area detection. For example, the same technique can be used for other particle beams to study activation distribution. Understanding the radionuclide and cross-section of nuclear interactions will aid the interpretation of more complicated images. There is no doubt that materials other than aluminium foil can be used as alternative radioactive sources. For biomedical application, autoradiography of animal or human tissues could be visualized more quickly in a wider dynamic range using less radioactivity. New radiopharmaceuticals including monoclonal antibodies are worth exploring further in connection with autoradiography using the SLSL system.

Acknowledgments

We thank Fuji Medical System Division for interest and assistance. The helpful advice of R. O. Kornelsen and the support, including computer programming, of R. Harrison are also acknowledged.

References

AMERIYA, Y., WAKABAYASHI, K., HAMANAKA, T., WAKABAYASHI, T., MATSUSHITA, T. & HASHIZUME, H., 1983. Design of a small-angle x-ray diffractometer using synchrotron radiation at the photon factory. *Nuclear Instruments and Methods*, *208*, 471–477.

FOWLER, P. H. & PERKINS, D. H., 1961. The possibility of therapeutic application of beams of negative π-mesons. *Nature*, *189*, 524–528.

GOODMAN, G. B., DIXON, P., LAM, G. K. Y., HARRISON, R., KORNELSEN, R. O., LUDGATE, C. M. & FLORES, A. D., 1985. Preparatory clinical studies of pi-mesons at TRIUMF. *Radiation Research*, *104*, S279–S284.

HOGSTROM, K. R. & AMOLS, H. I., 1980. Pion in vivo dosimetry using aluminium activation. *Medical Physics*, *7*, 55–60.

MIYAHARA, J., TAKAHASHI, K., AMERIYA, Y., KAMIYA, N. & SATO, Y., 1986. A new type of X-ray area detector utilizing laser stimulated luminescence. *Nuclear Instruments and Methods*, *A246*, 572–578.

SALZMANN, M., BLATTMANN, H., CRAWFORD, J., CORDT, I., PEDRONI, E., SEILER, P. G. & SCHAEPPI, K., 1982. The pion dosimetry program at SIN. In *Pion and Heavy Ion Radiotherapy: Pre-Clinical and Clinical Studies*, ed. by L. D. Skarsgard (Elsevier/North-Holland, New York), pp. 129–138.

SONODA, M., TAKANO, M., MIYAHARA, J. & KATO, H., 1983. Computed radiography utilizing scanning laser stimulated luminescence. *Radiology*, *148*, 833–838.

Primary orbital lymphoma: staging by computed tomographic scanning

By *P. Mills, BM, MRCP and C. A. Parsons, FRCS, FRCR

Department of Diagnostic Radiology, The Royal Marsden Hospital, Fulham Road, London SW3

(*Received July 1988 and in revised form October 1988*)

Primary orbital lymphoma is a rare form of extranodal lymphoma and accounts for only 1% of all orbital tumours (Calle et al, 1975). Recently reported series have dealt principally with the clinical and radiotherapeutic aspects of the disease, including risk factors for the development of systemic lymphoma (Knowles & Jakobiec, 1980; Fitzpatrick & Macko, 1984; Barthold et al, 1986; Gordon et al, 1986). Published data on the results of staging investigations have included little information on computed tomographic (CT) scanning (Henk, 1982; Bessell et al, 1989). Most patients undergo extensive investigation including a full blood count and erythrocyte sedimentation rate (ESR), liver function tests, bone marrow examination, chest radiography and, in recent years, abdominal and thoracic CT.

We have retrospectively studied a group of patients with primary orbital lymphoma, with particular reference to their staging investigations and to the factors affecting the development of systemic disease.

Methods

All patients with primary orbital lymphoma who were referred for abdominal and thoracic CT were included. This group did not include those patients with known non-Hodgkin's lymphoma and secondary orbital involvement. Many of these patients were referred by Mr J. Wright at the Orbital Clinic, Moorfields Eye Hospital for further management after initial investigation including open biopsy, pathology and orbital CT scanning.

Patients underwent a full clinical examination, blood count and ESR, liver function tests, bone marrow trephine and chest radiography. In addition, many patients seen since 1984 had abdominal and orbital CT scans performed at the time of presentation. Each patient was given local radiotherapy to the tumour to a dose of 20–30 Gy.

Results

A total of 24 patients were seen with an age range from 35 to 81 years (mean 60 years). The female to male ratio was 2 : 1. There were 17 patients with orbital lesions, one of whom had bilateral disease, and seven patients with conjunctival lesions, two of whom had bilateral disease. Twenty-one patients had

---

*Present address: Department of Radiology, St George's Hospital, Blackshaw Road, Tooting, London SW17. Correspondence to Dr P. Mills.

Table I. Histology of the orbital lymphomas

Histologic type	Number
Diffuse lymphocytic lymphoma	16
Nodular lymphocytic lymphoma	4
Histiocytic lymphoma	2
Indeterminate lymphocytic lesion	2

Table II. Results of staging investigations

Investigation	Number performed	Result	
		Positive	Negative
Chest radiograph	24	0	24
Lymphogram	1	0	1
Liver scan	1	0	1
CT (abdomen and pelvis)	19	1^a	18
CT (thorax)	3	0	3
Bone marrow trephine	24	0	24
Blood tests (blood count, ESR, liver function tests)	24	1^b	23

[a] Pelvic and para-aortic lymph nodes. [b] Elevated ESR.

low-grade and three had high-grade lymphoma. Details of the histologies encountered are shown in Table I. Most patients had CT performed at the time of initial diagnosis but in five cases this was not done, as they presented prior to the acquisition of the equipment. Others had CT performed after clinical evidence of relapse had occurred. The sequence of CT examinations in the group is shown in Fig. 1.

The results of the initial staging investigations are shown in Table II. Of the eight patients who had CT performed after relapse had occurred, four were positive. Of these, one revealed mediastinal lymphadenopathy in a patient with a pleural effusion (Case 8, Table III), the second para-aortic lymphadenopathy in a patient with widespread lymph node enlargement and an epigastric mass (Case 1, Table III), the third a para-aortic lymph node mass in a patient with "B" symptoms, skin involvement and a pleural effusion (Case 6, Table III), and the fourth showed a pelvic lymph node mass in a patient with liver enlargement (Case 7, Table III).

Four of 24 cases (16.5%) were found to have evidence of systemic lymphoma at the time of presentation. One had bilateral orbital tumours, an elevated ESR and Bence-Jones protein in the urine. Another had a unilateral orbital tumour and skin nodules on the face. The third had bilateral conjunctival lesions and palpable cervical lymphadenopathy, and the fourth had a unilateral orbital tumour and deep vein thrombosis with both pelvic and para-aortic lymph node disease shown by CT. The first two patients had low-grade diffuse lymphocytic lymphoma and the last two had low-grade nodular lymphocytic lymphoma.

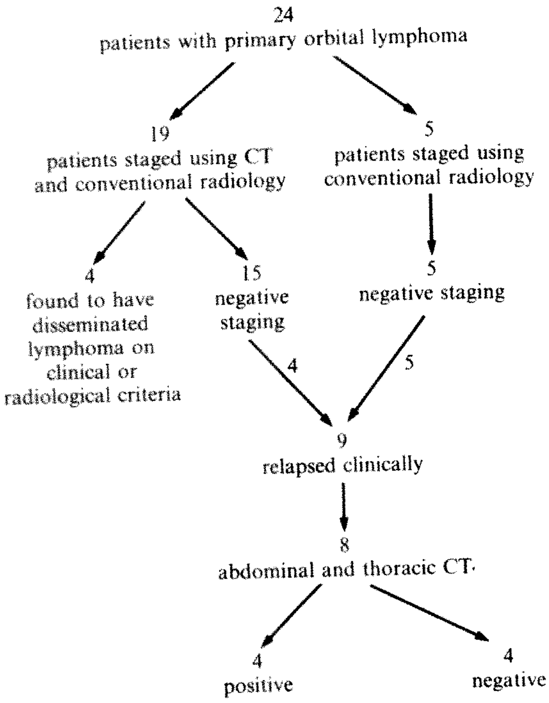
24
patients with primary orbital lymphoma
19
patients staged using CT and conventional radiology
5
patients staged using conventional radiology
4
found to have disseminated lymphoma on clinical or radiological criteria
15
negative staging
5
negative staging
4
5
9
relapsed clinically
8
abdominal and thoracic CT
4
positive
4
negative

Figure 1. Flow chart showing the sequence and results of staging investigations.

Nine of 24 patients (37.5%) subsequently developed systemic lymphoma after an interval of 1 month to 6 years (mean 4 years). Details of this group are shown in Table III. All nine patients had negative staging investigations when first seen. However, one patient had invasion of the maxillary antrum demonstrated on the orbital CT scan (Case 6, Table III), which does not alter the stage but is reported to be associated with a higher incidence of relapse.

Discussion

The age range, sex ratio and clinical features of this group of patients is similar to that reported by others (Kim & Fayos, 1976; Knowles & Jakobiec, 1980; Barthold et al, 1986; Mittal et al, 1986).

The initial staging investigations were negative in 20 of 24 cases (83.3%). Of the four patients who were found to have disseminated lymphoma at the time of presentation, in only one was the diagnosis made and the clinical stage altered by the radiological investigations. Two of the patients had bilateral tumours, which is reported to be associated with a higher incidence of systemic lymphoma (Blodi & Gass, 1968). The only evidence of extraorbital disease shown by the radiological staging investigations was local invasion of the maxillary antrum demonstrated on the orbital CT scan of one patient and pelvic and para-aortic disease shown on the abdominal CT scan of the patient with the deep vein thrombosis. The other radiological investigations did not show systemic lymphoma (see Table II). In view of these negative results, we suggest that radiological staging investigations in primary orbital lymphoma be confined to a chest radiograph and an orbital CT scan unless there is bilateral orbital involvement or clinical evidence of disseminated lymphoma. An orbital CT scan should be performed to aid radiotherapy planning. If bone destruction or bilateral disease are demonstrated on the scans, further investigation is indicated as these factors are known to be associated with a greater risk of developing systemic lymphoma (Knowles & Jakobiec, 1980).

Nine patients developed systemic lymphoma. Various authors have reported an incidence of progression to systemic disease from 5.8% to 71.4% (Ampil & Bahrassa, 1985). Knowles and Jakobiec (1980) have suggested that a 5-year disease-free period is sufficient to exclude associated systemic lymphoma, but in this series one patient developed systemic

Table III. Clinical details of the patients who developed systemic lymphoma

Case	Age	Sex	Site of primary	Time after presentation	Site of relapse	Abnormal blood tests	"B" symptoms	Histology
1	67	F	Orbit	2 years	LN neck, abdomen, groin	Alk. ph.	+	WDNL
2	75	F	Orbit	2.5 years	Larynx	Nil	–	DL
3	57	F	Orbit	3 years	Pleura	ESR	–	WDDL
4	59	F	Orbit	9 months	Skin, LN neck	Alk. ph.	–	NL
5	48	F	Conj.	1 month	LN	Nil	–	PDDL
6	80	F	Bil. conj.	1 year	LN neck, abdomen, skin, chest	ESR, +BJP, alk. ph.	+	WDDL
7	68	M	Orbit	6 years	Liver, pelvis	ESR, alk. ph.	–	H
8	61	F	Orbit	5 years	Pleura, mediastinum	ESR	–	DL
9	68	F	Orbit	6 years	Submandibular gland	Alk. ph.	–	WDDL

Key: LN, lymph node; alk. ph., alkaline phosphatase; BJP, Bence–Jones protein; WD, well differentiated; PD, poorly differentiated; NL, nodular lymphocytic; DL, diffuse lymphocytic; H, histiocytic.

disease after 5 years and a further two patients relapsed after 6 years. All nine patients that developed systemic lymphoma had clinical evidence of disease, such as symptoms (four patients), palpable lymph nodes (four patients), pleural effusion (two patients) and liver enlargement (one patient). Seven patients developed abnormal blood tests (elevated ESR or elevated alkaline phosphatase). In six cases the site of disease included the neck and in four it was confined to the neck. Only two patients developed systemic lymphoma at multiple sites.

In this series, six of 16 cases with diffuse lymphocytic lymphoma, two of four cases with nodular lymphocytic lymphoma and one of two cases with histiocytic lymphoma developed systemic disease. Several authors have stated that histiocytic orbital lymphoma is more likely to become disseminated (Case 7, Table III) (Kim & Fayos, 1976; Knowles & Jakobiec, 1980; Ampil & Bahrassa, 1985; Bessell et al, 1989). Patients with poorly differentiated orbital lymphomas have also been described as more likely to develop systemic disease (Knowles & Jakobiec 1980; Bessell et al, 1989) and at an earlier stage (Case 5, Table III). Conjunctival lymphomas have been noted to undergo dissemination at an early stage (Kim & Fayos, 1976), although the incidence of systemic disease is less common with conjunctival than with orbital lymphoma. In this series, there was a 42% rate of development of systemic lymphoma when the primary lesion was conjunctival and a 60% rate when the primary was orbital.

There were no local recurrences after radiotherapy. Follow-up at 3- to 6-monthly intervals with clinical examination, full blood count, ESR and liver function tests was carried out. Long-term follow-up from 1 month to 9 years (mean 2.5 years) was achieved. Nineteen of 24 (79%) are alive and disease-free at 1 month to 9 years, three of 24 are alive and on treatment for systemic lymphoma at 2 to 2.5 years and two of 24 died of unrelated disease.

Excluding the four patients who had systemic involvement at presentation, 45% of patients in this series with true primary orbital lymphoma subsequently developed systemic disease. This relatively high figure is a result of the selection method used in this study, as patients who are referred for CT scanning are those most likely to have disseminated disease. Factors which confer a higher risk of dissemination are bilateral disease, an orbital versus a conjunctival primary lesion, orbital bone destruction and a poorly differentiated and/or histiocytic tumour. We recommend a chest radiograph and an orbital CT scan as radiological staging investigations. Abdominal and thoracic CT should be reserved for patients in whom there is clinical or haematological suspicion of systemic lymphoma and for those young patients with high-grade lymphoma in whom high-dose chemotherapy is contemplated as an alternative to radiotherapy because they have a high risk of developing systemic disease.

Acknowledgments

We would like to thank Dr J. M. Henk, FRCR, Consultant Radiotherapist at the Royal Marsden Hospital, and Mr J. Wright, FRCS, Consultant Ophthalmic Surgeon at Moorfield's Eye Hospital, for granting permission to report these cases.

References

AMPIL, F. L. & BAHRASSA, F. S., 1985. Primary orbital lymphoma-pseudotumor (pseudolymphoma): case reports and review of the radiotherapy literature. *Journal of Surgical Oncology, 30,* 91–95.

BARTHOLD, H. J., HARVEY, A., MARKOE, A. M., BRADY, L. W., AUGSBURGER, J. J. & SHIELDS, J. A., 1986. Treatment of orbital pseudotumors and lymphoma. *American Journal of Clinical Oncology, 9,* 527–532.

BESSELL, E. M., HENK, J. M., WRIGHT, J. E. & WHITELOCK, R. A. F., 1989. Orbital and conjunctival lymphoma: treatment and prognosis. *Radiotherapy and Oncology,* in press.

BLODI, F. C. & GASS, J. D. M., 1968. Inflammatory pseudotumour of the orbit. *British Journal of Ophthalmology, 52,* 79–93.

CALLE, R., ZAJDELA, A., HAYE, C. & SCHLIENGER, P., 1975. Primary malignant lymphoma of the orbit: the eye and its adnexa. *Eye, Ear, Nose and Throat Monographs, 54,* 141–149.

FITZPATRICK, P. J. & MACKO, S., 1984. Lymphoreticular tumors of the orbit. *International Journal of Radiation Oncology, Biology, Physics, 10,* 333–340.

GORDON, P. S., JUILLARD, G. J., SELCH, M. T., PARKER, R. G. & FU, Y.-S., 1986. Orbital lymphomas and pseudolymphomas: treatment with radiation therapy. *Radiology, 159,* 797–799.

HENK, J. M., 1982. Radiotherapy for orbital lymphoma and pseudotumour. *Orbit, 1,* 71–74.

KIM, Y. H. & FAYOS, J. V., 1976. Primary orbital lymphoma: a radiotherapeutic experience. *International Journal of Radiation Oncology, Biology, Physics, 1,* 1099–1105.

KNOWLES, D. M. & JAKOBIEC, F. A., 1980. Orbital lymphoid neoplasms. A clinicopathologic study of 60 patients. *Cancer, 46,* 576–589.

MITTAL, B. B., DEUTSCH, M., KENNERDELL, J. & JOHNSON, B., 1986. Paraocular lymphoid tumours. *Radiology, 159,* 793–796.

1989, *The British Journal of Radiology*, 62, 290–292

Demonstration of vertebral body end plate veins by magnetic resonance imaging

By W. R. Saywell, MA, FRCR, *H. V. Crock, AO, MD, MS, FRCS, FRACS, *J. P. S. England, FRCS and †R. E. Steiner, CBE, MD, FRCR

Departments of Nuclear Magnetic Resonance and *Orthopaedic Surgery, Royal Postgraduate Medical School, Hammersmith Hospital, Du Cane Road, London W12 0MS

(*Received September 1988*)

The venous drainage of the vertebral end plate capillary bed is via a plexus of post-capillary venules in the subchondral region, which drains into a horizontal subarticular collecting vein. This vein then joins the anterior internal vertebral venous plexus. There are also anastomotic connections through vertical tributaries to the basi-vertebral system of veins (Crock et al, 1973; Crock, 1983) (Fig. 1).

The end plate venous plexus may be important in the pathogenesis of symptoms in the syndrome of internal disc disruption, in which catabolites and disc proteins leak out of the disc into the systemic circulation via the end plate veins, producing local and systemic features of hypersensitivity reactions (Gurdjian et al, 1961; Nachemson, 1969; Crock, 1970). The plexus is also important in maintaining the integrity of the normal intervertebral disc, as diffusion of nutrients takes place across the end plates (Urban et al, 1976; Bernick & Caillet, 1982).

Although demonstrated in dogs and post-mortem specimens, the end plate veins have not previously been demonstrated by *in vivo* imaging.

Methods

Patients with suspected internal disc disruption or isolated disc resorption (Crock, 1970) were referred by orthopaedic surgeons. Magnetic resonance imaging of the whole lumbar spine was performed on a Picker prototype cryogenic system operating at 0.15 T, as described in detail elsewhere (Young et al, 1982). All patients were examined with a planar surface coil, using five different pulse sequences ($SE_{544/44}$, $SE_{1500/80}$, $IR_{1500/100/44}$, $PS_{500/22}$ and $PS_{500/33}$), and some were given intravenous paramagnetic contrast enhancement with gadolinium-DTPA as part of another study. The relevant sequence for the demonstration of the end plate venous system is the partial saturation sequence with a repetition time (TR) of 500 ms and echo time (TE) of 22 ms. This value of TE was chosen to cause chemical shift phase cancellation of signal from the red marrow (which contains approximately equal proportions of its protons in fat and water), by collecting the signals from protons in water and protons in lipid when they are out of phase by 180° (Bydder & Young, 1985; Wiener et al, 1985; Bydder, 1988).

A further study was made on three patients and one volunteer, using the $PS_{500/22}$ sequence with the phase encoding gradient reversed. This enables differentiation between chemical shift artefacts and true structures as the cause of lines parallel to the end plates.

Results

The $PS_{500/22}$ sequence demonstrates the slow-flowing venous blood in the end plate venous plexus as a line of high signal against the low signal of red marrow (Fig. 2).

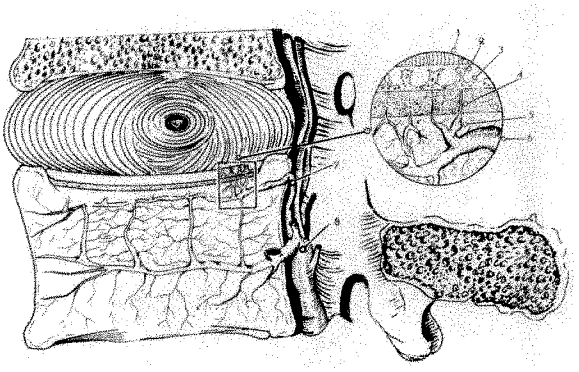

Figure 1. The veins of a typical vertebral body in sagittal section. (1) Intervertebral disc. (2) End plate capillary bed. (3) Subchondral venule. (4 & 5) Short vertical venous tributary. (6) End plate vein running horizontally in subarticular location. (7) End plate vein joining anterior internal vertebral plexus. (8) Basi-vertebral vein joining anterior internal vertebral plexus. (First published in the *Journal of Bone and Joint Surgery*, 1973 and reproduced by kind permission of the Editors.)

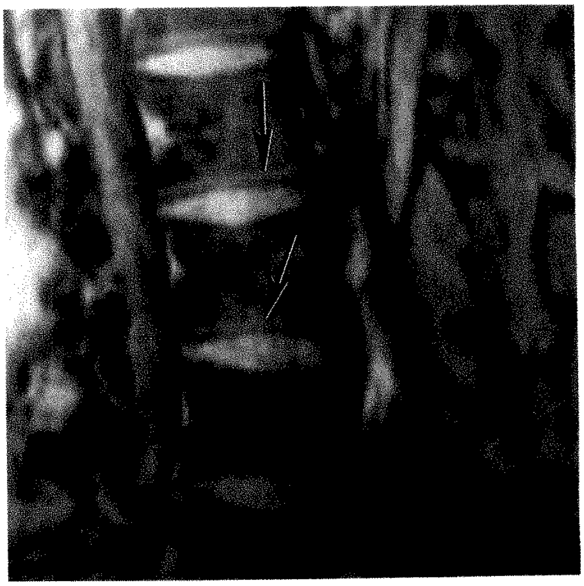

Figure 2. Horizontal subarticular end plate veins (arrows). The basi-vertebral veins may also be seen (arrowheads).

---

†Author for correspondence.

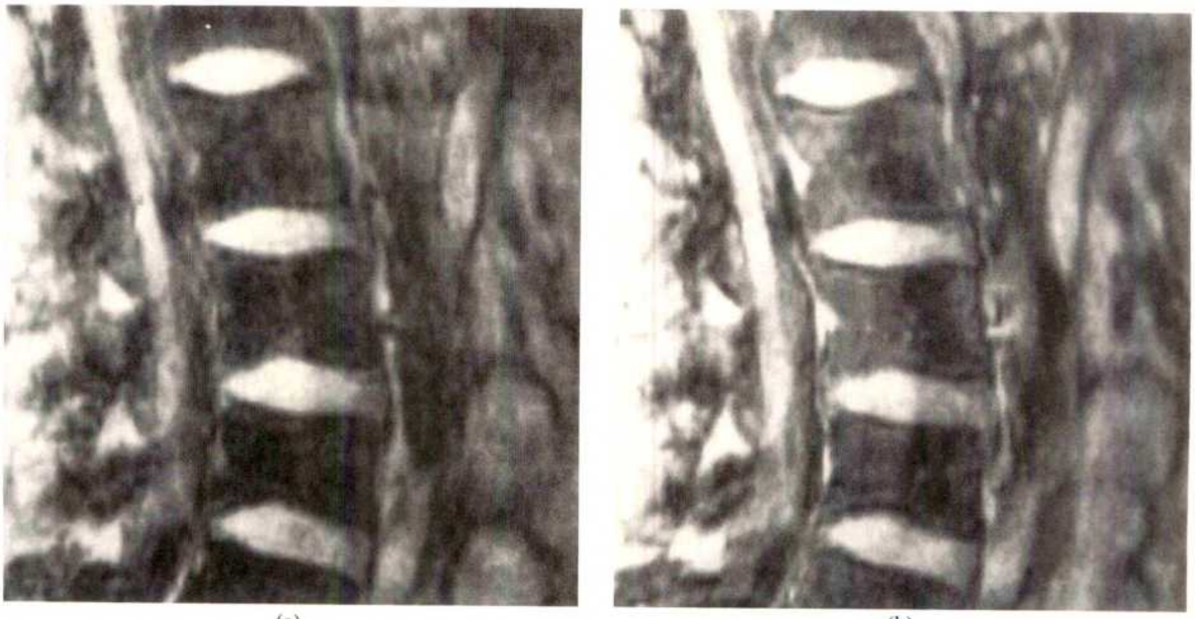
(a) (b)

Figure 3. (a) Unenhanced scan. The end plate veins are barely visible. (b) With gadolinium-DTPA enhancement the end plate veins are more clearly seen at all levels.

In 44 patients (mean age 38 years) examined without contrast enhancement, the end plate venous system is demonstrated in 31 cases (70%), though not necessarily at all levels (mean number of lumbar levels 2.6). In the six patients given gadolinium-DTPA enhancement, the end plate veins were seen in four before and five after contrast medium. In four patients the veins were seen better after enhancement than before (Fig. 3).

Reversal of the gradients in the $PS_{500/22}$ sequence caused no change in the appearances of the lines representing the end plate venous plexuses (Fig. 4). Other veins demonstrated are the

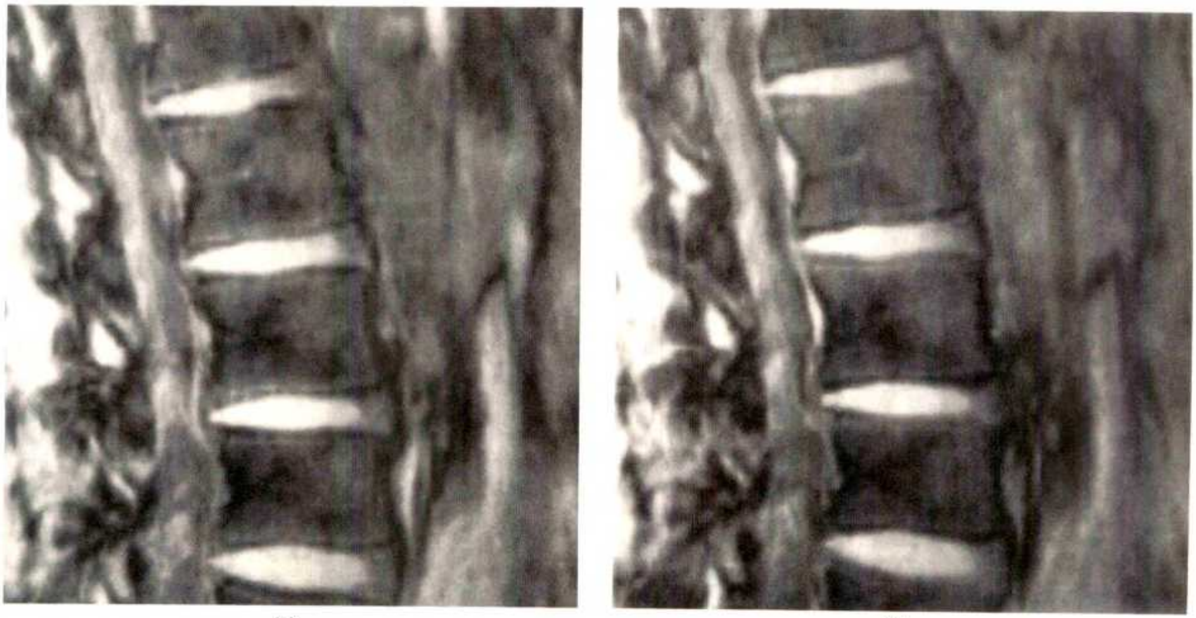
(a) (b)

Figure 4. End plate veins are shown with the phase encoding gradient in (a) normal and (b) reversed orientation. No change in appearance or position of the end plate veins is seen.

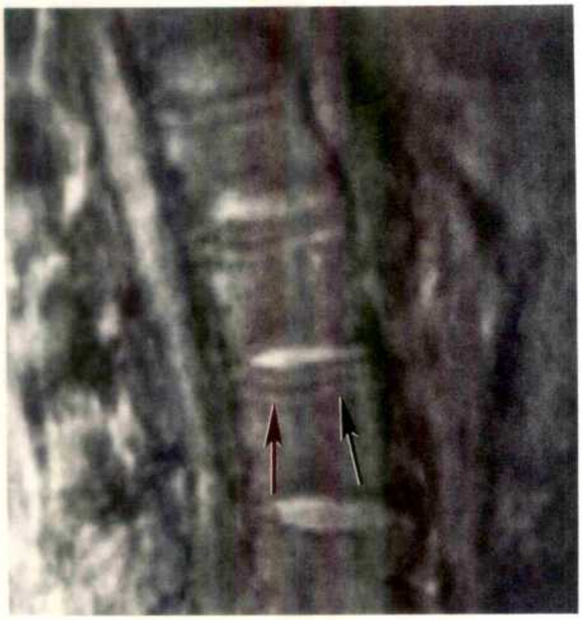

Figure 5. Typical chemical shift artefact (arrows). Note the high-signal line with low-signal "void" above.

anterior internal veins of the spinal canal, and the central vein of the vertebral body.

Discussion

Lines parallel to the end plates may be caused by chemical shift artefacts (Peck & Haughton, 1985) and it is important to differentiate these from the end plate veins. Chemical shift artefacts are due to the slightly different resonant frequencies of protons in fat and protons in water. This results in the signal from fat, which has a lower frequency, being spatially encoded by the Fourier transformation to a position apparently further down the magnetic gradient, leaving behind a "void" or black line bereft of signal (Fig. 5). These artefacts thus occur in one direction only, and hence are not seen on both sides of the disc (as the veins are). Furthermore, the chemical shift artefact would not be made more apparent by gadolinium enhancement. The constant appearance of the end plate veins despite reversal of the phase encoding gradients (Fig. 4) excludes the possibility of their being due to the chemical shift artefact.

It is thus concluded that the venous plexus draining the human vertebral body end plate is demonstrable by magnetic resonance imaging *in vivo*. Although all the patients in this series were referred with back pain, the plexus is visible in many patients at levels remote from the site of disc pathology. The clinical significance of showing or not showing the plexus at any particular level is as yet uncertain, and further work is in progress to correlate the appearances on magnetic resonance imaging with the clinical and operative findings.

Acknowledgments

The authors wish to thank the Editors of the *Journal of Bone and Joint Surgery* for their permission to reproduce Fig. 1, and Mrs D. Spencer for performing the imaging.

References

BERNICK, S. & CAILLET, R., 1982. Vertebral end plate changes with aging of human vertebrae. *Spine*, *7*, 97–102.

BYDDER, G. M., 1988. Clinical use of PS and SR sequences. In *Magnetic Resonance Annual 1988*, ed. by H. Y. Kressel (Raven Press, New York).

BYDDER, G. M. & YOUNG, I. R., 1985. Clinical use of the partial saturation and saturation recovery sequences in MR imaging. *Journal of Computer Assisted Tomography*, *9*, 1020–1032.

CROCK, H. V., 1970. A re-appraisal of intervertebral disc lesions. *Medical Journal of Australia*, *1*, 983–989.

—— 1983. *Practice of Spinal Surgery* (Springer Verlag, Wien/New York), Chapter 2, pp. 35–92.

CROCK, H. V., YOSHIZAWA, H. & KARNE, S. K., 1973. Observations on the venous drainage of the human vertebral body. *Journal of Bone and Joint Surgery*, *55B*, 528–533.

GURDJIAN, E. S., WEBSTER, J. E., OSTROWSKI, A. Z., HARDY, W. G., LINDNER, D. W. & THOMAS, L. M., 1961. Herniated lumbar intervertebral discs—an analysis of 1176 operated cases. *Journal of Trauma*, *1*, 158–176.

NACHEMSON, A., 1969. Intradiscal measures of pH in patients with lumbar rhizopathies. *Acta Orthopaedica Scandinavica*, *40*, 23–42.

PECK, P. & HAUGHTON, V. M., 1985. Lumbar intervertebral disk: correlative MR and anatomic study. *Radiology*, *156*, 699–701.

URBAN, J., HOLM, S., MAROUDAS, A. & NACHEMSON, A., 1976. An *in-vivo* study of the penetration of the sulphate ion into the canine intervertebral disc and of its incorporation into the matrix. *Journal of Bone and Joint Surgery*, *58B*, 255.

WIENER, G. C., ROSEN, B. R., BUXTON, R., STARK, D. D. & BRADLEY, T. J., 1985. Chemical shift imaging of bone marrow: preliminary experience. *American Journal of Roentgenology*, *145*, 1031–1037.

YOUNG, I. R., BAILES, D. R., BURL, M., COLLINS, A. G., SMITH, D. T., MCDONNELL, M. J., BYDDER, G. M., GREENSPAN, R. H. & STEINER, R. E., 1982. Initial clinical evaluation of a whole body nuclear magnetic resonance (NMR) tomograph. *Journal of Computer Assisted Tomography*, *6*, 1–18.

1989, *The British Journal of Radiology*, *62*, 293

Correspondence

(The Editors do not hold themselves responsible for opinions expressed by correspondents)

An analysis of referrals for primary diagnostic abdominal ultrasound to a general X-ray department

THE EDITOR—SIR,

We note with interest the findings of Drs Colquhoun, Saywell and Dewbury (1988).

It is our practice to promote ultrasound as the first-line investigation of abdominal symptoms, both for hospital and GP referrals. We are, however, concerned at their advice to perform partial examination. Little time will be saved and much may be missed.

Pelvic ultrasound, which omits a survey of the kidneys and abdomen, may be comparable to a clinical examination of the abdomen that omits the rectum.

Yours, etc.,
R. FITZGERALD
G. MACKIE
R. MANNS

Department of Radiology,
New Cross Hospital,
Wolverhampton WV10 0QP
(*Received June 1988*)

Reference

COLQUHOUN, J. R., SAYWELL, W. R. & DEWBURY, K. C., 1988. An analysis of referrals for primary diagnostic abdominal ultrasound to a general X-ray department. *British Journal of Radiology*, *61*, 297–300.

(*Author's reply*)

THE EDITOR—SIR,

Drs Fitzgerald, Mackie and Manns are clearly as enthusiastic users of ultrasound as am I. It is the great success of ultrasound that has led to ever increasing workloads. This prompted our detailed retrospective analysis of 1861 patients, which forms only a small proportion of the 23 000 diagnostic ultrasound scans carried out in the department per year.

They make the statement that little time will be saved and much may be missed if the whole abdomen and pelvis are not examined in each patient. This is an unsubstantiated opinion not borne out in our series, which is the largest published to date. The thrust of modern radiology is in its selective and effective use. Surely, it is better to spend more time on important areas than disperse the effort in unproductive ones. Ultrasound is an interactive examination and it is normal and sensible practice to extend the examination according to one's findings. I would agree that on finding a pelvic mass the liver should be checked for metastases and the kidneys for obstruction.

I was surprised to see Dr Fitzgerald et al state their policy of offering ultrasound as the first line of investigation for abdominal symptoms. Barium studies or endoscopy are surely more appropriate for gastrointestinal symptoms and an intravenous urogram for suspected renal colic.

Critical use of our diagnostic resources is essential for the future. Larger, preferably prospective, studies will be necessary to help us make sensible decisions.

Yours, etc.,
K. C. DEWBURY

X-Ray Department (Ultrasound),
Southampton General Hospital,
Tremona Road,
Southampton
(*Received September 1988*)

Sarcoidosis mimicking metastatic testicular tumour

THE EDITOR—SIR,

Drs Parr and Williams (1988) have omitted to mention in their paper the interesting possibility that the intrathoracic sarcoidosis of their two cases could represent a sarcoid-like granulomatous reaction to the testicular tumour. This response is well recognized with malignant lymphomas (Brincker, 1972; Kadin et al, 1980). A recent report in *Thorax* described a case with a prominent sarcoid-like pulmonary granulomatous reaction to Hodgkin's disease, diagnosed 6 months before the development of the extrathoracic lymphoma, and which recurred with the exacerbations of the lymphoma (Daly et al, 1988).

I am not aware whether such granulomatous reaction is exclusive to lymphomas or if it can occur with other malignant tumours such as testicular teratoma and seminoma. It is suggested by Daly et al (1988) that a low serum angiotensin-converting enzyme activity and negative Kveim-Siltzbach test may help in distinguishing pulmonary granulomatous reaction related to Hodgkin's disease from active sarcoidosis. The two cases reported by Parr and Williams (1988) could well represent a coincidental pulmonary sarcoidosis, which caused difficulty in assessing the intrathoracic spread of a malignant testicular tumour. Nevertheless, the possibility of a granulomatous reaction justifies consideration.

Yours, etc.,
S. K. MORCOS

Department of Radiology,
Lodge Moor Hospital,
Sheffield S10 4LH
(*Received August 1988*)

References

BRINCKER, H., 1972. Sarcoid reactions and sarcoidosis in Hodgkin's disease and other malignant lymphomata. *British Journal of Cancer*, *26*, 120–128.

DALY, P. A., O'BRIAIN, D. S., ROBINSON, I., GUCKIAN, M. A. & PRICHARD, J. S., 1988. Hodgkin's disease with a granulomatous pulmonary presentation mimicking sarcoidosis. *Thorax*, *43*, 407–409.

KADIN, M. E., DONALDSON, S. S. & DORFMAN, R. F., 1970. Isolated granulomas in Hodgkin's disease. *New England Journal of Medicine*, *283*, 859–861.

PARR, M. J. A. & WILLIAMS, M. V., 1988. Sarcoidosis mimicking metastatic testicular tumour. *British Journal of Radiology*, *61*, 516–518.

1989, *The British Journal of Radiology*, 62, 294–295

New developments in the field of acute myocardial infarction imaging

THE EDITOR—SIR,

We read with interest the article by Bell et al (1988) regarding the development of newer and more effective myocardial infarction imaging agents. $^{99}\text{Tc}^{\text{m}}$ pyrophosphate and its analogues have severe limitations for the imaging of acute myocardial infarction (Turi et al, 1985) because of low specificity, dependence on blood flow for its uptake by necrotic myocardium and poor image quality. We wish to draw your attention to the development of a promising new agent for the imaging of acute myocardial infarction: radiolabelled monoclonal antimyosin antibodies.

Experimental work (Khaw et al, 1982) has shown that antimyosin antibodies bind specifically to myocardial cells with acute irreversible damage to the cell membrane. Initial studies using the experimental animal model of acute myocardial infarction (Khaw et al, 1979) have shown that ^{125}I-labelled antimyosin antibodies localize specifically at the site of myocardial infarction in high concentrations and there is a close correlation between the site of radiotracer uptake and histological myocardial necrosis. Because of unsuitable physical characteristics, ^{125}I was not used for human studies. These were carried out using $^{99}\text{Tc}^{\text{m}}$- (Khaw et al, 1986) or ^{111}In-labelled (Khaw et al, 1987a) Fab fraction of antimyosin antibodies. The use of Fab fraction instead of the intact molecule reduces the immunogenicity, enhances renal clearance of the unbound antibodies and gives a greater target to background ratio.

In a direct comparison of ^{111}In-labelled antimyosin antibodies with $^{99}\text{Tc}^{\text{m}}$ pyrophosphate in the canine model of experimental myocardial infarction (Khaw et al, 1987b), a good correlation was obtained between the area of infarction detected by the two agents. However, $^{99}\text{Tc}^{\text{m}}$ pyrophosphate consistently overestimated the infarct size. ^{111}In-antimyosin uptake correlated more closely with the histochemically outlined area of myocardial necrosis and was found to bind specifically to the necrotic myocardium, whereas $^{99}\text{Tc}^{\text{m}}$ pyrophosphate was taken up not only by the necrotic tissue but also by the ischaemic but non-necrotic myocardium.

We have recently participated in a multicentre Phase III study to evaluate the clinical usefulness and safety of ^{111}In-labelled monoclonal murine antimyosin antibodies in the detection and localization of myocardial necrosis in patients admitted with suspected acute myocardial infarction or unstable angina. The results of our first 103 patients (Jain et al, 1988a) showed a 98% sensitivity and 91% specificity for this agent in the diagnosis of acute myocardial infarction. Even small myocardial infarctions were diagnosed accurately. The preliminary results of the multicentre study support our interim analysis and a high sensitivity and specificity of the technique in detecting acute myocardial infarction (Berger et al, 1988) has been confirmed. The uptake by the ribs and sternum is negligible and the images are therefore much clearer and easier to interpret than pyrophosphate images. Figure 1 shows ^{111}In-antimyosin images in the anterior and 45° left anterior oblique views of a patient with acute inferolateral myocardial infarction, obtained 48 h after the injection of the radiotracer. There is a clear delineation of the radiotracer in the inferior and posterolateral walls. The liver is visualized but does not interfere with image interpretation and there is little uptake elsewhere. The only drawback of the technique is that we have to wait for at least 18–24 h after the injection for the unbound tracer to clear from the blood pool. The persistence of blood pool activity may interfere with early image interpretation in about 20% of cases, but this problem is not present at 48 h.

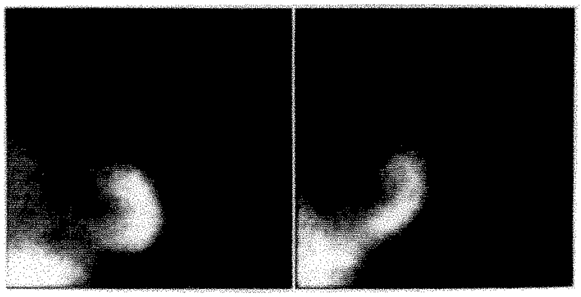

Figure 1. ^{111}In-antimyosin images in anterior (left) and 45° left anterior oblique (right) views of a patient with acute inferolateral myocardial infarction. There is intense tracer uptake in the inferior, posterolateral walls and the apex. Liver is visualized but does not interfere with image interpretation. Note the absence of uptake by ribs though there is minimal uptake by the sternum.

We have also observed different patterns of ^{111}In-antimyosin uptake in acute myocardial infarction which gave important prognostic information in these patients (Jain et al, 1988b). In a post-mortem study, we have observed a close correlation between the uptake of ^{111}In-antimyosin detected by autoradiography and the myocardial necrosis detected by histology (Jain et al, 1988c). Interestingly, we have noted an additional region of focal myocardial necrosis in a remote myocardial segment perfused by an unobstructed coronary artery; this region was correctly identified by ^{111}In-antimyosin imaging. Such a finding may give a new insight into the pathogenesis of acute myocardial infarction.

Currently, research is under way to replace ^{111}In with $^{99}\text{Tc}^{\text{m}}$ as the radiolabel for antimyosin, since $^{99}\text{Tc}^{\text{m}}$ is less expensive, has favourable physical characteristics and is more readily available. Further refinements in the technique which would result in early clearance from the blood pool will reduce the time to imaging. At present, antimyosin antibody imaging appears to be superior to pyrophosphate imaging for the detection and localization of acute myocardial necrosis. Other applications of this technique are also of interest, namely, detection of myocarditis and cardiac transplant rejection.

Yours, etc.,

DIWAKAR JAIN
AVIJIT LAHIRI
JOHN C. CRAWLEY
EDWARD B. RAFTERY

Department of Cardiology
and Divisions of Clinical Sciences
and Radioisotopes, Northwick Park Hospital
and Clinical Research Centre,
Harrow HA1 3UJ

(*Received August 1988 and in revised form October 1988*)

(*Authors' reply*)

THE EDITOR—SIR,

We note the reference to our paper (Bell et al, 1988) in the letter by Jain et al (above) and the ensuing discussion of their work with ^{111}In-antimyosin antibodies. We would point out that the aim of our study was to compare $^{99}\text{Tc}^{\text{m}}$-DMAD with

1989, *The British Journal of Radiology*, *62*, 295–296

^{99}Tc^{m}-PYP in myocardial infarction in the hope that the affinity for ^{99}Tc^{m}-DMAD for damaged myocardium compared with normal bone would facilitate better planar imaging. This was not the case and ^{99}Tc^{m}-PYP remains the standard imaging agent. We would agree that ^{99}Tc^{m}-PYP has limitations for the imaging of acute myocardial infarction, but it is cheap and readily available, and has the additional advantage that imaging is performed 2 h after administration. The sensitivity of ^{99}Tc^{m}-PYP imaging may well be improved through the use of single photon emission computed tomography.

The use of ^{111}In-labelled antimyosin antibody should improve the quality of image, owing to the absence of skeletal uptake, but has a number of disadvantages. It is expensive and not readily available making it less than ideal for the routine management of patients with acute myocardial infarction. A ^{99}Tc^{m} label should overcome the availability problem. A further delay is introduced by the fact that imaging cannot be performed until the day after injection because of circulating unbound tracer in the blood pool. The figures quoted by Jain et al shows a 98% sensitivity and 91% specificity for acute myocardial damage. This is an improved sensitivity compared with PYP (88%) but the same specificity (91%) as quoted in a large series (Turi, 1985). To state categorically that antimyosin antibody imaging is better than traditional PYP imaging in infarction requires a trial to compare both techniques in man. Khaw et al (1987) have published a comparative study in dogs showing a very good correlation between the two methods, though infarct size was overestimated by PYP. We have also used ^{111}In for myocardial imaging (Bell et al, 1987) and of course agree that ^{99}Tc^{m} labelling is desirable in view of its more favourable physical characteristics for gamma camera imaging, but would also suggest that single photon emission computed tomography is an important advance with regard to improved quality plus quantification of myocardial imaging (Jansen, 1985).

Yours, etc.,
D. Bell
A. M. Millar
R. Grayshan
A. L. Muir

Departments of Medicine and Radiopharmacy,
Edinburgh Royal Infirmary and Department of Pharmacy,
Heriot Watt University, Edinburgh
(*Received August 1988*)

References

Bell, D. et al, 1987. The acute inflammatory response to myocardial infarction: imaging with Indium-111 labelled autologous neutrophils.

Bell, D. M., Millar, A. M., Grayshan, R. & Muir, A. L., 1988. Radiopharmaceuticals for myocardial infarct imaging: a clinical comparison of ^{99}Tc^{m} pyrophosphate and ^{99}Tc^{m} dimethylaminoethylene disphosphonate. *British Journal of Radiology*, *61*, 646–648.

Berger, H., Lahiri, A., Leppo, J., Makler, T., Maddahi, J., Mintz, G. & Strauss, H. W., 1988. Antimyosin imaging in patients with ischaemic chest pain: initial results of Phase III multicentre trial. *Journal of Nuclear Medicine*, *29*, 805–806 (Abstract).

Jain, D., Lahiri, A., Ravl, U., James, C., Crawley, J. C. W. & Raftery, E. B., 1988a. Sensitivity and specificity of ^{111}In-labelled antimyosin for detection of acute myocardial infarction. *Nuclear Medicine Communications*, *9*, 148 (Abstract).

Jain, D., Lahiri, A., Crawley, J. C. W., Berger, H. & Raftery, E. B., 1988b. Significance of diffuse uptake of ^{111}In-labelled antimyosin in acute myocardial infarction. *Nuclear Medicine Communications*, *9*, 149 (Abstract).

Jain, D., Lahiri, A., Crawley, J. C. W. & Raftery, E. B., 1988c. Postmortem correlation between the histopathological and autoradiographic extent of myocardial necrosis detected by ^{111}In-antimyosin imaging in a patient with acute myocardial infarction. *American Journal of Cardiac Imaging*, *2*, 158–161.

Jansen, D. E., Corbett, J. R., Wolfe, C. L., Lewis, S. E., Gabliani, G., Filipchuk, N., Redish, G., Parkey, R. W., Buja, M., Jaffe, A. S., Rude, R., Sobel, B. E. & Willerson, J. T., 1985. Quantification of myocardial infarction: a comparison of single photo-emission computed tomography with pyrophosphate to serial plasma MB-creatine kinase measurements. *Circulation*, *72*, 327–333.

Khaw, B. A., Fallon, J. T., Beller, G. A. & Haber, E., 1979. Specificity of location of myosin specific antibody fragments in experimental myocardial infarction: histologic, histochemical, autoradiographic and scintigraphic studies. *Circulation*, *60*, 1527–1531.

Khaw, B. A., Scott, J., Fallon, J. T., Cahill, S. L., Haber, E. & Homey, C., 1982. Myocardial injury: quantitation by cell sorting initiated with antimyosin fluorescent spheres. *Science*, *217*, 1050–1052.

Khaw, B. A., Gold, H, K., Yasuda, T., Leinbach, R. C., Kanke, M., Fallon, J. T., Barlai-Kovach, M., Strauss, H. W., Sheehan, F. & Haber, E., 1986. Scintigraphic quantification of myocardial necrosis in patients after intravenous injection of myosin-specific antibody. *Circulation*, *74*, 501–508.

Khaw, B. A., Yasuda, T., Gold, H. K., Leinbach, R. C., Johns, J. A., Kanke, M., Barlai-Kovach, M., Strauss, H. W. & Haber, E., 1987a. Acute myocardial infarct imaging with In-111 labelled monoclonal antimyosin Fab. *Journal of Nuclear Medicine*, *28*, 1671–1678.

Khaw, B. A., Strauss, H. W., Moore, R., Fallon, J. T., Yasuda, T., Gold, H. K. & Haber, E., 1987b. Myocardial damage delineated by indium antimyosin Fab and technetium-99m pyrophosphate. *Journal of Nuclear Medicine*, *28*, 76–82.

Turi, Z. G., Rutherford, J. D., Roberts, R., Muller, J. E., Jaffe, A. S., Rude, R. E., Parker, C., Raabe, D. S., Stone, P. H., Hartwell, T. D., Lewis, S. E., Parkey, R. W., Gold, H. K., Robertson, T. L., Sobel, B. E. & Willerson, J. T., 1985. Electrocardiographic, enzymatic and scintigraphic criteria of acute myocardial infarction as determined from the study of 726 patients (a Milis study). *American Journal of Cardiology*, *55*, 1463–1470.

The unseen radiation hazards of ultrasound

The Editor—Sir,

The 1985 *Ionizing Radiations Regulations* (Health & Safety Commission, 1985) state that the dose limit for the abdomen of a pregnant woman shall be 10 mSv (1.0 rem) during the declared term of the pregnancy. If the declared term of the pregnancy is taken as 40 weeks and the women works a 40-h week, this figure works out to a dose limit of 50 μSv(5.0 mrem) per working day. Assuming a 36-week or 30-week declared term the dose limits would be 55.6 μSv (5.56 mrem) and 66.7 μSv (6.67 mrem), respectively, per working day. The National Radiological Protection Board (NRPB) in their recent publication *Interim Guidance on the Implications of Recent Revisions of Risk Estimates and the IRCP 1987 Como Statement* (NRPB, 1987), have made recommendations that all

1989, *The British Journal of Radiology*, *62*, 296–298

radiation workers keep within an average of 15 mSv (1.5 rem) effective dose-equivalent per year. This brings all workers down to the current legal maximum dose-rate during pregnancy.

In many hospitals it is common practice to book a patient in for more than one investigation in a day, saving the patient time and inconvenience. Where the investigations are for carcinoma of the breast or bronchus, the patient often visits the radioisotope department for a bone scan injection and immediately goes to the ultrasound department for a liver scan. This usefully fills in the time before bone imaging. Where such booking procedures are routine it is possible to find oneself scanning two or more radioactive patients in one day. Such an exposure may come close to the maximum permitted dose-rate to the abdomen if the ultrasound operator is pregnant, and close to the new NRPB recommended dose-rate if the exposure occurs on a regular basis.

Harding et al (1985) have estimated the dose-rates to nurses at 10 cm from a patient leaving the department after a bone scan to be at a maximum of 96 μSv (9.6 mrem) per hour. These rates were calculated from readings collected perpendicular to the mid-trunk of the patient within 10 min of injection. Using this data, assuming that a liver scan may take up to 15 min to perform and that the scan is performed promptly after the injection, the dose to any part of the operator within 10 cm of the patient will be 24 μSv (2.4 mrem) per patient. Thus scanning two such patients in a day will bring the pregnant operator close to or above the maximum permitted dose-rate.

In the light of the recent NRPB recommendations, the possibility of receiving significant amounts of ionizing radiation from radioactive patients assumes importance not only for pregnant radiologists and ultrasonographers but for all radiation workers. The Board emphasizes that as long as the legal dose limits remain at their present levels, it is important to "keep exposures as low as reasonably achievable, since continued exposure near to the dose limit represents a level of risk which verges on the unacceptable". It goes on to recommend that the dose to individual workers should be controlled so as not to exceed an average of 15 mSV (1.5 rem) effective dose-equivalent per year. This works out as 57 μSv (5.7 mrem) per working day, a level which may be achieved by any ultrasound operator routinely scanning two or more radioactive patients per day.

These are simple extrapolations but it may be that dose-rates are even higher. Harding took his data above the abdomen of his patients at 10 min after injection and not above the ribs where the radiopharmaceutical is concentrating and where the ultrasonographer is in closest contact during a liver scan. In cases where there are rib metastases the doses could be even higher. The pregnant abdomen may easily be within 10 cm of the ribs, especially when reaching around the patient to examine the spleen and left kidney.

Perhaps it is time to review the practice of booking radioactive patients for ultrasound. The problem is not limited to bone scanning. Patients do occasionally leave the isotope department with a full bladder (probably containing 50% of the dose) after a DTPA study in order to have kidneys and pre- and post-micturition bladder volumes assessed by ultrasound. The hazard is an unseen one as most patients do not volunteer the information that they are radioactive. Therefore the pregnant ultrasonographer is unaware that she is in close proximity to a source of ionizing radiation. This is doubly important as many radiologists and radiographers consider the ultrasound department as a safe haven and elect to do more sessions in ultrasound during pregnancy in order to avoid the risks of exposure from other radiological procedures.

Obviously there is scope for collecting accurate data on this subject but until such information is available, pregnant radiologists or radiographers or indeed anyone wishing to remain within the newly advised 15 mSV (1.5 rem) effective dose-equivalent per year should be advised to ask patients about prior radionuclide administration before scanning them. Alternatively, perhaps the practice of double booking any radioactive patient should simply be abandoned.

Yours, etc.,
A. C. HAVARD

Department of Radiology,
Charing Cross Hospital,
London W6 8RF

(*Received August 1988*)

References

HARDING, L. K., MOSTAFA, A. B., RODEN, L. & WILLIAMS, N., 1985. Dose rates from patients having nuclear medicine investigations. *Nuclear Medicine Communications*, *6*, 191–194.

HEALTH & SAFETY COMMISSION, 1985. *Ionizing Radiations Regulations, 1985* (HMSO, London).

NRPB, 1987. *Interim Guidance on the Implications of Recent Revisions of Risk Estimates and the IRCP 1987 Como Statement*, November 1987 (HMSO, London).

Incorporating the time factor into the linear-quadratic model

THE EDITOR—SIR,

In recent years the linear-quadratic (LQ) model (Kellerer et al, 1971; Chadwick & Leenhouts, 1973) has become the model of choice for the description of single-dose radiation damage in *in vitro* as well as *in vivo* biological systems. This model has been used to describe both tumour and normal-tissue responses to fractionated radiotherapy and continuous low-dose-rate irradiation. A useful overview can be found for instance in Thames and Hendry (1987), which also contains further references. In particular, work by Douglas and Fowler (1976), Thames et al (1982) and Barendsen (1982), and more recently by Dale (1986a, b; Dale et al, 1988) has been of great influence.

A potential shortcoming of the LQ model as it is presently used is the inability to address the issue of proliferation during treatment of both tumour cells and early reacting normal tissues. In a recent paper (van de Geijn, 1988), a new model was introduced that also describes damage to both tumours and early reacting (ER) normal tissues to fractionated radiotherapy, in terms of either the two-component or the linear-quadratic model, but with the added advantage of incorporating the effects of proliferation and time. In the course of further developing this model it was realized, however, that the simple exponential form of the LQ model would allow for an elegant and powerful incorporation of the time parameter for both tumour and normal-tissue reactions. As is shown below, under certain conditions the extended LQ model for survivals from agimen of n equal fractions of dose d over a total time t_n takes the simple form

$$S_n(d, t_n) = \exp(-n\alpha d - n\beta d^2 + \lambda t_n)$$

for tumour as well as for normal tissues.

Tumour response

Single-dose survival of clonogenic (C) cells from a dose d is, in the LQ model, given by

$$S_1(d) = \exp(-\alpha_C d - \beta_C d^2) \qquad (1)$$

Let fractionated treatment start at $t = 0$, and equal fractions be delivered at times t_i, at intervals Δt_i large enough so that repair of sublethal damage can be considered substantially completed. Let $T_{2(C)}$ be the characteristic doubling time so that the growth rate is given by

$$\lambda_C = 0.693/T_{2(C)}$$

Incorporating the exponential growth over the time interval Δt_1 after the first fraction, delivered at $t_1 = 0$

$$S_1(d, t_1 + \Delta t_1) = \exp(-\alpha_C d - \beta_C d^2)\exp(\lambda_C \Delta t_1)$$

or

$$S_1(d, t_1 + \Delta t_1) = \exp(-\alpha d - \beta d^2 + \lambda_C \Delta t_1) \qquad (2)$$

After the second dose, delivered at $t_2 = t_1 + \Delta t_1$, after completion of the sublethal damage repair

$$S_2(d, t_2) = \exp(-2\alpha_C d - 2\beta_C d^2)\exp(\lambda_C \Delta t_1)$$

At Δt_2 later, that is, at $t_2 + \Delta t_2$

$$S_2(d, t_2 + \Delta t_2) = \exp[-2\alpha d - 2\beta d^2 + \lambda_C(\Delta t_1 + \Delta t_2)] \qquad (3)$$

Similarly, after n doses, over a total time $t_n = \Sigma_{i=1}^{n-1} \Delta t_i$

$$S_n(d, t_n) = \exp(-n\alpha_C d - n\beta_C d^2 + \lambda_C t_n) \qquad (4)$$

If there is a delay time $T_{\mathrm{delay(C)}}$ in the onset of the "acute" C-cell proliferation, Equation 4 becomes

$$S_n(d,t_n) = \exp[-n\alpha_C d - n\beta_C d^2 + \lambda_C(t_n - T_{\mathrm{delay(C)}})] \qquad (5)$$

So far, both the acute doubling rate and the fraction dose are assumed to be constant. It is clear that in that case, Equations 4 and 5 can easily be used to investigate, for any given regimen, the influence of C-cell doubling time and the delayed onset of characteristic proliferation on the C-cell survival at the end of the treatment.

In a more general case the dose per fraction may vary over time. This is easily represented by replacing, in Equations 4 and 5, nd and nd^2 by $\Sigma_{i=1}^{n} d_i$ and $\Sigma_{i=1}^{n} d_i^2$, respectively. In case the C-cell doubling rate changes over time, λ_C becomes a function of time and $\lambda_C t_n$ has to be replaced by $\Sigma_{i=1}^{n-1} \lambda_C(t_i)\Delta t_i$. In the case of a delayed onset of C-cell proliferation, an initial set of the $\lambda_C(t_i)$ is equal to zero.

Normal-tissue reactions

From the start of treatment, dividing stem (S) cells and transitional cells are subject to radiation damage. Until the acute proliferation of the S cells is triggered at some time $T_{\mathrm{delay(S)}}$ after the start of treatment, the survival of these cells is governed by the basic LQ equation (Barendsen, 1982), with their own characteristic α_S and β_S. Let k fractions have been delivered at the time $T_{\mathrm{delay(S)}}$, the onset of acute S-cell proliferation. At that time the survival of the S-cell/transitional cell system will then be given by the conventional LQ expression

$$S_k(d, T_{\mathrm{delay(S)}}) = \exp(-k\alpha_S d - k\beta_S d^2) \qquad (6)$$

It may be, as is assumed to be the case for late reacting (LR) tissues, that T_{delay} is longer than the duration of the treatment; alternatively, treatment may be delivered in such a short overall time that even for ER tissue the onset of acute proliferation occurs only after the completion of treatment. In those cases, the conventional LQ model applies during the whole treatment, and for some time after. An excellent overview of ranges of doubling times and delay times for several normal tissues can be found in Thames and Hendry (1987), Chapter 4, which also refers to pertinent original investigations. Usually, for ER tissue $T_{\mathrm{delay(S)}}$ is shorter than the overall duration of the treatment. Then, according to the scenario presented in van de Geijn (1988), the surviving fraction after each subsequent fraction grows over the interfraction interval Δt_i according to

$$S_i(d, t_i + \Delta t_i) = \frac{S_i(d, t_i)}{S_i(d, t_i) + (1 - S_i(d, t_i))\exp(-\lambda_S \Delta t_i)} \qquad (7)$$

with $\lambda_S = 0.693/T_{2(S)}$, $T_{2(S)}$ being the acute S-cell doubling time. This expression describes the homeostatic control governing repopulation. It was first introduced by Cohen and Scott (1968). After the next fraction

$$S_{i+1}(d, t_{i+1}) = S_i(d, t_i + \Delta t_i)\exp(-\alpha_S d - \beta_S d^2) \qquad (8)$$

and Equation 7 applies again over the next interval. For oral mucosa and for skin, $T_{2(S)}$ is of the order of 1 day, and interfraction times are of the same order. Then, for $\Delta t = 1$ day, $\exp(-\lambda_S \Delta t) \sim 0.5$ and cannot be simplified. However, at time $T_{\mathrm{delay(S)}}$ the surviving fraction $S_k(d, T_{\mathrm{delay(S)}})$ is usually already very small (van de Geijn, 1988), that is, much smaller than 0.5. As long as that is the case, Equation 7 may be approximated by

$$S_i(d, t_i + \Delta t_i) = S_i(d, t_i)\exp(\lambda_S \Delta t_i) \qquad (9)$$

Thus, after n fractions over a total time t_n

$$S_n(d, t_n) = \exp[-n\alpha_S d - n\beta_S d^2 + \lambda_S(t_n - T_{\mathrm{delay(S)}})] \qquad (10)$$

which is entirely similar to Equation 5 for the tumour.

It should be realized, however, that for early reacting normal tissues this approximation holds only as long as the surviving fraction $S_i(d, t_i)$ remains really small, as indicated above. In reality, depending on the α_S, β_S, the fraction size and the interfraction intervals Δt_i, the effective repopulation rate may decrease during the course of the treatment, as was demonstrated by van de Geijn (1988).

In conclusion, Equation 5 and its equivalent Equation 10 would seem to be useful extensions of the basic LQ model. The time parameter becomes non-zero for the tumour once the characteristic C-cell proliferation has been triggered. For normal tissues the same applies, within certain constraints, after the triggering of the acute stem cell proliferation. It is difficult to determine characteristic S-cell and C-cell doubling times in practice, and it may be impossible to determine variations over time, if any, but calculations on the basis of Equations 5 and 10 allow at least for "bracketing" the magnitudes of their effects, that is, making useful estimates of the influence of doubling times within reasonable limits, in any given or proposed treatment regimen.

Yours, etc.,
J. VAN DE GEIJN

Radiation Oncology Branch,
Division of Cancer Treatment,
National Cancer Institute,
Bethesda MD 20892,
USA

(Received August 1988 and in revised form October 1988)

Acknowledgments

The author is greatly indebted to J. F. Fowler and J. B. Mitchell for their interest and encouragement.

1989, *The British Journal of Radiology*, *62*, 298–299

References

Barendsen, G. W., 1982. Dose fractionation, dose rate and iso-effect relationships for normal tissue responses. *International Journal of Radiation Oncology, Biology, Physics*, *8*, 1981–1999.

Chadwick, K. M. & Leenhouts, H. P., 1973. A molecular theory of cell survival. *Physics in Medicine and Biology*, *18*, 78.

Cohen, L. & Scott, M. J., 1968. Fractionation procedures in radiation therapy, a computerized approach to evaluation. *British Journal of Radiology*, *41*, 529–533.

Dale, R. G., 1986a. The application of the linear-quadratic model to fractionated radiotherapy when there is incomplete normal tissue recovery between fractions, and possible implications for treatments involving multiple fractions per day. *British Journal of Radiology*, *59*, 919–927.

——1986b. A graphical method to simplify the application of the linear-quadratic dose–effect equation to fractionated radiotherapy. *British Journal of Radiology*, *59*, 1111–1115.

Dale, R. G., Huczkowski, J. & Trott, K. R., 1988. Possible dose rate dependence of recovery kinetics as deduced from a preliminary analysis of the effects of fractionated irradiations at varying dose rates. *British Journal of Radiology*, *61*, 153–157.

Douglas, B. G. & Fowler, J. F., 1976. The effect of multiple small doses of X-rays on skin reactions in the mouse and a basic interpretation. *Radiation Research*, *66*, 401–426.

van de Geijn, J., 1988. Time-dose-response of human tumors and normal tissues during and after fractionated radiotherapy. A new model. *Radiotherapy and Oncology*, *12*, 57–78.

Kellerer, A. M. & Rossi, H. H., 1971. RBE and the primary mechanism of radiation action. *Radiation Research*, *47*, 15–34.

Thames, H. D. & Hendry, J. H., 1987. In *Fractionation in Radiotherapy* (Taylor and Francis, London), pp. 166–169, 226–237.

Thames, H. D., Withers, H. R., Peters, L. J. & Fletcher, G. H., 1982. Changes in early and late radiation responses with altered dose fractionation: implications for dose-survival relationships. *International Journal of Radiation Oncology, Biology, Physics*, *8*, 219–226.

Post-operative neutron irradiation

The Editor—Sir,

Glaholm and Harmer (1988) reported a prospective study of post-operative irradiation with neutrons (five patients) or photons (nine patients) in patients with soft-tissue sarcomas. The unacceptable late tissue damage in the neutron group led to the termination of the trial.

These results, although based on a small number of patients, support the radiobiological data. Absence of a gross tumour may not be a proper indication of neutron therapy, since it deprives the radiotherapist of both the hypoxic and kinetic gain factors. When a bulky tumour is present, as in definitive or pre-operative irradiation, the following conditions are fulfilled, at least theoretically: (i) the amount of hypoxic cells is greatest, an optimum situation for high linear energy transfer radiation; (ii) a bulky tumour is supposed to repair photon-induced potentially lethal damage efficiently (Little et al, 1973; Guichard et al, 1984) and less repair is observed after neutron irradiation (Rasey & Nelson, 1981); (iii) sarcomas are likely to contain a large number of non-cycling cells (Malaise et al, 1973), which do not redistribute efficiently between fractions, and therefore would exhibit less resistance to fractionated neutron therapy as compared with photon treatment (Withers & Peters, 1979); and (iv) the α/β ratio for dose effect is generally higher for tumours than for late-responding tissues (Fowler, 1984). The relative biological effectiveness (RBE) is expected to be higher in tissues with a low α/β ratio as compared with populations with a high α/β ratio (Withers et al, 1982).

For all these reasons, a therapeutic gain would be achieved if the ratio of the amount of tumour to the amount of late-responding tissue is highest in the irradiated volume, such as in pre-operative or definitive irradiation of bulky tumours. These conditions are not fulfilled in post-operative irradiation, where the few remaining clusters of cells (if any) are expected to be well oxygenated, to have a short doubling time and to redistribute between fractions. These factors contribute to a low neutron RBE for the tumour population, and therefore a therapeutic loss.

The authors' conclusion that there is no biological advantage in the use of fast neutrons for the treatment of soft-tissue sarcoma is not substantiated in their report. It should be recalled that good results have been observed by others in these particular tumours (Cohen et al, 1985; Schmitt et al, 1986; Pickering et al, 1987).

Yours, etc.,
A. Courdi

Centre A. Lacassagne,
36 Voie Romaine,
06054 Nice Cedex,
France

(*Received October 1988*)

References

Cohen, L., Hendrickson, F. R., Kurup, P. D., Mansell, J. A., Awschalom, M., Rosenberg, I. & Ten Haken, R. K., 1985. Clinical evaluation of neutron beam therapy. Current results and prospects, 1983. *Cancer*, *55*, 10–17.

Fowler, J. F., 1984. Total doses in fractionated radiotherapy. Implications of new radiobiological data. *International Journal of Radiation Biology*, *46*, 103–120.

Glaholm, J. & Harmer, C., 1988. Soft-tissue sarcoma: neutrons versus photons for post-operative irradiation. *British Journal of Radiology*, *61*, 829–834.

Guichard, M., Weichselbaum, R. R., Little, J. B. & Malaise, E. P., 1984. Potentially lethal damage repair as a possible determinant of human tumour radiosensitivity. *Radiotherapy and Oncology*, *1*, 263–269.

Little, J. B., Hahn, G. M., Frindel, E. & Tubiana, M., 1973. Repair of potentially lethal radiation damage *in vitro* and *in vivo*. *Radiology*, *106*, 689–694.

Malaise, E. P., Chavaudra, N., Battaglini, F., Richard, J. M. & Tubiana, M., 1973. Cinétique de prolifération cellulaire des divers types anatomo-pathologiques des tumeurs humaines. *Bulletin du Cancer*, *60*, 119–130.

Pickering, D. G., Stewart, J. S., Rampling, R., Errington, R. D., Stamp, G. & Chia, Y., 1987. Fast neutron therapy for soft-tissue sarcoma. *International Journal of Radiation Oncology, Biology, Physics*, *13*, 1489–1496.

Rasey, J. S. & Nelson, N., 1981. Repair of potentially lethal damage following irradiation with X rays or cyclotron neutrons: response of the EMT-6/UW tumor system treated under various growth conditions *in vitro* and *in vivo*. *Radiation Research*, *85*, 69–84.

Schmitt, G., Fürst, G. & Bamberg, M., 1986. The value of neutron- and neutron-boost irradiation for the local control of advanced soft-tissue sarcomas. *Bulletin du Cancer*, *73*, 577–581.

WITHERS, H. R. & PETERS, L. J., 1979. The application of RBE values to clinical trials of high LET radiation. In *High LET Radiations in Clinical Radiotherapy*, ed. by G. W. Barendsen, J. Broerse & K. Breur (Pergamon Press, New York), pp. 257–261.

WITHERS, H. R., THAMES, H. D. & PETERS, L. J., 1982. Biological bases for high RBE values for late effects of neutron irradiation. *International Journal of Radiation Oncology, Biology, Physics*, *8*, 2071–2076.

(*Authors' reply*)

THE EDITOR—SIR

The theoretical advantages for the use of external-beam fast neutron therapy in the treatment of soft-tissue sarcoma are not in dispute, indeed these were the rationale for conducting the reported randomized study of neutrons versus photons.

As we discussed in our paper, a number of centres have reported improved local control with neutron irradiation (Franke, 1979; Salinas et al, 1980; Cohen et al, 1984; Pickering et al, 1987). However, other attempts using neutrons have been less encouraging (Batterman & Breuer, 1981; Duncan et al, 1982, 1986). The incidence of serious late tissue damage following irradiation with pure neutron beams has been reported to be as high as 28.6% (Schmitt et al, 1983, 1984; Richard et al, 1985; Pickering et al, 1987).

It is conceivable that a greater therapeutic gain may be achieved if the ratio of tumour to normal tissue was large, as in the case of pre-operative irradiation or in the treatment of inoperable disease. However, wide tumour excision and in particular compartmental resection followed by high-dose external-beam irradiation is the treatment policy of the Royal Marsden Hospital Sarcoma Unit for operable soft-tissue sarcoma. We remain unconvinced of any advantage resulting from the use of external-beam fast neutron irradation in this circumstance.

Yours, etc.,
J. GLAHOLM
C. HARMER

Sarcoma Unit,
The Royal Marsden Hospital,
Fulham Road,
London SW3 6JJ

(*Received November 1988*)

References

BATTERMAN, J. J. & BREUER, K., 1981. Fast neutron therapy for locally advanced sarcomas. *International Journal of Radiation Oncology, Biology, Physics*, *7*, 1051–1053.

COHEN, L., HENDRICKSON, F., MANSELL, J. O. A., KURUP, P., AWSCHALOM, M. & ROSENBERG, I., 1984. Response of sarcomas of bone and soft tissue to neutron beam therapy. *International Journal of Radiation Oncology, Biology, Physics*, *10*, *821–824*.

DUNCAN, W., ARNOTT, S. J. & LACK, W. J. L., 1986. The Edinburgh experience of treating sarcomas of soft tissues and bone with neutron irradiation. *Clinical Radiology*, *37*, 317–320.

DUNCAN, W., ARNOTT S. J., ORR, J. A. & KERR, G. R., 1982. The Edinburgh experience of fast neutron therapy. *International Journal of Radiation Oncology, Biology, Physics*, *8*, 2155–2157.

FRANKE, H. D., 1979. Results of clinical applications of fast neutrons at Hamburg–Ependorf. In *High LET Radiations in Clinical Radiotherapy*, ed. by G. W. Barendsen, J. J. Broerse & K. Bruer (Pergamon Press, Oxford), pp. 51–59.

PICKERING, D. G., STEWART, J. S., RAMPLING, R., ERRINGTON, R. D., STAMP, G. & CHIA, Y., 1987. Fast neutron therapy for soft tissue sarcoma. *International Journal of Radiation Oncology, Biology, Physics*, *13*, 1489–1495.

RICHARD, F. R., RENARD, L. & WAMBERSIE, A., 1985. Results of neutron therapy of locally advanced soft tissue sarcomas at Louvain-La-Neuve. *Strahlentherapie*, *161*, 794–796.

SALINAS, R., HUSSEY, D. H., FLETCHER, G. H., LINDBERG, R. J., MARTIN, R. G. & PETERS, L. J., 1980. Experience with fast neutron therapy for locally advanced sarcomas. *International Journal of Radiation Oncology, Biology, Physics*, *6*, 267–272.

SCHMITT, G., RASSOW, J., SCHNABEL, K., BORMANN, R., BAMBERG, M., SCHERER, E. & STREFFER, C., 1984. Radiotherapy of soft tissue sarcomas with neutrons or a neutron boost. *British Journal of Radiology*, *57*, 247–250.

SCHMITT, G., SCHNABLE, K., SAUERWEIN, W. & SCHERER, E., 1983. Neutron and neutron boost irradiation for soft tissue sarcomas. 4.5 year analysis of 139 patients. *Radiotherapy and Oncology*, *1*, 23–29.

1989, *The British Journal of Radiology*, 62, 300–304

Book reviews

Doppler Echocardiography. The Quantitative Approach, 2nd edn. By Arthur J. Labovitz and George A. Williams, pp. x + 121, 1988 (Lea & Febiger, Philadelphia), $22.95.
ISBN 0–8121–1105–2

This book aims to provide a basic primer in the clinical applications of Doppler ultrasound in cardiology. To understand how Doppler ultrasound is used to measure blood velocity and, in particular, to appreciate its limitations, requires some appreciation of the physical principles of the method. Thus, many clinicians find the opening chapters of texts on Doppler rather daunting. To try to overcome this difficulty, the authors have compressed the discussion of blood flow and the theory of continuous-wave and pulsed Doppler into a total of eight pages. The problem is that this leaves several aspects unmentioned and what is provided contains half-truths and even fallacies.

The normal examination is described with the aid of recordings keyed to clear diagrams. It is, however, unclear why examples of pathological valve regurgitation are given in this chapter when there is no mention of the "physiological" tricuspid and pulmonary valve regurgitation reported to be present in the majority of normal subjects.

The chapters on aortic and mitral valve lesions and prosthetic valve applications cover the basic needs and include a number of "case studies", with spaces for the reader to fill in answers obtained from inspection of the accompanying illustration. The chapter on left ventricular function describes methods of measurement of cardiac output but also includes a number of other Doppler derived parameters which will not be of great interest to the newcomer. There is a brief treatment of congenital heart disease in the adult. References are appended to each chapter but, since they are not cited in the text, their relevance is frequently obscure.

This book is clearly written and the illustrations are mainly of good quality, but not very well positioned in relation to the accompanying text. A slim paperback, aimed at broad readership, it offers a superficial treatment of a complex subject which may appeal to small-town US cardiologists but is unlikely to satisfy a serious student, who would be better advised to consult one of the more detailed and authoritative texts already available.

Graham J. Leech

Ultrasonography of the Neck. By J.-N. Bruneton, pp. xiv + 118, 1987 (Springer-Verlag, Berlin), DM118.
ISBN 3–540–17039–1 (Berlin)
0–387–17039–1 (New York)

This short book covers virtually all aspects of neck ultrasound, with the notable exception of assessment of the carotid arteries and the use of Doppler. It is made up of seven chapters, the first of which describes the anatomy of the neck and examination techniques. There are then chapters on the thyroid, parathyroids and salivary glands, discussing the clinical features, pathology and, to some extent, the management of conditions likely to be encountered. There is also some discussion of the role of other imaging techniques although, surprisingly, a relatively small amount of space is allocated to describing the ultrasound appearances; there are, however, numerous illustrations. The remaining chapters cover miscellaneous conditions, including the assessment of oral tumours, lymph nodes and paediatric problems.

This is a multi-author book, although Dr Bruneton is the principal author of most chapters. Despite this, there is an unnecessary degree of repetition in the text. The illustrations, although numerous, have not always reproduced well and in some chapters, too many similar examples are shown.

The author has considerable personal experience in the field of tumour assessment and this aspect is stressed throughout the book. Those involved in the staging of ENT tumours by ultrasound should therefore find it useful. For beginners in the field of neck ultrasound, the clinical material could provide useful background reading but overall, as this is such a slim volume, I do not feel that it is particularly good value for money.

F. E. White

The Use of Transrectal Ultrasound in the Diagnosis and Management of Prostate Cancer. Ed. by Fred Lee and Richard D. McLeary, pp. xii + 228, 1987 (Alan R. Liss, New York), £23.00.
ISBN 0–8451–5087–1

In considering the choice of new textbooks for the departmental library the average United Kingdom radiologist, working with diminishing budget and increasing prices, may be forgiven for quickly dismissing a 228-page textbook concerned solely with transrectal ultrasound of the prostate. Thirty per cent of males over the age of 50 will, however, show latent carcinoma of the prostate and perhaps radiologists should be taking both this disease and its method of imaging more seriously.

The book represents the proceedings of a symposium held in Detroit in late 1986 and the format of the text is variable, being made up of facsimiles of the author's own submissions. Great care has, however, been taken by the publishers to ensure that both the text and, more particularly, the illustrations are clearly and faithfully reproduced.

The collected reports are not solely concerned with clinical aspects of transrectal ultrasound examination and the first two chapters are a historical review of the technique and a description of the pathological processes that occur within the prostate. Subsequent contributions discuss the pertinent physics of an optimal examination and its performance, before the discussion focuses on diagnostic considerations in transrectal ultrasound imaging of the prostate and the use of this technique in screening for carcinoma. There are short contributions describing needle biopsy techniques for both cytological and histological material, but the concluding third of the book is devoted to four chapters describing the experience of differing clinical groups within the United States, the United Kingdom, Japan and Germany. In all, there are 18 chapters covering this interesting and somewhat controversial subject.

Of necessity, publication of symposium proceedings results in variable literary style as well as degree of overlap of the content. In this case this is by no means to the detriment of the book, as it is only by considering the varying and sometimes opposing views of different contributors that a reader, inexperienced in prostatic ultrasound, can form a balanced view as to its relevance.

Whilst the book might not be everyone's choice of bedtime reading, nor is its inclusion in every departmental library to be advised, nevertheless, if this imaging service is contemplated then the radiologist might be wise to examine this textbook before he commences.

D. M. King

Cerebral Angio-CT. By Kazuhiko Sadamoto and Keiji Fukui, pp. x + 102, 1988 (Raven Press, New York), $61.50.
ISBN 0–88167–403–6

"Cerebral angio-CT" is the name given by the authors to the technique of rapid sequential scanning through a region of interest in a variety of planes following an intravenous infusion of contrast medium. Infusion rates, scan planes and scanning intervals are given in quite exhaustive detail although these relate only to the General Electric 9800 and 9000-2 CT scanners. The protocols will need to be adapted for other scanners.

The volume is profusely illustrated with high-quality scans and clear expositions of intracranial vascular anatomy. Conversely, the text falls far short of what might be reasonably expected from an American publisher. The standard of the translation from the Japanese is poor, resulting in many very clumsy and sometimes barely comprehensible statements. Spelling errors are frequent.

After the "basics", the authors go on to relate their experience with angio-CT in screening mainly for aneurysms and in the demonstration of a variety of conditions following initial diagnosis. The final sections are devoted to illustrative case histories and pitfalls for the unwary. Throughout the text, one is aware of some repetition and "padding".

Quite where angio-CT might find a place in British practice is problematic. Suffice to say the reviewer does not share the authors' missionary zeal. Its adoption as a screening method will undoubtedly overburden most scanners and there is (as yet) no clinical demand for the diagnosis of essentially asymptomatic intracranial aneurysms.

This is a specialized CT technique and should be used as such. It may be of some value in the demonstration of rather subtle, isodense subdural haematomas or in clinically dubious cases of subarachnoid haemorrhage prior to angiography.

This is not a book for the individual to purchase. It may nevertheless find a place in the departmental library, simply because the concept of angio-CT is a sound one and the book is sufficiently well illustrated for its literary failings not to matter too much. For a hard-bound book, albeit a slim one, the price is not unreasonable, and with proper editing a second edition could be greatly improved.

P. Butler

Normal Anatomy for Multiplanar Imaging. By Bharat Raval, Joel W. Yeakley and John H. Harris Jr, 1987 (Williams & Wilkins, Baltimore)
The Trunk and Extremities, pp. xiv + 199, £43.00.
ISBN 0–683–07154–8
Head, Neck and Spine, pp. xiv + 433, £90.00.
ISBN 0–683–07153–X

These two companion volumes provide an anatomical atlas based mainly on computed tomography but also including some magnetic resonance images. There are clearly annotated line drawings on the pages facing the images. The illustrations are uniformly clear and large. Where appropriate, scout views show the sectional level of the CT scans. There is a good balance between unenhanced and contrast-enhanced scans. A useful feature is the explanatory notes which advise on positioning and scanning technique. The volume on the head, neck and spine contains considerable detail, particularly applied to the sellar region, temporal bone, paranasal sinuses and nasopharynx.

There are a few criticisms. The identification of blood vessels in the superior mediastinum is not complete; more coronal MR images of the chest and abdomen as well as sagittal sections of the knee would have been helpful inclusions. The important retroperitoneal fascial compartments could have been illustrated in more detail.

These atlases are highly recommended as reference books within imaging departments. Trainee radiologists would also greatly benefit from their availability.

G. H. Whitehouse

Computed Tomography of the Chest: a Teaching File. By M. Elon Gale and Joel B. Karlinsky, pp. xviii + 254, 1988 (Year Book Medical Publishers, Chicago), £41.50.
ISBN 0–8151–3322–7

The book starts with a nicely annotated section on normal anatomy of the mediastinum, bronchi and fissures. The remainder of the book is divided into chapters on parenchyma, hila and airways, mediastinum, cardiovascular system, pleura, diaphragm and chest wall. There are 209 cases, all well illustrated, each with a short and cogent description. Most cases are supplemented by references which are listed by chapter at the end of the book.

A volume such as this stands or falls on the quality of its images. The mediastinal window images are uniformly good and although the lung window images are generally acceptable, very high resolution lung window images have not been included which, I think, accounts for the erroneous statement on p. 69 that "the earliest pulmonary manifestation of scleroderma is a fine, reticular pattern on chest film. At this initial stage, the appearance of the lung on CT is relatively normal because the interstitial changes are below the resolution of the technique."

The cases have been well chosen and the selected images all make their respective points. The accompanying text is both lucid and well written. The book will be of use to FRCR candidates and should find a place in X-ray Department and CT Unit libraries. It is reasonably priced at £41.50. The authors say in their preface that they hope that both the experienced and inexperienced reader will find the book clear, informative and above all, useful. I think that they have succeeded in their aim but it is more likely that this book will be purchased by libraries and institutions than by individuals.

Denis H. Carr

Renal and Adrenal Tumors: Pathology, Radiology, Ultrasonography, Magnetic Resonance (MRI), Therapy, Immunology, 2nd edn. Ed. by Eberhard Löhr and Lutz-Dietrich Leder, pp. xv + 275, 1987 (Springer-Verlag, Berlin), DM298.
ISBN 3–540–16554–1 (Berlin)
0–387–16554–1 (New York)

This is the second edition of a book which first appeared in 1979. Comparing the list of chapters of the two editions, there has been a considerable shift in the emphasis given to the various imaging techniques described. In their foreword to the current edition the editors contend that the newer techniques of ultrasound, computed tomography and magnetic resonance imaging have completely supplanted intravenous urography and arteriography in the detection of renal tumours. Indeed, intravenous urography does not seem to merit much attention anywhere in this edition and it is not even given an entry in the index; this is a sign of the times. All of the 23 contributors are either German or American. There is no noticeable repetition of material but the style of English is sometimes poor; on the first page there is a reference to bioptic material and other irritating examples of faulty anglicization are scattered throughout the book.

The imaging of renal and adrenal tumours makes up the bulk of the book. This is sandwiched between an account of the pathology of these neoplasms and a few brief final chapters on their treatment and immunology. This first chapter on pathology is a joy to read; it is succinct and beautifully illustrated and includes a few choice colour plates. Each of the many tumour types is given concise macroscopic and microscopic descriptions and a useful feature is an assessment of their likely malignant potential or otherwise under the sub-heading of "Biological Behavior".

The name of Springer-Verlag has become synonymous with first-rate image reproduction, but the sheer quality of the illustrations throughout this book never fails to surprise. The chapter on computed tomography of adrenal tumours is particularly fine in this respect. The chapter on magnetic resonance imaging is comprehensive but the concluding remarks are disconcertingly vague. Apart from detecting tumour thrombus in the intrarenal part of the renal veins and possibly elucidating the natural history of haemorrhagic renal cysts, there is no evidence in this chapter to suggest that MRI has anything, as yet, to offer over CT in the imaging of renal tumours. Childhood renal tumours are well covered but there is an odd little chapter towards the end of the book on prenatal Wilms' tumours which is based on three case reports. Although the discussion on the pathogenesis of these tumours is fascinating, this barely justifies a separate chapter.

If the style of the text could have been refined to match the elegance of the illustrations, this book would have been difficult to better. As it is, this handsome but justifiably expensive volume will appeal to anybody who has more than a passing interest in the imaging of renal and adrenal tumours.

David Hansell

Rational Use of Diagnostic Imaging in Paediatrics. Report of a WHO Study Group. World Health Organization Technical Report Series 757, pp. 102, 1987 (World Health Organization, Geneva), Sw Fr. 14, US $8.40.
ISBN 92-4-120757-4

This is the report of a WHO study group, consisting of some of the most eminent paediatric radiologists from around the world. Their brief was to try to establish how diagnostic imaging should be used in paediatrics, taking into account the widely differing resources available across the world.

Inevitably such a document cannot be too controversial, and whilst the reviewer would not accept all the statements made nor all the recommendations, most of the criticisms would be minor. For example, whilst "routine" radiography of the chest is deprecated there are several occasions in which the left lateral chest radiograph together with a PA (or AP) view in cardiac disease is recommended. I do not think many paediatric radiologists in the UK would agree that the lateral view is particularly helpful in most instances. Again, AP chest tomography is recommended in cases of Wilms' tumour if CT is not available but there is no mention of the difficulties of tomography in the particular age group in which this problem is likely to occur. Isotope studies to examine the renal parenchyma are recommended "because they subject the patient to a lower radiation dose". This is not true of the renal dose in DMSA scanning and is therefore misleading.

Although other radiologists are bound to find statements with which they disagree, the study group is to be commended for accomplishing so much of a virtually impossible task, in giving so much useful advice and guidance to clinicians as well as those involved in imaging in paediatrics. It will also help those radiologists for whom paediatric practice is only a small part of their work to realize what is going on in "mainstream" paediatric imaging.

D. W. Pilling

Books received

Impact of Functional Imaging in Neurology and Psychiatry. Current Problems in Neurology 5. Ed. by J. Wade, S. Knezevic, V. A. Maximilian, Z. Mubrin and I. Prohovnik, pp. viii + 199, 1987 (John Libbey, London), £26.00, US$46.00, FF345.
ISBN 0-86196-106-4

Radiology: Faculty Proceedings of the VI European Congress of Radiology, Lisbon, Portugal, 31 May–6 June 1987. Ed. by M. E. Silvestre, F. Abecasis and J. A. Viega-Pires, pp. xv + 673, 1987 (Excerpta Medica, Amsterdam).
ISBN 0-444-80947-3

The Use of Ultrasound in Patients with Clinical Signs of Appendicitis. By J. B. C. M. Puylaert, pp. 91, 1988 (Drukkerij de Kempenaer, Oegstgeest).

Applications of Thermal Imaging. By S. G. Burnay, T. L. Williams and C. H. N. Jones, pp. xi + 248, 1988 (Adam Hilger, Bristol), £45.00.
ISBN 0-85274-421-8

Developments in Preventive Oncology. Parts A and B (2 volumes). Ed. by Herbert E. Nieburgs, pp. xvii + 548 (Part A), xvi + 471 (Part B), 1987 (Alan R. Liss, New York), $96.00.
ISBN 0-8451-4299-2 (set)
0-8451-4231-3 (Part A)
0-8451-4232-1 (Part B)

Prostaglandins, Leukotrienes and Cancer Eicosanoids and Radiation. Ed. by Peter Polgar, pp. x + 195, 1988 (Kluwer, Boston), £39.50, US$62.50, Dfl.145.00.
ISBN 0-89839-361-7

Clinics in Diagnostic Ultrasound 22. Intraoperative and Endoscopic Ultrasonography. Ed. by Matthew D. Rifkin, pp. xi + 244, 1987 (Churchill Livingstone, New York), £29.95.
ISBN 0-443-0822-6

Diagnosis and Differential Diagnosis of Breast Calcifications. By Marton Lanyi, pp. viii + 252, 1988 (Springer Verlag, Berlin), DM148.
ISBN 3-540-16949-0 (Berlin)
0-387-16949-0 (New York)

Frontiers of Clinical Neuroscience Volume 4: Clinical Neuroimaging. Ed. by William H. Theodore, pp. x + 288, 1988 (Alan R. Liss, New York), $62.50.
ISBN 0-8451-4503-7

Health Effects of Low Dose Ionising Radiation: Recent Advances and their Implications. Proceedings of an international conference held in London on 11–14 May 1987, pp. vi + 209, 1987 (British Nuclear Energy Society, London).
ISBN 0-7277-1302-7

PUBLICATIONS OF THE BRITISH INSTITUTE OF RADIOLOGY

	Price (p. & p. included)
BJR Supplements:	
22. Megavoltage Radiotherapy 1937-1987, 1988, 160 pp., ISBN: 0 905749 16 2	£28.50
21. Radionuclides in Brachytherapy: Radium and After, 1987, 64 pp., ISBN: 0 905749 15 4	£15.00
20. The Safety of Diagnostic Ultrasound, 1987, 48 pp., ISBN: 0 905749 14 6	£12.00
19. Radiation Damage to Skin Fundamentals and practical aspects, 1986, 159 pp., ISBN: 0 905749 13 8	£30.00
18. Criteria and Methods for Quality Assurance in Medical X-ray Diagnosis, 1985, 179 pp., ISBN: 0 905749 12 X	£27.50
17. Central Axis Depth Dose Data for use in Radiotherapy This standard work replaces BJR Supplement 11 (1972), 1983, 147 pp., ISBN: 0 905749 111	£25.00
Other publications:	
Assurance of Quality in the Diagnostic X-ray Department, 1988, 160 pp., ISBN: 0 905749 17 0	£20.00
Basic Clinical Ultrasound Hylton B Meire and Pat Farrant, 1982, (BIR Teaching Series No.4) 170 pp., ISBN: 0 905749 10 3	£12.50
Special Report 17: High Dose Rate Afterloading in the Treatment of Cancer of the Uterus, 1980, 200 pp., ISBN: 0 905749 07 3	£18.50
SI Unit Cards	.50
Review article: **The Radiological Effects of Nuclear War** (BJR, 1983, 56, 147-170) Report of a BIR Working Party	£1.00

Order Form

Please order these titles from your local bookseller — or in case of difficulty from: Butterworths, Borough Green, Sevenoaks, Kent TN15 8PH

Telephone Orders (0732) 884567
Telex Orders 95678

24-Hour Order Line (0732) 882566
This line gives immediate access at any hour: Orders can be placed over the telephone by using your Butterworths account number or by charging to your credit card account.

Please send me the following titles:

Qty	Title/ISBN	£ Price
....	....	....
....	....	....
....	....	....
....	....	....
....	....	....
....	....	....
....	....	....
....	....	....
....	....	....
	TOTAL £	....

Please select preferred method of payment

☐ I enclose remittance for £ ....

☐ Please debit my credit card as follows:

☐ Access/ Mastercard ☐ Barclaycard and other VISA cards ☐ American Express

Card number

☐☐☐☐☐☐☐☐☐☐☐☐☐☐☐☐

Expiry date ....

Signature .... Date...............

Name ....

Position ....

Address ....

....

.... Postcode ....

All prices are subject to change without notice and orders are subject to acceptance by Butterworths head office. Please allow 28 days for delivery in the UK.

Registered Office: 88 Kingsway, London, WC2B 6AB
Registered in England No 125354

25 AUG 1989

The dynamic Clinac
Varian introduces the Clinac 2100-C

Designed to match radiotherapy of today and tomorrow, the Clinac 2100-C performs the treatments of your choice with microprocessor controls.

Combining microprocessors with the proven yet unmatched beam performance of the switchguide results in the leading concept for modern dual modality therapy systems.

The Clinac 2100-C offers advanced application software modules supported by sound accelerator firmware. It's a design of choice – your choice.

varian

Varian – the Predictable Future

Scandinavia: Lyskaer 9 / DK-2730 Herlev / Denmark / Phone (02) 84 61 66
UK and Ireland: Gatwick Rd. / Crawley Sussex RH 10 2RG / Great Britain / Phone: (0293) 312 44
Europe: Steinhauserstrasse / CH-6300 Zug / Switzerland / Phone: (042) 44 88 44
Germany: Alsfelderstrasse 6 / Postfach 111435 / D-6100 Darmstadt / Phone: (06151) 7030
Asia: Room 1018-20 / Tower A / Mandarin Plaza / TST East / Kowloon / Hong Kong / Phone: 3-724-283
Australia: Unit 6 / Frenchs Forest Road (East) / French Forest, N.S.W. 2086 / Phone: 451-1933
USA: 611 Hansen Way / Palo Alto / California / Phone: (415) 424-6200